



LUND UNIVERSITY

Prediction models for chloride ingress and corrosion initiation in concrete structures

Nilsson, Lars-Olof

Published in:
P-01:6

2001

[Link to publication](#)

Citation for published version (APA):

Nilsson, L.-O. (2001). Prediction models for chloride ingress and corrosion initiation in concrete structures. In L.-O. Nilsson (Ed.), *P-01:6* Chalmers University of Technology.

Total number of authors:

1

General rights

Unless other specific re-use rights are stated the following general rights apply:

Copyright and moral rights for the publications made accessible in the public portal are retained by the authors and/or other copyright owners and it is a condition of accessing publications that users recognise and abide by the legal requirements associated with these rights.

- Users may download and print one copy of any publication from the public portal for the purpose of private study or research.
- You may not further distribute the material or use it for any profit-making activity or commercial gain
- You may freely distribute the URL identifying the publication in the public portal

Read more about Creative commons licenses: <https://creativecommons.org/licenses/>

Take down policy

If you believe that this document breaches copyright please contact us providing details, and we will remove access to the work immediately and investigate your claim.

LUND UNIVERSITY

PO Box 117
221 00 Lund
+46 46-222 00 00



Prediction models for chloride ingress and corrosion initiation in concrete structures

LARS-OLOF NILSSON

Department of Building Materials
CHALMERS UNIVERSITY OF TECHNOLOGY
Göteborg, Sweden 2001

Chalmers tekniska högskola
Institutionen för byggnadsmaterial

Publikation P-01:6
Arb nr 621

**PREDICTION MODELS FOR CHLORIDE INGRESS AND
CORROSION INITIATION IN CONCRETE STRUCTURES**

(Nordic Mini Seminar & *fib* TG 5.5 meeting, Göteborg, May 22-23, 2001)

Editor

Lars-Olof Nilsson

Göteborg, December 2001

Keywords:

Concrete
Chloride
Corrosion
Models
Test case

Publikation P-01:6
ISSN 1104-893X
Institutionen för Byggnadsmaterial
Chalmers Tekniska Högskola
S-412 96 GÖTEBORG
Tel: 031-7721000

LIST OF CONTENTS

- 1 Introduction
Lars-Olof Nilsson (seminar objectives)
- 2 Prediction Models for Chloride Ingress into Uncracked Concrete
 - 2.1 Lars-Olof Nilsson. Overview of Prediction models for chloride ingress into concrete structures
 - 2.2 Joost Gulikers. Historic Interpretation of Chloride Profiles for the Eastern Scheldt Storm Surge Barrier
 - 2.3 Steinar Helland. The Selmer Chloride Ingress Model
 - 2.4 Jens Frederiksen & Mette Geiker. On an Empirical Model for Estimation of Chloride Ingress into Concrete
 - 2.5 Sascha Lay. (Test application of) DuraCrete Models
 - 2.6 Michael Thomas, Evan Bentz & Per Fidjestøl. The Life-365 Chloride ingress and corrosion Model
 - 2.7 Tang Luping. The original and modified ClinConc model
 - 2.8 Björn Johannesson. An Overview of Models on Multi-species Diffusion in Pore Solution of Concrete
 - 2.9 Björn Johannesson. A theoretical model describing diffusion of a mixture of different types of ions in pore solution of concrete coupled to moisture transport
 - 2.10 Jens Frederiksen. How to Apply the Hetek Model in the Road Environment – 1999
 - 2.11 Gro Markeset. Consequences of Uncertainties in Model Parameters
- 3 Environmental Actions
 - 3.1 Anders Lindvall. Original quantification of the Environmental Parameters in the DuraCrete Chloride Ingress Model
 - 3.2 Bernt J. Leira. Service Life Prediction of Chloride Ingress by Probabilistic Methods
- 4 Concrete Transport Properties
 - 4.1 Bertil Persson. Chloride ingress properties of 63 SCC:s
- 5 Corrosion initiation
 - 5.1 Jens Frederiksen. Chloride Threshold Values for Service Life Design
 - 5.2 Raoul Francois. Threshold levels and effects of cracks on corrosion
 - 5.3 Ervin Poulsen, Jens Frederiksen & Leif Mejlbro. Characteristic value of the initiation time, with special reference to marine RC structures

6 Overview of Research, Research Needs

6.1 Watanabe Hiroshi. Chloride and corrosion research in Japan

7 Test Case

7.1 The Test Case

7.2 The Test Environments

7.3 Contributions

7.4 Comparison

7.5 Discussion and conclusion

8 Conclusions

APPENDIX – Contributions to the test case

1 INTRODUCTION

fib task group 5.5 and **Nordic Seminar on**

**PREDICTION MODELS FOR CHLORIDE INGRESS AND CORROSION INITIATION
IN CONCRETE STRUCTURES**

1 INTRODUCTION

Lars-Olof Nilsson

Objective

To summarize, discuss, question and conclude the present state-of-the-art on prediction models for corrosion initiation due to chloride ingress in structures exposed to sea water and de-icing salts.

Preliminary topics:

- Chloride ingress into un-cracked concrete
- The effect of cracks on chloride ingress
- Chloride ingress in various environments (marine submerged and splash, road, p-deck, etc.)
- Chloride threshold levels for corrosion initiation
- The effect of cracks on corrosion initiation (and rate of corrosion?)
- Corrosion initiation in various environments

***PREDICTION MODELS FOR CHLORIDE INGRESS AND CORROSION
INITIATION IN CONCRETE STRUCTURES***

Final PROGRAM

Tuesday May 22

11.00 Gathering, Restaurant Einstein, lunch

12.15 Introduction, presentation of participants, room 2003-2004

Lars-Olof Nilsson (seminar objectives) & Steen Rostam (updating EN206)

12.45 Prediction Models for Chloride Ingress into Uncracked Concrete

Lars-Olof Nilsson

Overview of Prediction models for chloride ingress into concrete structures

Joost Gulikers

Historic Interpretation of Chloride Profiles for the Eastern Scheldt Storm Surge Barrier

Steinar Helland

The Selmer Chloride Ingress Model

Jens Frederiksen & Mette Geiker

On an Empirical Model for Estimation of Chloride Ingress into Concrete

13.45 Coffee Break

Sascha Lay

(Test application of) DuraCrete Models

(Michael Thomas) Per Fidjestøl

The Life-365 Chloride ingress and corrosion Model

Tang Luping

The original and modified ClinConc model

Nick Buenfeld

The Imperial College Chloride Ingress Model

Björn Johannesson

An Overview of Models on Multi-species Diffusion in Pore Solution of Concrete

Björn Johannesson

A theoretical model describing diffusion of a mixture of different types of ions in

pore solution of concrete coupled to moisture transport

Jens Frederiksen

How to Apply the Hetek Model in the Road Environment - 1999

Discussion

Consequences of Uncertainties in Model Parameters (Gro Markeset)

Time and concentration dependent diffusion coefficients and chloride binding (Harald Justnes)

16.30 Chloride Ingress into Cracked Concrete

Leif Mejlbro

A solution to Fick's 2nd law for cracked concrete

Discussion

19.00 Dinner, Ahlströms Pir, Eriksberg (boat trip from Lilla Bommen 18.30)

Wednesday May 23

08.30 Environmental Actions

Anders Lindvall

Original quantification of the Environmental Parameters in the DuraCrete Chloride Ingress Model

Response to chloride environments by seven Swedish road bridges

Per Fidjestöl

Recent chloride profiles from a quay in Göteborg

Bernt J. Leira

Service Life Prediction of Chloride Ingress by Probabilistic Methods

Discussion

09.15 Concrete Transport Properties

Bertil Persson

Chloride ingress properties of 63 SCC's

Doug Hooton, M. Geiker and M. Nokken

Effects of Curing Regimes on Transport properties and Service Life

Mette Geiker & Erik Pram Nielsen

Effect of degree of saturation on transport in cementitious materials

Discussion

Coffee break

10.30 Corrosion initiation

Henrik E Sørensen

The HETEK SoTA on corrosion initiation

Jens Frederiksen

Chloride Threshold Values for Service Life Design

Raoul Francois (written)

Threshold levels and effects of cracks on corrosion

Ervin Poulsen, Jens Frederiksen & Leif Mejlbro

Characteristic value of the initiation time, with special reference to marine RC structures

Discussion

11.45 Lunch break

13.00 Test Case

Summary and discussion of contributions by

Marianne Tange Jepsen	Predictions for the Test case
Sascha Lay	Test application of DuraCrete Models
Jens Frederiksen	The HETEK model
Steinar Helland	The Selmer Model
Tang Luping	The ClinConc Models
Lars-Olof Nilsson	An Incorrect Empirical ERFC-Model
Mike Thomas	The 365 LIFE-model
Lars-Olof Nilsson	The NIST- model
Doug Hooton	The Toronto Model
others	

Discussion

Overview of Research, Research Needs

Watanabe Hiroshi (written)

Chloride and corrosion research in Japan

Discussion

15.00 CLOSURE

Participants:

Anders Lindvall	lindvall@bm.chalmers.se
Bernt J. Leira	bernt.leira@marin.ntnu.no
Bertil Persson	bertil.persson@byggtek.lth.se
Björn Johannesson	bjorn.johannesson@byggtek.lth.se
Doug Hooton	hooton@civ.utoronto.ca
Erik Pram Nielsen	erik_pram_nielsen@hotmail.com
Ervin Poulsen	ervin-poulsen@get2net.dk
Gro Markeset	gro.markeset2fbt.mil.no
Harald Justnes	harald.justnes@civil.sintef.no
Henrik E Sørensen	hes@force.dk
Jens Frederiksen	jmf@aec-dk.com
Joost Gulikers	j.gulikers@bwd.rws.minvenw.nl
Leif Mejlbro	l.mejlbro@mat.dtu.dk
Lars-Olof Nilsson	nilsson@bm.chalmers.se
Tang Luping	tang.luping@sp.se
Marianne Tange Jepsen	Marianne.T.Jepsen@teknologisk.dk
Mette Geiker	mge@byg.dtu.dk
Michael Thomas (corr.)	michael.thomas@utoronto.ca
Nick Buenfeld	n.buenfeld@ic.ac.uk
Per Fidjestol	per.fidjestol@elkem.no
Raoul Francois (corr)	francois@lmdc.insa-tlse.fr
Sascha Lay	lay@bsi.bv.tum.de
Steen Rostam	sro@cowi.dk
Steinar Helland	steinar.helland@selmer.skanska.no
Watanabe Hiroshi (corr.)	

2 PREDICTION MODELS FOR CHLORIDE INGRESS INTO UNCRACKED CONCRETE

Overview of

PREDICTION MODELS FOR CHLORIDE INGRESS INTO CONCRETE STRUCTURES

Lars-Olof Nilsson

Different prediction models have a number of similarities and differences. They require different input data that look alike, but sometimes are quite different. A structure of the available methods is:

A. EMPIRICAL METHODS.

“Empirical methods” are methods where chloride profiles are predicted from analytical or numerical solutions (true or false!) to Fick’s 2nd law of diffusion.

1. ERFC-methods

- a. Constant D_a & C_{sa} (traditional, Collepardi, Japan)
- b. $D_a(t)$ & constant C_{sa} (Selmer-Poulsen, Bamforth, DuraCrete)
- c. $D_a(t)$ & $C_{sa}(t)$ (Nilsson)

2. Analytical solutions to Fick's 2nd law (other than *erfc*)

- a. $D(t)$ & $C_s(t)$ (Mejlbro-Poulsen, Hetek)

3. Numerical solutions to Fick's 2nd law

- a. $D_{F2}(t)$ & $C_{sf}(t)$, binding isotherm (NIST)
- b. $D_{F2}(t)$ & $C_s(t)$ (Life-365)

B. PHYSICAL METHODS

“Physical methods” are methods where chloride transport and chloride binding are described with separate, physical expressions.

1. based on Fick's 1st law

- a. Binding isotherm (ClinConc)
- b. Convection models (Hetek, Imperial, Toronto)

2. based on the Nernst-Planck flow equation

- a. Binding isotherm (Truc)
- b. Ion-solid equilibrium (Johannesson)
- c. Chemically bound Cl (Samson)

HISTORIC INTERPRETATION OF CHLORIDE PROFILES FOR THE EASTERN SCHELDT STORM SURGE BARRIER

Joost Gulikers
Research Department
Ministry of Transport, Public Works and Water
Management
3502 LA UTRECHT
THE NETHERLANDS
E-mail: j.gulikers@bwd.rws.minvenw.nl

ABSTRACT

The Eastern Scheldt Storm Surge Barrier located in the south-western part of The Netherlands is designed for a service life of 200 years. Although there was a lack of practical experience with respect to such a long service life for structures continuously exposed to an aggressive marine environment, an attempt was made to meet this requirement by analysing the process of corrosion initiation by chlorides.

In view of the function of the structure reliable information on the actual performance over time is considered of vital importance. This will allow cost-effective preventive measures to be taken without impairing flood protection. Although there are yet no visible signs of distress after more than 20 years of exposure, an urgent need has emerged to validate the model which has been used to describe the process of chloride penetration through the concrete cover. To this end previous measurements have been evaluated in order to arrive at a better procedure for chloride determination in view of service life prediction.

Keywords: chloride, concrete, durability, models

1 INTRODUCTION

The storm surge barrier across the Eastern Scheldt is the most impressive part of the so-called Delta project which started one year after the catastrophic flooding disaster of 1953. This project aimed to protect the low-lying polders in the south-western part of The Netherlands against flooding from the rivers and the sea water and to enable fresh water and salt water to be separated and controlled. Probabilistic methods were introduced in the design with a probability of exceeding of 2.5×10^{-4} time per annum as the criterion according to the Delta Committee. After a construction period of approximately 5 years the barrier was officially opened in October 1986.

A significant part of the barrier is made of steel reinforced concrete structures. Even though reinforced concrete structures did not have a track record in excess of 100 years the barrier was specified for a service life of 200 years. Due to this rather unusual service life requirement the Eastern Scheldt Storm Surge Barrier was probably one of the first large scale marine structures in the world in which explicitly attention had been devoted to durability in the design process aimed at achieving the target service life. Since durability was not covered explicitly by prescriptive code recommendations at the time of design and construction of the barrier, predictive models to describe the destructive impact of the aggressive marine environment on the structure were developed. At present, after nearly 20 years of continuous exposure, an urgent need has emerged to develop a maintenance and repair strategy on a probabilistic basis.

2 DESCRIPTION OF THE STRUCTURE

The storm surge barrier has a total length of 2800 m, thereby crossing 3 tideways (Hammen, Schaar and Roompot). In Fig. 1 the major components of the barrier are shown. The complete barrier comprises 66 monolithic concrete piers with a centre to centre distance of 45 m, heights ranging from 35 to 45 m and base plates of 25×50 m².

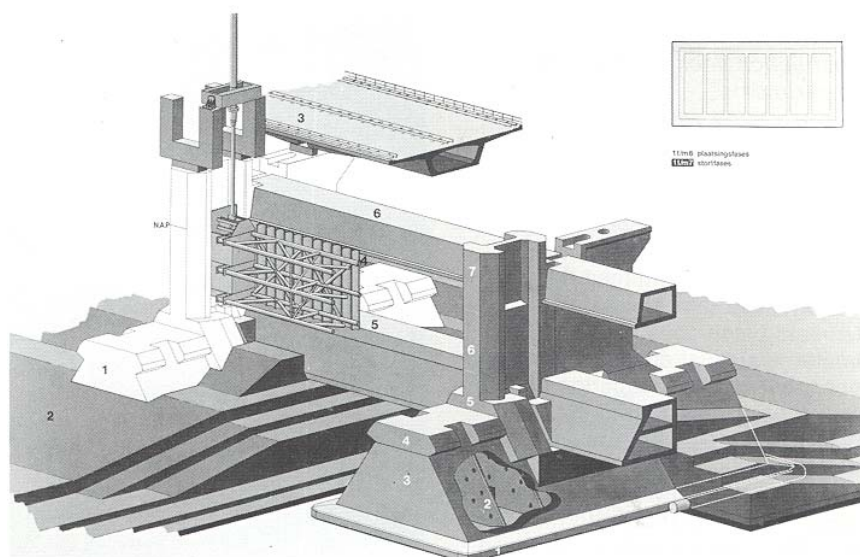


Fig. 1 Components of the storm surge barrier

The piers are linked by the threshold beams placed on the seabed and upper beams located approximately 1 m above mean tide level. The piers, threshold beams and upper beams are manufactured from normal weight concrete reinforced with mild and prestressing steel. A motorway is built over the storm surge barrier. The road bridge sections over the piers are constructed from prestressed concrete box girders, which house the machinery for operating the gates. At the abutments the box girder sections are fabricated from light weight concrete (expanded clay) whereas the remaining 63 sections are manufactured from normal weight concrete. The concrete piers are

considered to be the backbone of the storm surge barrier, supporting the superstructure, guiding the steel gates for closing the apertures, and transferring the forces exerted by a superstorm to the foundation.

3 DESIGN FOR DURABILITY

The concrete components of the storm surge barrier are designed for a service life of 200 years. In view of the lack of practical experience with regard to such a long service life, there was an urgent need to predict the durability requirements. Given the continuous exposure to an aggressive marine environment, initiation of reinforcement corrosion by penetration of chlorides through the concrete cover was considered the prevalent mode of deterioration. Therefore the design was directed at achieving structures with a minimum amount of cracks in the concrete cover. This was effected by extensive artificial cooling during the cement hydration process, adequate detailing and quality control during execution, as well as provisions for prestressing to prevent shrinkage cracks and crack development during service conditions. In addition blast furnace slag cement with a slag content of 75% was used which exhibits a lower heat of hydration and has proven to be superior to ordinary Portland cement when exposed to marine exposure conditions.

In order to establish the relevant parameters regarding chloride penetration into concrete and corrosion of the embedded reinforcing steel a literature review was performed /1/. Based on these findings an extension of the schematic phasing model introduced by Beeby /2/ and Tuutti /3/ has been used to distinguish between the subsequent stages of the deterioration process. In addition to the initiation stage in which chloride ions penetrate the concrete cover in sufficient amount to depassivate the steel the propagation stage has been subdivided into two time periods. A distinction has been made between active reinforcement corrosion in the presence of a concrete cover and when freely exposed to the ambient atmosphere.

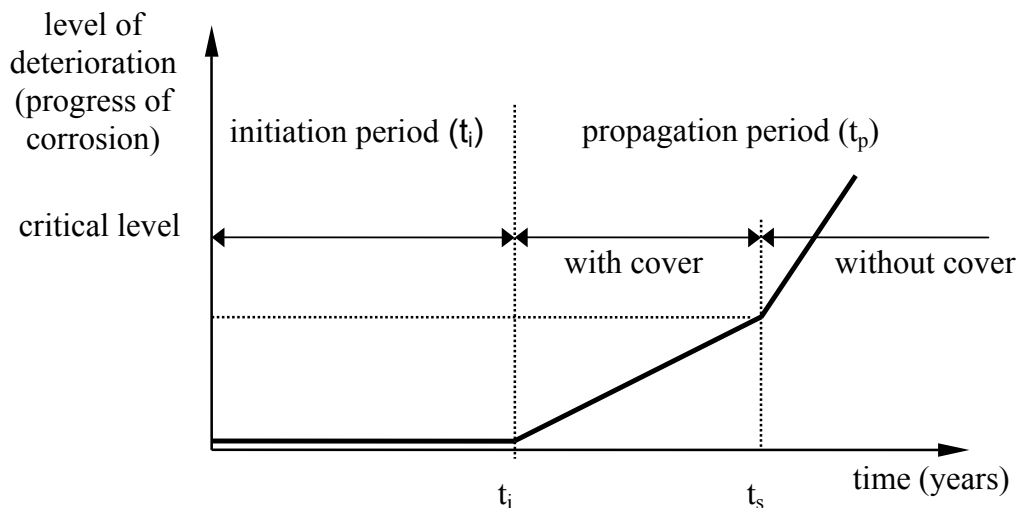


Fig. 2 Stages during service life with respect to corrosion of reinforcement

With respect to the exposure conditions a subdivision in three zones is made, i.e. the submerged, the tidal and the splash zone. The submerged zone is characterised by a high chloride and a low oxygen diffusion rate. In the splash zone the penetration of chloride is considered to be relatively low, but the oxygen flux is high. For the tidal zone intermediate conditions apply. The penetration rate of chloride is decisive for the initiation stage, whereas oxygen diffusion determines the rate of reinforcement corrosion during the propagation stage.

For the initiation stage of deterioration the standard solution to Fick's 2nd law of diffusion for an isotropic, semi-infinite medium is adopted. The process of chloride penetration into the concrete cover as a function of time, is described by:

$$c(x,t) = c_s \cdot \left[1 - \operatorname{erf} \left(\frac{x}{2\sqrt{D_c t}} \right) \right] \quad [\% \text{ m/m}] \quad (1)$$

where $c(x,t)$ is the chloride concentration at depth x from the exposed concrete surface after time t for a steady state chloride concentration c_s at the exposed surface; erf is the error function. All chloride concentrations refer to the total (acid-soluble) chloride level and are expressed as a percentage with respect to mass of cement [% m/m]. The initial chloride concentration due to contamination of the mix ingredients is considered to be 0%.

The input data regarding threshold and surface chloride content, oxygen content, and diffusion coefficients for chlorides and oxygen were obtained from the literature review. A compilation of the input values for these relevant parameters is given in Table 1.

	exposure zone		
parameter	splash	tidal	submerged
c_s (%)	2.4	2.4	2.4
c_{crit} (%)	0.5	0.5	0.5
D_c (mm ² /year)	20	20	50

Table 1 Input values for the determination of the initiation and propagation period

For the chloride concentration, c_s , at the exposed concrete surface a fixed value of 2.4% was assumed for the three exposure zones. This value was considered to be a safe estimate. Taking into account the high quality of the cover concrete the threshold level, c_{crit} , for the depassivation of steel was fixed at 0.5%. Substitution of these values in (1) yields an expression for the initiation time as a function of effective chloride diffusion coefficient, D_c , and depth of cover, d :

$$t_i = 0.316 \cdot \frac{d^2}{D_c} \quad [\text{year}] \quad (2)$$

Based on unknown considerations a minimum cover depth of 70 mm had been specified. This resulted in a prediction for the initiation time of 77.4 years for the splash and tidal zone, and 31.0 years for the submerged zone. It was emphasised that near cracks the local initiation time could be reduced to 30% if the extensive precautions regarding crack width limitation would prove to be not effective.

The acceptable degree of corrosion is expressed as an average loss in rebar diameter and is arbitrarily set at 0.2 mm. Since it is anticipated that this value will not result in cracking of the concrete cover, this criterion is considered as a “warning limit”. Predictions for the corrosion rate ranged from 91.74 $\mu\text{m}/\text{year}$ for the splash zone, 18.64 $\mu\text{m}/\text{year}$ for the tidal zone, and 0.84 $\mu\text{m}/\text{year}$ for the submerged zone. According to the theory adopted the corrosion rate of reinforcing steel in the splash zone approaches that of unprotected steel which is in the order of 100 $\mu\text{m}/\text{year}$, independently of the thickness of the concrete cover. The predicted development of the deterioration process is shown in Fig. 3.

Thus the estimated service life of the concrete components located in the splash and tidal zone is significantly less than the target service life used in the design. Consequently, loss of cover by cracking and spalling may be expected to occur within 80 and 95 years of service life in these zones. In view of this extensive repair is not precluded during the design stage, but this action is considered practically feasible for the tidal and splash zone.

Due to the continuous lack of oxygen, the corrosion rate of reinforcing steel embedded in the submerged zone is restricted. Although the initiation time is relatively short, the propagation period is expected to increase the service life beyond 200 years.

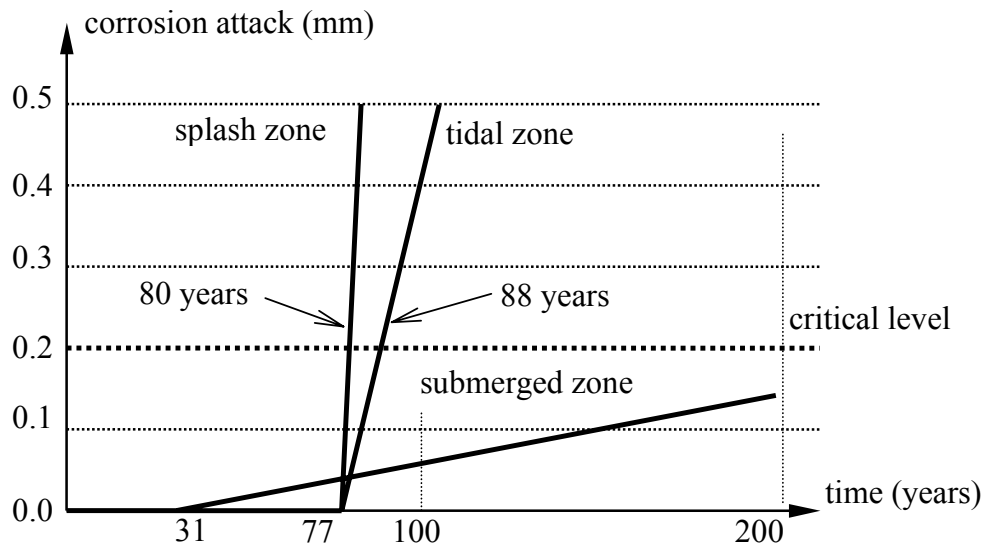


Fig. 3 Predicted development of the deterioration for the splash, tidal and submerged zone

In view of the uncertainties in the mathematical modelling and consequently uncertainties regarding the duration of the initiation period, a regular condition assessment is performed. This involves determination of the chloride profile of a limited number of concrete cores retrieved from selected locations every 5 years. In 1991 the last chemical analysis of the chloride content was performed on concrete disks of approximately 10 mm thickness. Given the high concrete quality and the relative short exposure period this approach resulted in 2 or 3 values for individual cores representing the local chloride profile. Given the relatively slow process of chloride penetration it was decided to wait until 2001 to execute new measurements.

In order to arrive at a prediction of the initiation period for reinforcement corrosion, to date the following procedure has been adopted:

- the chloride penetration follows Fick's 2nd law of diffusion corresponding to expression (1);
- all factors used in (1) have constant values in time;
- the diffusion coefficient, D_c , is independent of depth;
- the average chloride content of the first slice is substituted for the surface chloride concentration, c_s ;
- deeper values for the chloride profile are not taken into account;
- the value for the effective chloride diffusion coefficient used in the initial penetration model, i.e. $D_c = 20 \text{ mm}^2/\text{yr}$, is maintained.

Based on measurements of 1989 and 1991 it was anticipated that corrosion initiation would be delayed by approximately 20 years corresponding to an initiation period of 100 years. However, a critical evaluation of this procedure reveals several major pitfalls.

At first it has to be realised that all models are a simplification of actual processes occurring in practice. In this respect the solution to Fick's 2nd law of diffusion may be considered a practical and sufficiently reliable mathematical description for chloride ingress on the long term for exposure conditions where diffusion is the prevalent transport mechanism. Departing from this model, it is obvious that equating the chloride content of the outer disk to the content of the concrete surface, could seriously underestimate the actual value of c_s . Based on (1) the ratio of the average chloride content of the first disk, c_1 , to the real surface content, c_s , can be calculated. In Fig. 4 the ratio's are shown for a disk thickness of 10 mm as a function of exposure time for two values of D_c . Especially for short exposure times significant differences will occur, i.e. after 5 years the average content amounts to 73 and 91% of the "real" surface content, for $D_c = 20$ and $D_c = 200 \text{ mm}^2/\text{yr}$, respectively. Accordingly, a longer initiation period will be predicted if c_s is underestimated. As an example a comparison for the corrosion initiation period of the storm surge barrier is demonstrated between the "real" duration based on the extrapolated surface content and the duration based on

the average chloride content of the first slice. For the situation found in practice, with $c_1 = 1.6\%$ after an exposure period of 10 years this would imply a difference in initiation period of approximately 50 years (Fig. 5). Moreover, it has to be borne in mind that the chloride distribution in the outer concrete layer is very much dependent on exposure conditions and will normally not demonstrate ideal “Fickian” behaviour.

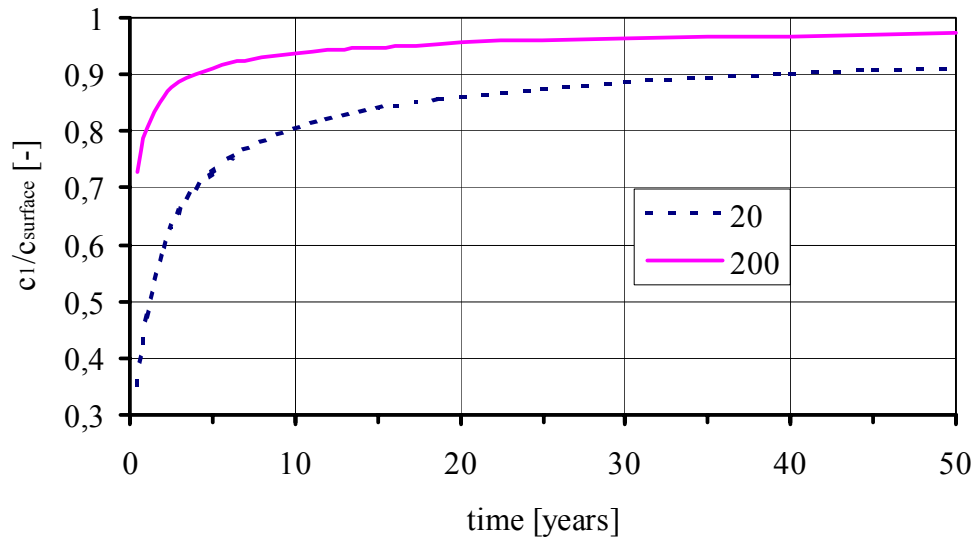


Fig. 4 Ratio of average chloride content of disk 1 (thickness 10 mm) and surface chloride content as a function of time

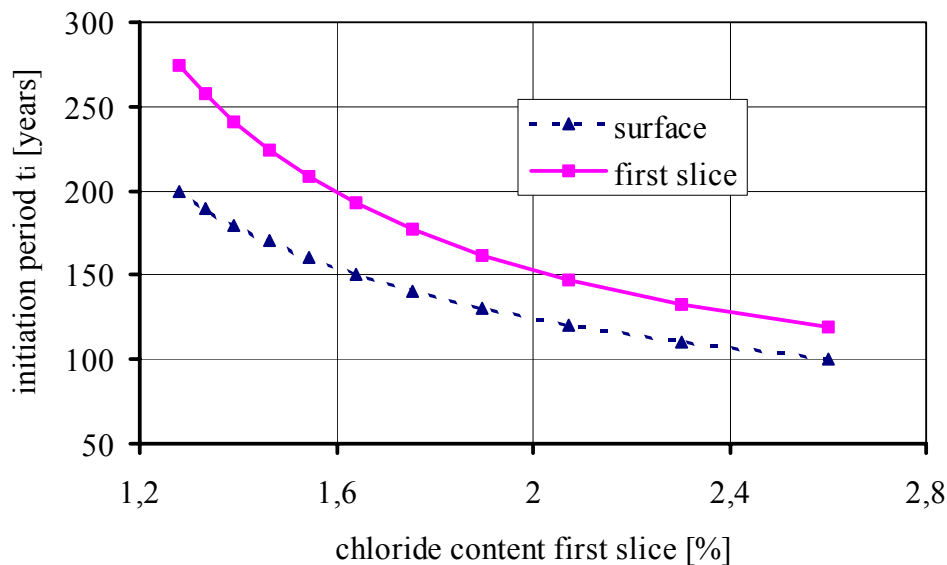


Fig. 5 Influence of equating chloride content of first disk (thickness 10 mm) to surface chloride content on the corrosion initiation period

Leaching, carbonation, evaporation, and washing off are known to affect the near surface chloride distribution.

With respect to corrosion initiation, the presence of surface cracks will influence the local penetration rate and average values for the chloride content will not reflect variations on a smaller scale.

The actual effective chloride diffusion coefficient is not taken into account. This would require fitting of the chloride profile, but considering that only 2 or 3 values are provided this will probably not result in a reliable value for D_c .

5 RECOMMENDATIONS

Based on the evaluation of the measurement procedure adopted to date the following recommendations are suggested:

- More detailed determination of the existing chloride profiles in order to arrive at a more reliable prediction of chloride penetration over time. However, this would require slices of 5 and preferably 2 mm thickness and consequently a decreasing amount of material for chemical analysis. The disturbing influence of physical and chemical phenomena acting at the outer concrete layer has to be avoided by discarding the outer surface layer of approximately 5 mm thickness.
- Critical evaluation of the aggressivity of the local exposure conditions, taking into account shielding effects, wind direction, and height above mean tide level.
- Formulation of requirements for a statistical analysis of chloride penetration addressing number, location and frequency of measurements.
- Execution of a statistical analysis of the actual cover depths in order to predict the probability of initiation of reinforcement corrosion. This requires extensive non-destructive measurements to be executed on all concrete components of the structure.
- Execution of accelerated laboratory tests on concrete specimens retrieved from several parts of the structure to obtain a realistic value for the actual chloride transport coefficient.

6 CONCLUDING REMARKS

Generally, after 14 years of marine exposure no signs of serious deterioration due to reinforcement have been identified. Chloride profiles obtained until now indicate a very slow penetration rate in the components made from normal concrete. However, the light weight concrete box girders of the bridge revealed significant contamination with chlorides. As the design was mainly focused on the durability of the structural components of the barrier, little attention has been paid to the performance characteristics of components made of light weight concrete. This situation has now been recognised and future investigations will be primarily directed at quantitative assessment of the box girder components.

It must be borne in mind that the major transport parameters, i.e. effective diffusion coefficient and chloride surface concentration, can be adjusted in the course of time by fitting to the measured chloride profile. However, the threshold level remains a rather

uncertain factor. In view of the significant impact of this parameter on service life prediction further research is urgently needed.

A proposal has been drafted in order to arrive at a more reliable prediction of the future performance of the concrete structure regarding chloride penetration and subsequent corrosion. The proposal adopts the approach developed in the European DuraCrete project /4/ for a probabilistic performance based durability design of concrete structures. The Eastern Scheldt Storm Surge Barrier will be used as a case study for implementation of this probabilistic approach to an existing structure.

REFERENCES

- /1/ Reijgersberg, A.A.J. (1982) *The life time of the Eastern Scheldt Barrier, Part I: An arithmetical approach of the corrosion process in reinforced concrete*. Report nr. 1337-1-0.
- /2/ Beeby, A.W. (1978) *Cracking and corrosion*, Concrete in the Oceans, Technical Report No. 1.
- /3/ Tuutti, K. (1982) *Corrosion of steel in concrete*. Swedish Cement and Concrete Research Institute, Stockholm. Report No. CBI Research FO 4:82.
- /4/ DuraCrete (1998) *Modelling of degradation*. Document BE95-1347/R4-5.

THE “SELMER” CHLORIDE INGRESS MODEL

Steinar Helland
Head - Concrete Technology Group
Selmer Skanska AS
P.O.Box 12175 – Sentrum,
N - 0107
Oslo
NORWAY
E-mail: steinar.helland@selmer.skanska.no

ABSTRACT

In the 1970s, Collepardi introduced Fick's second law of diffusion for describing the ingress of chlorides in concrete. During the 1980s the researchers gradually realised that the application of this model gave an unrealistic rapid transport of chloride ions when long-term predictions were based on short-term characterisation of the material's diffusion coefficient.

In the late 1980s Selmer started work to improve the model. The basis was characteristics measured on a number of Norwegian coastal bridges /1/ and cast and exposed concrete specimens subject to various laboratory and field conditions.

Due these experimental data, the so-called “Selmer” model was derived as an empirical “curve-fitting” to the observations.

Due to the well-established literature and database worldwide linked to Fick's second law, we did choose to base our model on this equation, and just modify one parameter, the diffusion coefficient.

The “Selmer model” therefore does not state whether the chloride transport is due to a diffusion process or a combination of different phenomena. It just considers this equation as a convenient one for “curve-fitting”.

During the 1990s we have experience a fairly good correlation between our observations and the model.

This paper is mainly based on the EuroLightCon report BE96-3942/R3, “Chloride penetration into concrete with lightweight aggregates”, March 1999 /2/. The full report on the model and its application is downloadable from www.sintef.no/bygg/sement/elcon

Keywords: chloride, models

1 THEORETICAL BACKGROUND

The development of the theoretical model is described more in detail in /3/.

It is assumed that chloride ingress into concrete obeys Fick's second law of diffusion for a semi-finite medium with constant exposure, and that there is a critical value of the chloride content in the concrete, $C = C_{cr}$, leading to the corrosion of steel:

$$C(x,t) = C_i + (C_s - C_i) \cdot \operatorname{erfc}\left(\frac{x}{\sqrt{4tD}}\right)$$

where:

$C(x,t)$ = Chloride content at depth x at time t .

C_i = Initial chloride content.

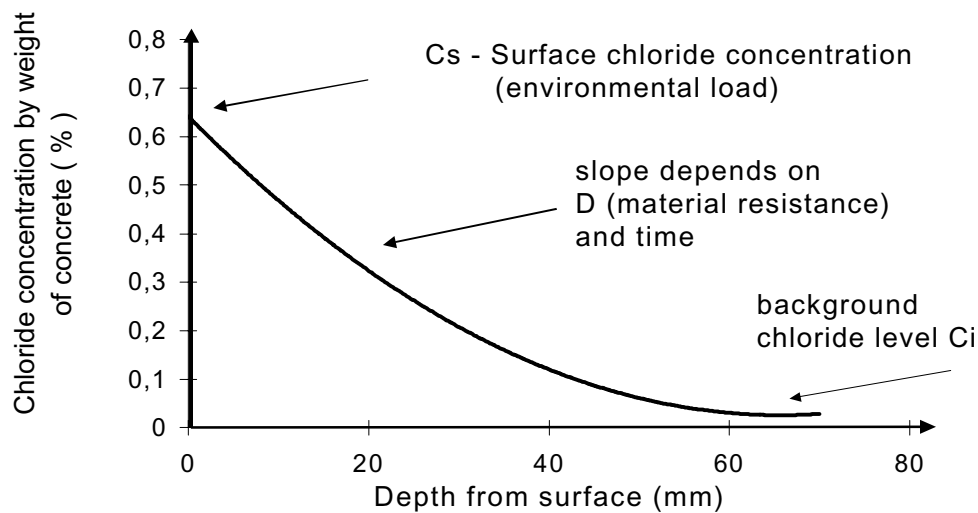
C_s = Chloride content on the exposed surface.

t = Exposure time.

x = Depth.

erfc = Error function.

D = Chloride diffusion coefficient.



The chloride diffusion coefficient, D , is an important material parameter that has been

considered as a time independent parameter. However, laboratory testing /4/, /5/ and results from existing structures /5/ show that the concrete age dependency of the coefficient obeys a straight line in a double logarithmic coordination system. This means that a general mathematical model may be expressed as:

$$D(t) = D_R \cdot \left(\frac{t_R}{t}\right)^k \quad (2)$$

where:

$D(t)$ = Time dependant chloride diffusion coefficient.

t = Time when $D(t)$ is valid.

t_R = Time when reference diffusion coefficient D_R was measured.

D_R = Reference diffusion coefficient at time t_R .

k = Parameter to be determined by regression analysis of test results.

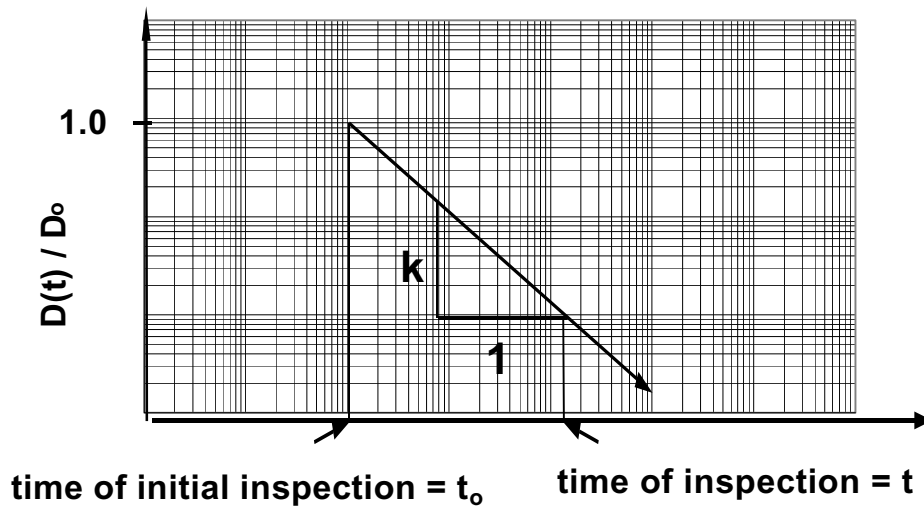


Figure 2 The decrease of achieved diffusion coefficient D over time compared with a reference diffusion coefficient D_o measured at time of inspection t_o . The decrease is linear in a log – log diagram.

2. POTENTIAL CHLORIDE DIFFUSIVITY, $D_p(t_0)$

Potential chloride diffusivity, $D_p(t_0)$, is a time dependant inherent material parameter according to Eq. (2). This is because chloride diffusion takes place in the capillary pores of the cement paste and the width of the pores decreases with age due to continued hydration. $D_p(t_0)$ may be expressed as:

$$D_p(t_0) = D_{pR} \cdot \left(\frac{t_{0R}}{t_0}\right)^\beta \quad (3)$$

where:

$D_p(t_0)$ = Potential diffusion coefficient after curing time t_0 .

D_{pR} = "Reference" potential diffusion coefficient at curing reference time t_{0R} .

β = Material parameter depending on concrete composition.

For practical reasons, a direct measurement of $D_p(t)$ must include a certain period of exposure to chlorides to derive the material's resistance. In our studies, we include 35 days exposure (t_b) according to NT Build tst procedure 443 /6/.

The total age $t_T = t_0 + t_b$ and the reference total age $t_{TR} = t_{0R} + t_b$ of the concrete may be introduced in Eq. (3):

$$D_p(t_T) = D_{pR} \cdot \left(\frac{t_{TR} - t_b}{t_T - t_b} \right)^\beta \quad (4)$$

where:

t_b = Exposure time in the short time test method used (35 days in NT Build 443).

t_T = Total age of concrete ($t_T = t_0 + t_b$).

t_{TR} = Reference total age of concrete ($t_{TR} = t_{0R} + t_b$).

By choosing t_{0R} equal to 1 in the time system used (year, month or day), the potential diffusion coefficient $D_p(t_T)$ of the concrete may be calculated according to equation (5):

$$D_p(t_T) = D_{pR} \cdot (t_T - t_b)^{-\beta} \quad (5)$$

It is clear that t_T always has to be equal to or larger than t_b which means that $D_p(t_T)$ may be calculated at any time $t > t_b$. Eq. (5) shows that $D_p(t_T) \Rightarrow \infty$ when $t_T \Rightarrow t_b$.

$D_p(t_0)$ may be tested both on laboratory cured samples or on virgin inner part of drilled cores from real structures. In both situations t_0 is the (curing) age of the concrete before it is exposed to the short time test.

When testing laboratory cured samples, the curing time t_0 and the total age t_T may be short compared to the exposure time t_b , and the curve will be non linear in a double logarithmic system as shown by Eq. (5) and demonstrated in Fig. 3.

When testing samples from existing structures, the (curing) age is normally long compared to the exposure time t_b in the bulk diffusion test. This means that $t_T \cong t_0$, and Eq. (4) may be simplified to:

$$D_p(t_0) = D_{pR} \cdot \left(\frac{t_{0R}}{t_0} \right)^\beta \quad t_T \cong t_0 \gg t_b \quad (6)$$

This is the same equation as given in chapter 6.3.1 in reference (1). When $t_T \cong t_0 \gg t_b$, Eq. (4) will be a straight line in a double logarithmic system as shown by Eq. (6) and demonstrated in Fig. 3.

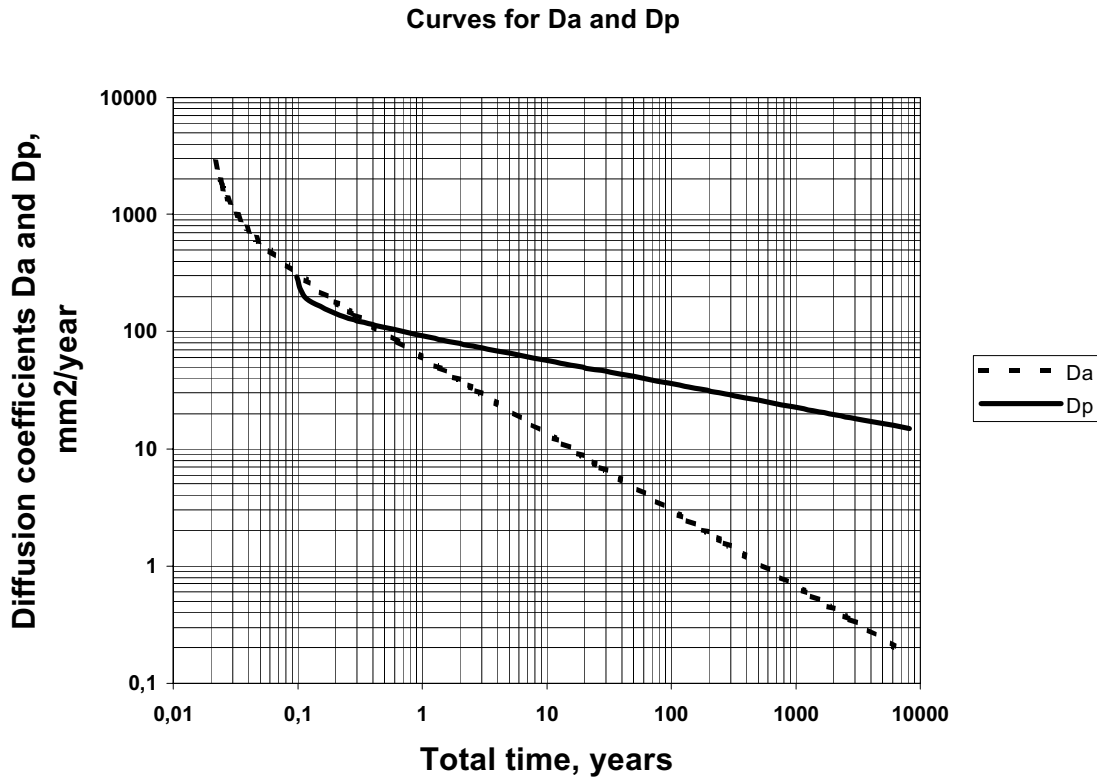


Figure 3

Example of calculation of curves for D_a and D_p . In this example, the following numbers have been used:

D_a -curve: t_0 (cur. time) 7 days, t_{eR} (ref. time) one year, D_{aR} (ref. D) 60 mm²/year, parameter $\alpha = 0,65$, Eq. (8).

D_p -curve: t_b (test time) 35 days, t_{0R} (ref. time) one year, D_{pR} (ref. D) 90 mm²/year, parameter $\beta = 0,20$, Eq. (4).

3 ACHIEVED or INSITU CHLORIDE DIFFUSIVITY, $D_a(t_e)$

The achieved or in-situ chloride diffusivity for the skin concrete, $D_a(t_e)$, exposed to sea water is a time dependant parameter depending on concrete composition and environmental conditions according to Eq. (2). The permeability in the concrete skin is reduced due to beneficial interaction with the sea water. $D_a(t_e)$ may be expressed as:

$$D_a(t_e) = D_{aR} \bullet \left(\frac{t_{eR}}{t_e}\right)^\alpha \quad (7)$$

where:

$D_a(t_e)$ = "Achieved" diffusion coefficient after exposure time t_e .

D_{aR} = "Reference" achieved diffusion coefficient at reference exposure time t_{eR} .

α = Parameter depending on concrete composition and environment.

The total age $t_T = t_e + t_0$ and the reference total age $t_{TR} = t_{eR} + t_0$ of the concrete may be introduced in Eq. (7):

$$D_a(t_T) = D_{aR} \bullet \left(\frac{t_{TR}-t_0}{t_T-t_0}\right)^\alpha \quad (8)$$

where:

t_0 = Curing time before exposure to saline water.

By choosing t_{eR} equal to 1 in the time system used (year, month or day), the achieved diffusion coefficient $D_a(t_T)$ at any total age t_T of the concrete may be calculated according to equation (9):

$$D_a(t_T) = D_{aR} \bullet (t_T - t_0)^{-\alpha} \quad (9)$$

From Eq. (9), it is clear that $t_T > t_0$ and that $D_a(t_T) \Rightarrow \infty$ when $t_T \Rightarrow t_0$.

$D_a(t_e)$ may be tested both on laboratory cured samples or on drilled cores from real structures. In both situations t_e is the time the concrete has been exposed to saline water.

When testing laboratory cured samples, the exposure time t_e , the total time t_T and the curing time t_0 may be of the same order of magnitude, and the curve will be non linear in a double logarithmic system as shown by Eq. (8) and demonstrated in Fig. 1.

When testing samples from existing structures, the exposure time t_e is normally much longer than the curing time t_0 . This means that $t_T \cong t_e$ and Eq. (8) may be simplified to:

$$D_a(t_T) = D_{aR} \bullet \left(\frac{t_{eR}}{t_T}\right)^\alpha \quad t_T \cong t_e \gg t_0 \quad (10)$$

This is the same equation as given in chapter 6.3.2 in reference /3/. When $t_T \cong t_e \gg t_0$, Eq. (8) will be a straight line in a double logarithmic coordination system as shown by Eq. (10) and demonstrated in Fig. 3.

It can be shown /3/ that the concrete is "self blocking" if $[t_e * D_a(t_e)]$ does not vary with time, which means that $\alpha = 1.0$. This means that chloride ingress is terminated. Such effect has been observed for some concrete mixtures including silica fume and fly ash with a very low w/b-ratios (6).

4 PARAMETERS IN THE MODEL

The exponent α governs how fast the diffusion coefficient is improved over time. The physical explanation for this effect is two-fold. The water-binder reaction of the concrete is a long going process. As the hydration goes on, the porosity of the paste decreases. This has a well-known beneficial effect on the long-term strength gain, but the reduced porosity also improves the resistance towards ingress of chloride ions. The second effect is the beneficial effect of contact with the seawater itself. For mature material Helland and Maage /7/ demonstrated that an ion exchange occurred between the seawater and the surface layer. Magnesium and potassium gradually blocked the pore system and then further improved the resistance to chloride ingress.

The α exponent reflects the decrease of the achieved diffusion coefficient with age due to the combined effect of hydration and all other mechanisms acting in-field as ion exchange with the seawater. Thus

$$\alpha = \beta + \gamma$$

where β represents the effect of continued hydration of the cement and γ represents the beneficial effect on the concrete skin by being in contact with the seawater.

Values for the γ , α and β exponents

Fig 4 represents the results from laboratory and in-field exposed panels and structures. The population with higher age than 2 years represents old Norwegian bridges exposed to coastal environment /1/. Characteristics for the mix composition of these are the use of unblended cements and a fairly high water-binder ratio. The γ for the concrete in these structures varies from 0.32 to 0.96 with the majority around the best curve-fit of $\gamma = 0.64$

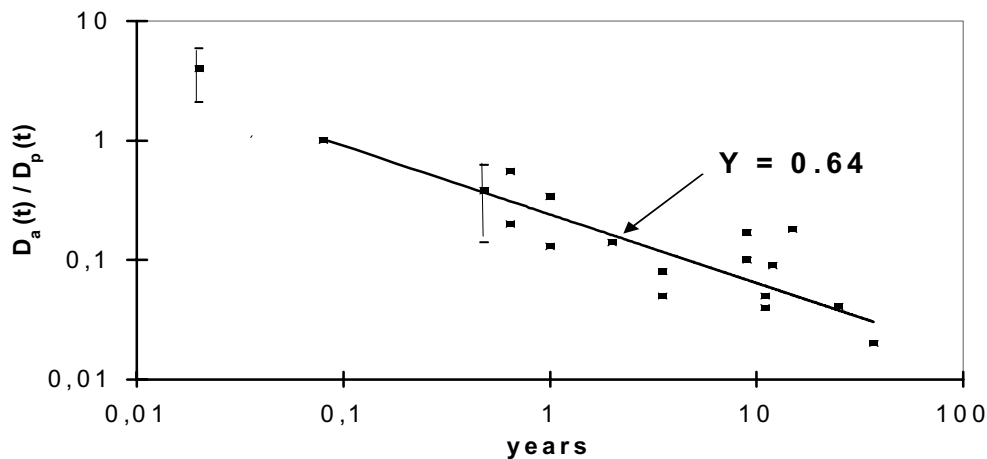


Figure 4 Experience from Scandinavian laboratory and in-field exposed marine concrete structures /5/

Figure 5 demonstrates the decrease of D_a for some LWAC mixes reported in /2/. In these series, the α is in the range of 0.52 – 0.61

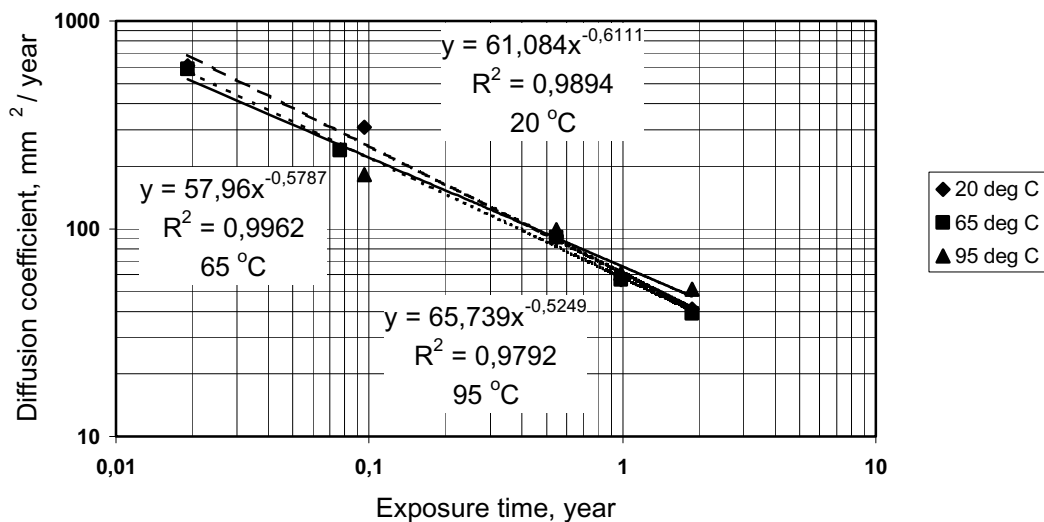


Figure 5 Effect of curing temperatures of 20 °C and semiadiabatic to 65 °C and 95 °C on diffusion coefficients for mix A. /2/

We have fewer measurements on the β exponent. However in the Norwegian research programme on lightweight concrete, "LettKon", we have mapped the decrease of $D_p(t)$ by letting the concrete pre-cure in fresh water for various periods from 1 to 365 days. The decrease then represented the sole result of continued hydration and the consequent refinement of the pore system.

On these mixes with effective water-binder ratios < 0.40 and about 8 % of silica fume, the β exponents were found to be in the range of 0.10 to 0.15.

An example is given in the figure.

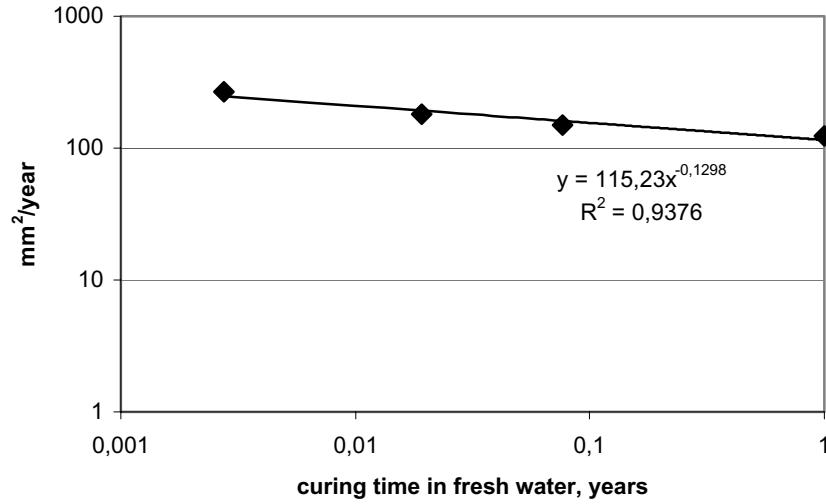


Figure 6 Decrease in $D_p(t)$ due to increased curing time in fresh water. Series “G” from /2/. $\beta = 0.13$

Based on the average values of the β and γ reported above, a rough estimate for α might then be $\alpha = \beta + \gamma = 0.64 + 0.20 \approx 0.85$

However, a broad variation should be expected depending on the cement type, type and amount of additions and water-binder ratio.

In addition, we have a number of in-field measurements on the α from the above-mentioned LWAC test panels produced with a modern mix design of low water-binder ratio and the addition of silica fume. These experienced a somewhat lower $\alpha \approx 0.70$ after 5 years of exposure /2/, /8/.

Environmental load

The effect of the environment is represented in the C_s in Fick’s second law. This parameter identifies the representative chloride concentration at the concrete surface during the time of exposure. The C_s depends both on the salinity of the water, the porosity of the surface layer (and thus the amount of saline pore water) and the length of wetting versus drying in the splash zone.

While calculating the D_s from a measured chloride profile, the C_s is represented as the chloride concentration at the surface (fig 1).

We have compiled a number of our observations from marine structures. Most of the results are from the splash zone.

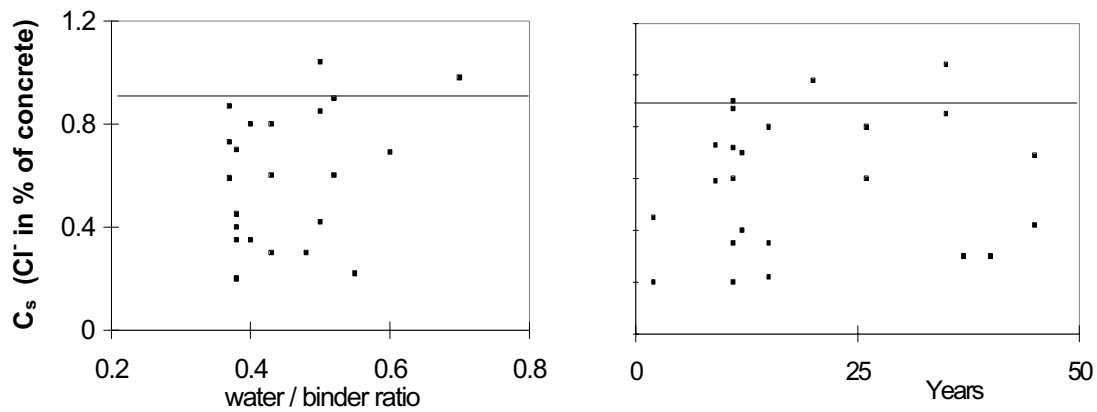


Figure 7 Registered surface chloride concentrations, C_s , at a number of Norwegian marine structures /9/

In Fig 7 these results of C_s , are plotted versus water-binder ratio and age. In these cases the structures themselves have acted as sensor. However, for the range of variables covered by these registrations, no significant dependency on these two parameters is found.

The scatter reflects the variations in microclimate even at the same structure.

For a structure located in the most harsh splash zone, a $C_s = 0.9\%$ of the concrete weight, seems to be a valid design value.

Figure 8 gives an example of the C_s as a function of maximum curing temperature, exposure length for submerged samples.

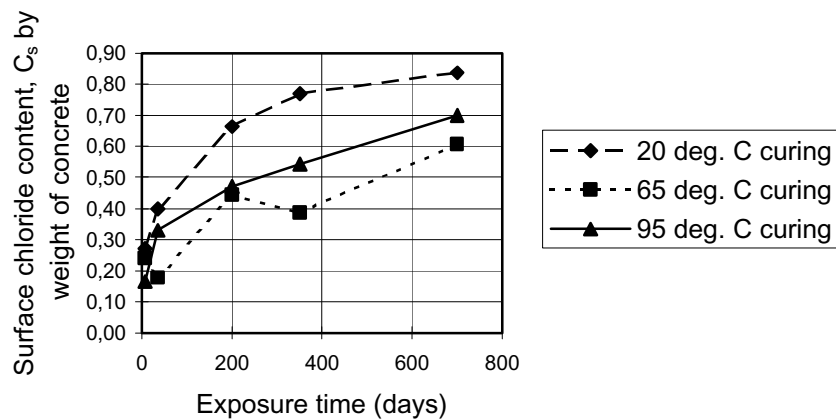


Figure 8 Effect of exposure length and maximum curing temperature on surface chloride content in % by weight of concrete. Based on mixes E and G from /2/.

Fig 9 from /10/ gives an example of the influence of the microclimate for a box-girder bridge in Northern Norway.

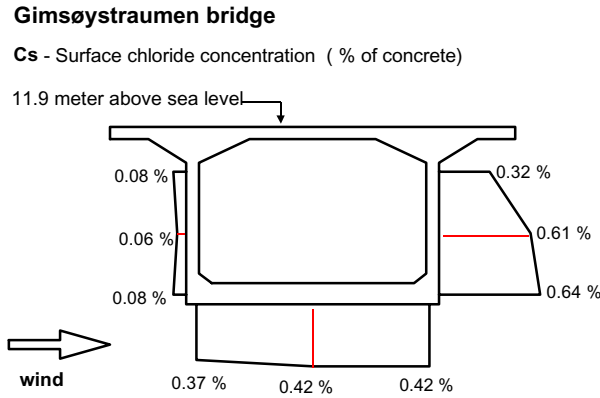


Figure 9 Gimsøystraumen bridge in Northern Norway. Typical influence of the micro climate for the box-girder /10/

5 CALCULATION OF INITIATION TIME

The service lifetime t_{LT} in this model is defined as the age of the structure when the chloride concentration $C_a(c, t_{LT})$ at the depth of the rebar with cover c reaches the critical (threshold) chloride concentration C_{cr} for initiating corrosion.

$$C_a(x, t) = C_a(c, t_{LT}) = C_{cr} \quad (11)$$

Reference /2/ gives the full mathematical solution.

For practical use, the EuroLightCon report /2/ also gives a number of nomogrammes enabling the engineer to perform the calculations only by hand calculation.

The minimum needed information for such an exercise is a given set of D_r and t_r and the parameters α , and in some cases β .

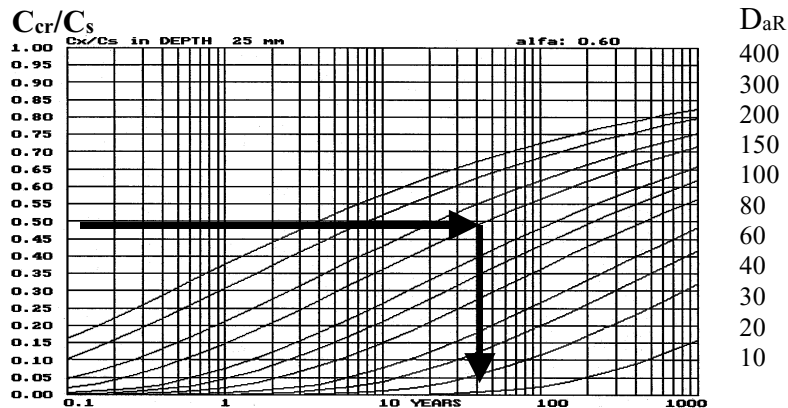
If this is a diffusion coefficient mapped from an exposed structure, the $D_{aR} = D_a$ (1 year) is extrapolated by the help of Eq. (7) by the exponent α .

If the known diffusion coefficient is from a bulk diffusion test, $D_{aR} = D_a$ (1 year) might be derived by “tracing” the history back to a curing period similar to the field exposed structure by the means of Eq. (3) and the exponent β , and then extrapolated with Eq. (7) to a reference period of exposure equal to 1 year.

Knowing the reference diffusion coefficient at 1 year (D_{aR}) and the α exponent, nomogrammes like the one in the figure might be used to map the situation at 25 mm depths.

Concrete cover: 25 mm

$\alpha = 0.60$



The example gives a chloride concentration of 50 % of C_s at the depth of 25 mm after close to 45 years for a concrete with a $D_{aR} = D_a (1 \text{ year}) = 150 \text{ mm}^2/\text{year}$ and $\alpha = 0.60$. Nomogrammes for other depths and α exponents are given in /2/

REFERENCES :

- 1 T. Farstad og S. Jacobsen: "Kystbruprosjektet." NBI/Vegdirektoratet, Statens Vegvesen, Vegdirektoratet, Oslo, Norway, 1993. (In Norwegian).
- 2 S. Helland, M. Maage, J. E. Carlsen, EuroLightCon report BE96-3942/R3, "Chloride penetration into concrete with lightweight aggregates", March 1999
- 3 M. Maage, E. Poulsen, Ø. Vennesland and J. E. Carlsen: «Service Life Model for Concrete Structures exposed to Marine Environment. Initiation period.» SINTEF report STF70 A94082. Trondheim, Norway, 1994
- 4 T. Luping. and L.-O.Nilsson.; "Chloride Diffusivity in High Strength Concrete at different Ages," Nordic Concrete Research, Publication No. 11, 1:1992. Oslo, Norway
- 5 M. Maage, S. Helland and J. E. Carlsen ; "Chloride penetration in High Performance Concrete exposed to Marine Environment," Symposium on Utilization of High Strength Concrete. Lillehammer, Norway, 1993.
- 6 NT BUILD 443; «Concrete, hardened: Accelerated chloride penetration.» NordTest, VTT, Finland, 1995.
- 7 M. Maage, S. Helland "Quality Inspection of "Shore Approach" High strength concrete". Proceedings Second CANMET/ACI International Conference on Durability of Concrete, Montreal 1991, ACI SP 126, Detroit USA
- 8 S. Helland, M. Maage, J. E. Carlsen "Service life predictions of LWA concrete in chloride environment". Proceedings International Symposium on Structural Lightweight Concrete. Sandefjord Norway 1995

- 9 S. Helland et al., “Service life of concrete offshore structures”. Offshore West Africa '99 Conference and Exhibition, March 23 – 25, 1999 Abidjan, Ivory Coast
- 10 F. Fluge “Environmental loads on coastal bridges” Proceedings from International Conference on repair of concrete structures, Svolvær, Norway. May 1997

ON AN EMPIRICAL MODEL FOR ESTIMATION OF CHLORIDE INGRESS INTO CONCRETE

(This paper is a reprint of an identical paper first presented at the RILEM Workshop TMC in Paris, September 2000)



Jens M. Frederiksen
B.Sc.Eng.(hon.)
Civil Engineer
jmf@aec-dk.com
AEClaboratory (Ltd.) A/S
Denmark
www.aec-dk.com



Mette Geiker
Associate Prof. Ph.D. M.Sc.
Chemical Engineer
Technical University of Denmark
mge@byg.dtu.dk
www.byg.dtu.dk

ABSTRACT

This paper presents the results from a comprehensive study of chloride ingress into concrete. Repeated measurements of chloride profiles taken in trial slabs of 13 different types of concrete naturally exposed in three different marine environments are analysed. Based on 114 chloride profiles obtained over five years, and a few laboratory studies, modified empirical models for estimating input parameters for an analytical ingress model are derived. The analytical model describes the result of chloride ingress into concrete, when both the surface chloride concentration and the diffusion coefficient are allowed to vary in time. The combined input parameters and model can be used directly for estimating chloride ingress into concrete exposed in South Scandinavian marine environments and with modifications also in other parts of the World.

Key words: Concrete, durability, chloride, model, ingress, penetration, time-dependency

1. INTRODUCTION

As part of the Swedish project *Durability of Marine Concrete Structures* (BMB) an exposure station, the Träslövsläge Marine Exposure Station, was established in 1991 on the South Swedish West Coast 10 km south of Varberg. A large number of different types of concrete are exposed there. Chloride profiles have been measured three or four times in the first five years of exposure in selected concrete types. In Frederiksen et al. [1997a] it was demonstrated that data from a 2½ years period could be utilised as a basis for empirical models for estimating the decisive parameters when modelling chloride ingress into concrete. The analytical model used to describe the chloride profiles was the general solution to Fick's 2nd law of diffusion – the so-called Mejlbro-Poulsen Model, cf. Mejlbro [1996] and Poulsen [1996].

The Mejlbro-Poulsen Model does not model the actual physical and chemical processes involved in the chloride ingress into concrete. The aim of the model is to describe the resulting chloride profiles. However, as the combined empirical models for estimation of input parameters and analytical model – the HETEK Model - is based directly on measured chloride profiles the result may be satisfactory from an engineering point of view. The fact that a relation between the field exposure and the laboratory exposure according to the NT BUILD 443 Accelerated Chloride Penetration test has been found for plain concrete, cf. Frederiksen et al. [1997b], facilitates the formulation of acceptance criteria for practical purposes. Thus the entire HETEK Model allows the owner, the designer, or the contractor to estimate the chloride ingress into a given concrete in a given environment and at the same time to define the requirements to be met in a relatively fast laboratory test, cf. Frederiksen et al. [1997c].

Parallel to the HETEK project guidelines for probabilistic based durability design has been made under the DuraCrete project, cf. COWI [1999]. These guidelines make use of a chloride ingress model assuming that the surface concentration is constant in time. The present paper demonstrates that experimental data suggest that the surface concentration *is* time dependent during the five first years of exposure.

Now data after five years of exposure are available, cf. Sandberg et al. [1998] and added to the data based on 2½ years of exposure, cf. Frederiksen et al. [1997a], which should improve the validity of the HETEK Model, even though much longer exposure times really are wanted. The Swedish BMB project has supplied the data, cf. Sandberg et al. [1998], and they may be the best data of its kind available right now. It is the aim of the paper to present a way of separating the different effects of the concrete composition and the environment. To illustrate the applicability of the updated HETEK Model chloride profiles measured in selected existing marine concrete structures are compared with estimated chloride profiles.

A list of symbols is given at the end of the paper.

2. TEST SPECIMEN, EXPOSURE AND RAW DATA

The concrete test specimens have the dimensions: $1000 \times 700 \times 100$ mm. Selected information on the concrete compositions investigated are given in Table 1.

Table 1. Composition of concrete test specimens at the Träslövsläge Marine Exposure Station.

ID Number	w/b ratio	Cement	Silica fume	Fly ash	Water	Cement paste	Cementitious content	Calculated density
1-50	0.50	370.0	0.0	0.0	185.0	30.2	17%	2152
3-50	0.50	351.5	18.5	0.0	185.0	30.5	17%	2145
Ô	0.38	420.0	0.0	0.0	159.6	29.3	19%	2217
2-40	0.40	420.0	0.0	0.0	168.0	30.1	19%	2217
3-40	0.40	399.0	21.0	0.0	168.0	30.4	19%	2210
H4	0.40	399.0	21.0	0.0	168.0	30.4	19%	2210
10-40	0.35	345.0	20.5	75.0	155.2	30.8	20%	2205
12-35	0.33	382.5	22.5	45.0	146.5	29.9	20%	2245
H3	0.30	492.0	0.0	0.0	148.0	30.4	20%	2460
H1	0.30	475.0	25.0	0.0	150.0	31.2	20%	2448
H2	0.30	450.0	50.0	0.0	150.0	31.6	21%	2439
H8	0.26	493.0	0.0	123.0	159.0	37.1	26%	2399
H5	0.25	525.0	26.3	0.0	137.8	31.6	22%	2501
Unit	by mass	Kg/m ³ Concrete	kg/m ³ concrete	kg/m ³ concrete	kg/m ³ concrete	% volume concrete	% mass concrete	kg/m ³ concrete

A specimen of each composition is mounted in an upright position at a pontoon in such a way that three local environments are formed:

- Marine atmospheric zone
- Marine splash zone
- Marine submerged zone.

The pontoons are placed at a marine exposure station at Träslövsläge Harbour at the south west coast of Sweden, near Varberg. The chloride content the seawater in Träslövsläge Harbour (14 ± 4 g/l) represents an average marine environment from a Danish point of view, i.e. the marine environment lies between the environment of the North Sea and the Baltic Sea.

Sandberg et al. [1998] describe the exposure station in Träslövsläge in more details and give a more detailed description of the test programme carried out at the Träslövsläge Marine Exposure Station.

3. MATHEMATICAL MODEL

The applied model is based upon Fick's 2nd law of diffusion that implies only one assumption, namely that the flow of chloride in concrete is proportional to the gradient of the chloride concentration in the medium; i.e. concrete. Fick's 2nd law of diffusion is a partial differential equation, which cannot be solved without specifying the material parameters, i.e. the chloride diffusion coefficient, and the initial and boundary conditions.

Inspection of marine concrete structures has shown that:

- The achieved chloride diffusion coefficient D_a of the concrete is time-dependent. Takewaka et al. [1988] proposed to describe $D_a(t)$ as a power function of time, and Maage et al. [1995] proposed the following power function:

$$D_a(t) = D_{aex} \left(\frac{t_{ex}}{t} \right)^a, \text{ where } 0 \leq a \leq 1 \quad (1)$$

- The chloride concentration C_{sa} of the exposed concrete surface is time-dependent. Mejlbro [1996] proposed C_{sa} to be described by the following family of functions:

$$C_{sa} = C_i + S \times \left((t - t_{ex}) \times D_{aex} \times \left(\frac{t_{ex}}{t} \right)^a \right)^p, \text{ where } 0 \leq p \leq 1 \quad (2)$$

or:

$$C_{sa} = C_i + S_p \times t^p, \text{ where} \quad (3)$$

$$S_p = S \times (t_{ex} D_{aex})^p \text{ and} \quad (4)$$

$$t = \left(\frac{t}{t_{ex}} \right)^{1-a} - \left(\frac{t_{ex}}{t} \right)^a \quad (5)$$

The application of the above functions to describe the time-dependency of the diffusion coefficient and the surface concentration in the solution of Fick's 2nd law is the so-called Mejlbro-Poulsen Model, cf. Mejlbro [1996] and Poulsen [1996], Frederiksen et al. [1997a]. Mejlbro [1996] proposed the “complete solution” of Fick's 2nd law:

$$C(x, t) = C_i + (C_{sa} - C_i) \times \Psi_p(z), \text{ where} \quad (6)$$

$$z = \frac{0.5x}{\sqrt{(t - t_{ex}) D_a(t)}} = \frac{0.5x}{\sqrt{t \times t_{ex} D_{aex}}} \quad (7)$$

The Ψ_p functions in (6) are defined as:

$$\Psi_p(z) = \sum_{n=0}^{+\infty} \frac{p^{(n)} (2z)^{2n}}{(2n)!} - \frac{\Gamma(p+1)}{\Gamma(p+0.5)} \sum_{n=0}^{+\infty} \frac{(p-0.5)^{(n)} (2z)^{2n+1}}{(2n+1)!} \quad (8)$$

In (8) $\Gamma(y)$ is the Gamma function defined as:

$$\Gamma(y) = \int_0^{+\infty} u^{y-1} \exp(-u) du \quad (9)$$

for $y \geq 0$. The notation used in (8) should be noted:

$$p^{(0)} = 1; p^{(1)} = p; p^{(2)} = p \times (p-1); \dots p^{(n)} = p \times (p-1) \times \dots \times (p-n+1) \quad (10)$$

where $p^{(n)}$ has $n \geq 1$ factors.

In the case where the chloride concentration of the chloride exposed concrete surface is constant; i.e. $p=0$ in the general solution (6), the chloride profile is described by the well-known error-function solution, cf. Poulsen [1993]:

$$C(x,t) = C_{sa} - (C_{sa} - C_i) \operatorname{erf} \left(\frac{0.5x}{\sqrt{(t-t_{ex})D_a(t)}} \right) \quad (11)$$

If the achieved chloride diffusion coefficient D_a of the concrete is *not* time-dependent, i.e. $\mathbf{a}=0$ in the general solution (6) $D_a(t)$ is simply replaced by D_a in (11) and we have the simplest form of the solution to Fick's 2nd law when diffusion into a half-space is considered.

4. CONVERSION FORMULAS

It is seen that four parameters govern the chloride profiles defined by the general solution (6). The four parameters are S_p , p , D_{aex} and \mathbf{a} . Here D_{aex} and \mathbf{a} mainly describe the magnitude and the time-dependency of the transport coefficient, cf. (1), while S_p and p (together with D_{aex} and \mathbf{a}) describe the magnitude and the time-dependency of the boundary condition, cf. (3).

Instead of estimating the four decisive parameters \mathbf{a} , D_{aex} , S_p and p of the concrete and it's local environment, it is more convenient to estimate the achieved chloride diffusion coefficients D_1 and D_{100} at time $t_1 = 1$ year and $t_{100} = 100$ years respectively, and the corresponding chloride concentrations of the exposed concrete surface C_1 and C_{100} . The estimation of these parameters can be based on data from natural exposure, ref. Step 1 and Step 2 below and Chapter 5:

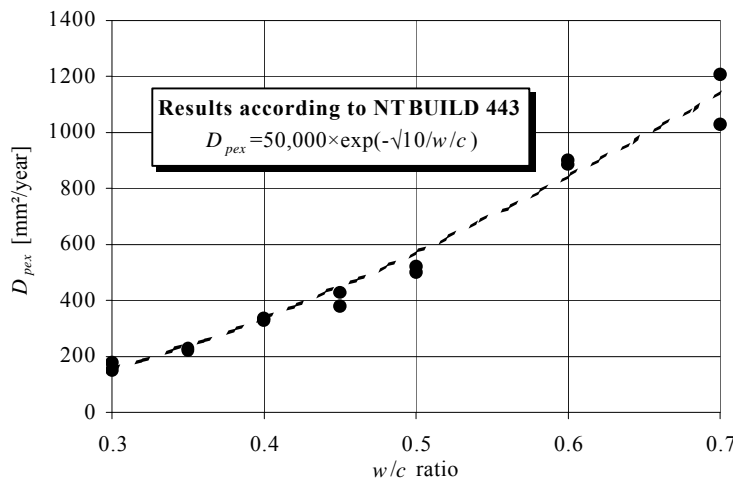


Figure 1. Correlated values of the transport coefficient measured by NT BUILD 443 and the w/c ratio (Danish Low Alkali Sulphate Resisting Portland Cement, constant cement paste volume at 27%). Cf. Frederiksen et al. [1997b].

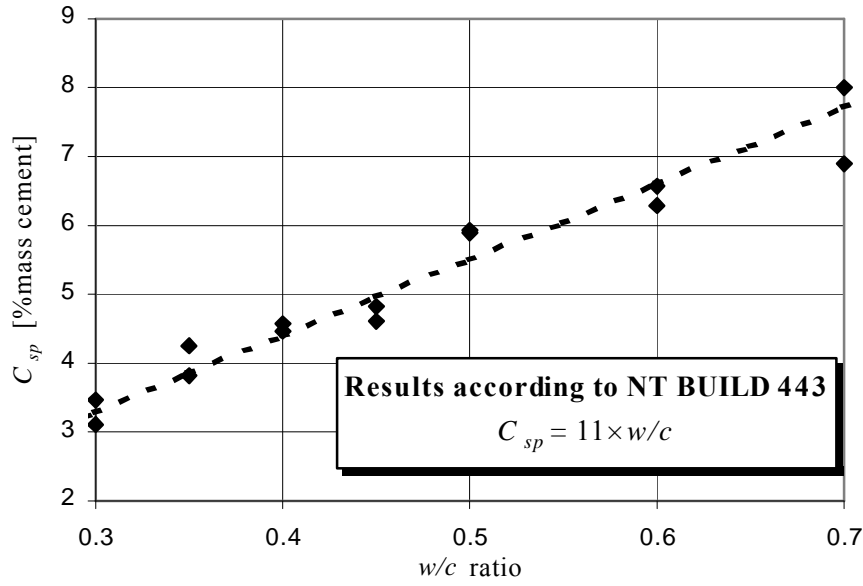


Figure 2. Correlated values of the surface concentration measured by NT BUILD 443 and the w/c ratio (Danish Low Alkali Sulphate Resisting Portland Cement, constant cement paste volume at 27%).
Cf. Frederiksen et al. [1997b]

Step 1. Estimate the achieved chloride diffusion coefficient D_1 and D_{100} at exposure time 1 year and 100 years respectively

Step 2. Estimate the achieved chloride concentration of the concrete surface C_1 and C_{100} at exposure time 1 year and 100 years respectively

From D_1 , D_{100} , C_1 and C_{100} it is possible to estimate the corresponding values of a , D_{aex} , S_p and p by a step wise determination using the following formulae, cf. Frederiksen et al. [1997a]:

Step 3. Calculate: $q = \frac{1}{2} \times \log_{10} \left(\frac{1}{t_{ex}} \right)$ (12)

Step 4. Calculate: $a = \frac{1}{2} \times \log_{10} \left(\frac{D_1}{D_{100}} \right)$ (13)

Step 5. Calculate: $D_{aex} = D_1 \times \left(\frac{D_1}{D_{100}} \right)^q$ (14)

Step 6. Calculate: $p = \frac{\log_{10}(C_{100}/C_1)}{\log_{10} \left(\frac{100 - t_{ex}}{1 - t_{ex}} \times \frac{D_{100}}{D_1} \right)}$ (15)

Step 7. Calculate: $S_p = C_1 \times \left(\left(\frac{D_1}{D_{100}} \right)^q \times \frac{t_{ex}}{1 - t_{ex}} \right)^p$ (16)

It is seen that these formulas are suitable for calculation by means of a spreadsheet and/or a programmable pocket calculator.

5. EMPIRICAL MODELS FOR ESTIMATION OF PARAMETERS AND METHODOLOGY

Empirical models for generating expectation values of C_1 , C_{100} , D_1 , and α (and with that D_{100}) for the Träslövsläge data were proposed in Frederiksen et al. [1997a]. The “ideas” came from the experiments carried out and reported in Frederiksen et al. [1997b], who performed laboratory test with different methods for determining diffusivity of concrete without silica fume and fly ash. One of the applied methods was NT BUILD 443. Figures 1 shows the relation between the transport coefficient and the w/c ratio for plain concrete. The correlation between surface concentration and w/c is given in Figure 2. It is assumed that the type of correlation observed for plain concrete is valid for concretes with puzzolanas too.

Figures 2 and 1 suggest that the effect of the w/c ratio on the surface concentration and the diffusivity, respectively, could be functions of the types given below:

$$C_1 = A \times \text{eqv } (w/c)_b \times k_{Cl, env} \text{ [% mass binder]} \quad (17)$$

$$C_{100} = C_1 \times k_{C100, env} \text{ [% mass binder]} \quad (18)$$

$$D_1 = B \times \exp \left(- \sqrt{\frac{10}{\text{eqv } (w/c)_D}} \right) \times k_{D1, env} \text{ [mm}^2\text{/yr]} \quad (19)$$

$$a = (U \times \text{eqv } (w/c)_D + V) \times k_{a, env} \quad (20)$$

From (19) and (20) D_{100} is derived from:

$$D_{100} = D_1 \left(\frac{1}{100} \right)^a \quad (21)$$

Frederiksen et al. [1997a] introduced environmental parameters in order to make the formulas (17) to (20) applicable for natural exposures and efficiency factors of puzzolanas. The efficiency factor related to a property of concrete is defined as the mass of cement that can be replaced by one unit mass of puzzolana while maintaining the property. When taking the efficiency factors in to account a so-called equivalent w/c ratio is obtained. The parameters of the empirical models are shown in Table 2.

The parameters of the HETEK Model, cf. Frederiksen et al. [1997a] have been optimised directly against the measured chloride profiles, cf. the example in Figure 3. A total of 978 chloride measurements distributed on three local marine environments, three exposure times covering a period of five years and 13 types of concrete formed the basis for optimising the 20 parameters in the HETEK Model. For each of the three exposure times the error function solution to Fick's 2nd law was used to derive the

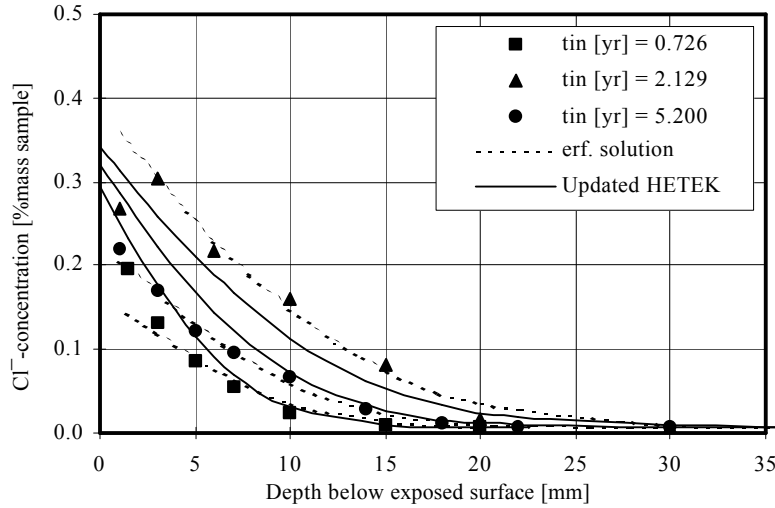


Figure 3. An example from the raw data for concrete ID 12-35 Splash. The measured data points are showed together with the error-function solution graphs and the updated HETEK Model graphs. Note that the chloride profile measured at 2.129 years of exposure shows the most pronounced chloride penetration.

parameters D_a and C_{sa} in all the concretes in Table 1 and in all three marine environments. The first point of all chloride profiles was omitted when fitting.

By double-linking all the spreadsheets dealing with the error-function solution and the Mejlbro-Poulsen Model with one spreadsheet dealing with the empirical models (17) to (21), the conversion formulas (12) to (16) and information on the types of concrete involved (cf. Table 1) it was possible to perform one “super-multiple” regression analysis.

No significant changes to the parameters governing the first years estimate were necessary, but the parameters governing the long-term estimates was changed, see Table 2.

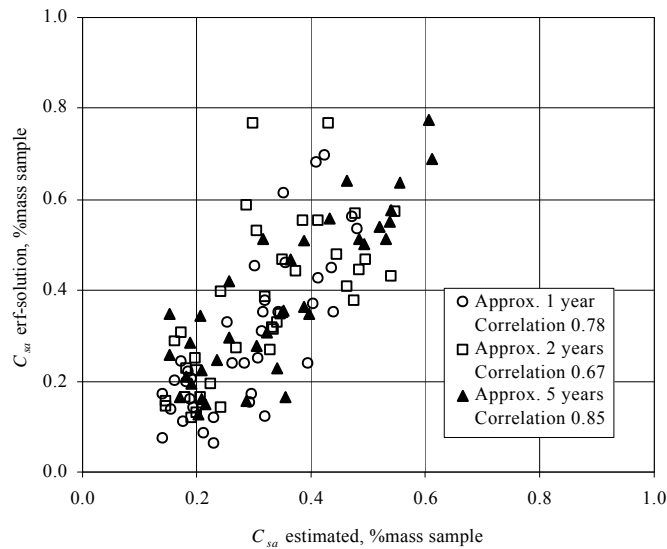


Figure 4. Correlation between the parameter C_{sa} estimated by the updated HETEK Model and the error-function solution.

Table 2. The parameters of the HETEK Model are given as the values before and after updating with the data for 5 years of exposure (cf. the enclosed list of symbols).

Parameter	Value		Remarks
Factor B in (19) formula for transport coefficient	25000		No change
Factor A in (17) formula for surface concentration	3.7		No change
Factor U in (20) formula for decrease parameter of transport coefficient	1.5		No change
Constant V in (20) formula for decrease parameter of transport coefficient	1		No change
	Before	Now	
Efficiency factor, transport, k_{MS} , cf. (19) and (20)	7	7.3	Small increase
Efficiency factor, transport, k_{FA} , cf. (19) and (20)	1	1.4	Small increase*
Efficiency factor, binding, k_{MS} , cf. (17)	-1.5	-0.8	Increase
Efficiency factor, binding, k_{FA} , cf. (17)	0.75	0	Reduction*)
Environmental parameters (first year of exposure), cf. (17) and (19)			
<i>Submerged zone</i>			
	$k_{DI, env}$	1	No change
	$k_{CI, env}$	1.4	No change
<i>Splash zone</i>			
	$k_{DI, env}$	0.6	No change
	$k_{CI, env}$	0.4	No change
<i>Atmosphere zone</i>			
	$k_{DI, env}$	0.4	No change
	$k_{CI, env}$	0.6	No change
Parameters that are decisive for the time dependency (100 years of exposure), cf. (18) and (20)			
<i>Submerged zone</i>			
	Before	Now	
	$k_{a, env}$	0.6	0.3 a becomes smaller and hence D_a becomes less time dependent
	$k_{C100, env}$	1.5	1.8 C_{100} becomes bigger and the time dependency becomes stronger
<i>Splash zone</i>			
	$k_{a, env}$	0.1	0.7 a becomes bigger and hence D_a becomes more time dependent
	$k_{C100, env}$	4.5	1.4 C_{100} becomes smaller and the time dependency becomes weaker
<i>Atmosphere zone</i>			
	$k_{a, env}$	1	0.2 a becomes smaller and hence D_a becomes less time dependent
	$k_{C100, env}$	7	1.3 C_{100} becomes smaller and the time dependency becomes weaker

Note: * Only few concrete types with fly ash, ref. Table 1

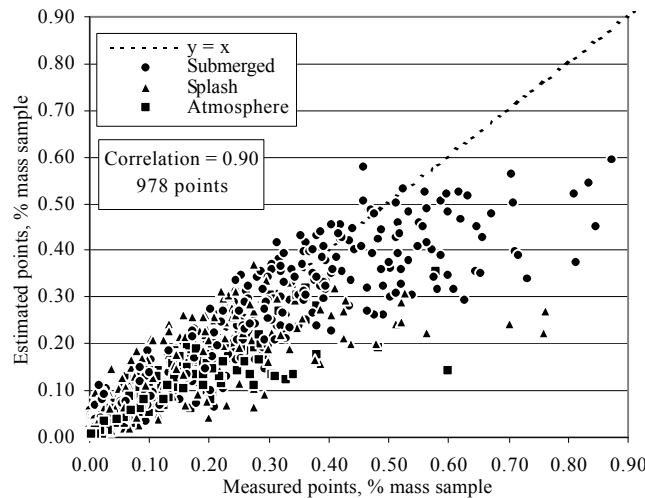


Figure 6. Correlation between estimated and the measured chloride content.

The correlations between the parameters D_a and C_{sa} estimated by the updated HETEK Model and the parameters derived by use of the error-function are shown on the Figures 4 and 5.

The correlation between the surface concentration after five years estimated according to the updated HETEK Model and the error-function solution, respectively, is slightly improved compared to the correlation after one or two years, cf. Figure 4. On the other hand, the correlation between the diffusion coefficient after five years estimated according to the updated HETEK Model and the error-function solution, respectively, is *not* improved when compared to results after one and two years, cf. Figure 5.

The correlation between the estimated and the measured data is shown in Figure 6. The over-all correlation of 0.90 may be satisfactory, but it is clear from the graph that the updated model is skewed. The estimate is slightly conservative for chloride contents up to approximately 0.1% by mass and reasonable until 0.4 % chloride by mass of sample. At higher chloride contents the updated HETEK Model provides too low chloride contents. The skew modelled chloride contents may be due to:

1. A relatively high number of very small chloride contents with a high relative measurement error, and
2. The systematic omission of the first point of all chloride profiles during the optimisation.

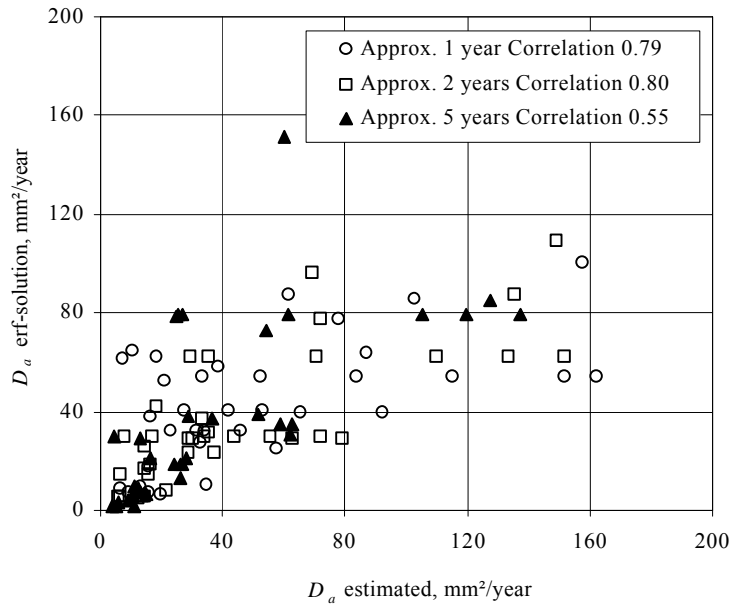


Figure 5 Correlation between the parameter D_a estimated by the updated HETEK Model and the error-function solution

None of the above effects have been studied here.

In Table 2 are given estimated values of the parameters in the formulas for estimating the diffusion coefficient (19) and the surface concentration (17) after 1 year of exposure. If the values are compared to the corresponding values from the laboratory test, cf. Figure 1 and 2 it is seen that there apparently is simple relation between the laboratory test and the natural exposure: $D_{pex} = 2 \times D_1$ and $C_{sp} = 3 \times C_1$ for the given

concrete and test method. These simple relations must be considered as the best estimates at this stage.

6. COMPARISON BEFORE AND AFTER THIS UPDATE

A comparison is made between measurements on selected existing Danish marine structures and chloride profiles estimated by the first and the updated versions of the HETEK Model, cf. Figure 7. Both the exposure type and the cementitious binder type vary, cf. Table 3.

Table 3. Information on selected Danish marine structures, cf. Frederiksen et al. [1997a].

Structure	Exposure	Binder type	Age at testing, years
Vejle Fjord Bridge	Above level +2.3 m, i.e.: Atmospheric	Low alkali, sulphate resisting cement	17
Farø Bridges	Water line, i.e.: Splash	Low alkali, sulphate resisting cement and 14% fly ash	9
Esbjerg Harbour	Submerged	Ordinary Portland cement	37

A rather poor correlation is observed, the updated HETEK Model resulting in estimates differing most from the measured chloride profiles. The estimated chloride profiles are higher than the measured chloride profiles in Esbjerg Harbour, i.e. a conservative estimate, whereas the estimated chloride profiles in the Vejle Fjord Bridge and the Farø Bridge are lower than the measured values.

As mentioned in Chapter 5, neither the possible effect of the relatively high number of very small chloride contents with a high relative measurement error, nor the effect of the omission of the first point of all chloride profiles during the optimisation have been studied here. This will be looked into in a consecutive paper.

Furthermore, the environmental exposures at Träslövsläge may not be fully representative for the in-situ exposure conditions where the chloride measurements have been made.

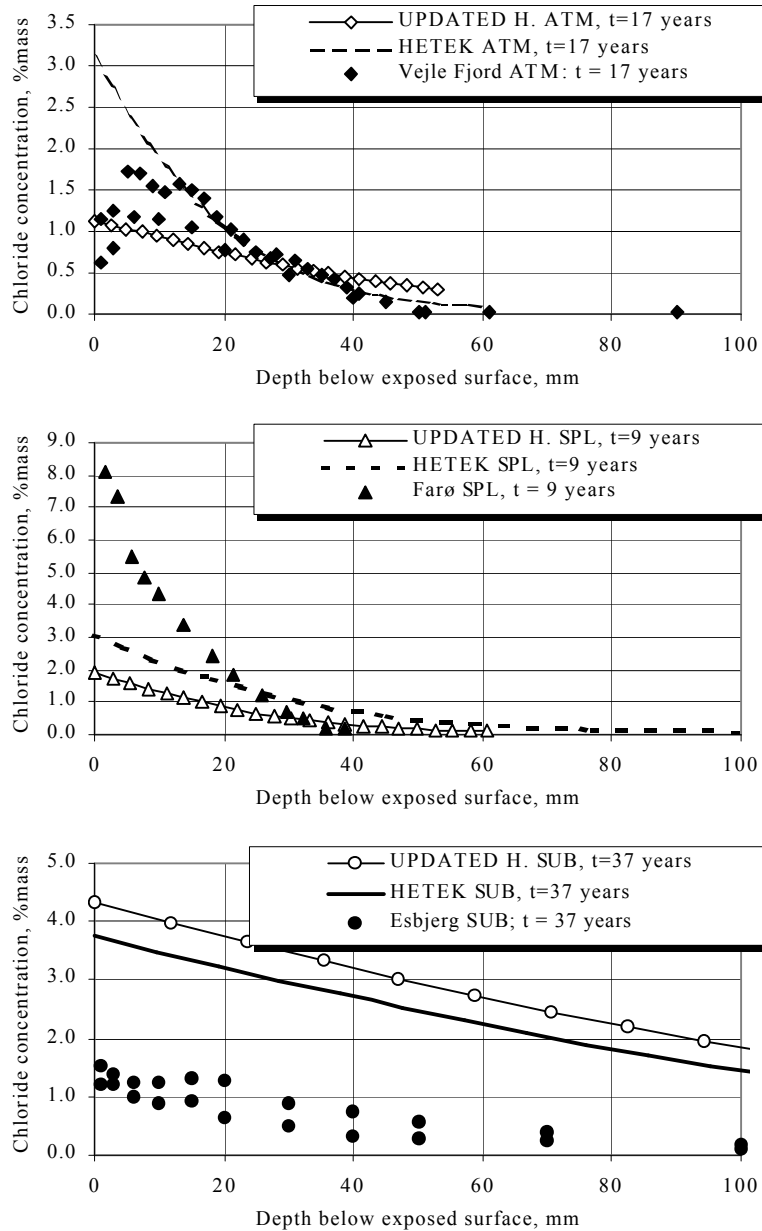


Figure 7. Comparison of data from real structures with estimates made with the HETEK Model and the updated HETEK Model respectively. The data are from Frederiksen et al. [1997a] and given in per cent of binder content.

7. SUMMARY AND CONCLUSION

Based on 114 chloride profiles obtained over five years in trial slabs of 13 different types of concrete naturally exposed at Träslövsläge Marine Exposure Station and data from a few laboratory studies, updated empirical models for estimating input parameters for an analytical ingress model have been derived. The analytical model applied describes the result of chloride ingress into concrete, when both the surface chloride concentration and the diffusion coefficient are allowed to vary in time. Details on the empirical models and the methodology applied are presented.

Chloride profiles estimated by the combined empirical models for input parameters and the analytical model - the HETEK Model - have been compared with measurements on three selected Danish marine structures. The updated version of the HETEK Model does not provide improved estimates of the measured chloride profiles when compared to the first version, which was based on a shorter exposure period. Both estimates higher and lower than the measured profiles have been obtained.

8. REFERENCES

- 1999 **COWI: BE95-1347/R14: General Guidelines for Durability Design and Redesign.** Task 7 Report
- 1997a **Frederiksen, J. M., Nilsson, L.-O., Poulsen, E., Sandberg, P.; Tang L. & Andersen, A.: HETEK, A system for estimation of chloride ingress into concrete, Theoretical background.** The Danish Road Directorate, Report No. 83.
- 1997b **Frederiksen, J. M.; Sørensen, H. E.; Andersen, A.; Klinghoffer, O.: HETEK, The effect of w/c ratio on chloride transport into concrete,** The Danish Road Directorate, Report No. 54.
- 1997c **Frederiksen, J.M.; Poulsen, E.: HETEK, Chloride penetration into concrete - Manual,** The Danish Road Directorate, Report No. 123.
- 1995 **Maage, M.; Poulsen, E.; Vennesland, Ø.; Carlsen, J.E.: Service life model for concrete structures exposed to marine environment initiation period.** LIGHTCON Report No. 2.4, STF70 A94082 SIN-TEF, Trondheim, Norway.
- 1996 **Mejlbro, L.: The Complete Solution of Fick's Second Law of Diffusion with Time-dependent Diffusion Coefficient and Surface Concentration,** Durability of Concrete in Saline Environment. Cementa. Danderyd Sweden.
- 1993 **Poulsen, E: On a model of chloride ingress into concrete having time dependent diffusion coefficient.** Proceeding if the Nordic Miniseminar in Gothenburg Dept. of Building Materials, Chalmers University of Technology, Gothenburg Sweden. Publication P-93:1.
- 1996 **Poulsen, E.: Estimation of Chloride Ingress into Concrete and Prediction of Service Lifetime with Reference to Marine RC Structures,** Durability of Concrete in Saline Environment. Cementa. Danderyd Sweden.
- 1998 **Sandberg, P., Tang, L. & Andersen, A.: Recurrent Studies of Chloride Ingress in Uncracked Marine Concrete at Various Exposure Times and Elevations,** Cement and Concrete Research, Vol. 28, No. 10, pp. 1489-1503
- 1988 **Takewaka, K.; Mastumoto, S.: Quality and cover thickness of concrete based on the estimation of chloride penetration in marine environments.** American Concrete Institute. Detroit USA. ACI SP 109-17, pp. 381-400.

9. LIST OF SYMBOLS

Symbol	Unit	Description and reference to definition in text
$C(x,t)$	mass%	Chloride concentration of concrete at a depth x beyond the concrete surface at the time t
C_i	mass%	Initial chloride content of concrete
C_s	mass%	Surface chloride concentration of concrete
C_{sa}	mass%	Surface chloride concentration of concrete, determined by regression analysis of an achieved chloride profile from natural exposure

C_{sp}	mass%	Surface chloride concentration of concrete, determined by regression analysis of a chloride profile from a standard laboratory exposure
C_1	mass%	Surface chloride concentration (boundary condition) of an achieved chloride profile after one year of natural exposure
C_{100}	mass%	Surface chloride concentration (boundary condition) of an achieved chloride profile after 100 years of natural exposure
D	m ² /s	Diffusion coefficient
D_a	m ² /s	Achieved transport coefficient characterising a chloride profile after a natural exposure for a non-specified time
D_1	m ² /s	Achieved transport coefficient characterising a chloride profile after one year of natural exposure
D_{100}	m ² /s	Achieved transport coefficient characterising a chloride profile after 100 years of natural exposure
D_{aex}	m ² /s	Achieved transport coefficient characterising a chloride profile after a natural exposure at time t_{ex}
D_{pex}	m ² /s	Potential transport coefficient characterising a chloride profile after a standard exposure in laboratory at time t_{ex}
eqv (w/c) _b	1	The equivalent w/c ratio with respect to the surface boundary conditions C_1 and C_{100}
eqv (w/c) _{cr}	1	The equivalent w/c ratio with respect to the threshold value for corrosion initiation
eqv (w/c) _D	1	The equivalent w/c ratio with respect to the achieved diffusion coefficient after one year of exposure D_1
$k_{a, env}$	1	Factor encountering the effect of a local environment on the “time decrease factor” a .
$k_{C1, env}$	1	Factor encountering the effect of a local environment on the surface boundary conditions C_1 and C_{100}
$k_{D1, env}$	1	Factor encountering the effect of a local environment on the achieved diffusion coefficient after one year of exposure D_1
k_{FA}	1	Efficiency factor of fly ash for chloride ingress
k_{MS}	1	Efficiency factor of silica fume for chloride diffusivity
$k_{C100, env}$	1	Factor encountering the effect of time for a local environment on the surface boundary condition C_{100}
S_p	mass%	Parameter in the Mejlbro-Poulsen Model described the magnitude of the surface chloride concentration.
t_{ex}	s	The time of exposure (to a chlorine environment)
x	m	Distance below the exposed concrete surface
a	1	A parameter describing the decrease with time of the achieved chloride diffusion coefficient
t	1	Time parameter
p		Potential and base of Mejlbro’s Λ and Ψ functions
x		Depth
min		Minimum
max		Maximum
i		Initial
cr		Critical
erf		Error function
erfc		Error function complement (1-erf)
exp		Natural exponential function (exp 1 = 2.718281828...)
inv		Inverse function
log ₁₀		Logarithm to the base 10
Ψ_p		Mejlbro’s Ψ functions

<i>w/b</i>	kg/kg	Water/binder ratio (<i>water</i> : the total amount of free water in the mixture; <i>binder</i> : Portland cement, pulverised fuel ash, micro silica, and/or ground granulated blast furnace slag)
<i>w/c</i>	kg/kg	Water/cement ratio (<i>water</i> : the total amount of free water in the mixture; <i>cement</i> : Portland cement)
ATM		Atmospheric exposure
BMB		“ <u>B</u> eständighet <u>M</u> arina <u>B</u> etongkonstruktioner” - A Swedish research programme
eqv		Equivalent
FA		Fly ash
HETEK		The abbreviation for the Danish research project High Performance Concrete - Contractor Technology (in Danish: <u>H</u> øjkvalitetsbeton - <u>E</u> ntreprenørens <u>T</u> EKnologi.)
NT		Nordtest
OPC		Ordinary Portland cement
RH		Relative humidity
SF		Silica fume
SRPC		Sulphate-resisting Portland cement
SPL		Splash zone exposure
SUB		Submerged exposure

Nordic Mini Seminar on

Prediction Models for Chloride Ingress and Corrosion Initiation in Concrete Structures

Test application of DuraCrete Models

Sascha Lay, Institute for Building Materials of the Technical University of Munich, Germany

1 Model

The applied model for the prediction of chloride ingress has been developed in the Brite EuRam project DuraCrete /1/ and further sophisticated by Gehlen /2/:

$$C(x, t) = (C_{s, \Delta x} - C_i) \cdot \left[1 - \operatorname{erf} \left(\frac{x - \Delta x}{2\sqrt{t \cdot D_{\text{eff}}(t)}} \right) \right] + C_i \quad \text{Eq. 1-1}$$

and,

$$D_{\text{eff}}(t) = k_{RH} \cdot D_{RCM,0} \cdot k_t \cdot k_T \cdot \left(\frac{t_0}{t} \right)^n \quad \text{Eq. 1-2}$$

$C(x, t)$	chloride concentration in depth x at time t [M.-%/b]
$C_{s, \Delta x}$	chloride concentration in depth Δx at time of inspection [M.-%/b]
C_i	initial chloride concentration [M.-%/b]
erf	error function
x	depth with corresponding chloride concentration $C(x, t)$ [m]
Δx	depth of the "convection" zone in which the chloride profile deviates from behavior according to the 2 nd law of diffusion [m]
t	age of concrete [s]
$D_{\text{eff}}(t)$	effective diffusion coefficient of concrete at time t [10^{-12} m ² /s]
k_{RH}	environmental parameter accounting for the influence of the degree of saturation on D_{eff} [-]
$D_{RCM,0}$	chloride migration coefficient of water saturated concrete prepared and stored under predefined conditions, determined at the reference time t_0 [10^{-12} m ² /s]
k_t	test parameter to account for deviations of the chloride migration coefficient, determined under accelerated condition with the Rapid Chloride Migration method (RCM), and a diffusion coefficient determined under natural conditions [-]
k_T	temperature parameter, introduced in /2/ [-]

with

$$k_T = \exp \left(b_T \left(\frac{1}{T_{\text{ref}}} - \frac{1}{T} \right) \right) \quad \text{Eq. 1-3}$$

b_T	regression parameter [K]
T_{ref}	reference temperature [K]
T	temperature of the environment (micro climate) [K]

and

n	exponent regarding the time-dependence of D_{eff} [-]
t_0	reference time [s]

The applied model is probabilistic, i.e. each parameter is inserted in terms of a mean value, standard deviation and distribution type.

Depassivation of the reinforcement will start when the critical corrosion inducing chloride content C_{crit} will be exceeded in the depth of the concrete cover d_c , expressed by the limit state function given in Eq. 1-4:

$$p_f = p \left\{ C_{crit} - C_i - (C_{s,\Delta x} - C_i) \cdot \left[1 - \operatorname{erf} \left(\frac{d_c - \Delta x}{2 \sqrt{k_{RH} \cdot k_t \cdot k_T \cdot D_{RCM,0} \cdot t \cdot \left(\frac{t_0}{t} \right)^n}} \right) \right] < 0 \right\} \quad \text{Eq. 1-4}$$

p_f	failure probability [-]
p	probability of a certain event to occur [-]
C_{crit}	critical chloride concentration [M.-%/b]
d_c	cover depth [mm]

2 Assumptions and Source of data

2.1 Substituted Surface Chloride Concentration $C_{s,\Delta x}$

For the marine environment the mean value was set to be the largest value of the “peak” concentration in depth Δx of the given chloride profiles /3/, whereas the co-variance was assumed to be 30%.

For the road environment a transition function, determined by a regression analysis of data from Tang and Utgenannt /4/, was applied:

$$k_{Cl} = \frac{Q_{Cl}}{M_{Cl}} = 20,67 - 0,90 \cdot a - 5,40 \cdot h \quad \text{Eq. 2-1}$$

k_{Cl}	ratio of chlorides reaching the concrete surface and the amount of chlorides spreaded [$10^{-3}/m$]
Q_{Cl}	chloride flow reaching the concrete surface [g Cl/m ²]
M_{Cl}	spreaded chloride [t/km]
a	horizontal distance from road [m]
h	vertical distance from road level [m]

The given distance of 3 m /3/ from the nearest lane was assumed to be the horizontal distance (safe side). The vertical distance was set to zero, as the chloride loading decreases more with increasing vertical as with horizontal distance.

The width of the street has been assumed to be 10 m leading to M_{Cl} in [t/km] with a given salt application m_{Cl} in [g/m²]. The co-variance (CoV) of $C_{s,\Delta x}$ was set to be 30%, since reliable data is yet lacking.

2.2 Migration Coefficient $D_{RCM,0}$

The migration coefficient $D_{RCM,0}$ measured at an age of 0,5 a was used for the calculations, assuming normal distribution. A clear age effect was not obvious throughout the given data. The CoV was set to 20% according to /2/.

2.3 Relative Humidity Factor k_{RH}

So far, reliable data on the influence of the saturation degree on the effective diffusion coefficient is scarce but nevertheless has to be accounted for. For the submerged (Sub), tidal (Tid) and splash (Sph) marine environment, full saturation was assumed on the safe side, giving a value of $k_{RH} = 1$. For the atmospheric marine environment (Atm) and the road-environment (road) a value of $k_{RH} = 0,5$ has been guessed, since data is not yet available.

2.4 Temperature Factor k_T

For the sea water the temperature input data was given. For the road environment the temperature was set to be equal to the sea water for comparison purposes.

2.5 The test method factor k_t and age factor n

Values for k_t and n were taken from DuraCrete /5/.

2.6 Depth Δx

For the submerged and tidal conditions Δx was set to be 4 mm according to the "peak" of the given chloride profiles. The "peak" of the profile is probably caused by an aggregation of cement paste in the surface area, since the specimens were stored submerged in seawater. Therefore Δx is assumed to remain constant over time for submerged and tidal conditions. The co-variance was set according to /2/.

For the splash, atmospheric and road-environment mean value and co-variance were chosen according to /2/, hereby accounting for possible effects as convection, chloride wash-off and carbonation in the surface near concrete layer.

2.7 Critical Chloride Concentration C_{crit} , initial concentration C_i and concrete cover d_{cover}

Values for C_{crit} were taken from /5/. The initial concentration was set constant to $C_i = 0,07$ M.-%/b. The mean of the concrete cover was given, whereas the co-variance was set to 8 mm according to /2/, assuming "standard" workman ship.

3 Input parameters

			D-Type	Sub	Tid	Sph	Atm	Road
$C_{s,\Delta x}$	[M.-%/b]	Mean	LogN	3,20	3,20	3,20	3,20	0,84
		StD		0,96	0,96	0,96	0,96	0,25
$D_{RCM,0}$	$[10^{-12} \text{ m}^2/\text{s}]$	Mean	ND	2,70	2,70	2,70	2,70	2,70
		StD		0,54	0,54	0,54	0,54	0,54
k_{RH}	[-]	Mean	Const	1,00	1,00	1,00	0,50	0,50
		StD		0,0	0,0	0,0	0,0	0,0
b_T	[K]	Mean	ND	4800	4800	4800	4800	4800
		StD		700	700	700	700	700
T_{ref}	[K]	Mean	Const	293	293	293	293	293
		StD		0,0	0,0	0,0	0,0	0,0
T	[K]	Mean	ND	284	284	284	284	284
		StD		9,00	9,00	9,00	9,00	9,00
k_t	[-]	Mean	ND	0,832	0,832	0,832	0,832	0,832
		StD		0,024	0,024	0,024	0,024	0,024
n	[-]	Mean	ND	0,30	0,30	0,30	0,65	0,65
		StD		0,12	0,12	0,12	0,05	0,05
t_0	[a]	Mean	Const	0,50	0,50	0,50	0,50	0,50
		StD		0,0	0,0	0,0	0,0	0,0
Δx	[mm]	Mean	BetaD	4,00	4,00	8,90	8,90	8,90
		StD	$0 \leq \Delta x \leq 50$	2,52	2,52	5,60	5,60	5,60
C_{crit}	[M.-%/b]	Mean	ND	2,10	0,80	0,80	0,80	0,80
		StD		0,20	0,10	0,10	0,10	0,10
d_c	[mm]	Mean	BetaD	60,00	60,00	60,00	60,00	60,00
		StD	$0 \leq d_c \leq 300$	8,00	8,00	8,00	8,00	8,00
C_i	[M.-%/b]	Mean	Const	0,07	0,07	0,07	0,07	0,07
		StD		0,0	0,0	0,0	0,0	0,0

D-Type: distribution type

StD: standard deviation

LogN: logarithmic normal distributed

ND: normal distribution

BetaD: beta distribution

4 Estimated Chloride Profiles

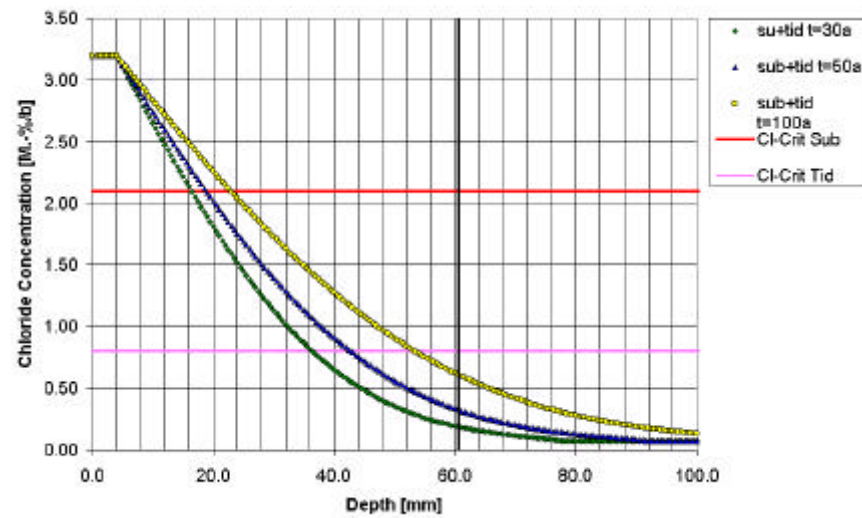


Figure 1: Submerged (Sub) and tidal (Tid) conditions

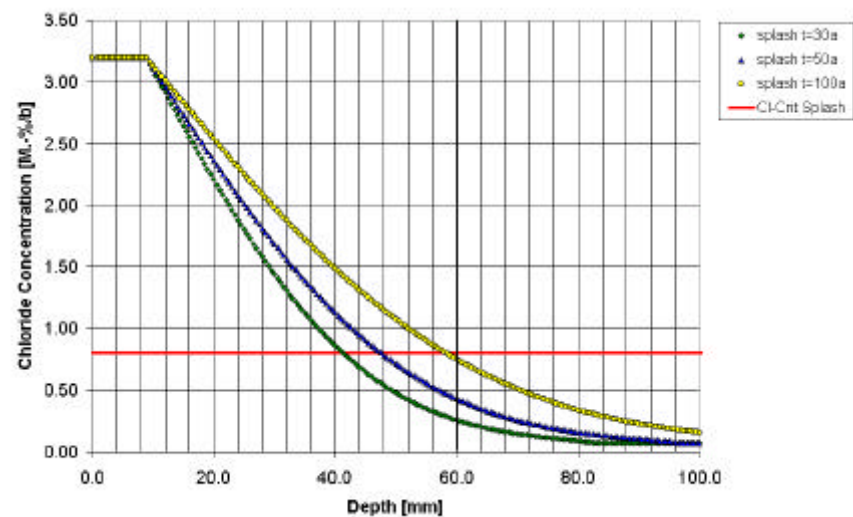


Figure 2: Marine splash conditions (Sph)

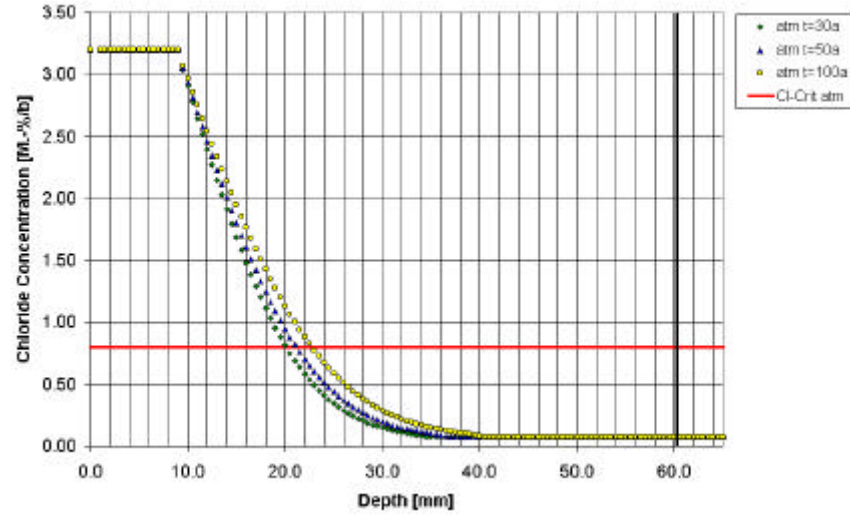


Figure 3: Marine atmospheric conditions (Atm)

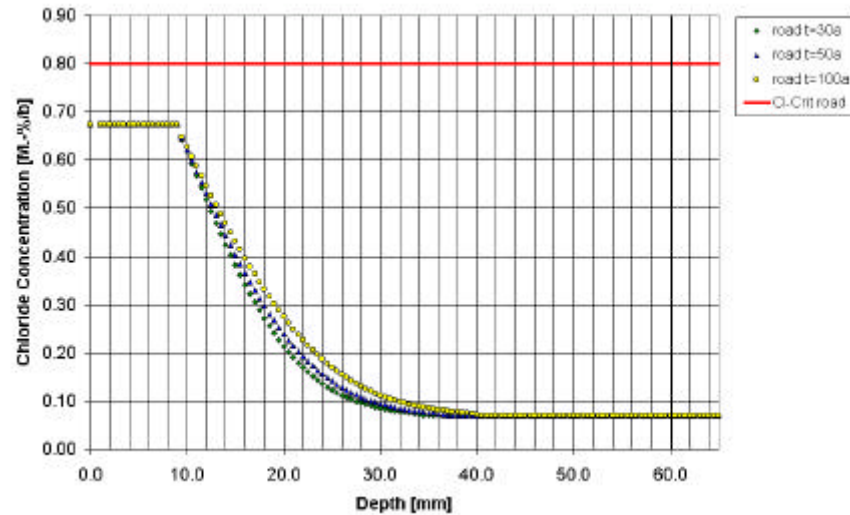


Figure 4: Estimated chloride profiles of a bridge column in a road environment (horizontal distance $a=3$ m from lane; $0,15 \text{ kg/m}^2$ NaCl spreaded)

5 Estimated Service Life

For the estimation of the service life of the case study structures, a safety requirement has to be introduced. Here, the chloride induced depassivation has been chosen as the limit state, which is regarded as a Serviceability Limit State (SLS 2 according to /2/). The required reliability index was set to $\beta_{\text{SLS}} = 2$, yielding a failure probability of $p_f = 2,275 \%$. The desired service life was assumed to be 100 years. Figure 5 to Figure 9 show the reliability index versus time for each environment. Table 1 depicts the reliability index after 100 years, and the service life yielding the reliability requirement.

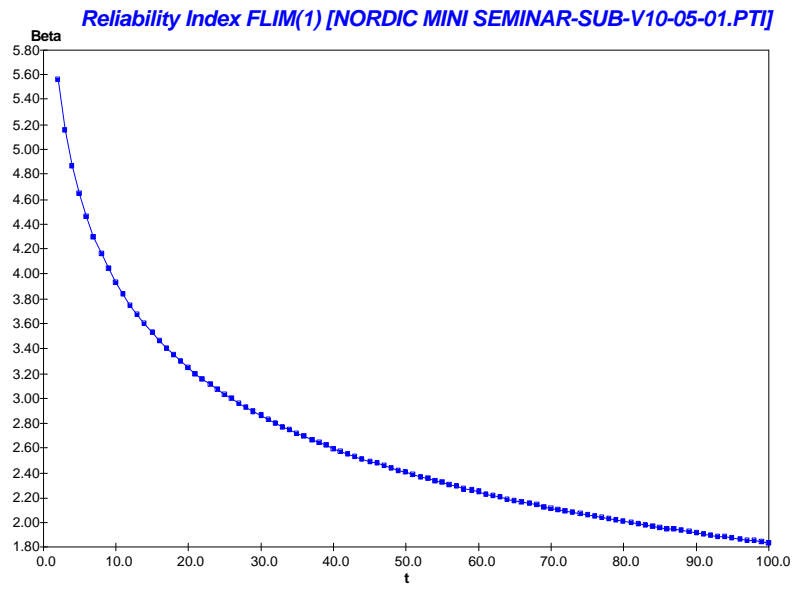


Figure 5: Reliability index for submerged marine conditions

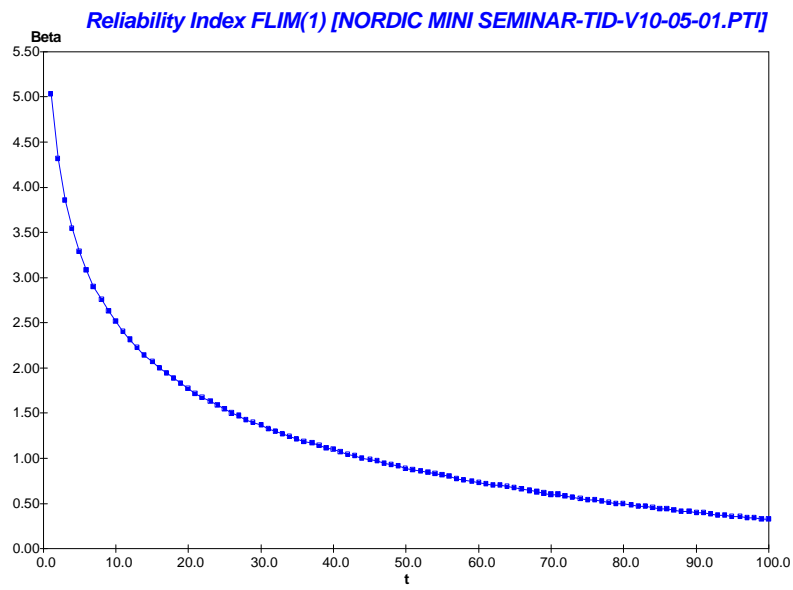


Figure 6: Reliability index for tidal marine conditions

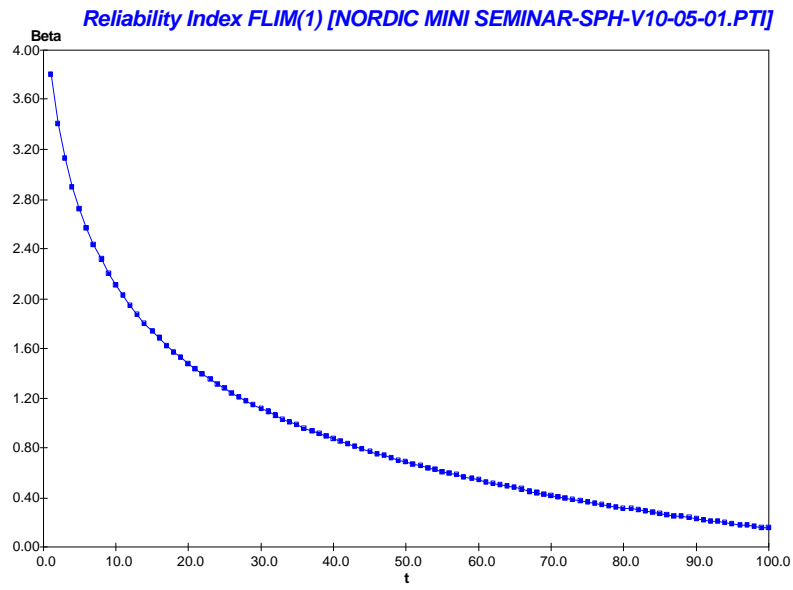


Figure 7: Reliability index for splash marine conditions

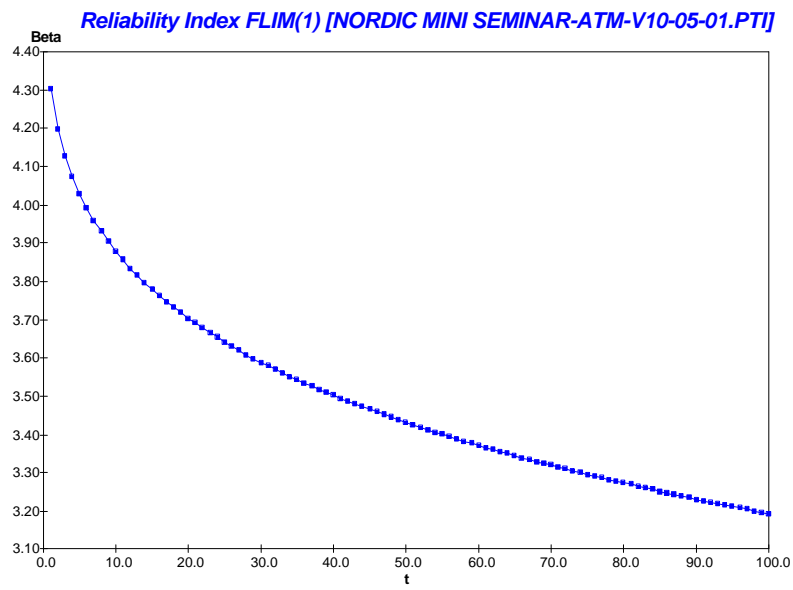


Figure 8: Reliability index for atmospheric marine conditions

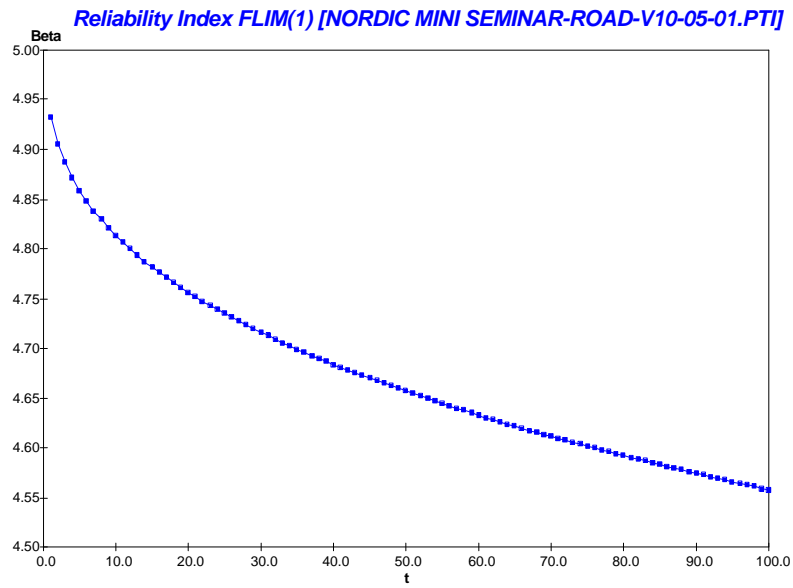


Figure 9: Reliability index for a road environment

Table 1: Estimated Service Life with a reliability $\mathbf{b}^3 2$ and reliability after 100 years $\mathbf{b}(t = 100a)$

		Submerged	Tidal	Splash	Atmospheric	Road
Service Life	[a]	81	16	11	>100	>100
$\beta(t = 100a)$	[-]	1,837	0,329	0,157	3,194	4,558

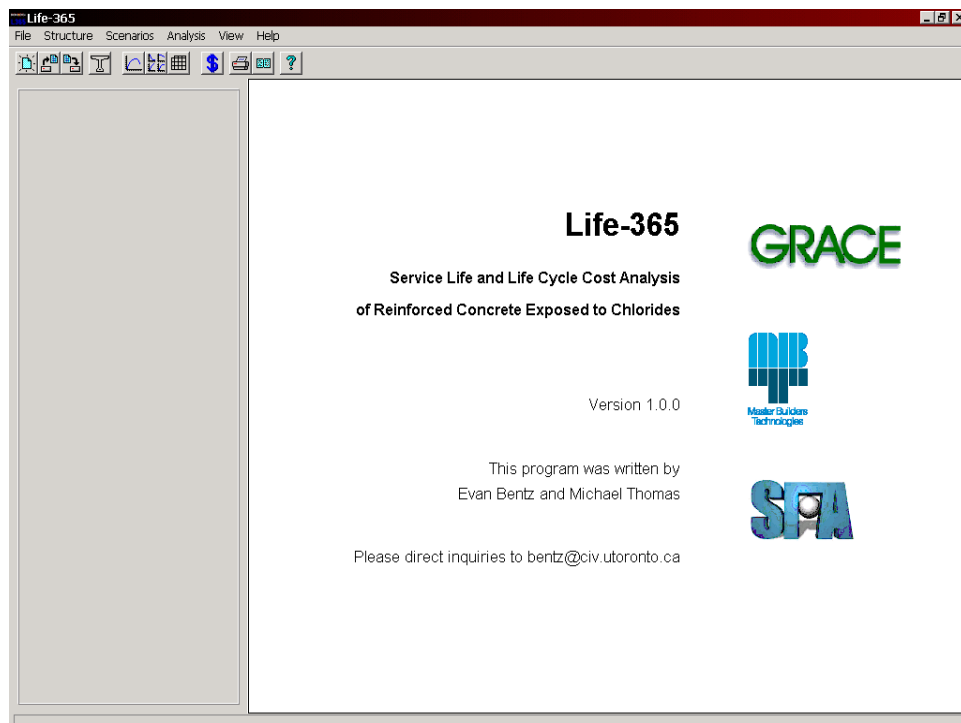
REFERENCES

- 1 BE95-1347: Modelling of Degradation – Report 4-5, 1998
- 2 Gehlen, C.: Probabilistische Lebensdauerbemessung von Stahlbetonbauwerken – Zuverlässigkeitsbetrachtungen zur wirksamen Vermeidung von Bewehrungskorrosion, Deutscher Ausschuss für Stahlbeton, Heft 510, Beuth Verlag, Berlin 2000
- 3 Nilsson, L.O.: Nordic Mini Seminar on Prediction Models for Chloride Ingress and Corrosion initiation in Concrete Structures – Data of the Case Studies, Göteborg, Sweden, 5/2001
- 4 Tang, L., Utgenannt, P.: Characterization of Chloride Environment along a Highway. In: Durability of Building Materials and Components 8 (Volume One), 1999
- 5 BE95-1347: Statistical Quantification of the Variables in the Limit State Functions – Report 9, 2000

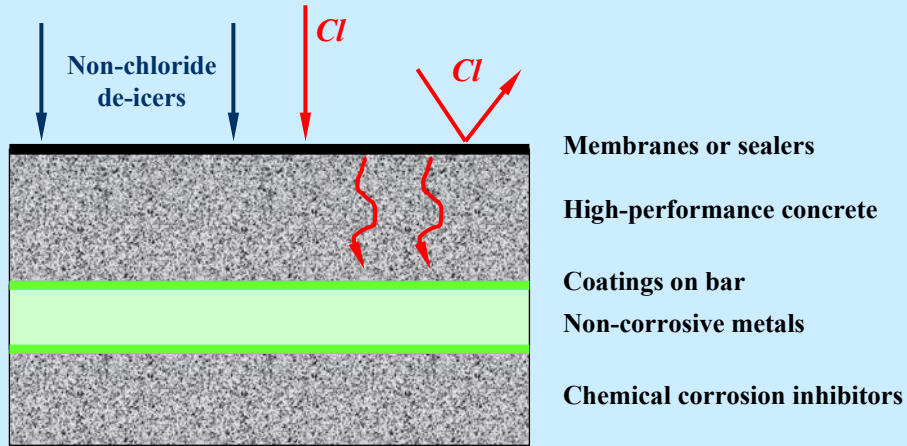
Predicting the Service-Life and Life-Cycle Costs of Reinforced Concrete Structures Exposed to Chlorides

*Michael Thomas & Evan Bentz
University of Toronto*

*Per Fidjestol
Elkem Materials*

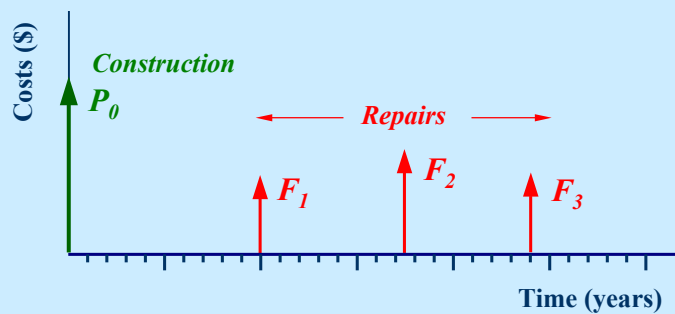


Corrosion Protection Strategies

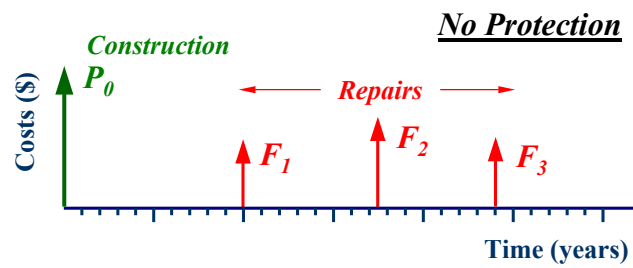


All of these strategies raise the initial cost of construction, but how do they influence the overall costs over the life of the project ?

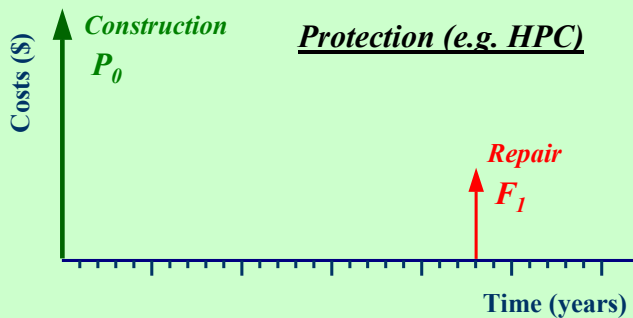
Cash-Flow Diagram



Total Costs includes Initial Construction & Future Repair Costs



*Which option
is the most
economic ?*



Time value of money

If an amount of money, P , is invested at an interest rate, i , (compounded annually) then in n years time the future value, F , is given by:

$$F = P \cdot (1 + i)^n$$

Same approach is taken in life-cycle cost analysis.

A future repair cost, F , spent in year, n , is converted to a “present worth”, PW , using a discount rate, i , as follows:

$$PW = \frac{F}{(1 + i)^n}$$

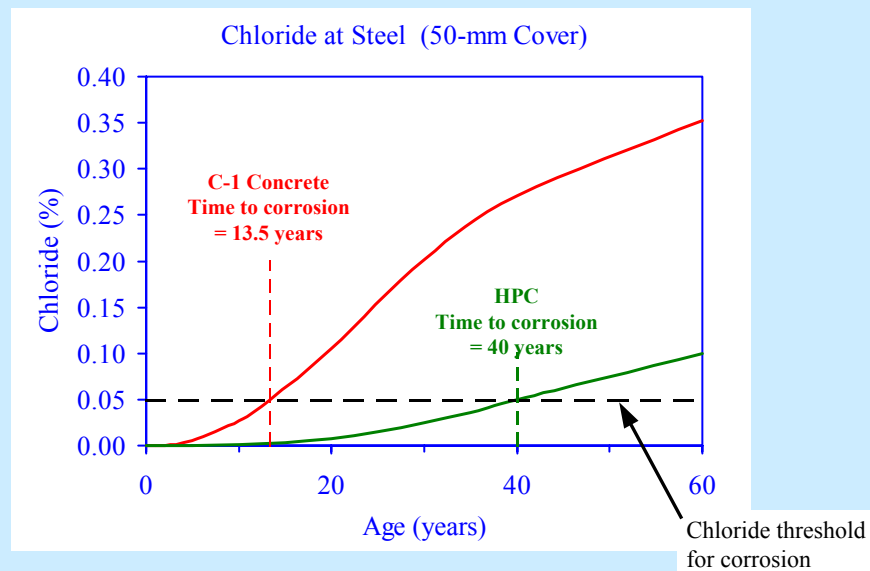
Example

HPC vs. C-1 Concrete for exposed bridge deck

Mix	Cement	W/CM	Cost (\$/m ³)	Cost (\$/m ²) ¹
C-1	T10	0.42	120	30
HPC	T10SF	0.36	160	40

¹ Cost/area for a 250-mm-thick slab

Service life model: used to calculate time for chlorides to reach the steel in sufficient quantity to initiate corrosion

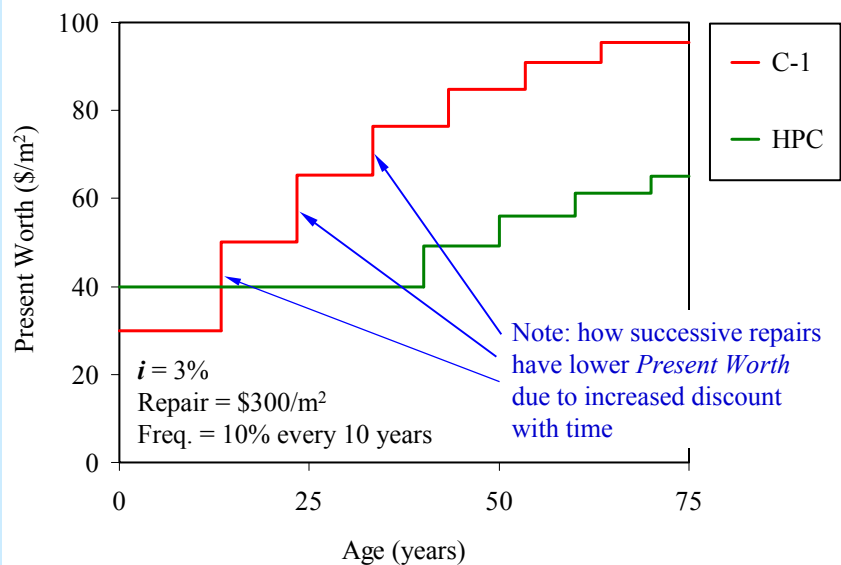


HPC has a lower permeability (and diffusivity) than regular C-1 concrete.

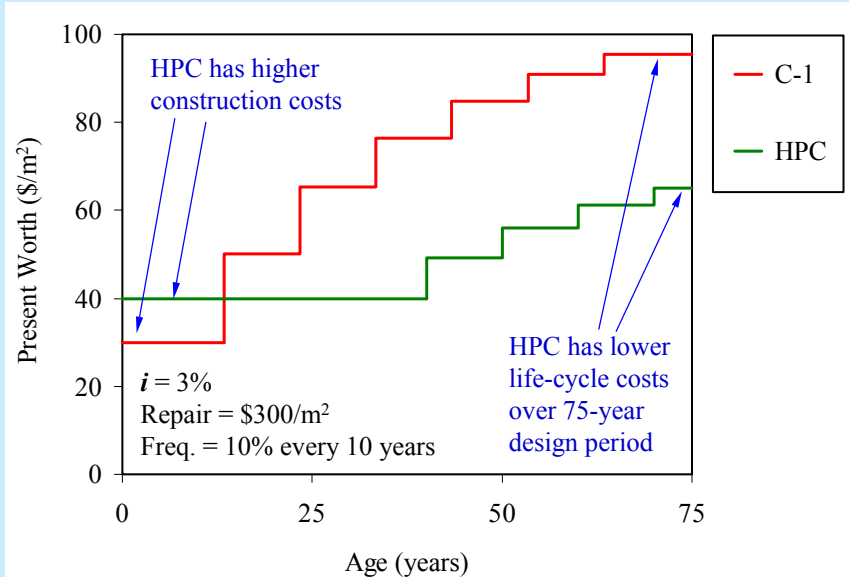
In other words, HPC has a higher resistance to the penetration of chlorides from de-icing salts (or seawater).

This means it takes longer for the chlorides to get to the embedded steel and initiate corrosion in HPC.

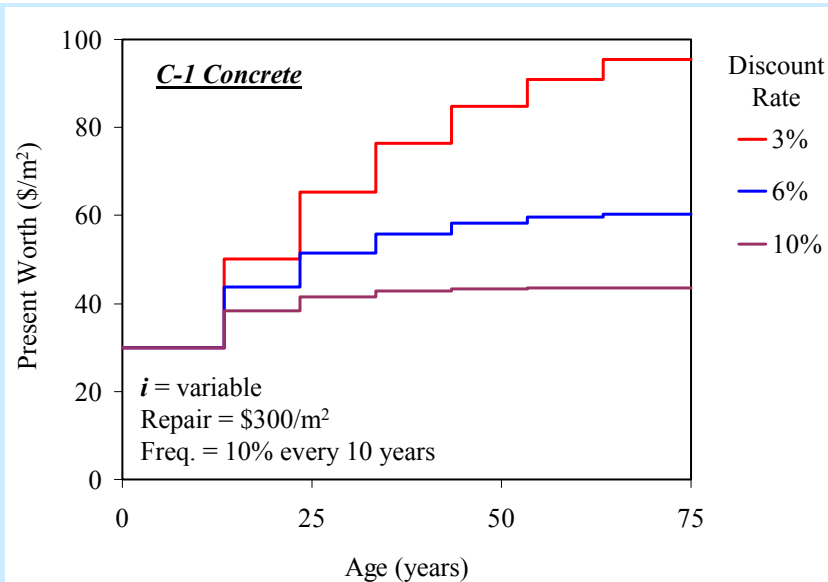
Life-Cycle Cost Analysis: used to calculate costs (construction and repair) over the life of the project.



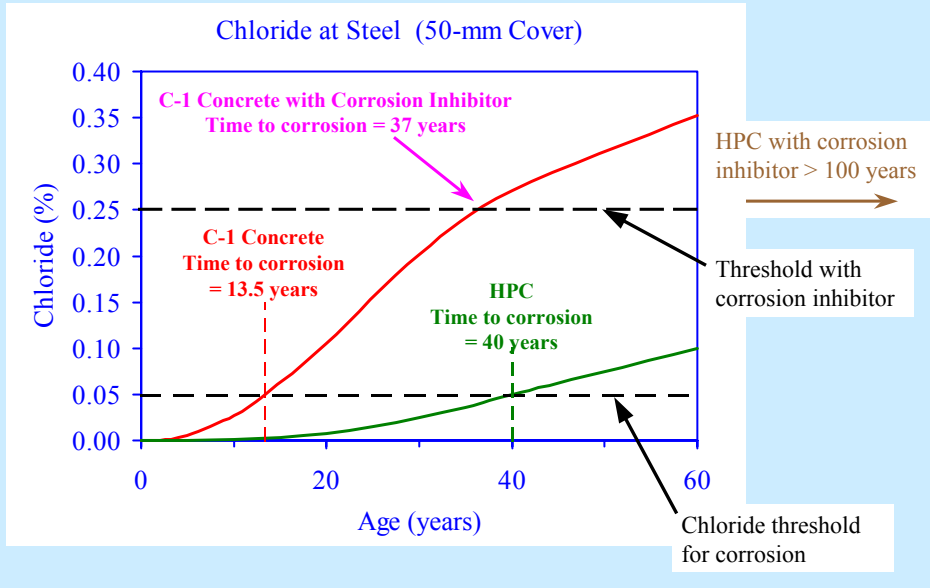
Life-Cycle Vs. Construction Costs.



Discount Rates: the final results of the life-cycle cost analysis are sensitive to the values used as inputs.



Service life model: used to calculate time for chlorides to reach the steel in sufficient quantity to initiate corrosion

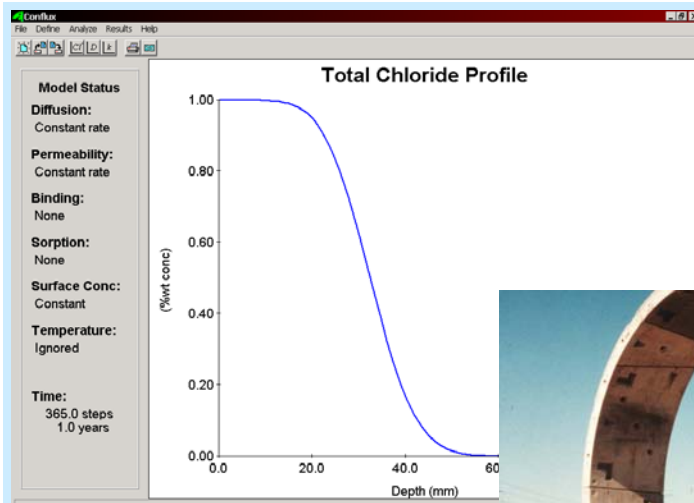


Life-365 specifically aimed at:

Bridge Decks



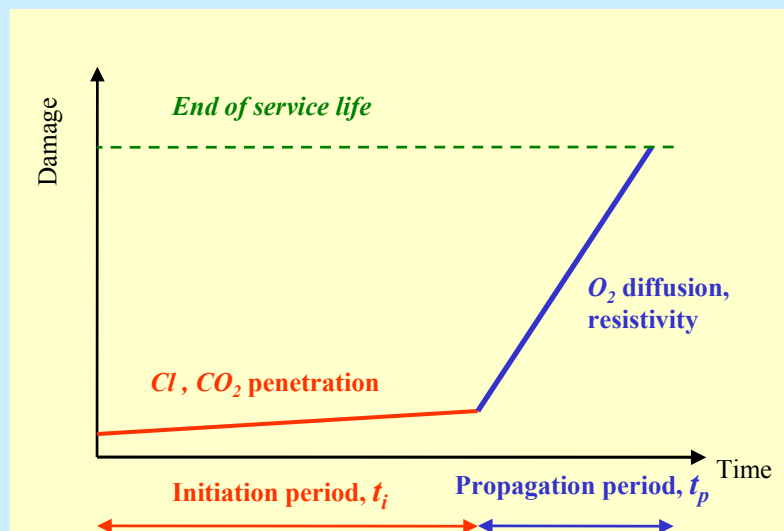
Parking Decks



Conflux: *Multi-mechanistic chloride transport model*



Simplified Service-Life Model



(Tuutti, 1982)

**Governing
Equation:**

$$\frac{dC}{dt} = D \cdot \frac{d^2C}{dx^2}$$

C	=	total Cl in concrete
D	=	diffusion coefficient
v	=	average linear velocity

Diffusion Coefficient

$$D(t, T) = D_{ref} \cdot \left(\frac{t_{ref}}{t} \right)^m \cdot \exp \left[\frac{U}{R} \cdot \left(\frac{1}{T_{ref}} - \frac{1}{T} \right) \right]$$

$D(t, T)$	=	diffusion coeff. at time t and temp. T
D_{ref}	=	diffusion coeff. at reference time and temp
m	=	constant (depending on mix prop.)
U	=	activation energy of diffusion process
R	=	gas constant

Initial Diffusion Coefficient, D_{28}

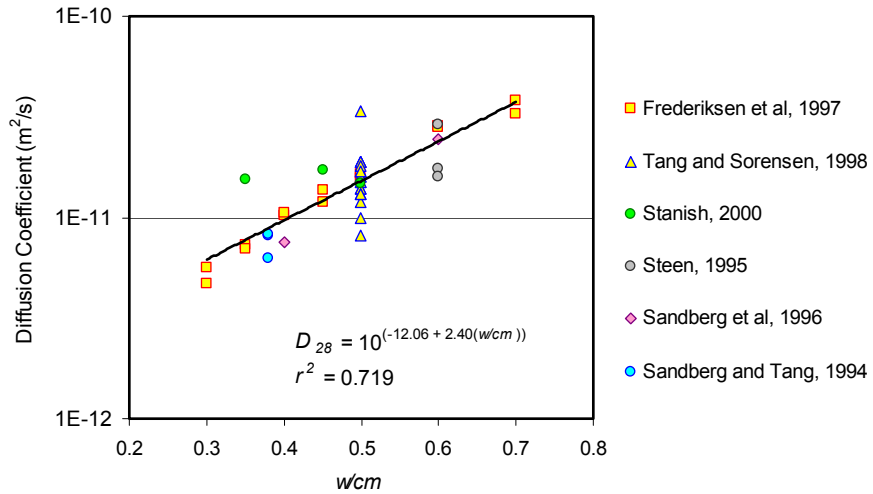


Figure 4.3 Relationship between D_{28} and w/cm for concrete at 20°C

Effect of Silica Fume

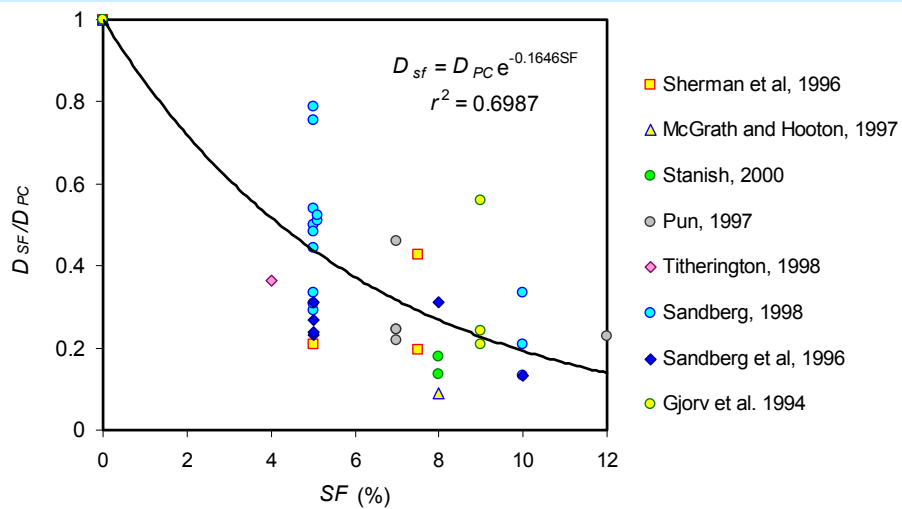
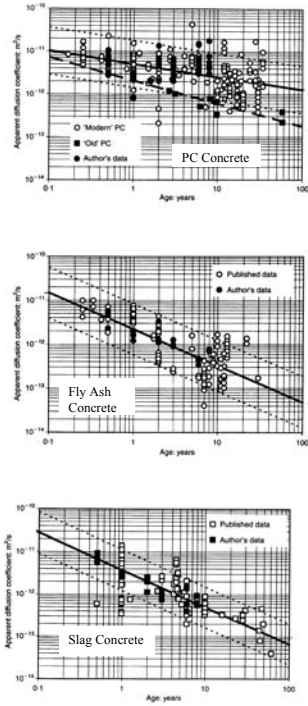


Figure 4.4 Effect of silica fume content on diffusion coefficient



Bamforth, 1999

	<i>m</i>
PC Concrete	0.264
Fly Ash Concrete	0.700
Slag Concrete	0.620

$$D_{28} = 10^{-12.06 + 2.40(w/cm)}$$

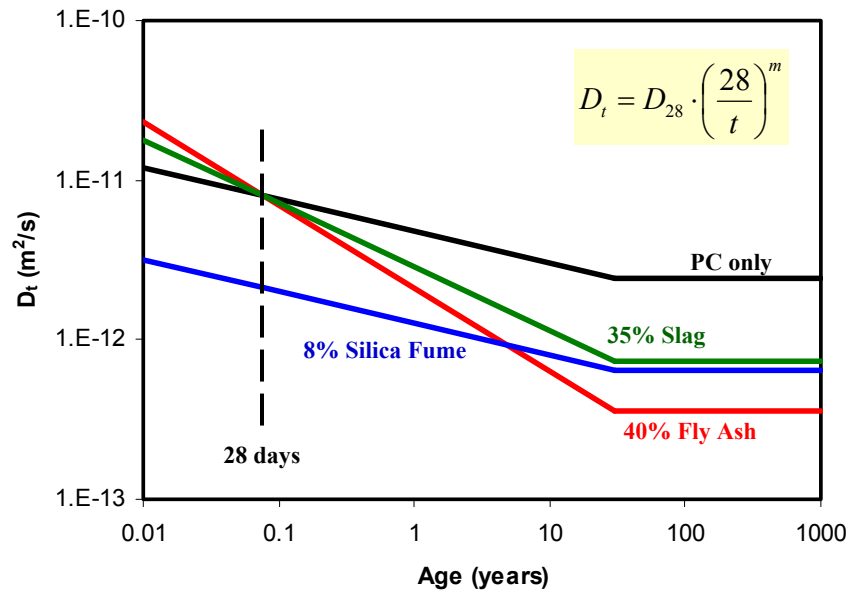
$$D_{SF} = D_{PC} e^{-0.165 SF}$$

$$D_t = D_{28} \cdot \left(\frac{28}{t} \right)^m$$

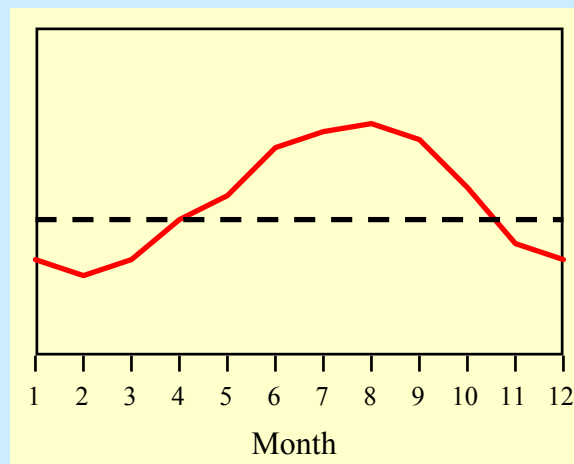
$$m = 0.2 + 0.4 \times (FA/50 + SG/70)$$

$$D_t = D_{30y} \quad \text{For } t \geq 30 \text{ years}$$

Effect of SCM on D vs t

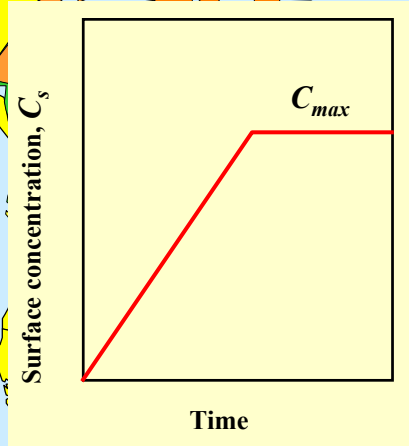


Temperature Profile



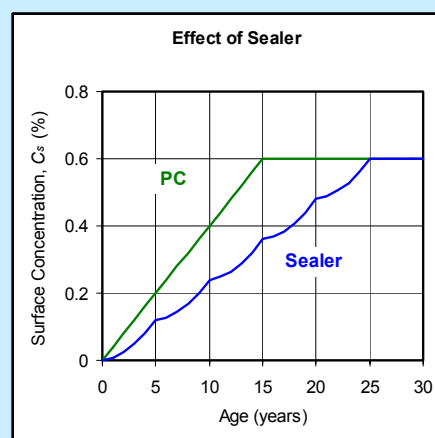
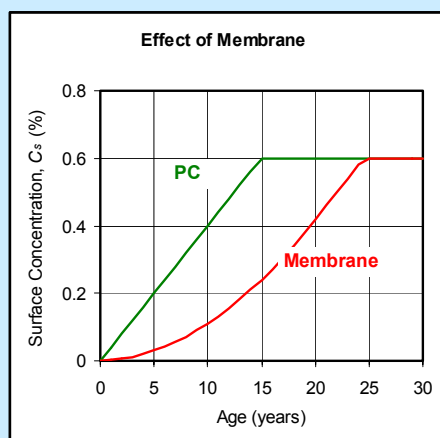
Surface Concentration

Key	Build-up (kg/m ³ yr)	C _s (kg/m ³)
	< 0.5	5
	0.5 to 1.0	10
	1.0 to 2.0	15
	2.0 to 3.0	20
	> 3.0	25
	No data available	



Miltenberger, 1999

Membranes & Sealers



Other Protection Strategies

Epoxy-coated rebar

Initiation period, t_i , unaffected

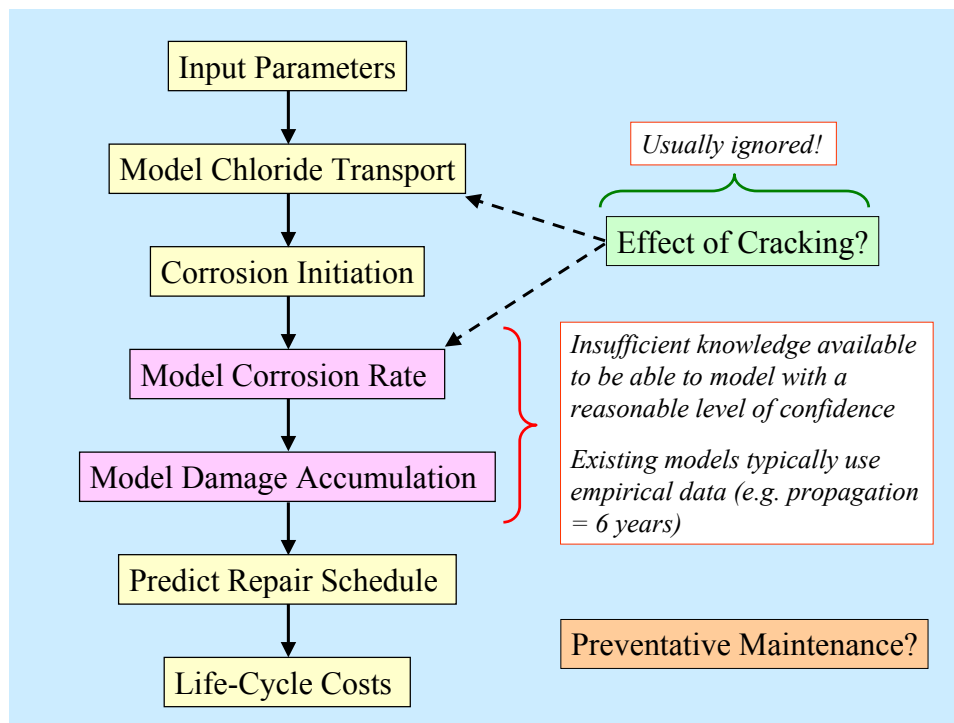
Propagation period, t_p , increased (default $t_p = 20$ years)

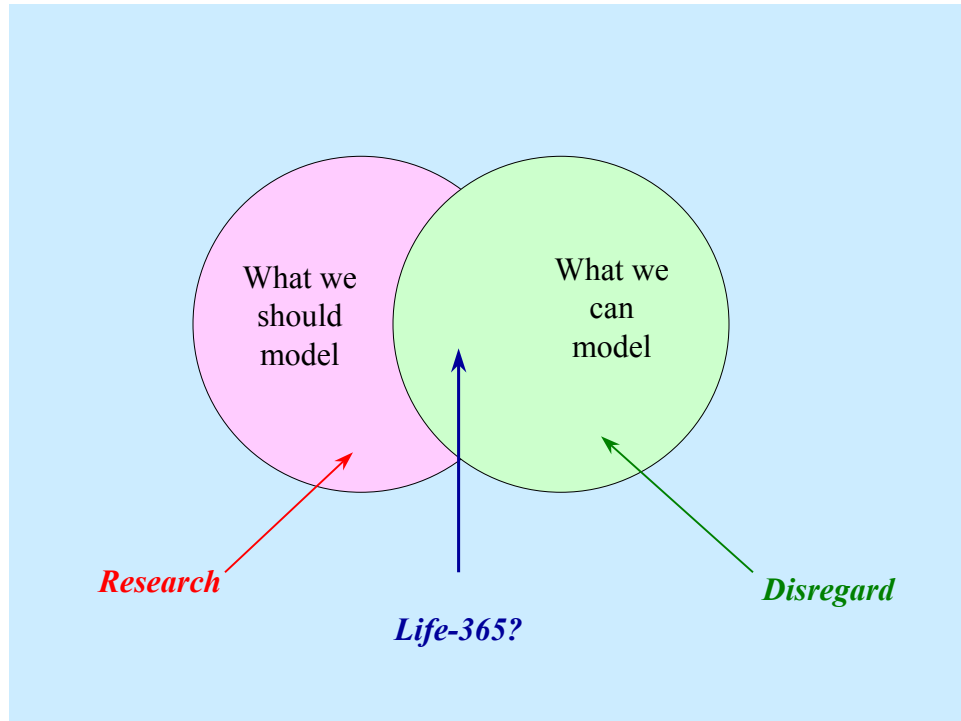
Corrosion Inhibitors

Increase chloride threshold concentration, C_t , depending on the type and dose of admixture

Stainless Steel

Increase chloride threshold concentration, $C_t = 0.50\%$





Version 2

- Probabilistic approach
- Model propagation period
- Validation (calibration)
- ?

Ongoing Research

- Effect of cracking
- Other transport mechanisms (unsaturated flow)
- ?

CLINCONC MODEL FOR PREDICTION OF CHLORIDE PENETRATION INTO CONCRETE – FROM THE ORIGINAL TO THE LATEST MODIFICATIONS

.....

Tang Luping
PhD
Dept. of Building Materials
Chalmers University of Technology
S-412 96 GÖTEBORG
SWEDEN
E-mail: tang@bm.chalmers.se

ABSTRACT

This paper presents the historical review of the prediction model ClinConc for chloride penetration into concrete. In the middle of 1990's, a scientific model called ClinConc was first presented. The model is essentially based on the knowledge of physical and chemical processes involved in the chloride transport and binding in concrete. The original model was for prediction of chloride penetration under submerged conditions only. After a number of modifications during the past years the model can in principle be used for different dry-and-wet environments, such as splash zone and road environment. In this paper different versions of ClinConc will be briefly reviewed and the latest modifications will be presented.

Keywords: chloride, concrete, models

1 INTRODUCTION

The numerical model ClinConc (*Cl in Concrete*) for prediction of chloride penetration into concrete was first presented in the middle of 1990's /1,2/. The model consists of two main procedures:

- 1) Simulation of free chloride penetration through the pore solution in concrete using a genuine flux equation based on the principle of Fick's law with the free chloride concentration as the driving potential, and
- 2) Calculation of the distribution of the total chloride content in concrete using the mass balance equation combined with non-linear chloride binding.

Not like other models, a unique character of the model ClinConc is that the chloride diffusivity, which can be determined by, e.g. the CTH method, is considered as a material property. It changes only when concrete is young, like many other material properties,

such as porosity and strength. After an age of a half of year, this diffusion coefficient becomes more or less constant according to the experiments /3,4/. Another unique character of the model ClinConc is that the climatic parameters, such as chloride concentration and temperature, are used in both the flux and the mass balance equations. Thus the model can well describe the effects of exposure conditions on chloride penetration.

The original version of ClinConc was developed based on the field data up to two years exposure under seawater. Due to the difficulties in combining moisture transport, the application of the original ClinConc was limited to submerged zone only. Very recently, a modification in climatic parameters makes the model applicable to different wet-and-dry environments including de-icing salt environment.

2 THE ORIGINAL CLINCONC

The original versions of ClinConc were based on MS Visual Basic /2,5/. There were no essential differences between different versions up to version 2.2b. The most of upgrading was for debugging and for making the program better user-friendly. In those versions, chloride binding was considered as temperature and alkali dependent, but not time-dependent. The exposure temperature and chloride concentration were described by a sine function, respectively. The model was verified using experimental data from the one-year laboratory exposure and the two-years field exposure. With the help of this model, it was demonstrated that the shape of a chloride penetration profile, especially a free chloride profile, is strongly dependent on the season /6/, as shown in Fig. 1. This is because of the effects of temperature on chloride binding as well as chloride diffusivity. In the summer (July), the high temperature decreases chloride binding capacity and increases chloride diffusivity. Some bound chlorides become unbound, resulting in higher free chloride concentrations in the pore solution and deeper penetration in the concrete. In the winter (January), most of the chlorides in the pore solution become bound, resulting in a lowest free chloride distribution during the year. This may explain some phenomena that, e.g. the corrosion is active only in the summer, not in the winter.

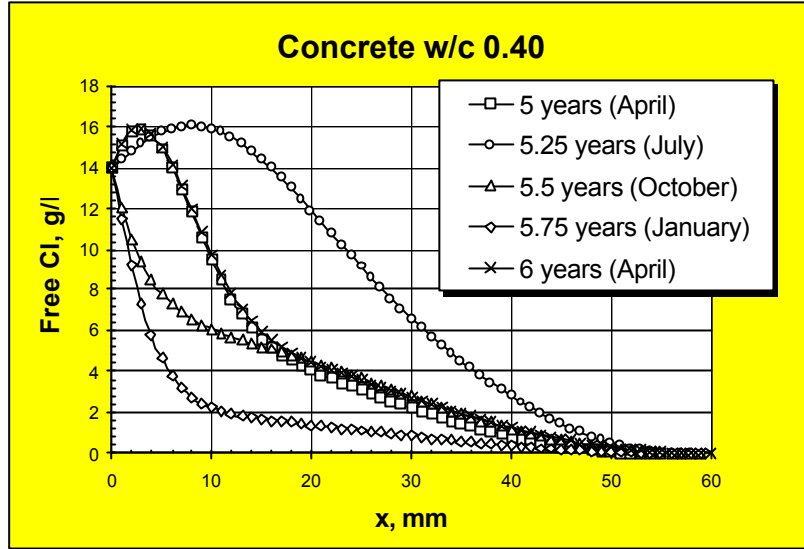


Fig. 1. Example of calculated free chloride profiles after exposure of 5 ~6 years /6/.

3 MODIFICATION FOR THE INCREASED SURFACE CHLORIDE CONTENT

When five-years field exposure data were available /7/, it was found that the original ClinConc underestimated the chloride content in the zone closer to the exposure surface, even though it fairly predicted the penetration depth. In other words, the surface chloride content tends to increase with exposure time even under submerged conditions. This increased chloride content cannot be explained by drying-and-wetting effect, like in the splash zone. Time-dependent chloride binding might be a potential reason, since the chloride binding isotherms used in the original ClinConc were those obtained in the laboratory after about two weeks equilibrium /8/. The effect of alkalinity on chloride binding was also based on a limited investigation /9/. In reality, the pore solution compositions may change due to leaching and penetration of different substances, resulting in different characteristics of chloride binding. Another possible reason is an increased saturation degree of the air voids near the surface. The saturation degree of the air voids will increase after such a long period of immersion, especially in contact with a salt solution. It is difficult, however, to model the saturation degree of the air voids. Thus the time-dependent chloride binding was assumed as a dominant reason for the increased chloride contents in the surface zone.

Since the current knowledge and quantitative information about the time effect of chloride binding is very limited, a simple modification was made in the MS Excel based version of ClinConc (version 3b), that is, to multiply the present binding function by a factor of f_t , which can be expressed as /10/

$$f_t = a \ln(t_{Cl} + b) + 1 \quad (1)$$

where t_{Cl} is the local chloride contamination time in years, and a and b are time-dependent coefficients. It should be noticed that, in the above equation, the time t_{Cl} does not mean the exposure duration, but means the duration of chloride contamination. No matter how long the exposure time is, at the depth where chlorides have not yet penetrated, the time t_{Cl} is always zero. Attention should be paid to this in computing. According to the measured chloride profiles /7/, the values of a and b could be assumed as 0.36 and 0.5, respectively. An example of f_t - t_{Cl} curve is illustrated in Fig. 2.

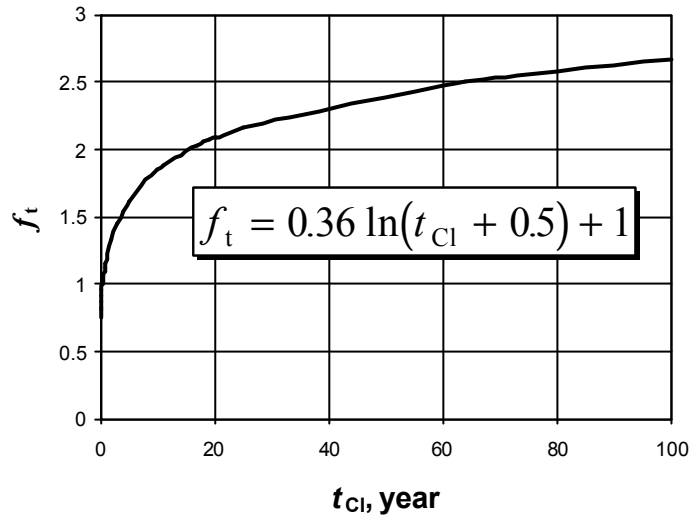


Fig. 2. Example of correction factor for time-dependent chloride binding /10/.

After this modification, the agreement between modelled and measured chloride profiles becomes better /11/.

3 THE LATEST MODIFICATION – FOR DIFFERENT EXPOSURE ENVIRONMENTS

Very recently, the model ClinConc was modified again in order to make it applicable to different exposure environments. In fact, nothing except for the exposure conditions has been modified in the latest version (MS Excel based version 4b, May 2001). In this latest modification, the exposure conditions were defined in a better and more precise way.

3.1 Exposure conditions for submerged zone

In the previous versions, both the exposure temperature and chloride concentration were described by a sine function, respectively. The problem occurred in combination of these two sine functions: Should these two sine functions be synchronous or not? Why? The sine function of annual average temperature has been well verified, but not the chloride concentration in seawater. Therefore, it was suggested in the latest version that average chloride concentration in seawater should be used unless the actual function of chloride concentration is known. An example of the exposure conditions for submerged zone is shown in Fig. 3.

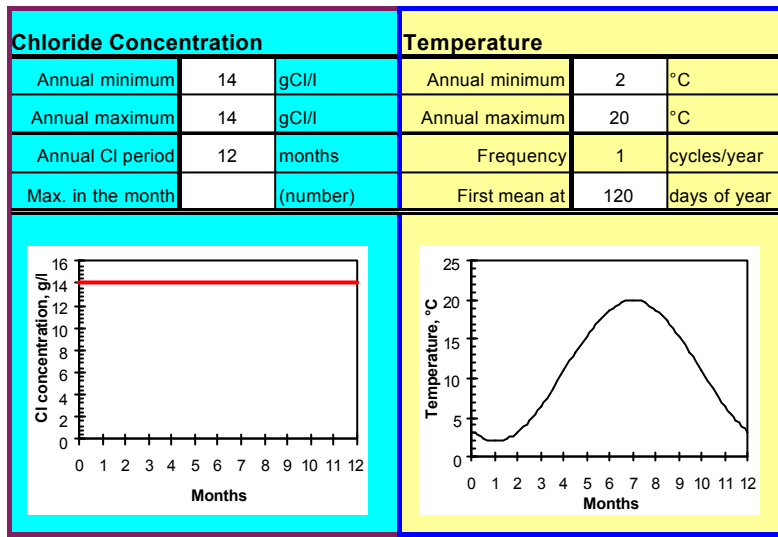


Fig. 3. Example of exposure conditions for submerged zone (Swedish west coast).

3.2 Exposure conditions for the marine environment above seawater

In the marine environment above seawater, such as splash zone or atmospheric zone, concrete is subjected to the alternative wetting-and-drying. The wetting includes both salt water and rain. Owing to the complicated mechanisms involved in both the moisture and chloride transport, it is not an easy task to combine both moisture and chloride transports into a single model, even though some attempts have been done [12,13]. On the other hand, it could be reasonable to assume that, under such a wet-and-dry environment, the chloride concentration in contact with the concrete surface alters between zero and a specified level. The wick effect due to drying is compensated by the effect of capillary suction due to re-wetting. Thus the chloride transport could be assumed dominated by diffusion in a saturated pore system, despite of wetting-and-drying processes. In this way the difficulties in modelling of moisture transport could be skipped and the question becomes how to define the chloride concentration curve. In the latest modification, a normal distribution function was used to describe the annual chloride concentration, that is,

$$c_{0s} = \bar{c}_0 \exp\left(-\frac{\tau^2}{2\sigma^2}\right) \quad (2)$$

where c_{0s} is the chloride concentration in contact with the concrete surface, \bar{c}_0 is the average annual chloride concentration in seawater, σ ($= 0.15$) is the standard deviation of time difference τ , the latter is expressed as

$$\tau = \begin{cases} \frac{t - t_m}{L} & (t - t_m) \leq \frac{L}{2} \\ 1 - \frac{t - t_m}{L} & (t - t_m) > \frac{L}{2} \end{cases} \quad (3)$$

where t is the actual time, t_m is the time when the chloride concentration reaches maximum during the period, and L is the period, which could be in hours, days or months. Since the actual repetition of chloride concentration in splash zone is unknown, L was simply assumed to be 12 months, that is, annually repeated in order to simplify the calculation. In this case the sine function of temperature is inapplicable, thus an average annual temperature should be used. Some examples of exposure conditions for the marine environment above seawater are given in Figs. 4 and 5.

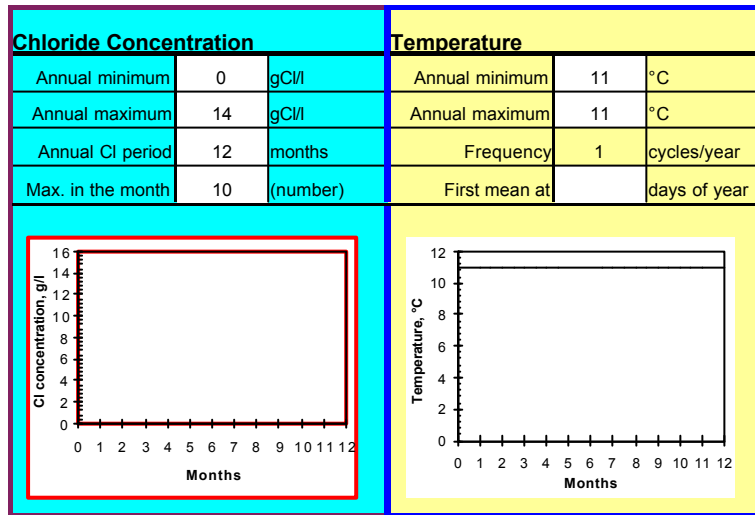


Fig. 4. Example of exposure conditions for splash zone (0~30 cm above seawater in Swedish west coast).

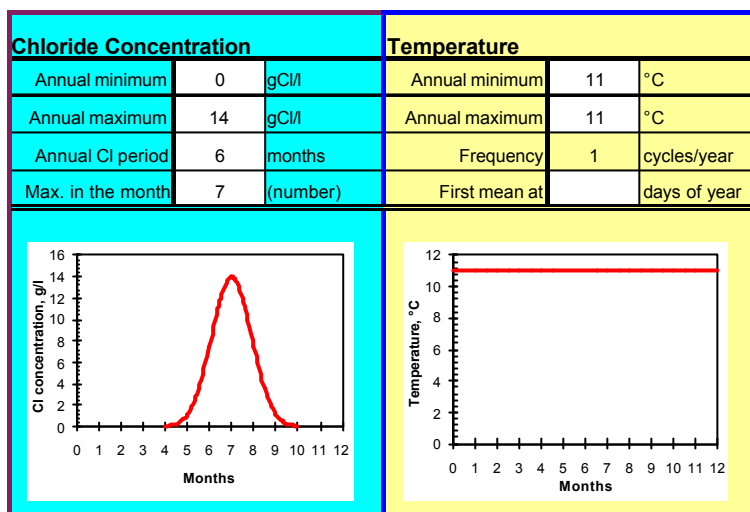


Fig. 5. Example of exposure conditions for atmospheric zone (30~60 cm above seawater in Swedish west coast).

3.3 Exposure conditions for the road environment using de-icing salt

The same principles as described in 3.2 can be used for the road environment. Difference is that the chloride period (application of de-icing salt) is a more or less known parameter. Thus the sine function of temperature can be applied. However, the maximum chloride concentration in this case becomes unknown. From the field data obtained from the two-winters exposure along the highway Rv 40 between Borås and Göteborg it was found that, when assuming a maximum concentration of 50 g Cl per litre, the predicted profiles correspond fairly well with the field data, which will be presented later. An example of exposure conditions for the road environment is shown in Fig. 6.

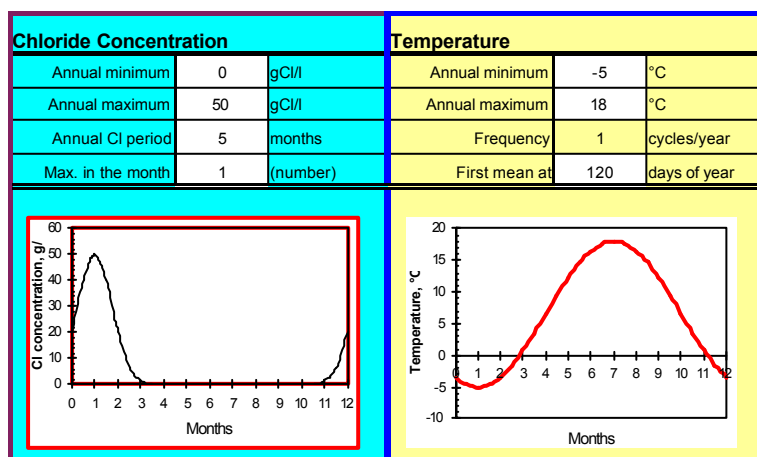


Fig. 6. Example of exposure conditions for a road environment (Highway Rv 40 between Borås and Göteborg, Sweden).

4 SOME EXAMPLES OF PREDICTED CHLORIDE PROFILES

From two Swedish national projects a lot of chloride profiles obtained after five years exposure under the marine environment and after two winters exposure under the road environment are available /7,14/. These chloride profiles were utilised to verify the modified ClinConc. The concrete mixture proportions were previously published elsewhere /15/. Some of the results are shown in Figs. 7-10. It can be seen that the predictions are in general fairly well in agreement with the field data, especially the shapes of chloride profiles from alternative wet-and-dry environments, indicating that the assumptions made in 3.2 and 3.3 are reasonable.

5 CONCLUDING REMARKS

The latest modification has made the model ClinConc applicable to both marine environment, including submerged, splash and atmospheric zones, and the road environment using de-icing salt in the winter. The verifications up to five-years marine exposure data and two-winters road exposure data show that the predictions of chloride penetration into concrete structures are, in general, fairly well in agreement with the measured chloride profiles.

The exposure environment can be described the combination of temperature function and concentration function. The former can be expressed as a sine function, while the latter expressed by a normal distribution function. With such a combination, the chloride ingress into concrete under various environments could be approximated by diffusion in a saturated pore system, thus the actual wetting-and-drying processes could be skipped.

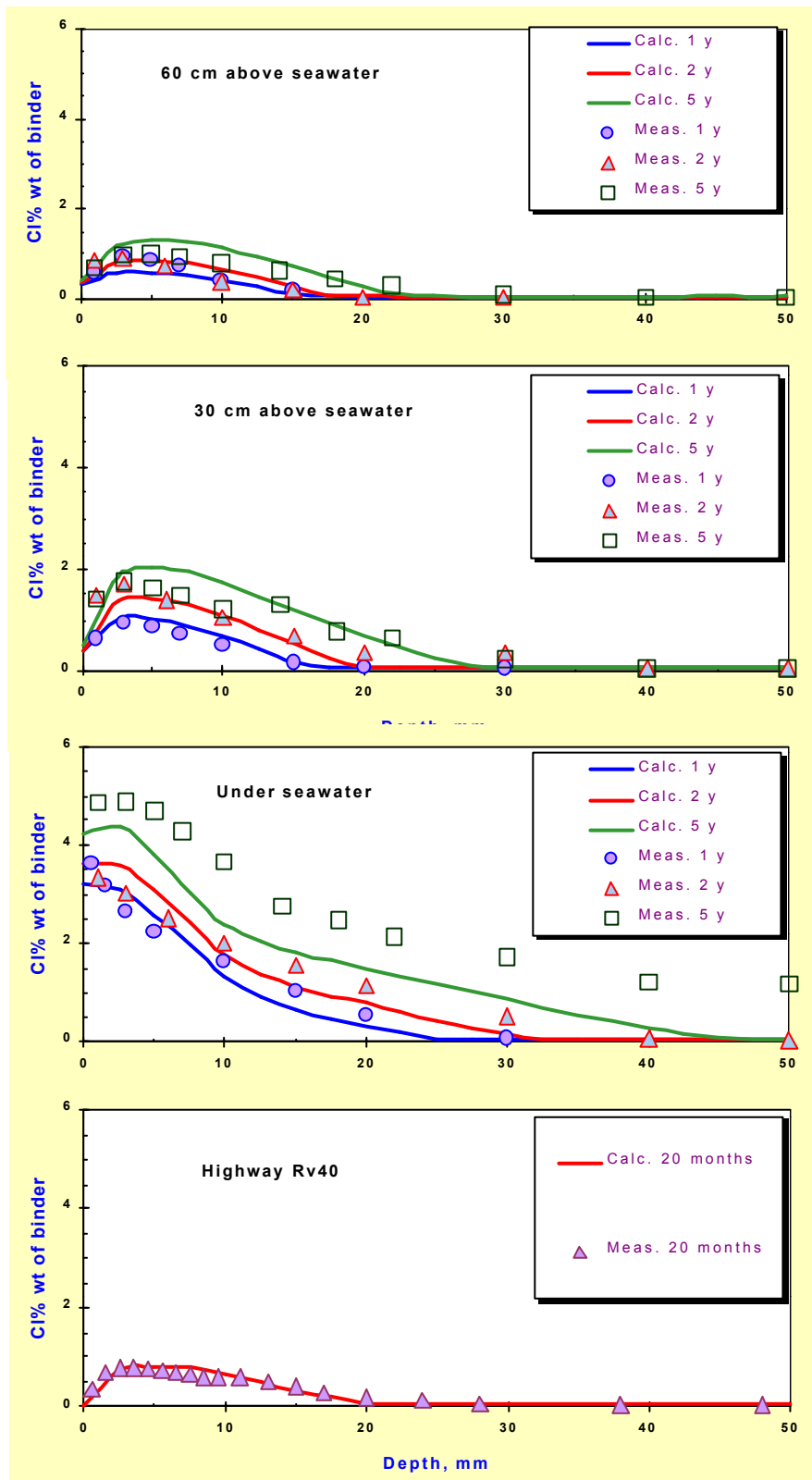


Fig. 7. Example of the predicted chloride profiles. SRPC w/b 0.40.

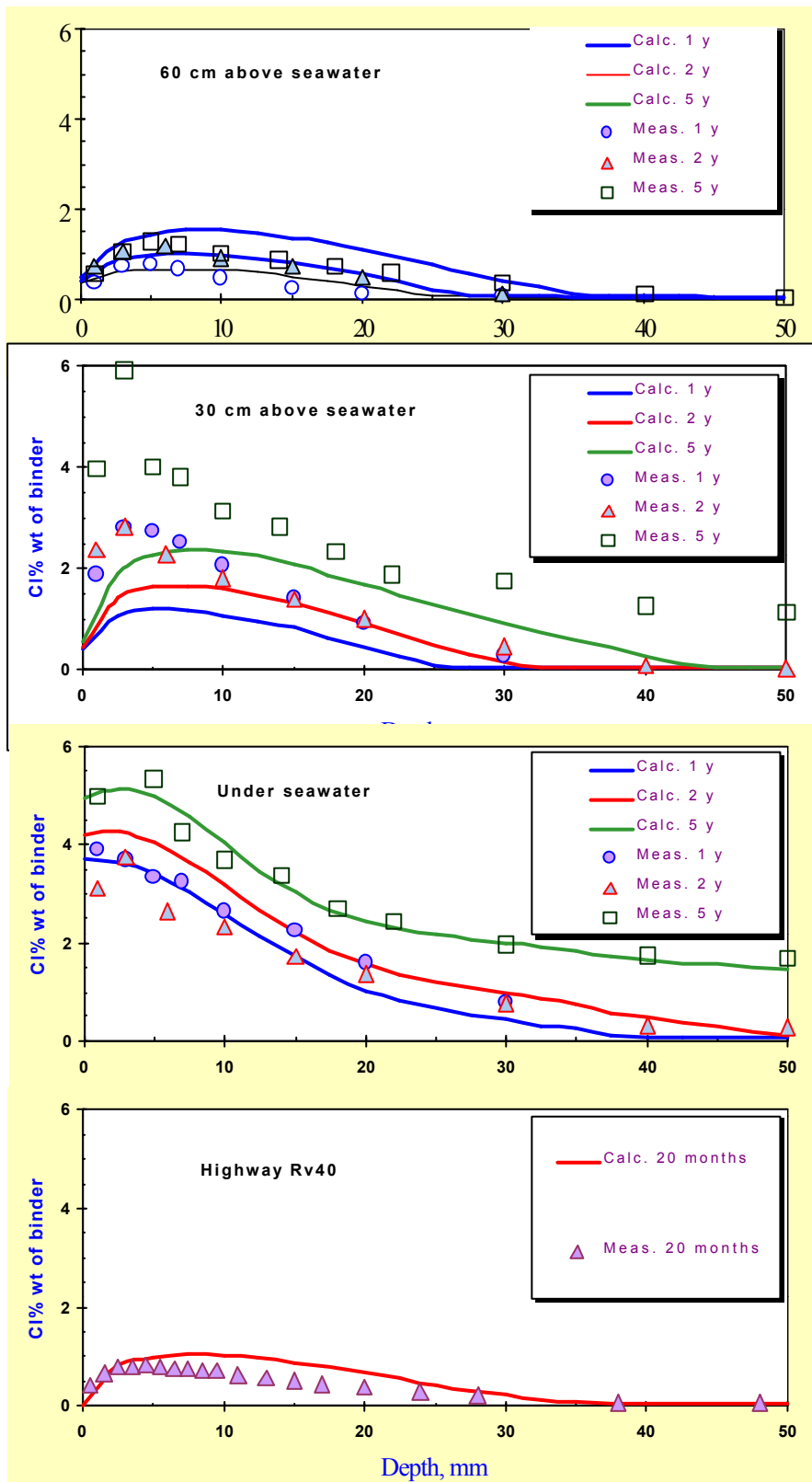


Fig. 8. Example of the predicted chloride profiles. SRPC, w/b 0.50.

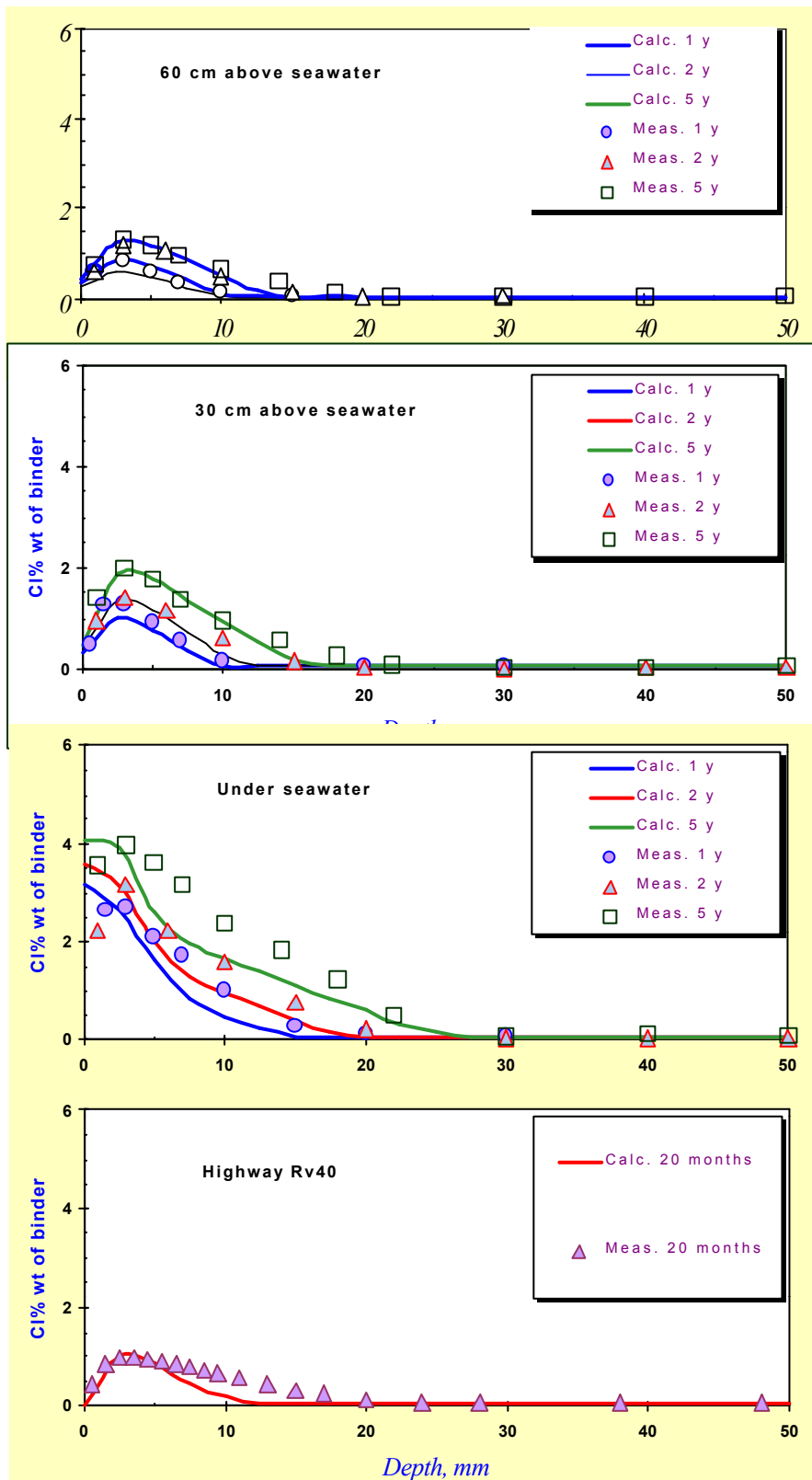


Fig. 9. Example of the predicted chloride profiles. SRPC + 5%CSF, w/b 0.40.

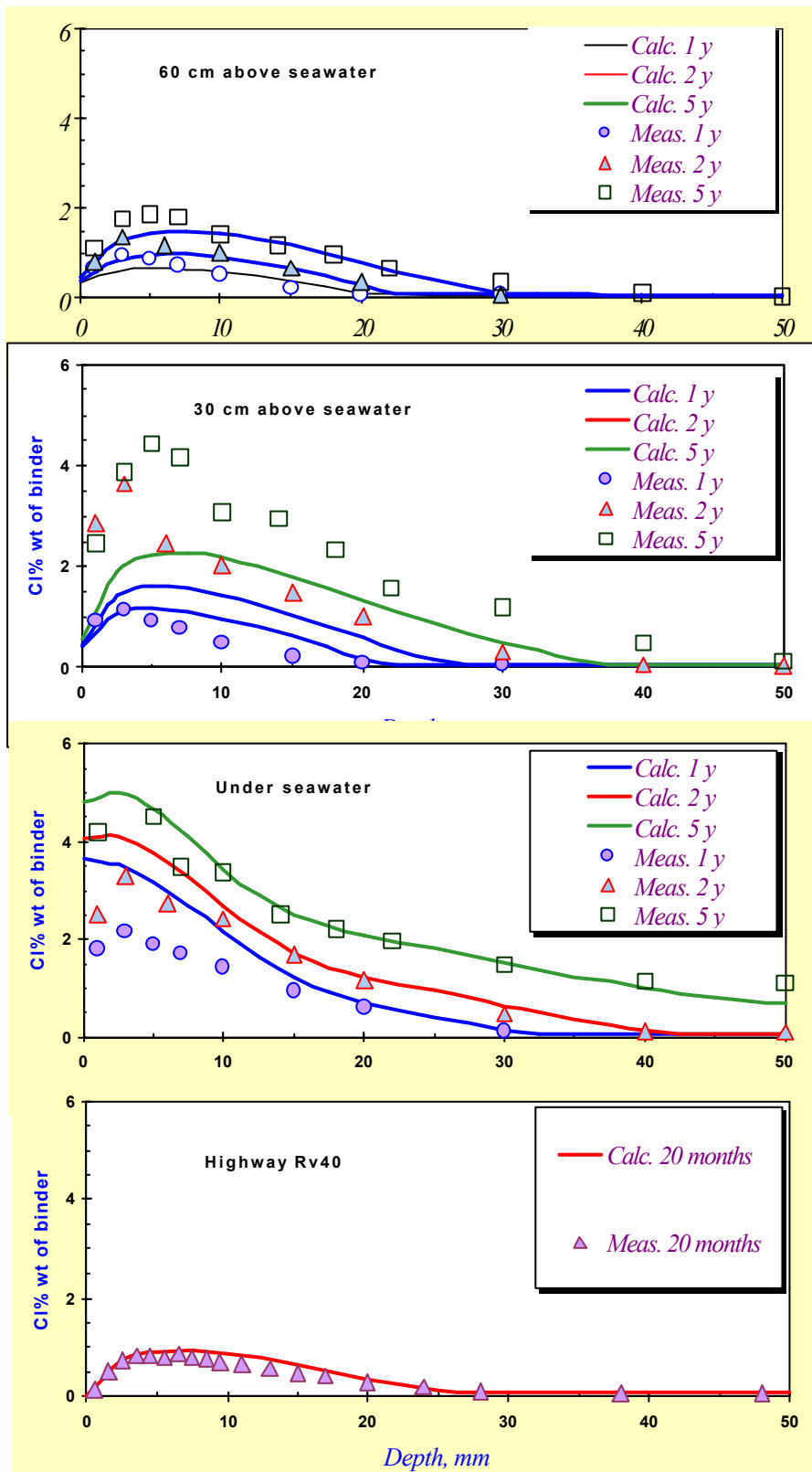


Fig. 10. Example of the predicted chloride profiles. SRPC + 5%CSF, w/b 0.50.

REFERENCES

- /1/ Tang, L. and Nilsson, L.-O. (1994), *A numerical method for prediction of chloride penetration into concrete structures*, in The Modelling of Microstructure and its Potential for Studying Transport Properties and Durability, ed. H. Jennings et al, Kluwer Academic Publisher, pp. 539-552.
- /2/ Tang, L. (1995), *A Windows program for the prediction of chloride penetration into submerged concrete*, Proceedings of the RILEM International Workshop on Chloride Penetration into Concrete, Oct. 15-18, 1995, St. Rémy-lès-Chevreuse, France, ed. by L.-O. Nilsson and J.P. Ollivier, pp. 206-215.
- /3/ Tang, L. and Nilsson, L.-O. (1992), *Chloride diffusivity in high strength concrete at different ages*, Nordic Concr. Res., Publication No. 11, pp. 162-171.
- /4/ Tang, L. (1996), *Electrically accelerated methods for determining chloride diffusivity in concrete*, Magazine of Concrete Research, Vol. 48, No. 176, pp. 173-179.
- /5/ Tang, L. (1996), *Chloride transport in concrete - Measurement and prediction*, Dept. of Building Materials, Chalmers University of Technology. Publication P-96:6.
- /6/ Tang, L. and Nilsson, L.-O. (1998), *Prediction of chloride penetration into concrete by using the computer program CLINCONC*, Proceedings of the 2nd International Conference on Concrete under Severe Conditions, June 21-24, 1998, Tromsø, Norway.
- /7/ Andersen, A., Hjelm, S., Janz, M., Johannesson, B., Pettersson, K., Sandberg, P., Sørensen, H., Tang, L. And Woltze, K. (1998), *Total chloride profiles in uncracked concrete exposed at Träslövsläge marine field station - Raw data from 1992 to 1997*, Report TVBM-7126, Division of Building Materials, Lund Institute of Technology, Lund, Sweden, 1998.
- /8/ Tang, L. and Nilsson, L.-O. (1993), *Chloride binding capacity and binding isotherms of OPC pastes and mortars*, Cement and Concrete Research, Vol.23, No.2, pp. 347-353.
- /9/ Sandberg, P. and Larsson, J. (1993), *Chloride binding in cement pastes in equilibrium with synthetic pore solutions as a function of [Cl] and [OH]*, in Chloride Penetration into Concrete Structures - Nordic Miniseminar, ed. by L.-O. Nilsson, Publication P-93:1, Division of Building Materials, Chalmers University of Technology, pp. 98-107, Gothenburg, Sweden, 1993.
- /10/ Tang, L. and Nilsson, L.-O. (2000), *Modeling of chloride penetration into concrete - Tracing five years field exposure*, Concrete Science and Engineering, Vol.2, No. 8, pp. 170-175.
- /11/ Tang L. and Nilsson, L.-O. (2000), *Current development and verification of the numerical model ClinConc for predicting chloride penetration into concrete*, Proceedings of the 2nd International RILEM Workshop on Testing and Modelling the Chloride Ingress into Concrete, Paris, 11-12 September 2000, pp. 305-316.
- /12/ Nilsson, L.-O. (2000) *A numerical model for combined diffusion and convection of chloride in non-saturated concrete*. Proceedings of the 2nd International

- RILEM Workshop on Testing and Modelling the Chloride Ingress into Concrete, Paris, 11-12 September 2000, pp. 261-275.
- /13/ Francy, O., Bonnet, S., Francois, R. and Perrin, B. (1996), Modelling of chloride ingress into cement-based materials due to capillary suction, Proceedings of the 10th ICCI. 4iv078.
- /14/ Lindvall, A., Adersen, A. and Nilsson, L.-O. (2000) *Chloride ingress data from Danish and Swedish road bridges exposed to splash from de-icing salts*. Proceedings of the 2nd International RILEM Workshop on Testing and Modelling the Chloride Ingress into Concrete, Paris, 11-12 September 2000, pp. 85-103.
- /15/ Tang L. and Andersen, A. (2000), *Chloride ingress data from five years field exposure in a Swedish marine environment*, Proceedings of the 2nd International RILEM Workshop on Testing and Modelling the Chloride Ingress into Concrete, Paris, 11-12 September 2000, pp. 105-119.

An Overview of Models on Multi-Species Diffusion in Pore Solution of Concrete

Björn Johannesson

Lund Institute of Technology, Division of Building Materials

Box 118, SE-221 00 Lund, Sweden

May 14, 2001

Abstract

In order to understand the durability problems related to diffusion and chemical reactions in pore solution of concrete it is important to establish hypothesizes (i.e. physically adequate models) to which experimental results can be compared. Recently attention has been drawn towards the description of models dealing with multi-species diffusion in pore solution of concrete, which is suppose to have an important effect contributing to mechanisms being of importance in durability considerations. One advance with this approach is that several different mechanisms can be studied, such as reinforcement corrosion, sulfate attack, carbonation and hydroxide leaching.

1. Introduction

The last year attention has been drawn to the description of diffusion of different types of ions in pore solution of concrete. The subject is important since the diffusion behavior of ions such as hydroxide, chlorides and sulfates determines important deterioration processes in concrete.

Classical theories has been adopted, i.e. diffusion theories where both concentration and internal electrical potential gradients are included in the description of the diffusion velocities. In pore solution of concrete there are, however, two important mechanisms not included in these classical theories, i.e. the effect of

homogeneous reactions, heterogeneous reactions and surface reactions involving ions in pore solution and the effect of convection on ions due to capillary suction of water in pore system. How to involve such mechanisms in the governed equations for the ion constituents will be discussed.

The models dealing with multi-species ion diffusion always demands solutions based on numerical methods since the equation system, defining the models, are non-linear and coupled. Therefore, the knowledge of different numerical techniques, involving both time and spatial domain discretizations, becomes very crucial. That is, reliable solution procedures for solving the suggested equations in models must be established, otherwise the demanded calibrations against experimental data can not be performed.

2. Two ion constituent method

Two types of ions in solution such as for example a sodium chloride solution must fullfil certain conditions with regard to diffusion. The two separate types of ions must be transported in solution in a way that the electron neutrality is very close to zero. For a 1-1 electrolyte such as a pure sodium chloride solution the sodium ions must follow the chloride ions during the diffusive flow. The classical condition for this case will be derived in this section.

Consider the classical constitutive relation for the diffusive flow $\rho_1^p \mathbf{u}_1^p$ for a type of ion denoted 1, as

$$\rho_1^p \mathbf{u}_1^p = -D_1^p n_1^p m_1 \text{grad} (\ln \gamma_1^p n_1^p) - A_1^p m_1 n_1^p \text{grad} \varphi^p \quad (2.1)$$

where ρ_1^p [kg/m³] is the mass density concentration of the ion type in the pore solution, \mathbf{u}_1^p [m/s] is the so-called diffusion velocity vector related to the velocity of the whole mixture, D_1^p [m²/s] is the diffusion constant, n_1^p [mol/m³] is the mole concentration in pore solution, m_1 [kg/mol] is the mole weight of ion type denoted 1, γ_1^p is the activity which is a function of ion concentrations in solution, A_1^p [m²/s/V] is the ionic mobility, φ^p is the electrical potential which is momentarily induced by the mixture of positively and negatively charged ions in solution.

The same assumption is used for the constituent denoted 2, which has an opposite charged than compared with constituent 2, i.e.

$$\rho_2^p \mathbf{u}_2^p = -D_2^p n_2^p m_2 \text{grad} (\ln \gamma_2^p n_2^p) - A_2^p m_2 n_2^p \text{grad} \varphi^p \quad (2.2)$$

The classical assumed relation between the ionic mobility and the diffusion constant will be adopted, i.e.

$$A_1^p = \frac{D_1^p v_1 F}{RT}; \quad A_2^p = \frac{D_2^p v_2 F}{RT} \quad (2.3)$$

where v_1 is the valence number (with correct sign), F [C/mol] is the Faraday's constant, R the gas constant and T the absolute temperature.

It is explicitly assumed that the mole flow of the two considered ions must fulfill the following condition

$$\frac{\rho_1^p \mathbf{u}_1^p v_1}{m_1} + \frac{\rho_2^p \mathbf{u}_2^p v_2}{m_2} = 0 \quad (2.4)$$

That is, the charge is zero during the diffusive mole flow.

By combining (2.1), (2.2), (2.3) and (2.4) one obtain

$$\sum_{i=1}^{\Re=2} D_i^p v_i n_i^p \left(\text{grad} (\ln \gamma_i^p n_i^p) + \frac{v_i F}{RT} \text{grad} \varphi^p \right) = 0 \quad (2.5)$$

Solving for $\text{grad} \varphi^p$ in this expression yields

$$\text{grad} \varphi^p = -\frac{RT}{F} \frac{\sum_{i=1}^{\Re=2} D_i^p v_i n_i^p \text{grad} (\ln \gamma_i^p n_i^p)}{\sum_{i=1}^{\Re=2} v_i^2 D_i^p n_i^p} \quad (2.6)$$

The solution will be assumed ideal which in this context means that the activity for the two considered constituents are equal to unity, i.e.

$$\gamma_1^p = 1; \quad \gamma_2^p = 1 \quad (2.7)$$

Furthermore, this example will be restricted to a case where the two ions have the valencies $v_1 = 1$ and $v_2 = -1$, that is a 1-1 electrolyte is under consideration only. By combining the restriction (2.7) with expression (2.6), the following is obtained

$$\text{grad} \varphi^p = -\frac{RT}{F} \frac{(D_1^p \text{grad} n_1^p - D_2^p \text{grad} n_2^p)}{D_1^p n_1^p + D_2^p n_2^p} \quad (2.8)$$

It will also be assumed that no net charge can be developed in any spatial material point in the domain of interest, which can be written as

$$n_1^p v_1 + n_2^p v_2 = 0 \quad (2.9)$$

That is, for this case $n_1^p = n_2^p = n^p$, which follows directly from (2.9). By using (2.8) and (2.9) the expression for the gradient of the electrical potential in solution can be formulated as

$$\text{grad}\varphi^p = -\frac{RT}{F} \frac{(D_1^p - D_2^p) \text{grad}n^p}{(D_1^p + D_2^p) n^p} \quad (2.10)$$

Consider, next, the constitutive relation (2.1) written as

$$\rho_1^p \mathbf{u}_1^p / m_1 = -D_1^p n_1^p \text{grad}(\ln \gamma_1^p n_1^p) - A_1^p n_1^p \text{grad}\varphi^p \quad (2.11)$$

By combining the expression for $\text{grad}\varphi^p$ in (2.10) and (2.11) the following is obtained

$$\rho_1^p \mathbf{u}_1^p / m_1 = \left(\frac{D_1^p (D_1^p - D_2^p)}{(D_1^p + D_2^p)} - \frac{D_1^p (D_1^p + D_2^p)}{(D_1^p + D_2^p)} \right) \text{grad}n^p \quad (2.12)$$

This expression is the condition for the flow of constituent 1 due to the presence of constituent 2. From (2.4, (2.11) for a 1-1 electrolyte one obtain

$$\rho_1^p \mathbf{u}_1^p / m_1 = \rho_2^p \mathbf{u}_2^p / m_2 = -\frac{2D_1^p D_2^p}{(D_1^p + D_2^p)} \text{grad}n^p \quad (2.13)$$

This expression is written as

$$\rho_1^p \mathbf{u}_1^p / m_1 = \rho_2^p \mathbf{u}_2^p / m_2 = -D_{12}^p \text{grad}n^p \quad (2.14)$$

where

$$D_{12}^p = \frac{2D_2^p D_1^p}{(D_1^p + D_2^p)} \quad (2.15)$$

That is, for a 1-1 electrolyte, the weighed diffusion constant D_{12}^p should be adopted when calculating $n_1^p(\mathbf{x}, t) = n_2^p(\mathbf{x}, t) = n^p(\mathbf{x}, t)$ with the Fick's second law.

It should be remarked that it is simple to rewrite the condition (2.15) for two constituents not necessarily being a 1-1 electrolyte. Further, it is noted that the use of the demonstrated method is too much simplified to be used in the application of diffusion of different types of ions in pore solution of concrete. An attempt has, however, been performed where different ions in solution was collected in neutral packages consisting of pairs of ions in which the weighting method illustrated in (2.15) was adopted, see [1]. Problems of motivating the specific choices used for distribute the neutral packages is, however, an issue.

3. Explicit internal electrical potential gradient method

A method which has been used in the application of diffusion of different type of ions in pore solution, which accounts for more than two constituents has been described in [2]. The method differs from the classical methods in the sense that the full set of equations is reduced by developing an explicit expression for the gradient of the electrical potential, instead of solving the whole equation system in an direct manner. The method can be seen as an generalization of the two constituent approach which was described in the previous section.

The classical constitutive assumption for the mass density flow $\rho_i^p \mathbf{u}_i^p$ of ion type i , is the assumption

$$\rho_i^p \mathbf{u}_i^p = -D_i^p n_i^p m_i \text{grad} (\ln \gamma_i^p n_i^p) - A_i^p m_i n_i^p \text{grad} \varphi^p; \quad i = 1, \dots, \mathfrak{R} \quad (3.1)$$

which is (2.1) for a case of \mathfrak{R} number of different ions in solution.

Again, the assumption (2.4) will be used now for a case of \mathfrak{R} number of constituents

$$\sum_{i=1}^{\mathfrak{R}} \frac{v_i \rho_i^p \mathbf{u}_i^p}{m_i} = 0 \quad (3.2)$$

The mass balance equation for the i th constituent can be written as

$$\frac{\partial \rho_i^p}{\partial t} = -\text{div} (\rho_i^p \mathbf{x}_i^p) + \hat{c}_i^p; \quad i = 1, \dots, \mathfrak{R} \quad (3.3)$$

where $\partial \rho_i^p / \partial t$ denotes the spatial time derivative of the mass density concentration ρ_i^p , \mathbf{x}_i^p is the velocity of i th constituent in solution, \hat{c}_i^p [kg/m³/s] denotes the supply or consumption rates of ions to pore solution from the solid hydration products of the concrete.

The mass balance equation for the \mathfrak{N} number of solid hydration products in concrete is written as

$$\frac{\partial \rho_h^c}{\partial t} = \hat{c}_h^c; \quad h = 1, \dots, \mathfrak{N} \quad (3.4)$$

where the super-script c is included to stress that the properties in (3.4) are related to solid constituents with no diffusion velocities. The property \hat{c}_h^c denotes the supply or consumption rates of ions from pore solution to the solid hydration product denoted h .

There can not be any net production of mass due to the chemical reactions. This can be formulated as

$$\sum_{h=1}^{\aleph} \hat{r}_h^c + \sum_{i=1}^{\aleph} \hat{r}_i^p = 0 \quad (3.5a)$$

Combining (3.1) and (3.2) yields

$$\sum_{i=1}^{\aleph} \frac{v_i \rho_i^p \mathbf{u}_i^p}{m_i} = \sum_{i=1}^{\aleph} v_i (-D_i^p n_i^p \text{grad}(\ln \gamma_i^p n_i^p) - A_i^p v_i n_i^p \text{grad} \varphi^p) = 0 \quad (3.6)$$

From (3.6) it is, further, directly concluded that the expression for $\text{grad} \varphi^p$ when considering \aleph number of ion constituents, can be written as

$$\text{grad} \varphi^p = - \frac{\sum_{i=1}^{\aleph} v_i D_i^p \left(\frac{n_i^p}{\gamma_i^p} \text{grad} \gamma_i^p + \text{grad} n_i^p \right)}{\sum_{i=1}^{\aleph} A_i^p v_i^2 n_i^p} \quad (3.7)$$

Using the classical relation

$$A_i^p = \frac{D_i^p v_i F}{RT} \quad (3.8)$$

expression (3.7) takes the form

$$\text{grad} \varphi^p = - \frac{RT \sum_{i=1}^{\aleph} v_i D_i^p \left(\frac{n_i^p}{\gamma_i^p} \text{grad} \gamma_i^p + \text{grad} n_i^p \right)}{F \sum_{i=1}^{\aleph} D_i^p v_i^2 n_i^p} \quad (3.9)$$

For the $i = 1, \dots, \aleph$ number of ion constituent considered it will be assumed that the velocity of constituents is approximately equal to its corresponding diffusion velocities $\dot{\mathbf{x}}_i^p \approx \mathbf{u}_i^p$, which in essence means that no convection is included in the flow behavior of the ions. By relating the mass density concentrations and the mole density concentrations as $\rho_i^p = n_i^p m_i$, where m_i is the mole weight the mass balance equation (3.3) can be replaced by

$$\begin{aligned} \frac{\partial n_i^p}{\partial t} &= \text{div} (D_i^p n_i^p \text{grad}(\ln \gamma_i^p n_i^p)) \\ &\quad + \text{div} \left(D_i^p v_i \frac{F}{RT} n_i^p \text{grad} \varphi^p \right) + \hat{r}_i^p \end{aligned} \quad (3.10)$$

where the chemical reaction rate \hat{r}_i^p is related to \hat{c}_i^p as: $\hat{r}_i^p = \hat{c}_i^p / m_i$.

The equation (3.10) with $\text{grad}\varphi^p$ calculated from (3.9) is the governing equation which is used, in for example, [2]. In this work also the effect of chloride binding was introduced.

It should be noted that a proper constitutive equation must be assumed for the reaction rates and equilibrium conditions, i.e. a complete description of \hat{r}_i^p must be done, which, for example can be the description of chloride ion binding in concrete.

In [2] the condition

$$\sum_{i=1}^{\mathfrak{R}} v_i n_i^p = 0 \quad (3.11)$$

is used to eliminate one of the ion constituents, i.e. one equation is eliminated. It is, however, realized that the solution for all concentration fields can be obtained solely by equations (3.9) and (3.10), therefore equation (3.11) can be used as a control of the performance of the needed numerical scheme, rather than an equation included in the system.

It can be argued that there may be some physical inconsistencies with the explicit use of the condition (3.11) in the numerical scheme. Consider one of Maxwell's balance principles, i.e. the balance of charge

$$\text{div}(\mathbf{d}^p) = q^p \quad (3.12)$$

where \mathbf{d}^p [C/m²] is the electric displacement vector for the ion solution and q^p is the charge density [C/m³]. The classical assumption for the electric displacement vector is

$$\mathbf{d}^p = -\tilde{\varepsilon}\varepsilon_o \text{grad}\varphi^p \quad (3.13)$$

where $\tilde{\varepsilon}\varepsilon_o$ [C/V] is the dielectric coefficient of the solution. In the case studied the charge density is solely developed by momentarily imbalances in neutrality in the solution. This charge density can be constituted as

$$q^p = F \sum_{i=1}^{\mathfrak{R}} n_i^p v_i \quad (3.14)$$

Combining the charge balance postulate (3.12) with (3.13) and (3.14) results in the governing equation for the determination of the electrical potential φ^p , i.e.

$$\text{div}(\tilde{\varepsilon}\varepsilon_o \text{grad}\varphi^p) = -F \sum_{i=1}^{\mathfrak{R}} v_i n_i^p \quad (3.15)$$

By comparison with the proposed condition (3.11) reveals that

$$\text{grad}\varphi^p = \text{const.} \quad (3.16)$$

in this case, which is a very strong restriction on, for example, the equation (3.9).

4. Complete equation system method

A method that has been applied to diffusion of different types of ions in pore solution of concrete is the complete equation system method. This name is used to stress that the electrical potential is calculated, using the classical charge equation, e.g. see equation (3.15). The computed values of the electrical potential at every material point are used in the diffusion equations for the ion constituents. In this approach the equation for determining the electrical potential and the equations determining the ion concentration profiles are coupled in both directions, i.e. the diffusion equations needs information from the charge equation and the charge equation need information from all diffusion equations. This type of method has been developed and solved for diffusion problems related to concrete durability, see [1], [3], [4] and [5].

The standard assumption concerning the mass density flow of ion i is used, i.e.

$$\begin{aligned} \rho_i^p \mathbf{u}_i^p &= -D_i^p m_i \text{grad} n_i^p - A_i^p n_i^p m_i \text{grad} \varphi^p \\ &\quad - (\gamma_i^p)^{-1} D_i^p n_i^p m_i \text{grad} \gamma_i^p \end{aligned} \quad (4.1)$$

which is (2.1) rewritten with aid of partial differentiation. The mass balance expressed in terms of mole density concentrations of the $i = 1, \dots, \aleph$ constituents is the postulate

$$\frac{\partial n_i^p}{\partial t} = -\text{div}(\rho_i^p \mathbf{u}_i^p m_i) + \hat{r}_i^p; \quad i = 1, \dots, \aleph \quad (4.2)$$

where it is assumed that $\dot{\mathbf{x}}_i^p \approx \mathbf{u}_i^p$. Assuming no diffusion for the \aleph number of solid components of concrete, the mole balance principals for the hydration products of interest becomes

$$\frac{\partial n_h^c}{\partial t} = \hat{r}_h^c; \quad h = 1, \dots, \aleph \quad (4.3)$$

No net production of mass can occur due to chemical reactions, therefore one must add the condition

$$\sum_{h=1}^{\aleph} \hat{r}_h^c + \sum_{i=1}^{\aleph} \hat{r}_i^p = 0 \quad (4.4)$$

to the balance principles illustrated in (4.2).

The charge balance postulate (3.12) and the two constitutive equations (3.13) and (3.14) was earlier shown to result in the equation for determination of the electrical potential φ^p , the derived equation is

$$\operatorname{div}(\tilde{\varepsilon}\varepsilon_o\operatorname{grad}\varphi^p) = -F \sum_{i=1}^{\mathfrak{R}} v_i n_i^p \quad (4.5)$$

which is (3.15) repeated.

By combining the constitutive relation (4.1) and the mass balance principle one obtain the governing equations for the $n_i^p(\mathbf{x}, t)$, $i = 1, \dots, \mathfrak{R}$, concentration profiles, i.e.

$$\begin{aligned} \frac{\partial n_i^p}{\partial t} = & \operatorname{div}(D_i^p \operatorname{grad} n_i^p) \\ & + \operatorname{div}\left(\frac{D_i^p v_i F n_i^p}{RT} \operatorname{grad} \varphi^p\right) \\ & + \operatorname{div}\left((\gamma_i^p)^{-1} D_i^p n_i^p m_i \operatorname{grad} \gamma_i^p\right) \\ & + \hat{r}_i^p \end{aligned} \quad (4.6)$$

where the equation (3.8) has been used. It is noted that the equation for determining the electrical potential (4.5) and the equations for the $n_i^p(\mathbf{x}, t)$, $i = 1, \dots, \mathfrak{R}$, concentration profiles, see (4.6), are coupled in both directions.

5. Concentration dependent diffusion, ionic strength and multi-species ion diffusion

The fact that the concentrations of ions such as hydroxide and potassium almost always are high in the pore solution of concrete means that the ideal conditions with regard to diffusion and standard assumptions concerning the chemical equilibrium constants can be questioned. No such effects can be included in ion diffusion models if not all the different ions, having a significant concentration, are accounted for.

The classical concept of introducing the activity parameter γ_i^p when modelling the diffusion behavior of ions in strong electrolytes is to include the gradient of γ_i^p when constituting the mass density flow of different types of ions. This was

accounted for in the previous sections, e.g. see equation (4.1). According to the classical concept of calculate the value of γ_i^p , the result will be that the activity parameter for an ion type is a function of the composition of the electrolyte, i.e. $\gamma_i^p = \gamma_i^p(n_1^p, n_2^p, \dots, n_{\mathfrak{R}}^p)$. This means, in turn, that the diffusion of a type of ion not only is dependent on its concentration gradient but also on the concentrations of all types of ions in solution.

The most common assumption for the value of γ_i^p is

$$\ln \gamma_i^p = -\frac{Cv_i^2\sqrt{I}}{I + a_iB\sqrt{I}} \quad (5.1)$$

where C and B are temperature dependent parameters, v_i is the valence number, a_i is a material constant specific to the ionic species related to the ionic radius, I is the so-called ionic strength. For cases where experimental observations are different from the relation proposed in (5.1), terms are added to fit the experiments. Examples of different modifications of (5.1) can be found in [6].

The ionic strength is defined to be a function of the valence number and the concentration of all ions in solution, i.e.

$$I = \frac{1}{2} \sum_{i=1}^{\mathfrak{R}} v_i^2 n_i^p \quad (5.2)$$

This means, for example, that ions with two valence electrons are weighted four times higher than ions with one valence electron with regard to the ionic strength. The material parameters C and B are given by the expressions

$$C = \frac{\sqrt{2}F^2e_o}{8\pi(\tilde{\varepsilon}\varepsilon_oRT)^{3/2}} \quad (5.3)$$

and

$$B = \sqrt{\frac{2F^2}{\tilde{\varepsilon}\varepsilon_oRT}} \quad (5.4)$$

where e_o is the electrical charge of one electron.

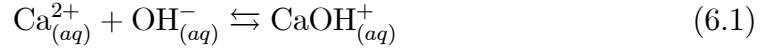
The use of the equation (5.1), or any modified version, to calculate the chemical activity coefficients can be used in equation (4.6) whenever the gradient of γ_i^p is suspected to significantly affect the diffusion behavior of ions in the solution.

The only missing description of properties in the governing equations for calculating the concentration profiles of the different types of ions in solution are

the supply/sink terms, \hat{r}_i^p . The equilibrium conditions for these properties are in the existing classical approaches assumed to be affected by the ionic strength and hence also dependent on the value of γ_i^p as calculated from equation (5.1). Such equilibrium (and non-equilibrium conditions) equations will be discussed in next section. Of course, the description of these properties are of importance when studying diffusion of ions in concrete since it involves mechanisms such as dissolution of hydroxide and binding of chlorides.

6. Homogeneous reactions in pore solution and its effect on the multi-species ion diffusion

The previous described methods to tackle multi-species ion diffusion did not include any explicit descriptions of the mass exchanges between ions in pore solution or between ions in solid components and ions in pore solution. In this section some examples, studied in [6], will be out lined concerning homogeneous reactions in pore solution. Examples of such reactions are



and



Due to the existence of reactions, such as the ones illustrated in (6.1) and (6.2), the multi-species ion diffusion will be affected since, in this case, the constituents $\text{CaOH}_{(aq)}^+$ and $\text{CaCl}_{(aq)}^+$ will be included in the diffusion equations with its own diffusion and ion mobility constants.

For simplicity the equilibrium mole concentration for $\text{Ca}_{(aq)}^{2+}$ will be denoted by n_1^{eq} , n_2^{eq} as the mole concentration of $\text{OH}_{(aq)}^-$, n_3^{eq} as the mole concentration of $\text{Cl}_{(aq)}^-$, n_{12}^{eq} as the mole concentration of $\text{CaOH}_{(aq)}^+$ and n_{13}^{eq} as the mole concentration of $\text{CaCl}_{(aq)}^+$.

The equilibrium relation for the reaction (6.1) is defined, e.g. see [9], as

$$K_1^H = \frac{\gamma_1^{eq} n_1^{eq} \gamma_2^{eq} n_2^{eq}}{\gamma_{12}^{eq} n_{12}^{eq}} \quad (6.3)$$

where K_1^H is the equilibrium constant for the reaction and γ_1^{eq} is the activity parameter corresponding to the equilibrium value n_1^{eq} . The equilibrium relation

for the reaction (6.2) is defined, in the same manner, as

$$K_2^H = \frac{\gamma_1^{eq} n_1^{eq} \gamma_3^{eq} n_3^{eq}}{\gamma_{13}^{eq} n_{13}^{eq}} \quad (6.4)$$

In order to incorporate the these types of reactions into the diffusion equations the mole supply/sink term \hat{r}_i^p must be described. One possible way to do this is to allow for a slightly momentarily deviation from equilibrium. The approach is to use the current calculated values of mole concentrations and its corresponding activity parameters, calculated with equation (4.6), except for one constituent included in the reaction, which instead are calculated for equilibrium. That is, for reaction (6.1) one uses a slightly modified version of (6.3) to, for example, calculate the equilibrium value of n_{12}^p , which corresponds to the current values of n_1^p and n_2^p , i.e.

$$n_{12}^{eq} = \frac{\gamma_2^p n_2^p \gamma_1^p n_1^p}{K_1^H \gamma_{12}^{eq}} \quad (6.5)$$

It should be observed that n_{12}^p must be solved for using a numerical iterative method since the activity parameters γ_1^p , γ_2^p and γ_{12}^{eq} are functions of all mole concentrations including n_{12}^{eq} , i.e. compare with equations (5.1) and (5.2). For reaction (6.2) the equilibrium value n_{13}^{eq} is searched for using the expression

$$n_{13}^{eq} = \frac{\gamma_1^p n_1^p \gamma_3^p n_3^p}{K_1^H \gamma_{13}^{eq}} \quad (6.6)$$

which is in analogy with equation (6.6).

The approach is, further, based on the current values of n_{12} and n_{13} , calculated with the diffusion equations, i.e. (4.6), and the corresponding equilibrium values n_{12}^{eq} and n_{13}^{eq} . The method is to use the difference in the current value of n_{12} and n_{12}^{eq} to calculate how much the reaction must continue to establish equilibrium. This can be done by constituting the rate of supply or consumption of $\text{CaOH}_{(aq)}^+$ according to (6.1), i.e.

$$\hat{r}_{12a}^p = R_{12a} (n_{12}^p - n_{12}^{eq}) \quad (6.7)$$

where R_{12a} is the constant describing the kinetics of reaction. The sign of \hat{r}_{12a}^p determines the direction of the reaction. It is extremely important to observe that when R_{12a} exceeds a certain value the reaction becomes more or less instantaneous which is the desired situation in this case. The same way of constituting \hat{r}_{13b}^p for reaction (6.2) is used as for constituting \hat{r}_{12a}^p , i.e.

$$\hat{r}_{13b}^p = R_{13b} (n_{13}^p - n_{13}^{eq}) \quad (6.8)$$

From the chemical reactions (6.1) and (6.2) it follows directly that the kinetics is related as

$$\hat{r}_{12a}^P = -\hat{r}_{1a}^P = -\hat{r}_{2a}^P \quad (6.9)$$

$$\hat{r}_{13b}^P = -\hat{r}_{3b}^P = -\hat{r}_{1b}^P \quad (6.10)$$

and

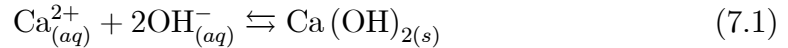
$$\hat{r}_1^P = \hat{r}_{1a}^P + \hat{r}_{1b}^P \quad (6.11)$$

The method presented treating the homogeneous reactions in pore solution results in that diffusion and reactions occurs simultaneously where the true chemical equilibrium is followed very closely, meaning that the reactions is instantaneous.

7. Dissolution/precipitation reactions in pore solution and its effect on the multi-species ion diffusion

For the case of cement based materials the pore solution contains a very high concentration of ions, especially potassium and hydroxide are at high concentrations. It is important to check whether or not the solution becomes over saturated or not, i.e. if dissolution or precipitation reactions in pore solution are active. In order to study such mechanisms together with diffusion a multi-species approach must be used. The dissolution/precipitation reactions in pore solution are separated from the reactions between ions in pore solution and the solid components of concrete, which are discussed in next section.

The following dissolution/precipitation reaction will serve as an example



where, again, n_1^{eq} will be denote the equilibrium mole concentration of $\text{Ca}_{(aq)}^{2+}$, and n_2^{eq} as the mole equilibrium concentration of $\text{OH}_{(aq)}^-$. The equilibrium concentration of the new introduced constituent $\text{Ca}(\text{OH})_{2(s)}$ will be denoted with n_4^{eq} . It should be observed that n_1^{eq} and n_2^{eq} defined in this section, related to reaction (7.1), is different from the same properties defined in the previous section.

The chemical equilibrium constant $K_1^{D/P}$ for reaction (7.1) is defined as, see [6], [7] and [8],

$$K_1^{D/P} = \gamma_1^{eq} n_1^{eq} (\gamma_2^{eq})^2 (n_2^{eq})^2. \quad (7.2)$$

It is clear that the equilibrium condition (7.2) is independent of the concentration of $\text{Ca}(\text{OH})_{2(s)}$.

The equilibrium value of the mole concentration of $\text{Ca}_{(aq)}^{2+}$ in reaction (7.1) is calculated with the current values of n_2^p and its corresponding chemical activity γ_2^p , i.e.

$$n_1^{eq} = \frac{K_1^{D/P}}{\gamma_1^{eq} (\gamma_2^p)^2 (n_2^p)^2} \quad (7.3)$$

The reaction kinetics will be constituted in the same manner as constituting reactions (6.1) and (6.2), i.e.

$$\hat{r}_{1c}^p = R_{1c} (n_1^p - n_1^{eq}) \quad (7.4)$$

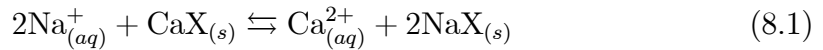
And the dissolution/precipitation reaction (7.1) immediately validates that \hat{r}_{1c}^p , \hat{r}_{2c}^p and \hat{r}_{4c}^p , are related as

$$\hat{r}_{1c}^p = 2\hat{r}_{2c}^p = -\hat{r}_{4c}^p \quad (7.5)$$

By including changes in concentrations of ions in pore solution due to dissolution/precipitation reaction the estimation of the ionic strength will be more adequate. Furthermore, the overall behavior of the multi-species diffusion of ions in pore solution will be affected since the ion diffusion mechanisms will be over or under estimated if not including dissolution and precipitation reactions.

8. Surface chemical reactions between ions in pore solution and solid surfaces and its effect on the multi-species ion diffusion

A typical surface chemical reaction in concrete is the binding and dissolution of chlorides. Here, however, a similar reaction will be considered, i.e.



where $\text{Na}_{(aq)}^+$ and $\text{Ca}_{(aq)}^{2+}$ in the pore solution competes for available sites in the hydration products denoted, in this case, by $\text{X}_{(s)}^{2-}$. In contrast to the homogeneous reactions occurring in pore solution, discussed earlier, the surface reaction (8.1) can be referred to as a heterogenous reaction.

A definition of the chemical equilibrium constant for the surface reaction (8.1) has been proposed [6], [9] and [10], where no consideration to ionic strength is taken, i.e.

$$K_1^S = \frac{n_5^{eq}}{n_6^{eq}} \left(\frac{n_1^{eq}}{n_7^{eq}} \right)^2 \quad (8.2)$$

where n_1^{eq} is the equilibrium concentration of $\text{Ca}_{(aq)}^{2+}$ in pore solution with respect to reaction (8.1) (which again is noted to be different from n_1^{eq} defined in previous sections), n_7^{eq} is the equilibrium concentration of $\text{CaX}_{(s)}$, n_6^{eq} is the equilibrium concentration of $\text{Na}_{(aq)}^+$ and n_5^{eq} is the equilibrium concentration of $\text{NaX}_{(s)}$. The equilibrium condition for the surface reaction (8.1) is concluded to be non-linear due to the format of equation (8.2). The equilibrium condition for chloride binding in concrete, which is a reaction with similarities with (8.1), has been experimentally proven to be non-linear, e.g. see [11].

With the computed current values of n_5^p , n_6^p and n_7^p the corresponding equilibrium value n_1^{eq} can be calculated as

$$n_1^{eq} = \sqrt{\frac{K_1^S (n_7^p)^2 n_6^p}{n_5^p}} \quad (8.3)$$

The constitutive relation for the reaction kinetics is determined by how far from equilibrium the current state is, i.e.

$$\hat{r}_{1d}^p = R_{1d} (n_1^p - n_1^{eq}) \quad (8.4)$$

The relations between the mass exchange terms becomes

$$\hat{r}_{1d}^p = -\hat{r}_{7d}^p = -2\hat{r}_{5d}^p = \hat{r}_{6d}^p \quad (8.5)$$

which follows directly from (8.1).

It should be remarked that the surface reactions not need to be instantaneous since important effects on the reaction kinetics can be obtained due to the diffusion driven nature of the surface reaction. That is the rate constant need not to be specified to a value where the reaction (8.4) becomes instantaneous.

9. Multi-species ion diffusion coupled to moisture transport

In concrete construction it is a very common condition that the outer climate is changed with time. Not only the outer concentration of different types of ions dissolved in water are changed but the construction is also exposed to wetting

and drying. This contributes to capillary suction and drying which affects the concentrations and flow of ions. That is, in most real constructions not only diffusive flow are active but also flows of ions induced by capillary suction, i.e. convection.

It is possible to establish a mass balance equation for a case where convection, diffusion and chemical reactions are included. This balance equation, for the \mathfrak{R} number of considered types of dissolved ions, could be written as

$$\frac{\partial n_i^p}{\partial t} = -\frac{1}{m_i} \operatorname{div}(\rho_i^p \mathbf{u}_i^p) - \dot{\mathbf{x}}_w^p \cdot \operatorname{grad} n_i^p - n_i^p \operatorname{div} \dot{\mathbf{x}}_w^p + \hat{r}_i^p; \quad i = 1, \dots, \mathfrak{R} \quad (9.1)$$

where $\dot{\mathbf{x}}_w^p$ denotes the velocity of pore solution in pore system, For the derivation of the \mathfrak{R} number of balance equations for the different types of dissolved ions, see [12]. For a more general description of the underlying theory, see [13].

The term $n_i^p \operatorname{div} \dot{\mathbf{x}}_w^p$, in equation (9.1), represents the change in the mass density concentration of ion i in a pore solution due to a change in the mass density concentration of the pore solution caused by drying or capillary suction. The mass balance equation (9.1) for the mole density concentration of the ion type i dissolved in the pore solution is a generalization of the standard diffusion-convection equation, e.g. see [14], in the sense that the change of the reference volume, i.e. the volume change of pore water phase, and the mass exchanges between phases and within phases are included.

The mass balance equation for the pore solution phase is

$$\frac{\partial \rho_w^p}{\partial t} = -\operatorname{div}(\rho_w^p \dot{\mathbf{x}}_w^p) \quad (9.2)$$

where ρ_w^p [kg/m³] is the mass density concentration of pore water in concrete and $\dot{\mathbf{x}}_w^p$ is the velocity of pore water, which is assumed to approximately equal to the so-called mean velocity of the mixture.

Next, consider the constitutive relations for the constituents. The velocity of the pore water in material is the assumption

$$\dot{\mathbf{x}}_w^p = -\frac{D_w^p(\rho_w^p)}{\rho_w^p} \operatorname{grad} \rho_w^p \quad (9.3)$$

where $D_w^p(\rho_w^p)$ is the nonlinear material parameter relating the gradient of the mass density concentration of water in pores with the velocity $\dot{\mathbf{x}}_w^p$. Methods to evaluate $D_w^p(\rho_w^p)$ from capillary suction experiments have been proposed, e.g. see

[15] and [16], further, methods using steady state conditions to evaluate $D_w^p(\rho_w^p)$ have been developed, see [17]. The effect on $\mathbf{\tilde{x}}_w^p$ caused by an external applied pressure is not included in the present model.

The assumptions for the diffusion velocity flows for the \mathfrak{R} considered types of ions in a pore solution are

$$\begin{aligned} \rho_i^p \mathbf{u}_i^p = & -\tilde{D}_i^p(\rho_w^p) m_i \text{grad} n_i^p - \tilde{A}_i^p(\rho_w^p) m_i v_i n_i^p \text{grad} \varphi^p \\ & - (\gamma_i^p)^{-1} \tilde{D}_i^p(\rho_w^p) m_i n_i^p \text{grad} \gamma_i^p \end{aligned} \quad (9.4)$$

where $\tilde{D}_i^p(\rho_w^p)$ (m^2/s) is the diffusion parameter for ion type i , dissolved in the pore solution, which is assumed to be dependent on the moisture condition ρ_w . The property $\tilde{A}_i^p(\rho_w^p)$ ($\text{m}^2/(\text{Vs})$) is the ion mobility parameter for ion type i in pore solution. If effects caused by corrosion of reinforcement bars embedded in concrete are also included, an extra term must be added in (9.4), since an electrical potential (which is different from φ^p) will develop in the domain surrounding the anodic and cathodic area, i.e. in the corrosion zone. The gradient of the electric potential caused by reinforcement corrosion will affect the diffusion of all ions dissolved in pore solution near the corrosion zone. This phenomena has been theoretically studied in [18].

The chemical reactions \hat{r}_i^p can be treated as proposed in the examples in the previous sections, and will not be discussed further in the context of diffusion coupled to moisture transport.

Combining the mass balance equation (9.2) and the constitutive relation (9.3) for the mass density flow of the water phase, one obtains

$$\frac{\partial \rho_w^p}{\partial t} = \text{div} (D_w^p(\rho_w^p) \text{grad} \rho_w^p) \quad (9.5)$$

which is the governing equation determining $\rho_w^p(\mathbf{x}, t)$.

Combining the constitutive relation (9.4), for the diffusion velocity for the ion type i , and the assumption (9.3) with the mass balance equation (9.1) for the same ion type, one obtains for all $i = 1, \dots, \mathfrak{R}$ ion types considered.

$$\begin{aligned} \frac{\partial n_i^p}{\partial t} = & \text{div} \left(\tilde{D}_i^p(\rho_w^p) \text{grad} n_i^p \right) + \\ & \text{div} \left(\tilde{A}_i^p(\rho_w^p) v_i n_i^p \text{grad} \varphi^p \right) + \\ & \text{div} \left((\gamma_i^p)^{-1} \tilde{D}_i^p(\rho_w^p) n_i^p \text{grad} \gamma_i^p \right) + \end{aligned} \quad (9.6)$$

$$\begin{aligned} & \frac{D_w^p(\rho_w^p)}{\rho_w^p} \text{grad} \rho_w^p \cdot \text{grad} n_i^p + \\ & n_i^p \text{div} \left(\frac{D_w^p(\rho_w^p)}{\rho_w^p} \text{grad} \rho_w^p \right) + \\ & \hat{r}_i^p \end{aligned}$$

which is the governing equation determining $n_i^p(\mathbf{x}, t)$.

The first term on right-hand side of (9.6) describes the effect of normal diffusion, i.e. diffusion which is ideal, the second term describes the effect on diffusion caused by the internally induced electrical imbalance among positively and negatively charged ions in pore solution phase, the third term models the effect of the ionic strength on the diffusion, i.e. the non-ideal part of the diffusion, the fourth term gives the change of concentration of ion type i due to a motion of the pore solution phase in the concrete pore structure, the fifth term models the effect of the change in concentration of ions in pore solution due to drying (or an increase in water content) of the pore water and, finally, the last term on the right-hand side of (9.6) is the loss or gain of ions due to mass exchanges between pore solution and solid hydration product of concrete or due to reactions within the pore solution.

10. Numerical methods and multi-species ion diffusion

The equations that needs to be solved in problems related to multi-ionic diffusion with inclusions of chemical reactions can not be solved analytically. Two different types of methods to solve equation systems dealing with diffusion and durability of concrete has been used, i.e. explicit time integration schemes using the finite difference methods, e.g. see [2] and implicit time integration schemes using the finite element methods, e.g. see [1] and [4].

One of the problems that must be tackled is the coupling between the different constituent equations. When using the finite element method these couplings can be treated in a rather direct manner since the chemical reactions and dielectric effects on the diffusion can be included as off-diagonal terms in the global stiffness matrix. This method is robust since no staggering procedure has to be used, i.e. the whole set of equations can be solved in one step (for each time level) without sending coupling information between the different equations during the time step.

When solving the complete equation system, described in section 4, an implicit

time integration scheme has to be used. An implicit scheme do not suffer from being dependent on any critical time step length, in contrast to the explicit time integrations most often adopted within the finite difference methods. The use of a implicit time integration scheme is required in order to be able to solve the full set of equations as described in section 4. The reason for this is the extreme time scale difference in the mechanisms of diffusion and dielectric properties.

Special numerical problems must be considered when including for convection of ions in pore solution. Within finite elements the normal spatial weighting has to be exchanged by, for example, a so-called Petrov-Galarkin weighting. The method steams from finite volume techniques and when used in the finite difference schemes they are referred to as up-winding approaches. Simple examples of these kind of numerical issues can be studied in [18] [19] and [20].

11. Identification of values of material constants

Very few comparisons between multi-species diffusion models and experiments, in the field of concrete durability, has been performed. Computer runs presented in [2] indicates, however, that the mechanism is important. In [3] a model similar to the one presented in section 4 was compared to measured chloride ion profiles at water saturated conditions, see [21]. This study gave one possible explanation for the peak in chloride profile near the exposed surface which occurs even when the outer chloride solution is constant. According to the established model the peak is obtained due to dielectric effects of different considered types of ions in pore solution combined with the fact that calcium and hydroxide are leached out from solid hydration products, changing the overall diffusion behavior in pore solution. These kind of consideration can not be adequately studied if not establishing models including all different types of ions appearing in pore solution of concrete. Other conclusions drawn in this study is that the leaching of hydroxide from pore solution is slowed down due to dielectric effects in the pore solution electrolyte.

In [3] tortuosity factors for ion diffusion was obtained for different concrete qualities being saturated by fitting the multi-species ion diffusion model to experiments. In [22] tortuosity factors for concrete are determined by a gas diffusion technique. The tortuosity factors obtained for concrete with the cement content 400 kg/m^3 having water to cement ratios 0.40 and 0.55 were 0.007 and 0.011, respectively. These values are in good agreement with the ones obtained in [3], where similar concrete samples with water to cement ratios 0.40 and 0.55 were 0.007 and 0.090, respectively. Special theoretical arguments leading to the concept

of tortuosity can be also be obtained using a so-called homogenization technique, e.g. see [23].

The inclusion of the concept behind the tortuosity factors are advantageous if also assuming that all different types of ions in pore solution are affected by the pore system in an identical manner. This means that the known measured values of diffusion constants and ionic mobilities in bulk water can be used together with only one tortuosity factors. Then using this strategy it is clear that the multi-species diffusion problem in concrete is directed more towards the description and verification of the chemical reactions always taking place in the pore system and at surfaces of concrete pores.

The inclusion of convection of ions in pore solution do not generate any new unknown material property into the model under the condition that one assumes the ions in pore solution themselves do not affects the moisture transport. This means that established properties for moisture transport can be incorporated into the diffusion models in a direct manner, see section 9.

12. Conclusions

In order to study the degradation of concrete, due to changes in the composition of ions in pore solution, in a stringent manner, account must be taken to the dielectric nature of diffusion of the charged species of interest. In this work some of the proposed models for this kind of diffusion problems has been discussed. The models are far from being novel in its structure, many of the discussed models has, for example, earlier been applied to diffusion of ions in groundwater.

The most marked differences in the proposed models are the descriptions of the chemical reactions. The most common approach is to involve the mass exchange terms in the diffusion parameters, i.e. the so-called effective diffusion constant concept. When including more than one chemical reaction (such as chloride binding) and including more than two constituents (i.e. bound and free chloride) the effective diffusion concept cannot be derived theoretically. It is, therefore, advantageous to describe the equilibrium and kinetic relations in an explicit manner using the constitutive dependent mass supply/sink terms. When using this approach no restrictions on the number of reactions and diffusion equations, included in the model, for the constituents exists. That is, several of the important mass exchange mechanisms of ions in pore solution, and between ions in pore solution and solid components of concrete, can be studied in a stringent manner.

It is of importance to be able to solve the theoretical models, using adequate

boundary conditions, and compare the results to experiments, which is a method to identify proper values of the included material constants and parameters. The numerical solution procedure for the addressed problem is, however, not straight forward and a lot of work still remain to make the proposed time stepping schemes optimized.

The models for multi-species diffusion demands calibrations against experiments where all concentration profiles in concrete and its evolution with time must be measured. Very few attempts has been done to perform such measurements.

In real conditions, concrete structures are often exposed to variation in moisture content, due to changes in relative humidity and due to capillary suction. The diffusion in pore solution of concrete are highly affected by such phenomena. A model describing this situation is included in this review. The classical theory for moisture transport was incorporated in the ion diffusion equations in an explicit manner, without introducing any new material constants. The numerical solution of this problem, however, demand special types of weighting parameters, since the equation system include derivatives of first-order. A method valid for this case was proposed.

References

- [1] Johannesson, B.F. (1999). *Diffusion of a Mixture of Cations and Anions Dissolved in Water*, Cement and Concrete Research, Vol. 29. pp. 1261-1270.
- [2] Truc. O. (2000). *Prediction of Chloride Penetration into Saturated Concrete - Multi-Species Approach*, Department of Building Materials, Chalmers University of Technology Göteborg, Sweden.
- [3] Johannesson, B.F. (2000). *Transport and Sorption Phenomena in Concrete and Other Porous Media*, Lund Institute of Technology, Division of Building Materials, Lund.
- [4] Samson, E. and Marchand, J. (1999). *Numerical Solution of the Extended Nernst-Planck Model*, Journal of Colloid and Interface Science 215, pp. 1-8.
- [5] Samson, E., Marchand, J. Robert, J.-L. and Bournazel, J.-P. (1999). *Modelling Ion Diffusion Mechanisms in Porous Media*. International Journal for Numerical Methods in Engineering, 46, pp. 2043-2060.

- [6] Samson, E., Marchand, J. and Beaudoin, J.J. (2000). *Modeling the Influence of Chemical reactions on the Mechanisms of Ionic Transport in Porous Materials, An overview*. Cement and Concrete Research, Vol. 30. pp. 1895-1902.
- [7] Kirkner, D.J., Reeves, H.W., (1988). *Multicomponent Mass Transport with Homogeneous and Heterogeneous chemical reactions: Effect of the Chemistry on the Choice of Numerical Algorithm - 1. Theory.*, Water Resour. Res. 24 (10), pp. 1719-1729.
- [8] Kirkner, D.J., Reeves, H.W., Jennings, A.A., (1984). *Finite Element Analysis of Multicomponent Contaminant Transport Including Precipitation - Dissolution Reactions*, in: J.L. Laible, et. al. (Eds.), *Finite Elements in Water Resources*, Springer-Verlag, USA, pp. 309-318.
- [9] Rubin, J. (1983). *Transport of Reacting Solutes in Porous Media: Relation between Mathematical Nature of Problem Formulation and Chemical Nature of Reactions*, Water Resour. Res. 19 (5), pp. 1231-1252.
- [10] Valocchi, A.J., Street, R.L., Roberts, P.V., (1981). *Transport of Ion-exchanging Solutes in Groundwater: Chromatographic Theory and Field Simulation*, Water Resour. Res. 17 (5), pp. 1517-1527.
- [11] Nilsson, L.O., Massat, M. and Tang, L. (1994). *The Effect of Non-linear Chloride Binding on the Prediction of Chloride Penetration into Concrete Structures*, In *Durability of Concrete: Proc. 3rd. Int. Conf.*, Edited by Malhotra, ACI SP 145, Detroit, pp. 469-486.
- [12] Johannesson, B. (2001). *A Theoretical Model Describing Diffusion of a Mixture of Different Types of Ions in Pore Solution of Concrete Coupled to Moisture Transport*, Lund Institute of Technology, Division of Building Materials, Lund.
- [13] Bowen, R.M. (1976). *Theory of Mixtures*, Part 1, in *Continuum Physics*, Edited by A. Cemal Eringen, Princeton University of Technology.
- [14] Bear, J. (1979). *Hydraulics of Groundwater*, McGraw-Hill, Inc. New York.
- [15] Janz, M. (1997). *Methods of Measuring the Moisture Diffusivity at High Moisture Levels*, Lund Institute of Technology, Division of Building Materials, Lund.

- [16] Arvidsson, J. (1998). *Moisture Transport in Porous Media, Modelling Based on Kirchhoff Potentials*. Lund University of Technology, Department of Building Technology, Building Physics, Lund.
- [17] Hedenblad, G. (1993). *Moisture Permeability of Mature Concrete, Cement Mortar and Cement Paste*, Lund Institute of Technology, Division of Building Materials, Lund.
- [18] Johannesson, B. (1998). *Modelling of Transport Processes Involved in Service Life Prediction of Concrete, Important Principles*, Lund Institute of Technology, Division of Building Materials, Lund.
- [19] Johannesson, B.F. (1997). *Nonlinear Transient Phenomena in Porous Media with Special Regard to Concrete and Durability*, Advanced Cement Based Materials, Vol. 6. pp. 71-75.
- [20] Johannesson, B.F. (1996). *Convection-diffusion Problems with Significant First-order Reversible Reactions*, Ninth Nordic Seminar on Computational Mechanics, Technical University of Denmark, Edited by Lars Damkilde.
- [21] Janz, J and Johannesson, B.F. (1993). *A Study of Chloride Penetration into Concrete* (in Swedish), Lund Institute of Technology, Division of Building Materials, Lund.
- [22] Alfarabi Sharif, Loughlin, K.F., Azad, A.K. and Navaz C.M. (1997). *Determination of the Effective Chloride Diffusion Coefficient in Concrete via a Gas Diffusion Technique*. ACI Materials Journal, Vol. 94, No. 3.
- [23] Samson, E., Marchand, J. and Beaudoin, J.J. (1999). *Describing Ion Diffusion Mechanisms in Cement-based Materials Using the Homogenization Technique*. Cement and Concrete Research, Vol. 29. pp. 1341-1345.

A Theoretical Model Describing Diffusion of a Mixture of Different Types of Ions in Pore Solution of Concrete Coupled to Moisture Transport

B.F. Johannesson

Lund Institute of Technology, Division of Building Materials

Box 118, SE-221 00 Lund, Sweden

Abstract

A theoretical model is established for diffusion of different types of ions in pore solution of concrete and the coupling to moisture flow and moisture content. Mass exchanges between ions in pore solution and solid hydration products in the concrete are also considered. The basic concepts behind the so-called mixture theory are used. The development of a mass balance principle for ions in pore solution is established. This principle accounts for *(i)* diffusion caused by concentration gradients of ions and gradients of the so-called internal electrical potential, *(ii)* convection i.e. the effect on the motion of ions due to a motion of the pore solution in concrete, *(iii)* the effect on the concentration due to changes in the moisture content and, finally, *(iv)* the effect of mass exchange of ions between solid hydration products and the pore solution phase. The model is general in the sense that all different types of ions appearing in pore solution phase can be included and computed for during quite arbitrary boundary conditions.

1. Introduction

Most concrete constructions subjected to harmful ions such as chlorides, sulfates and carbonic acid are also exposed to variations in moisture content. Phenomena such as capillary suction and drying will affect the diffusion of different types of

ions dissolved in a pore solution. A stringent model of this problem should result in one equation for each type of ion appearing in a pore solution, one equation describing the moisture transport and one equation for each solid component being formed from ions in the pore solution or being dissolved into the pore solution from solid components.

The need for knowledge about how the pore solution of concrete is changed due to different environmental conditions is crucial since most of the degradation mechanisms are dependent on the pore solution composition. Examples of such degradation mechanisms are: chloride-induced reinforcement corrosion, see e.g. [1], [2] and [3], carbonation, see e.g. [4], sulfate attack, see e.g. [5], salt frost scaling, see e.g. [6], and leaching of hydroxide from pore solution, see e.g. [7].

A quite general model is established by considering mass balance equations for constituents building up two phases, a pore solution phase and a solid phase. The mass balance principles obtained for the different types of ions in pore water phase are supplemented with constitutive assumptions making the equation system complete.

2. Diffusion of a mixture of different types of ions coupled to moisture transport in concrete

The basic concept behind the so-called mixture theory will be used, see e.g. [8], in order to establish a model describing diffusion of a mixture of different types of ions in a pore solution of concrete, and its couplings to the moisture condition and moisture flow. Each constituent is assigned a mass density concentration. The mass density concentration of the $i = 1, \dots, \mathfrak{R}$ dissolved ions considered in pore solution will be denoted ρ_i^p (kg/m³) and the $s = 1, \dots, \mathfrak{S}$ solid precipitated combinations of ions in pore solution will be denoted ρ_s^p . The $h = 1, \dots, \mathfrak{N}$ solid components of the concrete will be denoted ρ_h^c and the mass density concentration of liquid water in the material volume will be denoted ρ_w^p . The total mass density of the mixture ρ is the sum of all constituents. Two phases will be considered, the pore solution phase p and the solid phase of the concrete c . Reactions within and between the phases will be considered in the general case. The only balance principles that will be considered are the mass balance equations for the constituents, the two phases and the whole mixture, i.e. the momentum balance equation, energy balance equation and the second axiom of thermodynamics are ignored in this presentation.

It will be seen that the complexity of the problem considered grows drastically

as compared to, for example, the isothermal moisture transport problem which only includes one mass balance principle and one constitutive equation.

The mass density concentration of solid component phase ρ^c , i.e. the ‘dry’ concrete density, is the sum of the \aleph number of individual solid constituents, i.e.

$$\rho^c = \sum_{h=1}^{\aleph} \rho_h^c \quad (2.1)$$

where ρ_h^c is the mass density concentration of the h th solid component.

The mass density concentration of the pore solution phase ρ^p is the sum of the \aleph number of dissolved ion constituents, the sum of the \Im number of solid precipitated combinations of ions and the water itself, i.e.

$$\rho^p = \sum_{i=1}^{\aleph} \rho_i^p + \sum_{s=1}^{\Im} \rho_s^p + \rho_w^p \quad (2.2)$$

where ρ_i^p is the mass density concentration of the i th dissolved ion constituent, ρ_s^p is the mass density concentration of the s th precipitated constituent in pore water phase and ρ_w^p is the mass density concentration of the ‘pure’ water in material. The total mass density concentration of the mixture ρ is

$$\rho = \rho^c + \rho^p = \sum_{h=1}^{\aleph} \rho_h^c + \sum_{i=1}^{\aleph} \rho_i^p + \sum_{s=1}^{\Im} \rho_s^p + \rho_w^p \quad (2.3)$$

The mean velocity of the pore solution phase $\dot{\mathbf{x}}^p$ is defined as the mass weighted average of individual constituent velocities $\dot{\mathbf{x}}_i^p$ (m/s), $\dot{\mathbf{x}}_s^p$ and $\dot{\mathbf{x}}_w^p$, i.e.

$$\dot{\mathbf{x}}^p = \frac{1}{\rho^p} \sum_{i=1}^{\aleph} \rho_i^p \dot{\mathbf{x}}_i^p + \frac{1}{\rho^p} \sum_{s=1}^{\Im} \rho_s^p \dot{\mathbf{x}}_s^p + \frac{\rho_w^p \dot{\mathbf{x}}_w^p}{\rho^p} \quad (2.4)$$

The mixture velocity of the solid phase $\dot{\mathbf{x}}^c$ is the mass weighted average of individual solid constituent velocities $\dot{\mathbf{x}}_h^c$, i.e.

$$\dot{\mathbf{x}}^c = \frac{1}{\rho^c} \sum_{h=1}^{\aleph} \rho_h^c \dot{\mathbf{x}}_h^c \quad (2.5)$$

The velocity of the whole mixture $\dot{\mathbf{x}}$ is defined to be the sum of $\dot{\mathbf{x}}^p$ and $\dot{\mathbf{x}}^c$, that is

$$\dot{\mathbf{x}} = \frac{1}{\rho} \sum_{i=1}^{\aleph} \rho_i^p \dot{\mathbf{x}}_i^p + \frac{1}{\rho} \sum_{s=1}^{\Im} \rho_s^p \dot{\mathbf{x}}_s^p + \frac{\rho_w^p \dot{\mathbf{x}}_w^p}{\rho} + \frac{1}{\rho} \sum_{h=1}^{\aleph} \rho_h^c \dot{\mathbf{x}}_h^c \quad (2.6)$$

In a general case where $\dot{\mathbf{x}}_h^c$ is different from zero, the mass balance principle for the \aleph number of solid constituents of the concrete phase c can be written as

$$\frac{\partial \rho_h^c}{\partial t} = -\text{div}(\rho_h^c \dot{\mathbf{x}}_h^c) + \hat{c}_h^c + \hat{r}_h^c; \quad h = 1, \dots, \aleph \quad (2.7)$$

where \hat{c}_h^c is the gain of mass from all $\aleph - 1$ number of solid constituents present in phase c . The term \hat{r}_h^c is the gain of mass to the h th constituent from the $\Re + \Im + 1$ number of constituents building up the pore solution phase p .

The postulate for the mass balance for the solid phase c is

$$\frac{\partial \rho^c}{\partial t} = -\text{div}(\rho^c \dot{\mathbf{x}}^c) + \hat{r}^c \quad (2.8)$$

where \hat{r}^c is the total gain of mass to the solid concrete phase from the pore solution phase, i.e. \hat{r}^c is related to \hat{r}_h^c , as

$$\hat{r}^c = \sum_{h=1}^{\aleph} \hat{r}_h^c \quad (2.9)$$

In mixture theory it is postulated that the sum of the constituent balance principles in a phase should be equal to the mass balance equation for the whole phase. Summing the \aleph number of balance principles in (2.7), therefore, results in

$$\sum_{h=1}^{\aleph} \hat{c}_h^c = 0 \quad (2.10)$$

where (2.6), (2.7), (2.8) and (2.9) are used.

The mass balance for the pure water w in the pore solution phase p is the postulate

$$\frac{\partial \rho_w^p}{\partial t} = -\text{div}(\rho_w^p \dot{\mathbf{x}}_w^p) + \hat{c}_w^p + \hat{r}_w^p \quad (2.11)$$

where \hat{c}_w^p and \hat{r}_w^p are the gain of mass to the w constituents from constituents within phase p and from phase c , respectively.

The mass balance principle for the different types of dissolved ions in pore solution is

$$\frac{\partial \rho_i^p}{\partial t} = -\text{div}(\rho_i^p \dot{\mathbf{x}}_i^p) + \hat{c}_i^p + \hat{r}_i^p; \quad i = 1, \dots, \Re \quad (2.12)$$

where \hat{c}_i^p is the mass gain to the dissolved ion constituent i from all constituents in the pore solution, i.e. in phase p . The property \hat{r}_i^p is the mass gain to the dissolved ion constituent i from the solid phase c .

The mass balance principle for the solid precipitated neutral combinations of ions in pore solution is

$$\frac{\partial \rho_s^p}{\partial t} = -\text{div}(\rho_s^p \dot{\mathbf{x}}_s^p) + \hat{c}_s^p + \hat{r}_s^p; \quad s = 1, \dots, \mathfrak{S} \quad (2.13)$$

where \hat{c}_s^p is the mass gain to the solid constituent s in the pore solution from the i number of dissolved ions also present in the pore solution. The term \hat{r}_s^p is the mass gain to the solid constituent s in the pore solution, i.e. in phase p , from the solid phase c .

The mass balance for the whole pore solution phase p is the postulate

$$\frac{\partial \rho^p}{\partial t} = -\text{div}(\rho^p \dot{\mathbf{x}}^p) + \hat{r}^p \quad (2.14)$$

where \hat{r}^p is the total gain of mass to the pore solution phase p from the solid phase c , i.e.

$$\hat{r}^p = \sum_{i=1}^{\mathfrak{R}} \hat{r}_i^p + \sum_{s=1}^{\mathfrak{S}} \hat{r}_s^p + \hat{r}_w^p \quad (2.15)$$

The sum of equation (2.11), the \mathfrak{R} number of equations in (2.12) and the \mathfrak{S} number of equations in (2.13) should result in satisfying the condition

$$\sum_{i=1}^{\mathfrak{R}} \hat{c}_i^p + \sum_{s=1}^{\mathfrak{S}} \hat{c}_s^p + \hat{c}_w = 0, \quad (2.16)$$

since it is postulated that equation (2.14) is the sum of the constituent equations in phase p .

The postulated mass balance for the whole mixture, including both the pore solution phase p and the solid phase c , is

$$\frac{\partial \rho}{\partial t} = -\text{div}(\rho \dot{\mathbf{x}}) \quad (2.17)$$

Summation of the mass balance equations for the c and p phases, i.e. equation (2.7) and (2.14), results in the relation

$$\hat{r}^p + \hat{r}^c = 0 \quad (2.18)$$

where (2.4), (2.5) and (2.6) are used.

Yet another balance principle will be invoked for the pore solution phase p , the continuity equation for the charge, which is

$$\operatorname{div}(\mathbf{d}^p) = q^p \quad (2.19)$$

where the electrical displacement field is denoted by \mathbf{d}^p (C/m²) and the charge density by q^p (C/m³). This equation will control the condition of the pore solution in terms of an electrical potential φ^p . The reason for obtaining an electrical potential in a pore solution is a momentarily unbalancing number of positive and negatively charged dissolved ions in a representative volume being much larger than the size of the ions themselves.

In this application it is convenient to introduce the so-called diffusion velocity \mathbf{u} , which is the velocity of a constituent in relation to the phase mixture velocity.

$$\mathbf{u}_i^p = \dot{\mathbf{x}}_i^p - \dot{\mathbf{x}}^p \quad (2.20)$$

$$\mathbf{u}_h^c = \dot{\mathbf{x}}_h^c - \dot{\mathbf{x}}^c \quad (2.21)$$

It will be explicitly assumed that different dissolved ions in a pore solution cannot react with each other, i.e. the problem will be restricted to a case where precipitation of combinations of ions cannot occur. This means that the mass exchange terms $\hat{c}_i^p(\mathbf{x}, t)$, $i = 1, \dots, \mathfrak{R}$ are set to zero. The unknown quantities for the \mathfrak{R} number of different types of ions dissolved in the pore solution, therefore, are

$$\rho_i^p(\mathbf{x}, t); \quad \mathbf{u}_i^p(\mathbf{x}, t); \quad r_i^p(\mathbf{x}, t); \quad i = 1, \dots, \mathfrak{R} \quad (2.22)$$

where ρ_i^p is the mass density concentration of an arbitrary type of ion dissolved in the pore solution, \mathbf{u}_i^p is the corresponding diffusion velocity, i.e. the velocity of the ion type i in relation to the velocity of the phase mixture, i.e. in relation to $\dot{\mathbf{x}}^p$.

For the ‘pure’ water in a pore solution it will be explicitly assumed that $\hat{c}_w^p(\mathbf{x}, t) = 0$. Furthermore it will be assumed that $r_w^p(\mathbf{x}, t) = 0$, i.e. effects such as loss of water due to hydration or gain of water due to carbonation, will not be included in the model. The unknown properties left for the ‘pure’ water in the pore solution are

$$\rho_w^p(\mathbf{x}, t) \quad \text{and} \quad \dot{\mathbf{x}}_w^p(\mathbf{x}, t) \quad (2.23)$$

For the \mathfrak{S} number of solid components in the pore solution phase p , denoted by a subscript s , it will be assumed that the velocities $s = 1, \dots, \mathfrak{S}$ are zero, i.e. $\dot{\mathbf{x}}_s^p(\mathbf{x}, t) = 0$, and that no mass exchanges take place within the phase or between

the two phases, i.e. $\hat{c}_s^p(\mathbf{x}, t) = 0$ and $r_s^p(\mathbf{x}, t) = 0$ for all $s = 1, \dots, \mathfrak{S}$ constituents. This means that the mass densities for the precipitated combinations of ions in a pore solution will be entirely given by its initial values. For simplicity these initial values will be set to zero.

The properties of the solid constituents in concrete will be restricted in the sense that the velocities for \aleph number of constituents are set to zero, i.e. $\dot{\mathbf{x}}_h^c(\mathbf{x}, t) = 0$. Further, no reactions between the \aleph number of solid constituents within the phase c will be included, i.e. $\hat{c}_h^c(\mathbf{x}, t) = 0$. The unknown properties of the solid constituents in phase c , therefore, are

$$\rho_h^c(\mathbf{x}, t); \quad r_h^c(\mathbf{x}, t); \quad h = 1, \dots, \aleph \quad (2.24)$$

The unknown properties for the whole mixture, including both phase p and c , are

$$\rho(\mathbf{x}, t); \quad \dot{\mathbf{x}}(x, t) \quad (2.25)$$

where ρ and $\dot{\mathbf{x}}$ are defined in (2.3) and (2.6).

In order to study the influence of the charge of the different kinds of ions in the pore solution phase on the diffusion behavior, the electrical potential φ^p (V), the electrical displacement field \mathbf{d}^p (C/m²) and the charge density q^p (C/m³) must be added to the list of unknown properties in the problem studied.

$$\varphi^p(\mathbf{x}, t); \quad \mathbf{d}^p(\mathbf{x}, t); \quad q^p(\mathbf{x}, t) \quad (2.26)$$

The number of unknown properties in the reduced problem is $7 + 3\aleph + 2\mathfrak{S}$.

With the above assumptions the balance principles for the constituents are simplified. For the solid components in the phase c , one obtains the mass balance equations

$$\frac{\partial \rho_h^c}{\partial t} = \hat{r}_h^c; \quad h = 1, \dots, \aleph \quad (2.27)$$

The simplified mass balance equation for the pure water constituent becomes

$$\frac{\partial \rho_w^p}{\partial t} = -\text{div}(\rho_w^p \dot{\mathbf{x}}_w^p) \quad (2.28)$$

The mass balance for the \aleph number of dissolved ions in the pore solution is

$$\frac{\partial \rho_i^p}{\partial t} = -\text{div}(\rho_i^p \dot{\mathbf{x}}_i^p) + \hat{r}_i^p; \quad i = 1, \dots, \aleph \quad (2.29)$$

The conditions imposed by the mass balance for the whole mixture imply that no net production of mass can take place during mass exchange between the two phases. That is, the mass balance condition

$$\sum_{i=1}^{\mathfrak{R}} \hat{r}_i^p + \sum_{h=1}^{\aleph} \hat{r}_h^c = 0 \quad (2.30)$$

must hold.

The last balance principle considered is the condition for the electrical potential, which is

$$\text{div}(\mathbf{d}^p) = q^p \quad (2.31)$$

In the application to be presented it will be of interest to use a mol density concentration definition of the ion constituents dissolved in pore water, instead of the mass density concentration definition. The relation between the mass density concentration ρ_a and the mol density concentration n_i^p (mol/m³) is

$$\rho_i^p = n_i^p m_i; \quad (2.32)$$

where m_i (kg/mol) is the mass of one mol of the i th constituent which is a constant property. By definition (2.32) the mass balance equation for the ion constituents (2.29) can be written

$$m_i \frac{\partial n_i^p}{\partial t} = -m_i \text{div}(n_i^p \mathbf{x}_i^p) + m_i \hat{n}_i^p; \quad i = 1, \dots, \mathfrak{R}, \quad (2.33)$$

where the mass gain density to the i th constituent \hat{r}_i^p is related to the mol gain density \hat{n}_i^p (mol/(m³s)) as $\hat{n}_i^p = \hat{r}_i^p / m_i$. That is, the mass balance principle for the ion constituents (2.33) can be written as

$$\frac{\partial n_i^p}{\partial t} = -\text{div}(n_i^p \mathbf{x}_i^p) + \hat{n}_i^p; \quad i = 1, \dots, \mathfrak{R}, \quad (2.34)$$

This equation will be rewritten in yet another way in order to facilitate the description of the diffusion velocities of the different types of dissolved ions. Consider the concentration c_i^p (-) of the ion constituents, defined as

$$c_i^p = \rho_i^p / \rho^p = n_i^p m_i / \rho^p \quad (2.35)$$

This definition together with equations (2.20) and (2.29) can be combined to yield

$$\frac{\partial (c_i^p \rho^p)}{\partial t} = -\text{div}(\rho_i^p \mathbf{u}_i^p) - \text{div}(c_i^p \rho^p \mathbf{x}_i^p) + \hat{r}_i^p; \quad i = 1, \dots, \mathfrak{R} \quad (2.36)$$

Partial differentiation of the terms

$$\frac{\partial (c_i^p \rho^p)}{\partial t} = c_i^p \frac{\partial \rho^p}{\partial t} + \rho^p \frac{\partial c_i^p}{\partial t} \quad (2.37)$$

and

$$\operatorname{div} (c_i^p \rho^p \dot{\mathbf{x}}^p) = c_i^p \operatorname{div} (\rho^p \dot{\mathbf{x}}^p) + \rho^p \dot{\mathbf{x}}^p \cdot \operatorname{grad} c_i^p \quad (2.38)$$

makes it possible to write equation (2.36) as

$$\begin{aligned} c_i^p \left(\frac{\partial \rho^p}{\partial t} + \operatorname{div} (\rho^p \dot{\mathbf{x}}^p) \right) + \rho^p \frac{\partial c_i^p}{\partial t} &= -\operatorname{div} (\rho_i^p \mathbf{u}_i^p) - \\ \rho^p \dot{\mathbf{x}}^p \cdot \operatorname{grad} c_i^p + \hat{r}_i^p; \quad i &= 1, \dots, \mathfrak{R} \end{aligned} \quad (2.39)$$

The first term on the left-hand side of (2.39) can be identified with the aid of the mass balance equation for the phase p , i.e. equation (2.14), as

$$c_i^p \left(\frac{\partial \rho^p}{\partial t} + \operatorname{div} (\rho^p \dot{\mathbf{x}}^p) \right) = c_i^p \hat{r}^p = c_i^p \sum_{i=1}^{\mathfrak{R}} \hat{r}_i^p \quad (2.40)$$

where (2.14) with $\hat{r}_s^p = 0$, for $s = 1, \dots, \mathfrak{S}$, and $\hat{r}_w^p = 0$ are used. The equations (2.39) and (2.40) combine to yield

$$\rho^p \frac{\partial c_i^p}{\partial t} = -\operatorname{div} (\rho_i^p \mathbf{u}_i^p) - \rho^p \dot{\mathbf{x}}^p \cdot \operatorname{grad} c_i^p + \hat{r}_i^p - \frac{\rho_i^p \sum_{i=1}^{\mathfrak{R}} \hat{r}_i^p}{\rho^p}; \quad i = 1, \dots, \mathfrak{R} \quad (2.41)$$

Using the mol density concentration, as defined in (2.32), instead of the concentration c_a , the equation (2.41) takes the form

$$\begin{aligned} \rho^p m_i \frac{\partial (n_i^p / \rho^p)}{\partial t} &= -\operatorname{div} (\rho_i^p \mathbf{u}_i^p) - \rho^p m_i \dot{\mathbf{x}}^p \cdot \operatorname{grad} (n_i^p / \rho^p) + \\ \hat{r}_i^p - \frac{n_i^p \sum_{i=1}^{\mathfrak{R}} m_i \hat{r}_i^p}{\rho^p}; \quad i &= 1, \dots, \mathfrak{R} \end{aligned} \quad (2.42)$$

Partial differentiation of the term

$$\operatorname{grad} (n_i^p / \rho^p) = \frac{1}{\rho^p} \operatorname{grad} n_i^p - \frac{n_i^p}{(\rho^p)^2} \operatorname{grad} \rho^p \quad (2.43)$$

and

$$\frac{\partial (n_i^p / \rho^p)}{\partial t} = \frac{1}{\rho^p} \frac{\partial n_i^p}{\partial t} - \frac{n_i^p}{(\rho^p)^2} \frac{\partial \rho^p}{\partial t} \quad (2.44)$$

in (2.42) means that the mass balance equation for the $i = 1, \dots, \mathfrak{R}$ types of ions dissolved in pore water can be written as

$$\begin{aligned} \frac{\partial n_i^p}{\partial t} - \frac{n_i^p}{\rho^p} \frac{\partial \rho^p}{\partial t} = & -\frac{1}{m_i} \operatorname{div}(\rho_i^p \mathbf{u}_i^p) - \dot{\mathbf{x}}^p \cdot \operatorname{grad} n_i^p + \\ & \frac{n_i^p \dot{\mathbf{x}}^p}{\rho^p} \cdot \operatorname{grad} \rho^p + \\ & \hat{n}_i^p - \frac{n_i^p \sum_{i=1}^{\mathfrak{R}} \hat{r}_i^p}{\rho^p} \end{aligned} \quad (2.45)$$

The assumption that the mass density concentration for the pure water phase is much greater than any of the mass density concentrations of the dissolved ions will be used, i.e.

$$\rho_w^p \gg \rho_{i=1, \dots, \mathfrak{R}}^p; \quad (2.46)$$

This results in the mean velocity of the pore solution phase $\dot{\mathbf{x}}^p$ being approximately equal to the velocity $\dot{\mathbf{x}}_w^p$ of the pore solution, i.e. compare with (2.4). Furthermore, the mass density of the pore solution phase is approximately equal to the mass density of pure water, i.e. the approximation in (2.46) results in

$$\dot{\mathbf{x}}^p \approx \dot{\mathbf{x}}_w^p; \quad \rho^p \approx \rho_w^p \quad (2.47)$$

The approximative version of the balance principle for the ion constituents in pore solution becomes with (2.47)

$$\begin{aligned} \frac{\partial n_i^p}{\partial t} - \frac{n_i^p}{\rho_w^p} \frac{\partial \rho_w^p}{\partial t} = & -\frac{1}{m_i} \operatorname{div}(\rho_i^p \mathbf{u}_i^p) - \dot{\mathbf{x}}_w^p \cdot \operatorname{grad} n_i^p + \\ & \frac{n_i^p \dot{\mathbf{x}}_w^p}{\rho_w^p} \cdot \operatorname{grad} \rho_w^p + \hat{n}_i^p; \quad i = 1, \dots, \mathfrak{R} \end{aligned} \quad (2.48)$$

for all \mathfrak{R} considered ions. It is noted that the term

$$\frac{n_i^p \sum_{i=1}^{\mathfrak{R}} \hat{r}_i^p}{\rho_w^p} = \frac{\rho_i^p \sum_{i=1}^{\mathfrak{R}} \hat{r}_i^p}{m_i \rho_w^p} \approx 0 \quad (2.49)$$

in (2.45) is approximately zero due to the conditions in (2.47).

Consider the mass balance equation for the pure water constituent, i.e. (2.28), written as

$$\frac{n_i^p}{\rho_w^p} \frac{\partial \rho_w^p}{\partial t} = -\frac{n_i^p}{\rho_w^p} \operatorname{div}(\rho_w^p \dot{\mathbf{x}}_w^p) \quad (2.50)$$

i.e.

$$\frac{n_i^p}{\rho_w^p} \frac{\partial \rho_w^p}{\partial t} = -\frac{n_i^p \dot{\mathbf{x}}_w^p}{\rho_w^p} \cdot \text{grad} \rho_w^p - n_i^p \text{div} \dot{\mathbf{x}}_w^p \quad (2.51)$$

This means that the \Re equations in (2.48) can be written as

$$\frac{\partial n_i^p}{\partial t} = -\frac{1}{m_i} \text{div} (\rho_i^p \mathbf{u}_i^p) - \dot{\mathbf{x}}_w^p \cdot \text{grad} n_i^p - n_i^p \text{div} \dot{\mathbf{x}}_w^p + \hat{n}_i^p; \quad i = 1, \dots, \Re \quad (2.52)$$

The term $n_i^p \text{div} \dot{\mathbf{x}}_w^p$, in equation (2.52), represents the change in the mass density concentration of ion i in a pore solution due to a change in the mass density concentration of the pore solution caused by drying or capillary suction. The mass balance equation (2.52) for the mole density concentration of the ion type i dissolved in the pore solution is a generalization of the standard diffusion-convection equation, e.g. see [9], in the sense that the change of the reference volume, i.e. the volume change of pore water phase, and the mass exchanges between phases are included.

To show the meaning of the term $n_i^p \text{div} \dot{\mathbf{x}}_w^p$, consider again the mass balance for the ‘pure’ water in the pore solution phase, i.e.

$$\frac{\partial \rho_w^p}{\partial t} = -\text{div} (\rho_w^p \dot{\mathbf{x}}_w^p) = -\dot{\mathbf{x}}_w^p \cdot \text{grad} \rho_w^p - \rho_w^p \text{div} \dot{\mathbf{x}}_w^p \quad (2.53)$$

Note that the material derivative of ρ_w^p , denoted $(\rho_w^p)'$, is the change in mass density concentration related to the motion $\dot{\mathbf{x}}_w^p$ given as

$$(\rho_w^p)' = \frac{\partial \rho_w^p}{\partial t} + \dot{\mathbf{x}}_w^p \cdot \text{grad} \rho_w^p \quad (2.54)$$

That is, by combining (2.53) and (2.54), the mass balance equation using the material description becomes

$$(\rho_w^p)' = -\rho_w^p \text{div} \dot{\mathbf{x}}_w^p \quad (2.55)$$

This means that the ratio between the change in mass density concentration of the pore water, following its own motion, and the actual mass density concentration, in this case, is proportional to $\text{div} \dot{\mathbf{x}}_w^p$, i.e.

$$\frac{(\rho_w^p)'}{\rho_w^p} = -\text{div} \dot{\mathbf{x}}_w^p \quad (2.56)$$

Hence the term $n_i^p \text{div} \dot{\mathbf{x}}_w^p = n_i^p (\rho_w^p)' / \rho_w^p$, in equation (2.52), is the absolute change of the mass concentration of ion i dissolved in a pore solution, due to changes in mass concentration of pore water ρ_w^p only, following the motion of the pore water.

3. Constitutive relations

Next, consider the constitutive relations for the constituents. The velocity of the pore water in material is the assumption

$$\dot{\mathbf{x}}_w^p = -\frac{D_w^p(\rho_w^p)}{\rho_w^p} \text{grad} \rho_w^p \quad (3.1)$$

where $D_w^p(\rho_w^p)$ is the nonlinear material parameter relating the gradient of the mass density concentration of water in pores with the velocity $\dot{\mathbf{x}}_w^p$. Methods to evaluate $D_w^p(\rho_w^p)$ from capillary suction experiments have been proposed, e.g. see [10] and [11], further, methods using steady state conditions to evaluate $D_w^p(\rho_w^p)$ have been developed, see [12]. The effect on $\dot{\mathbf{x}}_w^p$ caused by an external applied pressure is not included in the present model.

The assumptions for the diffusion velocity flows for the \mathfrak{R} considered types of ions in a pore solution are

$$\rho_i^p \mathbf{u}_i^p = -\tilde{D}_i^p(\rho_w^p) m_i \text{grad} n_i^p - \tilde{A}_i^p(\rho_w^p) m_i v_i n_i^p \text{grad} \varphi^p; \quad i = 1, \dots, \mathfrak{R} \quad (3.2)$$

where $\tilde{D}_i^p(\rho_w^p)$ (m^2/s) is the diffusion parameter for ion type i , dissolved in the pore solution, which is assumed to be dependent on the moisture condition ρ_w . The property $\tilde{A}_i^p(\rho_w^p)$ ($\text{m}^2/(\text{Vs})$) is the ion mobility parameter for ion type i in pore solution. The valence number for ion type i (to be used with the correct sign) is denoted by v_i ($-$), and φ^p (V) denotes the electrical potential in the pore solution. If effects caused by corrosion of reinforcement bars embedded in concrete are also included, an extra term must be added in (3.2), since an electrical potential (which is different from φ^p) will develop in the domain surrounding the anodic and cathodic area, i.e. in the corrosion zone. The gradient of the electric potential caused by reinforcement corrosion will affect the diffusion of all ions dissolved in pore solution near the corrosion zone. This phenomena has been theoretically studied in [13].

The constitutive assumption for the mass flow of ions in water-filled pore system in concrete has been used by, for example, [14], [15] and [16]. In [14] the gradient of the chemical activity is also included in the constitutive function for the mass density flow. The chemical activity is assumed to be a function of the concentration and temperature, i.e. the so-called Debye-Hückel model. The extended Debye-Hückel model also considers the radius of the various ions in solution.

The mass exchange rate for the ion type i with solid constituents can, in a somewhat general case, be described as functions of all \mathfrak{R} number of mol density concentrations of the different types of ions in phase p and all \mathfrak{N} number of mass densities of solid components in phase c . The mol density gain of mass to the i th ion constituent dissolved in a pore solution from the solid phase is written, in a general fashion, as

$$\hat{n}_i^p = f_i \left(n_{i=1, \dots, \mathfrak{R}}^p, \rho_{h=1, \dots, \mathfrak{N}}^c \right) \quad (3.3)$$

And the mol density gain of mass to the h th constituent in solid phase from ions in the pore solution is written as

$$\hat{n}_h = f_h \left(n_{i=1, \dots, \mathfrak{R}}^p, \rho_{h=1, \dots, \mathfrak{N}}^c \right) \quad (3.4)$$

where it should be noted that the function f_i is related to f_h through the chemical reaction assumed to be taking place. Typical mass exchanges to be described with the constitutive functions in (3.3) and (3.4), for the studied case, are binding and leaching of chloride, hydroxide and calcium ions. Explicit assumptions for this kind of reactions can be found in [17]. Properties related to chloride binding and its equilibrium conditions in concrete can be studied in, for example, [18].

The assumption for the electric displacement field \mathbf{d}^p in a pore solution is

$$\mathbf{d}^p = -\tilde{\varepsilon} \varepsilon_o \text{grad} \varphi^p \quad (3.5)$$

where ε_o (C/V) is the coefficient of dielectricity or permittivity of vacuum, $\varepsilon_o = 8.854 \cdot 10^{-12}$, and $\tilde{\varepsilon}$ (-) is the relative coefficient of dielectricity that varies among different dielectrics. For water at 25°C, $\tilde{\varepsilon} = 78.54$.

The charge density in the pore solution is the global imbalance of charge in a representative material volume given as

$$\mathbf{q}^p = F \sum_{i=1}^{\mathfrak{R}} n_i^p v_i \quad (3.6)$$

where $F = 96490$ (C/mol) is a physical constant describing the charge of one mol of an ion having a valence number equal to one.

4. Governing equations

Combining the mass balance equation (2.28) and the constitutive relation (3.1) for the mass density flow of the water phase, one obtains

$$\frac{\partial \rho_w^p}{\partial t} = \text{div} (D_w^p (\rho_w^p) \text{grad} \rho_w^p) \quad (4.1)$$

which is the governing equation determining $\rho_w^p(\mathbf{x}, t)$.

Combining the constitutive relation (3.2), for the diffusion velocity for the ion type i , and the assumption (3.1) with the mass balance equation (2.52) for the same ion type, one obtains for all $i = 1, \dots, \aleph$ ion types considered.

$$\begin{aligned} \frac{\partial n_i^p}{\partial t} = & \operatorname{div} \left(\tilde{D}_i^p(\rho_w^p) \operatorname{grad} n_i^p \right) + \\ & \operatorname{div} \left(\tilde{A}_i^p(\rho_w^p) v_i n_i^p \operatorname{grad} \varphi \right) + \\ & \frac{D_w^p(\rho_w^p)}{\rho_w^p} \operatorname{grad} \rho_w^p \cdot \operatorname{grad} n_i^p + \\ & n_i^p \operatorname{div} \left(\frac{D_w^p(\rho_w^p)}{\rho_w^p} \operatorname{grad} \rho_w^p \right) + \\ & f_i \left(n_{i=1, \dots, \aleph}^p, \rho_{h=1, \dots, \aleph}^c \right) \end{aligned} \quad (4.2)$$

which is the governing equation determining $n_i^p(\mathbf{x}, t)$.

The first term on right-hand side of (4.2) describes the effect of normal diffusion, the second term describes the effect on diffusion caused by the internally induced electrical imbalance among positively and negatively charged ions in pore solution phase, the third term gives the change of concentration of ion type i due to a motion of the pore solution phase in the concrete pore structure, the fourth term models the effect of the change in concentration of ions in pore solution due to drying (or an increase in water content) of the pore water and, finally, the last term on the right-hand side of (4.2) is the loss or gain of ions due to mass exchanges between pore solution and solid hydration product of concrete.

The equation determining the mass density field $\rho_h^c(\mathbf{x}, t)$, i.e. the mass density concentration of solid component h in concrete, is obtained by combining the mass balance equation (2.27) and the constitutive assumption (3.4), i.e.

$$\frac{\partial \rho_h^c}{\partial t} = \xi_h \left(n_{i=1, \dots, \aleph}^p, \rho_{h=1, \dots, \aleph}^c \right); \quad h = 1, \dots, \aleph \quad (4.3)$$

where the function ξ_h is related to f_h , in (3.4), by the mol weight involved in the reaction. Examples of reactions are binding of chlorides and leaching of hydroxide.

The governing equation for the electric potential $\varphi^p(\mathbf{x}, t)$ is obtained by inserting the two constitutive assumptions (3.5) and (3.6) into the continuity equation (2.31), i.e.

$$-\operatorname{div}(\tilde{\varepsilon} \varepsilon_o \operatorname{grad} \varphi^p) = F \sum_{i=1}^{\aleph} n_i^p v_i \quad (4.4)$$

According to the mass balance principle for the local mass exchanges between pore solution phase and solid phase, i.e. (2.30), the following should also hold

$$\sum_{i=1}^{\mathfrak{R}} f_i \left(n_{i=1, \dots, \mathfrak{R}}^p, \rho_{h=1, \dots, \mathfrak{S}}^c \right) = \sum_{b=1}^{\mathfrak{S}} f_b \left(n_{i=1, \dots, \mathfrak{R}}^p, \rho_{h=1, \dots, \mathfrak{S}}^c \right) \quad (4.5)$$

One of the main ideas behind this method of treating multicomponent ion diffusion in concrete pore solutions is that the diffusion parameters $\tilde{D}_i^p(\rho_w)$ and ion mobility parameters \tilde{A}_i^p for all i th types of ions considered can be scaled with the same tortuosity factor t , which is assumed to be a function of the pore structure and moisture content ρ_w . That is,

$$\tilde{D}_i^p = t(\rho_w) D_i; \quad \tilde{A}_i^p = t(\rho_w) A_i; \quad i = 1, \dots, \mathfrak{R} \quad (4.6)$$

where D_i and A_i are the bulk diffusion and ion mobility coefficient in water, respectively. The values of these bulk coefficients for different types of ions can be found in, for example, [19]. The experimental work concerning the diffusion characteristics, therefore, consists of determining only one parameter, i.e. $t(\rho_w)$ for the material in question. The main experimental and theoretical work, due to this choice of approach, is directed more toward describing the mass exchanges between ions in pore solution and the solid components of concrete, i.e. the description of f_i and f_h .

Solutions to the presented equation system have been reported for cases where the concrete is saturated, i.e. the convection is excluded, e.g. see [14], [16], [17] and [20]. Solutions for cases considering only concentration gradient driven chloride diffusion and convection due to motion of the pore water phase in concrete have been studied in [21] and [22].

Studies conducted in [17] reveal that the dielectric effects in the pore solution phase play a significant rule in describing the chloride ion diffusion in the water-filled pore system of concrete, especially in cases where the concrete samples were dried and re-wetted in tap water before exposure to a chloride solution. The obtained tortuosity factors from this study were in the range 0.006-0.009, in saturated conditions, for water to binder ratios 0.35-0.55. Chloride profiles reported in [23] were used together with the model described in this work, to obtain these tortuosity factors. These results are in accordance with tortuosity factors determined by a gas diffusion technique [24]. The tortuosity factors obtained for concrete with the cement content 400 kg/m³ having water to cement ratios 0.40 and 0.55 were 0.007 and 0.011, respectively.

5. Conclusions

A theoretical model describing penetration and leaching of different types of ions in pore solution of concrete was established. The model accounts for: (i) diffusion of different types of ions caused by its concentration gradient, (ii) diffusion caused by the gradient of the electrical potential which is determined from the momentarily developed imbalance of charge among positive and negative ions in pore solution, (iii) mass exchange between ions in pore solution and hydration products in concrete, e.g. binding and leaching of chloride, hydroxide, carbonic-acid, sulfate and calcium ions, (iv) convective flows caused by a motion of the pore solution phase, e.g. motion of ions dissolved in pore solution caused by capillary suction, (v) the effect on the ion concentration due to a change in the mass concentration of pore water in the concrete, i.e. when drying of pore solution occurs the concentration of ions in the water phase increases and when the water content increase the solution becomes more dissolute. The derived mass balance principle for the different types of ions appearing in the pore solution phase, i.e. equation (2.52), includes all these important phenomena. The mass balance equation for the ion constituents dissolved in the pore solution was established by considering two phases, i.e. the pore solution phase and the solid phase using the basic assumptions defined in mixture theory as described in [8].

It is assumed that the different types of ions in pore solution are affected by the pore system in an identical manner with regard to diffusion caused by concentration and electric-potential gradients. This way of simplifying the problem very much turns the problem toward describing the correct equilibrium and kinetic conditions for the mass exchanges processes occurring between ions in pore solution and solid components of the concrete.

The convection of ions was introduced by using the so-called diffusion velocities, that is, the velocity relative to the velocity of the mixture (in this reduced problem the velocity of pore solution phase) together with the use of a proper equation for the mass balance for the ion constituents dissolved in pore water. The method for calculating the velocity of pore phase, see equations (4.1) and (3.1), may be criticized, since at relatively low moisture contents in concrete the distribution of moisture is mainly due to vapor diffusion in air-filled space in pore system not contributing to a motion of pore water phase. That is, the convection of ions in pore solution phase is most likely overestimated at medium and low water contents in pore system, for concrete exposed to drying or wetting, in the model described.

References

- [1] Sandberg, P. (1998). *Chloride Initiated Reinforcement Corrosion in Marine Concrete*, Lund Institute of Technology, Division of Building Materials, Lund.
- [2] Tuutti, K. (1982). *Corrosion of Steel in Concrete*, Swedish Cement and Concrete Institute (CBI), Royal Institute of Technology, Stockholm, Sweden.
- [3] Page, C.L., Short, N.R. and El-Tarras, A. (1981). *Diffusion of Chlorides in Hardened Cement Pastes*, Cement and Concrete Research, Vol. 11. pp. 751-757.
- [4] Ho, D.W.S and Lewis, R.K. (1987). *Carbonation of Concrete and its Predictions*, Cement and Concrete research, Vol. 17, pp. 489-504.
- [5] Taylor, H.F.W. (1990). *Cement Chemistry*, Academic Press.
- [6] Lindmark, S. (1998). *Mechanisms of Salt Frost Scaling of Portland Cement-bound Materials: Studies and Hypothesis*, Lund Institute of Technology, Division of Building Materials, Lund.
- [7] Ekström, T. (2000). *Leaching of Concrete, Experiments and modelling*, Lund Institute of Technology, Division of Building Materials, Lund
- [8] Bowen, R.M. (1976). *Theory of Mixtures*, Part 1, in Continuum Physics, Edited by A. Cemal Erigen, Princeton University of Technology.
- [9] Bear, J. (1979). *Hydraulics of Groundwater*, McGraw-Hill, Inc. New York.
- [10] Janz, M. (1997). *Methods of Measuring the Moisture Diffusivity at High Moisture Levels*, Lund Institute of Technology, Division of Building Materials, Lund.
- [11] Arvidsson, J. (1998). *Moisture Transport in Porous Media, Modelling Based on Kirchhoff Potentials*. Lund University of Technology, Department of Building Technology, Building Physics, Lund.
- [12] Hedenblad, G. (1993). *Moisture Permeability of Mature Concrete, Cement Mortar and Cement Paste*, Lund Institute of Technology, Division of Building Materials, Lund.

- [13] Johannesson, B. (1998). *Modelling of Transport Processes Involved in Service Life Prediction of Concrete, Important Principles*, Lund Institute of Technology, Division of Building Materials, Lund.
- [14] Samson, E. and Marchand, J. (1999). *Numerical Solution of the Extended Nernst-Planck Model*, Journal of Colloid and Interface Science 215, pp. 1-8.
- [15] Samson, E., Marchand, J. Robert, J.-L. and Bournazel, J.-P. (1999). *Modelling Ion Diffusion Mechanisms in Porous Media*. International Journal for Numerical Methods in Engineering, 46, pp. 2043-2060.
- [16] Truc. O. (2000). *Prediction of Chloride Penetration into Saturated Concrete - Multi-Species Approach*, Department of Building Materials, Chalmers University of Technology Göteborg, Sweden.
- [17] Johannesson, B.F. (2000). *Transport and Sorption Phenomena in Concrete and Other Porous Media*, Lund Institute of Technology, Division of Building Materials, Lund.
- [18] Nilsson, L.O., Massat, M. and Tang, L. (1994). *The Effect of Non-linear Chloride Binding on the Prediction of Chloride Penetration into Concrete Structures*, In Durability of Concrete: Proc. 3rd. Int. Conf., Edited by Malhotra, ACI SP 145, Detroit, pp. 469-486.
- [19] Weast, R.C, Lide, D.R., Astle, M.J. and Beyer, W.H. (1989). *Handbook of Chemistry and Physics*, 70th edition, CRC Press, Inc. Boca Raton, Florida.
- [20] Johannesson, B.F. (1999). *Diffusion of a Mixture of Cations and Anions Dissolved in Water*, Cement and Concrete Research, Vol. 29. pp. 1261-1270.
- [21] Johannesson, B.F. (1997). *Nonlinear Transient Phenomena in Porous Media with Special Regard to Concrete and Durability*, Advanced Cement Based Materials, Vol. 6. pp. 71-75.
- [22] Johannesson, B.F. (1996). *Convection-diffusion Problems with Significant First-order Reversible Reactions*, Ninth Nordic Seminar on Computational Mechanics, Technical University of Denmark, Edited by Lars Damkilde.
- [23] Janz, J and Johannesson, B.F. (1993). *A Study of Chloride Penetration into Concrete* (in Swedish), Lund Institute of Technology, Division of Building Materials, Lund.

- [24] Alfarabi Sharif, Loughlin, K.F., Azad, A.K. and Navaz C.M. (1997). *Determination of the Effective Chloride Diffusion Coefficient in Concrete via a Gas Diffusion Technique*. ACI Materials Journal, Vol. 94, No. 3.

HOW TO APPLY THE HETEK MODEL IN THE ROAD ENVIRONMENT – 1999



Jens M. Frederiksen
B.Sc.Eng.(hon.)
Civil Engineer
jmf@aec-dk.com
AEClaboratory (Ltd.) A/S
Denmark
www.aec-dk.com

ABSTRACT

Environmental data for road structures are scarce. What is actually available and what can be concluded from them? This paper gives an overview of the State of the Art and some new data. Further more a suggestion is given for three environmental zones in the road environment. Finally the HETEK model for marine concrete is slightly modified for the road environment where de-icing salt is the chloride source.

Keywords: Concrete, durability, chloride, model, ingress, penetration, time-dependency

1. INTRODUCTION

The conditions in the road environment are summarised in Nilsson et al. [1996]. The distribution of chloride (concentrations at different depths) is a function of the environmental conditions, the design of the structure and the material properties. The mechanisms of chloride transport and binding involved are complicated and usually combined in a complicated way, cf. Chapter 7 in Frederiksen et al [1997].

The transport and distribution of chloride in a concrete structure is very much a function of the environmental conditions, mainly the duration of the contact and the concentration of the solutions in contact with the concrete surface. The conditions are quite different in different exposure situations.

Salt water can be sucked into the concrete surface. Rainwater washes the surface free from chloride and may remove some. Evaporation increases the chloride concentration. Chloride moves inwards and outwards due to moisture flow and ion diffusion.

The conditions are different at different heights from the road level. A maximum chloride content may be found at a height where salt water is frequently supplied to the surface but where the surface intermittently dries out.

Bridges and road structures that are exposed to de-icing salts have boundary conditions that vary extensively with time. In wintertime parts of the structure are exposed to saturated salt solutions that are rapidly diluted as the ice and snow melts. This exposure can be repeated frequently, sometimes once a day. Rainwater washes the surfaces and move salt water to drains and/or other parts of the structure.

Salt water penetrates cracks and joints. Consequently, the occurrence and the effect of defects must be considered in the evaluation of the behaviour of a structure. These effects are described in Chapter 8 and 9 of Frederiksen et al [1997].

2. THE EFFECT OF RADIATION

Radiation gives a major contribution to the energy balance of surfaces. The radiation is traditionally divided into two components: Short wave radiation from the sun and long wave radiation which have origin in “black body” radiation from surfaces and long wave transparent volumes. Long wave radiation is a function of surface temperature and emission properties.

The long-wave radiation exchange with the sky lowers the temperature in night-time on horizontal surfaces. Bridge columns are often covered by the bridge deck and are therefore protected both from driving rain and long wave radiation exchange with sky, the so called sky temperature are normally several degrees lower than the ambient temperature. But the columns still absorb the short-wave solar radiation from the low standing sun. Such parts of a bridge could therefore be warmer than the surrounding air. This can explain the low relative humidity measured in columns under Danish road bridges by Andersen [1996]. The bridge deck is extremely exposed to radiation, both short-wave radiation from the sun and to long-wave radiation towards a clear sky. That lead to extreme variations in surface temperature over a 24-h period every cloud-free day of the year.

3. DE-ICING SALT

When the temperature drops below 0°C or if it is raining under cold rain, de-icing salt (NaCl) is sprayed on the road as a NaCl solution or as dry salt. Sometimes de-icing salts are applied in the beginning of a snow period. Salting are mostly performed in night-time or in the early morning hours. In the Nordic countries de-icing salts are spread around 30 to 60 times each season and each time 10 to 25 g/m² NaCl are spread depending on the meteorological conditions.

There could be a relationship between the frequency of de-icing salt exposure and chloride penetration according to Kamiya et al. [1995].

Tang [1996] studies combined effects of splash and air-borne salt. The experimental set-up cf. Figure 1 collects the salt water and chloride content are analysed, and the total chloride exposure on a vertical surface close to the road was calculated. Wirje [1996] measured the adsorption of chloride in mortar specimens on the same location. The correlation between in chloride exposure and absorption in mortar specimens are shown in Figure 1.

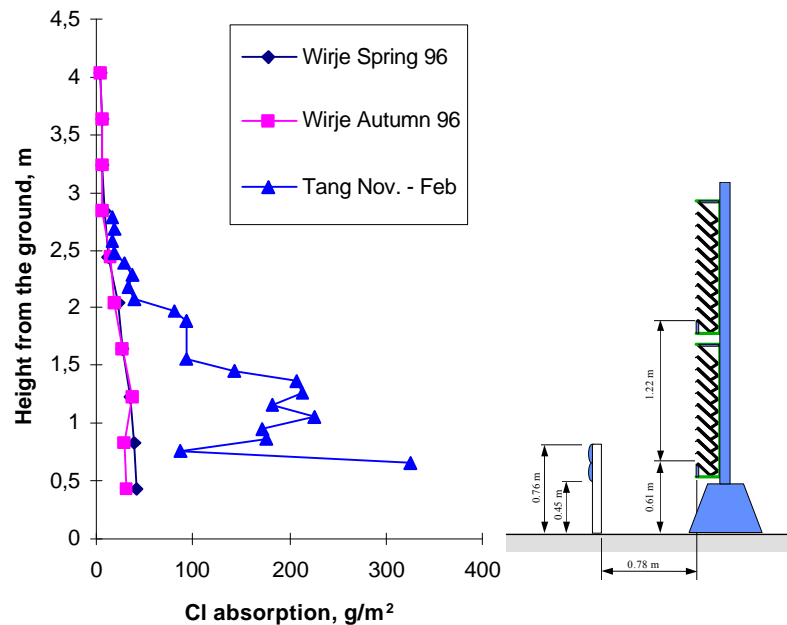


Figure 1. Chloride exposure on a vertical surface at Rv40, in the SW part of Sweden. Under the winter 1995-1996 869 g Cl/m^2 (1432 g NaCl/m^2) was applied. Tangs [1996] experimental set-up measures the chloride exposure. Wirje's [1996] experimental set-up measures the chloride absorbed into mortar specimens.

4. AIR BORNE SALT

Small water drops will be created when mechanical energy or moving air are added to wet surfaces or to larger water drops. Small water drops do not have enough kinetic energy and will easily follow moving air.

In the road environment the definition of “air borne salt” should be used on small salt water drops and dry salt that easily follow the drag from vehicles. They move parallel to the traffic and can be lifted in the turbulent zone behind the car. When the car has passed, it will follow the wind and be deposited close to the road. At a distance of more than 100 m from the road the airborne salt level is close to the background level, Eliasson [1996]. About 20% of the salt will deposit within 3 meters from the road according to Dragstedt [1980], and 25% will deposit within 7 meters according to Pedersen & Forstad [1994].

5. THE ROAD BRIDGE ENVIRONMENT

The microenvironment surrounding a road bridge could be divided into two principal zones, the dry zone and the zone exposed to rain. These zones could be identified in

data from Wirje [1996] shown in Figure 2. It is important to note that the data are obtained from only one exposure season and in a location where the other parameters (car speed, location...) are constants.

The height above the road is the most decisive parameter in this and other studies. The C_{sa} value varies from 0.4 % down to 0.05 % in the wet zone and from 0.15% down to the detection limit in the dry zone. The C_{sa} values in Andersen [1996] are higher.

This could be explained with the lack of leaching in the dry zone and it would be natural with a slow increase with time in C_{sa} in the dry zone. In the wet zone a steady state in the C_{sa} value would probably be reached after a couple of seasons due to leaching of chloride out of the concrete in the summer and autumn periods. In Wirje [1996] approximately 20 % of the chloride leached out in the wet zone and less than 5 % in the dry zone during the first season.

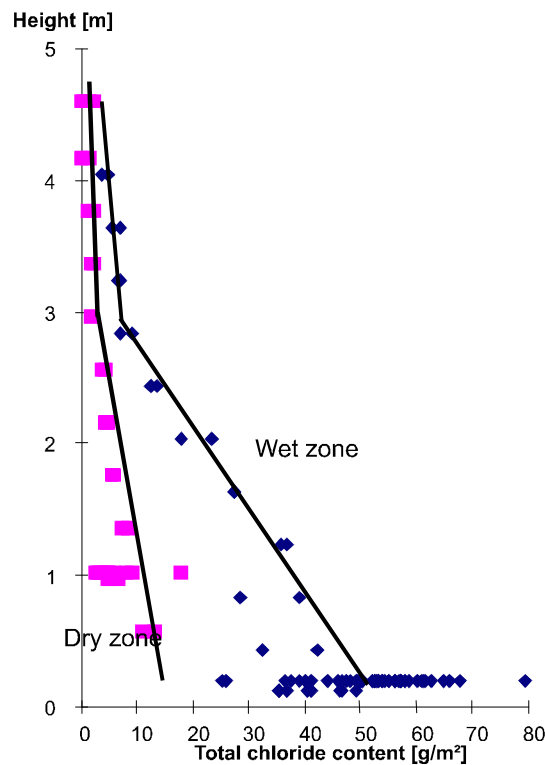


Figure 2. The amount of chloride absorbed in mortar specimens close to highway Rv40 in Sweden during the winter 1995-1996 as a function of height above the road for dry and wet road structures. The data are from Wirje [1996].

6. THE “DRY” ROAD ENVIRONMENT

It is characteristic for the dry zone that it is not exposed to direct rain, and therefore the concrete has a relative low relative humidity, less than 90% RH. Sometimes it could have a lower relative humidity than the surrounding air, because of the low radiation from a low standing sun and lack of radiation towards the sky, which leads to a higher temperature than the surrounding air.

Splash and aerosols from the road make the microclimate very complex on these parts of the structure. It is not straightforward to evaluate the chloride penetration in these parts of a bridge structure.

Measurements by Volkwein [1986] and Andersen [1996] indicate that it is not the surface facing the road, the traditionally examined surface, which has the highest chloride penetration depth. Instead, the leeward surfaces have higher chloride contents, this phenomenon is also observed in some RC structures exposed to marine environment Maage et al. [1995].

The height dependence is however relatively clear. From the road level up to around 3 meters the chloride exposure decreases to almost a background level, cf. Weber [1982] and Figure 3. This is also confirmed by Wirje [1996], cf. Figure 2. The salt exposure is relatively low but leaching of salt from the concrete in the dry parts is also low according to Wirje [1996].

Parts of a concrete structure in the dry environment just below joints are exposed to running salt water and are typical damaged areas according to West [1996]. This indicates that special concern should be taken when designing these parts of de-icing salt exposed structures.

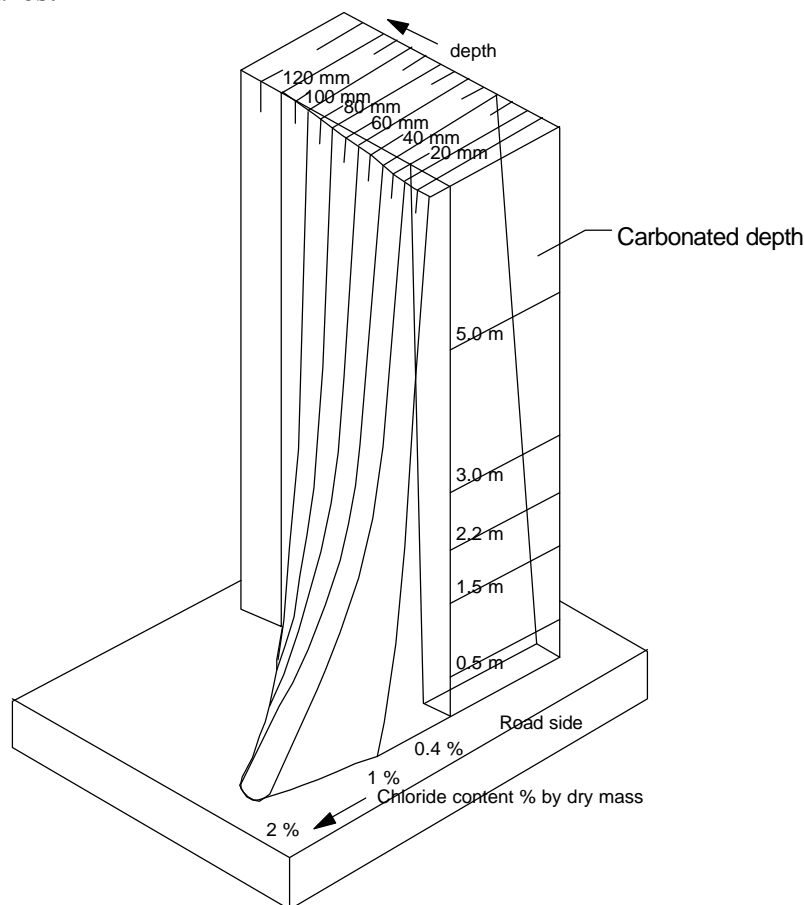


Figure 3. Height dependence of chloride penetration profiles close to a road. Data from Weber [1982].

7. THE WET ROAD ENVIRONMENT

The wet road environment is directly exposed to rain, and therefore the relative humidity in the concrete often exceeds 90 % RH. The wet environment is also exposed to radiation, which could lead to extreme temperature variations on some of these parts. The road surface is also wet close to these parts. Consequently there will be significant splash of rain water and salt water from the road surface to the concrete surfaces. These parts of the structure often have the highest chloride exposure but chloride could be extensively washed out according to Wirje [1996].

8. RESPONSE FROM DANISH ROAD BRIDGES

The responses of road bridges are complex but they seem to follow a pattern. The simplest way to summarise the response is to use the parameters C_{sa} and D_a defined as the achieved surface concentration and diffusion coefficient respectively. The inner part of the chloride profiles from Andersen [1996] fits well the error function. Curve fitting of the inner part of the profile and the outer part of the profile separately gives approximately the same C_{sa} value but the D_a value differs in the inner and outer part of the profile. One interpretation of this phenomenon is the chloride profile's inner part is a response from the bridge's lifetime. The outer part of the chloride profile changes over a year cycle. This change is larger in the wet zone. In the inner part of the structure the chloride transport mechanism is a diffusion process. In the outer part convection contributes to the chloride transport. The cores are all from columns supporting road bridges and **they are situated in the dry road environment**.

Table 1. Chloride penetration depths, carbonation depths and chloride diffusion coefficients for cores taken from bridges. From Andersen [1996]. The C_{sa} and D_a values are fitted from the inner part of the profiles. The C_{sa} values from the outer part of the profile are almost the same as the C_{sa} values from the inner part.

Bridge no./ built	Sampling date	Core Mark	Height above road level [m]	x_{CO_3} [mm]	D_{CTH} [$10^{-12} m^2/s$]	C_{sa} [% Cl by dry mass]	D_a [$10^{-12} m^2/s$]
10-0031/ 1968	960512	1	0.2	2	8.2	0.15	0.06
	960512	2	0.2	0		0.33	0.15
	960512	3	0.0	0		0.17	0.80
	9103		0.2			0.17	0.80
30-0016/ 1972	960425	1	0.5	-	10	0.13	0.18
	9103		0.2			0.06	0.05
20-0085/ 1963	960511	1	0.3	7-14	35 and 32 79 and 37	0.07	0.30
	960511	3	0.1	5-15		0.16	0.25
	960511	4	0.7	7-10		0.20	0.40
	9103		0.3			0.07	0.25
40-0004/ 1956	960526	"20"	0.2	0		0.16	0.19
	960526	"33"	0.3	0		0.16	0.22
	9103		0.15			0.12	0.15
14-0036/ 1956	960619	S	1.3	4	7.5	0.41	0.083
	960619	N1	1.3	2	9.0	0.44	0.009
	960619	N3	0.2	2	4.6	0.46	0.086
	960619	N4	1.9	3		0.27	0.035
	911002	S	1.0			0.48	0.042
	911002	N	1.0			0.39	0.021
	920520	S	1.0			0.33	0.066
	920520	N	1.0			0.21	0.033

The results presented in Table 1 may belong to the better part of the available published data from the road environment.

9. COMPARISON WITH THE MARINE ENVIRONMENT

Although it is far from the same a direct comparison of the severity of the marine atmosphere exposure in Träslövsläge are made with the “dry” road environment along a motorway in Copenhagen. The data are from Frederiksen [1998]. In Table 2, 3 and in Figure 4 the comparison is shown.

Table 2. The measured chloride profiles of specimens exposed in Träslövsläge. (The abbreviations U and L stand for the upper or the lower 15 cm of the samples). The data are from Frederiksen [1998].

Exp. start:	18-01-94	Exp. end:	27-08-97	Exp. time	1317	days =	3.61years
Trä 0-3U		Trä 0-4U		Trä 0-3L		Trä 0-4L	
0.55	0.102	0.60	0.125	0.50	0.182	0.50	0.197
1.95	0.139	2.40	0.154	2.10	0.211	2.10	0.203
3.90	0.150	4.55	0.164	4.50	0.226	4.30	0.211
6.40	0.135	6.85	0.146	6.90	0.195	6.90	0.195
9.40	0.112	9.90	0.121	9.45	0.171	9.85	0.172
13.05	0.083	13.60	0.089	12.70	0.154	13.15	0.147
16.95	0.057	17.60	0.053	16.85	0.117	16.85	0.109
		21.90	0.019	21.55	0.080	21.40	0.072
D , mm ² /yr	39		30		61		59
C_s , %mass	0.187		0.225		0.268		0.261
K , mm/ $\sqrt{\text{yr}}$	10		10		15		15

Table 3. The measured chloride profiles of specimens exposed at the motorway M3. (The abbreviations U and L stand for the upper or the lower 15 cm of the samples). The data are from Frederiksen [1998].

Exp. start	30-11-93	Exp. end	15-08-97	Exp. time	1354	days =	3.71 years
235-1 U		235-2 U		235-1 L		235-2 L	
0.55	0.082	0.45	0.090	0.55	0.145	0.45	0.125
1.90	0.130	1.85	0.118	1.95	0.176	1.80	0.123
3.65	0.139	3.75	0.134	3.85	0.225	3.90	0.134
6.05	0.142	6.00	0.121	5.80	0.223	6.40	0.120
8.80	0.122	8.45	0.103	8.25	0.201	9.25	0.106
12.05	0.092	11.40	0.076	12.00	0.177	12.80	0.081
16.20	0.049	15.15	0.042	16.30	0.132	16.85	0.047
20.15	0.017	18.95	0.019	20.50	0.090	20.50	0.024
D , mm ² /yr	27		20		66		29
C_s , %mass	0.195		0.184		0.274		0.176
K , mm/ $\sqrt{\text{yr}}$	8.9		7.5		16.2		8.8

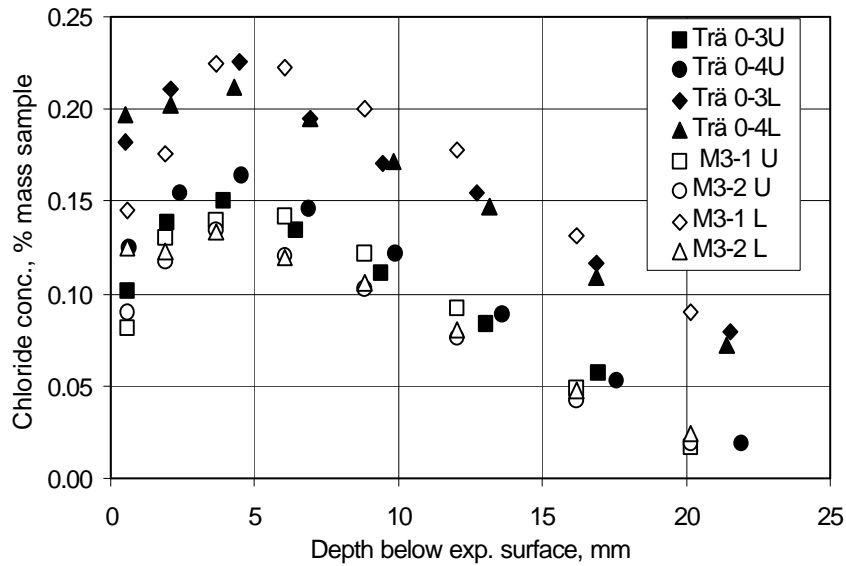


Figure 4. Measured chloride profiles of the reference specimens exposed under natural conditions in Träslövsläge and at motorway M3 around Copenhagen. (The abbreviations U and L stand for the upper or the lower 15 cm of the samples). The data are from Frederiksen [1998].

From Figure 4 it is seen that the concrete's response to the exposure is almost similar in Träslövsläge and at the motorway M3 except for one sample (M3-2 L) that responds differently compared to the other samples. There is no explanation for that result.

10. INTERPRETATION OF OBSERVATIONS FROM THE ROAD ENVIRONMENT

Above some indications were given of what was to be expected about the chloride ingress in the road environment. However the results of systematic investigations is still very few and not at all comparable to the quality of the data from the marine exposure station in Träslövsläge. The Swedish BTB project on the durability of concrete road structures exposed to de-icing salts, cf. Utgenannt et al. [1996] will hopefully provide data of a quality compared to those of the BMB project.

Some tendencies can be found in the available data and observations. A summary is listed below. The road environment must be divided into two separate groups: a "dry" and a "wet" road environment.

For the "dry" environment the following statements are given:

- C_{sa} can reach 0.5 % mass concrete at exposure periods up till approx. 40 years.
- C_{sa} will increase with time.
- C_{sa} will decrease linearly with the height above the road level.
- C_{sa} will decrease logarithmically with the distance from the road.
- C_{sa} will have a maximum on the leeward face.
- $D_a \times t$ will decrease and become a constant (i.e. $a \rightarrow 1$).

Correspondingly for the "wet" environment the following statements are given:

- The magnitude of C_{sa} is not known very well but values up to 2 % mass concrete have been reported.
- C_{sa} will decrease linearly with the height above the road level.
- C_{sa} will decrease logarithmically with the distance from the road.
- $D_a \times t$ will not become a constant (i.e. $a < 1$).

From this it is seen that the road environment may be more complicated to model than the marine environment. No safe conclusions can be drawn at this stage. For the time being it is recommended to adopt the results from the marine environment to the extend possible.

11. ENVIRONMENTAL ZONES

In order to take care of the above given statements in a way that is not more complicated than when handling the three marine environmental zones the road environment is separated into three different zones as follows:

1. *Wet splash (WRS)*: The wet road environment where the distance to the traffic is less than 4 m e.g. edge beams.
2. *Dry splash (DRS)*: The “dry” road environment where the distance to the traffic is less than 4 m e.g. pillars.
3. *Distant road atmosphere (DRA)*: The wet or the dry environment where the distance to the traffic is more than 4 m e.g. noise shelters or parts of the structure high above road level.

An approach similar to that made by Frederiksen et al. [1997] is used in order to make semi-objective estimates of the governing parameters.

12. REVISED HETEK MODEL

Because of the lack of data from the road environment there is only basis for slight modifications of the HETEK model for the marine environment. In figure 6 a plot of the chloride profiles from the M3 motorway, cf. Frederiksen [1998] are shown together

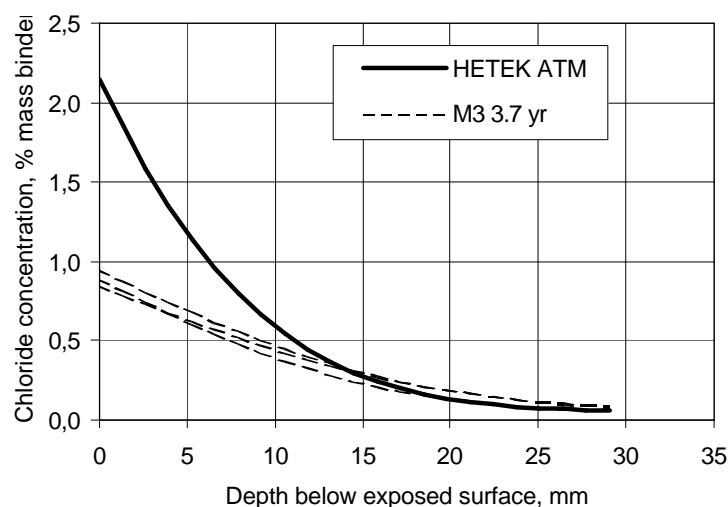


Figure 6. Plot of the chloride profiles from the M3 motorway, cf. Frederiksen [1998] are shown together with a profile estimated by the HETEK model for the marine atmosphere.

with a profile estimated by the HETEK model for the marine atmosphere. From Figure 6 it is obvious that the HETEK model for the marine atmosphere does not predict the chloride profile precisely but in a somewhat conservative way. As these data are the only data where the concrete composition and the exposure conditions are well known it is chosen to use these data for the first adjustment of the HETEK model for the marine environment to the road environment.

In the HETEK model the following expressions are used for the estimation of the various transport coefficients and time dependencies:

$$D_1 = 25,000 \times \exp \left(- \sqrt{\frac{10}{\text{eqv} \left(\frac{w}{c} \right)_D}} \right) \times k_{D,env} \quad [\text{mm}^2/\text{yr}] \quad (1)$$

$$a = (1 - 1.5 \times \text{eqv} (w/c)_D) \times k_{a,env} \quad (2)$$

The first estimates of the constants of (1) and (2) for are given in Table 6 and 7.

Table 6. The constants of (1) and (2).

Environment:	Wet Road environment	Dry Road environment	Distant Road Atmos-
Constant:	Splash (WRS)	Splash (DRS)	phere (DRA)
$k_{D,env}$	0.8	0.4	0.4
$k_{a,env}$	1	1	1

Table 7. The activity factors for diffusivity to be used when calculating the $\text{eqv} (w/c)_D$ ratio in (1) and (2).

Activity factor	Silica fume	Fly ash
k	7	1

$$C_I = 3.667 \times \text{eqv} (w/c)_b \times k_{b,env} \quad [\% \text{ mass binder}] \quad (3)$$

$$C_{100} = C_1 \times k_{time|env} \quad [\% \text{ mass binder}] \quad (4)$$

The constants of (3) and (4) are given in Table 8 and 9.

Table 8. The constants of (3) and (4).

Environment:	Wet Road environment	Dry Road environment	Distant Road Atmos-
Constant:	Splash (WRS)	Splash (DRS)	phere (DRA)
$k_{b,env}$	0.6	0.6	0.3
$k_{time env}$	4.5	3.5	3.5

Table 9. The activity factors for binding to be used when calculating the $\text{eqv} (w/c)_b$ ratio in 5).

Activity factor	Silica fume	Fly ash
k	-1.5	0.75

The quality of the suggested “models” can not be visualised for all the three suggested road environments because of the nature of these first rough estimates. It can however be visualised how the modified model works for the data (3.7 years) from the M3 motorway shown in Table 3 and Figure 6 and for the long time data given in Table 2.

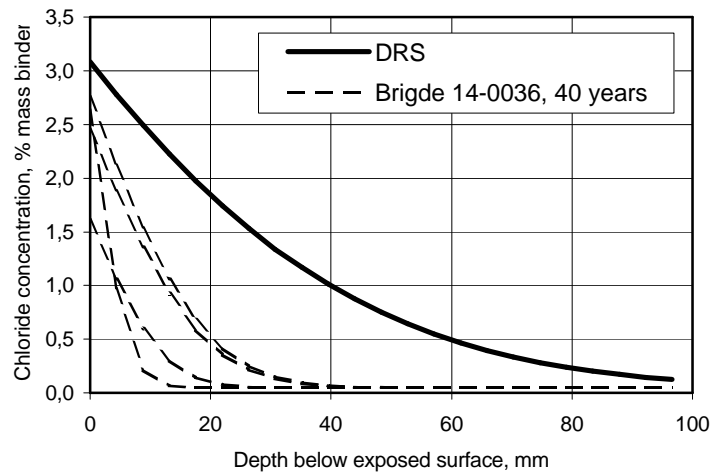


Figure 7. Comparison of some of the long time data given in Table 2 with the DRS environment of the modified HETEK model.

13. SPREADSHEET CALCULATION

The above suggested estimation formulas can be synthesised into a spreadsheet with the Mejlbro-Poulsen Model as the mathematical basis. That is done in the spreadsheet *BRIMEdei.xls*. A result of a calculation with this spreadsheet is presented in Figure 9. On the graph the difference between the three suggested road environments is shown.

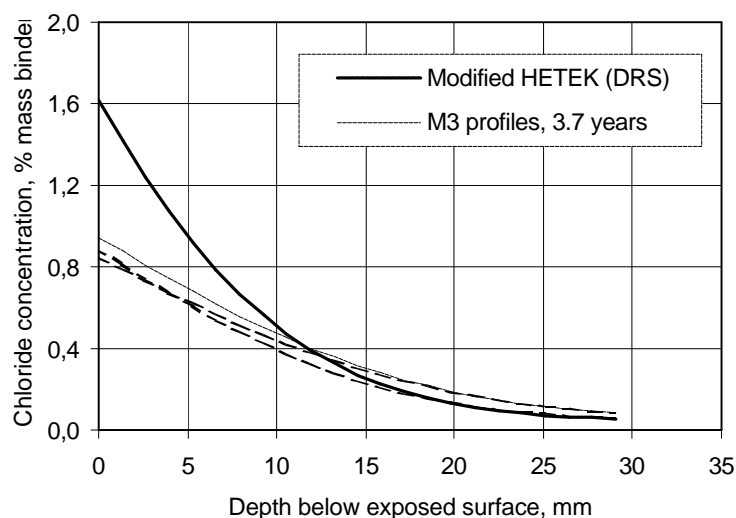
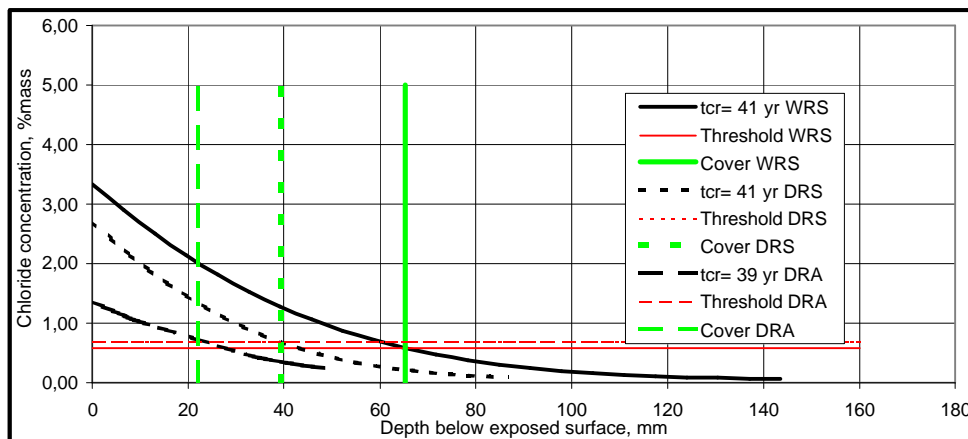


Figure 8. Comparison of the short time data given in Table 3 with the DRS environment of the modified HETEK model.

Estimation of decisive parameters and initiation time in the road environment (de-icing salt)							
Concrete composition	WRS	DRS	DRA Unit	Surface concentration	WRS	DRS	DRA Unit
Cement content	100	100	100 % PO	$k_{C1,env}$	0,6	0,6	0,3 -
Fly ash content	0	0	0 % PO	$k_{time env}$	4,5	3,5	3,5 -
Micro silica content	0	0	0 % PO	k_{MS}	-1,5	k_{FA}	0,75 -
Effective water content	42	42	42 % PO	eqv w/c	0,420	0,420	0,420 -
w/b ratio	0,42	0,42	0,42 -	C_1	0,9	0,9	0,5 % mass
Initial chloride content	0,048	0,048	0,048 % mass	C_{100}	4,2	3,2	1,6 % mass
Concrete age at Cl ⁻ -exp.	0,500	0,500	0,500 year	ID of structure:			
Diffusion coefficients				Part of structure:			
$k_{D,env}$	0,8	0,4	0,4 -	Min. concrete covers:			
$k_{a,env}$	1	1	1 -		65	39	22 mm
k_{MS}	7	k_{FA}	1 -	Expected init. time:			
eqv w/c	0,420	0,420	0,420 -		40,0	40,0	40,0 yr
D_1	152	76	76 mm²/yr	Threshold concentration			
a	0,370	0,370	0,370 -		WRS	DRS	DRA -
D_{100}	28	14	14 mm ² /yr	$k_{cr,env}$	0,7	0,6	0,6 -
				k_{MS}	-4,5	k_{FA}	-1,2 -
				eqv w/c	0,420	0,420	0,420 -
				C_{cr}	0,58	0,68	0,68 % mass



Acceptance criteria when testing acc. to NT BUILD 443			
Concrete for zone:	WRS	DRS	DRA Unit
Test parameter:			
Test parameter: $D_{per} <$	304	304	304 mm²/yr
Test parameter: $C_{sp} <$	2,8	2,8	2,8 %mass binder

Figure 9. A printout of the result after a calculation with the spreadsheet *BRIMEdei.xls*, which is synthesising the estimation formulas given in the text with the Mejlbro-Poulsen Model presented in Frederiksen et al [1997]. The difference between the three suggested road environments is visualised on the graph.

14. CONCLUSION

A reasonable approach to describe the environment for road structures is to separate the environments into two main groups, each having a height dependent chloride exposure with a maximum chloride exposure at the road level and decreasing almost linearly to near zero at some 3-4 m above road level.

The two environmental areas would be

- **Wet road structures:** parts of structures that are exposed to direct driving rain and direct splash from a wet road surface.
- **Dry road structures:** parts of structures that are exposed to airborne chloride, but sheltered from rain and close to relatively dry road surfaces that are sheltered from rain.

From this three different road environments appears:

1. *Wet splash (WRS)*: The wet road environment where the distance to the traffic is less than 4 m e.g. edge beams.
2. *Dry splash (DRS)*: The “dry” road environment where the distance to the traffic is less than 4 m e.g. pillars.
3. *Distant road atmosphere (DRA)*: The wet or the dry environment where the distance to the traffic is more than 4 m e.g. noise shelters or parts of the structure high above road level.

This paper gives the first rough estimates of how to modify the HETEK model in order to achieve reasonable results in the road environment.

15. REFERENCES

- [1996] **Andersen, A.:** *HETEK, Investigation of chloride penetration into bridge columns exposed to de-icing salt*. The Danish Road Directorate, Report No. 82.
- [1980] **Dragstedt, J.:** *Vejsalt och vejtræer. Resultat af et praktisk studie over vejsaltets vandring i jorden omkring vejtræer og indvirkning på disse*. (In Danish). Vejdirektoratet, Statens Vejlaboratorium, Laboratorierapport 46, 75 p.
- [1996] **Eliasson, Å.:** *Spridning av vägsalt kring vägar*. (In Swedish). Projektarbete, 20p. Naturgeografiska Institutionen. Göteborgs Universitet.
- [1997] **Frederiksen, J.M., Nilsson, L.-O., Poulsen, E., Sandberg, P., Tang L. & Andersen, A.:** *HETEK, A system for estimation of chloride ingress into concrete, Theoretical background*. The Danish Road Directorate, Report No. 83.
- [1998] **Frederiksen, J.M.:** *Test methods for measuring the chloride resistance properties of concrete coating systems*. NORDTEST project No. 1271-96. Report No. AEClab97-030.
- [1995] **Kamiya, M.; Iizuka, Y.; Watanabe, M.:** *Study on damaged concrete structures and their repair methods*. Concrete under severe conditions, environment and loading. E & F N Spon.
- [1995] **Maage, M.; Poulsen, E.; Vennesland, Ø.; Carlsen, J.E.:** *Service life model for concrete structures exposed to marine environment initiation period*. LIGHTCON Report No. 2.4, STF70 A94082 SIN-TEF, Trondheim, Norway.
- [1996] **Nilsson, L.O.; Poulsen, E.; Sandberg, P.; Sørensen, H.E.; Klinghoffer, O.:** *HETEK, Chloride penetration into concrete, State-of-the-Art, Transport processes, corrosion initiation, test methods and prediction models*. The Danish Road Directorate, Report No. 53.
- [1994] **Pedersen, P.; Forstad, O.:** *Effect av vejsaltning på jord, vand og vegetation. Jord- og vegetationsundersøkelser i 1993*. (In Norwegian). Statusrapport, Forskningsparken i Ås, Rapport 3/94, 30 p.
- [1996] **Tang, L.:** *Unpublished results*. SP, Borås, Sweden.
- [1996] **Utgenannt, P.; Petersson, P-E.; Malmström, K.:** *Fältextponering av betong - två nationella projekt (in Swedish) (Eng. title: “Field exposure of concrete - two national projects”)*. Bygg & Teknik, Nr. 7.
- [1986] **Volkwein, A.; Dorner, H.; Springenschmid, R.:** *Untersuchungen zur Chloridkorrosion der Bewehrung von Autobahn-Brücken aus Stahl- oder Spannbetong*. (In German). Forschung, Strassenbau und Strassen-

verkehrstechnik, Heft 460.

- [1982] **Weber, D.:** *Untersuchung von Umwelteinflüssen auf Ingenieurbauwerke der Berliner Stadsautobahn.* (In German). BAM 12, No. 2, Berlin, Germany.
- [1996] **West, G.:** *Alkali-aggregate reactions in concrete road bridges.* Thomas Telford, ISBN 07277 2069.
- [1996] **Wirje, A.; Offrell, P.:** *Kartering av miljölaster-kloridpenetration vid Rv 40.* (In Swedish). Lund, november 1996, report TVBM-7106.

Service Life Predictions of Marine Concrete Structures - Consequences of Uncertainties in Model Parameters

Gro Markeset

Visiting Professor, dr.ing.
Technical University of Denmark,
Department of Civil Engineering
e-mail: gm@byg.dtu.dk

ABSTRACT:

Chloride induced corrosion is generally acknowledged as the most critical cause of deterioration of concrete structures and warrants thus special attention. This is needed to provide reliable service life design of structures in chloride environments. Practical application of models for chloride penetration into concrete has highlighted the need for investigating the critical parameters and their uncertainties. The time dependent apparent diffusion coefficient, governed by the ageing factor, α , and the chloride threshold value for corrosion, C_{cr} , are identified as key parameters. Unfortunately, these are the parameters we know the least about. It turns out that, depending on the choice made of these values among currently available data, any required "design service life" could be achieved through "rational calculations".

This investigation has analysed the sensitivity of the critical parameters. Testing chloride profiles at different ages can provide information on the expected value of α . Corrosion sensors installed in existing structures can provide information on C_{cr} . These values are then specific for the individual structure tested.

The conclusion is, that special care shall be taken when determining, or selecting, or specifying these values if manipulation of the service life and residual service life calculations shall be avoided in practice.

Correctly chosen reliability based models, critical parameters and acceptance criteria can then be used to provide partial coefficients and entered into a service life design procedure performed identically to the well-known load-and-resistance-factor-design procedure for structural analysis.

1 INTRODUCTION

The dominant deterioration mechanism for marine concrete structures is chloride-induced corrosion. The time-dependent corrosion process in concrete is commonly modelled as occurring in two stages, defined as "initiation" and "propagation", see Figure 1. In the majority of situations the chlorides penetrate the surface layers of concrete by absorption and ion diffusion carries the chlorides to the level of the reinforcing steel. When the chloride level reaches a certain threshold limit, the reinforcing steel becomes depassivated, corrosion starts and this marks the beginning of the propagation period. During the propagation phase, the rate of oxy-

gen diffusion to the cathode, the electric resistivity of the concrete and the temperature level control the corrosion rate.

The initiation period is defined as the time until onset of corrosion. Further events will be cracking, spalling etc, which develops during the propagation period. Each of these events may in a design context be defined as a so-called limit state. If a limit state-related failure leads only to economic consequences, serviceability limit state (SLS) procedures should be applied (e.g. onset of corrosion). If failure leads to severe consequences (e.g. total loss of vital structural elements or human lives) ultimate limit state (ULS) procedures should be applied (collapse due to overloading or to excessive material degradation). The owner may define other intermediate stages mainly in order to reduce the operating costs or repair costs.

Acceptance limits for exceeding the various limit states (failure) may be defined by codes (e.g. Eurocode) or by the owner. The acceptance limits will vary depending upon the type of limit-state considered.

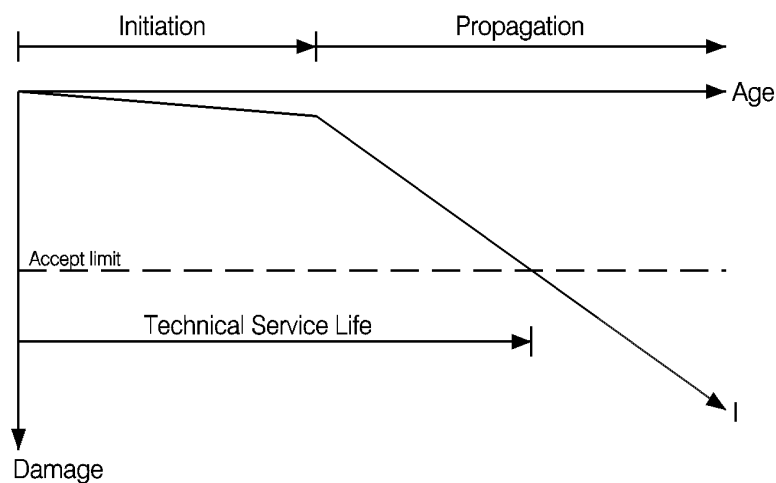


Figure 1: Service life of concrete structures, a two-phase modelling of deterioration.

For the design phase, a reasonable approach/simplification would be to include only the initiation period into calculations. Then a reliable model for predicting the chloride ingress into concrete and the limit state defining the onset of corrosion is needed. The defined events as time to onset of corrosion, called the design service life, may be calculated provided the concrete cover and its quality are known.

2 MODELLING OF THE PROPAGATION STAGE – DISCUSSION OF PARAMETERS

2.1 Chloride ingress

Different empirical prediction models for chloride ingress into concrete exist (DuraCrete 1998). However, they are all based on Fick's 2nd law of diffusion but may require different input data. The solution of this differential equation may be given as:

$$C(x, t) = C_0 + (C_s - C_0) \cdot \operatorname{erfc}\left(\frac{x}{2 \cdot \sqrt{D(t) \cdot t}}\right) \quad (1)$$

where,

$C(x, t)$:	chloride concentration at depth x at time t
C_s :	chloride concentration on the exposed surface (achieved best-fit value and not the true surface value)
C_o :	initial chloride concentration in the concrete
t	exposure time
x	depth
erfc	the error function complement
$D(t)$	diffusion coefficient

In this equation the calculated surface chloride concentration C_s represents the environmental loading and the chloride diffusion coefficient, $D(t)$, characterises the materials ability to withstand the ingress of chlorides.

The original solutions of the differential equation treated these parameters as time independent. More recent research indicates that both these parameters have some variation in time. However, for exposure time longer then 2-5 years sufficient accuracy may be achieved by treating the surface chloride concentration as time independent.

The calculated surface chloride concentration depends on the microclimate, such as distance to seawater, leeward-luward effects, and geometrical layout resulting in local differences in accumulation of chloride ions (e.g. splash zones). However, as illustrated in figure 2 the scatter in the data is often fairly high. The corresponding statistical data for surface chloride concentrations are listed in table 1. (Hofsøy et al. 1999). It may also be observed that e.g. data on surface chloride concentration reported by McGee (1999) for bridges in Australia is supporting or confirming these observations for quays.

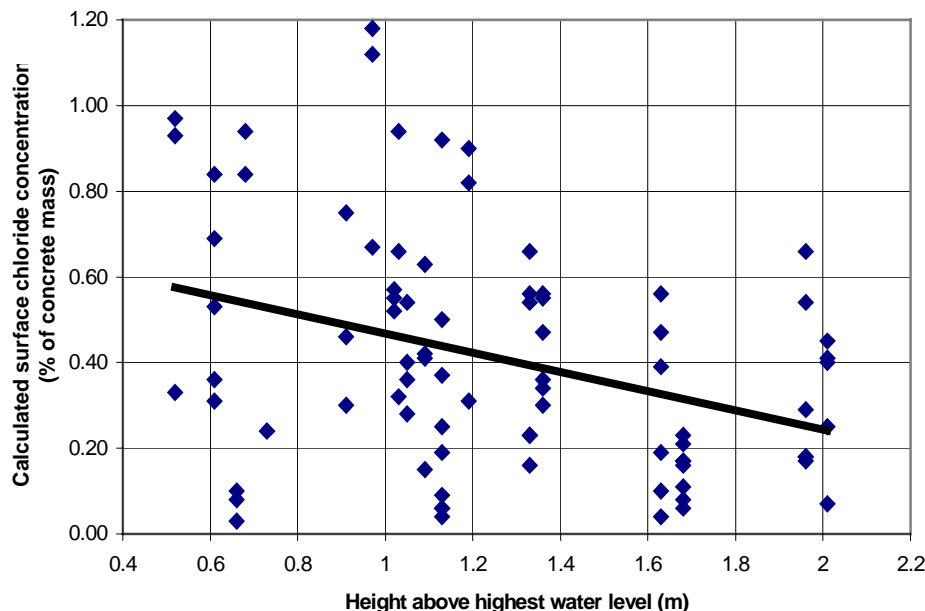


Figure 2: Surface chloride concentration above highest high water level determined from chloride profiles measured on different Norwegian quays and jetties (Hofsøy et al 1999)

Table 1: Statistical data for surface chloride concentration for Norwegian quays and jetties (based on Hofsføy et al. 1999)

Structural parts	No of data	Chloride content (% wt of concrete)		
		Mean	Stand.dev.	CoV
Deck slab				
All data	84	0.41	0.28	67 %
Data up to 1.4 m				
Above SWL	59	0.48	0.29	60 %
Deck beam				
All data	101	0.63	0.30	48 %
Data up to 1.4 m				
Above SWL	38	0.50	0.26	51 %

The chloride diffusion coefficient should on the other hand be treated as time dependent. It has been confirmed both in laboratory testing and by in-situ testing that this resistance is improved over time. A commonly used expression for the time dependent diffusion coefficient is:

$$D(t) = D_0 \left(\frac{t_0}{t} \right)^\alpha \quad (2)$$

where D_0 is a measured reference chloride diffusion coefficient at the age t_0 . The α exponent governs how fast the diffusion coefficient is improved over time. The decrease of the diffusion coefficient with age is due to a combined effect of hydration of the cement and all other mechanisms acting in the field as ion exchange takes place between concrete and seawater.

The aging factor α is proven to be a governing parameter in the service life prediction. However, data for this parameter are scarce. Figure 3 shows measured in-situ diffusion coefficients on quays and jetties with different ages. An α -factor of 0.3 is indicated for concrete with w/c less than 0.6. Somewhat higher values are reported for blastfurnace slag cement. The α -value is also found to be higher in the submerged part of the structure than in the tidal/plash zone (DuraCrete 2000).

In a design phase the concrete resistance against chloride penetration should be measured in the laboratory by e.g. a bulk diffusion test started at 28 days and lasting 35 days. But here a transition from laboratory conditions to in situ condition must be included. This problem may be solved by introduction of a transition parameter, k_{tm} , giving that $D_0 = k_{tm} \cdot D_{tm}$ where D_{tm} is the measured laboratory chloride diffusion coefficient by the selected procedure, ref. DuraCrete (1998 and 2000). The parameter k_{tm} will then obviously be dependent upon measurement procedure, microenvironment for the actual structural component, curing and concrete composition. Incorporating this into Eq.(2) gives:

$$D(t) = k_{tm} D_{tm} \left(\frac{t_0}{t} \right)^\alpha \quad (3)$$

A set of relevant parameters for the proposed model is given in Table 2.

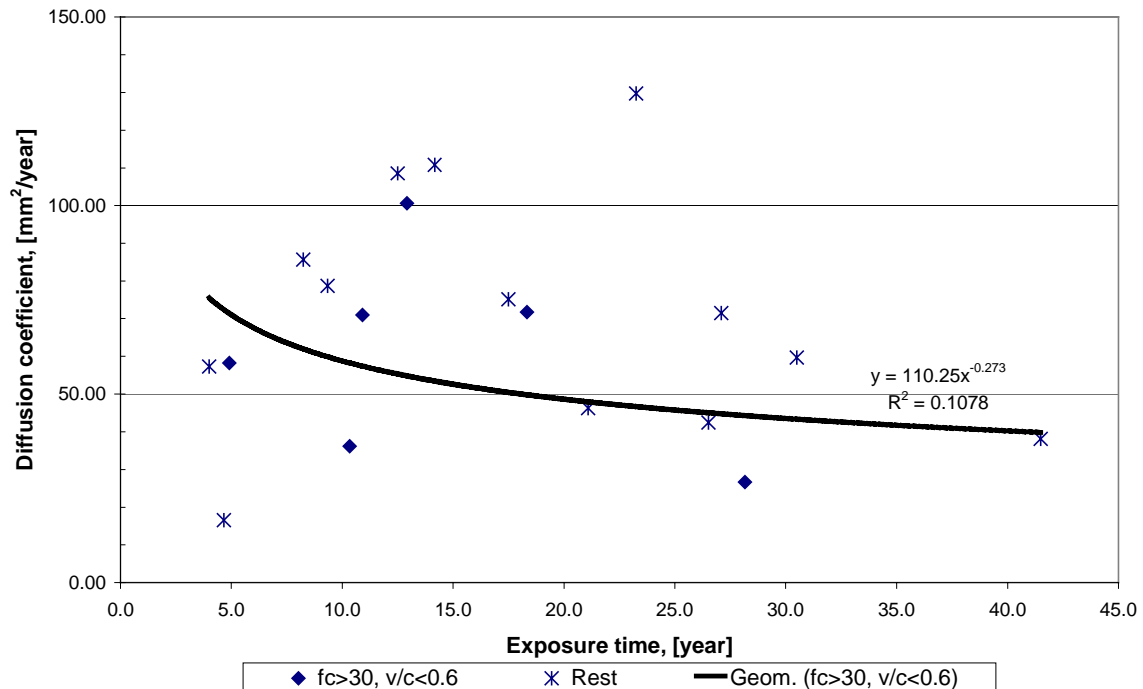


Figure 3: Diffusion coefficients measured on quays and jetties as a function of exposure time. The curve fit is done on data where strength is above 30 MPa and w/c is less than 0.6. (Hof-søy et al 1999)

Table 2: Parameter range of the diffusion coefficient model for two typical mixes of concrete (Larssen 2001)

Parameter	Concrete no 1	Concrete no 2
	moderate hostile environment	hostile environment
w/b ratio	0.45-0.55	0.40 – 0.42
Binder [kg/m ³]	325-375 cement	>350 cement and 0-5 % silica
Bulk diffusion (at 28 days) [10 ⁻¹² m ² /sec]	15 - 25	3 – 9
Transition parameter k_{tm}	0.9 – 0.6	0.9 – 0.6
Age factor α	0.1 – 0.4	0.4 – 0.6

2.2 Onset of corrosion – Chloride threshold value

The corrosion process starts (onset of corrosion), when the chloride concentration at the level of the reinforcement is higher than a critical value, C_{cr} :

$$C(x, t) \geq C_{cr} \quad (4)$$

This threshold level for chlorides is determined by a complex interplay of many factors:

- source of contamination (internal/external)
- condition of the steel and the steel/concrete interfacial zone
- concrete composition (binder type, binder content, water/binder ratio etc.)
- cover depth
- cracking (not induced by corrosion)
- exposure environment (moisture and oxygen availability, temperature, carbonation, sulphates)

In practice, it may not always be clear which factors are operating or predominant and a range of values have been reported in the literature. At present the chloride threshold level is maybe best considered in terms of associated corrosion risk. For temperate climates, Browne (1982) has suggested a risk classification as given in Table 3. These recommendations are broadly consistent with data for bridges both in UK and Scandinavia.

Table 3: Corrosion risk classification at different chloride threshold levels (Browne, 1982)

Risk of Corrosion	Chloride (% wt of cement)	Chloride (% wt of concrete) *
Negligible	< 0.4	< 0.07
Possible	0.4 – 1.0	0.07 – 0.17
Probable	1.0 – 2.0	0.17 – 0.35
Certain	>2.0	> 0.35

*) Based on 400 kg cement/m³

2.3 Probabilistic modelling

A deterministic way of calculating service life is by using the mean values or fixed characteristic values of the relevant parameters (concrete cover, surface chloride concentration, diffusion coefficient at different age, and critical chloride concentration). However, this type of calculation does not include the obvious uncertainty of the various parameters in a consistent manner.

In order to include the uncertainty of the various parameters in a consistent manner, probabilistic modeling must be utilized. Probabilistic modeling of the deterioration mechanisms has gained strong momentum during the past few years (DuraCrete 1999). This opens the possibility of using service life design methods being similar to the methods behind the well-established **load-and-resistance-factor-design** method used for structural calculations.

The major difficulties related to the use of probabilistic modelling of the deterioration mechanisms are connected to the lack of good relevant data. In order to achieve reliable results from the computations the applied uncertainty of the various parameters must be quantified. Generally a huge amount of data is available. The challenge is to sort out the reliable part of the data and to organise these in order to use them for probabilistic calculations. Up till now there have existed very scarce data for this purpose.

Probabilistic modeling uses the principles of limit states and structural reliability. In structural terms, the failure of an element occurs when the load effect (S) exceeds the resistance (R). Reliability can thus be expressed as a probability of failure (p_f) or by the 'reliability index' (β), defined:

$$p_f = Pb(R - S \leq 0) = Pb(g(R, S) \leq 0) = \int_{g(R, S) \leq 0} f_{RS}(r, s) dr ds = \Phi(-\beta) \quad (5)$$

where

- $f_{RS}(r, s)$ is the simultaneous probability density function of the stochastic variables R and S
- Φ is the standard normal distribution function
- $g()$ is the 'limit state function' of the of the stochastic variables [which is equal to R-S in this case],

Utilising this concept for chloride ingress in concrete means that the load effects are those of chloride penetration and the resistance is the concrete cover to reinforcement.

For service life calculations based on onset of corrosion, the probability of failure becomes the possibility of the chloride concentration at the reinforcement exceeding the critical chloride concentration at the time t. The limit state function may then be defined as the difference between the critical chloride concentration and the calculated chloride concentration at the reinforcement:

$$g(X) = C_{cr} - C(x, t) \quad (6)$$

where X is a vector of the statistical parameters as diffusion coefficient, surface chloride concentration, concrete cover etc.

3 SERVICE LIFE PREDICTION – AN EXAMPLE

Application of the probabilistic methodology described above is relevant for structures in a marine environment that should have specified life length like bridges and jetties. In this paper a rather large reinforced concrete jetty is used as an example. Results are just as relevant for concrete bridges.

The structure is to be designed for a service life of 50 years. The target service life is defined as the time to onset of corrosion. Based on this definition an acceptance limit for onset of corrosion is given by the owner as 10 %. The structural system of the jetty is a beam-slab type solution with concrete piles resting on rock surface, as illustrated in principle in Figure 4.

The structure may be divided into the following structural parts:

- vertical support system
- horizontal support system
- deck beams
- deck slab
- fender beam

In order to get an optimal design with respect to service life different strategies should be selected for different structural parts, as detailed in Markeset (2000).

Concrete piles with permanent steel casing are found to be a very durable solution for the vertical support system. Stainless steel reinforcement is used in critical zones/areas with respect to durability and safety, i.e.:

- tie back anchor slab
- retaining wall
- joint between tie back anchor slab and deck
- fender beam

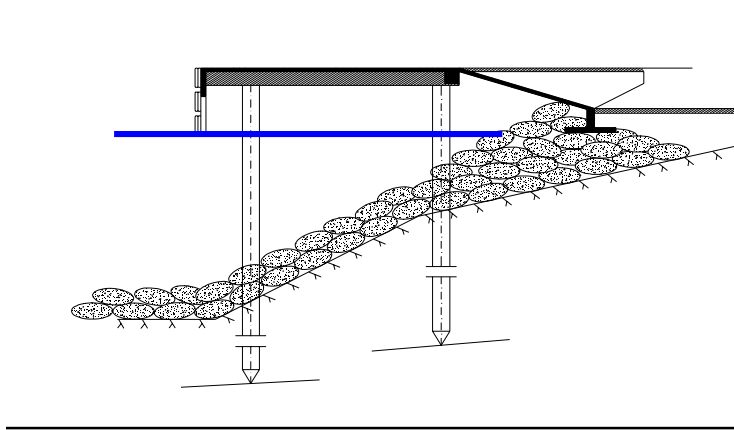


Figure 4: Principle section of the reinforced concrete jetty used for the example of service life calculation

For the remaining parts of the structure, required cover thickness and concrete quality is determined based on the probabilistic model presented above.

3.1 Sensitivity of the ageing factor α

The effect of different concrete quality would be reflected in the parameter values for the diffusion coefficient. Calculations are here presented for one set of diffusion coefficient parameters or one concrete quality.

In order to study the effect of the uncertainty of the parameters defining the time dependent diffusion coefficient, i.e. D_0 and α , an additional study is performed. The results of this study are illustrated in Figure 5.

Only the parameters D_0 and α are treated as statistical variables. The remaining parameters are taken as:

- surface chloride concentration of 1.0 % of concrete weight
- critical chloride concentration of 0.10 % of concrete weight

The parameters D_0 and α are both taken as normal distributed with the following set of statistical parameters:

- D_0 has a mean value of $7.0 \cdot 10^{-12} \text{ m}^2/\text{s}$ and a standard deviation of $1.05 \cdot 10^{-12} \text{ m}^2/\text{s}$ giving a coefficient of variation, CoV (standard deviation/mean value), of 15 %
- α are investigated for two sets of parameters, the first having a mean value of 0.4 and standard deviation of 0.06 or 0.04 (CoV 15 % and 10 %) and the second set having a mean value of 0.6 and standard deviation of 0.09 or 0.06 (CoV 15 % and 10 %)

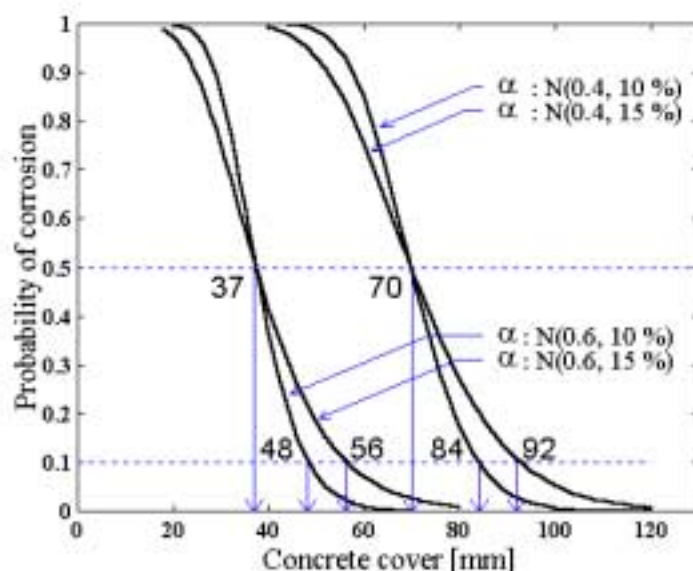


Figure 5: Calculated concrete cover for different mean values and CoV of the time dependent diffusion coefficient (both α and D_0 as statistical parameters). Results based on 50 years of exposure.

The probabilistic modelling gives, in addition to the analogous results from the deterministic modelling (50% probability), a probability for exceeding the given result. For a mean value of 0.6 for the α -parameter, the probability of corrosion after 50 years in service is 50 % for a 37 mm concrete cover. A probability of 50 % of not achieving the required service life is rather high. If this event should be treated as a SLS limit state, an acceptance limit of approx. 7 % should be used according to the Eurocode. For the calculations reported here, an acceptance limit of 10 % is chosen.

Using this acceptance limit, the necessary concrete cover increases from 37 mm to 48 mm if the CoV of the α -parameter is only 10 % and the mean value is 0.6. For a CoV of 15 %, the needed cover increases to 56 mm, i.e. an increase of more than 50 % from the deterministic value (50 % probability). Corresponding results are given for the mean value of 0.4 for the α -parameter in Figure 5.

Due to the uncertainties in the value of the aging parameter, α , the owner would not accept a higher value of this parameter than 0.4.

3.2 Statistical input parameters

The statistical parameters approved by the owner and used in the calculations of required cover thickness for the remaining part of the concrete structure are:

$$C_s = N(0.4, 60 \%) \text{ [% of concrete weight]}$$

$$D_0 = N(7.0 \cdot 10^{-12}, 15 \%) [\text{m}^2/\text{s}]$$

$$\alpha = N(0.4, 15 \%)$$

$$x = \text{LN}(x, 10) [\text{mm}]$$

where N indicate a normal distribution statistical model and LN a lognormal model.

For the critical chloride concentration reliable statistical data are not readily available. Due to that two deterministic values are selected for the calculations:

$$C_{cr} = 0.05 [\% \text{ of concrete weight}]$$

$$0.10 [\% \text{ of concrete weight}]$$

3.3 Results from the service life calculation

Based on these data a probabilistic calculation of required concrete cover was performed. The results of these calculations are shown in Figure 6. With a probability of 50% for initiation of corrosion the needed concrete cover varies between 50 and 66 mm for a service life of 50 years. This corresponds to the deterministic results.

For the given acceptance limit (probability of corrosion initiation) of 10 % the cover thickness needed for 50 years service life becomes 75 and 93 mm for a critical chloride concentration of 0.10 and 0.05 %, respectively. For a 100 year design service life the corresponding cover thickness becomes 92 mm and 115 mm respectively.

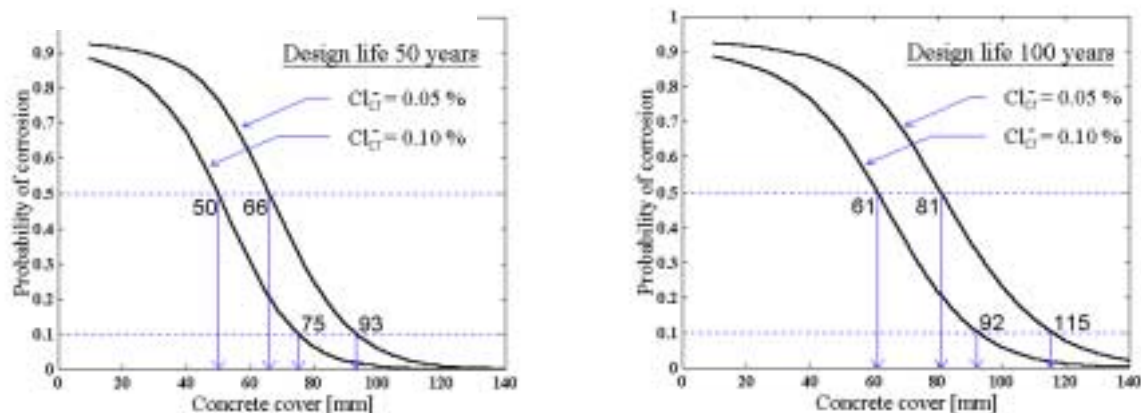


Figure 6: Required concrete cover for service life of 50 and 100 years for the concrete jetty in the example

The sensitivity of the critical chloride concentration C_{cr} is clearly illustrated by the following observations:

- If the critical chloride concentration is 0.05 % the required cover thickness becomes 93 mm for achieving the target service life of 50 years.
- If the critical chloride concentration is 0.10 % a cover thickness of 93 (92) mm gives 100 years service life.

From this it is evident that C_{cr} is a value needing much more attention than recognized at present. C_{cr} shall be investigated for different types of cement, concrete mixes, and for different types of environments.

4 DURABILITY MONITORING AND PREVENTIVE MAINTENANCE

As presented in the previous Section it has been recognised that the rate of chloride penetration (diffusion coefficient with ageing factor α) and the local chloride threshold value for corrosion initiation (C_{cr}) constitute the two most important parameters.

Therefore, it is essential to determine these values as reliably as possible. Present day research has had considerable difficulties in determining reliable in-situ values for the time dependent diffusion coefficients and in particular in determining the corrosion threshold values. This is mainly due to the fact that testing focusing on a reliability based treatment of the results have only come into focus during the past few years.

4.1 Corrosion sensors

In particular, the threshold value is a parameter, which has not received much attention when investigating existing structures. Installing corrosion sensors in existing structures exposed to chloride environments is one very practical means of determining the corrosion threshold value in an actual structure. Proprietary corrosion sensors of the type illustrated in Figure 7 seem to be able to provide valuable information on the threshold value in a given structure.

The corrosion sensors constitute six separate thin steel rings spaced at 10 mm and mounted in a stainless steel cylinder in such a way that they are electrically isolated from each other but wired up to a socket at the end surface, see Figure 7. The sensor is placed in a hole drilled into the concrete at the place selected for monitoring. The cylinder guiding the steel rings can be compressed longitudinally thus squeezing the steel rings tightly against the concrete surface. The uncarbonated and chloride free concrete will passivate the steel rings as it also does with the steel reinforcement cast into the concrete.



Figure 7: Mounting of proprietary corrosion sensors in existing quays. The picture to the right shows the sensor, a temporary micro-amp meter and the small titanium pin as cathode placed just above the instrument. The system is a further development from the system in Schiessl and Raupach 1992.

However, when chlorides in sufficient quantity penetrate to the level of one of the rings depassivation will occur and corrosion may take place on this ring. Close to the sensor a small platinised titanium pin is pressed into a small drilled hole in the concrete, see Figure 7, just above the measuring instrument. When linked electrically to the steel rings his noble metal will provide a strong driving force for a corrosion current when depassivation has occurred. If the concrete passivates the steel no current will flow. By linking the different rings of the sensor with the coated titanium pin through a micro-amp-meter the corrosion current can be measured, and the depth of the depassivation front can be determined within the 10 mm spacing of the rings.

The particularly valuable information, which can be gained through such sensors, are the following:

- **General:** The sensor records the depth of penetration of the critical chloride content able to depassivate steel in the actual concrete in the special local- or microenvironment of the specific structure. The penetration of the depassivation front is determined. Hence the major uncertainty related to determining the critical chloride concentration is eliminated.
- **Chloride threshold value:** By mounting the sensor in a structure where chlorides already have penetrated some way into the concrete cover, the actual level of the critical chloride concentration can be determined. This can be achieved by comparing the detailed chloride profile in the core from the hole cored for the sensor with the level of corrosion currents for each sensor ring measured shortly after installation.
- **Residual service life updating:** By taking sensor readings as part of a regular inspection routine, say each half-year or so, the rate of chloride penetration can be determined with time, and updating of the assumed chloride diffusion coefficient - or of the value of the ageing factor α - can be made. This will then provide data for an updating of the residual service life of the structure.

These sensors represent a new development of similar ladder type sensors developed a decade ago and used for monitoring new structures. They shall be placed in the cover and cast into the structure together with casting of the structure.

Three existing quays aged 37, 18 and 12 years respectively, have been monitored with the special corrosion sensors in order to determine the values of the two critical parameters in marine environment, see Figure 8. The concrete in all three structures is based on Ordinary Portland Cement, but with some microsilica added to the concrete in the youngest quay.

It is the intention to utilise such information as feed-back data for further improving the service life designs of new structures as well as to optimise the operation, maintenance and repair costs throughout the lifetime of the structure, through a rational life cycle cost optimisation.



Figure 8: Installation of corrosion sensors in Norwegian quays, see also Figure 7.

It is the overall intention to evaluate the potentials of using such corrosion sensors placed in parts of structures exposed to chloride containing aggressive environments where access for inspection, maintenance and repair is difficult or not possible. The benefits should be a noticeable reduction in needed inspection and testing activities and reduced costs.

5 CONCLUSIONS

The following conclusions can be drawn from the above investigations and calculations:

- **The ageing factor, α** , modifying the apparent diffusion coefficient is a critical value in determining the rate of chloride penetration into concrete. The value of α depends on, among others the cement type, the concrete mix and the environmental exposure. The chloride penetration is very sensitive to the choice of this value, and caution shall govern the selection of α in each individual case. The determination of this value warrants considerable attention within research and in practical investigations.
- **The critical chloride concentration, C_{cr}** , triggering corrosion (the threshold value) is another very critical parameter with high sensitivity with respect to forecasting corrosion initiation. Also this value warrants additional attention. Corrosion sensors mounted in existing structures, with chlorides already penetrating the concrete cover, may be one means of determining insitu the threshold value for individual structures. This is an area already being investigated in detail. However, the influence of the electric resistivity of the concrete on the rate of corrosion is equally an issue needing further detailed investigation.
- **Reliability based service life design**, considering the uncertainties associated with the governing parameters seems to become more and more valuable as basis for design new structures for required durability performance, and for upgrading the service life calculation of existing structures.
- **The load-and-resistance-factor-design** approach seems to be a valuable future formulation of the design for durability and performance.

REFERENCES

- Browne, 1982. Design prediction of the life of reinforced concrete in marine and other chloride environments, in *Durability of Building Materials*, Vol. 3, Elsevier Publishing Co., Amsterdam
- DuraCrete, 1998. *Modelling of Degradation*, The European Union – Brite EuRam III, Project No. BE95-1347, Probabilistic Performance based Durability Design of Concrete Structures, Report No. R4-5
- DuraCrete, 1999. *General Guidelines for Durability Design and Redesign*. The European Union - Brite EuRam III, Project No.BE95-1347, "Probabilistic Performance based Durability Design of Concrete Structures", Report No.T7-01-1
- DuraCrete, 2000. *Statistical Quantification of the Variables in the Limit State Functions*. The European Union - Brite EuRam III, Project No.BE95-1347, Probabilistic Performance based Durability Design of Concrete Structures, Report No.R9
- Hofsøy, A., Sørensen, S.I. & Markeset, G. 1999 *Experience from long term performance of quays and jetties* (in Norwegian). Report No. 2.2, National R&D Project "Durable Concrete Structures"
- Larssen, R.M. 2001. *Parametervariasjon i levetidsmodeller for marine betongkonstruksjoner* (in Norwegian) Dr.Ing. A.Aas-Jakobsen AS, Oslo, Norway.
- Markeset, G. 2000. *Cost Optimal Design, Construction and Maintenance of Concrete Quays and Jetties*. Presentation at the Seminars on "Concrete Remediation, Design & Long Life Solutions", Melbourne, Sydney, Brisbane and Auckland, May 2000. 27 pp.
- M^cGee, R. 1999. Modelling of durability performance of Tasmanian bridges. Proceedings of *The 8th International Conference on the Application of Statistics and Probability*, Sydney, Australia
- Schiessl, P. and Raupach, M., 1992. Monitoring system for the corrosion risk of steel in concrete structures. *Concrete International* V. 14, No. 7, July 1992, pp 52-55.

3 ENVIRONMENTAL ACTIONS

ORIGINAL QUANTIFICATION OF THE ENVIRONMENTAL PARAMETERS IN THE DURACRETE CHLORIDE INGRESS MODEL

(from chapter 5 of DuraCrete work report BE95-1347/TG4/C)

.....

Anders Lindvall
PhD student
Lars-Olof Nilsson
Professor, PhD
Dept. of Building Materials
Chalmers University of Technology
S-412 96 GÖTEBORG
SWEDEN
E-mail: lindvall@bm.chalmers.se

ABSTRACT

Literature data on chloride ingress was collected and compared with the DuraCrete Chloride Ingress Model. By regression analysis the environmental parameters in the model were statistically quantified to give a statistical distribution, a mean value and a measure of the scatter for each parameter.

To make a good quantification of environmental parameters, observations from different environments on the same concrete, cured under the same conditions, must be used. That kind of data is, however, not available from any of the observations in the present chloride-ingress database. In the quantifications of the different environmental parameters large differences in the result have been observed, mainly depending on the variations in the methods used by each reference-source.

Keywords: concrete, chloride, models, environments,

1 INTRODUCTION

In Task 4 of DuraCrete a statistical quantification of the parameters in the design models, which have been chosen for further investigation within Task 2, was made. In this paper some of the work done by Chalmers University of Technology is presented. The work involved statistical quantification of the environmental parameters in the carbonation and chloride ingress models. Only chloride is dealt with in this paper, limited to marine environments.

To make the statistical quantification a database has been established within Task 4. The data in the database is taken from the following different sources:

- Literature data, both laboratory and field data.
- Unpublished data (provided from the partners in the DuraCrete-project), both laboratory and field data.
- Data produced within the DuraCrete-project, mainly laboratory data.

In the statistical quantification the following influencing parameters are also considered, besides the time-dependencies:

- Environmental influences.
- Material influences.
- Execution effects.

2 DETERIORATION MODEL

The DuraCrete Chloride Ingress Model is based on the traditional error function solution to Fick's 2nd law, with a time dependent apparent diffusion coefficient

$$C_x = C_{SN} \cdot \operatorname{erfc} \left(\frac{x}{2 \cdot \sqrt{k_{e,Cl} \cdot k_{t,Cl} \cdot D_{ce,m} \cdot \left(\frac{t_m}{t} \right)^{n_{Cl}} \cdot t}} \right) \text{ (wt-\%)} \quad (1)$$

However, the application of this model is different from most previous cases. A material parameter $D_{ce,m}$ is to be measured in an independent test, at an age of t_m , and used for predictions or selected in a design procedure. Parameters $k_{e,Cl}$ and $k_{t,Cl}$ give the effect of curing different from the test procedure and test results from another test method than the specified.

The environmental parameters in the chloride ingress model are:

- n_{Cl} . A parameter, which takes the influence of age on the effective diffusion coefficient into account. The factor is divided in one part influenced by the material and one part influence by the environment.
- $k_{e,Cl}$. A parameter, which considers the influence of the environment on the effective diffusion coefficient at defined compaction, curing and environmental conditions.
- C_{SN} . The surface chloride level. This is a combined material and environmental factor.
-

3 STATISTICAL QUANTIFICATION

The statistical quantification of the environmental parameters is based on the data available in the database established within the DuraCrete project.

The statistical quantification of the environmental parameters is made in three different ways:

- The quantified parameter values are given as a statistical distribution with mean value and standard deviation. The data available in one class in the database are used for the quantification.
- The quantified parameter values are given as a function of time. A Bayesian regression analysis is used to statistically quantify the relationship. The data available in one class in the database are used for the quantification.
- The quantified parameter values are given as a function of two (or more) material or environmental parameters. A multiple regression analysis is used to statistically quantify the “constants” in the function.

Required data

Each of the parameters can be quantified from observations where all parameters except one at a time are kept constant. If more than one parameters is varying, the quantification can be

made if the other parameters are quantified separately or, if non-systematic data are available, with a multiple regression analysis.

Required observations are:

- Achieved diffusion coefficients, D_a , for the same concrete in one exposure environment (Marine environment: submerged, tidal, splash and atmospheric) observed at at least three different times.
- Surface chloride concentrations for the same concrete in different exposure conditions (Marine environment, submerged, tidal, splash and atmospheric) observed at different times.

Available data

In order to get data as a foundation for the quantification, it was agreed in the DuraCrete-project to establish a database. In the database data from field and laboratory exposure are collected, mainly from literature but also some data from observations made in the DuraCrete-project.

In the database the reference sources given in Table 1 are used.

Table 1: The available data in the database for the marine environment.

Marine-Submerged	Marine-Tidal	Marine-Splash	Marine-Atmospheric
Andersen	Bijen	Andersen	Andersen
Gjorv	Gedge	Bamforth	Sörensen
Gorley	Hansen et al	Bijen	Jägermann
Maage and Hella	Lea and Watkins	Gautefall	Kamiya
Makita	Liam et al	Liam et al	Macecknie
Osborne	Macecknie	Maage and Hella	Mustafa et al
Polder	Mangat et al	Macecknie	Nagano
Roy et al	Matthews	Nagano	Oshiro et al
Sakoda	Osborne	Polder	Roy et al
Sandberg (1998)	Roy et al	Sagues et al	Sagues et al
Sandvik	Sagues et al	Sandberg (1998)	Sakado et al
Takeda	Tang (1997)	Sandvik et al	Sandberg (1998)
Tang (1997)	Taywood	Sasaki	Sandvik et al
Taywood	Thomas and Malt	Suzuki et al	Statens Vegvesen
	Thomas et al	Takeda	Takeda
	Uji	Tang (1997)	Tang (1997)
	Vennesland et al	Taywood	Taywood
		Uji	Uji
		Vassie	

Classification

There is only a limited amount of data available in the database. To be able to make a reasonable quantification, a classification of the available data has been made. In the classification only field data is taken into account.

The classification of the data available in the database is made in the following four steps:

- Type of Binder.

- Exposure environment.
- Water-Binder ratio.
- Quality check of data.

The first step in the classification is to subdivide the data available in the database depending on the binder used. The following types of binders are included in the database:

- Portland Cement (OPC).
- Portland Cement with Blast Furnace slag (GGBS).
- Portland Cement with Fly Ash (PFA).
- Portland Cement with Silica Fume (SF).
- Binder not recorded. This class is not included in the classification.

The second step in the quantification is to divide the data available in the database into classes depending on the exposure environment. In the DuraCrete-project the following marine environmental classes have been used:

Marine environment

- Submerged zone.
- Tidal zone.
- Splash zone.
- Atmospheric zone.

In the third step, the data were classified with respect to w/b intervals, i.e. 0.40-0.45.

The fourth step in the classification is the check the quality of the data in the different classes. The quality-check means that data, which differ a lot from the expected values, are removed from the database. The quality check is performed in two different ways; either by examining if the mean value of the chosen distribution is too small or large or if the standard deviation of the chosen distribution are too large.

Quantification

Age factor

In the chosen deterioration model the material is characterised by the achieved chloride diffusion coefficient, D_a . It has been shown that the resistance against chloride penetration increases with age. This age-dependency of the diffusion-coefficient is not only depending on the concrete composition, but also on the environmental conditions.

The quantification is made in two steps:

1. A linear regression analysis is made to find the age-dependency of the achieved diffusion-coefficient. The regression analysis is made on data from one concrete-mix in one environment, where the diffusion coefficient is observed at at least three different times.
2. On the age-factors calculated with the regression analysis a statistical quantification is made, to find statistical distribution function of the age-factor. In the statistical quantification each binder and each environmental zone is treated separately.

The quantification of the age factor is made by expressing the diffusion coefficient as a function of the exposure time. This is done by applying a 10-logarithm on the expression under the square-root sign. The model presented in (2) is used for the quantification.

$$\log_{10}(D_a) = \log_{10}(k_{c,Cl} \cdot k_{e,Cl} \cdot k_{t,Cl} \cdot D_{ce,m}) + n_{Cl} \cdot [\log_{10}(t_m) - \log_{10}(t)] \quad (2)$$

From (2) a linear regression analysis is performed for each of the material classes. From this linear regression analysis, the offset, the regression parameter and the precision are calculated.

An example of a quantification is shown in Figure 1a.

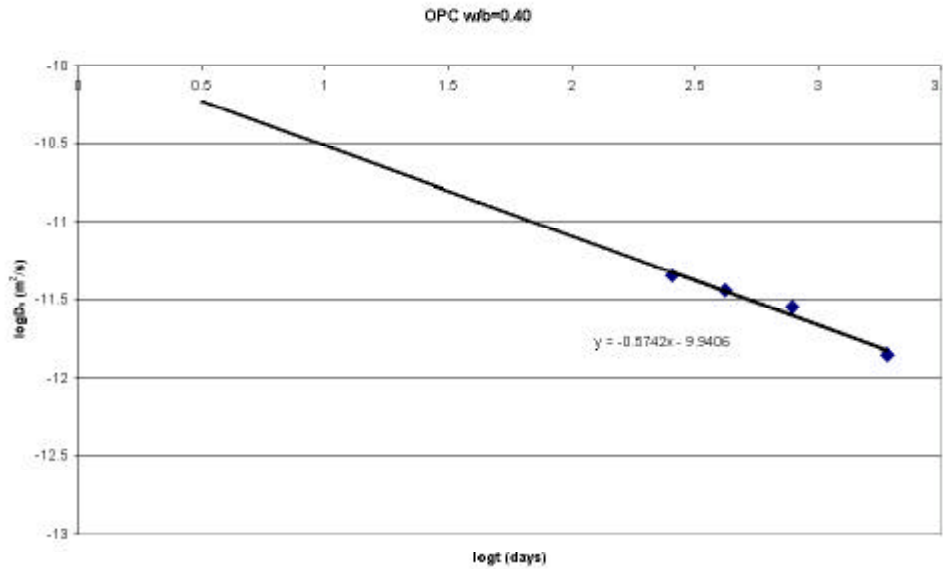


Figure 1a: The quantification of the age-factor. In this case the age-factor is equal to 0.574.

In Frederiksen et al (1997) the age-factor is expressed as a function of equivalent w/b. The intention in the DuraCrete-project is to use this approach but add an error-term, see (3).

$$\text{Age - factor} = \text{Offset} + A \cdot (w/b) + e \quad (-) \quad (3)$$

where *Offset* is an offset, *A* is a regression parameter and *e* is an error-term.

Environmental factor

To make the diffusion coefficient applicable in other environmental conditions as well, an environmental factor has been introduced in the model. The diffusion coefficient, $D_{ce,m}$, measured in the compliance test after 28 days, is used as a reference value. The quantification is made with (4), where S, Sp, T and A denote the Submerged, Splash, Tidal and Atmospheric zones.

$$k_{e,Cl} = \frac{D_{a,28}(S, Sp, T, A)}{D_{ce,m}} \quad (-) \quad (4)$$

The achieved diffusion coefficient after 28 days is calculated with (16).

$$D_{a,28} = 10^{Offset - n_{Cl} \cdot \log(28)} \quad (\text{m}^2/\text{s}) \quad (5)$$

where $Offset = \log[k_{e,Cl} \cdot k_{e,Cl} \cdot k_{t,Cl} \cdot D_{ce,m}]$ and n_{Cl} is the age factor, determined with a Bayesian Regression Analysis. In Figure 1b an example of how $D_{a,28}$ is determined is shown.

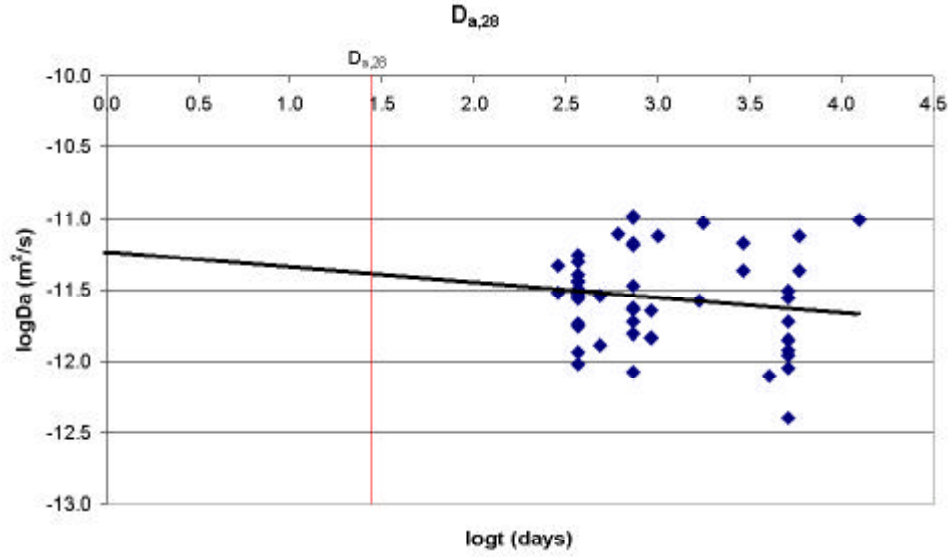


Figure 1b: Example of determination of $D_{a,28}$. In this case $D_{a,28}$ is equal to $8.05E-12$

Surface chloride concentration

The quantification of the surface chloride concentrations is made with surface chloride concentrations expressed in weight-% per binder. The surface chloride concentration is described as a function of w/b and an error-term, see (6). This approach is used by Frederiksen et al (1997), where the surface chloride concentration is described as a function of an equivalent w/b .

$$C_{SN} = A \cdot (w/b)_{eqv} + e \quad (6)$$

The quantification is made in the following way:

- A Bayesian regression analysis is made to find a relationship between w/b and C_{SN} . Each binder and environment is treated separately.

An example of what a quantification can look like is shown in Figure 2.

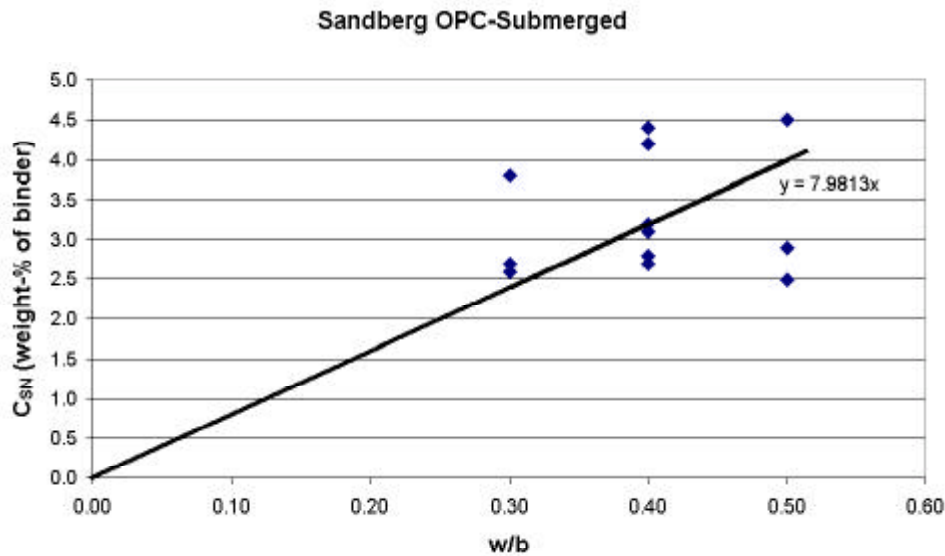


Figure 2: The quantification of the surface chloride concentration. In this case the regression parameter is equal to 7.98 and the standard deviation of the regression parameter equal to 0.58.

4 RESULTS OF QUANTIFICATIONS – MARINE ENVIRONMENT

In the following section the result of the final quantification in the marine environment is given. The complete quantification can be found in the Appendix of the DuraCrete report.

Classification

Age factor

The data used for the quantification of the age factor have been classified in such way that observations of the diffusion coefficient have been made for the same concrete-mix in the same environment at at least three different times. The classification ended up with the following result, see Table 2a (OPC-concrete), 6b (PFA-concrete), 6c (GGBS-concrete) and 6d (SF-concrete).

Table 2a: The classification used in the quantification of the age factor for OPC-concrete.

OPC - Submerged	OPC - Tidal	OPC - Splash	OPC - Atmospheric
Frederiksen et al (1997)	No data available	Taywood	Takeda
Sandberg (1998)		Sandberg (1998)	
Takeda		Takeda	
		Vassie	

Table 2b: The classification used in the quantification of the age factor for PFA-concrete.

PFA - Submerged	PFA - Tidal	PFA - Splash	PFA - Atmospheric
Sandberg (1998)	No data available	Taywood	No data available

Table 2c: The classification used in the quantification of the age factor for GGBS-concrete.

GGBS - Submerged	GGBS - Tidal	GGBS - Splash	GGBS - Atmospheric
Polder	No data available	Taywood Vassie	No data available

Table 2d: The classification used in the quantification of the age factor for SF-concrete.

SF - Submerged	SF - Tidal	SF - Splash	SF - Atmospheric
Frederiksen et al (1997) Sandberg (1998)	No data available	Frederiksen et al (1997) Sandberg (1998)	No data available

The final classification is given in Table 2e, where a subdivision is made in submerged, tidal, splash and atmospheric zones. In the table the number of available and used data is given. One set of data is observations of the diffusion coefficient for the same concrete in the same environment at at least two different times. Used data is observations of the diffusion coefficient at at least three different times.

Table 2e: The final classification of the data used for the quantification of the age factor, divided in different binders and environments. # denotes the number of observations used in the quantification.

Author	Binder	Env.	#
Given in Table 2a	OPC	Submerged	13 (7)
Given in Table 2a	OPC	Tidal	4 (0)
Given in Table 2a	OPC	Splash	19 (15)
Given in Table 2a	OPC	Atmospheric	6 (1)
Given in Table 2b	PFA	Submerged	2 (1)
Given in Table 2b	PFA	Tidal	9 (0)
Given in Table 2b	PFA	Splash	5 (3)
Given in Table 2b	PFA	Atmospheric	1 (0)
Given in Table 2c	GGBS	Submerged	2 (2)
Given in Table 2c	GGBS	Tidal	No data available
Given in Table 2c	GGBS	Splash	5 (5)
Given in Table 2c	GGBS	Atmospheric	1 (0)
Given in Table 2d	SF	Submerged	13 (10)
Given in Table 2d	SF	Tidal	No data available
Given in Table 2d	SF	Splash	18 (9)
Given in Table 2d	SF	Atmospheric	10 (0)

Environmental factor

The classification used in the quantification of the environmental factor is the original classification, but only OPC-concrete and GGBS-concrete are considered. A subdivision is made in submerged, tidal, splash and atmospheric zones. The classification is shown in Table 3.

Table 3: The classification of the data used in the quantification of the environmental factor.

Author	Binder	Env.	#
All data w/b=0.40	OPC	Submerged	51
All data w/b=0.40	OPC	Tidal	74
All data w/b=0.40	OPC	Splash	67
All data w/b=0.40	OPC	Atmospheric	19
All data w/b=0.50	GGBS	Submerged	11

All data mean the data available in the database established within the DuraCrete-project.

Surface chloride concentration

The classification used in the quantification of the surface chloride concentration is the original classification, but some of the data are excluded. Since the quantification is made in two steps, two classifications are made. The classification is shown in Table 4.

Table 4: The classification used in the Bayesian regression analysis of the surface chloride concentration in the marine environment. The tidal and splash zones are treated as one zone.

Author	Binder	Env.	#
Sandberg (1998), 5 years	OPC	Submerged	4
Sandberg (1998), 5 years	OPC	Tidal+Splash	4
Frederiksen et al (1997)	OPC	Atmospheric	8
All	PFA	Submerged	5
All	PFA	Tidal+Splash	23
All	PFA	Atmospheric	2
Polder	GGBS	Submerged	15
Taywood, t>6 years	GGBS	Tidal+Splash	6
All	GGBS	Atmospheric	2
Sandberg (1998), 5 years	SF	Submerged	6
Sandberg (1998), 5 years	SF	Tidal+Splash	6
Frederiksen et al (1997)	SF	Atmospheric	10

Age factor

The quantification of the age factor is made separately for each exposure environment and binder.

A division has been made in three different exposure zones:

- A submerged zone (S).
- A combined tidal and splash zone (T+Sp)
- An atmospheric zone (A).

In the quantification no significant correlation between the age-factor and the w/b was found, see Figure 3a (OPC-concrete), 8b (PFA-concrete), 8c (GGBS-concrete) and 8d (SF-concrete). Thus, a reasonable approach would be to quantify the age-factor without a w/b dependency.

It should be noticed that in Figure 3a and 3d some of the quantified age-factors have negative values, i.e. the diffusion coefficient increases with time. This is not in accordance with the theory, where the diffusion coefficient should decrease with time. A possible explanation for the negative age-factors could be differences between the methods used to calculate the diffusion coefficients at different times.

The final result of the quantification is given in Table 5¹. Each binder and environment is quantified separately and there is no w/b dependency. STATREL has been used for the quantification and the used method is the maximum likelihood method. For some of the binder and environments a statistical quantification was not possible due to lack of reliable data. For these materials and environments “expert opinion” have been used to make the quantification.

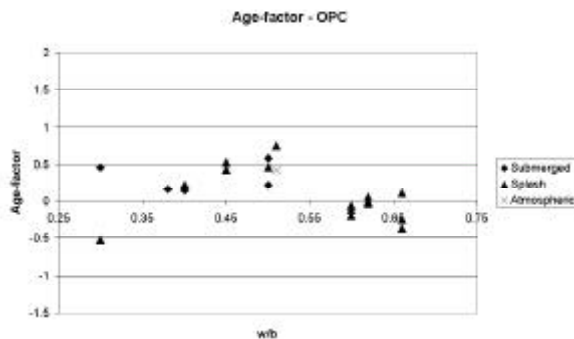


Figure 3a: The age-factor for OPC-concrete.

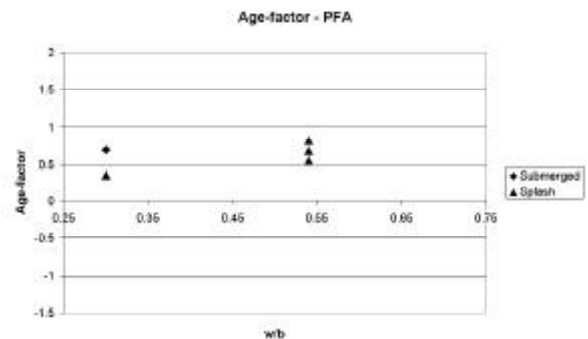


Figure 3b: The age-factor for PFA-concrete

¹ The result from this quantification differs from the result presented in the report “Statistical Quantification, Onset of Corrosion”. This difference may be caused by that the quantification made in that report is based on both field and laboratory data and only the submerged zone is covered.

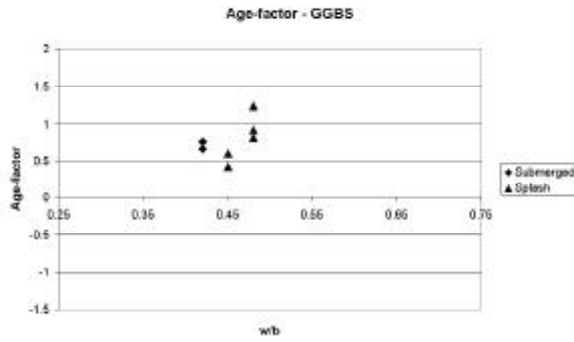


Figure 3c: The age-factor for GGBS-concrete.

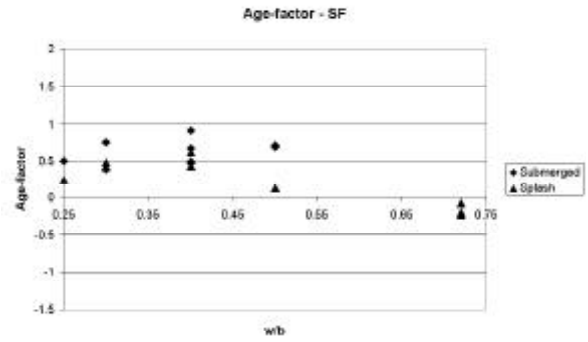


Figure 3d: The age-factor for SF-concrete

Table 5: The quantification of the age factor. The rows marked with grey are quantified from field-data.

Binder	Environment	Type of dist.	Mean	S. dev	a	b
OPC	Submerged	Beta	0.30	0.05	0	1
OPC	Tidal+Splash	Beta	0.37	0.07	0	1
OPC	Atmospheric	Beta	0.65	0.07	0	1
PFA	Submerged	Beta	0.69	0.05	0	1
PFA	Tidal+Splash	Beta	0.93	0.07	0	1
PFA	Atmospheric	Beta	0.66	0.07	0	1
GGBS	Submerged	Beta	0.71	0.05	0	1
GGBS	Tidal+Splash	Beta	0.80	0.07	0	1
GGBS	Atmospheric	Beta	0.85	0.07	0	1
SF	Submerged	Beta	0.62	0.05	0	1
SF	Tidal+Splash	Beta	0.39	0.07	0	1
SF	Atmospheric	Beta	0.79	0.07	0	1

In the Beta-function the first two parameters are the mean-value and the standard deviation. The two last parameters are the minimum and maximum in the data. In the chloride ingress-model chosen in the DuraCrete-project the minimum in the data is 0 and the maximum 1.0.

The age-factors for the OPC- and GGBS-concrete are given in Figure 4.

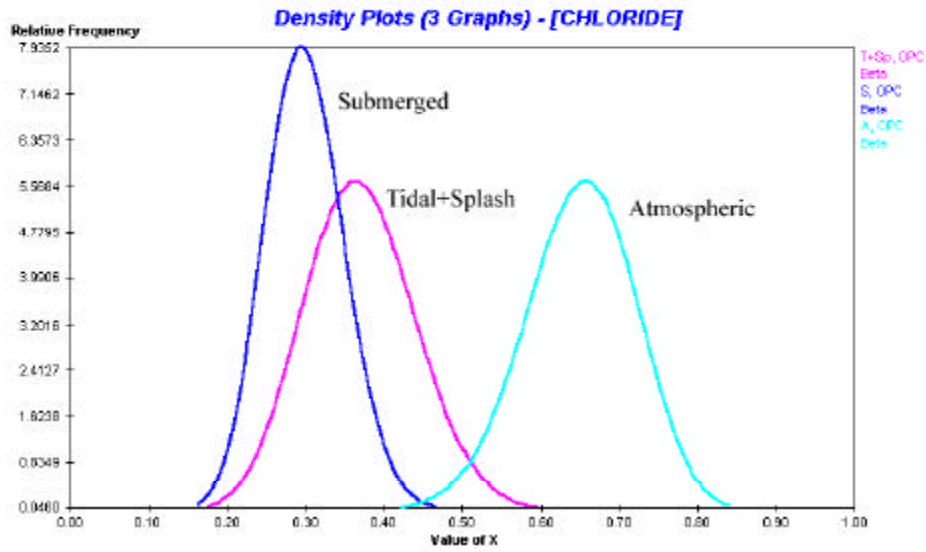


Figure 4a: The age-factors for OPC-concrete.

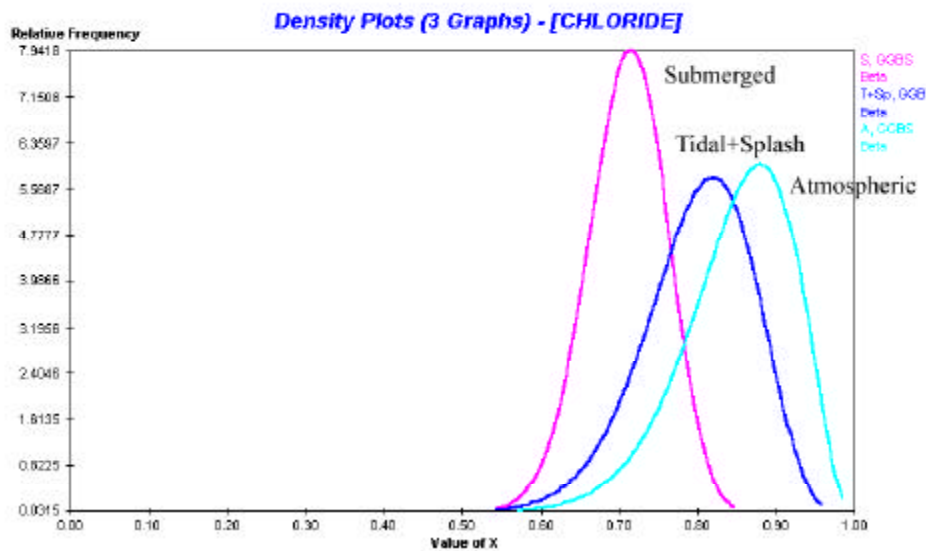


Figure 4b: The age-factors for GGBS-concrete.

Environmental factor

The quantification of the age factor is made in the four different exposure zones used in the quantification of the age factor, where the results from the compliance test is used as a reference value, i.e. $k_{e,Cl} = 1$. The quantification ended up with the results presented in Table 6 and Figure 5a and 10b. STATREL has been used for the quantification and the used method is the maximum likelihood method.

Table 6: The quantification of the environmental factor for OPC-concrete and GGBS-concrete. The rows marked with grey are quantified with field data.

Binder	Environment	Type of dist.	Mean	Standard dev.
OPC	Submerged	Gamma	1.325	0.223
OPC	Tidal	Gamma	0.924	0.155
OPC	Splash	Gamma	0.265	0.045
OPC	Atmospheric	Gamma	0.676	0.114
GGBS	Submerged	Gamma	3.877	1.292
GGBS	Tidal	Gamma	2.704	1.292
GGBS	Splash	Gamma	0.777	1.292
GGBS	Atmospheric	Gamma	1.978	1.292

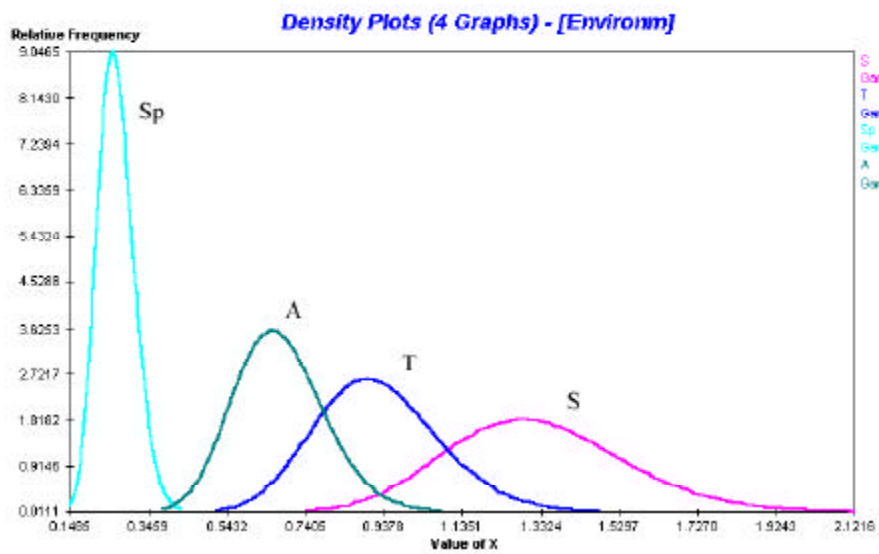


Figure 5a: The result of the quantification of the environmental factor for OPC-concrete.

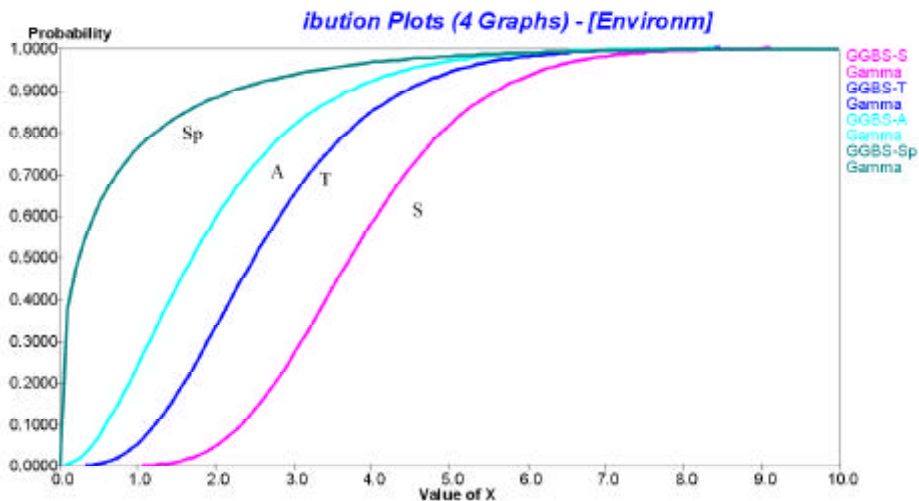


Figure 5b: The result of the quantification of the environmental factor for GGBS-concrete.

Surface chloride concentration

One has to consider that the chosen model for chloride penetration does not take observed time-dependencies of the notional surface chloride concentration into account.

It can be shown that there is a relationship between the concrete compositions, the amounts of binders and the surface chloride concentrations. Depending on how the classification of the data is made, this dependency is more or less obvious.

There is relationship between the surface chloride concentration and the type of binder used. If the data are classified in a more crude way (only by considering the different binders used) this dependency is more obvious.

The quantification of the surface chloride concentration in the DuraCrete-project is made in a similar way. The surface chloride concentration is assumed as a function of w/b and an error-term, see (18). This approach has also been used in Frederiksen et al (1997) where a relationship between the surface chloride concentration and w/b has been quantified. The regression parameter A was found equal to 3.667.

$$C_{SN} = A \cdot w/b + e \quad (18)$$

where A is a regression parameter and e is an error-term.

Using this approach the quantification of the surface chloride concentration ends with the result given in Table 7 and in Figure 6a (OPC-concrete), 6b (PFA-concrete), 6c (GGBS-concrete) and 6d (SF-concrete).

Table 7: The result of the Bayesian regression analysis made for the surface chloride concentration.

Binder	Env	Author	A	$sd^*(A)$	h	$sd(A)$
OPC	S	Sandberg (t=5 years)	10.348	1.231	2.971	0.714
OPC	T+Sp	Sandberg (t=5 years)	7.758	1.231	0.819	1.360
OPC	A	HETEK	2.565	0.881	6.106	0.356
PFA	S	All data	10.843	1.571	0.713	1.860
PFA	T+Sp	All data	7.464	0.421	1.772	0.316
PFA	A	HETEK	4.418	- ²	-	-
GGBS	S	Polder	5.059	0.615	0.863	0.662
GGBS	T+Sp	Taywood (t>5 years)	6.767	0.851	9.367	0.278
GGBS	A	All data	3.046	-	-	-
SF	S	Sandberg (t=5 years)	12.462	1.109	0.521	1.537
SF	T+Sp	Sandberg (t=5 years)	8.960	1.094	0.405	1.744
SF	A	HETEK	3.228	0.943	16.155	0.235

In Table 7 A is the regression parameter, h is the precision of the estimation and $sd^*(A)$ is the standard deviation from the Bayesian regression analysis. This standard deviation, however, is not taking the precision of the regression analysis into account. To get the true standard deviation, $sd(A)$, the standard deviation from the regression analysis has to be corrected. This is done by dividing $sd^*(A)$ with the squareroot of the precision, h .

² No statistical quantification possible, due to lack of data.

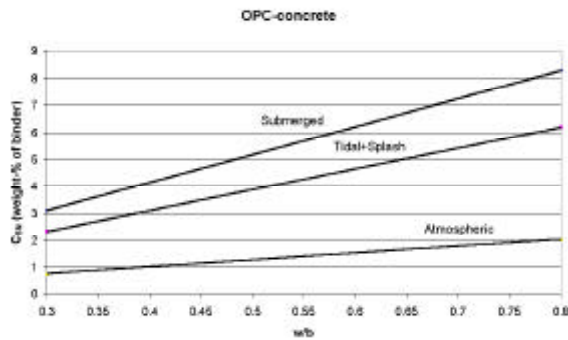


Figure 6a: The quantification of surface chloride concentrations for OPC-concrete

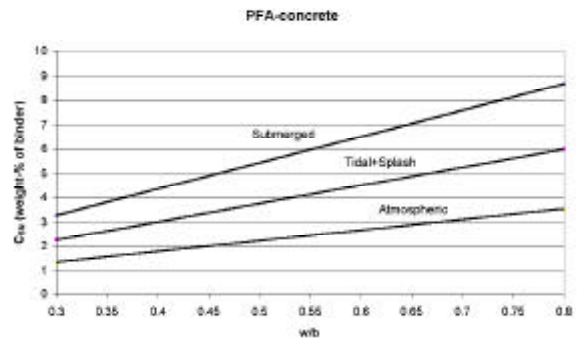


Figure 6b: The quantification of surface chloride concentrations for PFA-concrete

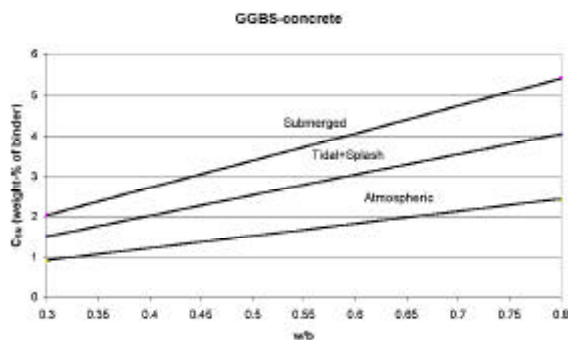


Figure 6c: The quantification of surface chloride concentrations for GGBS-concrete

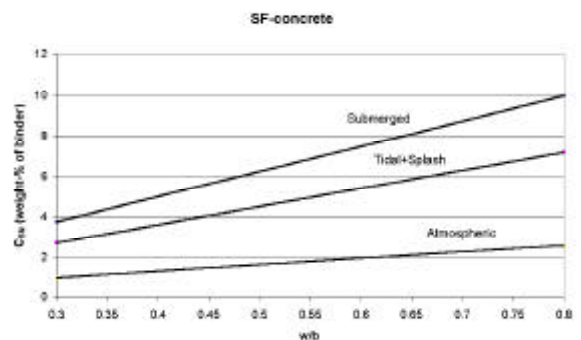


Figure 6d: The quantification of surface chloride concentrations for SF-concrete

CONCLUSIONS

The task of Chalmers University of Technology within Task 4 is to make a quantification of the environmental parameters in the design models. To make a good quantification of environmental, observations from different environments on the same concrete-mix cured under the same conditions. This is, however, not the case for any of the observations in the chloride-ingress database.

In the quantifications of the different environmental parameters large differences in the result have been observed, depending on the used reference-source. There are also differences depending on which parts of the data that are used. In the first quantification all data were included, ending with a very large scatter giving an uncertain end-result. In many cases this scatter is a result of differences between the reference-sources used. These differences are caused by:

- The used sampling-methods.
- The exposure site - laboratory or field exposure?
- The method used in the laboratory-analysis.
- The methods in evaluating the result from the laboratory-analysis.

Thus the quantification is not made on the influence from curing, environmental or material but on the differences between different reference-sources. A possible solution to this problem could be to introduce a "reference-source parameter" in the deterioration models. This parameter should cover the differences between different reference sources. To avoid this "reference source parameter" and make observations from different reference-sources comparable methods of observations should be standardised.

REFERENCES

- Andersen, A., Investigations of chloride penetration into bridge columns exposed to de-icing salt, Report No. 82, Danish Road Directorate, Copenhagen, 1997.
- Andersen, A., Unpublished data, Chalmers University of Technology, Department of Building Materials, Göteborg, 1996.
- CEB, New Approach to Durability Design – An Example for Carbonation Induced Corrosion, Bulletin d'Information 1997:238, Lausanne, 1997.
- Danmarks Meteorologiska Institut (DMI), Jordens Klima (The climate of the Earth), København, 1994. (in Danish)
- Harderup, E., Klimatdata för fuktberäkningar (Climate data for moisture calculations), Report 3025, Lunds University, Department of Building Physics, Lund, 1995. (in Swedish).
- Frederiksen, J.M., Nilsson, L.-O., Sandberg, P., Poulsen, E., Tang, L. & Andersen, A. HETEK, A system for estimation of chloride ingress into concrete. Theoretical background, Report No. 83, Danish Road Directorate, Copenhagen, 1997.
- Mejlbro, L., The complete solution of Fick's second law of diffusion with time-dependent diffusion coefficient and surface concentration, Durability of Concrete in Saline Environment, Cementa AB, Danderyd, 1996. pp. 127-158.
- Nilsson, L-O. & Rodhe, M., The CTH carbonation model – a micro-level model for carbonation in natural climate, New approach to durability design, CEB Bulletin No. 238, Lausanne, 1997. Appendix 2.
- Sandberg, P., Chloride initiated reinforcement corrosion in marine concrete, Report TVBM-1015, Lunds Institute of Technology, Department of Building Materials, Lund, 1998.
- Sørensen, B. & Maahn, E., Penetration rate of chloride in marine concrete structures, Nordic Concrete Research, Publication no. 1, The Nordic Concrete Federation, Stockholm, 1982. pp. 24:1-24:18.
- Tang, L., Chloride Penetration Profiles and Diffusivity in Concrete under different Exposure Conditions, Report E-97:3, Chalmers University of Technology, Department of Building Materials, Göteborg, 1997.
- WeatherDisc Associates, World Weather Disc (WWD), Seattle, 1994.
- Wierig, H-J., Long-time studies on the carbonation of concrete under normal outdoor exposure, Proceedings of the RILEM seminar on Durability of concrete structures under normal outdoor exposure, 26th-29th March 1994, Hannover, 1994. pp. 239-249.

PROBABILISTIC MODELING OF CHLORIDE SERVICE LIFETIME



Bernt J. Leira
Professor, Dr. Ing.
Dept. of Marine Structures
NTNU
N-7491 TRONDHEIM
NORWAY
E-mail: Bernt.Leira@marin.ntnu.no

ABSTRACT

The parameters relevant for prediction of service lifetime with respect to chloride ingress are associated with large uncertainties. Full-scale measurements for conditions which are as homogeneous as possible are in demand.

The present paper summarizes statistical distributions which are obtained based on measurements from the Gimsøystraumen bridge in Norway. A large number of chloride profiles are available, and for each of these the diffusion coefficient and surface concentration are estimated. Extensive measurements of concrete cover are also performed.

These probability distributions are subsequently employed as input to a prediction model for chloride concentration at the steel reinforcement. Since the input parameters are represented in probabilistic terms, the chloride concentration is also a stochastic quantity. Furthermore, introducing the critical chloride concentration on a similar form, the probability of exceeding the critical threshold is determined as a function of time.

Keywords: full-scale measurements, probabilistic, chloride, lifetime

1 INTRODUCTION

A large number of chloride profiles have been obtained from the Gimsøystraumen bridge which is located in the Northern part of Norway. For the superstructure profiles from 725 locations were collected, and for the columns sampling was performed for 168 locations, ref/1/. For each of the profiles, the corresponding diffusion coefficient

and the chloride surface concentration were estimated. Extensive measurements of concrete cover were also performed. (Note: The values for statistical values given herein may deviate slightly from those of ref/1/ due to further refinement of the chloride profile data in that report).

These probability distributions are subsequently employed as input to a model for prediction of chloride concentration at the steel reinforcement. As the input parameters are represented in probabilistic terms, the chloride concentration accordingly becomes a stochastic quantity. The critical chloride concentration is also introduced on a similar form. As the next step, the resulting probability that the concentration at the reinforcement exceeds the critical threshold is then determined as a function of time, ref/2/.

Parameter variations are performed with respect to the input statistical models. In particular, the effect of introducing a diffusion coefficient which varies with time is investigated.

2 PROBABILISTIC MODELING BASED ON FULL - SCALE MEASUREMENTS

For each of the three parameters that were measured or estimated based on the measurements (i.e. diffusion coefficient, surface concentration and concrete cover), the applicability of various analytical probability distributions were tested by plotting in different types of probability paper. A ranking was performed based on the regression coefficients. As an example, a summary of the results are shown in Table 1 for the diffusion coefficients obtained for the east side of the columns.

Table 1 Diffusion coefficient (Multiplication by 10^{-12} gives the values in m^2/s)

Prob. model	Regression line	Mean value	Standard deviation	Sample variance	R ²
Normal	$y = 1.6051x - 2.0384$	1.27	0.64	0.41	0.9815
Gamma	$y = 0.7388x - 0.6466$				0.7934
Gumbel	$y = 2.1481x - 2.1085$				0.9899
Weibull	$y = 2.3307x - 0.8316$				0.9948
Lognormal	$y = 1.9765x - 0.1641$				0.9809

As observed, the Weibull distribution gives the highest regression coefficient, R². The measured and analytical distribution functions as plotted in Weibull probability paper are compared in Figure 1. However, in general all the different distributions give quite high values for the regression coefficient.

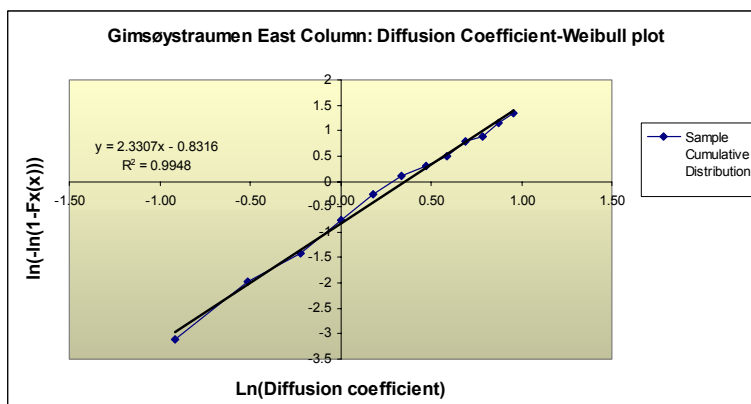


Fig. 1. Comparison between sample distribution function and fitted Weibull distribution for the diffusion coefficient, east side of columns.

A more direct comparison between the analytical model and the observed data is provided by considering the density function, i.e. the expected number versus the observed number of samples within each discretized interval. Such a comparison is provided by Figure 2. The overall comparison is quite good, but with some “oscillations” around the theoretical curve

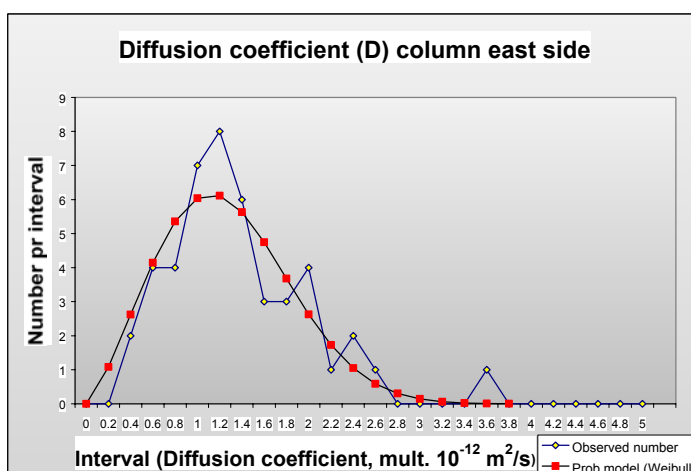


Figure 2. Observed versus predicted number of samples for the diffusion coefficient within each interval, east side of columns. Theoretical model is based on regression curve in Figure 1.

Although the Weibull model gave the best fit for this specific case, it is found that on the average, the lognormal probability distribution gives the best fitting. Furthermore, there are reasons of convenience for selecting this model when calculating the probabilistic lifetime distributions. Hence, the lognormal distribution is applied for the present calculations of lifetime distributions.

The regression coefficients obtained from a similar fitting of probability distributions for the *chloride surface concentration* are shown in Table 2. It is observed that the lognormal distribution gives the highest value for the regression coefficient. However, all the distributions have regression coefficients higher than 0.9, which in general is quite acceptable.

Table 2 Surface concentration, C_s (% of concrete weight)

Probabilistic model	Regression line	Mean value	Standard deviation	Sample variance	R^2
Normal	$y = 3.5447x - 1.5979$	0.50	0.34	0.11	0.9156
Gamma	$y = 1.4932x - 0.3422$				0.9352
Gumbel	$y = 4.0841x - 1.3635$				0.9716
Weibull	$y = 1.9038x + 1.2355$				0.9338
Lognormal	$y = 1.4879x + 1.3571$				0.9826

The corresponding sample distribution function and the fitted lognormal model are shown in Figure 3. It is seen that the upper part of the empirical distribution (which is most relevant for the shortest lifetimes) is also fitted well by this analytical model.

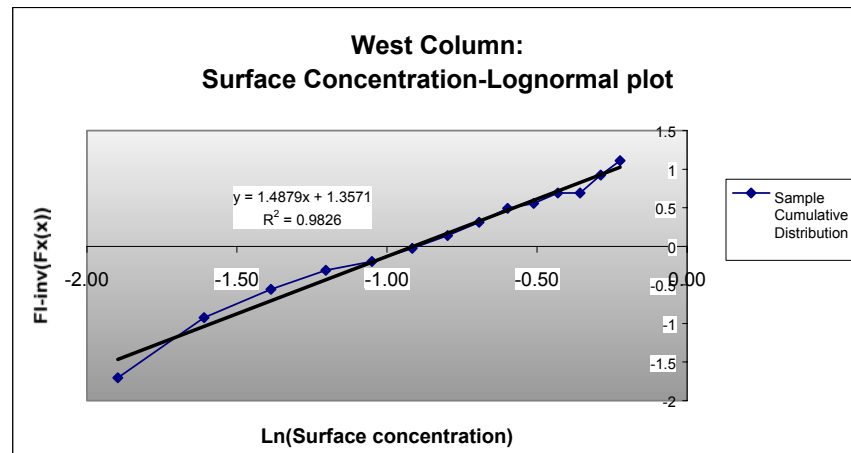


Figure 3. Cumulative distributions for measured surface concentration plotted in lognormal scale, and resulting fitted lognormal model. West side of columns.

Measurements of concrete cover depth were also performed. A lognormal model was found to give the best fit to the measurements. Based on the full-scale measurements and consideration of the additional parameters entering into the computation of chloride lifetime, corresponding probabilistic models are established. The relevant

parameters are defined in relation to the solution of Fick's second law for the chloride concentration $c(x,t)$ at position x and at time t :

$$c(x,t) = c_i + (c_s - c_i) \cdot \operatorname{erfc}\left(\frac{x}{2\sqrt{D \cdot t}}\right)$$

where c_i is the initial chloride concentration in the concrete, c_s is the chloride concentration at the surface, and D is the diffusion coefficient. The concentration at the position of the reinforcement is subsequently compared to the critical chloride concentration for onset of corrosion. The diffusion coefficient may furthermore be time-dependent. The time variation is here expressed by the so-called alfa-factor, refs/3,4/.

The probabilistic models which applied for the superstructure are summarized in Table 3. The model uncertainty factor which occurs both in Table 3 and Table 4 is introduced in order to account for deviations between model predictions and observed diffusion rates. The lowest value is taken to represent lifetime calculations performed for the bridge from which the measurement were performed. The highest value could e.g. represent a situation where these particular data were applied for calculations of a "similar" bridge.

Table 3. Statistical distributions for superstructure

Statistical variable	Distribution type	Mean value	Standard deviation
Surface concentration	Lognormal	0.25 (% concrete weight)	0.18 (% concrete weight)
Diffusion coefficient	Lognormal	0.88 (m ² /sec, mult 10 ⁻¹²)	0.68 (m ² /sec, mult 10 ⁻¹²)
α-factor (time-variation of diffusion coef.)	Deterministic	0.0	-
Initial concentration	Normal	0.015 (% concrete weight)	0.0015 (% concrete weight)
Concrete cover	Lognormal	23 mm	6 mm
Critical chloride concentration	Lognormal	0.18 (% concrete weight)	0.06 (% concrete weight)
Model uncertainty	Normal	1.0	0.01/0.10

Corresponding models which apply to the columns are given in Table 4. As observed, both the diffusion coefficient and the surface concentration are higher for this case. However, the concrete cover is also considerably thicker than for the superstructure.

Table 4. Statistical distributions for columns

Statistical variable	Distribution type	Mean value	Standard deviation
Surface concentration	Lognormal	0.50 (% concrete weight)	0.34 (% concrete weight)
Diffusion coefficient	Lognormal	1.27 (m ² /sec, mult 10 ⁻¹²)	0.64 (m ² /sec, mult 10 ⁻¹²)
α-factor (time variation)	Deterministic	0.0	-
Initial concentration	Uniform	0.015 (% concrete weight)	0.0015 (% concrete weight)
Concrete cover	Lognormal	45 mm	6 mm
Critical chloride concentration	Lognormal	0.18 (% concrete weight)	0.06(% concrete weight)
Model uncertainty	Normal	1.0	0.01/0.10

3 LIFETIME DISTRIBUTIONS

The cumulative distribution functions for chloride lifetime which are obtained by calculating probabilities of the type: $P(\text{chloride concentration at reinforcement at time } t < \text{critical chloride concentration})$. These probabilities are computed repeatedly for a number of different values of the time parameter. The calculations are performed by application of so-called First Order Reliability Methods (FORM), see e.g. ref/5/.

The probability distribution that results from the input data which are given in Table 3 (superstructure), is shown in Figure 4. The corresponding probability density function is obtained by numerical differentiation and is given in Figure 5. As observed, the peak of the latter occurs for a lifetime of 6 years. However, the shape of the upper tail is such that it decays very slowly. This implies a large standard deviation for the lifetime. This is also reflected by the distribution function rising very slowly.

This distribution function obtains a value of 0.4 for a duration of 80 years. This implies that the probability for the lifetime to be smaller than this value is 40%.

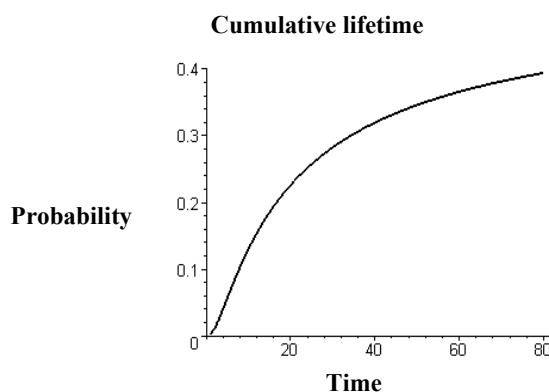


Figure 4 Probability distribution of lifetime (superstructure) corresponding to input statistical models given in Table 3.

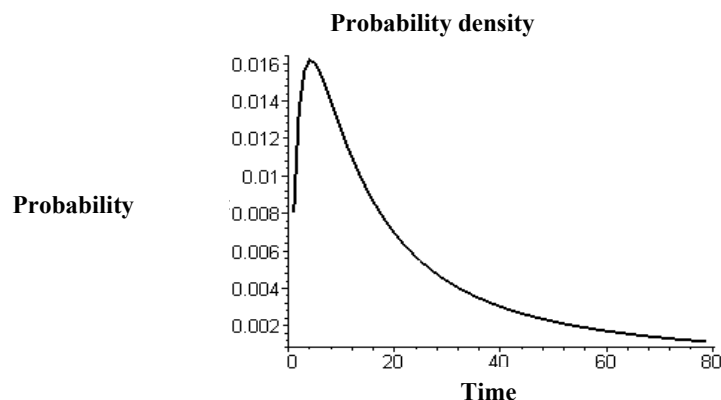


Figure 5. Probability density function obtained by differentiation of distribution function in Figure 4.

4 PARAMETER STUDIES

The effect of varying the statistical parameters of the input models can be readily studied. The effect of including a probabilistic time varying diffusion is accounted for by introducing the alfa-parameter as discussed above. This is presently done by modelling this parameter as a random variable. The mean value is taken to be 0.4, and the standard deviation is 0.1. A lognormal distribution is assumed to apply. The resulting cumulative distribution of the lifetime and the corresponding density function are shown in Figures 6 and 7. These should be compared to the distribution and density functions presented in Figures 4 and 5.

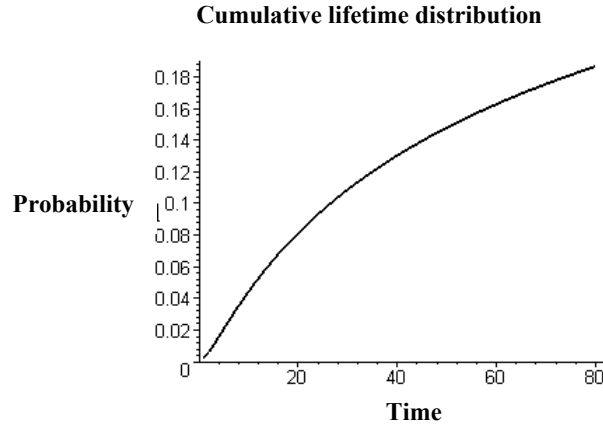


Figure 6. Cumulative distribution function for chloride lifetime. Alfa-parameter which defines variation of diffusion coefficient with time is represented by a lognormal distribution with mean value 0.4 and a standard deviation of 0.1

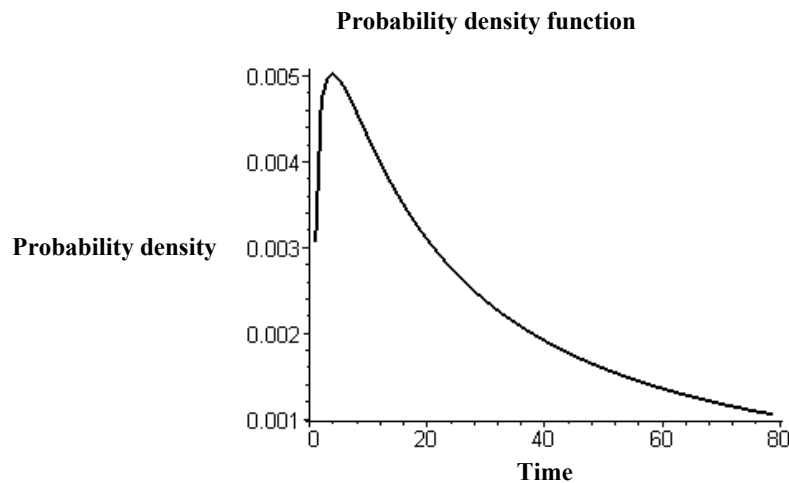


Figure 7. Probability density function corresponding to the distribution function in Figure 6.

The peak of the density function is still located at 6 years. However, the peak is now much smaller than in Figure 4. The upper tail of the density is also higher, and the corresponding distribution function in Figure 6 is “stretched” towards higher lifetimes as could be anticipated.

5 CONCLUDING REMARKS

In the present paper, probabilistic models based on full-scale measurements from the Gimsøystraumen bridge are addressed. These models apply to the diffusion coefficient, the chloride surface concentration and the concrete cover. Based on these models and supplementary models for other parameters affecting chloride diffusion, probabilistic lifetime calculations are performed.

In order to apply the present methodology more extensively, e.g. based on laboratory tests taken prior to construction of a new structure, probabilistic models of conversion factors between lab/full-scale need to be established. This is obviously a challenging task which requires both high quality data and extensive statistical analysis.

ACKNOWLEDGEMENTS

The present work was supported by the project “The lifetime of concrete structures” (Betong-konstruksjoners Livsløp) which is run by the Norwegian Public Roads Administration. The background material for the present paper was contributed by a number of persons, in particular Finn Fluge, Ola Skjølsvold, Trine Hynne, and Jan-Erik Carlsen. Their contributions are greatly acknowledged.

REFERENCES

- /1/ Skjølsvold, Ola: “Gimsøystraumen Bru. Spesialinspeksjon 1992 – kloridprofiler. Vurdering av kloridbelastning og – diffusjonskoeffisient” (in Norwegian), Internal Report no. 2196, Road Technology Department (NRRL), Norwegian Public Roads Administration, April, 2001.
- /2/ Hynne, T.; Leira, B.J.; Carlsen, J.E. and Lahus, O.: “Statistiske levetidsberegninger for betongkonstruksjoner utsatt for kloridinntrengning” (in Norwegian), SINTEF Report, STF22 F01613, Project report no DP1 B1, "The lifetime of concrete structures", Trondheim, 2001.
- /3/ Maage, M; Poulsen, E.; Vennesland, Ø and Carlsen J.E.: "Service Life Model for Concrete Structures exposed to Marine Environment", LIGHTCON report DP 2-7, STF70 94082, SINTEF, Trondheim, Norway, 1994.
- /4/ Poulsen, E.: "Estimation of Chloride Ingress into Concrete and Prediction of Service Lifetime with reference to Marine RC Structures", Proceedings of CEMENTA's Workshop on "Durability of Concrete in Saline Environment", Danderyd, Sweden, 1996.
- /5/ Madsen, H.O.; Krenk, S.; Lind, N.C.: "Methods of Structural Safety", Prentice-Hall, Englewood Cliffs, NJ, 1986.

4 CONCRETE TRANSPORT PROPERTIES

CHLORIDE DIFFUSION COEFFICIENT AND SALT FROST SCALING OF SELF-COMPACTING CONCRETE AND OF NORMAL CONCRETE



Bertil Persson
Senior Lecturer, PhD Eng.
Dept. of Building Materials
Lund Institute of Technology
P. O. Box 118
SE-221 00 LUND
SWEDEN
E-mail: bertil.persson@byggtek.lth.se

ABSTRACT

The project includes laboratory studies of chloride diffusion coefficient, *c_{dc}*, and salt frost scaling of Self Compacting Concrete, SCC, as compared with the corresponding properties of normal compacting concrete, NC. The strength development of the concretes was followed in parallel. Both 28 and 90 days' age applied at the start of the testing. Six SCCs were studied and 2 NCs, all with water-cement ratio, $w/c = 0.39$. The concretes were sealed from casting until testing. The effect of normal and reversed order of mixing (filler last), increased amount of filler, crystalline or sedimentary limestone powder, increased air content and large fresh concrete pressure was studied. The results indicate that *c_{dc}* of SCC was somewhat 60% larger than that of NC probably due to the inability of limestone powder to bind chlorides. It was also observed that at constant cement content the same *c_{dc}* was obtained, after recalculation, of SCC and NC. The difference between the salt frost scaling of SCC and NC was small.

Keywords: chloride diffusion, limestone filler, frost scaling, SCC.

1. INTRODUCTION, LIMITATIONS AND OBJECTIVE

1.1 Introduction

Concrete that does not require any energy for compacting in order to cover the reinforcement or fill out the mould has attracted a great deal of interest. Experiences now exist from 19 full-scale bridges and other full-scale projects with SCC in Sweden /1/. The technique has also been introduced for dwelling houses and office buildings. Regarding concrete for construction of bridges, dams, tunnels and so forth, the requirements of durability are greater since the conditions are essentially more severe /2/. Therefore a higher level of documentation is required for outdoor constructions than for dwelling houses or office buildings. It was the objective of the project to document *c_{dc}* and salt frost scaling for SCC that contains limestone filler, is cast with different methods and varying air content and compare the results with the corresponding properties of NC to give advices for mix composition and production.

1.2 Limitations

Both 28 and 90 days' age applied at the start of the testing of *cdc* and salt frost scaling. Eight concretes were studied, 2 were NCs and the rest SCCs, with water-cement ratio, $w/c = 0.39$. The concretes were sealed from casting until testing. All the specimens were core drilled from a large mass of concrete. In this way the effect of concrete skin, segregation and so forth was avoided. The following parameters were studied:

1. normal and reversed order of mixing (filler last)
2. increased amount of filler
3. crystalline or sedimentary limestone powder
4. increased air content
5. large fresh concrete pressure

1.3 Objective

The following objectives were settled on the project:

- to investigate the *cdc* of SCC in order to give recommendations for the choice of materials and mix composition at ready mixing
- to determine the salt frost scaling of SCC that contains increased amount of filler, different types of casting and air content in order to give recommendations for the chose of materials and mix composition at manufacture
- to compare the result of *cdc* and salt frost resistance of SCC with the corresponding properties of NC

2. PREVIOUS RESEARCH

2.1 *cdc* and w/c

Figure 1 shows *cdc* of SCC with quartzite filler and of NC. All concrete contained Slite Std cement except for concrete with $w/c = 0.27$, in which Degerhamn Std cement was used, Appendix 1-2. The measurement was performed with CTH Rapid Test Method [3,4]. For SCC with $w/c = 39\%$, $cdc = 14 \cdot 10^{-12} \text{ m}^2/\text{s}$ was obtained. The following expression for *cdc* at 3 years' age was obtained ($10^{-12} \text{ m}^2/\text{s}$, w/c in %):

$$cdc = 0.97 \cdot w/c - 25 \quad \{R^2 = 0.96\} \quad (1)$$

2.2 *cdc* and additives

Tang and Nilsson [5] studied *cdc* for 4 concretes of which one included silica fume, Appendix 3. *cdc* was substantially decreased in concrete with silica fume. On the other hand the chloride binding ability of the concrete probably decreased due to reduce of calcium hydroxide in concrete with silica fume during the pozzolanic interaction [6]. Geiker, Thaulow and Andersen studied the amount of current passing through dishes of NCs meant for the Great Belt Link according to [7], [8,9], Appendix 4. Especially when silica fume was introduced in the mix composition, the number of coulombs passing the NCs was reduced [8], Figure 2. However, the workability of the NCs on site was poor leaving remaining honeycombs and cracking in the cover layer to be repaired. A couple of large structures had to be discarded at the start of the project [9].

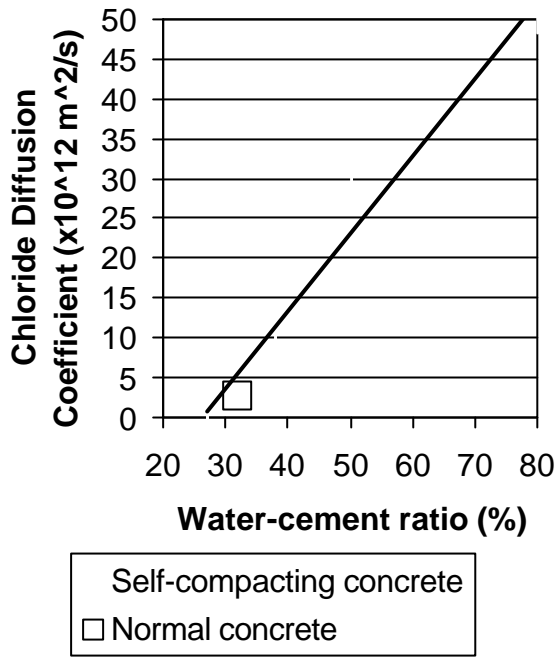


Figure 1 – *c_{dc}* versus w/c [4].

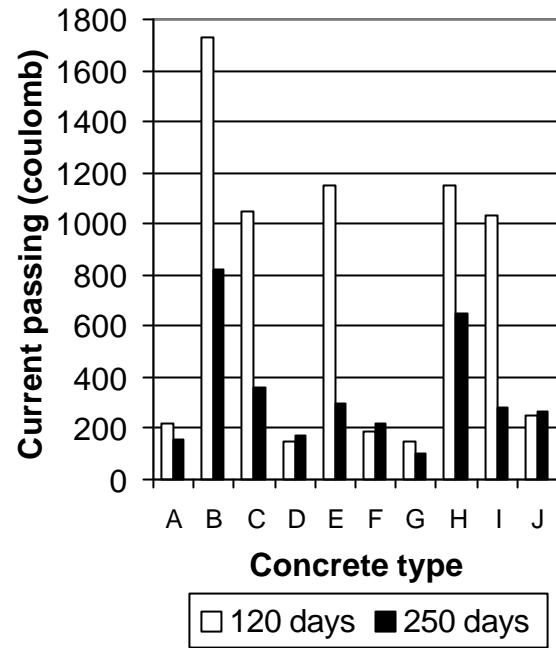


Figure 2 - Coulombs passing dishes [8].

Boubitsas and Paulou [10] studied 4 SCCs for Marine Environment and one NC, Appendix 5. A great decrease of *c_{dc}* was observed when using cement with slag or silica fume in SCC. The effect of fly ash on *c_{dc}* was more dubious [10]. However, when using as much as 68% slag of the binder, the chloride binding ability of the concrete more or less vanished which in turn increase the amount of free chlorides [6] and lowered the threshold chloride level for corrosion of reinforcement to commence.

2.3 Salt frost scaling and internal frost resistance

Rougeau, Maillard and May-Dippe studied salt frost scaling and internal frost resistance of SCC and NC [11]. Mix composition, properties, salt frost scaling and internal transversal resonance of [11] is shown in Appendix 6. The internal transversal resonance matches well to the dynamic elastic modulus that in turn corresponds to internal damage from frost, Appendix 6. The loss of salt frost scaling and internal transversal resonance was much larger for NC than for SCC [11]. The salt frost scaling was increasing with time for NC but remained constant at 0.9 kg/m³ for SCC after 28 cycles [11]. NC exhibited a total loss of internal frost resistance after 150 cycles while SCC only lost 7% under the corresponding period of time [11]. After 300 cycles the drop of the elastic modulus only was 12% [11]. Most probably the vibration technique more or less damaged the air void system in NC [11]. In SCC, however, the entrained air was unaffected since no vibration took place in this kind of concrete. Boubitsas and Paulou [10] found that the salt frost scaling increased in concretes with large amounts of slag compared with a reference concrete without slag, Appendix 5. However, for concrete with less than 12% fly ash and less than 5% silica fume as estimated on the cement content, less salt frost scaling was observed than for the reference concrete without those additives. For 24% fly ash and less than 10% silica fume larger salt frost scaling was obtained than for the reference concrete, Appendix 5.

3. MATERIAL AND METHODS

3.1 Material

Crushed gneiss, two types of natural sand, crystalline and sedimentary limestone filler and Degerhamn cement was used in the mix composition, Appendices 1 and 7 [4]. Melamine based superplasticiser was used for NC (Flyt 97M), polycabroxylic superplasticiser for SCC (Glenium 51) and air-entertainment agent based on fir oil (Microair) completed the mixes [4]. Manufacture and curing of the large mass of concrete was performed in the following way:

- new mixing order (N) with dry material except for filler mixed for $\frac{1}{2}$ min. with water and air-entertainment [12]. Then half the amount of superplasticiser mixed for $\frac{1}{2}$ min. At last the remaining superplasticiser with filler mixed for 1 min. [12].
- ordinary mixing order (O) with all dry material at the start mixed for $\frac{1}{2}$ min. with water including air-entertainment. Then the superplasticiser was mixed for $2\frac{1}{2}$ min.
- steel mould with 0.23 m in diameter and 0.3 m in height. NC vibrated 10+10+10 s.
- sealed curing at 20 °C until the specimens were core drilled from the massive pour.

3.2 Methods

From the pour the following specimens were drilled cored at 28 and 90 days' age:

- *cdc*: 3 pieces of dishes 100 mm in diameter and 50 mm in height [3].
- Salt frost scaling: 3 pieces of dishes 94 mm in diameter and 40 mm in height [13].

The specimens were stored in water with lime stone powder between drilling and testing. NT BUILD 492 was used to obtain *cdc*, Figure 3. Salt frost scaling was studied at all sides of the specimen by a method developed by Lindmark [13]. Two frost cycles between -20 and 20 °C were used daily, Figure 4. The temperature was held at -20 and 20 °C internally for 3 h. The tests were started either at 28 and 90 days' age. Singly 100-mm cubes were used for studies of strength at 1, 7, 28 and 90 days' age.



Figure 3 – Experimental set-up for test of *cdc* [3].

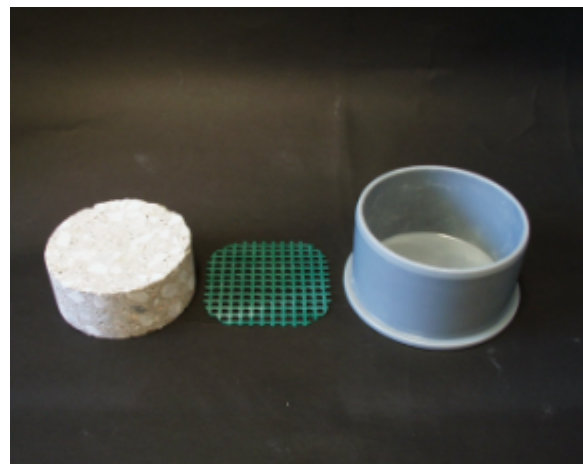


Figure 4 - Experimental set-up for test of salt frost scaling [3].

4. RESULTS AND ANALYSES

4.1 Strength and grading curves of particles in the fresh concrete

The choice of mix composition may be linked to strength and the grading curve of particles in the fresh concrete. The later properties of SCC were compared to the corresponding properties of NC, Figures 5 and 6. Gap-grading is not feasible for SCC. The filler had an substantial effect on strength of SCC since the particle packing improved. From figures 5 and 6 the following empirical relationships were obtained:

$$pm = 0.102 \cdot \ln(d) + 0.583 \quad \{R^2 = 0.96\} \quad (2)$$

$$f_{cc} = k_N \cdot k_S \cdot k_8 \cdot [(14.6 \cdot p + 12.3) \cdot \ln(t) + 51 \cdot p + 23] \quad \{R^2 = 0.70\} \quad (3)$$

f_{cc}	denotes compressive strength of 100-mm cube (MPa)
k_N	= 0.89 applies for new order of mixing (filler at last); $k_N = 1$ otherwise
k_S	= 0.82 applies for sedimentary lime stone filler; $k_S = 1$ otherwise
k_8	= 0.74 applies for sedimentary lime stone filler; $k_8 = 1$ otherwise
$\ln(d)$	denotes the natural logarithm of the sieve dimension ($0.002 < d < 10$ mm)
$\ln(t)$	denotes the natural logarithm of concrete age ($1 < t < 100$ days)
p	denotes content of limestone powder ($0.03 < p < 0.15$ by vol.)
pm	denotes the material passing through

4.2 *cdc*

Significant differences were obtained between *cdc* of SCC and that of NC, Figure 7. At 28 days' age *cdc* = 16 and 9 m²/s and at 90 days' age *cdc* = 10 and 7 m²/s respectively was observed, i.e. in all an 60% increase of *cdc* in SCC compared with NC [4]. The reason for lower *cdc* in SCC compared with *cdc* in NC was the lower cement content in SCC compared with NC, Figure 8 [4]. The filler effect on strength and also the improved workability invites contractors to use less cement in SCC than in NC. More cement in the concrete increased the ability of the concrete to bind chlorides. This studies and also those in Chapters 2.1 and 2.2 of concrete without additives were used to obtain the following empirically based eq. for *cdc*, Figures 9-11 (10⁻¹² m²/s) [5,8,9]:

$$cdc = [(0.0055 \cdot \ln(t) - 0.2122 \cdot c - 3.5 \cdot \ln(t) + 104] \cdot (4 \cdot w/b - 1.2) / 0.4 \quad \{R^2 = 0.88\} \quad (4)$$

c	denotes the cement content ($375 < c < 450$ kg/m ³)
<i>cdc</i>	denotes the chloride diffusion coefficient (x10 ⁻¹² m ² /s)
$\ln(t)$	denotes the natural logarithm of concrete age ($1 < t < 36$ months)
w/b	denotes the water-binder ratio, 1:1 ($0.35 < w/b < 0.50$)

4.2 Chloride binding ability

The pozzolanic reaction takes place under conditions similar to those required for carbonation to take place. Carbonation and pozzolanic reactions require calcium hydroxide to be present. When carbonation or pozzolanic reactions takes place no chlorides may be bound in the concrete [9]. At $w/c = 0.39$ about 16% silica fume is required to prevent the pozzolanic reaction [14]. Ten percent silica fume is required

estimated on the cement content to prevent pozzolanic reaction at $w/c = 0.31$, long-term, since hydration is slowed down substantially at low w/c [15]. The following equation was obtained for the chloride binding ability, cba Figure 12 [6,14,15]:

$$cba = 0.65 \cdot \ln(w/c) - 0.05 \cdot s + 1.3 \quad \{0.3 < w/c < 0.5\} \quad (5)$$

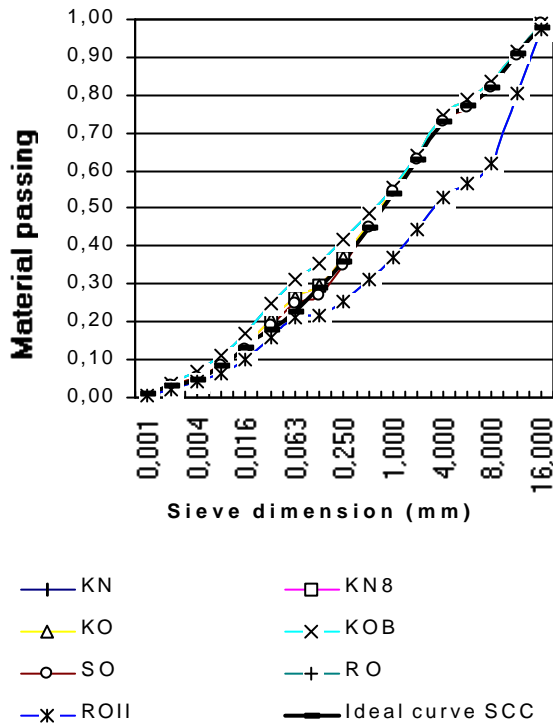


Figure 5 – Grading curve in fresh concrete [4].

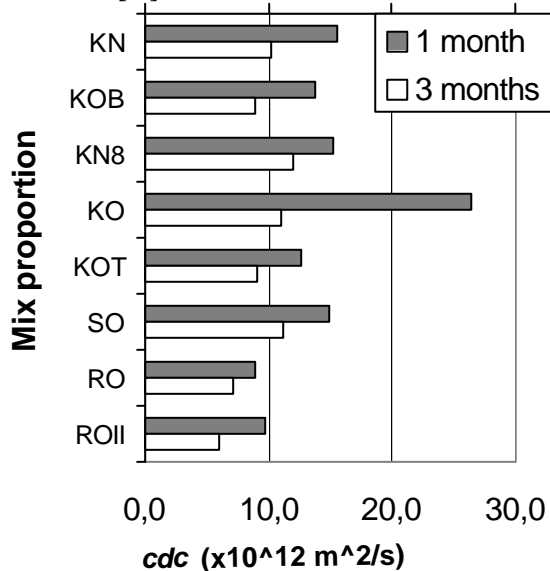


Figure 7 – cdc for tested concrete, Appendix 7 [4].

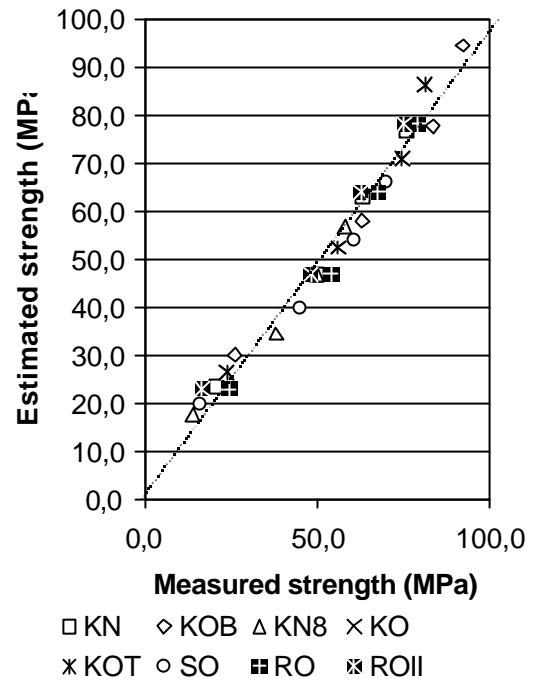


Figure 6 – Measured strength versus strength calculated by eq. (3) [4].

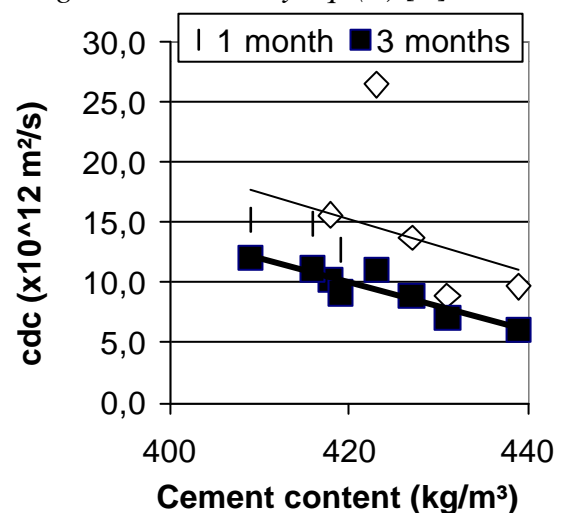


Figure 8 – cdc versus cement content, Appendix 7 [4].

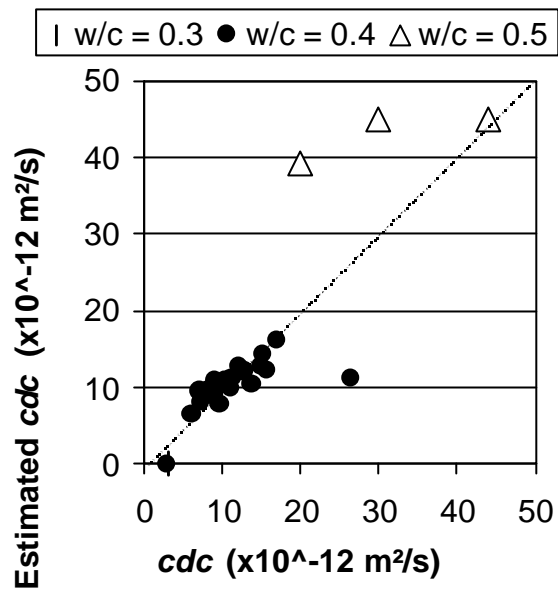


Figure 9 – cdc estimated with eq. (4) versus tested cdc [4,5,8,9].

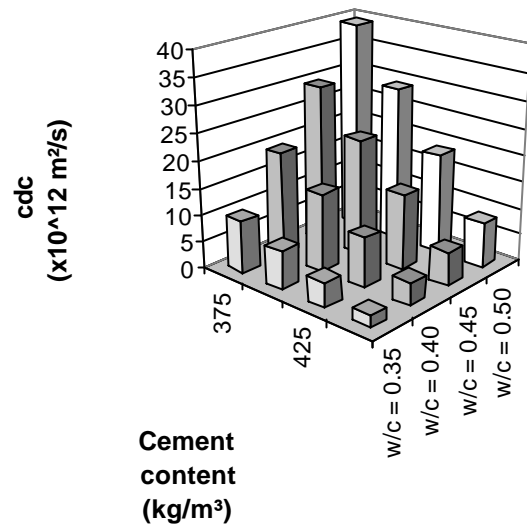


Figure 10 – 3 months- cdc estimated by eq. (4) vs cement content and w/c .

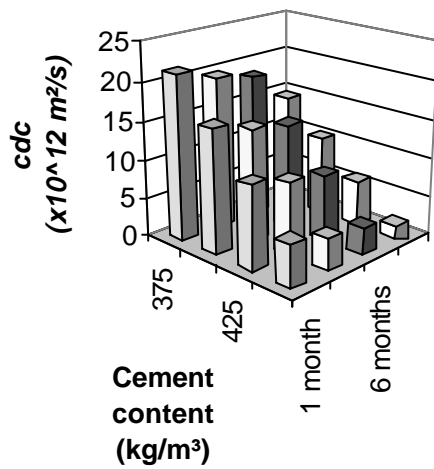


Figure 11 - cdc estimated with eq. (4) versus age and cement content ($w/c=0.4$)

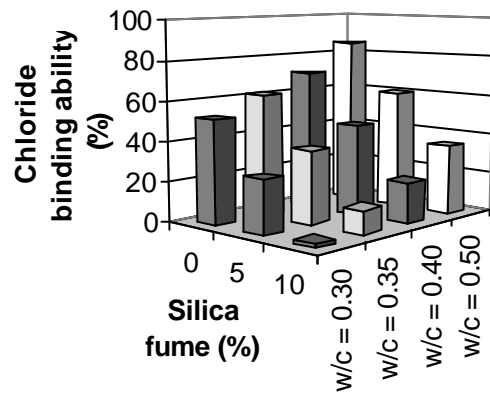


Figure 12 – Chloride binding ability, cba versus content of silica fume and w/c .

4.4 Salt frost scaling

Figure 13 shows salt frost scaling of all studied concrete at 28, 56 and 112 frost cycles [4]. SCC had more or less the same salt frost scaling like NC did. Based on the experiments the following conclusions were drawn after 112 cycles:

- at 28 days start age but not at 90 the salt frost scaling was larger in SCC than in NC
- increased amount of filler did not significantly increase the amount of scaling
- 5.5 m pouring pressure compared with 0.5 m did not change the salt frost scaling
- concrete with crystalline filler had larger salt frost scaling than with sedimentary
- concrete with 6% air content had larger frost scaling than concrete with 8% air

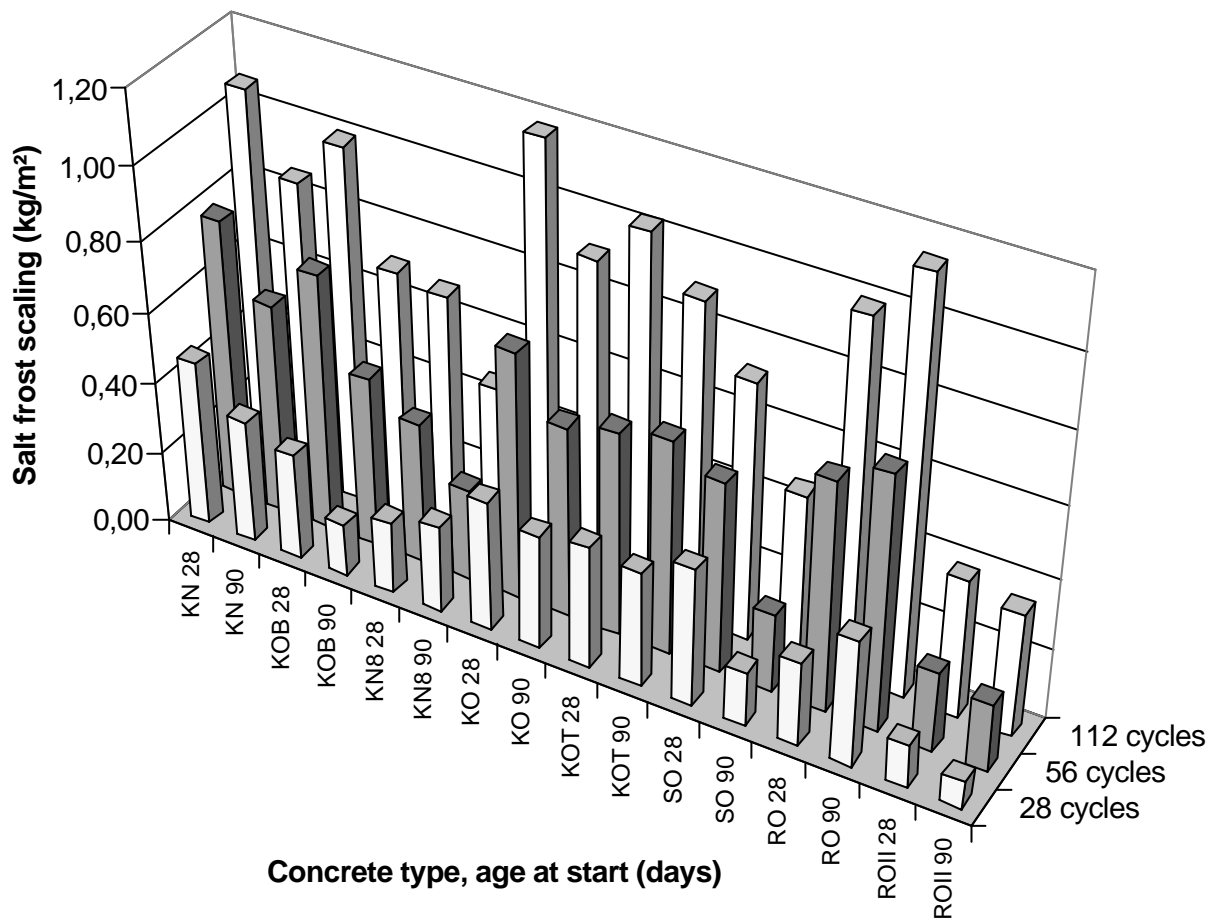


Figure 13 - Salt frost scaling of all studied concrete at 28, 56 and 112 frost cycles [4].

5. ACCURACY

In Table 1 the coefficient of variation (the standard deviation to average ratio) is given in order of estimating the accuracy. The following order of accuracy was found for the test of salt frost scaling: SO, KN8, KOB, KOT, KN, KO, ROII and RO. In all accuracy was better of the tests of SCCs than of the tests of NCs most probably to the fact that vibration was avoided in SCCs. The transition zone remained unaffected in SCC but was affected in NC due to different movements of cement paste and aggregate.

Table 1 - Coefficient of variation of *cdc*-tests given in order of accuracy [4].

Concrete	KOB	KOT	SO	KN8	KN	ROII	RO	KO
Coefficient of variation (%)	3.5	5.5	7.0	8.0	8.5	9.0	10.0	10.5

B = increased amount of filler; K = crystalline limestone filler; N = new way of mixing (filler at last); O = ordinary way of mixing (filler at first); S = sedimentary limestone filler; T = 5.5 m height of pouring instead of 0.5 m; II = second reference concrete.

6. DISCUSSION OF POZZOLANIC INTERACTION BETWEEN PORTLAND CEMENT, SILICA FUME, FLY ASH AND SLAG AS REGARDS *CDC*

From the results and from the references it was obvious that pozzolans like silica fume, fly ash and slag had an effect on *cdc*. On the other hand pozzolans consumed the calcium hydroxide in the cement paste which in turn lowered the chloride binding ability [6]. From the results obtained by Tang and Nilsson [5] and further by Boubitsas and Paulou [10] it was possible to estimate the effect of pozzolans on *cdc* assuming the concrete to perform in accordance with eq. (4) above. So called efficiency factors for the different additives were adjusting the cement content in eq. (4) for the measured results to coincide with the estimations. The Recalculation of the amount of cement into an equivalent amount did this. From previous research it was known that silica fume had a substantial effect on strength, self-desiccation and hydration [16,17]. For strength large efficiency factor were obtained at early ages but declining to less than 1 after about 90 months [16,17]. However, for hydration the opposite results were found. The present results were only obtained at 1 and 6 months' age, i.e. the efficiency factor maybe time dependent. The following results were obtained for the pozzolanic interaction between Portland cement, silica fume, fly ash and slag as regards *cdc*:

$$c_{eq.} = c + 0,21 \cdot fl + 1,6 \cdot sf + 1,03 \cdot sl \quad \{R^2 = 0,81\} \quad (5)$$

$c_{eq.}$	denotes the equivalent amount of cement
c	denotes the amount of Portland cement
fl	denotes the amount of fly ash
sf	denotes the amount of silica fume
sl	denotes the amount of slag

7. CONCLUSIONS

Tests on chloride diffusion coefficient, *cdc*, and salt frost scaling of Self Compacting Concrete, SCC, and normal compacting concrete, NC, gave the following conclusions:

- limestone filler additives increased the strength of SCC substantially compared with strength of NC even through the cement content was somewhat lower in SCC
- the packing close to an ideal packing was the reason for the enlarged SCC strength
- *cdc* of SCC was about 60% larger than in NC due to lower cement content in SCC
- the efficiency on *cdc* of silica fume seems to be 1,6, of slag about 1 and of fly ash 0,2 as compared with the effect of Portland cement on *cdc*.
- larger salt frost scaling was found for SCC at 28 days' starting age than for NC. In all no significant difference was found between salt frost scaling of SCC and NC.
- salt frost scaling increased in concretes with large amounts of slag compared with a reference concrete without slag.
- in concrete with less than 12% fly ash and less than 5% silica fume, less salt frost scaling was observed than for the reference concrete without those additives.

ACKNOWLEDGEMENT

Financial support from the Development Fund of the Swedish Construction Industry and from Skanska Sweden Ltd is gratefully acknowledged. Nordkalk Partek Ltd has performed an associated work about structure of concrete with limestone filler, which is also gratefully acknowledged. Thanks are also due to Professor Göran Fagerlund.

REFERENCES

1. Nilsson, M.; Petersson, Ö. *The First SCC Bridge*. VoV-byggaren 2/98, pp. 28-31.
2. Söderlind, L., *Full-scale tests for housing SCC*. RILEM symposium on SCC. Stockholm. Ed.: Skarendahl and Petersson. 1999, pp. 723-728.
3. *CTH Rapid Test for Determination of cdc in Concrete*. NT BUILD 492. 2000.
4. Persson, B. *SCC – cdc and Frost Resistance*. TVBM-30XX. Lund. 2001, 45 pp.
5. Tang, L.; Nilsson, L.-O., *Modelling of chloride penetration into concrete – Tracing five years' field exposure*. Concrete Science and Engineering. Vol. 2. 2000, 170-175.
6. Johannesson, B., *Transport and Sorption Phenomena in Concrete and Other Porous Media*. TVBM-1019. LTH Byggnadsmaterial. Lund. 1993, 491 pp.
7. AASHTO T 271-831. *Rapid Determination of Chloride Permeability of Concrete*.
8. Geiker, M.; Thaulow, N.; Andersen, P. J., *Assessment of Rapid Test of Concrete Permeability Test of Concrete with and without Mineral Admixtures*. Durability of Concrete and Components. Brighton. Chapman & Hall. 1990, 52-61.
9. Persson, B., *A Background for the Choice of Mix Design of the Concrete for the Great Belt Link*. Report U91.02 Div. Building Materials. 1991, 102 pp.
10. Boubitsas, D.; Paulou, K., *Self Compacting Concrete for Marine Environment*. TVBM-5048. Lund Institute of Technology. Lund University. Lund. 2000, 55 pp.
11. Rougeau, P.; Maillard, J. L.; Mary-Dippe, C., *Comparative Study on Properties of SCC and HPC Concrete Used in Precast Construction*. RILEM symposium on SCC. Stockholm. Ed.: Skarendahl and Petersson. 1999, 251-261.
12. Pettersson, Ö., *Dispersion and Frost Resistance. Investigation of Four Types of Limestone Filler for Self Compacting Concrete*. Report 2000-27. Cement and Concrete Research Institute. Stockholm. 2000, 14 pp.

13. Lindmark, S., *Mechanisms of Salt Frost Scaling of Portland Cement-bound Materials: Studies and Hypothesis*. TVBM-1017. Lund University. 1998, 266 pp.
14. Persson, B., Long-term Shrinkage of High Performance Concrete. 10th Congress on the Chemistry of Cement. 2ii073. Gothenburg. 1997. Ed.: Justnes, H., 9 pp.
15. Persson, B., Shrinkage of High Performance Concrete. Proc. RILEM Conference on early Age Cracking in Concrete. Haifa. 2001. Ed. by A Bentur. 2001, 301-311.
16. Persson, B., *Long-term Effect of Silica Fume on the Principal Properties of Low-Temperature-Cured Ceramic*. CCR 27. 1997, 1667-1680.
17. Persson, B., *Pozzolanic Interaction between Portland Cement and Silica Fume in Concrete*. Sixth CANMET/ACI Int. Conference. Bangkok. 1998, 631-660.

Appendix 1. The chemical composition and physical properties of cements (%).

Component	Slite Std, N	Degerhamn, SL
CaO	62	65
SiO ₂	20	21.6
Al ₂ O ₃	4.4	3.5
Fe ₂ O ₃	2.3	4.4
K ₂ O	1.4	0.58
Na ₂ O	0.2	0.05
MgO	3.5	0.78
SO ₃	3.7	2.07
Ignition losses	2.4	0.47
CO ₂	1.9	0.14
Clinker minerals:		
C ₂ S	14	21
C ₃ S	57	57
C ₃ A	8	1.7
C ₄ AF	7	13
Water demand	28%	25%
Initial setting time	154 min.	145 min.
Density	3122 kg/m ³	3214 kg/m ³
Specific surface	364 m ² /kg	305 m ² /kg

Appendix 2. Mix composition and strength of concretes (kg/m³, MPa) [4].

Mix	Cement, c	Type	Silica fume, s	w/(c+s)	Sand filler	Air (%)	Strength
27	500	SL	50	0.24	50	1.3	141
32	389	N		0.32	106	12	55
38N	360	N		0.38	68	12	42
38S	400	N		0.38	145	1.4	86
50N	285	N		0.50	33	13	30
50S	340	N		0.50	165	3.5	61
80N	250	N		0.80		1.2	24
80S	260	N		0.80	185	1.9	27

Appendix 3. Mix composition and *cdc* of NCs [5].

Material/mix- water-binder ratio (%)	1-40	1-50	H40	2-40
Cement Degerhamn	420	370	399	
Cement Slite Std				420
Silica fume			21	
Water	168	185	168	168
Air content (% vol.)	6	6.4	5.9	6.2
Aggregate	1692	1684	1685	1675
<i>cdc</i> (10^{-12} m ² /s)	8.1	19.9	2.7	7.1

Appendix 4. Mix composition NCs meant for Great Belt Link [8].

Material/mix	A	B	C	D	E	F	G	H	I	J
SRPC	310	405	370	345	370	345				
RPC							310	405	370	345
PFA	70		70		70		70		70	
SF	30			30		30	30			30
w/c	0.34	0.33	0.32	0.33	0.31	0.32	0.36	0.34	0.33	0.35
Current pass. (coulomb)	220	1730	1050	150	1150	190	150	1150	1030	250

PFA = fly ash; RPC = rapid cement; SF = silica fume; SRPC = sulphate resistant.

Appendix 5. Mix composition and *cdc* of SCCs [10].

Material/mix composition	D	F	G	R	T
Crushed aggregate Bålsta 8 -16	496	494	580	876	495
Natural sand Bålsta 0 -8	699	728	800	727	714
Natural sand SÄRÖ 0-2	505	465	220	149	521
Fly ash	89	55			
Glas filler			60		
Cement Aalborg (CEMI)	375				
Cement Degerhamn Std (CEMI)		440	420	438	
Slag cement (CEMIII, 68% slag)					470
Silica fume Elkem (granulate)	35	18	21		
Air-entrainment (wet, g, 10% dry)	0,498	0,501	0,500	482	0,498
Superplasticiser(wet, 35% dry)	5,25		4,24	5,92	3,52
Vatten	191	172	162	171	183
w/b	0,38	0,38	0,37	0,39	0,39
Slump flow (mm)	690	725	720	150	737
Flow time until diameter 500 mm (s)	7	8	8		6,5
Density	2247	2300	2306	2368	2281
Aggregate content (>0.125, % vol.)	0,64	0,64	0,60	0,66	0,65
Air content (%)	6,4	6,2	6,3	6,1	5,7
28-day cube strength (100 mm, MPa)	61	70	64	63	79
<i>cdc</i> ($\times 10^{12}$ m ² /s)	5,8	5,5	4,6	9,6	1,9
Salt frost scaling 112 cycles (kg/m ²)	0,461	0,174	0,182	0,387	0,509

Appendix 6. Mix composition and frost resistance of NC and SCC [11].

Material, cement type, w/c	BAP3	BAP5	HPC
Coarse aggregate 6-14 mm	267	267	
Sand 3-6 mm	543	544	
Sand 0-4 mm	886	887	
limestone powder	101	100	
Cement CEMI 52.5 R	352	350	323
Plasticiser	3.2	5.0	
Superplasticiser	2.3	0.9	
Water	197	190	
w/c	0.56	0.54	
Water-powder ratio, w/p	0.44	0.42	
Aggregate content (>0.125 mm, % vol.)	0.64	0.64	
Slump flow (mm)	600	580	
28-day strength (MPa)	56	58	72
Decrease of internal transversal resonance (%):			
150 frost cycles	0	13	100
300 frost cycles	7	18	-
Increase of length (%):			
150 frost cycles	0.01	0.13	0.39
300 frost cycles	0.01	0.22	-
Salt frost scaling (kg/m ²):			
28 frost cycles	0.9	1.3	1.8
56 frost cycles	0.9	1.4	3.7

Appendix 7. Mix composition and properties of NC and SCC [4].

Material/mix composition	KN	KOB	KN8	KO	KOT	SO	RO	ROII
Crushed aggregate Bålsta 8 -16	363	371	355	367	363	402	862	876
Natural sand Bålsta 0 -8	853	872	836	864	855	786	715	727
Natural sand SÄRÖ 0-2	316	135	309	320	316	422	146	149
Limestone filler Köping 500	183	375	180	186	184	94	0	
Cement Degerhamn Std	418	427	409	423	419	416	431	438
Microair (wet weight, g, 10% dry)	585	213	1203	106	117	125	474	482
Superplasticiser(wet, 35% dry)	2,97	4,13	3,2	3,39	3,69	2,99	7,32	5,92
Water	163	167	160	165	163	162	168	171
w/c	0,39	0,39	0,39	0,39	0,39	0,39	0,39	0,39
Air content (%)	5,6	4,9	8	5,5	6,3	5,6	5,8	6,1
28-day cube strength (MPa)	63	84	50	75	75	61	68	63
Slump flow (mm)	720	780	735	620	640	710	110	150
Flow time until 500 mm (s)	5	7	8	10	8	5	-	-
Density	2297	2348	2250	2323	2300	2285	2325	2368
Aggregate content (% vol.)	0,58	0,52	0,57	0,59	0,58	0,61	0,65	0,66

Notations: please see Table 5 above

fib55durscc.doc

5 CORROSION INITIATION

CHLORIDE THRESHOLD VALUES FOR SERVICE LIFE DESIGN

(This paper is a reprint of an identical paper first presented at the RILEM Workshop TMC in Paris, September 2000)



Jens M. Frederiksen
B.Sc.Eng.(hon.)
Civil Engineer
jmf@aec-dk.com
AEClaboratory (Ltd.) A/S
Denmark
www.aec-dk.com

ABSTRACT

An estimation of the chloride ingress into concrete has little value for practice until the threshold value in the particular situation is known. When chloride penetrates the concrete cover and reaches the steel reinforcement a corrosion process will initiate when a certain chloride concentration (*the threshold value*) is reached.

It is known from the literature that not only the type of concrete but also the exposure conditions (local environments) are decisive for the magnitude of the threshold value. Therefore results from natural exposure and laboratory exposure must be compiled together in order to estimate threshold values for the engineering service life design.

A new approach for laboratory experiments is being developed so that chloride threshold levels in laboratory tests can be measured as chloride concentrations in the bulk concrete.

The paper presents an engineering approach where threshold values for ordinary concrete with silica fume and/or fly ash can be calculated from a formula based on data from the literature. When new types of concrete shall be evaluated the presented laboratory test method can be used.

1. INTRODUCTION

The determination of chloride threshold values, i.e. the chloride concentration at which mild steel reinforcement will start corroding in concrete is the subject for a number of research projects. This paper reintroduces recent findings given in the HETEK project, cf. Frederiksen et al [1997] and presents a new attempt for reliable determination of chloride threshold values in laboratory experiments.

In Frederiksen et al. [1997], P. Sandberg estimated chloride threshold values for different binders and for different environments including those mentioned above. The estimates were made on the basis of experimental data reported in the literature. That review is reintroduced below and supplemented with more considerations for the road environment.

Unfortunately no simple way exists for the translation of short-term corrosion data from the laboratory, or even short-term data from field exposure, into values that can describe the long-term behaviour of a field exposed structure.

Chloride threshold levels and active corrosion rates depend strongly on the cover thickness, for a given concrete quality exposed to a given set of exposure conditions. Therefore it is not possible to obtain quantitative corrosion data from direct measurements on high performance concrete with thick covers, because of the very long initiation period required.

2. EVALUATION OF PUBLISHED CHLORIDE THRESHOLD LEVELS

Modern concrete structures exposed to a severe environment typically have a low water to binder ratio (often less than $w/b = 0.40$) and a thick specified cover (often more than 45 mm). These measures do not only increase the penetration time for the chloride to reach the steel surface, they also minimise moisture and temperature variations at the depth of the reinforcement, thereby increasing the chloride threshold.

Unfortunately field exposure tests with such thick covers would be extremely time consuming before any chloride thresholds could be evaluated. As a consequence, chloride thresholds have been estimated in basically four different ways of testing, none of them being capable alone to simulate the field conditions in a modern structure:

- A) Field testing of modern low w/b ratio laboratory cast concrete specimen, with small covers (normally in the range 10-20 mm) - *missing the effects of cover and of variable compaction in practise.*
- B) Laboratory testing of modern low w/b ratio concrete, sometimes with the environmental impact simulated by potentiostatically controlled steel potentials - *missing the effects of cover and of variable compaction, and usually also the effect of a varying microclimate and of leaching of alkali hydroxide.*
- C) Field studies of existing good quality old structures, with covers > 30 mm but with higher w/b ratios (typically > 0.5) - *missing the effect of a low w/b ratio and the effect of new binders.*

D) Laboratory or field testing of concrete with cast-in chloride, thereby allowing for the use of low w/b ratio concrete and a thick cover - *missing the effect of steel passivation in chloride free concrete*.

Procedure D) is considered to be the most erroneous one, since the presence of cast in chloride decrease the ability of the cement paste to passivate the steel. Furthermore, the concrete porosity and the composition of some of the cement hydrates are altered if cast-in chloride is present during most of the curing.

Results from procedure A) - C) will all give some erroneous conclusions if not evaluated with care. No procedure yet exists which has proven to be scientifically correct for the evaluation of long term threshold levels. Therefore, an engineering approach has been used as shown by the following examples:

Example 1

OPC Concrete with $w/b = 0.50$ exposed to a marine splash water, reported results on chloride threshold levels by weight of cement, according to procedure A-C):

A) 0.6-1.9 % Cl. Thomas [1995], Pettersson [1996].

B) 1.1-2.7 % Cl. Arup [1996], Breit [1994].

C) 0.3-1.4 % Cl. Henriksen [1993], Lukas [1985], Vassie [1984].

Chloride threshold levels < 0.4 % Cl reported from existing structures (procedure C) are generally associated with failure to comply with required cover, or associated with large compaction voids, a high w/c ratio, and similar major defects. On the other hand, threshold levels from “macro defect free” specimens exposed in the laboratory at constant exposure conditions seems to indicate far too optimistic threshold levels for a dynamic exposure zone such as the splash zone. The threshold levels obtained by field exposure of laboratory cast specimens seem to be the most suitable values for describing chloride threshold in high performance concrete which is cast and placed properly. Chloride thresholds according to procedure A should be on the safe side, since they do not take the stabilising effect of a thicker cover into account.

Example 2

OPC Concrete with $w/b = 0.50$ exposed in a marine submerged zone, reported results on chloride threshold levels by weight of cement, according to procedure A-C):

A) 1.5-2.0 % Cl^- Pettersson [1996].

B) 1.6-2.5 % Cl^- Arup [1996], Breit [1994].

C) > 2.0 % Cl^- Sandberg [1995], Pettersson [1996].

The chloride threshold levels found in submerged concrete with procedure A-C seem to vary less as compared to the thresholds in the splash zone. This is probably because of the stable and relatively similar exposure conditions. The lower values according to procedure A are probably a result of smaller cover and of hydroxide

leaching in the field exposure test. Therefore, these values should be on the safe side.

3. COMPILATION OF CHLORIDE THRESHOLD LEVELS

Some measured ranges of chloride threshold levels (black steel) in macro crack free concrete or mortar in various exposure regimes have been compiled and analysed in an excellent review by Glass and Buenfeld [1995], as shown in Table 1. Some additional chloride threshold levels have been reported as shown in Table 2.

Table 1. Measured ranges of chloride threshold levels (black steel) in macro crack free concrete in various exposure regimes, Glass & Buenfeld [1995].

Total chloride %Wt. cement	Free Chloride Mole/l	[Cl]/[OH]	Exposure Type	Reference
0.17 - 1.4	0.14 - 1.8	3 - 20 2.5 - 6 0.26 - 0.8 0.3 0.6 1 - 40	Field	Stratful et al. [1975]
0.2 - 1.5			Field	Vassie [1984]
0.25			Field	West & Hime [1985]
0.25 - 0.5			Laboratory	Elsener & Bönni [1986]
0.3 - 0.7			Field	Henriksen [1993]
0.4			Outdoors	Bamforth & Chapman-Andrews [1994]
0.4 - 1.6			Laboratory	Hansson & Sørensen [1990]
0.5 - 2			Laboratory	Schiessl & Raupach [1990]
0.5			Outdoors	Thomas et al. [1990]
0.5 - 1.4			Laboratory	Tuutti [1993]
0.6			Laboratory	Locke & Siman [1980]
1.6 - 2.5			Laboratory	Lambert et al. [1991]
1.8 - 2.2			Field	Lukas [1985]
			Laboratory	Pettersson [1993]
			Laboratory	Goni & Andrade [1990]
			Laboratory	Diamond [1986]
			Laboratory	Hausmann [1967]
			Laboratory	Yonezawa et al. [1988]

Table 2. Additional chloride threshold levels (black steel) in macro crack free concrete in various marine or laboratory exposure regimes, Pettersson [1996], Pettersson and Sandberg [1996], Sandberg [1995], Arup [1996], Thomas [1995] and by Breit [1994].

Concrete type	Submerged zone		Splash zone		Atmospheric zone	
	C_{cr} - %Cl of cement	Procedure	C_{cr} - %Cl of cement	Procedure	C_{cr} - %Cl of cement	Procedure
$w/b = 0.50$						
100 % CEM I	1.5-2.0	A	0.6-1.9	A		
100 % CEM I	1.6-2.5	B	1.2-2.7	B	1.5-2.2	B
100 % CEM I	>2.0	C	0.3-1.4	C		
5 % SF	1.0-1.9	A				
5 % SF	0.8-2.2	B				
20 % FA			0.3-0.8	C		
$w/b = 0.40$						
100 % CEM I	>2.0	A	0.9-2.2	A		
100 % CEM I	>2.2	B				
5 % SF	>1.5	A				
$w/b = 0.30$						
100% CEM I	>2.2	A	>1.5	A		
5% SF	>1.6	A	>1.0	A		
20 % FA	1.4	A	0.7	A		

3.1 The effect of the concrete moisture state

The effect of relative humidity on the chloride threshold level in laboratory exposed mortars is shown in Figure 1, as presented by Pettersson [1996].

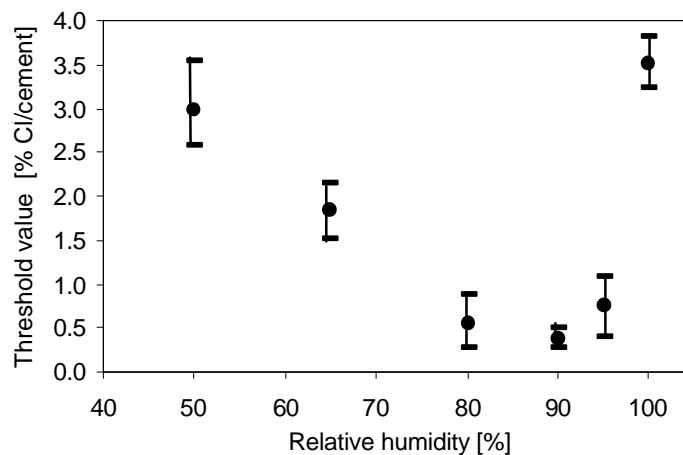


Figure 1. The effect of relative humidity on the chloride threshold level in laboratory exposed mortars, w/c ratio = 0.50, Pettersson [1996].

3.2 The effect of water to binder ratio

Pettersson and Sandberg [1996] as shown in Figure 2 illustrated the effect of water to binder ratio on the chloride threshold.

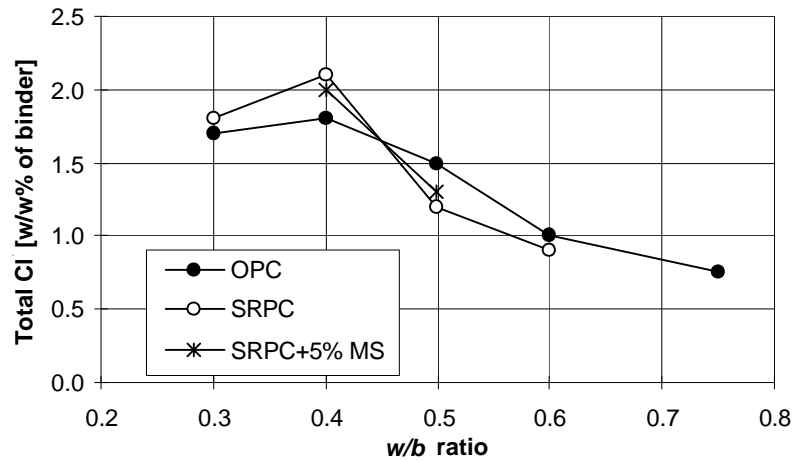


Figure 2. Chloride threshold levels measured on submerged concrete or mortar. Experimental results. Cover = 15 to 20 mm. Pettersson and Sandberg [1996].

3.3 The effect of mineral admixtures in concrete

Mineral admixtures have been found to decrease the chloride threshold level, as illustrated by Thomas [1996] for fly ash exposed in a marine splash zone, Figure 3. Pettersson [1993], [1996] has reported similar results for the effect of fly ash and silica fume.

Note that several investigations have indicated a very positive and decreasing effect of mineral admixtures on the corrosion rate. These findings are in most cases not related to direct studies of the chloride threshold, rather obtained from studies of the corrosion behaviour in the active state. The positive effect of mineral admixtures on the corrosion rate is attributed to the increase in concrete resistivity.

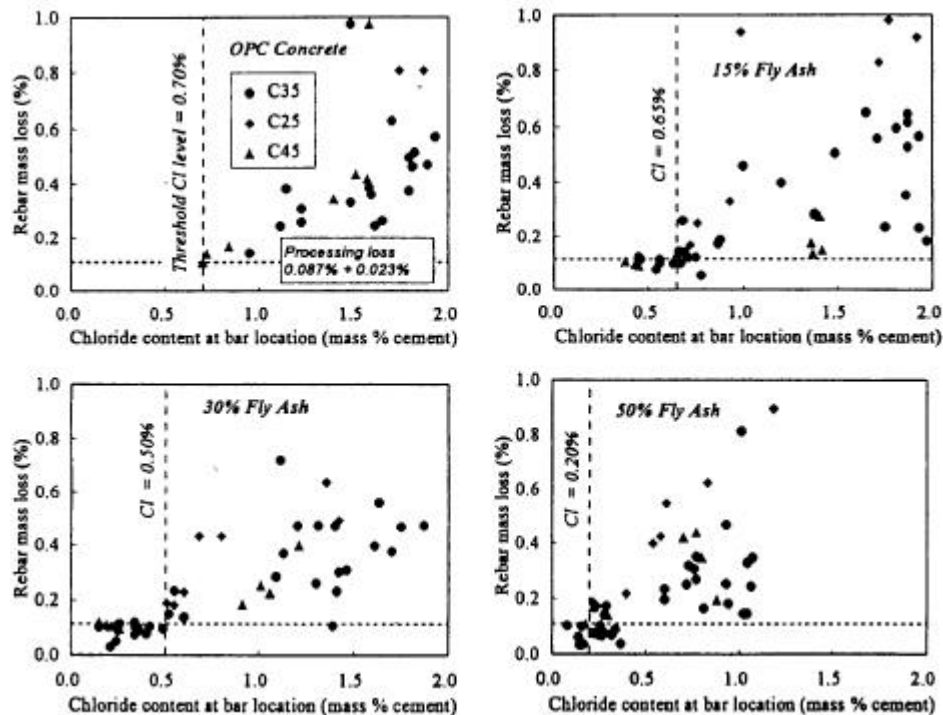


Figure 3. Chloride threshold levels and corrosion rates for OPC and fly ash concrete exposed in a marine splash zone in Canada, Thomas [1996].

The negative effect of mineral admixtures on the chloride threshold level is attributed to the decrease in alkalinity of the concrete pore solution, and to the decrease in calcium hydroxide at the steel-concrete interface, Sandberg [1995].

4. THE DEVELOPMENT OF CHLORIDE THRESHOLD LEVELS FOR DESIGN PURPOSES

The chloride threshold levels presented in Table 2 and Figures 1 and 3 indicate that the chloride threshold levels tend to decrease with the incorporation of mineral admixtures, and with an increasing w/c ratio. This behaviour is attributed to the decrease in the pH of the concrete pore solution caused by the incorporation of mineral admixtures, and by the diluting effect of an increasing w/c ratio, Sandberg [1995] and Pettersson [1996].

The threshold levels given in Table 1 are unfortunately presented in several different ways and sometimes lacking relevant information, which makes it very difficult to evaluate the results in a statistically correct way for design purpose. Therefore, a conservative engineering approach has been used as illustrated in the previous examples 1 and 2, to establish chloride threshold levels for design purpose as shown in Table 3. The relative differences in threshold levels between OPC and FA-concrete, between OPC and SF-concrete, and between OPC concrete of various w/c ratio, as found by Thomas [1996] and Pettersson [1996] respectively, has been maintained in the development of Table 3.

Table 3. Suggested design values for chloride threshold levels (black steel) in various Nordic exposure zones.*

Concrete type	submerged zone C_{cr} %Cl of PO (cement + puzzolanas)	marine splash zone C_{cr} %Cl of PO	de-icing salt splash zone C_{cr} %Cl of PO	atmospheric zone marine/de-icing C_{cr} %Cl of PO
w/b 0.50				
100 % CEM I	1.5 %	0.6 %	0.4 %	0.6 %
5 % SF	1.0 %	0.4 %	0.3 %	0.4 %
10 % SF	0.6 %	0.2 %	0.2 %	0.2 %
20 % FA	0.7 %	0.3 %	0.2 %	0.3 %
w/b 0.40				
100 % CEM I	2.0 %	0.8 %	0.6 %	0.8 %
5 % SF	1.5 %	0.5 %	0.4 %	0.5 %
10 % SF	1.0 %	0.3 %	0.2 %	0.3 %
20 % FA	1.2 %	0.4 %	0.3 %	0.4 %
w/b 0.30				
100% CEM I	2.2 %	1.0 %	0.8 %	1.0 %
5% SF	1.6 %	0.6 %	0.5 %	0.6 %
10% SF	1.2 %	0.4 %	0.3 %	0.4 %
20 % FA	1.4 %	0.5 %	0.4 %	0.5 %

*Chloride threshold levels vary extensively in field exposed concrete exposed to the air, as a consequence of the varying microclimate at the steel surface. As a consequence the chloride threshold level depends on the cover thickness and on the physical bonding between concrete and reinforcement. The chloride threshold levels are only valid for "macro crack free" concrete with a maximum crack width of 0.1 mm and a minimum cover of 25 mm. The data are not valid for calculations of the initiation time in cracked concrete with crack widths > 0.1 mm.

5. ENVIRONMENTAL ZONES

The environmental exposure to concrete structures in different exposure situations can be divided into different classes depending on the aggressiveness of the environment. This has been done in the Danish concrete standard, where four environmental classes is used: Passive, Moderate, Aggressive and Particular aggressive environmental class.

If moisture and chloride is present the environmental class is defined as aggressive or particular aggressive.

In Danish outdoor climate frost action also happens, which means that concrete in structures must be frost-resistant, if exposed to frost in a water-saturated condition during construction or in function.

The chloride-containing marine environment and the road environment can be subdivided into a number of local classes, while the chloride exposure is depending on the part of the structure. The distance to the waterline or the lane is one of the most important parameters. When striving towards an economical design of a structure one can group the individual structural parts/sections in different local environmental classes.

An appropriate division into local environmental classes, which is relevant in both marine environment and road environment, is given below. Besides, some examples on structural parts belonging to each local environmental class are stated. The purpose of this grouping is to exemplify the number of different chloride exposures, which can be seen on one structure. Among other things, the division is appropriate when planning inspection on a structure, while it for many (especially smaller) constructions will be too detailed as a paradigm for division into different environmental classes with varying covers and/or concrete qualities.

1. Road environment

- a) The “wet” road environment, i.e. structural parts, which are able to “see” the sky and which are subjected to direct rain. ***Wet splash (WRS)***: The distance to the traffic is less than 4 m e.g. edge beams.
- b) The “dry” road environment, i.e. structural parts, which are placed below a bridge deck and due to this not able to “see” the sky and not subjected to direct rain, but only to traffic splash. ***Dry splash (DRS)***: The distance to the traffic is less than 4 m e.g. pillars.
- c) The region outside the borders mentioned above. ***Distant road atmosphere (DRA)***: The wet or the dry environment where the distance to the traffic is more than 4 m e.g. noise shelters or parts of the structure high above road level.

Marine environment

- a) Submerged structures (***SUB***) placed below level -3 m with respect to the lowest minimum water level, e.g. caissons.
- b) Structures placed in the splash zone (***SPL***), here defined as being above level -3 m with respect to the lowest minimum water level and below level +3 m with respect to the highest maximum water level, e.g. bridge pier shafts.
- c) Structures placed in the atmosphere (***ATM***) above level +3 m with respect to the highest maximum water level, e.g. bridge piers and the underneath of decks on marine bridges.

6. ESTIMATION FORMULAS

An approach similar to that made by Frederiksen et al. [1997] is used in order to make semi-objective estimates for the threshold concentrations.

The values in Table 3 can be approximated by a formula of the type:

$$C_{cr} = k_{cr, env} \times \exp\left(K \times \text{eqv}\left(\frac{w}{c}\right)_{cr}\right) \quad (1)$$

A multiple regression analysis performed on the data in Table 3 is used to quantify the parameters. Based on that equation (1) is changed into (2) as follows:

$$C_{cr} = k_{cr, env} \times \exp\left(-1.5 \times \text{eqv}\left(\frac{w}{c}\right)_{cr}\right) [\% \text{ mass binder}] \quad (2)$$

The constants of (2) are given in Tables 4, 5 and 6.

Table 4. The constant $k_{cr, env}$ in (2) for the road environment.

Environ- ment:	Wet Road envi- ronment	Dry Road envi- ronment	Distant Road Atmosphere (DRA)
Constant:	Splash (WRS)	Splash (DRS)	
$k_{cr, env}$	1	1.25	1.25

Table 5. The constant $k_{cr, env}$ in (2) for the marine environment.

Environ- ment:	Submerged ma- rine environment (SUB)	Marine envi- ronment	Marine Atmos- phere (ATM)
Constant:		Splash (SPL)	
$k_{cr, env}$	3.35	1.25	1.25

Table 6. The activity factors for corrosion initiation in the road environment to be used when calculating the $\text{eqv}(w/c)_{cr}$ ratio in (2).

Activity factor	Silica fume	Fly ash
k	-4.7	-1.4

The quality of the suggested formula (2) can be visualised graphically by plotting the values of Table 3 versus the values obtained by calculations according to (2), cf. Figure 4 for the road environment and in Figure 5 for the marine environment.

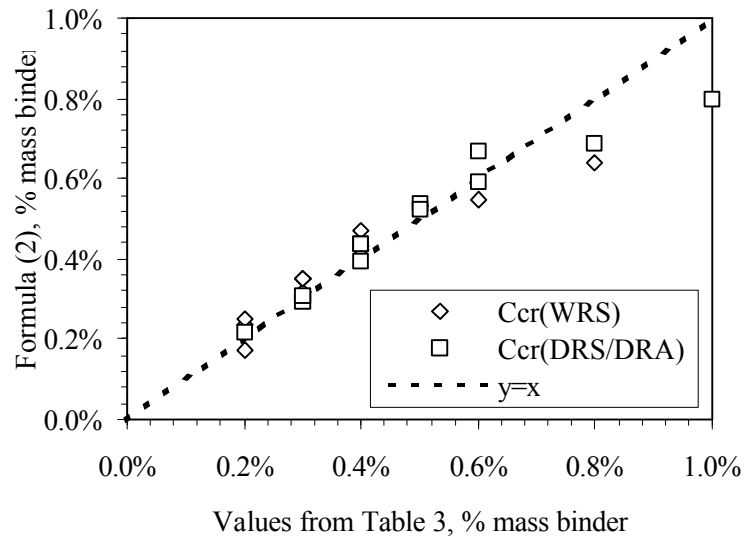


Figure 4. Plot of the values of Table 3 versus the values obtained by calculations according to the "model". The estimates of C_{cr} are seen to be in a fairly good agreement with the original data (Table 3, which are estimates too). **Road Environment.**

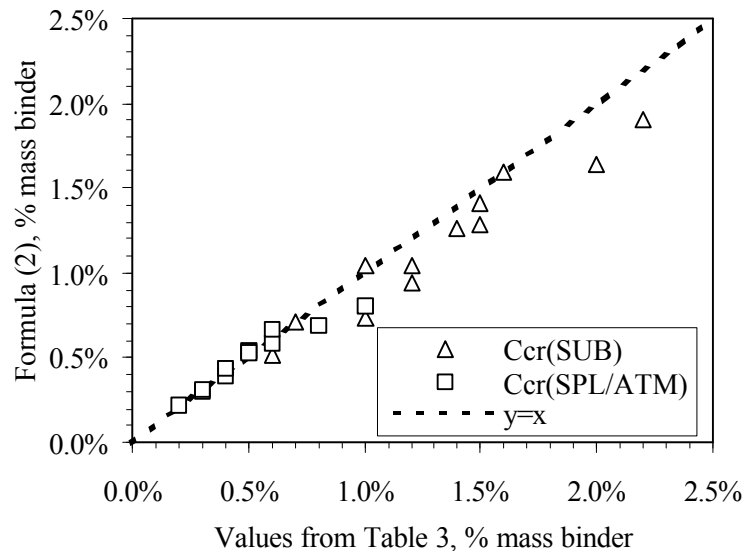


Figure 5. Plot of the values of Table 3 versus the values obtained by calculations according to the "model". The estimates of C_{cr} are seen to be in a fairly good agreement with the original data (Table 3, which are estimates too). **Marine environment.**

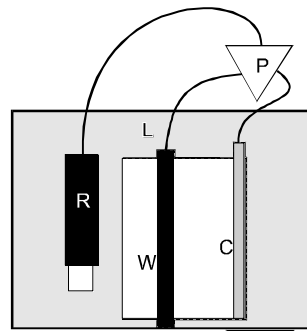
7. ATTEMPT TO DEVELOP A RELIABLE TEST METHOD

An ongoing NORDTEST project with the scope of developing/defining a test method for determination of chloride threshold values has been prolonged until mid 2000. Below some preliminary considerations and results are presented.

The first objective was to decide what is understood when using the term “Chloride Threshold Value”. The end-user of the result from such an experiment wants to know at what chloride concentration in the concrete the corrosion will initiate.

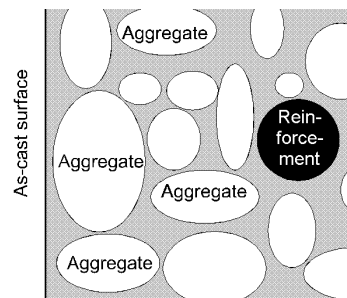
Many threshold value determinations have been concentrating on measuring the chloride concentration in the near by region of the steel reinforcement bar, e.g. by sophisticated techniques capable of measuring the chloride concentration exactly at the steel-concrete interface. This is in principle correct. All results from experiments trying to do this more or less precisely have the disadvantage that they are difficult to translate into reliable values also difficult to investigate.

The most simple and reliable technique to determine the corrosion on-set is to hold the steel potentiostatically controlled during the exposure, cf. figure. By “continuously” monitoring the current needed to maintain the passive steel at a certain potential, e.g. 0 mV vs. SCE, it can very precisely be monitored when the on-set of the corrosion appears because the current needed will rise one or two orders of magnitude.



determine the electrode exposure, cf. current needed certain potential,

By combining the above experience it is in fact natural to define the chloride threshold value as the concentration of chloride in the infinitesimal layer where the concrete cover of the reinforcement is measured at the time where the corrosion on-set is established. Therefore a new approach is introduced: *At the time of on-set of corrosion the chloride concentration in the undisturbed bulk concrete is measured at the depth of the reinforcement.* In other words: It is *not* considered what the chloride concentration is at the concrete-steel interface because that is not an interesting value for the end-user. The concentration appearing in the *undisturbed* bulk the steel.



not an interesting to consider is that concrete near to surface layer like the 10 mm from the more

Experience shows that the outermost (against a mould) of about 10 mm is not *undisturbed* bulk concrete. Having passed as-cast surface the concrete becomes

homogeneous, i.e. the cement paste volume becomes more constant with depth. The phenomenon behind this is the fact that large aggregate particles will only tend to touch the mould in a “point” so that the cement paste concentration in the surface is close to 100%. This changes dramatically when moving inward in the concrete. Therefore it is natural to regard the concrete cover from the surface to the reinforcement as an inhomogeneous material consisting of three layers with different characteristics:

1. The surface layers where a plane typically governs the position of the aggregate.
2. The bulk layers where the position of the aggregate is random.
3. The rebar layers where a circle typically governs the position of the aggregates.

To avoid disturbances in the chloride concentration measurement from the layers 1 and 3 above one needs to be away from disturbing bodies in the concrete. Experience from

chloride diffusion experiments says that 10 mm are sufficient to eliminate this problem. Therefore the specimen for the chloride threshold experiment now is designed to provide the needed space, cf. the sketch on the following page.

7.1 Test method

The project must result in a detailed description of how to perform the test. Therefore the test method is being prepared along with defining more and more of the test.

7.2 Test parameters

As quite a lot of experience exists of how to perform the corrosion on-set measurement the effort is at this stage concentrated on finding/defining:

- The level for the potential
- The needed cover thickness
- To determine the experimental scatter in-lab and between-labs.

To different levels of potentials were applied: 0 mV vs. SCE and +350 mV vs. SCE. Three cover thicknesses, 5 mm, 10 mm and 15 mm are used in one laboratory. Six specimens of three concrete mixes are to be tested in each laboratory.

7.3 Types of concrete investigated

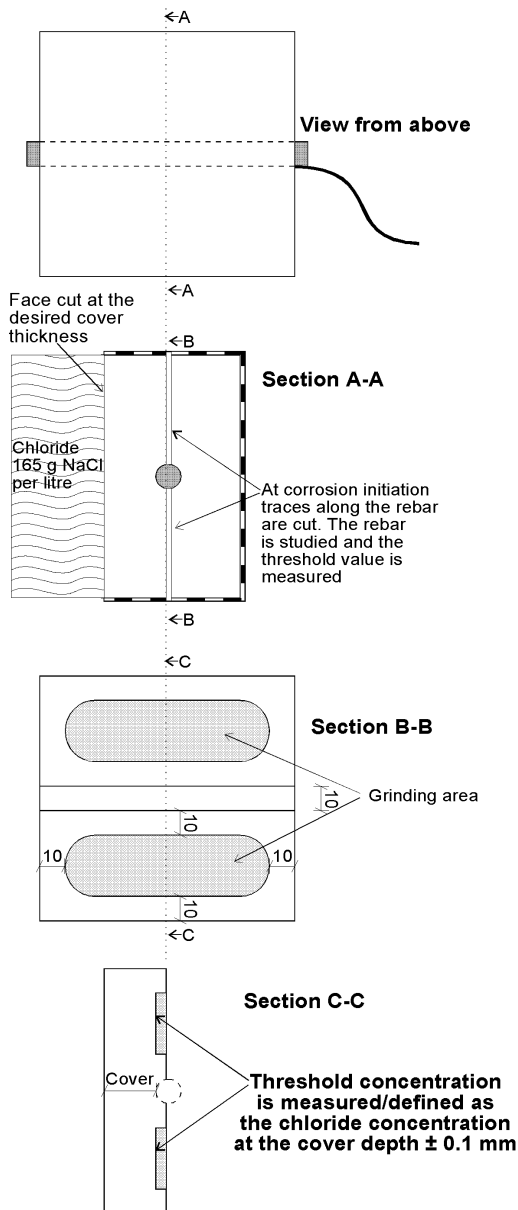
Three types of concrete have been cast for the experiments. The only difference between the concrete is the type of cement. Three Danish cement types were chosen:

- a) Low alkali sulphate resisting Portland Cement, CEM I 42.5
- b) Rapid Hardening Portland Cement, CEM I 52.5
- c) Portland Filler Cement, Cem II 52.5

Those cement types represent the most commonly used cements on the Danish market and at the same time comparison with other European countries is possible.

Three concretes were manufactured so that they had the same water-cement ratio (0.45), the same paste volume (27 %), the same aggregate size distribution, the same initial slump (45 mm) and the same natural air-content (1.5 %). The maximum aggregate size is 16 mm.

Principle for defining and measuring the chloride threshold value for corrosion initiation in concrete



AEC
laboratory

www.aec-dk.com
Phone: +45 45 66 12 66
Fax: +45 45 66 14 66

7.4 Some preliminary results

Until now only very few and rather uncertain data have been obtained from the tests. Problems have arisen with the protection of the steel concrete interface where the specimens are submerged into the sodium chloride solution. The results do however give some kind of information as seen below.

Only data from the specimens having a concrete cover of 5 mm have been obtained.

In the period from 2 to 5 months of exposure it was decided to stop five specimens in the test because the current needed to maintain the potentiostatic potential at +350 mV vs. SCE was too high, i.e. above 0.030 mA. The measured chloride concentrations at the rebar level are shown in Figure 6 together with some results from an earlier investigation carried out on mortar bars, at a potentiostatic potential at 0 mV vs. SCE and

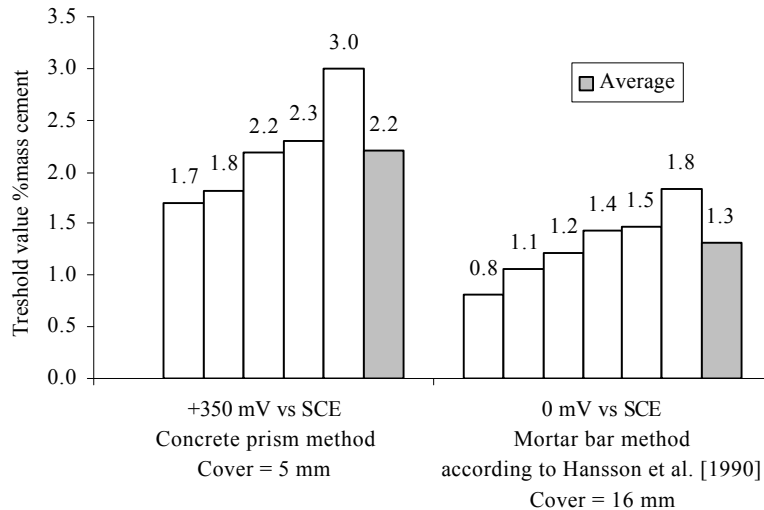


Figure 6. Results from the Nordtest project (left) versus results from some previous measurements (right). Both sets of data are from concrete with Danish Low Alkali Sulphate Resisting Cement (CEM with a cover thickness of 16 mm.

8. SUMMARY AND CONCLUSION

The established table and formula for estimation of chloride threshold values in different environments and for different concrete compositions is a step forward. Now threshold values depend logically on the type of exposure and type of concrete involved. By establishing a common test method for the determination of threshold values hopefully, more data and experience will sprout up.

Only few results from the ongoing experiments exist at this moment (ultimo March 2000). From the formula given above, the expected level of the chloride threshold value in the experiment can be found as follows:

The type of exposure in the test is constant submersion, but the potentiostatically controlled “artificial potential” may make the set-up comparable to the marine atmosphere (or any of the four environments SPL, ATM, DRS or DRA). The threshold value in the test is therefore assumed to be 0.64% mass cement or 0.094 % mass concrete (354 kg cement / 2385 kg concrete) if the test environment is similar to one of the four environments.

If instead the test environment is more like “SUB” the expected threshold value is 1.71% mass cement or 0.25% mass concrete. The preliminary results indicate that the test environment more likely is comparable to the submerged condition. This again indicates that the applied potential at or above 0 mV vs. SCE in the test has little or no effect in providing a situation similar to that of an aerated condition in a real structure.

An observation that supports the indication of the little relevance of the applied positive potential in the potentiostatic test is the finding of higher threshold values at higher potentials, cf. Figure 6.

The preliminary results also indicate that it should be “safe” to use a concrete cover of 5 mm when this is obtained by cutting away the excess cover after the concrete has hardened.

9. REFERENCES

- [1996] **Arup, H.:** *A new method for determining chloride thresholds as a function of potential in field exposure tests.* In Durability of Concrete in Saline Environment, pp. 107-112. Cementa AB, Box 144, S-182 12 Danderyd, Sweden.
- [1994] **Bamforth, P.B.; Chapman-Andrews, J.F.:** *Long term performance of R. C. elements under UK coastal exposure conditions.* In Corrosion and Corrosion Protection of Steel in Concrete, ed. R. N. Swamy, Sheffield Academic Press, Vol. 1, pp. 139-156.
- [1994] **Breit, W.:** *Untersuchungen über den kritischen, korrosionsauslösenden Chloridgehalt.* (In German). T 2614 IBAC Report F 355, IRB Verlag, Stuttgart.
- [1986] **Elsener, B.; Böhni, H.:** *Corrosion of steel in mortar studied by impedance measurements.* In Electrochemical Methods in Corrosion Research, ed. M. Duprat, Trans Tech Publications Ltd., Switzerland, Vol. 8, pp. 363-372.
- [1997] **Frederiksen, J.M., Nilsson, L.-O., Poulsen, E.; Sandberg, P.; Tang L. & Andersen, A.:** *HETEK, A system for estimation of chloride ingress into concrete, Theoretical background.* The Danish Road Directorate, Report No. 83.
- [1995] **Glass, G.K.; Buenfeld, N. R.:** *Chloride threshold levels for corrosion induced deterioration of steel in concrete.* In Chloride Penetration into Concrete, Proceedings of the International RILEM Workshop in Saint-Rémy-Les-Chevreuse, Oct. 15-18. RILEM Publications 1997, pp. 429-440.
- [1990] **Goni, S.; Andrade, C.:** *Synthetic concrete pore solution chemistry and rebar corrosion rate in the presence of chlorides.* Cement & Concrete Research, Vol. 20, No. 4, pp. 525-539.
- [1996] **Gustafsson, M.E.R.; Franzen, L.G.:** *Dry deposition and concentration of marine aerosols in a coastal area, SW Sweden.* Atmospheric Environment, Vol. 30, No. 6, pp. 977-989.
- [1990] **Hansson, C.M.; Sørensen, B.:** *Threshold concentration of chloride in concrete for the initiation of reinforcement corrosion.* In Corrosion Rates of Steel in Concrete, ed. N. S. Berke, V. Chaker, D. Whiting. ASTM STP 1065, pp. 3-16.
- [1967] **Hausmann, D.A.:** *Steel corrosion in concrete - How does it occur?* Mater. Protection, Vol. 6, pp. 19-23.
- [1993] **Henriksen, C.F.:** *Chloride corrosion in Danish bridge columns.* In Chloride Penetration into Concrete Structures, Proc. Nordic Miniseminar, Göteborg, edited by L-O Nilsson, Dept. of Building Materials, Chalmers University of Technology. Publication P-93:1.
- [1991] **Lambert, P.; Page, C. L.; Vassie, P.R.W.:** *Investigations of reinforcement corrosion. 2. Electrochemical monitoring of steel in chloride contaminated concrete.* Mater. Struct., Vol. 24, No. 143, pp. 351-358.
- [1980] **Locke, C. E.; Siman, A.:** *Electrochemistry of reinforcing steel in salt contaminated concrete.* In Corrosion of Reinforcing Steel in Concrete, ed. D.E. Tonini, J.M. Gaidis, ASTM STP 713, pp. 3-16.

- [1985] **Lukas, W.:** *Relationship between chloride content in concrete and corrosion in untensioned reinforcement on Australian bridges and concrete road surfings*. Betongwerk und Fertigteil-Technik, Vol. 51, No. 11, pp. 730-734.
- [1996] **Nilsson, L.O.; Poulsen, E.; Sandberg, P.; Sørensen, H.E.; Klinghoffer, O.:** *HETEK, Chloride penetration into concrete, state-of-the-art, Transport processes, corrosion initiation, test methods and prediction models*. The Danish Road Directorate, Report No. 53.
- [1993] **Pettersson, K.:** *Chloride threshold value and corrosion rate in reinforced concrete*. In Concrete 2000, ed. R.K. Dhir, M.R. Jones, E & F N Spon, London, Vol. 2, pp. 461-471.
- [1996] **Pettersson, K.:** *Service life of concrete structures - in a chloride environment*. Swedish Cement & Concrete Research Institute. CBI Report 3:96.
- [1996] **Pettersson, K.; Sandberg, P.:** *Chloride threshold levels and corrosion rates in cracked high performance concrete exposed in a marine environment*. Presented at the 4th CANMET/ACI Int. Conf. on Durability of Concrete, Sydney, Australia, August 17-22, 1997.
- [1995] **Sandberg, P.:** *Critical evaluation of factors affecting chloride initiated reinforcement corrosion in concrete*. Report TVBM-3068, Lund Institute of Technology, Building Materials.
- [1995] **Sandberg, P.; Pettersson, K.; Sørensen, H.E.; Arup, H.:** *Critical chloride concentrations for the onset of active reinforcement corrosion*. In Chloride Penetration into Concrete, Proceedings of the International RILEM Workshop in Saint-Rémy-Les-Chevreuse, Oct. 15-18. RILEM Publications 1997, pp. 453-459.
- [1990] **Schiessl, P.; Raupach, M.:** *The influence of concrete composition and microclimate on the critical chloride content in concrete*. In Corrosion of Reinforcement in Concrete, ed. C. L. Page, K.W.J. Treadaway, P.B. Bamforth, Elsevier Applied Science, London, pp. 49-58.
- [1975] **Stratful, R.F.; Jurkovich, W.J.; Spellman, D. I.:** *Corrosion testing of bridge decks*. Transportation Research Record No.539, pp 50-59.
- [1996] **Thomas, M.D.A.:** *Chloride thresholds in marine concrete*, Cement & Concrete Research, Vol. 26, No. 4, pp. 513-519.
- [1990] **Thomas, M.D.A.; Matthews, J.D.; Haynes, C.A.:** *Chloride diffusion and reinforcement corrosion in marine exposed concretes containing pulverised fuel ash*. In Corrosion of Reinforcement in Concrete, ed. C. L. Page, K.W.J. Treadaway, P.B. Bamforth, Elsevier Applied Science, London, pp. 198-212.
- [1993] **Tuutti, K.:** *Effect of cement type and different additions on service life*. In Concrete 2000, ed. R.K. Dhir, M.R. Jones, E & F N Spon, London, Vol. 2, pp. 1285-1295.
- [1984] **Vassie, P.:** *Reinforcement corrosion and the durability of concrete bridges*. Proc. Inst. Civil Engineers. Part 1. Vol 76, pp. 713-723.
- [1985] **West, R. E.; Hime, W.G.:** *Chloride profiles in salty concrete*. Mater. Perf. Vol. 24, No. 7, pp 29-36.
- [1988] **Yonezawa, T.; Ashworth, V.; Procter, R.P.M.:** *Pore solution composition and chloride effects on the corrosion of steel in concrete*. Corrosion, Vol. 44, No. 7, pp. 489-499.

A clarification of the corrosion of reinforcement of structures exposed in a chloride environment

A. Castel, R. François, G. Arliguie

LMDC, INSA-UPS Toulouse

Abstract

This article gives a progress report on the results obtained after about fifteen years experimentation. The main projections concern a description of the negligible role of bending cracks in the reinforced concrete (not just their widths) and the essential role of tensile concrete located between the bending cracks. Indeed, tensile concrete will continue to protect steel from corrosion as long as the bond between the steel and the concrete remains of good quality and it is the mechanical degradation of this connection beyond a certain level of loading that is responsible for corrosion of the reinforcements. This result allows for the introduction of mechanical criteria of durability making it possible to guarantee the service-life of the reinforced concrete structures exposed in a chloride environment.

Key-words : Cracks, corrosion, reinforced concrete, criteria, mechanical behavior, damage

Introduction

The LMDC began studies concerning durability and the relation between chemical degradation and mechanical behaviour fifteen years ago. The first topic developed was the corrosion of the reinforcements in reinforced concrete.

Initially, the project (supported by the French Ministry for Research) investigated the failings and contradictions characteristic of the experimental bases from which design rules are drawn up to ensure the durability of concrete structures. The initial objective of this work was to determine the influence of service cracking (due to the load) in the reinforced concrete and the damage possibly associated with this cracking on the corrosion process of the steels due to the incursion of aggressive agents through the concrete cover. One of the original features of this work was the fact that it took into account the real state of mechanical damage to the concrete with the use of large-sized reinforced concrete elements (3 m length with a cross-section of 15x30 cm) and stored in loaded state (three points bending and working load). Thus, the penetration of chlorides and the development of corrosion were studied taking into account the real condition of the concrete (cracking and damage due to the load and non saturated concrete) and its change over time, whereas this is impossible with low-size test specimens as used in most tests [1]. The research programme is still under way with the current objective being to predict the service-life of reinforced concrete structures exposed to chlorides.

This article gives a progress report on the results obtained after about fifteen years experimentation. The main projections concern a description of the negligible role of bending cracks in the reinforced concrete (not just their widths) and the essential role of tensile concrete located between the bending cracks. Indeed, tensile concrete will continue to protect steel from corrosion as long as the bond

between the steel and the concrete remains of good quality and it is the mechanical degradation of this connection beyond a certain level of loading that is responsible for corrosion of the reinforcements. This result allows for the introduction of mechanical criteria of durability making it possible to guarantee the service-life of the reinforced concrete structures exposed in a chloride environment.

1. False notions on cracking

All the current international regulations estimate that the risk of corrosion of reinforced concrete is related to the presence of service cracking and that we need to limit the width of these cracks to obtain good durability [2][3][4][5].

We shall show that these conclusions are false, being more myth than reality.

How has it come about that cracking of reinforced concrete is believed to represent a danger with respect to corrosion?

Firstly, cracking is visible to the naked eye and it seems obvious a priori that aggressive agents such as the chloride ion (10 nm) can readily penetrate these spaces and quickly reach the reinforcements to cause corrosion pitting at the bottom of crack.

Secondly, the use of crack models (usually 2 spaced concrete surfaces at a given distance from each other) as experimental studies into the development of corrosion at the bottom of cracks led to the obvious inference that cracking was to blame for subsequent weakness [6]. But in fact, this was, as we shall show, an incorrect interpretation of the phenomena.

Thirdly, the use of experimental results obtained too early (short term experiments) [7] or over the longer term but without taking the kinetic aspect into account also results in concluding as to an obvious influence of cracking (Figure 1). However, this is also an erroneous interpretation of the phenomena.

As an example, observation of figure 1 without information on the kinetics of the phenomena would lead us to conclude as to a correlation between the presence and even the opening up of the cracks with the development of reinforcement corrosion.

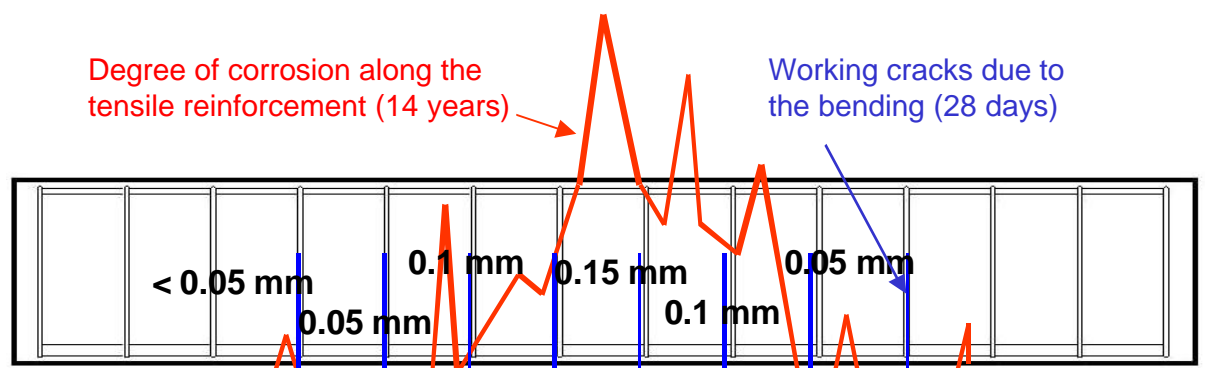


Figure 1: Comparison between the cracking map at 28 days and the corrosion map at 14 years for a 3 m long reinforced concrete beam stored under load (3 points bending) in a saline atmosphere. Examination of this figure alone suggests that corrosion is related to the presence of the cracks as also to their discontinuity of opening. However, examination of the development of corrosion

throughout the test led to a completely different conclusion, viz that cracks may or may not be indirectly responsible for corrosion of the tensile reinforcements according to the loading level [8].

2. The real nature and role of cracking

Cracking has 3 effects. Firstly, it leads to rapid penetration of aggressive agents into the bottom of the crack. Secondly, it allows for rapid initiation of corrosion at the crack tip. Thirdly, it allows expansive oxides to develop without creating additional stresses (and thus no additional cracking). Very quickly these oxides heal the cracks and lead to a halt in corrosion due to lack of chlorides. The result is shown in Figure 2: we can clearly see very low level corrosion at the crack tip (less than 1% in loss of mass) after a number of weeks. An obvious interpretation of the results in these terms would result in stating that there is a correlation between the presence of the cracks and the presence of corrosion. However, if you continue the experiment for a number of years, you will realise that the degree of corrosion is the same after 5 years as that obtained after one year and thus that corrosion has been halted [1].

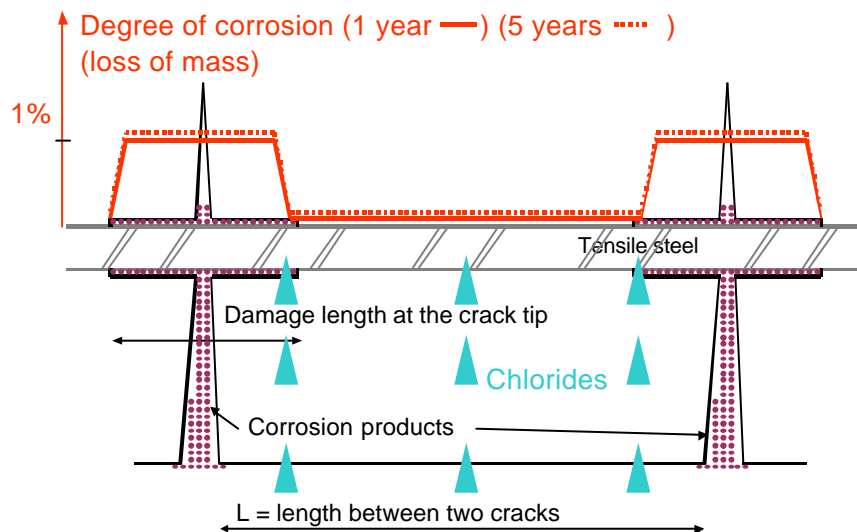


Figure 2: Schematic view of corrosion process in cracked concrete. Corrosion at the tip of the crack led to healing to protect the re-bars from corrosion. As a result, the degree of corrosion is the same after one year and five years of exposition to chloride environment. The aggressive agents then have to reach the reinforcements through the tensile concrete [8].

The service-life of the reinforced concrete thus proves to be independent of the functional cracking of the reinforced concrete.

A contrario, the tensile concrete between the cracks continues to ensure protection of the steel. This tensile concrete neglected by mechanical designers deserves in fact our full attention since the service-life of the reinforced concrete does in fact appear to be closely related to the quality of the bond between the steel and this tensile concrete.

3. Role of tensile concrete between the bending cracks

Whereas before cracking the mechanical behaviour of reinforced concrete is that of a homogeneous material, after cracking its behaviour is quite different. Indeed, after cracking the behaviour of the reinforced concrete between the cracks is the same as that for a tie (Figure 4), meaning that it is the steel that transmits part of its tensile load onto the concrete located between two cracks [13].

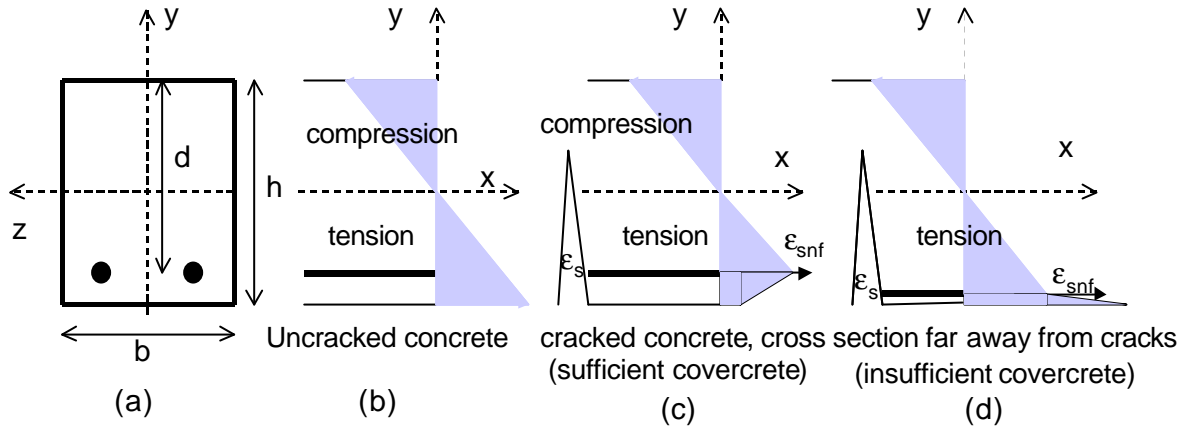


Figure 4: Schematic view of strains on a cross-section of a reinforced concrete beam before cracking (b) and after cracking but far away from cracks (c) and (d). After cracking, if the concrete cover is sufficient (c), the maximum strain in tension in the concrete will be at the level of the tensile reinforcement [13]. In this case, an increase of the load will lead to a damage of the interface between steel and concrete [13]. After cracking, if the concrete cover is insufficient (d), the maximum strain in tension will be at the bottom of the cross-section and will lead to the appearance of new cracks when increasing the load. ϵ_s is the tensile strain of re-bars in cracked cross-section and ϵ_{snf} is the tensile strain of re-bars in uncracked cross-section.

Mechanical behaviour of the reinforced concrete after cracking will be optimised if the maximum stress in the tensile concrete is located at the centre of gravity for tensile steels (Figure 4c). For this, we need a minimal cover so a sufficient field of tensile stress can be developed under the level of steels for the tie to function correctly. Where this is not the case (insufficient cover as in figure 4d), the level of tensile stresses in the concrete will increase in the concrete cover leading to the appearance of additional mini-cracks [9] resulting in the loss of mechanical contribution in this zone and in a reduction in the protection given to the steel by the tensile concrete.

After cracking, the level of tensile stress in the concrete located between two cracks will be limited by the possibility of transmission of the tensile load of the tensile steels towards the concrete. As soon as the strain of the tensile steel between two cracks (ϵ_{snf}) reaches the tensile failure limit for the concrete, damage to the steel-concrete interface will occur, corresponding to the appearance of a relative slipping between the two materials. The mechanical damage to the steel-concrete bond is modelled by a scalar variable d_M ranging between 0 and 1. When $d_M = 0$ there will be no damage and when $d_M = 1$ the steel-concrete bond will be completely degraded, corresponding to the steel sliding freely in the concrete [13].

This mechanical result has two very significant consequences on the physical-chemical behaviour of the reinforced concrete composite.

The first consequence is that the appearance of this mechanical damage to the steel-concrete bond allows the development of corrosion, all other parameters being equal. Figure 5 shows two reinforcements of two 12 year-old reinforced concrete beams. The real concrete cover is approximately 5 cm thick and the level of chlorides near the reinforcements is approximately 2% of the mass of the binder (i.e. 4 times greater than the currently accepted threshold for the start of corrosion [10]). Figure 5a shows a reinforcement with no mechanical damage ($d_M = 0$) while Figure 5b shows a reinforcement where mechanical damage is significant ($d_M = 0.7$) [9]. In the first instance, the reinforcement is not corroded whereas in the second, corrosion has been developing for a number of years.



(a)



(b)

Figure 5: Comparison of the state of corrosion between two reinforcements of two 12 year-old reinforced concrete beams. For both beams, the chloride rate at the vicinity of re-bars is the same and is higher than the chloride threshold currently accepted [10]. In the photograph on the left, absence of corrosion can be assigned to the good quality of the steel-concrete bond, whereas in the photograph on the right, corrosion of the reinforcements is related to preliminary mechanical damage to the steel-concrete bond [9].

Figure 6 shows the correlation between mechanical damage to the steel-concrete bond and the resulting corrosion, expressed in loss of mass. This result was obtained on a reinforced concrete beam stored in a loaded state (usual design loading) for 12 years in the presence of chlorides [9].

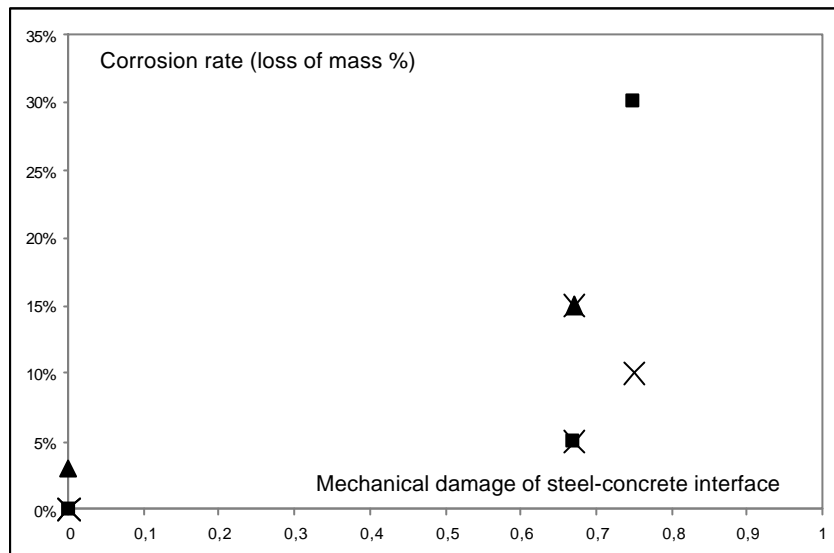


Figure 6: Correlation between mechanical damage to the steel-concrete bond and the degree of corrosion expressed in loss of mass.

The second consequence is that the appearance of irreversible non-elastic strain in tension in the concrete leads to a significant increase in the transfer properties of aggressive agents through the porous and damaged concrete. Calculation of the effective diffusion coefficient performed using experimental profiles of chloride ions obtained after 12 years exposure to chlorides actually showed an increase of 40% of the concrete zone having reached the limit of tensile failure in tension of the concrete [11].

4. Structural aspect of the service-life

The previous results, which showed the link between the mechanical behaviour of the structure and its service-life in the presence of chlorides, lead us to propose mechanical criteria of durability that are different from those relating to the limitation of the cracks' widths. The two criteria suggested are the direct consequence of the link between mechanical damage to the interface and corrosion of the reinforcements (Figure 6). The basic concept is that we shall need to limit degradation of the steel-concrete interface by limiting the strain of the tensile steels between the bending cracks at the limit of failure point for the tensile concrete. Further, to avoid degradation of the tensile concrete cover under the steel, we need to design the cross-section such that the maximum tensile stress is reached at the level of the reinforcement. We shall thus obtain two criteria known as DMC [Durability Mechanical Criteria] [12]: the first of these imposes a minimal cover, while the second imposes a maximum load so that the failure limit of the tensile concrete will not be reached between two cracks (no damage to the steel-concrete interface). The level of load will be limited through the tensile stress in the steels calculated on the cracked cross-section because, for one thing, this is a value easily determined using mechanical design models that neglect the tensile concrete (model used by civil engineers) which can be directly link to the bending moment M and also because it is already used in certain design codes to limit the width of cracks [5].

4.1. First mechanical criterion

The first criterion imposes a minimal cover on the reinforced concrete member as related to its geometrical characteristics (Figure 7).

In fact, the first criterion imposes positioning of the centre of gravity of tensile steels so that we can use appropriate constructional design to retain conventional covering as used for beams with a high vertical cross-section.

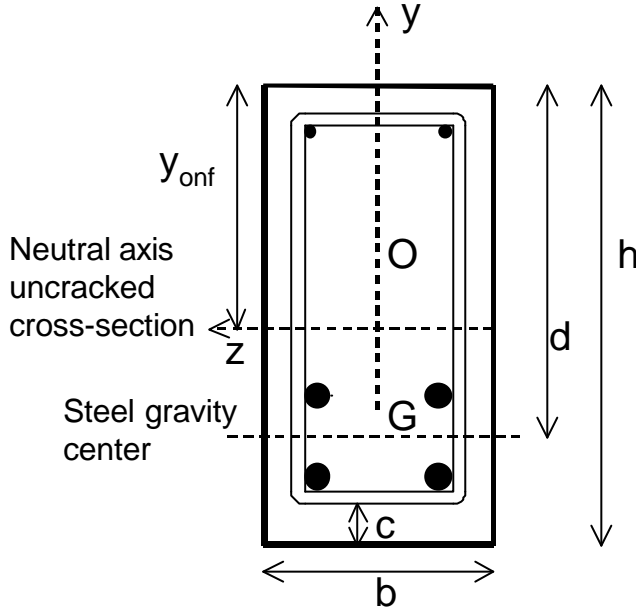


Figure 7: Geometrical parameters for the cross-section of a reinforced concrete beam, y_{onf} correspond to the position of the neutral axis calculated before cracking

The position of the centre of gravity of tensile steels must such that unequation 1 is verified [12] :

$$\frac{h - y_{onf}}{d - y_{onf}} \geq 1 + \frac{1}{\sqrt{3}} \quad (1)$$

4.2. Second mechanical criterion

This relation is obtained by comparing the internal loads between a cracked cross-section and a crack-free cross-section (Figure 8) and limiting the stress on the steels in the crack-free cross-section to the tensile limit of failure for the concrete (called f_{bt}). This calculation is performed assuming there is a perfect bond between the steel and concrete since the bond must not be damaged (i.e $d_M=0$).

For other applications, as with the change in mechanical behaviour of the reinforced concrete beyond the threshold of perfect bonding, the scalar damage parameter d_M for the steel-concrete interface can vary between 0 to 1 [13]. Further, to predict the service-life of the corroded structures, this mechanical damage variable can be coupled with an environmental damage variable d_c [13] enabling us to model the loss of bonding due to corrosion.

We consider two sections of beam stressed by the same bending moment M_{ser} : a first cross-section located adjacent to a crack where the steel is subject to stress σ_s , and a second cross-section, located between two bending cracks, where the steel is subject to stress σ_{snf}

(Figure 9).

The leverage of the internal forces on the cracked and crack-free sections are respectively noted z_f and z_{nf} ; they are calculated by using classics R-Concrete models. The resultant of tensile stresses N_{bt} is located on the steel. As these two sections of the beam are loaded by the same bending moment, we can therefore deduce a relation between unknown values to the load through σ_s , to the leverage of the internal forces and, finally, to a term C_{bt}/A , where A is the tensile steel cross-section and C_{bt} the mechanical contribution of the tensile concrete which is homogeneous to a surface. The sum $\sigma_{bti} \cdot C_{bt}$ will be equal to the resultant of tensile stresses in the concrete (N_{bt}), σ_{bti} is the tensile stress in the concrete at the level of the centre of gravity of tensile reinforcement. More details about this new mechanical model of reinforced concrete behaviour can be found in [13].

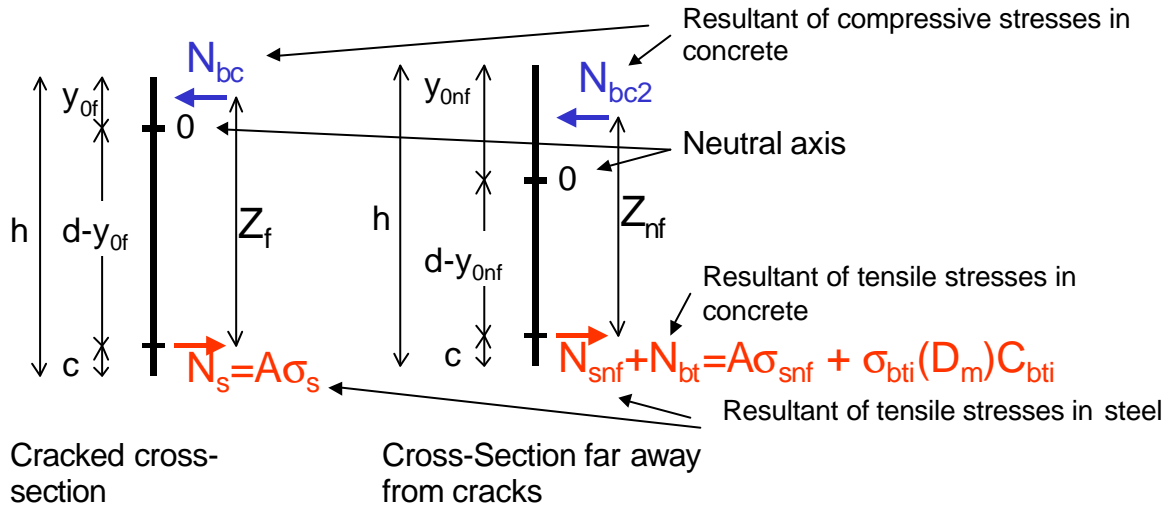


Figure 8: Parameters allowing internal forces to be calculated in cracked and crack-free cross-sections from [13]

To avoid mechanical degradation of the steel-concrete interface, mechanical loading of the reinforced concrete member must be limited to a value of bending moment M_{crit} or σ_{scrit} such that unequation 2 or 3 is verified [12] (I_f is the inertia of the cracked cross-section) :

$$M \leq f_{bt} \frac{I_f}{n(d - y_{of})} \frac{Z_{nf}}{Z_f} \left(n + \frac{C_{bt}}{A} \right) = M_{crit} \quad (2)$$

$$\sigma_s \leq f_{bt} \frac{Z_{nf}}{Z_f} \left(n + \frac{C_{bt}}{A} \right) = \sigma_{scrit} \quad (3)$$

This second durability mechanical criterion imposes a limitation on the stress σ_s in the steels located in the cracked cross section which will depend in particular on the quality of the concrete (modulus of elasticity and tensile strength) and more especially on the mechanical contribution of the tensile concrete. Indeed, we can note that an increase in the tensile concrete surface will allow the value for tolerated stress to be increased.

5. Experimental validation

Experimental validation without fitting parameters was carried out on one of the beams which had been stored for 12 years under loading in the presence of chlorides (Figure 9). The chloride content near the reinforcements was checked and was constant throughout the length of the beam, corresponding to approximately 2% as compared with the mass of binder. Although this rate is 4 times greater than that generally considered to be the threshold for the development of corrosion (i.e. 0.5%), corrosion did not develop along the length of the tensile reinforcements. Indeed, we noted that only the central zone was affected, and this over a length corresponding to that for which the second criterion of durability was not verified. It was thus only on the mechanically damaged interface zone of the steel-concrete bond, as determined by DMC model, that corrosion developed.

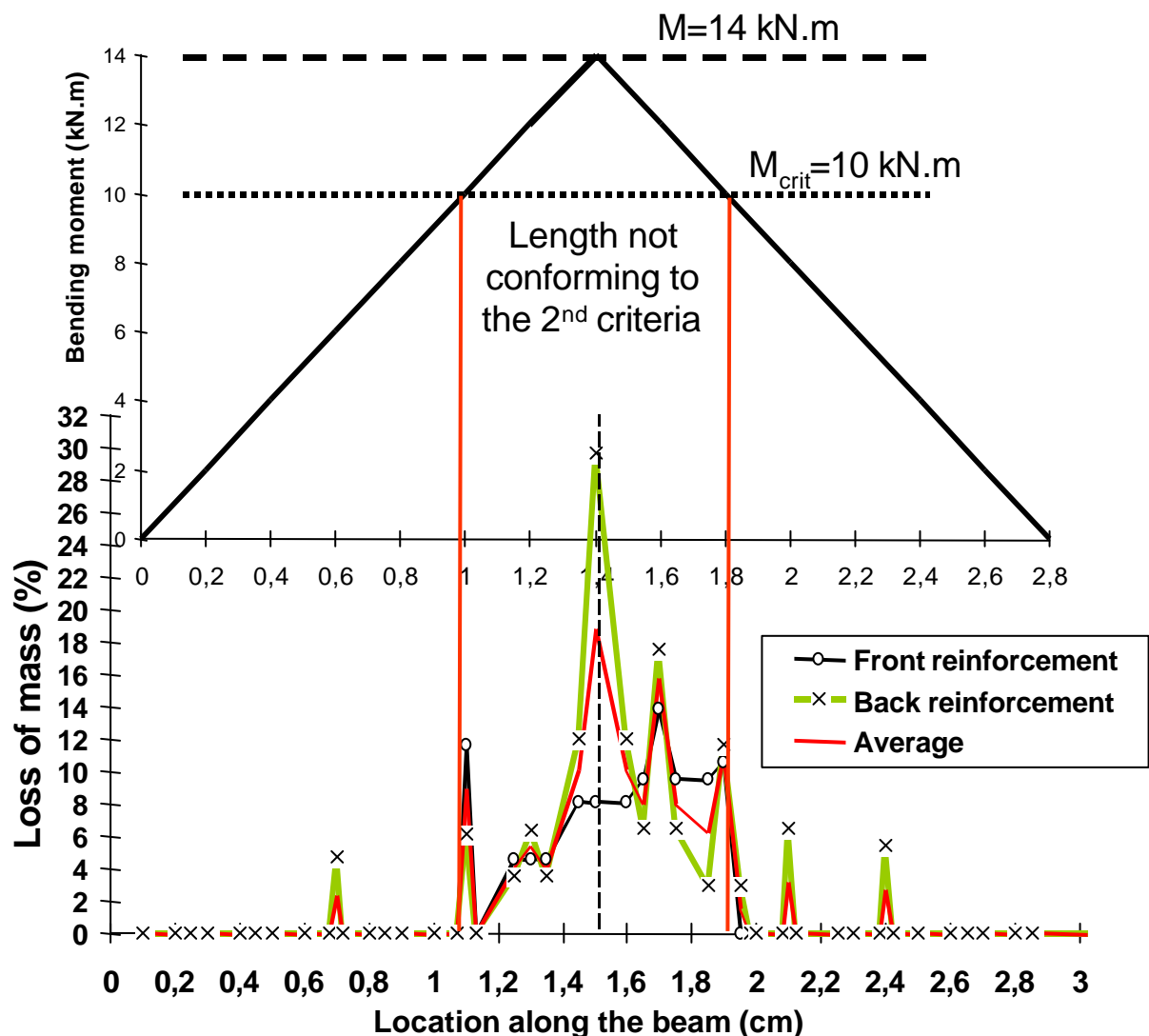


Figure 9: Comparison between the degree of corrosion (expressed in loss of mass) on the tensile reinforcements of a 12 year-old beam ageing in a chloride environment, with the zone where transmission of the stress of steel to the concrete led to exceeding the limit of failure of the concrete (length not conforming to the 2nd mechanical criterion).

Note: The mechanical criteria of durability represent a necessary condition for the initiation of corrosion in the presence of aggressive agents, with the proviso that we initially have good adhesion between the concrete and steel [14]. If the initial quality of the steel-concrete bond is not satisfactory (presence of holes or presence of a void under the reinforcement due to bleeding), corrosion can develop without the presence of mechanical damage.

6. Conclusion

Mechanical cracking of reinforced concrete does not have a direct influence on the corrosion process. Direct access to the reinforcements via the crack is not responsible for the development of corrosion. Moreover, if this was the case, as the structures in service were all cracked, degradations due to corrosion would be general after a few years. And this proved not to be the case [15]. The design rules to ensure durability of reinforced concrete structures with respect to corrosion are thus inappropriate, though limiting the width of cracks appears to be a psychological need.

However, the presence of cracks is the corollary to a modification of the mechanical behaviour of the reinforced concrete composite and in particular of the tensile concrete, which is not taken into account by the design rules because it is not considered necessary to determine reliability in relation to behaviour up to failure. It is this modification in behaviour that results in an accelerated corrosion process in the area of the reinforcements located between the cracks. This last point explains the interpretational errors that correlate corrosion with the presence of cracks and makes it clear that we need to define new design rules that explicitly take the role of the tensile concrete into account. The present article sought to provide an approach to this problem through examining the role of the two durability mechanical criteria (DMC criteria).

7. References

- [1] R. François, G. Arliguie, J.C. Maso - Durabilité du béton armé soumis à l'action des chlorures, Annales de l'I.T.B.T.P., n°529, pp. 1-48, 1994 (in French)
- [2] American Concrete Institute Committee 224 - Control of cracking in concrete structures. ACI journal Proceedings, 20, N°10, 10/1980. 1990 revisions published in ACI Materials Journal 07-08/1990
- [3] British Standards Institute - BS5400: Part 4 : Design of concrete bridges. London, BSI, **1990**
- [4] Comité Euro-International du Béton - CEB-FIP Model Code For Concrete Structures. International System of unified codes of practice for structures, 2, Paris **1978**
- [5] French Regulations for Reinforced Concrete Structures, **1983**.

- [6] Kondratova, I.L., Montes, P., Bremner, T.W., Accelerated corrosion testing results for specimens containing uncoated reinforcing steel and corrosion inhibitors, International Conference Durability of Concrete, Barcelone 2000, Editor : V.M. Malhotra, SP 192-48, pp.789-805, **2000**.
- [7] Otsuki, N., Miyazato, S., Diola, N., Suzuki, H., Influences of bending crack and water-cement ratio on chloride-induced corrosion of main reinforcing bars and stirrups. ACI Materials Journal, V. 97, No. 4, July-August 2000, pp. 454-464.
- [8] R. François, RF2B, 2000 (in french)
- [9] Castel, A. Couplage mécanique et corrosion dans les éléments de béton armé, PhD Thesis, Paul Sabatier University, 2000
- [10] Rilem Technical Committee 124-SRC. "Draft recommendation for repair strategies for concrete structures damaged by reinforcement corrosion" Material and Structures, vol. 27, 1994, pp. 415-436.
- [11] R. François, A. Castel, A discussion of the paper "Chloride diffusivity of concrete cracked in flexure" by N. Gowripalan, V. Sirivivatnanon, C.C. Lim, Cement and Concrete Research, to be published.
- [12] A. Castel, R. François, G. Arliguie, ELS du béton armé en environnement agressif: nouveaux critères mécaniques de durabilité (méthode D.M.C.) , Annales du BTP, to be published. (in French)
- [13] A. Castel, R. François, G. Arliguie, Modèle de comportement mécanique du béton armé après fissuration, Revue Française de Génie Civil, vol.5, 2001 (in French).
- [14] Yonzawa, T., Ashworth, V., Procter, R.P.M., Pore solution composition and chloride effects on the corrosion of steel in concrete, Corrosion Engineering, Vol. 44, No. 7, pp. 489-499, **1988**.
- [15] Gjorv Odd E., Steel corrosion in concrete structures exposed to Norwegian marine environment, P.K. Mehta symposium on durability of concrete "But concrete can be durable", Khayat, K.H., Aïtcin, P-C. Eds, pp.243-261, Nice, 05/1994.

CHARACTERISTIC VALUE OF INITIATION TIME

with special reference to marine RC structures



Ervin Poulsen
Professor Emeritus of Civil Engineering
8 Skovbrynet, Nødebo
DK-Fredensborg, DENMARK
E-mail: ervin-poulsen@get2net.dk



Jens M. Frederiksen B.Sc.Eng. (Hon.) Civil Engineer
AEClaboratory (Ltd) A/S, DENMARK. www.aec-dk.com
E-mail: jmf@aec-dk.com



Leif Mejlbro
Associate Professor, Department of Mathematics
Technical University of Denmark, DK-2800 Lyngby,
DENMARK
E-mail: L.Mejlbro@mat.dtu.dk

ABSTRACT

Research, tests and experience show that chloride ingress into a given concrete exposed to a given chloride laden environment is a stochastic variable. The rebar cover is also a stochastic variable. Therefore, one should have in mind that the initiation time ought to be determined by probabilistic methods.

However, the problem is that one does not know about the stochastic distribution of the chloride parameters and the rebar cover involved in the determination of the initiation time. Therefore, one has to make assumptions of the stochastic distributions. Once this has been done it is possible to calculate the stochastic distribution of the initiation time. However, for practical use the distribution of the initiation time is not necessary. Designers are used to design structures only on the basis of the characteristic value (i.e. the 5 % fractile) of the properties. While the determination of the stochastic distribution of the initiation time needs high computer power, the calculation of the characteristic value of the initiation time can be done by only simple calculation by hand or by spreadsheet.

This is convenient; it may take a long time before the distributions of the stochastic variables are known – if ever!

Keywords: Chloride ingress, Characteristic value, Initiation time, Marine RC structures, Probabilistic methods.

1 INTRODUCTION

Research into the phenomenon of chloride ingress into concrete of marine structures has led to rather reliable mathematical models. There is still a need for standard test methods to measure the various parameters of the chloride diffusivity of concrete exposed to a given chloride laden environment. It is however time to determine how the uncertain variables, which govern the chloride ingress into the concrete, can be taken into account by determining the initiation period of time by probabilistic methods.

Among civil engineers there is a long tradition for design of load bearing structures with a built-in safety against failure, e.g. the reinforcement of RC beams. Civil engineers have not gone to the limit of the bearing capacity of the structure, but they have always tried to have a certain margin between load and resistance. The determination of such a margin has varied, but typically an increasing knowledge about the uncertainties of the parameters involved has led to a more economical design.

Design of concrete having a certain durability is a fairly new discipline compared with the design of concrete having a certain compressive strength. In concrete mixture proportioning it has been common practice to design the compressive strength of concrete with a margin between the achieved strength and the required strength. Until now the understanding of the durability and deterioration of concrete has been so poor that a reliable mathematical model of concrete deterioration was not possible. However, an intensive research into concrete durability during the last period of time has changed this. Now there exist mathematical models for the most important types of concrete deterioration.

A *RILEM Technical Committee 130-CSL* about 'Durability Design of Concrete Structures', published its final report in 1996, cf. [1]. Here, one considers calculation of the stochastic distribution of the service lifetime of concrete members is dealt with on the basis of the stochastic distribution of the environmental parameters and the resistance of the concrete against the degradation. The development of the mathematical models is at present going on so fast that the model for chloride ingress into concrete described in [1] is now out-of-date.

Such a calculation of the stochastic distribution of the service lifetime is generally not familiar in use and appearance to the civil engineer at a typical design office. The current procedure in structural design is that the external dimensions of a structural component are chosen, the type of concrete (binder and w/c) and the rebar cover c in connection with the structural analysis of internal forces and deformations etc. The choice of the external dimensions may be supported by handbooks, while the choice of w/c and cover c are given as minimum values by tables in the Code of Practice. The design itself takes place without any probabilistic calculations, but after a simple and traditional method. However, the values of the involved parameters chosen by the civil engineer are in fact a result of probabilistic calculations, carried out once and for all by the responsible committee. The calculation of the service lifetime of a chloride exposed RC structure deviates in its form from the usual engineering practice – and this is not necessary!

This paper deals with the determination of the characteristic value (i.e. the 5 % fractile) of the initiation time. Until now the mathematical models have dealt with the determination of the expectation value of the initiation period of time. However, at the expectation time about 50 % of the reinforcement bars have initiated corrosion and nobody would accept this in practice to be a limit for the initiation time.

1.1 Types of structures

The marine RC structures of to day may be divided into three groups as follows:

- *Old RC structures*, i.e. RC structures that have been exposed to chloride for more than 25 years. For these RC structures it may be assumed that the chloride parameters will remain constant after the inspection at 25 years. The COLLEPARDI model with constant chloride parameters may be accepted, cf. [2] and [3].
- *RC structures*, which have been exposed to chloride for more than 10 years. For these RC structures it may be assumed that the chloride parameters will remain constant after the inspection at 10 years. The LIGHTCON model with constant surface chloride content and time-dependent diffusion coefficient may be accepted, cf. [4] and [5].
- *New RC structures*, e.g. under design. For these RC structures it may be assumed that the chloride parameters (surface chloride content and chloride diffusion coefficient) will be time-dependent. The HETEK model with time-dependent surface chloride content and time-dependent diffusion coefficient may be accepted, cf. [6].

Concrete is a kind of material which is characterised by an ongoing change of its microstructure, chemically as well as physically. The greatest change takes place immediately after casting when the hydration of the binders starts. However, the micro structural changes continues taking place even after 28 days, and even after several years there are notable changes in properties and characteristics of the concrete. After the development of the final microstructure an ageing process starts, also resulting in a change of properties and characteristics of the concrete.

The achieved chloride diffusion coefficient D_a of concrete is one of the time-dependent properties. However, when the concrete has been exposed to a chloride-laden environment for more than 25 years the change with time per year has slowed down. This means that it is possible to obtain a rough estimate of the future chloride ingress and the initiation period by neglecting the time dependency. Furthermore, the estimate is easy and usually on the safe side.

The chloride content of the exposed concrete C_s surface is also time-dependent. However, concrete submerged in seawater or exposed to the splash zone will reach its (almost) final value after 5-10 years, and it certainly will be a fair estimate to assume that the chloride content of the surface remains constant after a period of 25 years. On the other hand, concrete that is exposed to a marine atmosphere seems to show a time-dependent chloride surface content for a considerably longer time.

When the chloride parameters are time-dependent estimation of chloride ingress and prediction of the initiation period needs extensive calculations. Thus, rough estimates (on the safe side) are justified.

In the following such estimates are developed. When applying these estimates it should always be remembered that the assumptions made are approximations and that they are only valid in special cases.

Only old marine RC structures will be dealt with here. For structures younger than 25 years a proper model, e.g. the HETEK model, cf. [7], may estimate the stage of the chloride ingress into the concrete at an age of 25 years or more.

2 MARINE RC STRUCTURES OLDER THAN 25 YEARS

As stated in Clause 1.1 a rough estimate of the characteristic value of the initiation period of time may be found easily for marine RC structures older than 25. The marine structure is inspected and tested and the following procedure is applied. A more thorough explanation is given in the Appendix.

2.1 Deterministic determination of initiation time

Collepari et al in 1970 and 1972, cf. [2] and [3] introduced the equation of chloride ingress into concrete having constant chloride parameters. The chloride parameters C_{in} and D_{in} are measured at the inspection time $t_{in} \geq 25$ years. The equation yields

$$C(x,t) = C_i + (C_{in} - C_i) \operatorname{erfc} \frac{0.5x}{\sqrt{tD_{in}}} \quad (2.1:1)$$

where

- C_{in} surface chloride content determined at an age of 25 years or more
- D_{in} achieved chloride diffusion coefficient determined at an age of 25 years or more
- $C(x,t)$ chloride content of the concrete at location x and at time t
- C_i initial chloride content of the concrete
- t time, measured from first chloride exposure

By introducing the threshold value of chloride in concrete $C = C_{cr}$ at the depth x_{cr} of the concrete surface Eq (2.1:1) yields

$$C_{cr} = C_i + (C_{in} - C_i) \operatorname{erfc} \frac{0.5x_{cr}}{\sqrt{tD_{in}}} \quad (2.1:2)$$

By solving this equation with respect to x_{cr} we get

$$x_{cr} = 2\sqrt{tD_{in}} \times \operatorname{inv} \operatorname{erfc} \frac{C_{cr} - C_i}{C_{in} - C_i} = k_1 \sqrt{t} \quad (2.1:3)$$

When $x_{cr} = c$, where c is the rebar cover, the initiation period of time ends. Therefore, the initiation time yields

$$t_{cr} = \left(\frac{c}{k_1} \right)^2 \quad (2.1:4)$$

2.2 Procedure for the determination of the characteristic value of initiation time

It is assumed that the rebar cover c and the first year chloride ingress k_1 are lognormally distributed. Then the initiation time t_{cr} is also lognormally distributed, Therefore, the characteristic value (the 5 % fractile) yields

$$K[T_{cr}] = \exp(E[\ln T_{cr}] - 1.65 \times S[\ln T_{cr}]) \quad (2.2:1)$$

cf. Appendix. Since c , k_1 and t_{cr} are stochastic variables the notations C , K_1 and T_{cr} are used. Thus, to calculate $E[T_{cr}]$, $S[T_{cr}]$ and $K[T_{cr}]$, which will be of interest in practice, the following step-by-step procedure is used

Step 1. The expectation value of the initiation time is calculated by the following formula, cf. Appendix:

$$E[T_{cr}] = \left(\frac{m_c}{m_k} \right)^2 (1 + V_c^2) (1 + V_k^2)^3 \quad (2.2:2)$$

Note: since c and k_1 are lognormally distributed, the expectation of initiation time yields

$$E[t_{cr}] \neq \left(\frac{m_c}{m_k} \right)^2 \quad (2.2:3)$$

where the expectation values are: $E[c] = \mu_c$ and $E[k_1] = \mu_k$. The expectation value of the initiation time is found from Eq (2.2:2) and Eq (3:6).

Step 2. The coefficient of variation of the initiation time is calculated from the following formula, cf. Appendix:

$$V[T_{cr}] = \sqrt{[(1 + V_c^2)(1 + V_k^2)]^4 - 1} \quad (2.2:4)$$

Step 3. The standard deviation of the initiation time is calculated by the following formula, cf. Appendix:

$$S[T_{cr}] = E[T_{cr}] \times V[T_{cr}] \quad (2.2:4)$$

Step 4. Finally, the characteristic value (5 % fractile) of the initiation time is calculated by the following formula, cf. Appendix:

$$K[T_{cr}] = \frac{1 + V_k^2}{1 + V_c^2} \left(\frac{m_c}{m_k} \right)^2 \times \exp \left(-3.3 \sqrt{\ln[(1 + V_c^2)(1 + V_k^2)]} \right) \quad (2.2:6)$$

EXAMPLE 1. From pre-testing of concrete (at inspection time $t_{in} > 25$ years) from a reinforced concrete member exposed to a marine splash environment and an engineering interpretation the data shown in Table 1 is obtained including their standard deviations.

Table 1. Data from pre-testing and engineering interpretation, cf. Example 1

Stochastic parameter	Expectation value	Standard deviation	Unit	Coefficient of variation
k_1	$m_k = 4.50$	$s_k = 0.72$	mm/ $\sqrt{\text{yr}}$	$V_k = 16 \%$
c	$m_c = 50$	$s_c = 5.0$	mm	$V_c = 10 \%$

Step 1. Assuming constant chloride diffusivity the expectation value of the initiation period of time is, cf. Eq (2.2:2),

$$E[T_{cr}] = \left(\frac{50}{4.50} \right)^2 (1 + 0.10^2)(1 + 0.16^2)^3 = 134.5 \text{ years}$$

Step 2. The coefficient of variation of the initiation period of time is, cf. Eq (2.2:3),

$$V[T_{cr}] = \sqrt{[(1 + 0.10^2)(1 + 0.16^2)]^4 - 1} = 0.389 = 38.9 \%$$

Step 3. Thus, the standard deviation of the initiation period of time is, cf. Eq (2.2:4),

$$S[T_{cr}] = 134.5 \times 0.389 = 52.3 \text{ years}$$

Step 4. Finally, the characteristic value of the initiation time yields, cf. Eq (2.2:5),

$$K[T_{cr}] = \frac{1 + 0.16^2}{1 + 0.10^2} \left(\frac{50}{4.5} \right)^2 \exp\left(-3.3 \sqrt{\ln[(1 + 0.10^2)(1 + 0.16^2)]}\right) = 67.5 \text{ years}$$

Note. The data given in this example are all chosen for the purpose of illustration; laboratory tests or field inspection found none of the data.

EXAMPLE 2. From the Nordic Mini Seminar test case the Hetek model has predicted the chloride parameters at time of 25 years by *Frederiksen*, cf. [8]. The results were as follows

Table 2. Data at 25 years' age from HETEK prediction, cf. Example 2

Chloride parameters	Unit	Submerged zone	Splash zone	Atmospheric zone
Surface chloride, C_s	% mass binder	3.147	4.676	3.730
Diff. coefficient, D_a	mm ² /year	25.9	31.6	3.09
Threshold value, C_{cr}	% mass binder	1.45	0.54	0.54
Initial chloride, C_i	% mass binder	0.075	0.075	0.075

From an engineering interpretation the following data are obtained including their standard deviations.

Table 3. Data from pre-testing and engineering interpretation, cf. Example 2

Chloride parameters	Unit	Submerged zone	Splash zone	Atmospheric zone
$E[k_1]$	mm/ $\sqrt{\text{yr}}$	5.46	13.04	3.79
$S[k_1]$	mm/ $\sqrt{\text{yr}}$	0.764	1.826	0.531
$V[k_1]$	%	14	14	14
$E[c]$	mm	60	60	60
$S[c]$	mm	4.8	4.8	4.8
$V[c]$	%	8	8	8

The calculations takes place as shown in Example 1. The results of the calculations are shown in Table 4.

Table 4. Results from determination of initiation time according to the ‘Nordic Mini Seminar Test Case’, cf. Example 2

Parameters	Unit	Submerged zone	Splash zone	Atmospheric zone
$E[t_{cr}]$	years	129	23	267
$S[t_{cr}]$	years	43	8	88
$V[t_{cr}]$	%	33	33	33
$K[t_{cr}]$	years	72	13	149

Since the characteristic value of the initiation time for concrete in the splash zone is less than 25 years the result is not reliable. In order to get an impression of how much the characteristic value of the initiation time for concrete exposed to the submerged zone depends on the values of $V[c]$ and $V[k_1]$, $K[t_{cr}]$ is calculated versus these coefficients of variation. The results are shown in Table 5.

Table 5. Results from a sensitivity analysis of the initiation time (concrete in splash zone) with respect to the coefficients of variation $V[c]$ and $V[k_1]$ according to the ‘Nordic Mini Seminar Test Case’, cf. Example 2

$V[c]$	$V[k_1]$	5 %	6 %	7 %	8 %	9 %	10 %	11 %	12 %	13 %	14 %	15 %
5 %		96	93	91	89	87	84	82	80	77	75	73
6 %		93	91	89	87	85	83	81	78	76	74	72
7 %		91	89	87	85	83	81	79	77	75	73	71
8 %		88	87	85	83	81	79	78	76	74	72	70
9 %		86	84	83	81	79	78	76	74	72	71	69
10 %		83	82	80	79	77	76	74	73	71	69	68
11 %		80	79	78	77	75	74	72	71	69	68	66
12 %		78	77	76	75	73	72	71	69	68	66	65
13 %		75	74	73	72	71	70	69	67	66	65	63
14 %		73	72	71	70	69	68	67	66	64	63	62
15 %		70	70	69	68	67	66	65	64	63	61	60

3 DESIGN VALUE OF INITIATION TIME

In structural design the properties and the loads are handled as characteristic values, i.e. 5 % fractile for properties and 95 % fractile for the loads. *Eurocode No. 2* (1990), cf. [9], defines the characteristic values in the following way: ‘A material property is represented by a characteristic value X_k which in general corresponds to a fractile in the assumed statistical distribution of the particular property of the material, specified by relevant standards and under specified conditions’.

Eurocode No. 2 (1990), cf. [9] also defines the design value X_d of a material property in the following way: ‘the design value X_d of a material property is generally defined as

$$X_d = \frac{X_k}{g_M} \quad (3:1)$$

where g_M is the partial safety factor for the material property’ (given in EC2, where the fundamental values are $g_c = 1.5$ for concrete and $g_s = 1.15$ for steel reinforcement).

In the same way as RC structures are designed against failure according to the EC2 one can design RC structures against corrosion aiming at a given design value of the initiation time. The value of the partial safety factor g is given by the following formula, cf. *Mejlbro et al* [2002],

$$g = \exp \left[- (2b - 3.3) \times \sqrt{\ln[(1 + V_c^2)(1 + V_k^2)]} \right] \quad (3:2)$$

The conditions are that the rebar cover and the ‘first year chloride ingress’ are lognormally distributed and b is Cornell’s reliability index of corrosion, cf. *Mejlbro et al* [1999].

EXAMPLE 3. In Example 1 the characteristic value of the initiation time was found in the special case: $V_c = 10\%$ and $V_k = 16\%$. Corresponding to these values the partial safety factors are found for a probability of corrosion $0.1\% \leq p_F \leq 5\%$ (i.e. the interval: $1.64 \leq b \leq 3.09$) and given in Table 6

Table 6. Partial safety factors in relation to the probability of corrosion, cf. Example 1

$p_F, \%$	0.10	0.20	0.30	0.40	0.50	1.00	2.00	3.00	4.00	5.00
b	3.09	2.88	2.75	2.65	2.58	2.33	2.05	1.89	1.75	1.64
g	1.72	1.59	1.51	1.46	1.42	1.29	1.17	1.09	1.04	1.00

The partial safety factors ought to be specified by the Code of Practice.

4 APPENDIX

In Clause 2.1 the initiation time t_{cr} is handled with as a deterministic variable. However, the initiation time of an RC component is an uncertain variable. This is due to the fact that the chloride front is not a plane parallel with the concrete surface, that the positions of the reinforcement bars are uncertain, and that the threshold value of chloride in concrete is an uncertain variable. This means that the RC component will start corrosion of the reinforcement in spots located at defects and where the cover has a minimum value.

The initiation time when assuming constant chloride diffusivity (for an old RC structure), cf. Eq (2.1:4), is

$$t_{cr} = \left(\frac{c}{k_1} \right)^2 \quad (4:1)$$

From this equation it is possible to find the stochastic distribution of the initiation time when the distribution of the cover c and the ‘first year chloride ingress’ k_1 are known. Since the cover of the reinforcement c , the first year chloride ingress k_1 , and the initiation time t_{cr} are uncertain variables, the notation C , K_1 and T_{cr} are used to indicate that they are stochastic variables. It is assumed that the cover C of the reinforcement and the first year chloride ingress K_1 are not correlated.

In analogy with the characteristic strength of the concrete one could define the characteristic value of the initiation time, $K[T_{cr}]$, as the 5 % fractile. In order to be able to find the characteristic value of the initiation time it is necessary to know the statistic distribution of the cover c and the first year chloride ingress k_1 . To make this simple (but realistic) it is here assumed, that C and K_1 are lognormally distributed. This means that

the initiation period of time also becomes lognormal distributed. If $E[\ln(T_{cr})]$ and $S[\ln(T_{cr})]$ denote the expectation value and the standard deviation of the logarithm of the initiation period of time respectively, the characteristic initiation period of time (i.e. the 5 % fractile), $K[T_{cr}]$, yields, cf. e.g. *Ditlevsen et al* [1996] and *Toft-Christensen et al* [1982], Ref. [9] and [10],

$$K[T_{cr}] = \exp(E[\ln T_{cr}] - 1.65 \times S[\ln T_{cr}]) \quad (4:2)$$

The mean value of the logarithm of the initiation period of time (when assuming a constant chloride diffusivity and a lognormal distribution) is, cf. e.g. Ref. [11],

$$E[\ln T_{cr}] = \ln \frac{(1 + V_k^2) \mathbf{m}_c^2}{(1 + V_c^2) \mathbf{m}_k^2} \quad (4:3)$$

where V_k and V_c are the coefficient of variation for the ‘first year chloride ingress’ and the rebar cover respectively. The notations μ_c and μ_k are the expectation values of the rebar cover and the ‘first year chloride ingress’, respectively. Furthermore, the notations $\mathbf{m}_c = E[C]$, $\mathbf{s}_c = S[C]$, and $V_c = \mathbf{s}_c / \mathbf{m}_c$ are used for the concrete cover of the reinforcing bar and the following notations $\mathbf{m}_k = E[K_1]$, $\mathbf{s}_k = S[K_1]$, and $V_k = \mathbf{s}_k / \mathbf{m}_k$ for the ‘first year chloride ingress’. The standard deviation of the logarithm of the initiation period of time yields

$$S[\ln T_{cr}] = 2 \times \sqrt{\ln[(1 + V_c^2)(1 + V_k^2)]} \quad (4:4)$$

Thus, inserting Eq (4:3) and (4:4) into Eq (4:2), the characteristic value of the initiation period of time yields

$$K[T_{cr}] = \frac{1 + V_k^2}{1 + V_c^2} \left(\frac{\mathbf{m}_c}{\mathbf{m}_k} \right)^2 \exp\left(-3.3 \sqrt{\ln[(1 + V_c^2)(1 + V_k^2)]}\right) \quad (4:5)$$

The expectation value of the initiation period of time is

$$E[T_{cr}] = \left(\frac{\mathbf{m}_c}{\mathbf{m}_k} \right)^2 (1 + V_c^2)(1 + V_k^2)^3 \quad (4:6)$$

The coefficient of variation yields

$$V[T_{cr}] = \sqrt{[(1 + V_c^2)(1 + V_k^2)]^4 - 1} \quad (4:7)$$

Thus, the standard deviation of the initiation period of time yields

$$S[T_{cr}] = E[T_{cr}] \times V[T_{cr}] \quad (4:8)$$

where $E[T_{cr}]$ and $V[T_{cr}]$ refer to the above Eq (4:6) and Eq (4:7) respectively.

The characteristic value of the initiation period of time and other statistic parameters are easily found from four simple formulae, when it is assumed that the rebar cover and the first year chloride ingress are lognormally distributed and the chloride exposure has taken place at least in 25 years. However, the weak point of the method is that there is a lack of knowledge about the standard deviations.

6 ACKNOWLEDGEMENT

The authors thank Professor *Gunnar Mohr* at the Technical University of Denmark for constructive and helpful comments in preparation of this paper.

7 REFERENCES

- 1 A. SARJA, E. VESIKARI (EDITORS): »Durability Design of Concrete Structures«. *Report of RILEM Technical Committee 130-CSL*. E & FN SPON, 1996.
- 2 M. COLLEPARDI, A. MARCIALIS, R. TURRIZIANI: »The Kinetics of Chloride Ions Penetration in Concrete (in Italian)«. *Il Cemento*, Vol. **67**. Italy 1970.
- 3 M. COLLEPARDI, A. MARCIALIS, R. TURRIZIANI: »Penetration of Chloride Ions into Cement Pastes and Concrete«. *Journal of American Ceramic Society*, Vol. **55**. USA 1972
- 4 M. MAAGE, E. POULSEN, Ø. VENNESLAND, J. E. CARLSEN: »Service life model for concrete structures exposed to marine environment, Initiation period«. *LIGHTCON Report No. 2.4*, STF70 A94082 SINTEF. Trondheim, Norway 1995.
- 5 M. MAAGE, S. HELLAND, J. E. CARLSEN: »Chloride penetration into concrete with light weight aggregates«. *Report FoU Lightcon*, Report No. **3.6**, STF22 A98755 SINTEF. Trondheim, Norway 1999.
- 6 J. M. FREDERIKSEN, L.-O. NILSSON, P. SANDBERG, E. POULSEN, TANG L., A. ANDERSEN: »HETEK, a System of Estimation of Chloride Ingress into Concrete, Theoretical Background«. Report No. **83**:1997. *The Danish Road Directorate*. Copenhagen, Denmark 1997.
- 7 J.M. FREDERIKSEN, L. MEJLBRO, E. POULSEN: »The Hetek model of chloride ingress into concrete made simpler by approximations«. Proceedings of the 2nd International *RILEM Workshop on Testing and Modelling the Chloride ingress into Concrete*. France, Paris 2000.
- 8 J.M. FREDERIKSEN: »The Hetek chloride ingress model«. *Nordic Mini Seminar*, Göteborg 2001.
- 9 EUROCODE NO. 2: »Design of Concrete Structures, Part 1: General Ruled and Rules for Buildings«. Revised Final Draft, approved by the *EC2 Editorial Group*, 31 October 1990.
- 10 L. MEJLBRO, E. POULSEN: »Diffusion of Chloride in Concrete, Theory and Application«. SPON PRESS, London 2002.
- 11 L. MEJLBRO, E. POULSEN: »Design of Rebar Covers in Marine Structures by Probabilistic Modelling Applying Cornell's Reliability Index«. International Conference on *Ion and Mass Transport in Cement-Based Materials*. University of Toronto, Canada 1999
- 12 O. DITLEVSEN, H. O. MADSEN: »Structural Reliability Methods«. *Danish Institute of Building Research*, SBI report 211. Hørsholm, Denmark 1996.
- 13 P. TOFT-CHRISTENSEN, M. BAKER: »Structural Reliability Theory and its Applications. *Springer Verlag*, 1982.
- 14 GUNNAR MOHR: Clause 1.7 on Statistics of »Teknisk Ståbi« (in Danish). *Teknisk Forlag*. Edition No. 17, Copenhagen 1995.
- 15 INTERNATIONAL ORGANISATION FOR STANDARDISATION: »Guide to the Expression of Uncertainty in Measures«. Switzerland, 1993.

6 OVERVIEW OF RESEARCH, RESEARCH NEEDS

Chloride Ingress Model adopted in JSCE Standard Specification

Hiroshi Watanabe

Senior Research Engineer of Structure Management Team

Public Works Research Institute, Japan

1.Introduction

Chloride induced corrosion is one of the typical deterioration mechanism of concrete structures. Countermeasures for prevention of chloride-induced corrosion for Highway bridge structures have been enforced in Japan as follows from 1986.

- 1) Initial chloride content in freshly mixed concrete is generally not more than 0.3kg/m³ (Cl⁻).
 - 2) Designers have to choose one of the following countermeasures to construct concrete structures in marine environment, (a) enlarge cover thickness, (b)Coating surface of concrete structures, (c) use coated re-bar.
 - 3) w/c of concrete is not more than 50% for super-structures, 55% for sub-structures
- The enlargement of cover thickness has been most popularly adopted measures.

2.Method for Verification by JSCE Standard Specification

2.1 Outline of the verification method

The countermeasures described above must improve durability of concrete structures to salt attack. But the improvement of service lifetime of concrete structures by adopting these countermeasures was not clearly specified. It is said that the design service lifetime of newly constructed concrete structures should satisfy more than 100 years to reduce maintenance cost, therefore quantitative method is expected for the verification of service lifetime.

From this background, new verification method has been proposed in the revision of JSCE (Japan Society of Civil Engineers) Standard Specification for Design and Construction of Concrete Structures in 1999.

According to the revised JSCE specification, prediction of chloride distribution in concrete is based on Fick's 2nd law. i.e.,

$$C_d(x, t) = g_{cl} \cdot C_0 \cdot \left\{ 1 - \operatorname{erf} \left(\frac{x}{2\sqrt{D_d \cdot t}} \right) \right\} + C_i \quad (\text{eq.1})$$

$C_d(x, t)$; Design chloride content at depth of x and time of t (kg/m³; Cl)

g_{cl} ; Safety factor for taking into an account of the uncertainty of C_d and generally taken as 1.3.

D_d ; Design value of apparent chloride diffusion coefficient of concrete

C_0 ; Chloride content on the surface of concrete and the function of distance from the coastline

C_i ; Initial chloride content

Chloride content at the cover is not more than the threshold value (C_{lim}) , i.e.

$$g_i \frac{C_d}{C_{lim}} \leq 1.0 \quad (\text{eq.2})$$

g_i : structure factor and generally taken as 1.0. For important concrete structures $g_i = 1.1$

Threshold value of chloride content to corrosion of rebar is 1.2kg (Cl) per unit volume of concrete in spite of unit amount of binder. In case of concrete structures affected by freezing and thawing effect or carbonation, the threshold value should be less than 1.2kg/m³.

2.2 Apparent chloride diffusion coefficient

Design value of apparent chloride diffusion coefficient is obtained as follows.

$$D_d = g_c \cdot D_k \quad (\text{eq.3})$$

g_c ; material factor for concrete. Generally $g_c = 1.0$

D_k ; Characteristic value of apparent chloride diffusion coefficient. Characteristic value of the apparent chloride diffusion coefficient is obtained from the predicted chloride diffusion coefficient (D_p).

$$D_k = g_p \cdot D_p \quad (\text{eq.4})$$

g_p : safety factor taking into account of errors for predicted coefficient.

D_p is generally determined from the measured chloride profiles in real structures. The equation available to estimate D_p (cm²/sec) is given in the JSCE specification as follows.(Fig.1)

$$\text{For concrete using OPC} \quad \log_{10} D_p = 4.5(w/c)^2 + 0.14(w/c) - 8.47 \quad (\text{eq.5})$$

$$\text{For concrete using GGBS} \quad \log_{10} D_p = 19.5(w/c)^2 - 18.3(w/c) - 5.74$$

These equations were derived from the regression analysis between apparent diffusion coefficient and w/c. The apparent diffusion coefficient is obtained from results of chloride

profiles in real concrete structures and concrete specimens. (Fig.1)

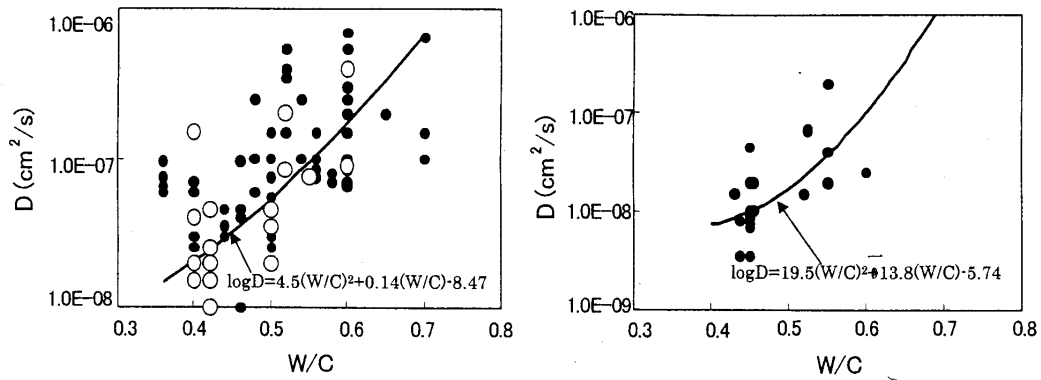


Fig.1 Relationship between w/c and apparent diffusion coefficient¹⁾
Left; OPC, Right; GGBS

It takes long time to obtain appropriate chloride profiles to derive the apparent diffusion coefficient by exposure test in marine environment. Therefore accelerated test method such as RCPT is studied to estimate the coefficient by many researchers in Japan. But the prediction of the apparent diffusion coefficient by accelerated test method has not been adopted in the specification, because the validity has not fully confirmed. Usage of accelerated test method is limited to only relative comparison of chloride diffusivity of concrete. One of the reasons why the accelerated test method is not adopted to estimate apparent diffusion coefficient, is that mechanisms of movement of ions under electrical field is so complicated and not clarified. Some experimental and theoretical research projects are undergoing in Japan to link the apparent diffusion coefficient and the charge passed by RCPT. These research projects are expected to make the accelerated test method possible for the

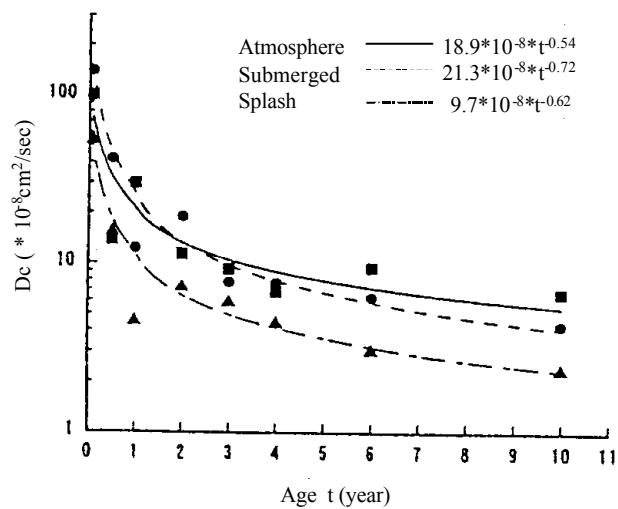


Fig.2 Relationship between D_c and age of concrete²⁾

practical application.

The apparent diffusion coefficient is also a function of age of concrete, which is not taken into account in eq.5. Results of long-term exposure tests show that the apparent diffusion coefficients decrease with age of concrete. Fig.2 shows the relationship between apparent diffusion coefficient and age of concrete in various exposure conditions. Tab.1 shows the results of estimation of D_c from measured chloride content by exposure test in atmosphere condition reported in ref3. D_c decreases as age of concrete increase though the tendency is not clear in the case of using blended cement.

But the amount of test data is so limited that effect of age on the apparent diffusion coefficient has not been taken into an account in the JSCE specification.

Tab.1 Results of exposure tests in marine environment

W/B	Cement	Year	$D_c (cm^2/sec)$	$C_o (kg/m^3)$	Cl^- Content(kg/m^3)			
					0-1cm	1-2cm	2-4cm	4-7cm
0.4	HPC	6	7.54E-09	6.5	5.5	3.1	0.6	0.1
		8	4.21E-09	9.6	8.1	3	1.1	0.1
		10	2.87E-09	8.5	7.2	2.2	0.8	0.1
0.5	HPC	6	1.53E-08	6.2	5.2	4.8	1.9	0.2
		8	1.29E-08	12.1	10.2	10	4.2	0.7
		10	6.86E-09	10.2	8.6	5.8	2.6	0.5
0.4	OPC	6	5.93E-09	12.2	10.3	4.4	1	0.1
		8	4.93E-09	12.3	10.4	5	1.1	0.1
		10	4.07E-09	13.6	11.5	5.7	1.3	0.1
0.5	OPC	6	1.40E-08	10.6	8.9	6.9	3.6	0.4
		8	8.72E-09	11.0	9.3	5.9	3.5	0.3
		10	5.93E-09	15.1	12.7	7.4	3.6	0.6
0.5	GBS+OPC	6	7.54E-09	12.2	10.3	5.7	1.2	0.3
		8	7.61E-09	9.2	7.8	5.6	1.5	0.1
		10	5.93E-09	13.2	11.1	7.6	2.1	0.4
0.3	SF+OPC	6	3.43E-09	7.9	6.7	1.3	0.1	0.1
		8	2.53E-09	11.1	9.4	1.1	0.1	0.1
		10	2.53E-09	10.3	8.7	1.8	0.4	0.1

2.3 Environmental load

Design values of C_o that means surface chloride content is specified as Tab.2 in JSCE specification. But the amount of chloride from environment is strongly affected by the geographical conditions and degree of a seasonal wind. Though amount of chloride supply itself do not affect chloride ingress mechanism, it is important to have information on a degree

of scattering in amount of chloride supply in order to estimate the precision of the prediction of chloride profiles in concrete structures.

Tab.2 Design value of surface chloride content

Splash zone	Distance from coastline (km)				
	<0.1	0.1	0.25	0.5	1.0
13.0	9.0	4.5	3.0	2.0	1.5

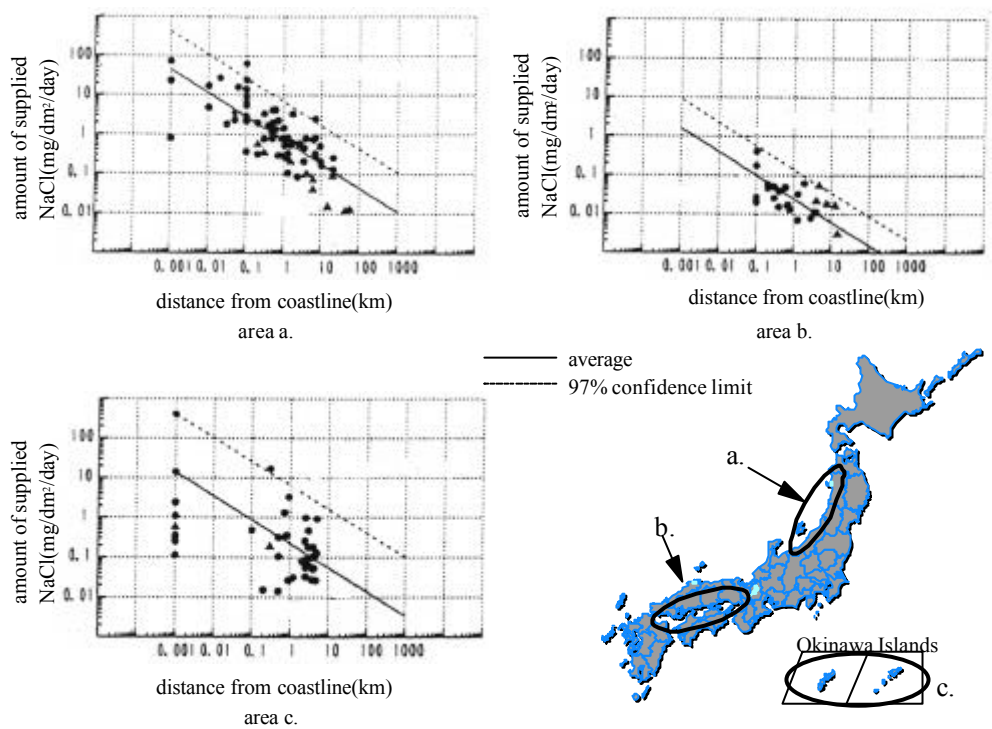


Fig.3 Chloride supplied from marine environmental⁴⁾

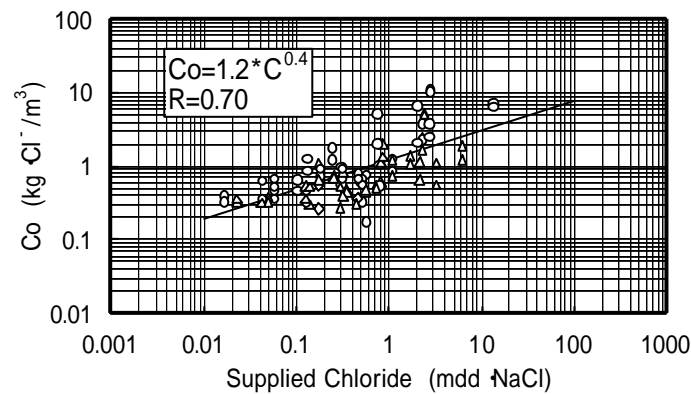


Fig.4 Relationship between C_0 and environmental load⁴⁾

Fig.3 shows the results of amount of chloride (NaCl $\text{mg}/\text{dm}^2/\text{day}$) supplied from marine environment measured in each districts in Japan. Plotted data are average values in 3 years measurement. Fig.4 shows the relationship between amount of chloride supplied from marine environment and measured surface chloride contents (C_o) of concrete specimens exposed for 3 years. Design values of C_o suitable for each district can be approximately obtained with the equation in Fig.4.

3. Summary

Existing practical design specifications for concrete structures, which consist of so-called deemed-to-satisfy provisions, are now moving into performance-based design specifications in Japan. JSCE specification revised in 1999 is the first one produced on the basis of performance-based design concepts for durability of concrete structures in Japan. The specification greatly affects the revisions of other practical design such as highway bridge structures and so on. But many uncertainties are still included in the JSCE specification, which results in introducing many safety factors for the verification of chloride contents in concrete and giving conservative output.

Recent research activity is focused on the threshold chloride content for initiation of corrosion, accelerated testing methods for the evaluation of diffusivity of concrete, interaction with other deterioration mechanism such as carbonation or freezing and thawing action, etc. Test results of chloride profiles in concrete cores sampled from real structures sometimes do not agree with the prediction by Fick's 2nd law. Understanding the transportation mechanism of chloride ion in concrete is important and also helpful for the practical use of the accelerated testing method.

4. Trial Prediction of Chloride Ingress Profiles in the Test Conditions

Though the test concrete contains Silica fume as in Table.I, we assume the test concrete is made of OPC since we don't have prediction models applicable to concrete with silica fume. According to the JSCE specification, the apparent chloride diffusion coefficient (D_c) is evaluated as $2.02(10^{-8} \text{ cm}^2/\text{sec})$, where the effect of humidity condition on D_c is not taken into an account. We conducted 3years exposure test in marine atmospheric zone and have derived experimentalequation for $D_c^{(5)}$. D_c calculated from the equation is $0.92(10^{-8} \text{ cm}^2/\text{sec})$, which is quite less than D_c by JSCE equation. The value of D_c estimated from JSCE is similar to the one obtained from exposure test in submerged condition from our experiment. Therefore D_c in submerged condition is assumed to be $2.02(10^{-8} \text{ cm}^2/\text{sec})$ and in atmospheric condition $0.92(10^{-8} \text{ cm}^2/\text{sec})$. Initial chloride content is assumed to zero in the prediction.

Chloride contents at the surface of concrete is assumed 3.63 wt-% of binder from the Table.III. As unit binder content in test concrete is 420kg, chloride content per unit volume of concrete is 15.2kg.

According to the JSCE specification, threshold chloride content for corrosion initiation is assumed 1.2 kg/m^3 , which corresponds to 0.28wt-% of binder. On the other hand, our results of observation of corrosion state of re-bars in old concrete bridge girders in marine environment, only slight surface corrosion occurred in some of the rebars where the chloride content reached the threshold value. And most of rebars showed corrosion where the chloride content exceeded 2.5 kg/m^3 . Therefore the threshold value is assumed to 2.5 kg/m^3 in this trial prediction for the atmospheric condition. In case of submerged condition, oxygen supply is not enough to activate cathode reaction, which inhibits corrosion reaction. Apparent threshold chloride value must be larger than in splash or tidal conditions. In this prediction threshold value in submerged condition was not defined.

Results of the predicted chloride profiles are shown in Fig.4

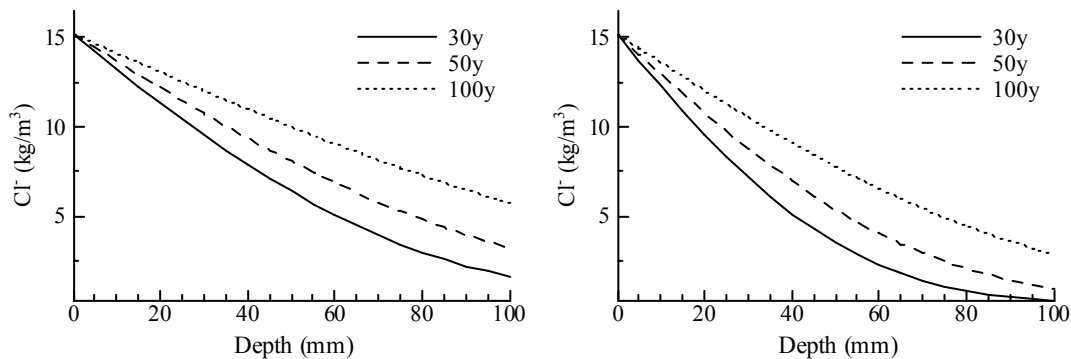


Fig.4 Predicted Chloride Profiles (Left: submerged, Right: atmospheric)

Cover thickness in concrete bridge piers is usually 80mm in Japan. Fig.5 shows a predicted chloride content change at the depth of 80mm in the atmospheric condition. The predicted time for initiation of corrosion in the atmospheric condition is about 58 years. If threshold value is assumed to 1.2kg/m³, the predicted initiation time is 36 years.

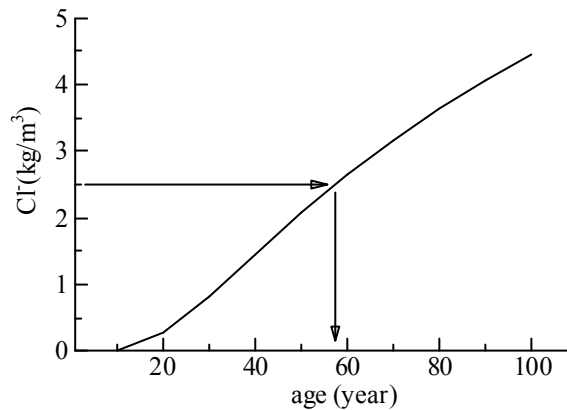


Fig.5 Predicted chloride content at 80mm depth

References

- 1) K.Takewaka, Investigation of chloride contents in concrete structures under marine environment, Proceedings of 43rd annual conference of civil engineer, 1988 (in Japanese).
- 2) N.Takeda, S.Sogo, S.Sakoda and T.Idemitsu, An experimental study on penetration of chloride ions into concrete and corrosion of reinforcing bars in various marine environment., Journal of Materials, Concrete Structures and Pavement, No.557, 1998 (in Japanese).
- 3) Public Works Research Institute and PC Contractor's Association, Cooperative Investigation on Protective Technologies for Concrete Structures in Marine Environment, Joint Research Report No.142, 1995 (in Japanese).
- 4) Public Works Research Institute, Investigation on chloride supply from marine environment in Japan, Technical Memorandum No.3157, 1993 (in Japanese)
- 5) Y. Tanaka, M. Fujita, K. Kawano and H. Watanabe, Chloride permeability of high strength concrete, Proceedings of Japan Concrete Institute, Vol.23, 2001 (in Japanese)

7 A TEST OF PREDICTION MODELS FOR CHLORIDE INGRESS AND CORROSION INITIATION

7 A TEST OF PREDICTION MODELS FOR CHLORIDE INGRESS AND CORROSION INITIATION.

1. Predict the chloride profiles after an exposure of 30, 50 and 100 years, and the time to initiation of corrosion, in the Test Concrete in a selection of Test Environments with your preferred prediction model(s)!
2. Describe briefly the model(s), the assumptions and the input data.
3. Show the predicted profiles, also numbers in an Excel sheet (for easy comparison)!
4. Use those data you need for the concrete and the environments from the description below!

7.1 THE TEST CONCRETE

A very well investigated concrete, in a well-known environment, (from the Nordic project BMB on Durability of Marine Concrete) has been chosen to quantify the differences between models. The mix composition is given in Table I.

Table I. Composition of the selected test concrete H4 [1].

w/b	Cement	Silica fume	Water	Cement paste	Binder content	Calc. density	Air
0.40	399.0	21.0	168.0	30.4	19	2210	5.9
	kg/m ³	kg/m ³	kg/m ³	vol-%	% mass	kg/m ³	vol-%
Cement: SRPC. Silica fume: slurry							

Various chloride migration and apparent diffusion coefficients have been determined for this concrete at different ages, cf. Table II. D_{CTH} is a migration coefficient determined by the “CTH method” [2], now NTBuild 492 [3]. D_{AEC} is determined in a five-week immersion test [4], similar to NTBuild 443 [5]. The results are given in Table II.

Table II. Diffusion coefficients for the test concrete H4 from accelerated tests

D_{CTH} (10^{-12} m ² /s) [2]				D_{AEC} (10^{-12} m ² /s) [5]
Unexposed Age 0.5 y	Exposed Age 1 y	Unexposed Age 1.3 y	Exposed Age 2y	Unexposed Age 0.5 y
2.7	3.2	3.7	3.1	1.7

Specimens of this concrete have been exposed to seawater in the Träslövsläge field exposure station since 1992 [2]. The salinity and water temperature were: $[Cl^-]=14\pm 4$ g/l, $T=11\pm 9$ °C. The specimens were exposed at an age of 14 days.

During a two-year period cores were taken to accurately determine the chloride profiles [2]. The profiles from the submerged zone for concrete H4 are shown in Figure 1 [2]. From those profiles the “achieved surface chloride contents” C_{sa} were determined by curve fitting. The results are shown in Table III.

Table III. Achieved Surface Chloride Contents C_{sa} for concrete H4 from a two-year exposure period in Träslövsläge [2]

Age [years]	0.63		1.05		2.03		0.6 - 2	
Exposure time [years]	0.59		1.01		1.99		Average	
Wt-% of binder	3.82	3.26	3.71	3.66	3.75	3.95	3.44	3.45
							3.63	

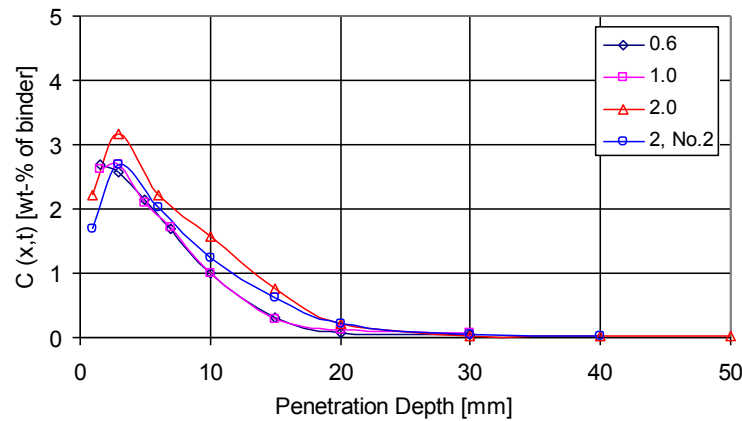


Fig. 1 Chloride profiles in the submerged zone for concrete H4 during a two-year field exposure period [2].

COVER: Assume a concrete cover of 60 mm in all environments!

7.2 THE TEST ENVIRONMENTS

A. Bridge column in a Marine Environment

The annual average and variation of salinity and water temperature are: $[Cl^-] = 14 \pm 4$ g/l, $T = 11 \pm 9$ °C. The concrete is assumed to be exposed at an age of 14 days.

Marine environment 1: Submerged zone

Marine environment 2: Tidal zone

Marine environment 3: Splash zone

Marine environment 4: Atmospheric zone

B. Bridge column in a Road Environment

Road Environment 1: A column at a distance from the road lane of 3 m. An average of totally 0.15 kg/m² NaCl is spread during five “winter” months each year. Make assumptions for other required climatic conditions!

References

1. Frederiksen, J. M. Nilsson, L.O., Sandberg, P., Poulsen, E., Tang, L. and Andersen, A. (1997), *HETEK, A system for estimation of chloride ingress into concrete, Theoretical background*, The Danish Road Directorate, Report No. 83.
2. Tang, L. (1997) *Chloride penetration profiles and diffusivity in concrete under different exposure conditions*. Dept. of Building Materials, Chalmers University of Technology. Publication P-97:3.
3. Nordtest (1999) ”Concrete, Mortar and Cement Based Repair Materials: Chloride Migration Coefficient from Non-steady State Migration Experiments”, NTBuild 492, Esbo, Finland, 1999.
4. Sørensen, H.E. (1992,1993), *Test Report. Project Durability of Marine Concrete Structures*, Test reports AECprov92-060, -074, -082 & 93-033, AEC, Vedbaek, Denmark
5. NordTest (1995), *Concrete, Hardened: Accelerated Chloride Penetration*. NTBuild 443, Esbo, Finland, 1995.

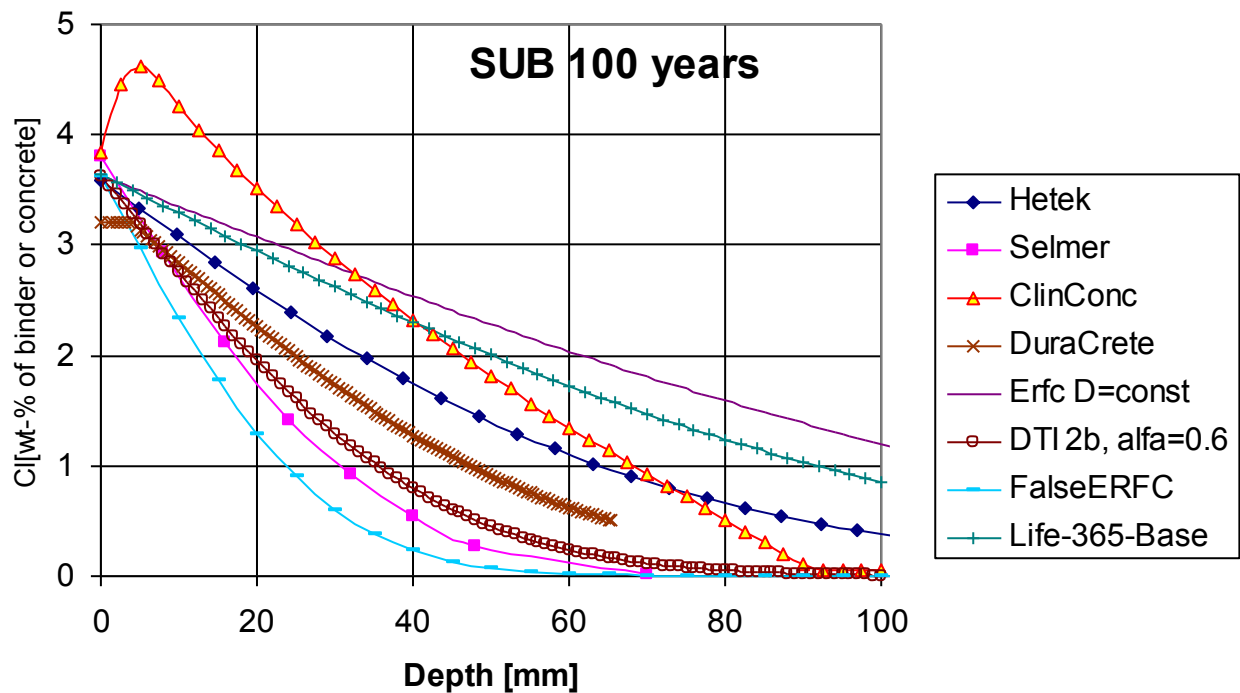
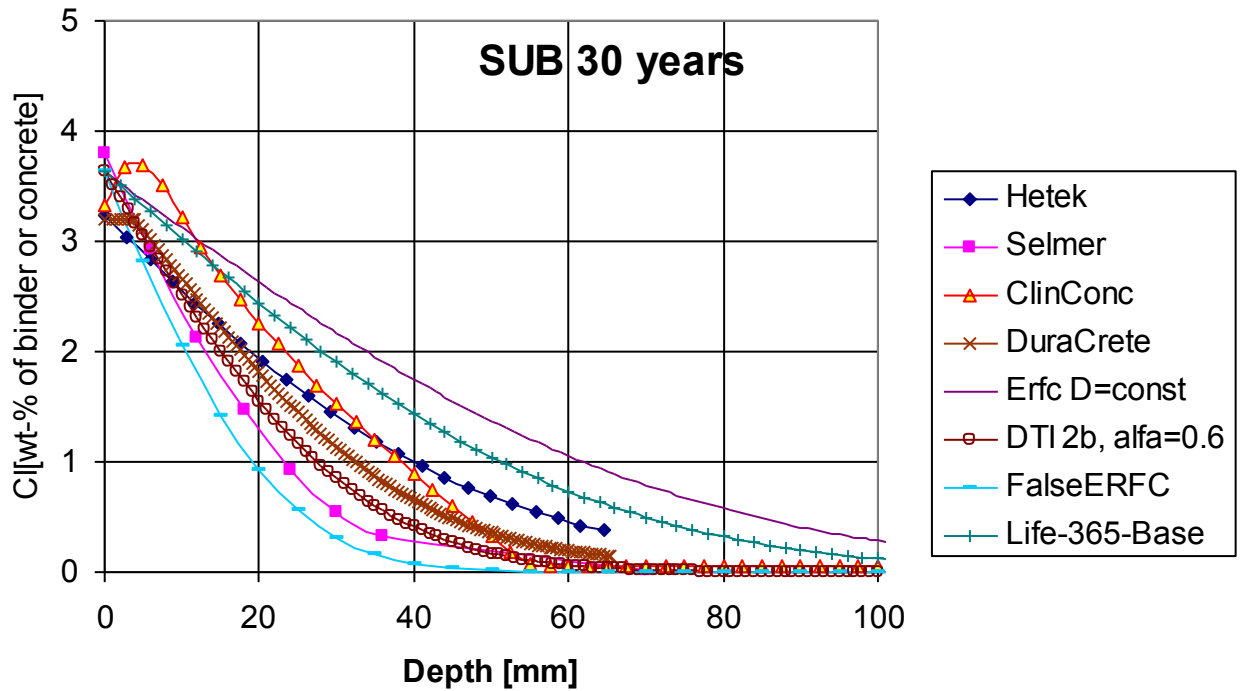
7.3 CONTRIBUTIONS

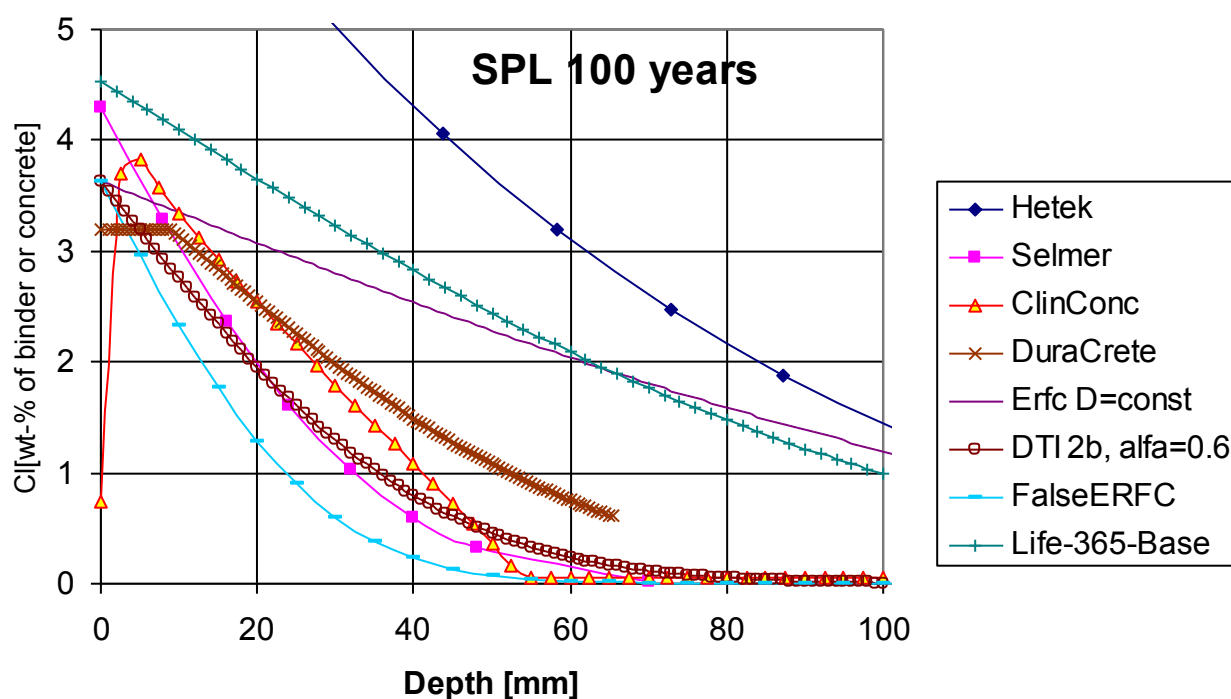
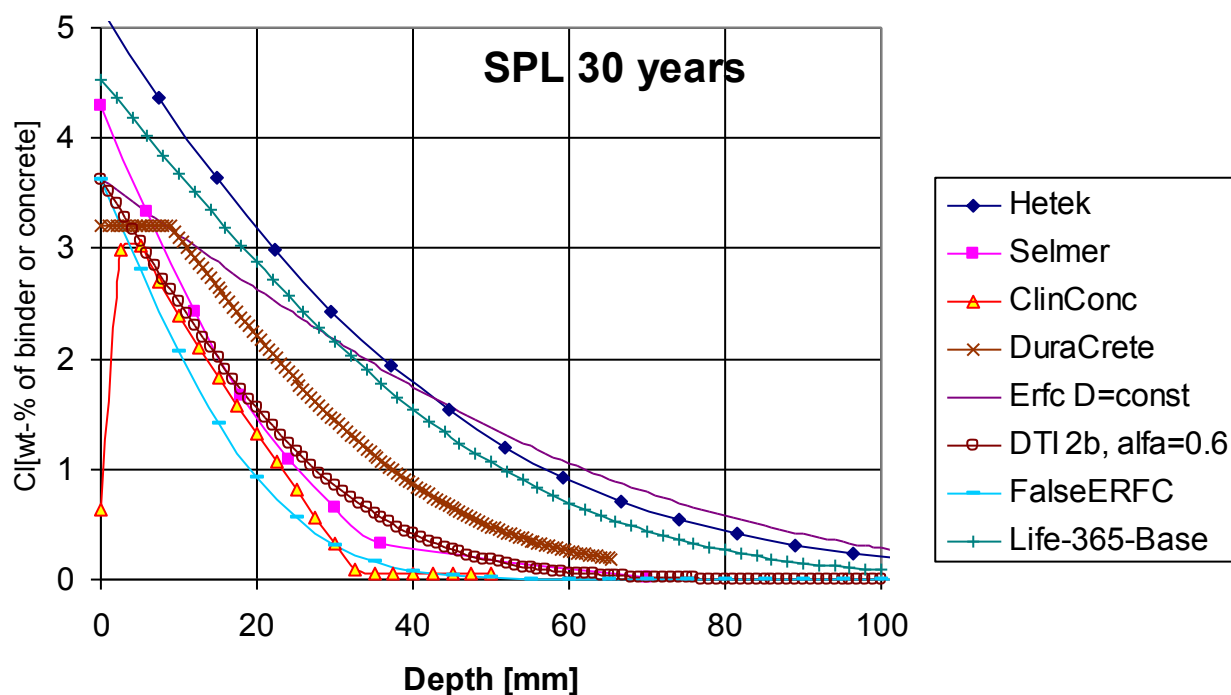
The contributions to the test case are described in detail in the Appendix.

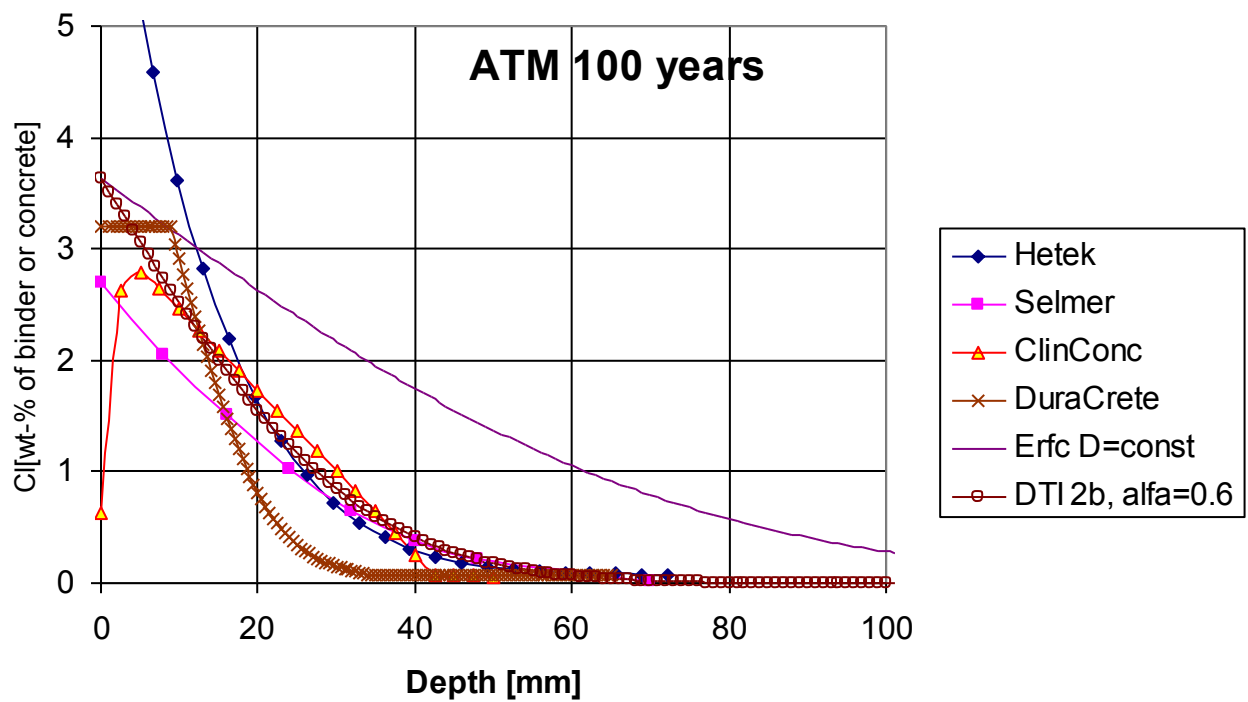
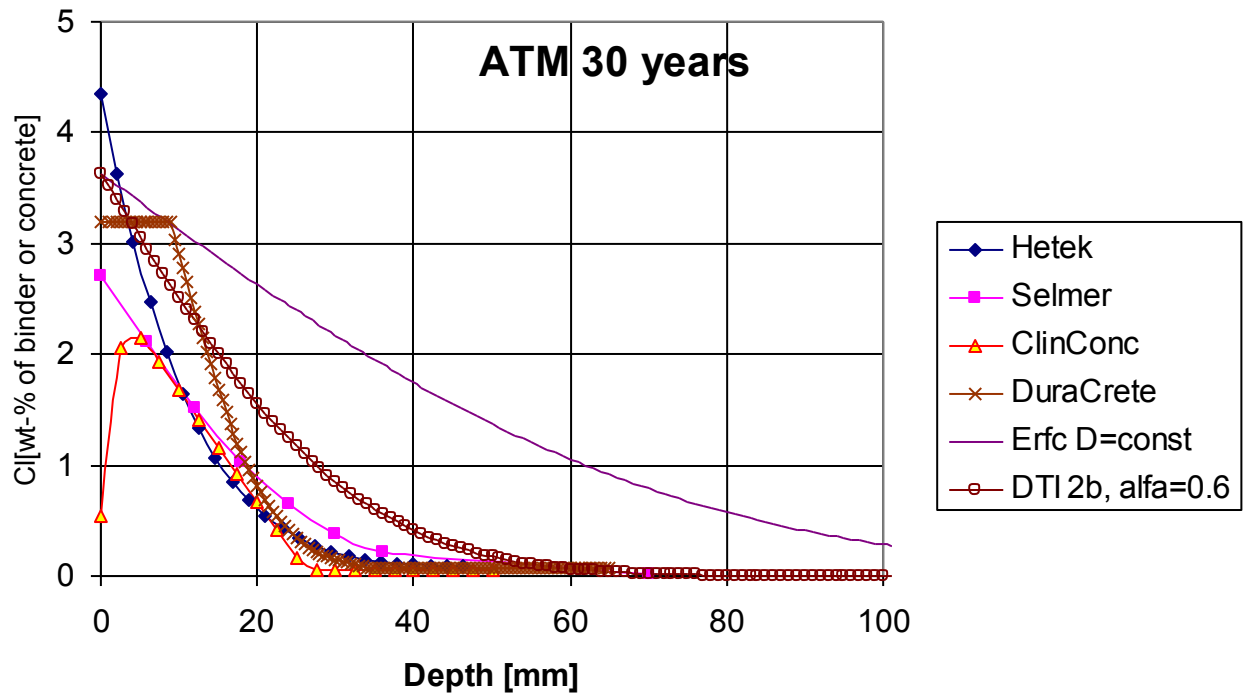
A TEST OF PREDICTION MODELS FOR CHLORIDE INGRESS AND CORROSION INITIATION.

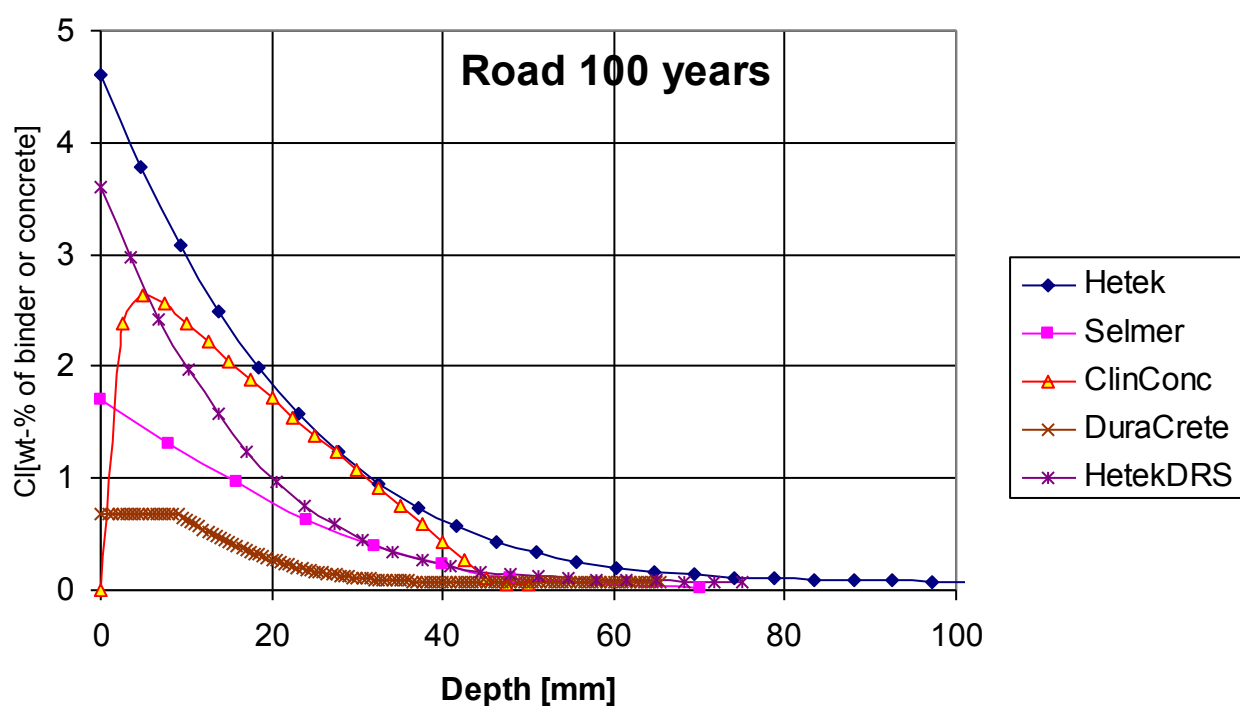
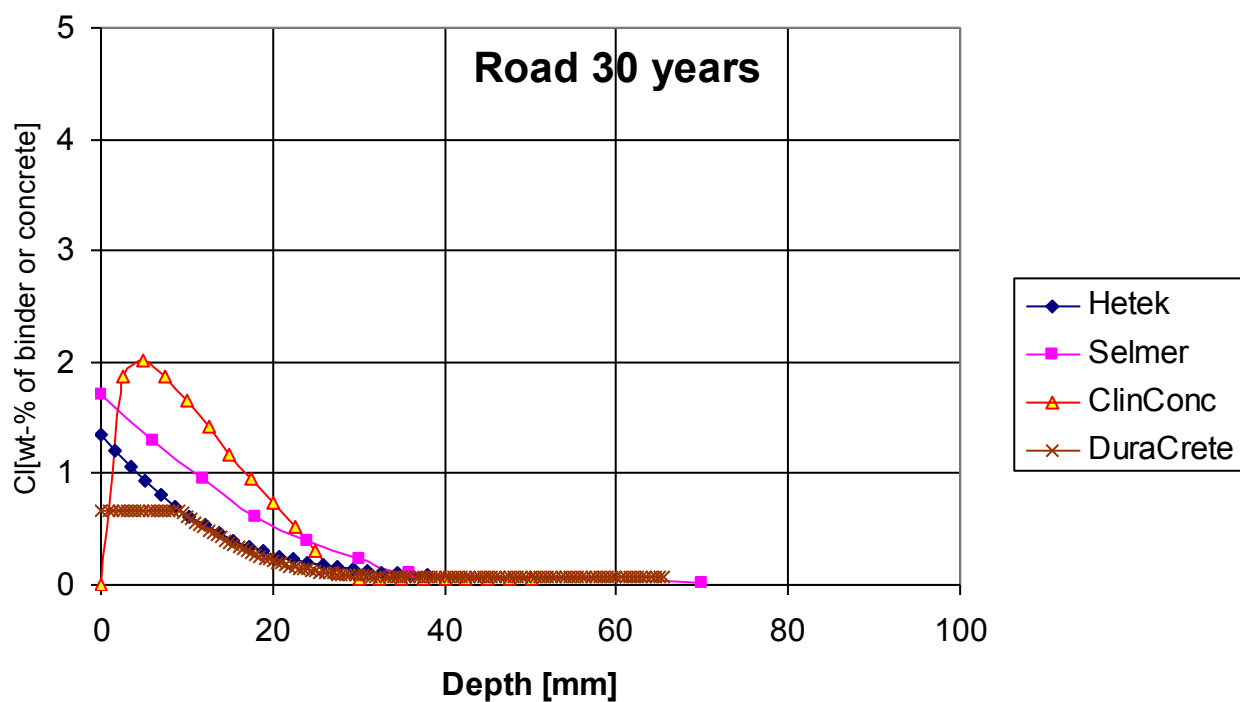
7.4 COMPARISON

The predictions of chloride ingress from the various models are compared in the next eight pictures.









7.5 DISCUSSION AND CONCLUSION

The conclusion is that the scatter is significant between the very best prediction models available today! Even for the most “simple” case, a concrete in the submerged zone with the surface chloride content and the apparent diffusion coefficient given for the first two years, the differences in predictions are really significant. For the splash zone the predictions of 100 years of chloride ingress differ tremendously!

The cause of these differences explains it all, of course. In fact, most models, except the ClinConc model, are more or less identical, with different assumptions on the variations with time of the apparent chloride diffusion coefficients and surface chloride contents. These differences in assumptions follow from the available exposure data for the development of each model.

8 CONCLUSIONS

A. GENERAL

1. Models should be able to reflect observations,
2. If they are not, we need better models OR better observations,
3. We may need different models for different applications,
4. We need alternative models (empirical and physical) for one application.
As long as they differ, we have a measure of the present uncertainty of the models.

B. EMPIRICAL MODELS

Empirical models (solving Fick's 2nd law, analytically or numerically, true or false)

1. shall allow for a time-dependent apparent diffusion coefficient*,
2. shall allow for a time-dependent surface chloride content C_{sa}^* ,
3. require methods to predict the surface concentration C_{sa} from local environmental (inter)actions and concrete mix,
4. are "mature" enough for most marine structures, but not yet for tunnels or road structures,
5. must consider the uncertainties of available data and execution in practice, i.e. being probabilistic,
6. require methods to determine the apparent D_a at some reference time.

(* BUT better data for the long-term dependency are required and the time-dependency must be much better understood!)

C. PHYSICAL MODELS

Physical models (describing the various, combined transport processes)

1. must contain material properties and boundary conditions that can be measured,
2. should be able to explain observations,
3. are required to understand and explain parts of empirical models,
 1. are required for calibration and understanding of empirical models.
4. require methods to predict the surface concentration C_{sa} from local environmental (inter)actions and concrete mix,
5. are "mature" enough for most marine structures, but not yet for tunnels or road structures,
6. must consider the uncertainties of available data and execution in practice, i.e. being probabilistic.

D. CORROSION INITIATION

1. The required conditions for corrosion initiation are extremely important for applications of empirical and physical models for service life estimations,
2. The models of those conditions must reflect local environmental actions, i.e. being different in various exposure classes,
3. The models of the environmental actions must consider not only chloride content, but also the state and variation of moisture, interfacial voids, stress distribution at the steel/concrete interface etc.,
4. A method for measuring necessary conditions for corrosion initiation is urgently required, including the effect of different reinforcement steels.

E. CRACKS (plus defects & joints)

1. Some research should be directed towards the effect of cracks,
2. Future ingress models shall be able to handle cracks, defects and casting joints.

F. CONCLUSIONS FROM THE TEST CASE

The conclusion from the contributions to the test case is that the scatter is significant between the very best prediction models available today! Even for the most “simple” case, a concrete in the submerged zone with the surface chloride content and the apparent diffusion coefficient given for the first two years, the differences in predictions are really significant. For the splash zone the predictions of 100 years of chloride ingress differ tremendously!

The cause of these differences explains it all, of course. In fact, most models, except the ClinConc model, are more or less identical, with different assumptions on the variations with time of the apparent chloride diffusion coefficients and surface chloride contents. These differences in assumptions follow from the available exposure data for the development of each model.

APPENDIX

Contributions To The Test Case

Jens Frederiksen. The Hetek Model

Steinar Helland. The Selmer Model

Doug Hooton. The Toronto Model

Björn Johannesson. Two Test Examples On Simulation Of Chloride Penetration: A Multi-Species Approach

Sascha Lay. Test Application Of Duracrete Models

Tang Luping. The Clinconc Models

Lars-Olof Nilsson. An Incorrect Empirical Erfc-Model

Marianne Tange Jepsen. Predictions For The Test Case

The 365 Life-Model

PREDICTION MODELS FOR CHLORIDE INGRESS AND CORROSION INITIATION IN CONCRETE STRUCTURES

A TEST OF PREDICTION MODELS FOR CHLORIDE INGRESS AND CORROSION INITIATION. Revised April 25

1. Predict the chloride profiles after an exposure of 30, 50 and 100 years, and the time to initiation of corrosion, in the Test Concrete in a selection of Test Environments with your preferred prediction model(s)!
2. Describe briefly the model(s), the assumptions and the input data.
3. Show the predicted profiles, also numbers in an Excel sheet (for easy comparison)!
4. Use those data you need for the concrete and the environments from the description below!

THE TEST CONCRETE

A very well investigated concrete, in a well-known environment, (from the Nordic project BMB on Durability of Marine Concrete) has been chosen to quantify the differences between models. The mix composition is given in Table I.

Table I. Composition of the selected test concrete H4 [1].

w/b	Cement	Silica fume	Water	Cement paste	Binder content	Calc. density	Air
0.40	399.0	21.0	168.0	30.4	19	2210	5.9
	kg/m ³	kg/m ³	kg/m ³	vol-%	% mass	kg/m ³	vol-%
Cement: SRPC. Silica fume: slurry							

Various chloride migration and apparent diffusion coefficients have been determined for this concrete at different ages, cf. Table II. D_{CTH} is a migration coefficient determined by the “CTH method” [2], now NTBuild 492 [3]. D_{AEC} is determined in a five-week immersion test [4], similar to NTBuild 443 [5]. The results are given in Table II.

Table II. Diffusion coefficients for the test concrete H4 from accelerated tests

D_{CTH} (10^{-12} m ² /s) [2]				D_{AEC} (10^{-12} m ² /s) [5]
Unexposed Age 0.5 y	Exposed Age 1 y	Unexposed Age 1.3 y	Exposed Age 2y	Unexposed Age 0.5 y
2.7	3.2	3.7	3.1	1.7

Specimens of this concrete have been exposed to seawater in the Träslövsläge field exposure station since 1992 [2]. The salinity and water temperature were: $[Cl^-]=14\pm4$ g/l, $T=11\pm 9$ °C. The specimens were exposed at an age of 14 days.

During a two-year period cores were taken to accurately determine the chloride profiles [2]. The profiles from the submerged zone for concrete H4 are shown in Figure 1 [2]. From those profiles the “achieved surface chloride contents” C_{sa} were determined by curve fitting. The results are shown in Table III.

Table III. Achieved Surface Chloride Contents C_{sa} for concrete H4 from a two-year exposure period in Träslövsläge [2]

Age [years]	0.63		1.05		2.03		0.6 - 2	
Exposure time [years]	0.59		1.01		1.99		Average	
Wt-% of binder	3.82	3.26	3.71	3.66	3.75	3.95	3.44	3.45
							3.63	

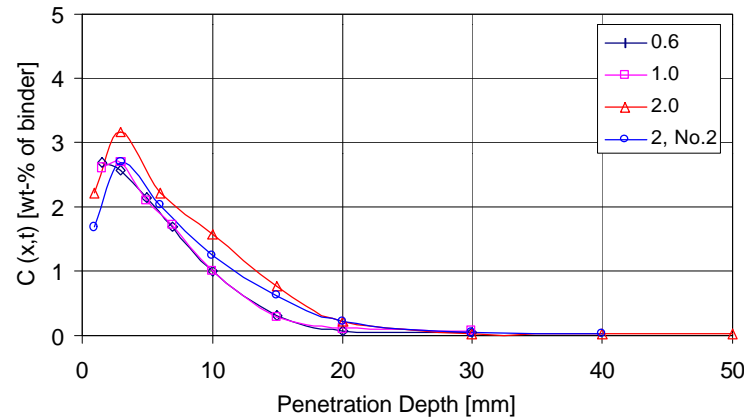


Fig. 1 Chloride profiles in the submerged zone for concrete H4 during a two-year field exposure period [2].

COVER: Assume a concrete cover of 60 mm in all environments!

THE TEST ENVIRONMENTS

A. Bridge column in a Marine Environment

The annual average and variation of salinity and water temperature are $[Cl^-] = 14 \pm 4$ g/l, $T = 11 \pm 9$ °C. The concrete is assumed to be exposed at an age of 14 days.

Marine environment 1: Submerged zone

Marine environment 2: Tidal zone

Marine environment 3: Splash zone

Marine environment 4: Atmospheric zone

B. Bridge column in a Road Environment

Road Environment 1: A column at a distance from the road lane of 3 m. An average of totally 0.15 kg/m² NaCl is spread during five “winter” months each year. Make assumptions for other required climatic conditions!

References

1. Frederiksen, J. M. Nilsson, L.O., Sandberg, P., Poulsen, E., Tang, L. and Andersen, A. (1997), *HETEK, A system for estimation of chloride ingress into concrete, Theoretical background*, The Danish Road Directorate, Report No. 83.
2. Tang, L. (1997) *Chloride penetration profiles and diffusivity in concrete under different exposure conditions*. Dept. of Building Materials, Chalmers University of Technology. Publication P-97:3.
3. Nordtest (1999) ”Concrete, Mortar and Cement Based Repair Materials: Chloride Migration Coefficient from Non-steady State Migration Experiments”, NTBuild 492, Esbo, Finland, 1999.
4. Sørensen, H.E. (1992,1993), *Test Report. Project Durability of Marine Concrete Structures*, Test reports AECprov92-060, -074, -082 & 93-033, AEC, Vedbaek, Denmark
5. NordTest (1995), *Concrete, Hardened: Accelerated Chloride Penetration*. NTBuild 443, Esbo, Finland, 1995.

Results according to the HETEK model (marine environment):

Marine environment

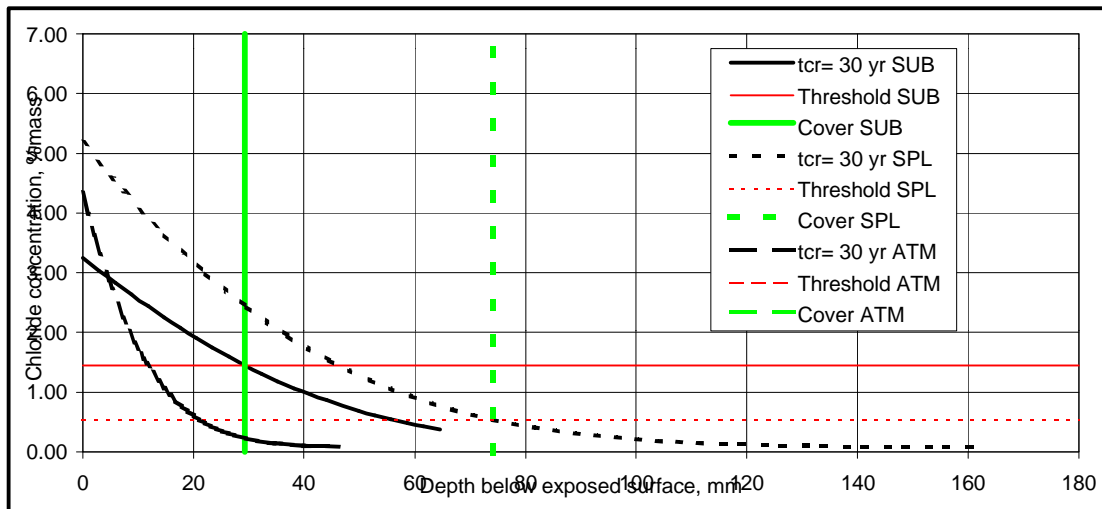
- Submerged structures (**SUB**) placed below level -3 m with respect to the lowest minimum water level, e.g. caissons.
- Structures placed in the splash zone (**SPL**), here defined as being above level -3 m with respect to the lowest minimum water level and below level +3 m with respect to the highest maximum water level, e.g. bridge pier shafts.
- Structures placed in the atmosphere (**ATM**) above level +3 m with respect to the highest maximum water level, e.g. bridge piers and the underneath of decks on marine bridges.

Estimation of decisive parameters and initiation time acc. to Frederiksen et al. [1997] (HETEK). Threshold value according to new formula.							
Concrete composition	SUB	SPL	ATM Unit	Surface concentration	SUB	SPL	ATM Unit
Cement content	95	95	95 % PO	$k_{C_1, env}$	1.4	1	0.6 -
Fly ash content	0	0	0 % PO	$k_{time env}$	1.5	4.5	7 -
Micro silica content	5	5	5 % PO	k_{MS}	-1.5	k_{FA}	0.75 -
Effective water content	40	40	40 % PO	eqv w/c	0.457	0.457	0.457 -
w/b ratio	0.40	0.40	0.40 -	C_1	2.3	1.7	1.0 % mass
Initial chloride content	0.075	0.075	0.075 % mass	C_{100}	3.5	7.5	7.0 % mass
Concrete age at Cl ⁻ -exp.	0.038	0.038	0.038 year	ID of structure:			
Diffusion coefficients	SUB	SPL	ATM -	Part of structure:			
$k_{D, env}$	1	0.6	0.4 -	Min. concrete covers:			
$k_{a, env}$	0.6	0.1	1 -	Expected init. time:			
k_{MS}	7	k_{FA}	1 -	5.0 5.0 5.0 yr			
eqv w/c	0.308	0.308	0.308 -	Threshold concentration	SUB	SPL	ATM -
D_1	84	50	33 mm ² /yr	$k_{cr, env}$	3.35	1.25	1.25 -
a	0.323	0.054	0.538 -	k_{MS}	-4.7	k_{FA}	-1.4 -
D_{100}	19	39	3 mm ² /yr	eqv w/c	0.559	0.559	0.559 -
				C_{cr}	1.45	0.54	0.54 % mass

Chloride profiles for 5 years of marine exposure:

SUB		SPL		ATM	
x, mm	C(x,t)	x, mm	C(x,t)	x, mm	C(x,t)
0.0	2.787	0.0	2.935	0.0	2.099
1.3	2.636	2.6	2.564	1.0	1.853
2.7	2.487	5.1	2.222	2.0	1.632
4.0	2.342	7.7	1.910	3.0	1.432
5.4	2.200	10.3	1.629	3.9	1.253
6.7	2.063	12.8	1.379	4.9	1.094
8.1	1.930	15.4	1.158	5.9	0.952
9.4	1.801	18.0	0.966	6.9	0.827
10.8	1.678	20.5	0.800	7.9	0.717
12.1	1.559	23.1	0.659	8.9	0.621
13.5	1.446	25.7	0.540	9.8	0.537
14.8	1.338	28.2	0.441	10.8	0.464
16.2	1.235	30.8	0.361	11.8	0.401
17.5	1.138	33.4	0.295	12.8	0.347
18.8	1.046	35.9	0.243	13.8	0.301
20.2	0.960	38.5	0.201	14.7	0.262
21.5	0.879	41.1	0.169	15.7	0.228
22.9	0.804	43.7	0.144	16.7	0.200
24.2	0.733	46.2	0.125	17.7	0.177
25.6	0.668	48.8	0.111	18.7	0.158
26.9	0.608	51.4	0.101	19.7	0.142
28.3	0.552	53.9	0.093	20.6	0.128
29.6	0.501	56.5	0.087	21.6	0.118

Estimation of decisive parameters and initiation time acc. to Frederiksen et al. [1997] (HETEK). Threshold value according to new formula.									
Concrete composition	SUB	SPL	ATM	Unit	Surface concentration	SUB	SPL	ATM	Unit
Cement content	95	95	95	% PO	$k_{C1,env}$	1.4	1	0.6	-
Fly ash content	0	0	0	% PO	$k_{time env}$	1.5	4.5	7	-
Micro silica content	5	5	5	% PO	k_{MS}	-1.5	k_{FA}	0.75	-
Effective water content	40	40	40	% PO	eqv w/c	0.457	0.457	0.457	-
w/b ratio	0.40	0.40	0.40	-	C₁	2.3	1.7	1.0	% mass
Initial chloride content	0.075	0.075	0.075	% mass	C₁₀₀	3.5	7.5	7.0	% mass
Concrete age at Cl ⁻ -exp.	0.038	0.038	0.038	year	ID of structure:				
Diffusion coefficients	SUB	SPL	ATM	-	Part of structure:				
$k_{D,env}$	1	0.6	0.4	-	Min. concrete covers:				29 74 21 mm
$k_{a,env}$	0.6	0.1	1	-	Expected init. time:				30.0 30.0 30.0 yr
k_{MS}	7	k_{FA}	1	-	Threshold concentration				SUB SPL ATM -
eqv w/c	0.308	0.308	0.308	-	$k_{cr,env}$	3.35	1.25	1.25	-
D₁	84	50	33	mm ² /yr	k_{MS}	-4.7	k_{FA}	-1.4	-
<i>a</i>	0.323	0.054	0.538	-	eqv w/c	0.559	0.559	0.559	-
D₁₀₀	19	39	3	mm ² /yr	C_{cr}	1.45	0.54	0.54	% mass



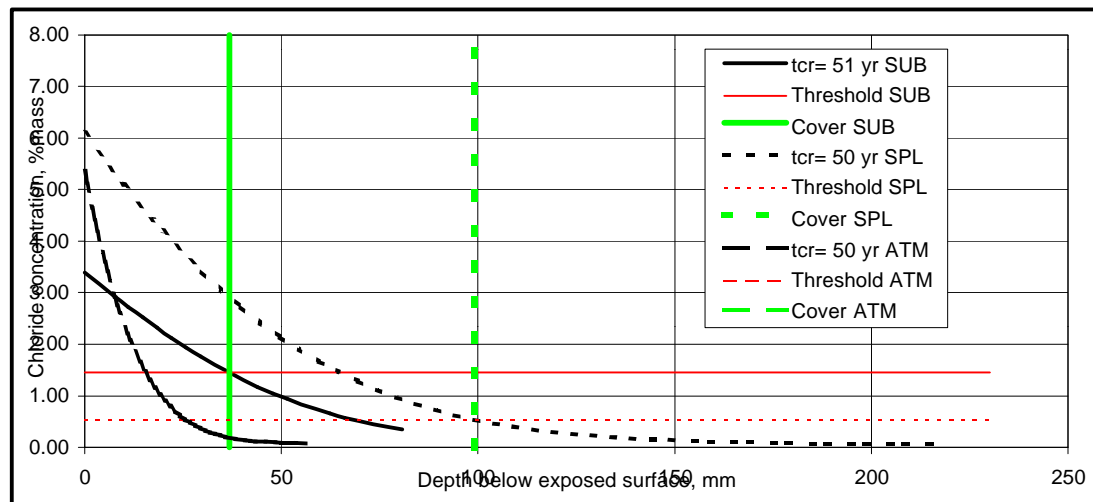
Acceptance criteria when testing acc. to NT BUILD 443						SUB	SPL	ATM
Concrete for zone:								
Test parameter:								
Test parameter: $D_{pex} <$								
Test parameter: $C_{sp} <$								

	SUB	SPL	ATM	Unit
a	0.323	0.054	0.538	
D_{aex}	239.7	59.8	193.5	
S_p	1.776	0.591	0.269	
p	0.128	0.342	0.899	

Chloride profiles for 30 years of marine exposure:

SUB		SPL		ATM	
x, mm	C(x,t)	x, mm	C(x,t)	x, mm	C(x,t)
0.0	3.245	0.0	5.184	0.0	4.345
2.9	3.036	7.4	4.371	2.1	3.628
5.9	2.831	14.8	3.640	4.2	3.009
8.8	2.632	22.2	2.992	6.3	2.477
11.7	2.439	29.6	2.427	8.4	2.026
14.7	2.254	37.1	1.943	10.5	1.646
17.6	2.076	44.5	1.536	12.6	1.329
20.5	1.906	51.9	1.200	14.7	1.067
23.5	1.744	59.3	0.927	16.8	0.853
26.4	1.591	66.7	0.710	18.9	0.679
29.3	1.447	74.1	0.540	21.0	0.540
32.3	1.312	81.5	0.409	23.2	0.429
35.2	1.186	88.9	0.311	25.3	0.342
38.1	1.069	96.3	0.239	27.4	0.274
41.1	0.960	103.8	0.187	29.5	0.222
44.0	0.861	111.2	0.150	31.6	0.183
46.9	0.770	118.6	0.124	33.7	0.153
49.8	0.686	126.0	0.107	35.8	0.131
52.8	0.611	133.4	0.095	37.9	0.115
55.7	0.543	140.8	0.087	40.0	0.103
58.6	0.482	148.2	0.075	42.1	0.094
61.6	0.427	155.6	0.075	44.2	0.088
64.5	0.379	163.0	0.075	46.3	0.084

Estimation of decisive parameters and initiation time acc. to Frederiksen et al. [1997] (HETEK). Threshold value according to new formula.									
Concrete composition	SUB	SPL	ATM	Unit	Surface concentration	SUB	SPL	ATM	Unit
Cement content	95	95	95	% PO	$k_{C\ 1,\ env}$	1.4	1	0.6	-
Fly ash content	0	0	0	% PO	$k_{time env}$	1.5	4.5	7	-
Micro silica content	5	5	5	% PO	k_{MS}	-1.5	k_{FA}	0.75	-
Effective water content	40	40	40	% PO	eqv w/c	0.457	0.457	0.457	-
w/b ratio	0.40	0.40	0.40	-	C_1	2.3	1.7	1.0	% mass
Initial chloride content	0.075	0.075	0.075	% mass	C_{100}	3.5	7.5	7.0	% mass
Concrete age at Cl ⁻ -exp.	0.038	0.038	0.038	year	ID of structure:				
Diffusion coefficients	SUB	SPL	ATM	-	Part of structure:				
$k_{D,\ env}$	1	0.6	0.4	-	Min. concrete covers:				37 99 26 mm
$k_{a,\ env}$	0.6	0.1	1	-	Expected init. time:				50.0 50.0 50.0 yr
k_{MS}	7	k_{FA}	1	-	Threshold concentration				SUB SPL ATM -
eqv w/c	0.308	0.308	0.308	-	$k_{cr,\ env}$	3.35	1.25	1.25	-
D_1	84	50	33	mm²/yr	k_{MS}	-4.7	k_{FA}	-1.4	-
a	0.323	0.054	0.538	-	eqv w/c	0.559	0.559	0.559	-
D_{100}	19	39	3	mm²/yr	C_{cr}	1.45	0.54	0.54	% mass

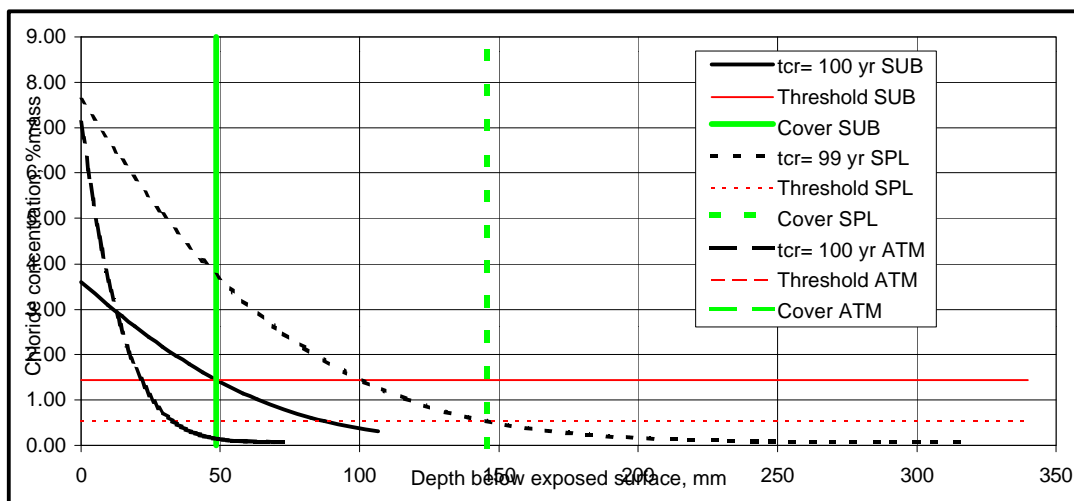


Acceptance criteria when testing acc. to NT BUILD 443						SUB	SPL	ATM
Concrete for zone:								
Test parameter:								
Test parameter: $D_{pex} <$	167	167	167	mm ² /yr	D_{aex}	0.323	0.054	0.538
Test parameter: $C_{sp} <$	5.0	5.0	5.0	%mass binder	S_p	1.776	0.591	0.269
					p	0.128	0.342	0.899

Chloride profiles for 50 years of marine exposure:

SUB		SPL		ATM	
x, mm	C(x,t)	x, mm	C(x,t)	x, mm	C(x,t)
0.0	3.395	0.0	6.103	0.0	5.355
3.7	3.166	9.9	5.098	2.6	4.405
7.3	2.942	19.8	4.199	5.1	3.593
11.0	2.725	29.7	3.410	7.7	2.907
14.7	2.516	39.6	2.728	10.2	2.332
18.3	2.314	49.6	2.151	12.8	1.856
22.0	2.122	59.5	1.671	15.3	1.466
25.7	1.938	69.4	1.281	17.9	1.150
29.3	1.765	79.3	0.970	20.4	0.897
33.0	1.601	89.2	0.727	23.0	0.697
36.7	1.447	99.1	0.541	25.5	0.540
40.3	1.304	109.0	0.401	28.1	0.419
44.0	1.171	118.9	0.299	30.6	0.326
47.7	1.049	128.8	0.226	33.2	0.256
51.3	0.936	138.8	0.175	35.7	0.204
55.0	0.833	148.7	0.139	38.3	0.166
58.7	0.739	158.6	0.116	40.8	0.138
62.3	0.655	168.5	0.100	43.4	0.119
66.0	0.579	178.4	0.090	46.0	0.105
69.7	0.511	188.3	0.075	48.5	0.095
73.3	0.450	198.2	0.075	51.1	0.088
77.0	0.396	208.1	0.075	53.6	0.084
80.6	0.349	218.0	0.075	56.2	0.080

Estimation of decisive parameters and initiation time acc. to Frederiksen et al. [1997] (HETEK). Threshold value according to new formula.									
Concrete composition	SUB	SPL	ATM	Unit	Surface concentration	SUB	SPL	ATM	Unit
Cement content	95	95	95	% PO	$k_{C1,env}$	1.4	1	0.6	-
Fly ash content	0	0	0	% PO	$k_{time env}$	1.5	4.5	7	-
Micro silica content	5	5	5	% PO	k_{MS}	-1.5	k_{FA}	0.75	-
Effective water content	40	40	40	% PO	eqv w/C	0.457	0.457	0.457	-
w/b ratio	0.40	0.40	0.40	-	C_1	2.3	1.7	1.0	% mass
Initial chloride content	0.075	0.075	0.075	% mass	C_{100}	3.5	7.5	7.0	% mass
Concrete age at Cl ⁻ -exp.	0.038	0.038	0.038	year	ID of structure:				
Diffusion coefficients	SUB	SPL	ATM	-	Part of structure:				
$k_{D,env}$	1	0.6	0.4	-	Min. concrete covers:				49 146 33 mm
$k_{a,env}$	0.6	0.1	1	-	Expected init. time:				100.0 100.0 100.0 yr
k_{MS}	7	k_{FA}	1	-	Threshold concentration	SUB	SPL	ATM	-
eqv w/c	0.308	0.308	0.308	-	$k_{cr,env}$	3.35	1.25	1.25	-
D_1	84	50	33	mm ² /yr	k_{MS}	-4.7	k_{FA}	-1.4	-
a	0.323	0.054	0.538	-	eqv w/c	0.559	0.559	0.559	-
D_{100}	19	39	3	mm ² /yr	C_{cr}	1.45	0.54	0.54	% mass



Acceptance criteria when testing acc. to NT BUILD 443						SUB	SPL	ATM
Concrete for zone:	SUB	SPL	ATM	Unit				
Test parameter:					a	0.323	0.054	0.538
Test parameter: $D_{pex} <$	167	167	167	mm ² /yr	D_{aex}	239.7	59.8	193.5
Test parameter: $C_{sp} <$	5.0	5.0	5.0	%mass binder	S_p	1.776	0.591	0.269
					p	0.128	0.342	0.899

Chloride profiles for 100 years of marine exposure:

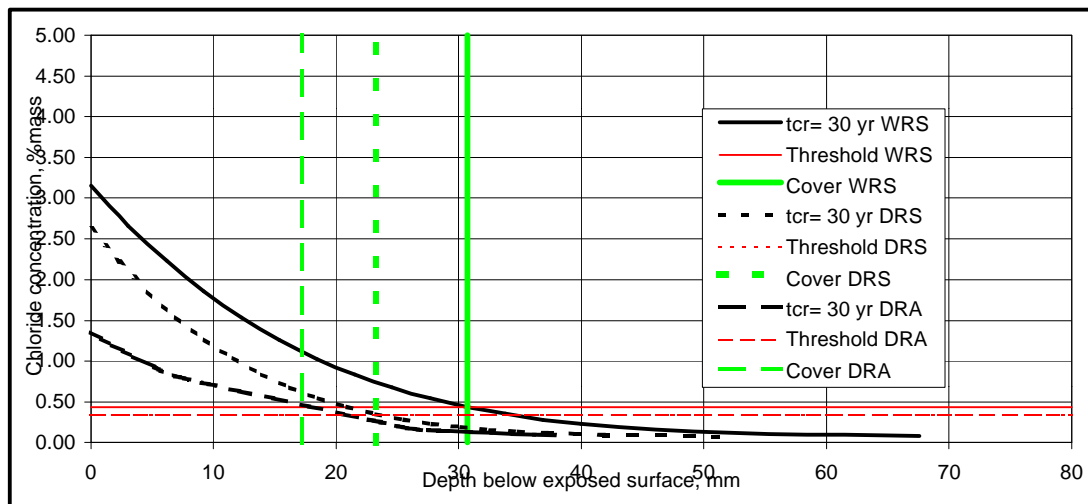
SUB		SPL		ATM	
x, mm	C(x,t)	x, mm	C(x,t)	x, mm	C(x,t)
0.0	3.595	0.0	7.595	0.0	7.116
4.9	3.339	14.6	6.267	3.3	5.738
9.7	3.090	29.1	5.089	6.6	4.580
14.6	2.849	43.7	4.065	9.8	3.618
19.4	2.616	58.2	3.192	13.1	2.829
24.3	2.394	72.8	2.464	16.4	2.190
29.1	2.182	87.3	1.871	19.7	1.679
34.0	1.980	101.9	1.398	23.0	1.276
38.8	1.791	116.4	1.029	26.2	0.963
43.7	1.613	131.0	0.749	29.5	0.722
48.5	1.448	145.5	0.541	32.8	0.540
53.4	1.294	160.1	0.390	36.1	0.405
58.2	1.153	174.6	0.283	39.4	0.306
63.1	1.023	189.2	0.210	42.7	0.234
67.9	0.905	203.7	0.160	45.9	0.183
72.8	0.798	218.3	0.127	49.2	0.147
77.6	0.702	232.8	0.107	52.5	0.123
82.5	0.616	247.4	0.094	55.8	0.106
87.3	0.539	261.9	0.075	59.1	0.095
92.2	0.471	276.5	0.075	62.3	0.087
97.0	0.412	291.0	0.075	65.6	0.083
101.9	0.360	305.6	0.075	68.9	0.075
106.7	0.314	320.1	0.075	72.2	0.075

Results according to the BRIME model (road environment):

1. Road environment

- The “wet” road environment, i.e. structural parts, which are able to “see” the sky and which are subjected to direct rain. **Wet splash (WRS)**: The distance to the traffic is less than 4 m e.g. edge beams.
- The “dry” road environment, i.e. structural parts, which are placed below a bridge deck and due to this not able to “see” the sky and not subjected to direct rain, but only to traffic splash. **Dry splash (DRS)**: The distance to the traffic is less than 4 m e.g. pillars.
- The region outside the borders mentioned above. **Distant road atmosphere (DRA)**: The wet or the dry environment where the distance to the traffic is more than 4 m e.g. noise shelters or parts of the structure high above road level.

Estimation of decisive parameters and initiation time in the road environment (de-icing salt)								
Concrete composition	WRS	DRS	DRA Unit	Surface concentration	WRS	DRS	DRA Unit	
Cement content	95	95	95 % PO	$k_{C1,env}$	0.6	0.6	0.3 -	
Fly ash content	0	0	0 % PO	$k_{time env}$	4.5	3.5	3.5 -	
Micro silica content	5	5	5 % PO	k_{MS}	-1.5	k_{FA}	0.75 -	
Effective water content	40	40	40 % PO	eqv w/c	0.457	0.457	0.457 -	
w/b ratio	0.40	0.40	0.40 -	C_1	1.0	1.0	0.5 % mass	
Initial chloride content	0.075	0.075	0.075 % mass	C_{100}	4.5	3.5	1.8 % mass	
Concrete age at Cl^- -exp.	0.038	0.038	0.038 year	ID of structure:				
Diffusion coefficients				Part of structure:				
$k_{D,env}$	0.8	0.4	0.4 -	Min. concrete covers:				
$k_{a,env}$	1	1	1 -		31	23	17 mm	
k_{MS}	7	k_{FA}	1 -	Expected init. time:				
eqv w/c	0.308	0.308	0.308 -		30.0	30.0	30.0 yr	
D_1	67	33	33 mm ² /yr	Threshold concentration				
a	0.538	0.538	0.538 -		WRS	DRS	DRA -	
D_{100}	6	3	3 mm ² /yr	$k_{cr,env}$	1	1.25	1.25 -	
				k_{MS}	-4.7	k_{FA}	-1.4 -	
				eqv w/c	0.559	0.559	0.559 -	
				C_{cr}	0.43	0.35	0.35 % mass	

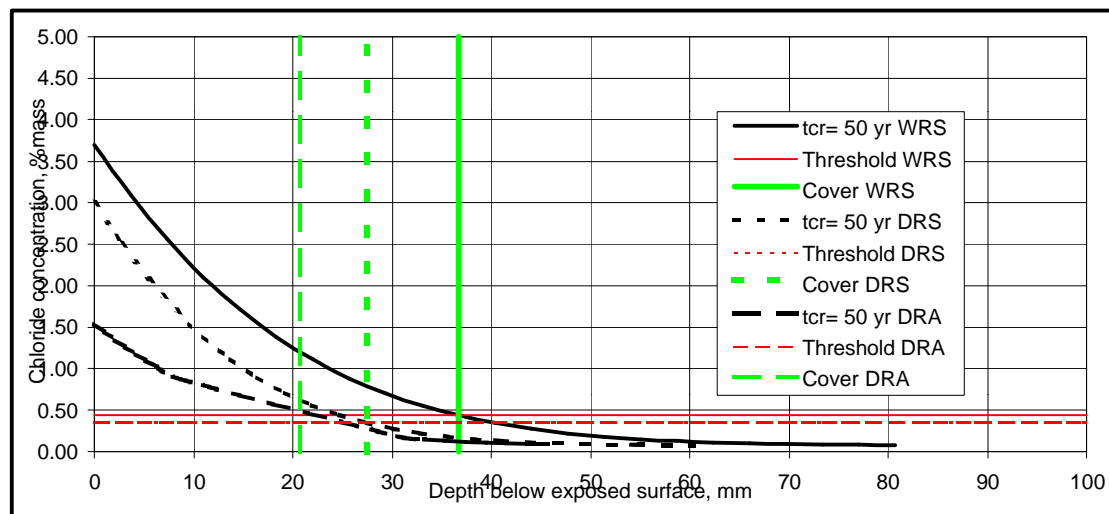


Acceptance criteria when testing acc. to NT BUILD 443						WRS	DRS	DRA
Concrete for zone:								
	WRS	DRS	DRA	Unit				
Test parameter:								
Test parameter: $D_{pox} <$	167	167	167	mm ² /yr	D_{aex}	0.145	0.118	0.334
Test parameter: $C_{sd} <$	5.0	5.0	5.0	%mass binder	S_p	0.000	0.000	0.000
					ρ	0.857	0.918	0.679

Chloride profiles for 30 years of exposure in the road environment:

WRS		DRS		DRA	
x, mm	C(x,t)	x, mm	C(x,t)	x, mm	C(x,t)
0.0	3.150	0.0	2.626	0.0	1.351
3.1	2.661	2.3	2.216	1.7	1.197
6.1	2.231	4.7	1.854	3.4	1.056
9.2	1.856	7.0	1.538	5.2	0.928
12.3	1.534	9.3	1.266	6.9	0.812
15.4	1.258	11.6	1.033	8.6	0.709
18.4	1.026	14.0	0.838	10.3	0.617
21.5	0.832	16.3	0.675	12.1	0.535
24.6	0.671	18.6	0.542	13.8	0.464
27.7	0.540	20.9	0.433	15.5	0.401
30.7	0.434	23.3	0.347	17.2	0.347
33.8	0.349	25.6	0.279	18.9	0.300
36.9	0.282	27.9	0.226	20.7	0.260
39.9	0.229	30.3	0.185	22.4	0.226
43.0	0.189	32.6	0.154	24.1	0.198
46.1	0.158	34.9	0.131	25.8	0.174
49.2	0.135	37.2	0.114	27.6	0.154
52.2	0.118	39.6	0.102	29.3	0.138
55.3	0.105	41.9	0.094	31.0	0.125
58.4	0.096	44.2	0.088	32.7	0.114
61.5	0.089	46.5	0.083	34.4	0.105
64.5	0.085	48.9	0.080	36.2	0.098
67.6	0.082	51.2	0.075	37.9	0.093

Estimation of decisive parameters and initiation time in the road environment (de-icing salt)							
Concrete composition	WRS	DRS	DRA Unit	Surface concentration	WRS	DRS	DRA Unit
Cement content	95	95	95 % PO	$k_{C1, env}$	0.6	0.6	0.3 -
Fly ash content	0	0	0 % PO	$k_{time env}$	4.5	3.5	3.5 -
Micro silica content	5	5	5 % PO	k_{MS}	-1.5	k_{FA}	0.75 -
Effective water content	40	40	40 % PO	eqv w/c	0.457	0.457	0.457 -
w/b ratio	0.40	0.40	0.40 -	C₁	1.0	1.0	0.5 % mass
Initial chloride content	0.075	0.075	0.075 % mass	C₁₀₀	4.5	3.5	1.8 % mass
Concrete age at Cl ⁻ -exp.	0.038	0.038	0.038 year	ID of structure:			
Diffusion coefficients				Part of structure:			
$k_{D, env}$	0.8	0.4	0.4 -	Min. concrete covers:			
$k_{a, env}$	1	1	1 -		37	27	21 mm
k_{MS}	7	k_{FA}	1 -	Expected init. time:			
eqv w/c	0.308	0.308	0.308 -		50.0	50.0	50.0 yr
D₁	67	33	33 mm²/yr	Threshold concentration			
a	0.538	0.538	0.538 -		WRS	DRS	DRA -
D₁₀₀	6	3	3 mm ² /yr	$k_{cr, env}$	1	1.25	1.25 -
				k_{MS}	-4.7	k_{FA}	-1.4 -
				eqv w/c	0.559	0.559	0.559 -
				C_{cr}	0.43	0.35	0.35 % mass

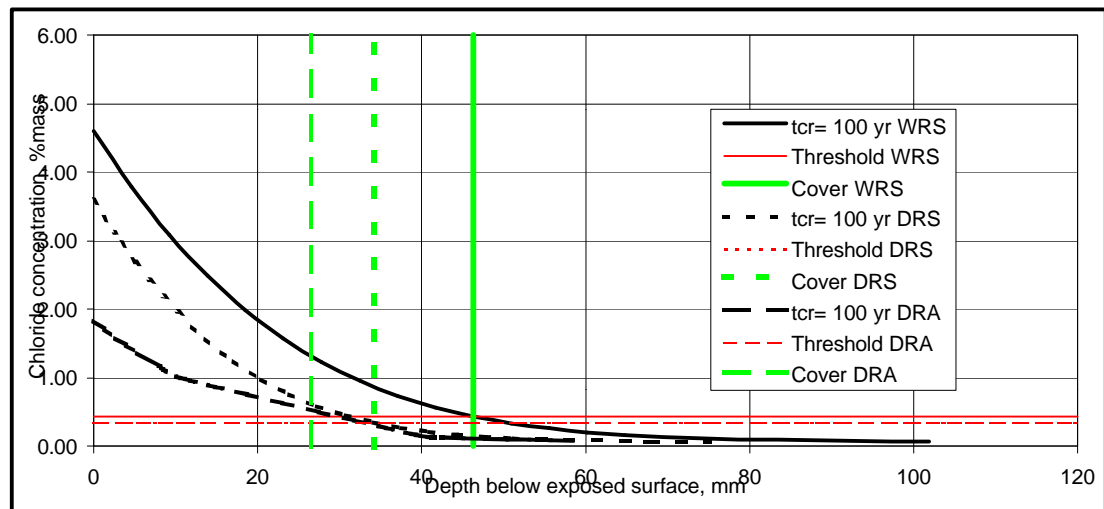


Acceptance criteria when testing acc. to NT BUILD 443						WRS	DRS	DRA
Concrete for zone:								
Test parameter:					a	0.113	0.097	0.268
Test parameter: $D_{pex} <$					D_{aex}	0.1	0.1	0.3
Test parameter: $C_{sp} <$					S_p	0.000	0.000	0.000
					p	0.909	0.962	0.729

Chloride profiles for 50 years of exposure in the road environment:

WRS		DRS		DRA	
x, mm	C(x,t)	x, mm	C(x,t)	x, mm	C(x,t)
0.0	3.699	0.0	3.000	0.0	1.537
3.7	3.089	2.7	2.509	2.1	1.349
7.3	2.558	5.5	2.078	4.2	1.177
11.0	2.100	8.2	1.705	6.2	1.023
14.7	1.710	11.0	1.386	8.3	0.885
18.3	1.381	13.7	1.117	10.4	0.762
22.0	1.107	16.5	0.893	12.5	0.654
25.7	0.881	19.2	0.708	14.5	0.560
29.3	0.698	21.9	0.559	16.6	0.478
33.0	0.551	24.7	0.441	18.7	0.407
36.7	0.434	27.4	0.347	20.8	0.347
40.4	0.342	30.2	0.275	22.9	0.296
44.0	0.272	32.9	0.220	24.9	0.253
47.7	0.218	35.7	0.178	27.0	0.217
51.4	0.178	38.4	0.147	29.1	0.188
55.0	0.148	41.1	0.125	31.2	0.164
58.7	0.126	43.9	0.109	33.3	0.144
62.4	0.110	46.6	0.098	35.3	0.129
66.0	0.099	49.4	0.090	37.4	0.116
69.7	0.091	52.1	0.085	39.5	0.106
73.4	0.086	54.9	0.081	41.6	0.099
77.0	0.082	57.6	0.075	43.6	0.093
80.7	0.075	60.3	0.075	45.7	0.088

Estimation of decisive parameters and initiation time in the road environment (de-icing salt)							
Concrete composition	WRS	DRS	DRA Unit	Surface concentration	WRS	DRS	DRA Unit
Cement content	95	95	95 % PO	$k_{C1, env}$	0.6	0.6	0.3 -
Fly ash content	0	0	0 % PO	$k_{time env}$	4.5	3.5	3.5 -
Micro silica content	5	5	5 % PO	k_{MS}	-1.5	k_{FA}	0.75 -
Effective water content	40	40	40 % PO	eqv w/c	0.457	0.457	0.457 -
w/b ratio	0.40	0.40	0.40 -	C₁	1.0	1.0	0.5 % mass
Initial chloride content	0.075	0.075	0.075 % mass	C₁₀₀	4.5	3.5	1.8 % mass
Concrete age at Cl ⁻ -exp.	0.038	0.038	0.038 year	ID of structure:			
Diffusion coefficients	WRS	DRS	DRA -	Part of structure:			
$k_{D, env}$	0.8	0.4	0.4 -	Min. concrete covers:			
$k_{a, env}$	1	1	1 -	Expected init. time:			
k_{MS}	7	k_{FA}	1 -	Threshold concentration			
eqv w/c	0.308	0.308	0.308 -	$k_{cr, env}$	1	1.25	1.25 -
D₁	67	33	33 mm²/yr	k_{MS}	-4.7	k_{FA}	-1.4 -
<i>a</i>	0.538	0.538	0.538 -	eqv w/c	0.559	0.559	0.559 -
D₁₀₀	6	3	3 mm²/yr	C_{cr}	0.43	0.35	0.35 % mass



Acceptance criteria when testing acc. to NT BUILD 443						WRS	DRS	DRA
Concrete for zone:								
Test parameter:					a	0.082	0.076	0.202
Test parameter: $D_{pex} <$					D_{aex}	0.1	0.1	0.2
Test parameter: $C_{sp} <$					S_p	0.000	0.000	0.000
					p	0.979	1.020	0.794

Chloride profiles for 100 years of exposure in the road environment:

WRS		DRS		DRA	
x, mm	C(x,t)	x, mm	C(x,t)	x, mm	C(x,t)
0.0	4.601	0.0	3.595	0.0	1.835
4.6	3.786	3.4	2.971	2.7	1.589
9.3	3.084	6.8	2.428	5.3	1.367
13.9	2.486	10.2	1.963	8.0	1.169
18.5	1.985	13.7	1.569	10.6	0.995
23.2	1.569	17.1	1.242	13.3	0.842
27.8	1.229	20.5	0.974	15.9	0.709
32.4	0.955	23.9	0.757	18.6	0.595
37.1	0.737	27.3	0.585	21.3	0.498
41.7	0.566	30.7	0.451	23.9	0.415
46.3	0.434	34.1	0.347	26.6	0.347
50.9	0.334	37.5	0.269	29.2	0.290
55.6	0.259	41.0	0.211	31.9	0.244
60.2	0.204	44.4	0.169	34.5	0.206
64.8	0.164	47.8	0.139	37.2	0.176
69.5	0.135	51.2	0.118	39.9	0.152
74.1	0.115	54.6	0.103	42.5	0.133
78.7	0.102	58.0	0.093	45.2	0.118
83.4	0.092	61.4	0.086	47.8	0.107
88.0	0.086	64.9	0.082	50.5	0.098
92.6	0.082	68.3	0.075	53.1	0.092
97.3	0.075	71.7	0.075	55.8	0.087
101.9	0.075	75.1	0.075	58.5	0.084

Data from Graph =====	Data from Graph =====	Data from Graph =====
30y : Total Chloride Profile	50y : Total Chloride Profile	100y : Total Chloride Profile
X Axis Title : Depth (mm) Y Axis Title : (%wt conc)	X Axis Title : Depth (mm) Y Axis Title : (%wt conc)	X Axis Title : Depth (mm) Y Axis Title : (%wt conc)
Depth (mm) (%wt conc) Line type : 0	Depth (mm) (%wt conc) Line type : 0	Depth (mm) (%wt conc) Line type : 0
0 3.63	0 3.63	0 3.63
1 3.5553	1 3.5692	1 3.5845
2 3.4807	2 3.5084	2 3.539
3 3.4062	3 3.4477	3 3.4936
4 3.3318	4 3.3871	4 3.4482
5 3.2577	5 3.3266	5 3.4028
6 3.1838	6 3.2662	6 3.3575
7 3.1101	7 3.2059	7 3.3123
8 3.0368	8 3.1459	8 3.2671
9 2.9639	9 3.0861	9 3.2221
10 2.8915	10 3.0265	10 3.1772
11 2.8195	11 2.9671	11 3.1324
12 2.748	12 2.9081	12 3.0878
13 2.6772	13 2.8494	13 3.0433
14 2.6069	14 2.791	14 2.999
15 2.5372	15 2.7329	15 2.9548
16 2.4683	16 2.6753	16 2.9108
17 2.4001	17 2.6181	17 2.8671
18 2.3327	18 2.5613	18 2.8236
19 2.266	19 2.5049	19 2.7802
20 2.2002	20 2.449	20 2.7372
21 2.1353	21 2.3936	21 2.6943
22 2.0712	22 2.3388	22 2.6518
23 2.0081	23 2.2844	23 2.6095
24 1.946	24 2.2306	24 2.5675
25 1.8848	25 2.1774	25 2.5258
26 1.8247	26 2.1248	26 2.4843
27 1.7656	27 2.0728	27 2.4432
28 1.7075	28 2.0214	28 2.4025
29 1.6505	29 1.9706	29 2.3621
30 1.5946	30 1.9205	30 2.322
31 1.5398	31 1.8711	31 2.2823
32 1.4861	32 1.8223	32 2.2429
33 1.4335	33 1.7743	33 2.2039
34 1.3821	34 1.7269	34 2.1653
35 1.3318	35 1.6803	35 2.1271
36 1.2827	36 1.6344	36 2.0894
37 1.2348	37 1.5892	37 2.052
38 1.188	38 1.5447	38 2.015
39 1.1424	39 1.5011	39 1.9785
40 1.098	40 1.4581	40 1.9424
41 1.0547	41 1.416	41 1.9068
42 1.0126	42 1.3746	42 1.8717

43	0.9716	43	1.334	43	1.8369
44	0.9318	44	1.2942	44	1.8027
45	0.8932	45	1.2552	45	1.769
46	0.8557	46	1.2169	46	1.7357
47	0.8193	47	1.1795	47	1.7029
48	0.7841	48	1.1429	48	1.6707
49	0.7499	49	1.107	49	1.6389
50	0.7169	50	1.072	50	1.6077
51	0.6849	51	1.0377	51	1.577
52	0.6541	52	1.0043	52	1.5468
53	0.6242	53	0.9716	53	1.5171
54	0.5955	54	0.9398	54	1.488
55	0.5677	55	0.9087	55	1.4595
56	0.5409	56	0.8784	56	1.4314
57	0.5152	57	0.849	57	1.404
58	0.4903	58	0.8203	58	1.3771
59	0.4665	59	0.7924	59	1.3507
60	0.4436	60	0.7652	60	1.325
61	0.4215	61	0.7389	61	1.2998
62	0.4004	62	0.7133	62	1.2752
63	0.3802	63	0.6885	63	1.2512
64	0.3607	64	0.6644	64	1.2277
65	0.3422	65	0.6411	65	1.2049
66	0.3244	66	0.6186	66	1.1826
67	0.3074	67	0.5967	67	1.161
68	0.2912	68	0.5757	68	1.1399
69	0.2757	69	0.5553	69	1.1195
70	0.2609	70	0.5357	70	1.0997
71	0.2469	71	0.5168	71	1.0805
72	0.2335	72	0.4986	72	1.0619
73	0.2208	73	0.4811	73	1.0439
74	0.2087	74	0.4643	74	1.0265
75	0.1973	75	0.4482	75	1.0098
76	0.1865	76	0.4328	76	0.9937
77	0.1762	77	0.418	77	0.9782
78	0.1665	78	0.404	78	0.9633
79	0.1574	79	0.3906	79	0.9491
80	0.1488	80	0.3778	80	0.9355
81	0.1408	81	0.3657	81	0.9226
82	0.1332	82	0.3543	82	0.9103
83	0.1261	83	0.3435	83	0.8986
84	0.1195	84	0.3333	84	0.8876
85	0.1134	85	0.3237	85	0.8772
86	0.1077	86	0.3148	86	0.8674
87	0.1024	87	0.3065	87	0.8583
88	0.0976	88	0.2988	88	0.8499
89	0.0932	89	0.2917	89	0.8421
90	0.0892	90	0.2853	90	0.8349
91	0.0855	91	0.2794	91	0.8284
92	0.0823	92	0.2741	92	0.8225
93	0.0795	93	0.2694	93	0.8173
94	0.077	94	0.2653	94	0.8127
95	0.0749	95	0.2618	95	0.8088
96	0.0731	96	0.2589	96	0.8056
97	0.0717	97	0.2566	97	0.803

98	0.0707
99	0.07

98	0.2548
99	0.2537

98	0.801
99	0.7997

Conflux model.

Boddy et al (1999), Cement & Concrete Research

CTH Test Case Doug.xls

Data from Graph

Data from Graph

Data from Graph

=====

=====

=====

100y, 500mm thick
: Total Chloride Profile

50y, 500mm thick
: Total Chloride Profile

30y,500mm thick
: Total Chloride Profile

X Axis Title : Depth (mm)

Y Axis Title : (%wt conc)

X Axis Title : Depth (mm)

Y Axis Title : (%wt conc)

X Axis Title : Depth (mm)

Y Axis Title : (%wt conc)

Depth (mm) (%wt conc)

Line type : 0

0	3.63
5	3.3999
10	3.1713
15	2.9455
20	2.724
25	2.5081
30	2.2988
35	2.0974
40	1.9047
45	1.7215
50	1.5484
55	1.3859
60	1.2344
65	1.094
70	0.9646
75	0.8462
80	0.7385
85	0.6411
90	0.5537
95	0.4757
100	0.4065
105	0.3454
110	0.292
115	0.2455
120	0.2053
125	0.1707
130	0.1412
135	0.1161
140	0.095
145	0.0773
150	0.0625
155	0.0503
160	0.0402
165	0.032
170	0.0253
175	0.0199
180	0.0155
185	0.0121
190	0.0093
195	0.0072
200	0.0055
205	0.0042
210	0.0031
215	0.0024

Depth (mm) (%wt conc)

Line type : 0

0	3.63
5	3.3263
10	3.026
15	2.7323
20	2.4481
25	2.1762
30	1.9189
35	1.6782
40	1.4553
45	1.2513
50	1.0665
55	0.9011
60	0.7545
65	0.6261
70	0.5148
75	0.4195
80	0.3386
85	0.2708
90	0.2145
95	0.1683
100	0.1308
105	0.1007
110	0.0768
115	0.058
120	0.0434
125	0.0321
130	0.0236
135	0.0171
140	0.0123
145	0.0088
150	0.0062
155	0.0043
160	0.003
165	0.0021
170	0.0014
175	0.0009
180	0.0006
185	0.0004
190	0.0003
195	0.0002
200	0.0001
205	0.0001
210	0
215	0

Depth (mm) (%wt conc)

Line type : 0

0	3.63
5	3.2574
10	2.891
15	2.5366
20	2.1996
25	1.8842
30	1.5941
35	1.3316
40	1.0979
45	0.8934
50	0.7173
55	0.5681
60	0.4438
65	0.3419
70	0.2598
75	0.1946
80	0.1438
85	0.1047
90	0.0752
95	0.0532
100	0.0371
105	0.0255
110	0.0173
115	0.0116
120	0.0076
125	0.0049
130	0.0032
135	0.002
140	0.0012
145	0.0008
150	0.0005
155	0.0003
160	0.0002
165	0.0001
170	0.0001
175	0
180	0
185	0
190	0
195	0
200	0
205	0
210	0
215	0

220	0.0018	220	0	220	0
225	0.0013	225	0	225	0
230	0.001	230	0	230	0
235	0.0007	235	0	235	0
240	0.0005	240	0	240	0
245	0.0004	245	0	245	0
250	0.0003	250	0	250	0
255	0.0002	255	0	255	0
260	0.0001	260	0	260	0
265	0.0001	265	0	265	0
270	0.0001	270	0	270	0
275	0	275	0	275	0
280	0	280	0	280	0
285	0	285	0	285	0
290	0	290	0	290	0
295	0	295	0	295	0
300	0	300	0	300	0
305	0	305	0	305	0
310	0	310	0	310	0
315	0	315	0	315	0
320	0	320	0	320	0
325	0	325	0	325	0
330	0	330	0	330	0
335	0	335	0	335	0
340	0	340	0	340	0
345	0	345	0	345	0
350	0	350	0	350	0
355	0	355	0	355	0
360	0	360	0	360	0
365	0	365	0	365	0
370	0	370	0	370	0
375	0	375	0	375	0
380	0	380	0	380	0
385	0	385	0	385	0
390	0	390	0	390	0
395	0	395	0	395	0
400	0	400	0	400	0
405	0	405	0	405	0
410	0	410	0	410	0
415	0	415	0	415	0
420	0	420	0	420	0
425	0	425	0	425	0
430	0	430	0	430	0
435	0	435	0	435	0
440	0	440	0	440	0
445	0	445	0	445	0
450	0	450	0	450	0
455	0	455	0	455	0
460	0	460	0	460	0
465	0	465	0	465	0
470	0	470	0	470	0
475	0	475	0	475	0
480	0	480	0	480	0
485	0	485	0	485	0
490	0	490	0	490	0

495

0

495

0

495

0

THE “SELMER” CHLORIDE INGRESS MODEL
APPLIED FOR THE TEST CASE OF THE NORDIC MINI SEMINAR
Chalmers May 2001

Steinar Helland
Head - Concrete Technology Group
Selmer Skanska AS
P.O.Box 12175 – Sentrum,
N - 0107
Oslo
NORWAY
E-mail: steinar.helland@selmer.skanska.no

ABSTRACT

At the Nordic Mini Seminar on “Prediction models for chloride ingress and corrosion initiation in concrete structures”, the organisers distributed to the participants a test case dated 25th April 2001.

This paper describes how Selmer Skanska AS solved the case based on the so-called “Selmer”-model.

The “Selmer” model is in detail described in another presentation at the mini seminar.

It is also available in more detail in the document EuroLightCon report BE96-3942/R3, “Chloride penetration into concrete with lightweight aggregates”, March 1999 /2/. The full report on the model and its application is downloadable from www.sintef.no/bygg/sement/elcon

Keywords: chloride, models

THE TEST CASE

The test case is given with two possible entries for the “Selmer” model

- 1 Diffusion coefficient obtained by a bulk diffusion test (NT Build 443 with 35 days exposure to 10 % NaCl). The specimen had been precured in fresh water for 0.5 years. The D_{AEC} was $1.7 \cdot 10^{-12} \text{ m}^2/\text{s} = 54 \text{ mm}^2/\text{year}$.
- 2 Chloride profiles from site exposed specimens after 0.59 - 1.01 and 1.99 years exposure. The specimens had been precured in fresh water for 14 days prior to exposure.

The best basis for extrapolation to 30, 50 and 100 years were the information from the site-exposed specimens.

INTERPRETATION OF THE SITE-EXPOSED SPECIMENS

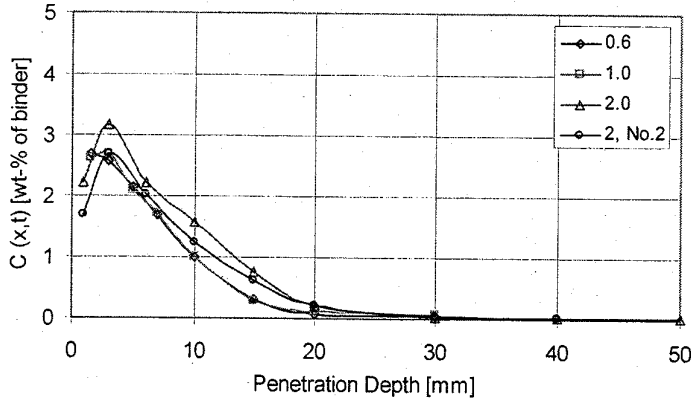


Fig. 1 Chloride profiles in the submerged zone for concrete H4 during a two-year field exposure period [2].

The 4 profiles were interpreted by a “semi”-automatic method by Selmer Skanska. The method includes a judgement of the “ideal” profile close to the surface and a best curve-fit to the solution of the Fick’s 2nd law.

The profiles and their interpretation with diffusion coefficient D_a and surface chloride concentration C_s are given in appendix 1 – 4.

The interpretation gave:

Exposure period years	$D_{achieved}$ $mm^2/year$	C_s % of binder
0,59	63	3,96
1,01	42	3,72
1,99	32	3,91
1,99	32	3,39

Based on these data, the reference $D_{aR} = D_a$ (1 year) and the α -exponent of the equation (1) were found by best curve-fit.

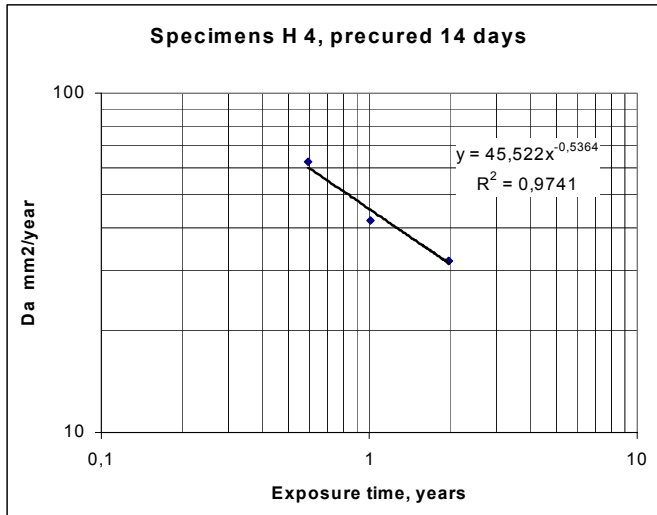
$$D_a(t_e) = D_{aR} \cdot \left(\frac{t_{eR}}{t_e}\right)^\alpha \quad (1)$$

where:

$D_a(t_e)$ = "Achieved" diffusion coefficient after exposure time t_e .

D_{aR} = "Reference" achieved diffusion coefficient at reference exposure time t_{eR} .

α = Parameter depending on concrete composition and environment.



The correlation is fairly good with $D_{aR} = D_a(t_R) = D_a(1 \text{ year}) = 46 \text{ mm}^2/\text{year}$ and $\alpha = 0.55$

Selmer Skanska has no own information on these properties for sulphate resistant cement as used in the mix H-4 as such cement is not applied for marine exposed structures in Norway. However, the parameters found for H-4 fit fairly well to similar concrete compositions where ordinary Portland cement has been used in combination with silica fume and the same range of water-binder ratios.

ENVIRONMENTAL LOAD C_s

From a number of Norwegian coastal structures, the environmental load C_s have been mapped at different levels above the sea. The results are given in the table. The C_s are calculated based on measured chloride profiles analysed according to Fick's 2nd law /Report 2.6 "Experience from sites" from R&D project "Durable concrete structures", Norway 1999/. The methodology is the same as used in appendix 1 - 4. This means that the C_s is not the measured surface level, but that according to the best curve-fit of the whole profile. The C_s thus correspond to the D_a as used to solve the equations.

As expected, the scatter is rather big

Meter above sea level	C_s (calculated) % of concrete	Stand. deviation	Number of data
0 - 2	0.51	0.23	62
2 - 4	0.41	0.22	277
4 - 6	0.35	0.22	125
6 - 8	0.35	0.24	127
8 - 10	0.43	0.27	71
10 - 12	0.25	0.24	60
12 - 14	0.31	0.27	41
14 - 16	0.20	0.18	17
16 - 18	0.20	0.21	33
18 - 20	0.18	0.12	15
20 - 24	0.23	0.16	11
24 -	0.17	0.10	8

Based on this experience, together with the reported C_s from the test-specimens, we have chosen the following C_s for the exposure conditions listed in this test:

<i>Environment</i>	<i>C_s (% of binder)</i>
Marine environment 1: submerged	3.8
Marine environment 2: tidal	3.8
Marine environment 3: splash	4.3
Marine environment 4: atmospheric	2.7
Road environment: 3 m from lane	1.7

We have in Selmer Skanska limited experience with C_s for concrete exposed to de-icing salts. Due to the long annual periods without salting, the deviation between an ideal chloride profile and the measured are also expected to be quite big in the surface zone. This effect will also lower the equivalent C_s (calculated as a continuous load) compared with the actual one during the relative short periods of salting. These two effects are expected to reduce the accuracy of the application of the "Selmer"-model.

The C_s chosen for the marine environment no 2, 3 and 4 are due to our Norwegian experience. The C_s chosen for the road environment is fairly representative for field measurements on 23 bridges in the Oslo area inspected in 1996-97.

EXTRAPOLATION

The D_a (30 years), D_a (50 years) and D_a (100 years) were then derived from Eq. 1

Years of exposure	D _a (t) mm ² /year
1 (reference)	46 (reference)
30	7.1
50	5.4
100	3.7

Selmer Skanska has no experience with how the de-icing environment influence the α - parameter compared to a marine environment. In the calculations in this test case we have therefore used α = 0.55 like for the other cases.

The predicted chloride profiles at 30, 50 and 100 years were then derived from the solution of Fick's 2nd law

$$C(x, t) = C_i + (C_s - C_i) \operatorname{erfc}\left(\frac{x}{\sqrt{4tD_a}}\right)$$

The results are given in appendix 5 (excel-sheets).

CALCULATIONS BASED ON THE BULK DIFFUSION TEST

The D_a (30 years), D_a (50 years) and D_a (100 years) could also be derived from the reported bulk diffusion test with $D_{AEC} = 1.7 \cdot 10^{-12} \text{ m}^2/\text{s} = 54 \text{ mm}^2/\text{year}$.

This D_{AEC} includes 0.5 years precuring and 35 days of exposure.

We then have to transform the situation from 0.5 year precuring plus 35 days exposure to 14 days precuring (like the real structure) plus 35 days of exposure.

According to the "Selmer"-model, this can be done by the Betta-parameter and Eq. 2

$$D_p(t_1) = D_p(t_2) \cdot \left(\frac{t_2}{t_1}\right)^\beta \quad (2)$$

where:

$D_p(t_1)$ = Potential diffusion coefficient after curing time $t_1 = 14 \text{ days}$.

$D_p(t_2)$ = Potential diffusion coefficient after curing time $t_2 = 182 \text{ days}$.

β = Material parameter depending on concrete composition.

An average β -exponent is 0.15

$D_p(t_2) = D_p(0.5 \text{ year}) = 54 \text{ mm}^2/\text{year}$.

$D_p(14 \text{ days}) = D_p \cdot (182/14)^{0.15}$

$D_p(14 \text{ days}) = 79 \text{ mm}^2/\text{year}$

(This is the calculated situation after 14 days curing + 35 days exposure)

By applying Eq. (1) this situation is again extrapolated to 14 days curing plus 1 year exposure

$$D_a(t_e) = D_{aR} \cdot \left(\frac{t_{eR}}{t_e}\right)^\alpha$$

where:

$D_a(t_e) = 79 \text{ mm}^2/\text{year}$ = calculated "Achieved" diffusion coefficient after exposure time $t_e = 35 \text{ days}$.

D_{aR} = "Reference" achieved diffusion coefficient at reference exposure time $t_{eR} = 1 \text{ year}$

$\alpha = 0.55$ = Parameter depending on concrete composition and environment

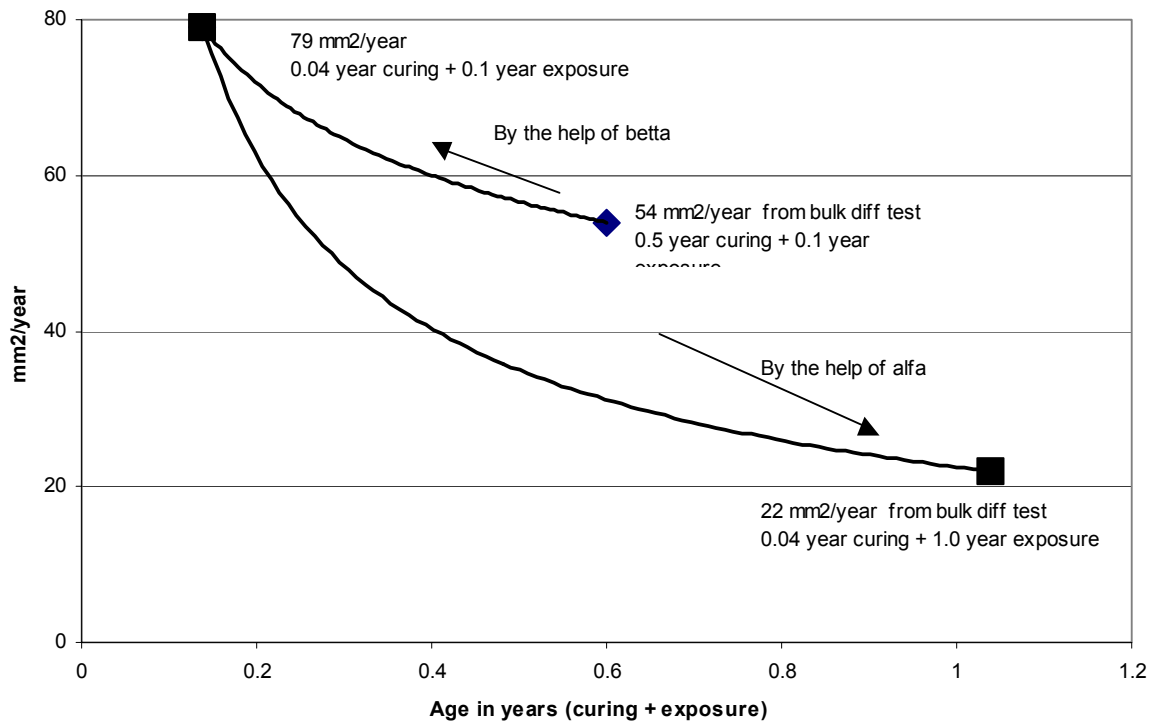
This gives $D_{aR} = D_a(1 \text{ year}) = 22 \text{ mm}^2/\text{year}$

$D_a = 22 \text{ mm}^2/\text{year}$ is far less than the $46 \text{ mm}^2/\text{year}$ derived from the field tests.

The data sets do therefore not correlate, or the transposition by help of β and α is not valid.

The general Norwegian experience is that we find a smooth transformation from bulk diffusion test results to field performance even if the accuracy is reduced as the gap in time and condition increases between those to be predicted and those of the input data.

Bulk diffusion test result transposed to D_a (1 year)



Betongteknologiavdelingen

-----d-m-år

Filnavn: CHALMERS

Utskrift-dato: 03.05.2001

Oppdrag: Test av levetidsmodell, Chalmers - mai 2001

Kloridprofil, beregning basert på Ficks 2. lov for diffusjon:

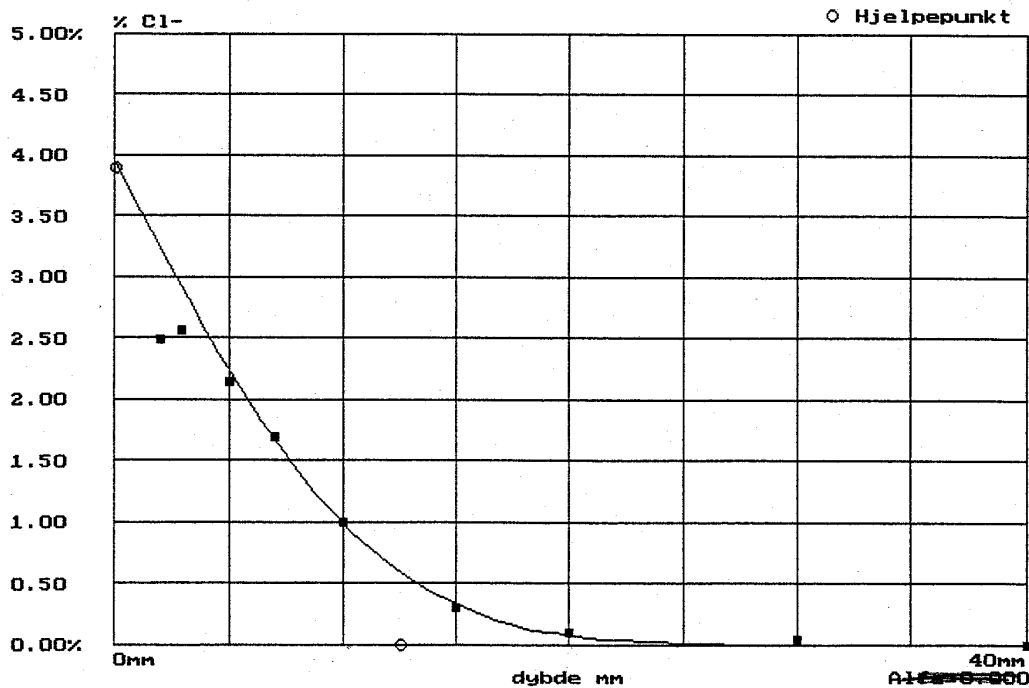
Datasett nr. 1 :

H4 Submerged 0,6 year

Antall dager utsatt for klorider :	220
Gitt indre kloridnivå (%) Ci :	0.00
Beregnet ytre kloridnivå (%) Cs :	3.96
KloridDiffusjonsKoeff. mm2/år D :	63
KloridDiffusjonskoeff. m2/sek D :	19.9E-13

Beregningen er basert på følgende data (punkter):

Data nr.	Dybde mm	Cl-%	
1	0.1	3.90	(hjælpepkt)
2	2.0	2.50	(ikke med)
3	2.9	2.56	(ikke med)
4	5.0	2.15	
5	7.0	1.70	
6	10.0	1.00	
7	12.5	0.00	(hjælpepkt)
8	15.0	0.30	
9	20.0	0.10	(ikke med)
10	30.0	0.05	(ikke med)
11	40.0	0.00	(ikke med)



Selmer Skanska AS

Betongteknologiavdelingen

Filnavn: CHALMERS

Utskrift-dato: 03.05.2001

Oppdrag: Test av levetidsmodell, Chalmers - mai 2001

Kloridprofil, beregning basert på Ficks 2. lov for diffusjon:

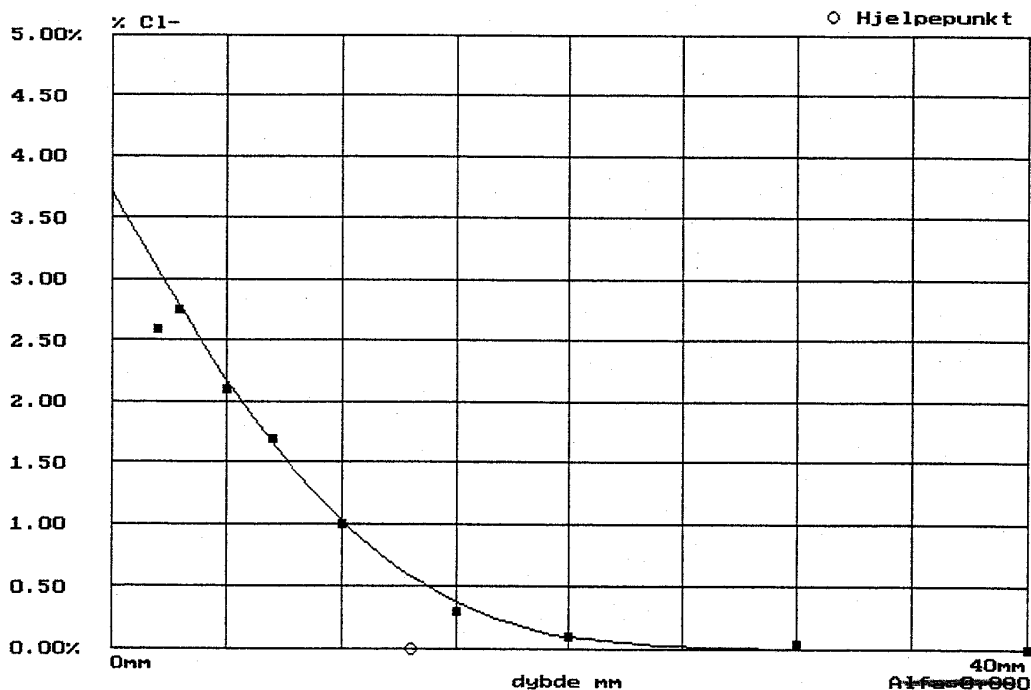
Datasett nr. 2 :

H4 Submerged 1,0 year

Antall dager utsatt for klorider :	365
Gitt indre kloridnivå (%) C_i :	0.00
Beregnet ytre kloridnivå (%) C_s :	3.72
KloridDiffusjonsKoeff. mm ² /år D :	42
KloridDiffusjonskoeff. m ² /sek D :	13.4E-13

Beregningen er basert på følgende data (punkter):

Data nr.	Dybde mm	Cl-%	
1	2.0	2.60	(ikke med)
2	2.9	2.75	
3	5.0	2.10	
4	7.0	1.70	
5	10.0	1.00	
6	13.0	0.00	(hjelpepkt)
7	15.0	0.30	
8	20.0	0.10	(ikke med)
9	30.0	0.05	(ikke med)
10	40.0	0.00	(ikke med)



Datasett : H4 Submerged 1,0 year

Selmer Skanska AS

Betongteknologiavdelinge

Filnavn: CHALMERS

Utskrift-dato: 03.05.200

Oppdrag: Test av levetidsmodell, Chalmers - mai 2001

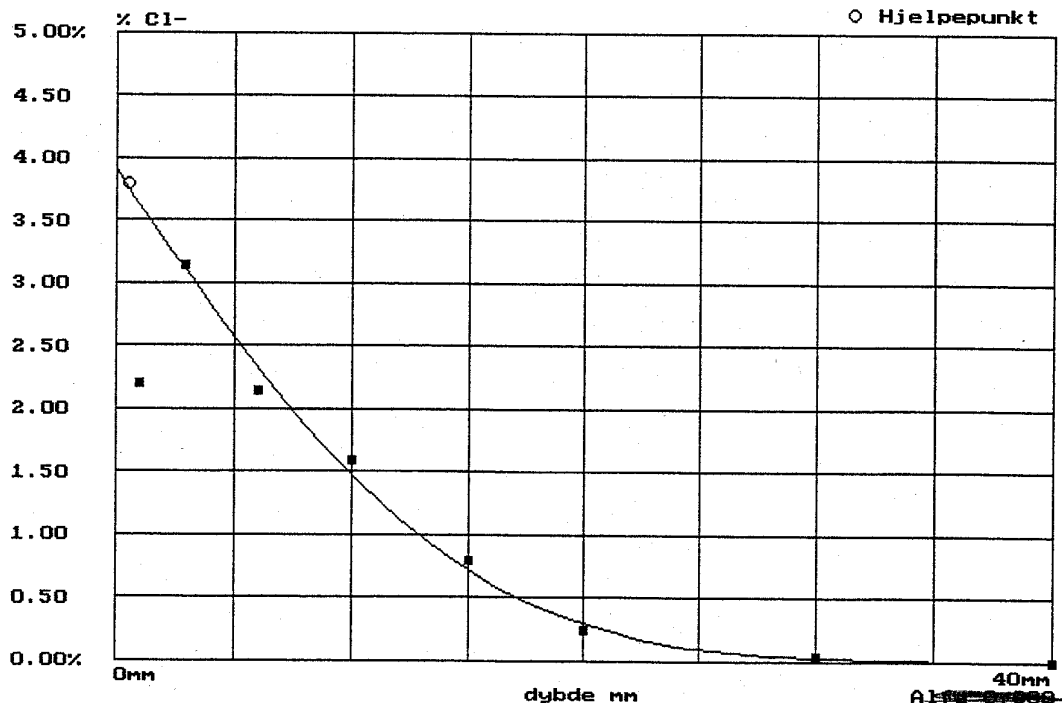
Kloridprofil, beregning basert på Ficks 2. lov for diffusjon
Datasett nr. 3 :

H4 Submerged 2,0 year

Antall dager utsatt for klorider : 730
Gitt indre kloridnivå (%) C_i : 0.00
Beregnet ytre kloridnivå (%) C_s : 3.91
KloridDiffusjonsKoeff. $\text{mm}^2/\text{år}$ D : 32
KloridDiffusjonskoeff. m^2/sek D : $10.2\text{E}-13$

Beregningen er basert på følgende data (punkter):

Data nr.	Dybde mm	Cl-%
1	0.5	3.80 (hjelpepkt)
2	1.0	2.20 (ikke med)
3	2.9	3.15
4	6.0	2.15
5	10.0	1.60
6	15.0	0.80
7	20.0	0.25 (ikke med)
8	30.0	0.05 (ikke med)
9	40.0	0.00 (ikke med)



Selmer Skanska AS

Betongteknologiavdelingen

Filnavn: CHALMERS

Utskrift-dato: 03.05.2001

Oppdrag: Test av levetidsmodell, Chalmers - mai 2001

Kloridprofil, beregning basert på Ficks 2. lov for diffusjon:

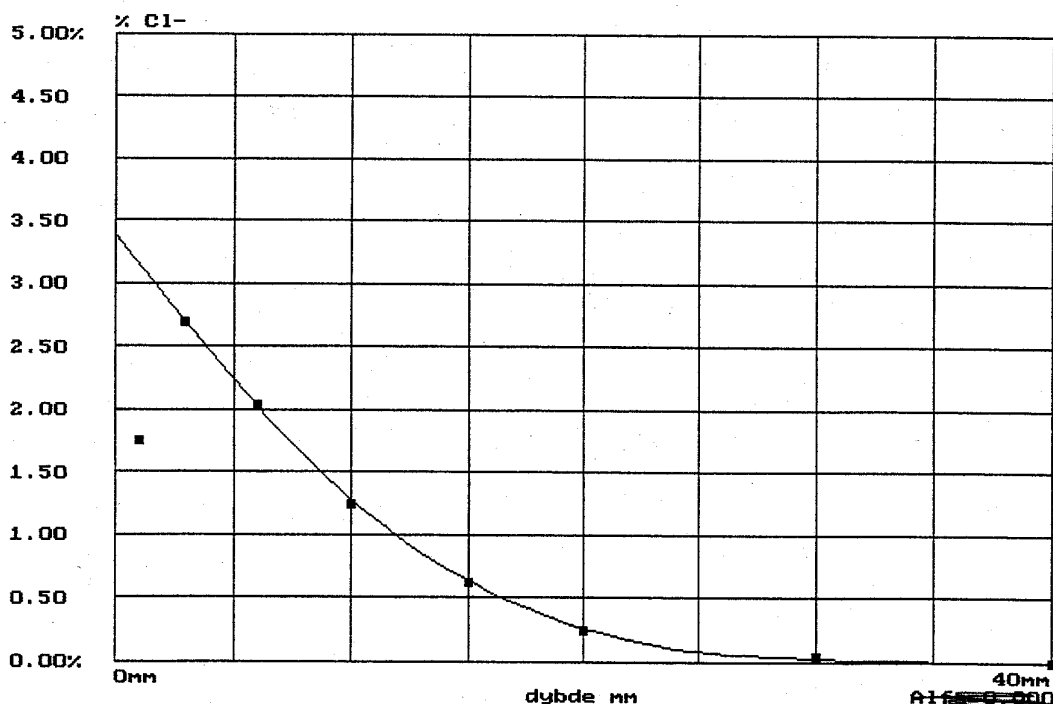
Datasett nr. 4 :

H4 Submerged 2,0 year (No. 2)

Antall dager utsatt for klorider : 730
Gitt indre kloridnivå (%) C_i : 0.00
Beregnet ytre kloridnivå (%) C_s : 3.39
KloridDiffusjonsKoeff. mm²/år D : 32
KloridDiffusjonskoeff. m²/sek D : 10.3E-13

Beregningen er basert på følgende data (punkter):

Data nr.	Dybde mm	Cl-%
1	1.0	1.75 (ikke med)
2	2.9	2.70
3	6.0	2.05
4	10.0	1.25
5	15.0	0.62
6	20.0	0.24
7	30.0	0.05 (ikke med)
8	40.0	0.00 (ikke med)



Datasett : H4 Submerged 2,0 year (No. 2)

Two Test Examples on Simulation of Chloride Penetration: A Multi-species Approach

Björn Johannesson

Lund Institute of Technology, Division of Building Materials

Box 118, SE-221 00 Lund, Sweden

May 18, 2001

Abstract

This report is written on demand by the organizers of the Nordic Mini Seminar: *Prediction Models for Chloride Ingress and Corrosion initiation in Concrete Structures*. The task is to model chloride ingress for a certain concrete quality exposed to different outer climate conditions.

The given material constant (i.e. the effective diffusion constant) is ignored since the model to be tested does not include this property. Furthermore, the variations in outer climate are not properly described. Due to this dilemma I have chosen to compare my simulations with indoor laboratory measurements where the variations of boundary conditions (outer climate) were controlled.

One important result from the performed test-runs is that convection of chlorides cannot be omitted from models when splash and tidal zones are considered.

1. Introduction

It is suggested that contributors to the *Nordic Mini Seminar on Prediction Models for Chloride Ingress and Corrosion Initiation in Concrete Structures, May 22-23 2001*, should simulate chloride ingress for different cases. My model include material constants and ion constituents in pore solution that not are given in the conditions. Due to this dilemma I have chosen to simulate chloride ingress in a concrete quality very similar to the one in the conditions, but the results are

compared with controlled laboratory tests for the submerge and tidal zone cases (i.e. the exact variations of outer climate are known). The needed initial conditions of concentrations are taken from pore solution extraction measurements. Since the model to be presented does not include the effective diffusion constant concept, the information regarding this, in the given conditions, is ignored. The material constants in use are instead the values giving the best fit to the presented experimental values.

The model in use is described in detail. In Section 3 the important physical balance laws for the constituents are presented. These balance laws are used together with the proposed constitutive relations described in Section 4. These assumptions constitute the hypothesis in use, which should be compared with experiments. In Section the details of the constitutive relations for the included chemical reactions between ions in pore solution and solid pore walls in concrete are described. The resulting equations which are obtained by combining the mass balance laws with the constitutive assumptions for the dielectric diffusion and chemical reactions are presented in Section 6. A very important issue, often not discussed in application of models within concrete durability, is the reliability of the adopted numerical method. The issue is important since no analytical solution to the kind of problems studied exist and therefore it is very important to show the extra assumptions that has to be introduced in the numerical analysis. This subject is discussed in Section 7. Test-runs of the described model are performed in Sections 8 and 9. In Section 8 a submerged case is considered and in Section 9 a cyclic case containing drying and exposure to a sodium chloride solution is studied. Both test examples are compared with controlled experiments performed in an identical manner as compared to the performed simulations.

2. Some thoughts about the suggested comparison of prediction models

The aim of the comparison of the models is not at all clear! Is it to show that different researchers have the ability to solve differential equations or is it to try to confirm the reliability of different proposed models. If it is the latter case I think the work of making these different simulations is quite a waste of time! The reason for this are:

1. It is stated that the material data for the concrete should be used (i.e. an effective diffusion constant). The problem is that different models demands

different types of material data besides an effective diffusion constant (or even not included at all). A model can for example include explicit descriptions of binding and leaching of ions which generates other material constants not described in the conditions.

2. The solutions to diffusion equations are very much determined by the boundary conditions. If different assumptions concerning the boundary conditions for the proposed examples, i.e. tidal zone, splash zone and atmospheric zone are chosen different solutions will be obtained and the comparison between them is useless.
3. Only one measured case is presented, i.e. the reliability of models cannot be tested in the other cases. The suggested diffusion constant and its time dependence should, further, be in accordance with the presented measured profiles. It can be immediately concluded that the effective diffusion constant used in Fick's second law cannot model the presented experimental data since the peak behavior of chlorides near surface is measured.
4. If considering effects on chloride diffusion caused by presence of other types of ions, then information concerning the initial concentrations of all different types of ions in pore solution must be known. Further, the composition of all different ions in sea-water will affect the chloride diffusion.
5. If studying cases where chlorides are effected by convection caused by capillary suction (i.e. at tidal zone, splash zone) a physical adequate model must include mechanisms related to moisture transport (not only D_{CTH}). No information regarding the moisture transport data, such as water diffusibility and sorption isotherms are included.
6. The preparation of the samples before exposure has been shown to effect the chloride penetration very much, i.e. depending on samples being dried before exposure (and re-wetted in tap water before exposure to a chloride solution) or stored in tap water (or membrane hardened) before exposure. No information about the preparation is given in the conditions.

Due to my doubts about the use of the kind of comparisons that are proposed I have made simulations on cases where experimental data on submerged and tidal zones exist. These experiments are performed under very controlled conditions in the laboratory.

3. Mass balance and the static continuity equation for the ionic charge

In this section the basic physical equations describing balance properties will be introduced. The only balance principles to be used are balance of mass and the continuity equation for the ionic charge. These equations must be supplemented by so-called constitutive relations, or equally material functions, in order to make the number of unknown properties and equations equal. A more simple approach whereby ‘convective’ velocities are ignored will be used. This means that the velocities of the constituents are assumed to be approximately equal to their corresponding so-called diffusion velocities.

In the so-called mixture theory, e.g. see [1], the mass balance for an individual constituent in a mixture, is the postulate

$$\frac{\partial \rho_a}{\partial t} = -\operatorname{div}(\rho_a \dot{\mathbf{x}}_a) + \hat{c}_a; \quad a = 1, \dots, \mathfrak{R}, \quad (3.1)$$

where ρ_a (kg/m³) is the mass density of the a :th constituent. The velocity is denoted $\dot{\mathbf{x}}_a$ (m/s), and \hat{c}_a (kg/m³s) the mass gain density to the a :th constituent from all other $\mathfrak{R} - 1$ constituents present in the mixture, where \mathfrak{R} is the number of constituents.

The total mass density of the mixture ρ is by definition

$$\rho = \sum_{a=1}^{\mathfrak{R}} \rho_a \quad (3.2)$$

One of the cornerstones in the theory of mixtures is that the postulated balance principals for the individual constituents should result in the classical principals used for single (constituent) materials when summing over all \mathfrak{R} constituents. The postulate for mass balance for a single material is

$$\frac{\partial \rho}{\partial t} = -\operatorname{div}(\rho \dot{\mathbf{x}}) \quad (3.3)$$

where ρ is the mass density of the mixture and $\dot{\mathbf{x}}$ is the mean velocity or simply the velocity of the mixture. By making a summation of all \mathfrak{R} constituent equations in (3.1) the equation (3.3) should be the result. This will be the case when defining the mean velocity $\dot{\mathbf{x}}$ as

$$\dot{\mathbf{x}} = \frac{1}{\rho} \sum_{a=1}^{\mathfrak{R}} \rho_a \dot{\mathbf{x}}_a \quad (3.4)$$

and also by applying the condition

$$\sum_{a=1}^{\mathfrak{R}} \hat{c}_a = 0 \quad (3.5)$$

This equation states that no net production of mass takes place due to exchange of mass among the constituents in the mixture.

In the application to be presented it will be of interest to use a mol density concentration definition of the constituents, instead of the mass density concentration definition. The relation between the mass density concentration ρ_a and the mol density concentration n_a (mol/m³) is

$$\rho_a = n_a m_a^c \quad (3.6)$$

where m_a^c (kg/mol) is the mass of one mol of the a :th constituent. The superscript c is included to stress that this property is constant. During mass exchange among constituents due to, for example, chemical reactions, the total mass is always conserved, i.e. see equation (3.5), but not necessarily the mol density concentrations. This will in turn mean that a different condition for conservation of mass must be used when using the mol density concentrations as state variables. This condition can easily be derived by considering equation (3.1) together with the definition (3.6), as

$$m_a^c \frac{\partial n_a}{\partial t} = -m_a^c \operatorname{div} (n_a \mathbf{x}_a) + m_a^c \hat{n}_a; \quad a = 1, \dots, \mathfrak{R}, \quad (3.7)$$

where the mass gain density to the a :th constituent \hat{c}_a is related to the mol gain density \hat{n}_a as: $\hat{c}_a = m_a^c \hat{n}_a$. Summing all \mathfrak{R} constituent equations in (3.7) should result in equation (3.3). This implies that the condition

$$\sum_{a=1}^{\mathfrak{R}} m_a^c \hat{n}_a = 0 \quad (3.8)$$

must hold. The mass balance principals for the constituents to be used is equation (3.7) rewritten as

$$\frac{\partial n_a}{\partial t} = -\operatorname{div} (n_a \mathbf{x}_a) + \hat{n}_a; \quad a = 1, \dots, \mathfrak{R}, \quad (3.9)$$

Equations (3.8) and (3.9) will be used together with constitutive equations for the mol density flows and mol density exchange rates for the constituents. The

application of diffusion and chemical reactions of ions in pore solution of concrete using constituent equations as described in (3.9) has been studied in [2].

Mass balance principals can also be expressed in terms of the diffusion velocity \mathbf{u}_a , which is defined as the difference between the velocity $\dot{\mathbf{x}}_a$ and the mean velocity $\dot{\mathbf{x}}$, i.e. $\mathbf{u}_a = \dot{\mathbf{x}}_a - \dot{\mathbf{x}}$. This kind of description is often used, for example, when having low mass concentration of dissolved diffusing ions in flowing water. Essentially the water velocity represents the mean velocity $\dot{\mathbf{x}}$; in this case contributing to convection of the dissolved ions.

Yet another balance principle will be invoked since positively and negatively charged ions dissolved in water will be studied. The principal to be used expresses the balance between the space charge density; in this case caused by not having positive and negative ions in solution balancing each other, and the electric displacement field vector. The local statement of the static continuity equation for the charge is one of Maxwell's equations, namely

$$\operatorname{div}(\mathbf{d}) = q, \quad (3.10)$$

where \mathbf{d} is the electric displacement field vector \mathbf{d} (C/m²) and q (C/m³) is the space charge density scalar.

4. Constitutive relations

In this section a tentative set of material assumptions will be described. The aim is to specify assumptions which are in accordance with general experimental observations concerning ion diffusion in porous cement-based materials, also including for mass exchange between solid constituents and ions dissolved in pore solution and, further, including electrical effects among the dissolved ions.

In every constitutive model, properties are divided into constitutive dependent and constitutive independent variables. In this model it will be assumed that the mol density concentration n_a , for all constituents, and the electric potential in solution φ are the constitutive independent properties. The constitutive dependent properties are: (i) the velocity $\dot{\mathbf{x}}_a$, (ii) the mass exchange rate among constituents \hat{n}_a , (iii) the electric displacement field vector \mathbf{d} and (iv) the space charge density q . The constitutive dependent properties are assumed to be given as a function of the independent properties and their corresponding gradients in the following manner

$$(\dot{\mathbf{x}}_a, \hat{n}_a, \mathbf{d}, q) = f(n_{a=1,\dots,\mathfrak{R}}, \operatorname{grad} n_{a=1,\dots,\mathfrak{R}}, \varphi, \operatorname{grad} \varphi) \quad (4.1)$$

Table 4.1: Example of material constants for ions dissolved in water.

Substance	Diffusion coeff. (m ² /s)	Ionic mobility (m ² /s/V)	Dielectric coeff. (C/V)
Cl ⁻	2.03·10 ⁻⁹	7.91·10 ⁻⁸	-
OH ⁻	5.30·10 ⁻⁹	20.64·10 ⁻⁸	-
Na ⁺	1.33·10 ⁻⁹	5.19·10 ⁻⁸	-
K ⁺	1.96·10 ⁻⁹	7.62·10 ⁻⁸	-
Ca ²⁺	0.79·10 ⁻⁹	6.17·10 ⁻⁸	-
H ₂ O	-	-	695.4·10 ⁻¹²

One important issue in constitutive modeling is to check that the material assumptions, as the one shown in expression (4.1), fulfill the requirements imposed by the second axiom of thermodynamics and the frame invariance. Such considerations do not, however, follow classical concepts when including electrical potential effects. One possibility is to treat the electric potential φ as a so-called hidden variable. The restrictions imposed by the second axiom of thermodynamics for the constitutive relations indicated in (4.1) will not be derived. This may be somewhat justified when thermal effects are excluded.

The $3\mathfrak{R} + 3$ unknown constitutive dependent and independent properties in this approach are

$$\begin{aligned}
 \mathfrak{R} \text{ number of : } & n_a(\mathbf{x}, t) \\
 \mathfrak{R} \text{ number of : } & \dot{\mathbf{x}}_a(\mathbf{x}, t) \\
 \mathfrak{R} \text{ number of : } & \hat{n}_a(\mathbf{x}, t) \\
 & \mathbf{d}(\mathbf{x}, t) \\
 & q(\mathbf{x}, t) \\
 & \varphi(\mathbf{x}, t)
 \end{aligned} \tag{4.2}$$

One mass balance equation for each constituent is defined in equation (3.9). The conservation of mass during the mass exchange among constituents, i.e. (3.8), gives one extra equation related to balance of mass. That is, $\mathfrak{R} + 1$ equations are available for describing mass balance of the mixture. Further, one equation describes continuity for the density of the electrical current. The total number of physical balance laws is therefore $\mathfrak{R} + 2$. The difference between the number of unknown constitutive dependent and constitutive independent properties, and the number of physical balance laws, must be constitutive relations, which in this case is $2\mathfrak{R} + 1$ assumptions.

The assumption for the electric displacement field vector \mathbf{d} is

$$\mathbf{d} = -\tilde{\varepsilon}\varepsilon_0\text{grad}\varphi \quad (4.3)$$

where ε_0 (C/V) is the dielectrics coefficient or permittivity of vacuum, $\varepsilon_0 = 8.854 \cdot 10^{-12}$, and $\tilde{\varepsilon}$ (-) is the relative dielectric coefficient of a given substance that varies among different dielectrics. For water at 25°C, $\tilde{\varepsilon}_w = 78.54$. The term $\text{grad}\varphi$ in equation (4.3) is the so-called electric field vector.

The charge density q is assumed to be given by the composition of positive and negative ions in solution in the following manner

$$q = F \sum_{a=1}^{\mathfrak{R}} n_a(\mathbf{x}, t) v_a \quad (4.4)$$

where $F = 96490$ (C/mol) is a physical constant (Faraday's constant) describing the charge of one mol of an ion having a valence number, denoted v_a , equal to one. In a solution not in contact with narrow pore walls the relation (4.4) is more or less a definition of the charge density q . When including the charge character of narrow pore walls in contact with solution, the relation (4.4) may, in fact, be questioned, at least when treating each small representative volume as being smeared, containing averaged values of all the state variables including q . The mass exchange between ions in solution and ions included in solids is, however, in this paper assumed to be caused by chemical reactions rather than caused by creations of double layers of positive and negative ions having their origin in a charged character of the solid pore walls.

The constitutive relation for the velocity for the \mathfrak{R} ions 1, ..., \mathfrak{R} is a Fick's first law type of equation with an extra term accounting for the effect of the electric field vector on the velocity. The following assumptions are used for the constituents:

$$\dot{\mathbf{x}}_a = -\frac{1}{n_a} \tilde{D}_a \text{grad} n_a - \tilde{A}_a v_a \text{grad} \varphi; \quad a = 1, \dots, \mathfrak{R} \quad (4.5)$$

where \tilde{D}_a (m²/s) and \tilde{A}_a (m²/s/V) are material constants. The tilde on top of D_a and A_a is used to stress that the values of D_a and A_a , given in Table 1, must be scaled to account for tortuosity effects in the pore system. Further, it should be noted that the diffusion coefficients D_a , presented in Table 1, are predicted values obtained by scaling the measured ionic mobilities A_a , e.g. see [3] and [4].

The material properties \tilde{D}_a and \tilde{A}_a are dependent on the shape and porosity of the pore system. It is, further, shown in [5] that pore size distribution and total porosity are changed during chloride penetration in concrete. This changes were measured with mercury porosimetry and X-ray diffraction. It was concluded that the change in the micro-structure is attributed to the formation of Friedel's salt.

The effect of the shape of the pore system on chloride diffusion in concrete has been investigated in [6] using a gas diffusion technique. The obtained tortuosity factor was in the range of 0.007-0.010 for a water to cement ratio 0.40 concrete, e.g. $\tilde{D}_a \approx 0.008D_a$ for this case.

Theoretical consideration using a homogenization technique on the physical balance laws and constitutive relations has been adopted for chloride diffusion in concrete [7]. In this method a tortuosity factor is used to describe the influence of the shape of the pore system on the ion diffusion.

The degree of saturation of water, further, affects the diffusion of dissolved ions in pore space. This phenomenon has been studied theoretically using a lattice Boltzmann method in order to model phase separation of a binary mixture, including wetting effects [8]. At high saturations a good agreement between the semi-empirical Archie's second law was found. At low saturations, however, the law breaks down as percolation effects were shown to be important. That is, diffusion of dissolved ions in pore solution cannot occur when the liquid water phase is not connected.

The mol density exchange rates among the constituents will be assumed to be given as functions of the composition of the mixture in terms of the all \mathfrak{R} individual mol densities, described in the following general manner

$$\hat{n}_b = f(n_1, n_2, \dots, n_{\mathfrak{R}}) \quad b = 1, \dots, \mathfrak{R} - 1 \quad (4.6)$$

where it should be noted that only $\mathfrak{R} - 1$ mol density exchange rates are to be described due to the relation (3.8). Further, the equilibrium condition for the reactions must be included as a special case.

The $2\mathfrak{R} + 1$ assumptions needed to make the equation system closed is the \mathfrak{R} number of assumptions of the velocities in (4.5), the $\mathfrak{R} - 1$ assumptions of the chemical reaction rates in (4.6) and the assumptions giving the electric displacement field \mathbf{d} and the charge density q , i.e. equations (4.3) and (4.4), respectively.

The equilibrium conditions and kinetics of chloride binding are of central interest in this investigation. This binding is, however, dependent on the conditions of the components present in the solid and in the pore solution. When accounting for dielectric effects in the pore solution it is important not only to consider the

chloride ions but also all other types of ions involved in chloride binding. A literature review of factors affecting chloride binding in cement-based materials can be found in [9]. Some of the main factors influencing binding of chlorides are the tricalcium aluminate content in cement, the water to binder ratio, the CaO/SiO₂ ratio, the pore solution alkalinity and cement replacement materials such as silica fume.

A general formulation for the aluminate phase can be described with the chemical formula $[\text{CaO}_2(\text{Al,Fe})(\text{OH})_6]^+ \text{Y}^- \cdot m\text{H}_2\text{O}$, where the brackets indicate the constitution of a positively charged layer unit. Molecular water is denoted by m . The excess positive charges are balanced by anions, denoted Y^- . These anions may typically be OH^- or externally supplied ions such as Cl^- , SO_4^{2-} and CO_3^{2-} . In [10] the Friedel's salt $\text{Ca}_2\text{Al}(\text{OH})_6\text{Cl} \cdot 2\text{H}_2\text{O}$ and its relations with hydroxy AF_m are studied. The Friedel's salt is important since it is more stable than the hydroxy aluminate AF_m and due to AF_m serves as a 'sink' for chloride ions and thereby retards diffusion of chlorides. An equilibrium condition between Friedel's salt found in AF_m and pore fluid chloride concentration is established.

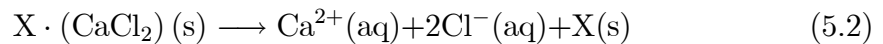
The kinetics of binding of chlorides is discussed in [11]. The time needed to reach equilibrium is observed to be in the range of 4 weeks, after which period the binding continues but is very slow. Measured relations, on different concrete qualities, between total chloride content and free dissolved chloride in pore solution can be found in, e.g. [12], [13], [14], [15], [16], [17] and [18].

5. Reaction kinetics and chemical equilibrium conditions

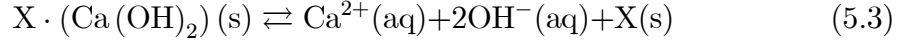
Only three different chemical reactions will be assumed to take place in the system considered. The first reaction, shown by equation (5.1), describes binding of chloride ions present in pore solution by ion-exchange of $\text{X} \cdot (\text{Ca}(\text{OH})_2)(\text{s})$ to form $\text{X} \cdot (\text{CaCl}_2)(\text{s})$. The symbol X is used as a general description for a more or less amorphous cement gel being interconnected with crystalline packages of calcium hydroxide. Further, this reaction is assumed to be irreversible, as



The second chemical reaction to be considered is dissolution of chloride ions from already formed calcium chloride being incorporated in the cement gel. This reaction is assumed to be irreversible:



The third and last chemical reaction considered is dissolution of calcium hydroxide from the hydration products. The reaction is assumed to be reversible, as



For easier notation, the constituents will be denoted by subscripts ranging from 1 to 7 as; Cl^{-} (1), Na^{+} (2), OH^{-} (3), Ca^{2+} (4), K^{+} (5), CaCl_2 (6), and $\text{Ca}(\text{OH})_2$ (7).

The equilibrium conditions in terms of the ion exchange equation (5.1) are the assumption

$$n_1^{eq} = (K + Zn_3) n_6; \quad (5.4)$$

where K and Z are positive constants. Under the condition that the actual value of n_1 is equal to n_1^{eq} the ion exchange equation (5.1) is assumed not to be active. This condition assumes that at a certain mol density of bound CaCl_2 and at a certain mol density of dissolved OH^{-} in pore solution, a given equilibrium mol density of dissolved Cl^{-} can be defined. Further, a high mol density of dissolved OH^{-} in pore solution gives a higher equilibrium value for the dissolved Cl^{-} than a low mol density of dissolved OH^{-} at a constant value of the mol density of bound CaCl_2 . The influence of hydroxide concentration in the pore solution of hardened cement paste on chloride binding is investigated in [19].

The reaction described in equation (5.3) is assumed to have an equilibrium condition expressed by n_3^{eq} , given as

$$n_3^{eq} = Wn_7 \quad (5.5)$$

When n_3^{eq} is equal to the actual value of n_3 the reaction (5.3) is assumed to be not active. That is, at a certain value of the mol density of solid $\text{Ca}(\text{OH})_2$ a corresponding equilibrium value of the mol density of dissolved OH^{-} in pore solution exists.

The ion exchange reaction (5.1) is assumed to be active when displaced from its equilibrium condition as described in equation (5.3) on condition that $n_1^{eq} \leq n_1$. That is, if the actual value of the mol density of dissolved Cl^{-} in pore solution, i.e. n_1 , is lower than the value of n_1^{eq} the solid product $X \cdot (\text{CaCl}_2)$ will be formed. The rate of formation or rate of consumption of Cl^{-} in this process will be assumed to be proportional to the ‘distance’ from equilibrium by using the constant R , as

$$\hat{n}_1^a = R(n_1^{eq} - n_1); \quad \text{if } n_1^{eq} \leq n_1 \quad (5.6)$$

where \hat{n}_1^a denotes the production of Cl^- in pore solution due to reaction (5.1) taking place. Having the constant R as a positive number, \hat{n}_1^a always becomes negative. The kinetic equation (5.6) describes the rate of mol density consumption of solid $\text{X} \cdot (\text{Ca}(\text{OH})_2)(\text{s})$ and dissolved Cl^- and the production of $\text{X} \cdot (\text{CaCl}_2)$ and dissolved OH^- in pore solution due to reaction (5.1) taking place. Due to the mol relation in equation (5.1) the following relation of rates can be established

$$\hat{n}_1^a = \frac{1}{2}\hat{n}_7^a = -\hat{n}_3^a = -\frac{1}{2}\hat{n}_6^a \quad (5.7)$$

The kinetic equation describing the rate of dissolution of chloride ions from already formed calcium chloride, being involved in the hydration products, is assumed to take place when $n_1^{eq} > n_1$, i.e. when the equilibration point for ion exchange according to equation (5.1) has been exceeded, at a rate proportional to the ‘distance’ from equilibrium as

$$\hat{n}_1^b = S(n_1^{eq} - n_1); \quad \text{if } n_1^{eq} > n_1 \quad (5.8)$$

where S is a positive number representing the rate constant for reaction (5.2) and where \hat{n}_1^b denotes the mol density rate of formation of dissolved Cl^- in pore solution. The value \hat{n}_1^b is always a positive number. Due to the mol relations in this reaction one can also establish the relations of rates as

$$\hat{n}_1^b = \frac{1}{2}\hat{n}_4^b = -\frac{1}{2}\hat{n}_6^b \quad (5.9)$$

The rate of the reversible reaction (5.3) is assumed to be constituted as

$$\hat{n}_3^c = Q(n_3^{eq} - n_3) \quad (5.10)$$

where \hat{n}_3^c denotes the mole density rate of production of dissolved OH^- . Under conditions where $n_3^{eq} < n_3$ the value \hat{n}_3^c becomes negative, i.e. binding of OH^- in solution onto the solid is assumed to be active. The mol density rates is in equation (5.3) related as

$$\hat{n}_3^c = \frac{1}{2}\hat{n}_4^c = -\frac{1}{2}\hat{n}_7^c \quad (5.11)$$

Finally, it is noted that the dissolved Na^+ and K^+ in pore solution is not involved in any chemical reactions, hence

$$\hat{n}_2 = 0; \quad \hat{n}_5 = 0 \quad (5.12)$$

It must be assured that no net production of mass occurs during the reactions according to the expression

$$\sum_{a=1}^6 \hat{n}_a m_a = 0 \quad (5.13)$$

where $m_5 = (m_4 + 2m_1)$ and $m_6 = (m_4 + 2m_3)$ in which the different m -values represent the mass per mol of the different constituents.

Depending on the relations of the different mol density concentrations, either the reactions behind equation (5.1) and (5.3) or (5.2) and (5.3) will take place. By first considering the reactions in (5.1) and (5.3), which are valid under condition $n_1^{eq} \leq n_1$, the condition in (5.13) must be fulfilled. This is the case, which can be seen by summarizing all the reaction rates multiplied by their corresponding mol mass, as

$$\begin{aligned}
0 = & -R(n_1^{eq} - n_1)m_1 \\
& + R(n_1^{eq} - n_1)m_3 - Q(n_3^{eq} - n_3)m_3 \\
& - \frac{1}{2}Q(n_3^{eq} - n_3)m_4 \\
& + \frac{1}{2}R(n_1^{eq} - n_1)(m_4 + 2m_1) \\
& - \frac{1}{2}R(n_1^{eq} - n_1)(m_4 + 2m_3) + \frac{1}{2}Q(n_3^{eq} - n_3)(m_4 + 2m_3)
\end{aligned} \tag{5.14}$$

The first to the last row in (5.14) represent the production of Cl^- , OH^- , Ca^{2+} , CaCl_2 and Ca(OH)_2 , respectively.

Under conditions described by $n_1^{eq} > n_1$ the reactions shown in (5.2) and (5.3) are assumed to take place. The condition in (5.13) is also fulfilled for this case, since

$$\begin{aligned}
0 = & -S(n_1^{eq} - n_1)m_1 \\
& - Q(n_3^{eq} - n_3)m_3 \\
& - \frac{1}{2}Q(n_3^{eq} - n_3)m_4 - \frac{1}{2}S(n_1^{eq} - n_1)m_4 \\
& + \frac{1}{2}S(n_1^{eq} - n_1)(m_4 + 2m_1) \\
& + \frac{1}{2}Q(n_3^{eq} - n_3)(m_4 + 2m_3)
\end{aligned} \tag{5.15}$$

where, again, the first to the last row in (5.15) represent the production of Cl^- , OH^- , Ca^{2+} , CaCl_2 and Ca(OH)_2 , respectively.

6. Governing equations

This section will summarize the governing equations given from using the mass balance laws defined in the mixture theory together with the proposed constitutive relations and also by using the charge balance equation together with its corresponding constitutive assumptions.

The concentration fields $n_a(\mathbf{x}, t)$ for the 7 considered constituents, Cl^- (1), Na^+ (2), OH^- (3), Ca^{2+} (4), K^+ (5), CaCl_2 (6), and $\text{Ca}(\text{OH})_2$ (7), are obtained by combining the mass balance equation (3.2) and the constitutive relation (4.5) describing the velocity and, further, by using the expressions for the chemical reaction rates described in section 4. It is also noted that the gradient of the electrostatic potential is involved to describe the velocity of the constituent. One extra equation is therefore necessary, to determine this potential. The differential equation determining the electrostatic potential φ becomes coupled to the diffusion equations and the diffusion equations are coupled to the electrostatic potential φ .

Since different chemical reactions are assumed to occur depending on whether $n_1^{eq} \leq n_1$ or $n_1^{eq} > n_1$, the equations shown will be related to one of these conditions and the other condition will be explained in the text.

The description of the chloride ions dissolved in the pore solution, denoted by the subscript 1, are under the condition $n_1^{eq} \leq n_1$ described as

$$\begin{aligned} \frac{\partial n_1}{\partial t} = & \text{div} \left(\tilde{D}_1 \text{grad} n_1 + \tilde{A}_1 v_1 n_1 \text{grad} \varphi \right) \\ & + R(n_1^{eq} - n_1) \end{aligned} \quad (6.1)$$

In cases where $n_1^{eq} > n_1$, the rate constant R is replaced by S . The equation (6.1) is obtained by combining equation (3.2) and the constitutive relations (4.5) and (5.6). When $n_1^{eq} > n_1$ the relation (5.6) is replaced by (5.8). The equilibrium value n_1^{eq} is given by the relation (5.4), which means that equation (6.1) is coupled to the equations determining the mol density of hydroxide, dissolved in pore solution, and solid calcium chloride.

Sodium ions, denoted by the subscript 2, appearing dissolved in the pore solution, are supposed not to take place in any chemical reactions. The governed equation for this constituent, therefore, is obtained by combining mass balance (3.2) and the constitutive relation (4.5) to obtain

$$\frac{\partial n_2}{\partial t} = \text{div} \left(\tilde{D}_2 \text{grad} n_2 + \tilde{A}_2 v_2 n_2 \text{grad} \varphi \right) \quad (6.2)$$

The concentration field of hydroxide ions n_3 , dissolved in the pore solution, are under the condition $n_1^{eq} \leq n_1$ described as

$$\begin{aligned} \frac{\partial n_3}{\partial t} = & \text{div} \left(\tilde{D}_3 \text{grad} n_3 + \tilde{A}_3 v_3 n_3 \text{grad} \varphi \right) \\ & - Q(n_3^{eq} - n_3) - R(n_1^{eq} - n_1) \end{aligned} \quad (6.3)$$

During conditions when $n_1^{eq} > n_1$ the material constant R is set to zero. Equation (6.3) is obtained by combining (3.2), (4.5), (5.6) and (5.10). When $n_1^{eq} > n_1$ equation (5.10) is not included. The equilibrium condition n_3^{eq} is given from equation (5.3) and n_1^{eq} from equation (5.4). That is, the differential equation (6.3) is coupled to the mol densities n_1 , n_5 and n_6 .

If the equilibrium condition for the chloride ions in pore solution is higher than the actual value, i.e. if $n_1^{eq} > n_1$, the equation governing the calcium ions in pore solution is obtained from the equations (3.2), (4.5), (5.8), (5.10), (5.9) and (5.11), as

$$\begin{aligned} \frac{\partial n_4}{\partial t} = & \operatorname{div} \left(\tilde{D}_4 \operatorname{grad} n_4 + \tilde{A}_4 v_4 n_4 \operatorname{grad} \varphi \right) \\ & - \frac{1}{2} Q (n_3^{eq} - n_3) + \frac{1}{2} S (n_1^{eq} - n_1) \end{aligned} \quad (6.4)$$

When $n_1^{eq} \leq n_1$ the rate constant S is set to zero due to the reaction described in (5.8) not being active in this case.

Combining the mass balance (3.9) with the constitutive assumptions (4.5) and (5.12) gives the governed equation for the dissolved K^+ ions in pore solution as

$$\frac{\partial n_5}{\partial t} = \operatorname{div} \left(\tilde{D}_5 \operatorname{grad} n_5 + \tilde{A}_5 v_5 n_5 \operatorname{grad} \varphi \right) \quad (6.5)$$

It will be explicitly assumed that the velocity for the solid $CaCl_2$ component is zero. That is, the differential equation describing the rate of change of the mol density of $CaCl_2$ is only due to chemical reactions. If the condition $n_1^{eq} \leq n_1$ holds, the mass balance (3.2), with inserted zero velocity, and with the chemical reaction rate assumption (5.6) together with the mol rate relation (5.7), gives the governed equation for the solid calcium chloride, as

$$\frac{\partial n_6}{\partial t} = -\frac{1}{2} R (n_1^{eq} - n_1) \quad (6.6)$$

When $n_1^{eq} > n_1$, R is replaced by S .

The solid calcium hydroxide constituent is also assumed to have zero velocity. During conditions when $n_1^{eq} \leq n_1$ the description of the solid calcium hydroxide is obtained by equation (3.2), with inserted zero velocity, and the description of the chemical reaction rate given from equations (5.8) and (5.10), together with the mol rate relations (5.7) and (5.11), as

$$\frac{\partial n_7}{\partial t} = \frac{1}{2} Q (n_3^{eq} - n_3) + \frac{1}{2} R (n_1^{eq} - n_1) \quad (6.7)$$

During situations when $n_1^{eq} > n_1$ the rate constant R is set to zero.

The last information needed is the equation describing the electrostatic potential φ , which is involved in all governing equations for the diffusing dissolved ions in the pore solution, i.e. the equations (6.1), (6.2), (6.3) and (6.4). By using the static continuity equation for the charge (3.10) together with the constitutive relations for the electric displacement field vector \mathbf{d} (4.3) and the charge density q (4.4) the governing equation for the electrostatic potential becomes

$$-\text{div}(\tilde{\varepsilon}\varepsilon_0\text{grad}\varphi) = F \sum_{a=1}^5 n_a(\mathbf{x}, t) v_a, \quad (6.8)$$

When using this method to calculate the 7 concentration fields $n_a(\mathbf{x}, t)$ the electroneutrality $\phi(\mathbf{x}, t)$ will not be satisfied, i.e.

$$\phi(\mathbf{x}, t) = \sum_{a=1}^5 n_a(\mathbf{x}, t) v_a \neq 0. \quad (6.9)$$

However, due to the time scale in the problem the potential $\phi(\mathbf{x}, t)$, as defined above, will be very close to the value zero.

Excluding the physical constant F , the model includes in total 17 material constants. The description of the velocity of the dissolved ions involves 5 diffusion constants and 5 ionic mobility constants, the description leading to a determination of the electrostatic potential involves one constant, i.e. the property $\tilde{\varepsilon}\varepsilon_0$, the description of the chemical equilibrium conditions involves 3 constants, i.e. K , Z and W , and the description of the kinetics of the considered chemical reactions involves 3 rate constants, i.e. R , S and Q .

7. Solution strategy

In order to check the reasonableness of the assumptions leading to the governing equations in section 5, a test example will be solved by giving numbers to the 17 defined material constants. The result from such a computation can be compared to general observations obtained from experiments. The 7 governed differential equations presented in section 5 are coupled and non-linear. A numerical method is therefore needed. Here the finite element method will be used. This concept can be studied in, e.g. [20], [21], [22] and [23].

The total equation system will be brought to the form

$$\mathbf{C}^t \dot{\mathbf{a}}^t + \mathbf{K}^t \mathbf{a}^t + \mathbf{f}^t = \mathbf{0}, \quad (7.1)$$

where \mathbf{C}^t , \mathbf{K}^t and \mathbf{f}^t are the total damping matrix, stiffness matrix and load/boundary vector, respectively. At a certain time level, the total concentration vector \mathbf{a}^t contains all spatial distributions of all 7 different constituents and the electrostatic potential. The property $\dot{\mathbf{a}}^t$ contains the corresponding time derivatives.

A finite time increment Δt will be considered, which is related to the time levels t_i and t_{i+1} as $t_{i+1} = t_i + \Delta t$, in order to obtain so-called recurrence relations. A time integration parameter Θ is introduced where $\Theta = 0$ is a truly explicit scheme, $\Theta = 1$ is a truly implicit scheme, $\Theta = 0.5$ is the Crank-Nicholson scheme and $\Theta = 0.878$ is the Liniger scheme in which Θ is chosen to minimize the whole domain error. Values of Θ greater than or equal to 0.5 are shown to be unconditionally stable for equation systems which are symmetric and positive definite. The time derivative is formed according to the one step scheme, i.e. $\dot{\mathbf{a}}^t = (\mathbf{a}_{i+1}^t - \mathbf{a}_i^t) / \Delta t$, where \mathbf{a}_i^t is given at time level t and \mathbf{a}_{i+1}^t at time level $t + \Delta t$. The concentration vector \mathbf{a}^t is weighted with the time integration parameter Θ as: $\mathbf{a}^t = \mathbf{a}_i^t + \Theta (\mathbf{a}_{i+1}^t - \mathbf{a}_i^t)$. Hence, (7.1) can be brought to the form

$$\begin{aligned} \mathbf{0} = & \frac{\mathbf{C}^t (\mathbf{a}_{i+1}^t - \mathbf{a}_i^t)}{\Delta t} + \mathbf{K}^t (\mathbf{a}_i^t + \Theta (\mathbf{a}_{i+1}^t - \mathbf{a}_i^t)) \\ & + \mathbf{f}_i^t + \Theta (\mathbf{f}_{i+1}^t - \mathbf{f}_i^t). \end{aligned} \quad (7.2)$$

where the load/boundary vector \mathbf{f}^t is weighted as $\mathbf{f}^t = \mathbf{f}_i^t + \Theta (\mathbf{f}_{i+1}^t - \mathbf{f}_i^t)$. The equation (7.2) is used to solve the unknown vector \mathbf{a}_{i+1}^t .

The matrix associated with the time derivative of the state variables is \mathbf{C}^t , formed by assembling the damping matrixes for the individual diffusion equations as block matrixes, is established as

$$\mathbf{C}^t = \begin{bmatrix} \mathbf{C}_1 & \mathbf{0} & \mathbf{0} & \mathbf{0} & \mathbf{0} & \mathbf{0} & \mathbf{0} & \mathbf{0} \\ \mathbf{0} & \mathbf{C}_2 & \mathbf{0} & \mathbf{0} & \mathbf{0} & \mathbf{0} & \mathbf{0} & \mathbf{0} \\ \mathbf{0} & \mathbf{0} & \mathbf{C}_3 & \mathbf{0} & \mathbf{0} & \mathbf{0} & \mathbf{0} & \mathbf{0} \\ \mathbf{0} & \mathbf{0} & \mathbf{0} & \mathbf{C}_4 & \mathbf{0} & \mathbf{0} & \mathbf{0} & \mathbf{0} \\ \mathbf{0} & \mathbf{0} & \mathbf{0} & \mathbf{0} & \mathbf{C}_5 & \mathbf{0} & \mathbf{0} & \mathbf{0} \\ \mathbf{0} & \mathbf{0} & \mathbf{0} & \mathbf{0} & \mathbf{0} & \mathbf{0} & \mathbf{0} & \mathbf{0} \\ \mathbf{0} & \mathbf{0} & \mathbf{0} & \mathbf{0} & \mathbf{0} & \mathbf{0} & \mathbf{C}_6 & \mathbf{0} \\ \mathbf{0} & \mathbf{0} & \mathbf{0} & \mathbf{0} & \mathbf{0} & \mathbf{0} & \mathbf{0} & \mathbf{C}_7 \end{bmatrix} \quad (7.3)$$

The time derivative of the total concentration vector \mathbf{a}^t is, further, arranged as

$$\dot{\mathbf{a}}^t = \begin{bmatrix} \dot{\mathbf{a}}_1 \\ \dot{\mathbf{a}}_2 \\ \dot{\mathbf{a}}_3 \\ \dot{\mathbf{a}}_4 \\ \dot{\mathbf{a}}_5 \\ \mathbf{0} \\ \dot{\mathbf{a}}_6 \\ \dot{\mathbf{a}}_7 \end{bmatrix} \quad (7.4)$$

where the subscripts, ranging from 1 to 7, denote the constituents, Cl^- (1), Na^+ (2), OH^- (3), Ca^{2+} (4), K^+ (5), CaCl_2 (6), and $\text{Ca}(\text{OH})_2$ (7).

The chemical reactions will be involved in the total stiffness \mathbf{K}^t , on condition that $n_1^{eq} \leq n_1$, as

$$\mathbf{K}_a^t = \begin{bmatrix} \mathbf{K}_1 + \mathbf{R}_1^a & \mathbf{0} & \mathbf{0} & \mathbf{0} & \mathbf{0} & \mathbf{V}_{\varphi 1}(\mathbf{a}_1) & -\mathbf{R}_6^a(\mathbf{a}_3) & \mathbf{0} \\ \mathbf{0} & \mathbf{K}_2 & \mathbf{0} & \mathbf{0} & \mathbf{0} & \mathbf{V}_{\varphi 2}(\mathbf{a}_2) & \mathbf{0} & \mathbf{0} \\ -\mathbf{R}_1^a & \mathbf{0} & \mathbf{K}_3 - \mathbf{R}_3 & \mathbf{0} & \mathbf{0} & \mathbf{V}_{\varphi 3}(\mathbf{a}_3) & \mathbf{R}_6^a(\mathbf{a}_3) & \mathbf{R}_7 \\ \mathbf{0} & \mathbf{0} & -\frac{1}{2}\mathbf{R}_3 & \mathbf{K}_4 & \mathbf{0} & \mathbf{V}_{\varphi 4}(\mathbf{a}_4) & \mathbf{0} & \frac{1}{2}\mathbf{R}_7 \\ \mathbf{0} & \mathbf{0} & \mathbf{0} & \mathbf{0} & \mathbf{K}_5 & \mathbf{V}_{\varphi 5}(\mathbf{a}_5) & \mathbf{0} & \mathbf{0} \\ \mathbf{E}_{\varphi 1} & \mathbf{E}_{\varphi 2} & \mathbf{E}_{\varphi 3} & \mathbf{E}_{\varphi 4} & \mathbf{E}_{\varphi 5} & \mathbf{K}_{\varphi} & \mathbf{0} & \mathbf{0} \\ -\frac{1}{2}\mathbf{R}_1^a & \mathbf{0} & \mathbf{0} & \mathbf{0} & \mathbf{0} & \mathbf{0} & \frac{1}{2}\mathbf{R}_6^a(\mathbf{a}_3) & \mathbf{0} \\ \frac{1}{2}\mathbf{R}_1^a & \mathbf{0} & \frac{1}{2}\mathbf{R}_3 & \mathbf{0} & \mathbf{0} & \mathbf{0} & -\frac{1}{2}\mathbf{R}_6^a(\mathbf{a}_3) & -\frac{1}{2}\mathbf{R}_7 \end{bmatrix} \quad (7.5)$$

where the stiffness matrix for the concentration gradient dependent diffusion is formed as $\mathbf{K}_a = \int_V \mathbf{B}^T \tilde{D}_a \mathbf{B} dV$, where $\mathbf{B}(\mathbf{x})$ is defined as the gradient of the shape function, i.e. $\mathbf{B}(\mathbf{x}) = \nabla \mathbf{N}(\mathbf{x})$. The stiffness matrix for the electrical displacement field is formed as $\mathbf{K}_{\varphi} = \int_V \mathbf{B}^T \tilde{\varepsilon} \varepsilon_0 \mathbf{B} dV$. The stiffness matrix for the part of the mass flow which is dependent on the gradient of the electrostatic potential φ is formed as $\mathbf{V}_{\varphi a}(\mathbf{a}_a) = \int_V \mathbf{B}^T \tilde{A}_a v_a(\tilde{a}_a) \mathbf{B} dV$ where the parameter \tilde{a}_a is a smeared element value of the nodal concentrations of the constituent a . The term related to the charge density q is $\mathbf{E}_{\varphi a} = \int_V \mathbf{N}^T F v_a \mathbf{N} dV$.

The chemical reactions, on condition that $n_1^{eq} \leq n_1$, are formed as $\mathbf{R}_1^a = \int_V \mathbf{N}^T R \mathbf{N} dV$, $\mathbf{R}_3 = \int_V \mathbf{N}^T Q \mathbf{N} dV$, $\mathbf{R}_5^a = \int_V \mathbf{N}^T R(K + Z(\tilde{a}_3)) \mathbf{N} dV$ and $\mathbf{R}_6 = \int_V \mathbf{N}^T Q W \mathbf{N} dV$.

On condition that $n_1^{eq} > n_1$, the total stiffness can be formulated as

$$\mathbf{K}_b^t = \begin{bmatrix} \mathbf{K}_1 + \mathbf{R}_1^b & 0 & 0 & 0 & 0 & \mathbf{V}_{\varphi 1}(\mathbf{a}_1) & -\mathbf{R}_6^b(\mathbf{a}_3) & 0 \\ 0 & \mathbf{K}_2 & 0 & 0 & 0 & \mathbf{V}_{\varphi 2}(\mathbf{a}_2) & 0 & 0 \\ 0 & 0 & \mathbf{K}_3 - \mathbf{R}_3 & 0 & 0 & \mathbf{V}_{\varphi 3}(\mathbf{a}_3) & 0 & \mathbf{R}_7 \\ \frac{1}{2}\mathbf{R}_1^b & 0 & -\frac{1}{2}\mathbf{R}_3 & \mathbf{K}_4 & 0 & \mathbf{V}_{\varphi 4}(\mathbf{a}_4) & -\frac{1}{2}\mathbf{R}_6^b(\mathbf{a}_3) & \frac{1}{2}\mathbf{R}_7 \\ 0 & 0 & 0 & 0 & \mathbf{K}_5 & \mathbf{V}_{\varphi 5}(\mathbf{a}_5) & 0 & 0 \\ \mathbf{E}_{\varphi 1} & \mathbf{E}_{\varphi 2} & \mathbf{E}_{\varphi 3} & \mathbf{E}_{\varphi 4} & \mathbf{E}_{\varphi 5} & \mathbf{K}_{\varphi} & 0 & 0 \\ -\frac{1}{2}\mathbf{R}_1^b & 0 & 0 & 0 & 0 & 0 & \frac{1}{2}\mathbf{R}_6^b(\mathbf{a}_3) & 0 \\ 0 & 0 & \frac{1}{2}\mathbf{R}_3 & 0 & 0 & 0 & 0 & -\frac{1}{2}\mathbf{R}_7 \end{bmatrix} \quad (7.6)$$

where the chemical reactions differ in \mathbf{R}_1^b and \mathbf{R}_5^b compared to \mathbf{R}_1^a and \mathbf{R}_5^a in (7.5). The properties \mathbf{R}_1^b and \mathbf{R}_5^b , associated with the reaction (5.1), are given as $\mathbf{R}_1^b = \int_V \mathbf{N}^T S \mathbf{N} dV$ and $\mathbf{R}_5^b = \int_V \mathbf{N}^T S (K + Z(\tilde{a}_3)) \mathbf{N} dV$.

The total load/boundary vector is expressed as

$$\mathbf{f}^t = \begin{bmatrix} \mathbf{f}_1 \\ \mathbf{f}_2 \\ \mathbf{f}_3 \\ \mathbf{f}_4 \\ \mathbf{f}_5 \\ \mathbf{f}_{\varphi} \\ \mathbf{f}_6 \\ \mathbf{f}_7 \end{bmatrix}. \quad (7.7)$$

The load/boundary vector for the diffusion equations is in general terms written as $\mathbf{f}_a = -\int_{S_h} \mathbf{N}^T h_a dS - \int_{S_{n=g}} \mathbf{N}^T q_a dS$, where h_a is a prescribed value of the normal flow of ions through the boundary surface S_h and q_a is the value of the flow through the boundary surface $S_{n=g}$ on which the concentration n_a has been prescribed. The values of q_a can be calculated whenever the concentration n_a is prescribed at the same material point.

The equation system (7.2) is solved directly, i.e. without using any staggered method, which means that all concentration fields for the different constituents and for the electric potential in the domain are evaluated in one step only, at each time level. No special methods are used to tackle the non-linearities by using iterations within time steps. A simple Euler forward approach is adopted in which the non-linear parameters are adjusted before proceeding to the next time step. The error made in this approach was tested, simply by checking the effect of

Table 8.1: Mix proportions, water to binder ratio 0.40.

	Weight (kg/m ³)	Weight in the mix (kg)	Moisture (kg)
Cement (SRPC)	399	8.778	-
Silica fume	21	0.462	-
Aggregate 0-8 mm	898	19.756	0.0790
Aggregate 8-12 mm	898	19.756	-
Water	168	3.5269	-
Plasticizer	6.3	0.138	0.0901

decreasing the time step length. A time step length was chosen so that a further decrease did not change the solution.

In order to obtain stable solutions an implicit time integration was used. This type of time integration method is, indeed, in conflict with the Euler forward method used for tackling the non-linearities. The errors introduced are, however, estimated to be rather small.

8. Example: Submerge case

A case where a concrete sample is exposed to a 3 wt% sodium chloride solution is studied. The sample was stored in room climate for two weeks after one day of membrane hardening after casting. After this preparation the concrete sample was stored in one week in tap water to prevent capillary suction of the chloride solution. The sample was then exposed to the 3 wt% sodium chloride solution for 119 days. The concrete tested, see Table 8.1, is the same as the one illustrated in: *A test of prediction models for chloride ingress and corrosion initiation*.

The model and numerical method described in previous section is used. The boundary conditions described are the essential conditions for the concentrations of Cl^- , Na^+ , OH^- , Ca^{2+} and K^+ in outer solution. The concentrations of Cl^- and Na^+ are set to 510 mol/m³ (3 wt%) and the other ion constituents are set to zero. The initial conditions in pore solution are for Na^+ , OH^- , Ca^{2+} and K^+ set to 31 mol/m³, 306 mol/m³, 10 mol/m³ and 255 mol/m³. These values are given from the pore expression data shown in Table 8.2. The initial value for solid $\text{Ca}(\text{OH})_2$ is set to $3 \cdot 10^4$ mol/m³ which is a value related to the volume of pore solution. No bound chlorides are assumed at the start of the simulation i.e. the initial condition for $\text{Ca}(\text{Cl})_2$ is zero.

Table 8.2: Pore extraction data for a 5-month-old concrete with water to binder ratio 0.40. The concrete was stored in water during the whole time. SRPC, with silica (5 mass percent of cement weight)

Material	K ⁺ (mmol/l)	Na ⁺ (mmol/l)	OH ⁻ (mmol/l)	(Error) -
<i>w/b</i> 0.40	255	34	286	3

Table 8.3: Material constants used for the concrete mixe based on SRPC with 5 percent silica fume. The sample were dried for two weeks and re-wetted for one week before exposure to a 3 weight percent sodium chloride solution. The constants presented are the ones giving the best fit with the measured total chloride profile when used in the proposed model.

Material constants	<i>w/b</i> 0.40
Tortuosity factor, (-)	0.00550
Binding cap., Cl ⁻ , $1/K$ (-)	1.25
Binding rate, Cl ⁻ , R (1/s)	0.0012
Binding cap., OH ⁻ , W (-)	0.0102
Binding rate, OH ⁻ , Q (1/s)	$1 \cdot 10^{-6}$
Measured active porosity	0.0788

The included material constants in the model was fitted against the performed experiment. This procedure involved several test run with different variations of the constants. In Figure 8.1 the results of the fitting of the model to the experiments are shown.

The coefficient of permittivity $\tilde{\epsilon}\epsilon_0$ is set to $6.95 \cdot 10^{-10}$ (C/V), which is the value of valid for bulk water at 25°C. No scaling of this coefficient is performed, since the determination of the electrostatic potential, which needs information of the value of the permittivity $\tilde{\epsilon}\epsilon_0$, is related to the ions dissolved in pore solution only.

The ‘best’ fitted simulation was performed using the material data shown in Table 8.3. It should be noted that the tortuosity factor are used for all types of ions in pore solution. The tortuosity factor are used together with the bulk diffusion and ion mobility constants presented in Table 4.1.

The measured data in Figure 8.1 are presented as total concentrations, at various depths from exposed surface, related to the active pore volume. The measured profile given as total chloride per mass of concrete are presented in

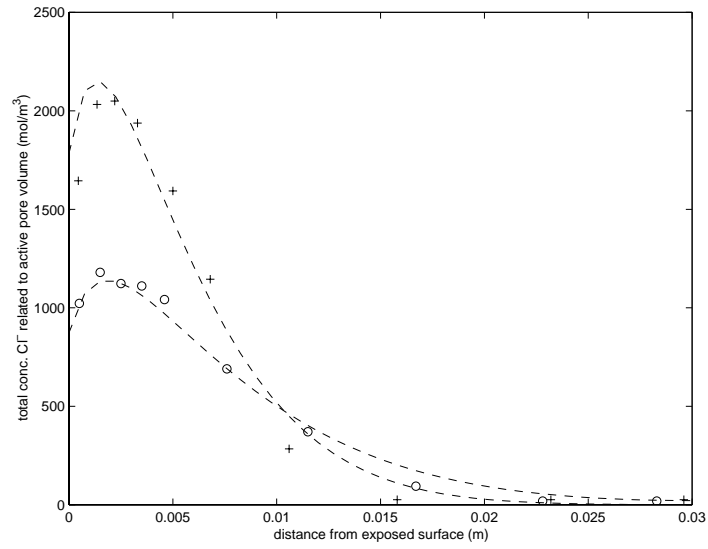


Figure 8.1: *Simulated and experimental total chloride profiles. The results of simulation using the material constants presented in Table 8.3. The + signs are the experimental values. Upper case is the experiment and simulation for the concrete quality presented in Table 8.1. The other case is the same type of concrete but with water to cement ratio 0.55. Samples were exposed for 119 days in a 3 wt% sodium chloride solution at room temperature.*

Table 8.4: Measured chloride profile in terms of total chloride (bound + free). Water to binder ratio 0.40. The sample was unidirectionally dried in room climate for two weeks and re-wetted for one week in tap water before being exposed to a 3 weight percent sodium chloride solution for 119 days.

Depth (mm)	U (mV)	Total Cl ⁻ (wt % of concrete)
0.0-0.9	19.0	0.191
0.9-1.8	14.1	0.236
1.8-2.6	13.9	0.238
2.6-4.0	15.2	0.225
4.0-6.0	19.8	0.185
6.0-7.5	27.6	0.133
10.1-11.0	60.7	0.003
15.1-16.5	116.6	0.003
22.1-24.3	120.9	0.003
28.9-30.2	121.1	0.003

Table 8.5: Amount of water absorbed during a capillary suction experiment expressed in terms of active porosity.

Concrete (w/b)	Active porosity (m ³ /m ³ of concrete)	Calc. capillary porosity (m ³ /m ³ of concrete)
0.40	0.0788	0.0740

Table 8.4.

The active porosity was measured with separated capillary suction tests, see Table 8.5. The active porosity is the measured volume occupied by water being capillary sucked in sample at equilibrium. In this Table also the calculated capillary porosity for the tested concrete is shown, where Power's formula is used. The degree of hydration at the time of exposure to the sodium chloride was used in this formula.

In Figure 8.2 the model is used to calculate the expected total chloride concentration related to active pore volume after one year of constant exposure to a 3 wt% sodium chloride solution. The same simulation for an exposure of two years are shown in Figure 8.3.

The whole idea with the model presented is that all types of ions of interest in

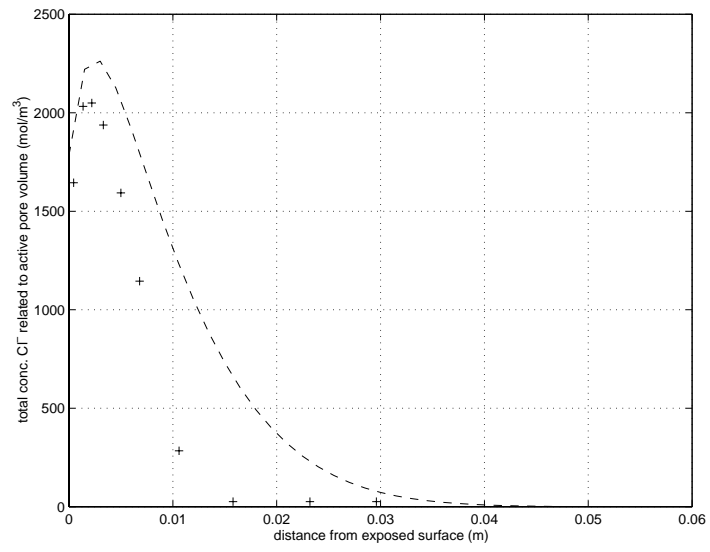


Figure 8.2: *Experimental values of total chloride penetration at 119 days in concrete described in Table 8.1. The dashed line shows the predicted total chloride profile after one year exposure.*

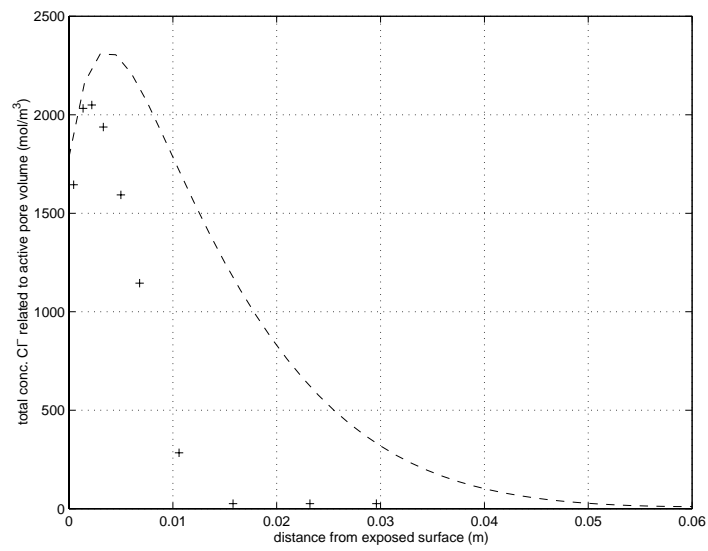


Figure 8.3: *Experimental values of total chloride penetration at 119 days in concrete described in Table 8.1. The dashed line shows the predicted total chloride profile after two years exposure.*

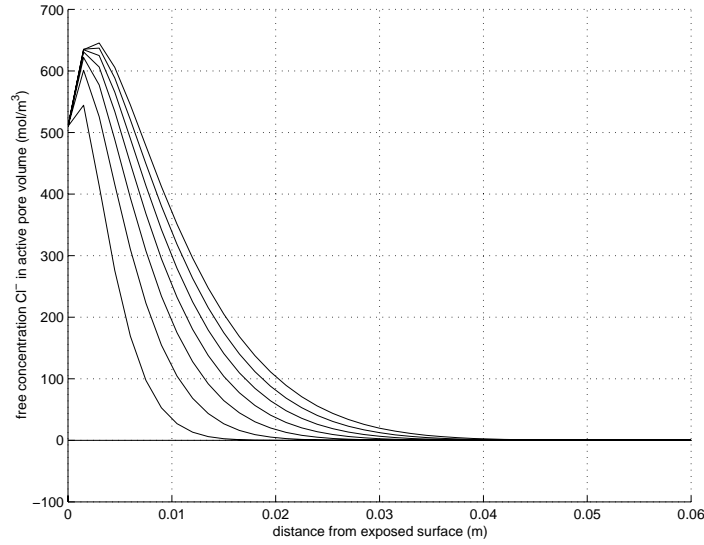


Figure 8.4: *Calculated free chloride concentration in pore solution up to one year exposure. The results corresponds to the simulation shown in Figure 8.2.*

the pore solution should be included. The concentration profiles, up to one year of exposure, of free chloride in pore solution are shown in Figure 8.4, where it is noted that a peaks in concentrations are obtained a few millimeters from surface. This behavior is due to dielectric effects in the pore solution combined with the fact the leaching of calcium and hydroxide are included in the model. The calcium profiles are shown in Figure 8.5. These profiles are withheld compare to the others which also is an effect caused by the dielectric nature of the problem.

The hydroxide leaching to the storage solution is shown in Figure 8.6. The simulation predicts that the leaching is quite small, which, among other things, is due to assuming a high buffer of solid calcium hydroxide in the solid concrete structure.

The free calcium ion concentration in pore solution is predicted to increase as shown in Figure 8.7, which is explained by the fact that calcium is supplied to the pore solution from the solid calcium hydroxide in concrete. The assumed leaching rate and the dielectric effects on the diffusion of calcium determines the behavior.

The potassium ions are leached out from the pore solution to the storage solution at a greater extent than the hydroxide ions, i.e. compare Figures 8.8 and 8.6. The reason is that no assumptions concerning leaching of potassium from

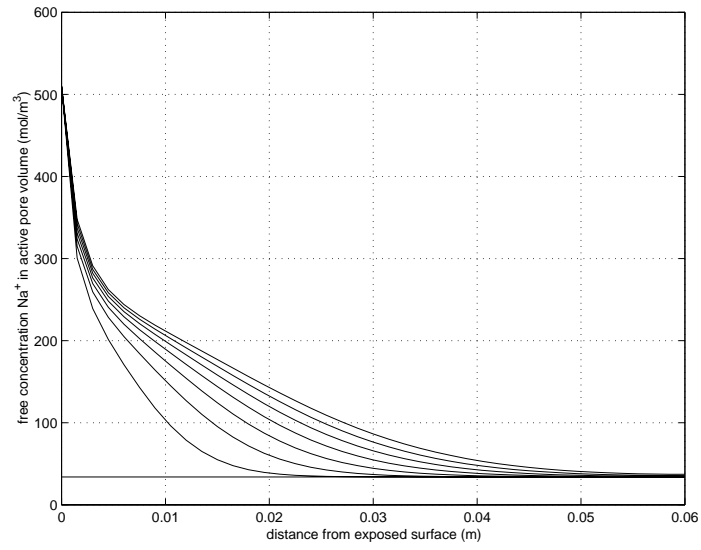


Figure 8.5: *Calculated free sodium concentration in pore solution up to one year exposure. The results corresponds to the simulation shown in Figure 8.2.*

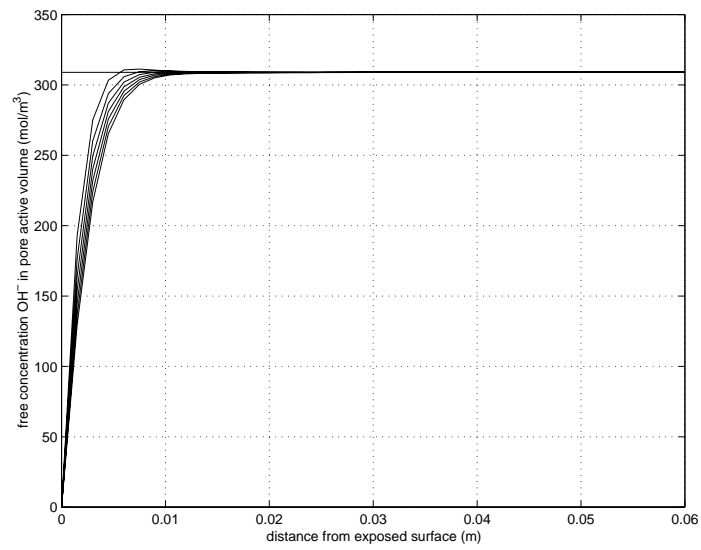


Figure 8.6: *Calculated free hydroxide concentration in pore solution up to one year exposure. The results corresponds to the simulation shown in Figure 8.2.*

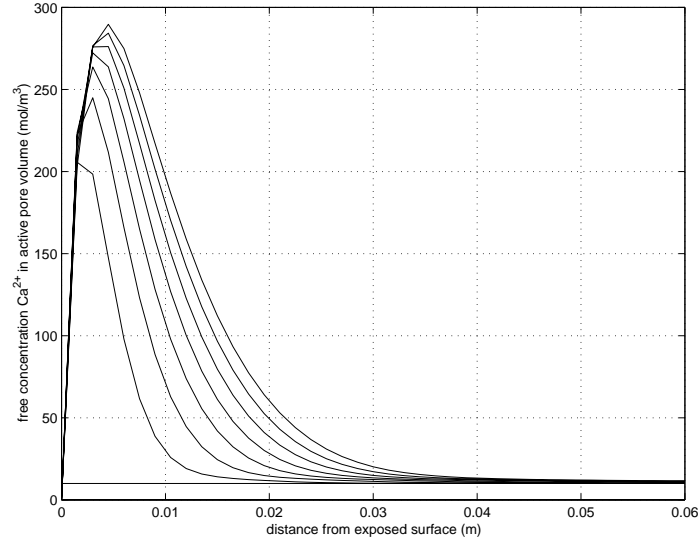


Figure 8.7: *Calculated free calcium concentration in pore solution up to one year exposure. The results corresponds to the simulation shown in Figure 8.2.*

solid constituents are included.

The concentration profiles for the solid $\text{Ca}(\text{Cl})_2$ is shown in Figure 8.9. The concentration values are related to the active pore volume of tested sample. It is noted that the total chloride profiles in Figure 8.2 constitute the sum of the free mole concentrations in Figure 8.4 and the bound concentrations in Figure 8.9. The bound chloride profiles has same peak behavior as the free chlorides, which is a result caused by assuming the linear binding equilibrium condition, see previous sections.

The decrease of the solid calcium hydroxide content due to dielectric diffusion and leaching is shown in Figure 8.10.

In order to compare the results from this simulation with classical models two different measures of the effective diffusion constants are calculated either from the obtained material constants in this investigation or from direct fitting of the measured profiles in a direct manner. The first, D_{eff} , is the most common used ‘effective’ diffusivity which is obtained by fitting the solution of Fick’s second law to the measured total chloride profile taken at a certain time from start of exposure. No special attention is paid in this method to the really occurring boundary condition, in terms of chloride ion concentration. The solution is rather

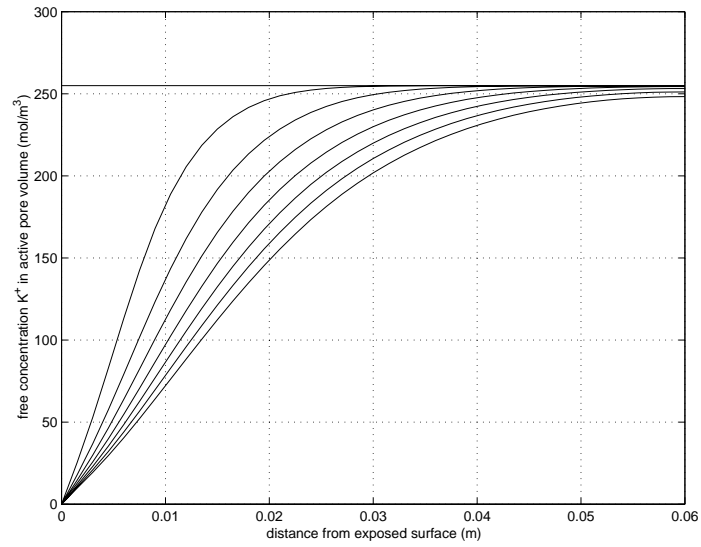


Figure 8.8: *Calculated free potassium concentration in pore solution up to one year exposure. The results corresponds to the simulation shown in Figure 8.2.*

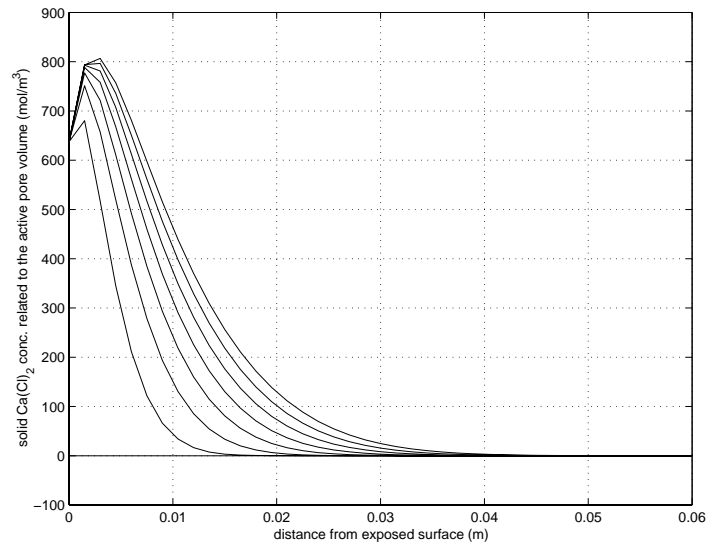


Figure 8.9: *Calculated bound chloride concentration, related to pore solution volume, up to one year exposure. The results corresponds to the simulation shown in Figure 8.2.*

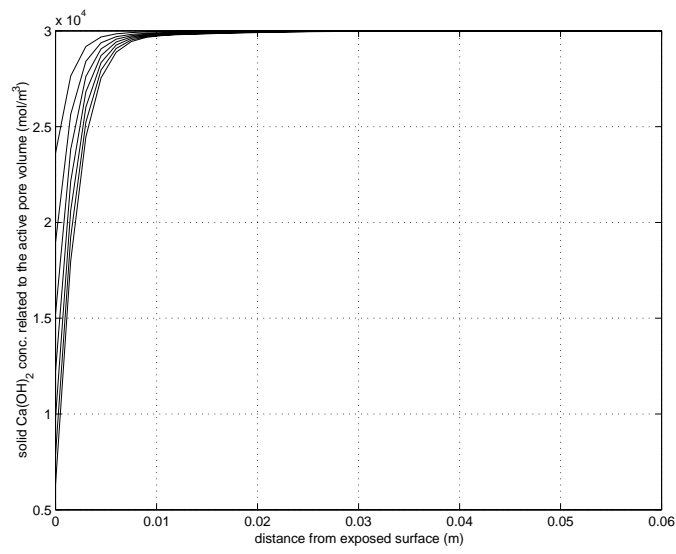


Figure 8.10: *Calculated bound calciumhydroxide concentration, related to pore solution volume, up to one year exposure. The results corresponds to the simulation shown in Figure 8.2.*

Table 8.6: SRPC with 5 wt chlorides. Sample were exposed to a 3 weight percent sodium chloride solution for 119 days.

Concrete mix	D_{eff}^* (m ² /s)	D_{eff} (m ² /s)
w/b 0.40	$3.19 \cdot 10^{-12}$	$1.73 \cdot 10^{-12}$

fitted to the total chloride content profile where concentrations measured near the exposed surface are ignored. This is, of course, a very rough approximation. The values of D_{eff} obtained by the above described method are presented in Table 8.6, for the examined concrete quality.

The obtained D_{eff} value is compared with value denoted D_{eff}^* which are calculated from results given from the simulation performed. The D_{eff}^* value is calculated by the formula: $D_{eff}^* = \tilde{D}_1 / (1 + 2K^{-1})$, where \tilde{D}_1 is the scaled diffusion constant for free chloride ions in the pore system and K is described in section 5. This formula can be derived by considering a ‘standard’ diffusion equation with mass exchange as: $\partial \rho_{cl} / \partial t = \tilde{D}_1 \partial^2 \rho_{cl} / \partial x^2 - \partial \rho_{cl}^b / \partial t$, where $-\partial \rho_{cl}^b / \partial t$ is the mass exchange rate between dissolved chlorides in pore solution and bound chlorides. The mass concentration of bound chlorides is denoted ρ_{cl}^b and the free chloride concentration with ρ_{cl} . Assume also a binding isotherm given as: $\rho_{cl}^b = 2K^{-1} \rho_{cl}$. That is, a given one-to-one relation between the mass concentration of free chlorides in pore solution and bound chlorides is assumed valid under all conditions. Combining the above two assumed relations, one obtains: $\partial \rho_{cl} / \partial t = \tilde{D}_1 / (1 + 2K^{-1}) \partial^2 \rho_{cl} / \partial x^2$. It is concluded that a high binding capacity reduces the effective diffusion constant D_{eff}^* , and the penetration rate, therefore, becomes small in this case.

9. Example: Tidal zone

The same material constants and model will be adopted for this case. The difference is that the boundary conditions will be altered simulating cycles of one week exposure in a 3 wt% sodium chloride solution and one week of drying in room climate. It is very important to observe that the adopted model does not include for the effects caused by convection due to the capillary suction of the sodium chloride solution. Using the same material constants as in the previous example results in a poor match of experiments obtained for the studied case

and the simulation. One possible explanation for the difference is, of course, that the convection is not included in the model. Furthermore, the concentration of ions is defined by the pore solution volume which in the experiment are changed which will affect the concentration of dissolved ions and the diffusion constants for ions in pore solution. The convection phenomena has never been combined with multi-species calculations when applied to concrete durability models. The theoretical model is, however, described in [31] and cases where only the chloride ions are considered together with convection can be studied in [29]. Numerical issues for this application can be found in [30].

The initial conditions for the tidal zone is the same as the previous example the boundary conditions must, however be changed to model the cyclic exposure of the sodium chloride solution. When submerged in the sodium chloride solution the boundary conditions for Cl^- and Na^+ are set to 510 mol/m^3 (3 wt%) and the other ion constituents are set to zero. When sample stored in room climate the out-flow of ions are set to zero for all free ion types considered in the model.

The comparison between the simulation of the tidal zone case and the experiments are shown in figure 9.1. One conclusion that can be drawn from this simulation is that the effects caused by capillary suction on the chloride diffusion is very important, since a model not included for this gives too low penetration depths.

In Figure 9.2 a three dimensional plot is used in order to illustrate the variation of the chlorides at surface due to the cyclic exposure. It can be noted that the model simulates that the concentration of free chlorides near surface increases during the drying periods. At the end of the simulation, i.e. at 119 days, the surface concentration in pore solution of concrete during the drying period are almost the same as when exposed to the sodium chloride solution.

The penetration of sodium ions into pore solution is shown in figure 9.3. The difference in surface concentration during drying and during exposure to the sodium chloride solution is seen to be more marked than for the chloride penetration shown in Figure 9.2. Furthermore, the sodium penetration at all depths is markedly different from the chloride penetration, i.e. the dielectric effects, caused by the presence of all different considered ions, is responsible for this behavior.

The leaching of hydroxide is presented in Figure 9.4. During exposure to the sodium chloride solution the hydroxide ions are allowed to diffuse to the outer storage solution by setting the boundary condition for hydroxide to zero at surface to zero.

An increase of calcium ions according to Figure 9.5 was obtained. The pen-

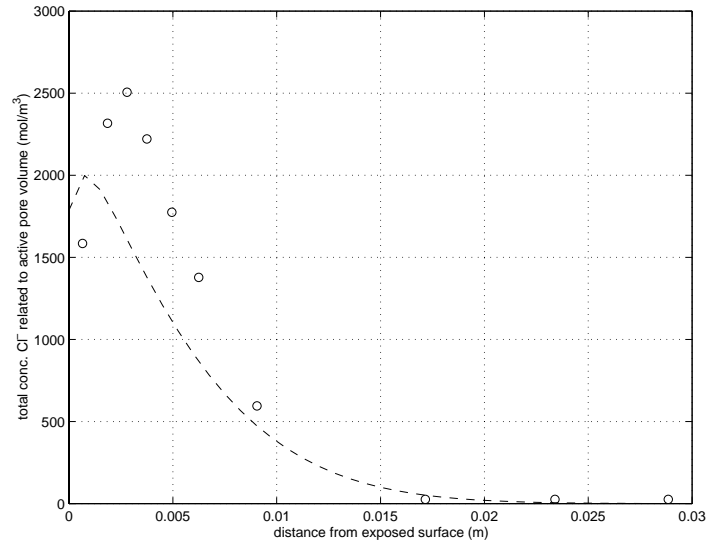


Figure 9.1: Circles, experimental values for a SRPC $w/b = 0.40$. The sample was exposed to cycles of one week of exposure to a 3 wt% sodium chloride solution and one week of storage in room climat during 119 days. The dashed lines shows the simulation using the material constants shown in Table 8.2. The boundary conditions where changed in accordance with the experiments. (Note that the flow of ions at boundary were set to zero during storage in air). The convection is not included in model, which partly explains the poor match.

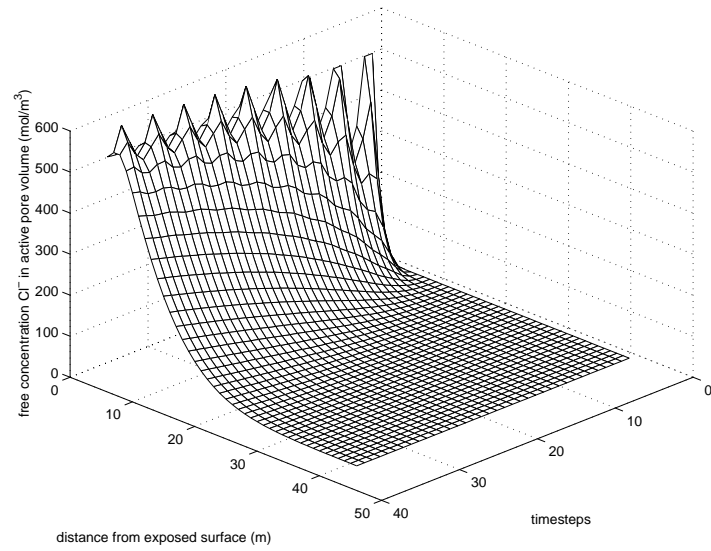


Figure 9.2: *Calculated free chloride concentration in pore solution up to 119 days of exposure. The test concerns an exposure of cycles of one week of exposure to a 3 wt% sodium chloride solution and one week of storage in room climat*

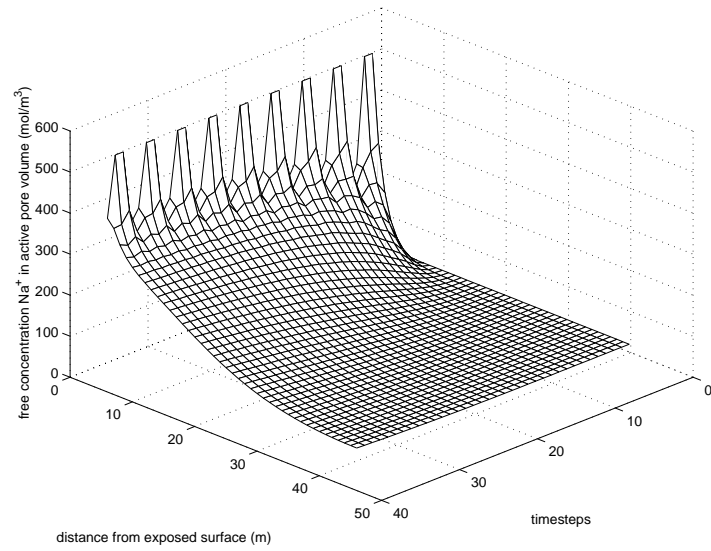


Figure 9.3: *Calculated free sodium ion concentration in pore solution up to 119 days of exposure. The test concerns an exposure of cycles of one week of exposure to a 3 wt% sodium chloride solution and one week of storage in room climate.*

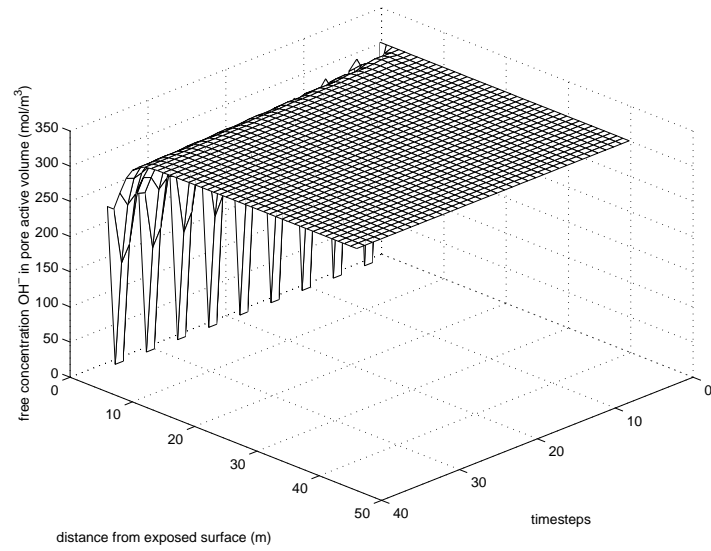


Figure 9.4: *Calculated free hydroxide ion concentration in pore solution up to 119 days of exposure. The test concerns an exposure of cycles of one week of exposure to a 3 wt% sodium chloride solution and one week of storage in room climate.*

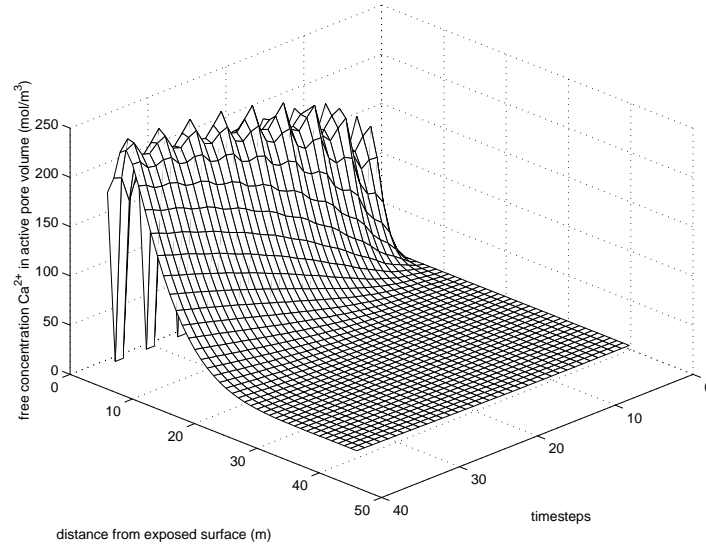


Figure 9.5: *Calculated free calcium ion concentration in pore solution up to 119 days of exposure. The test concerns an exposure of cycles of one week of exposure to a 3 wt% sodium chloride solution and one week of storage in room climate.*

etration of calcium ions into the pore solution is greater than the leaching of hydroxide. The leaching of potassium is shown in Figure 9.6.

The concentration profiles of the bound constituents, i.e. $\text{Ca}(\text{Cl})_2$ and $\text{Ca}(\text{OH})_2$, are shown in Figures 9.7 and 9.8, respectively. Again, it is noted that the total concentration of chlorides constitute the sum of bound and free chlorides, see Figure 9.1.

The simulations performed in this section show that the material constants obtained for the submerged case in the previous section can not alone model the behavior for the tidal zone case, i.e. see the poor match in figure 9.1. It is supposed that the material constants, in use, not should be dependent on the boundary conditions adopted. Therefore a model which also including mechanisms caused by the moisture flow and the change of moisture content must be established. This is the main conclusion drawn from this simulation.

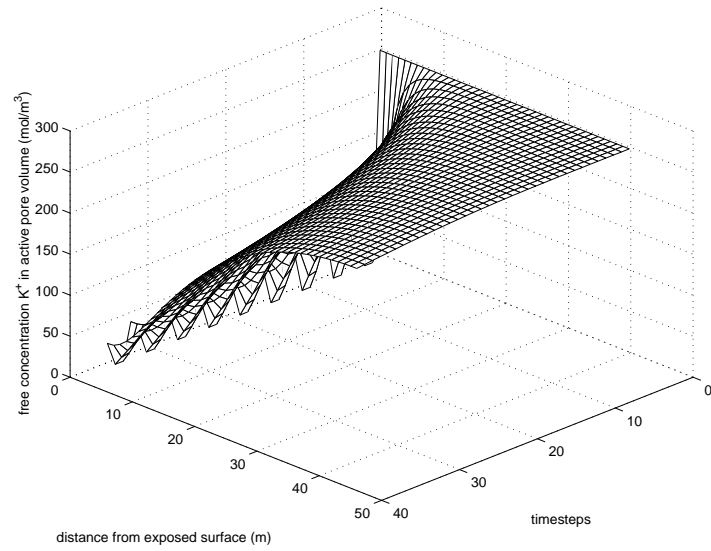


Figure 9.6: *Calculated free potassium ion concentration in pore solution up to 119 days of exposure. The test concerns an exposure of cycles of one week of exposure to a 3 wt% sodium chloride solution and one week of storage in room climate.*

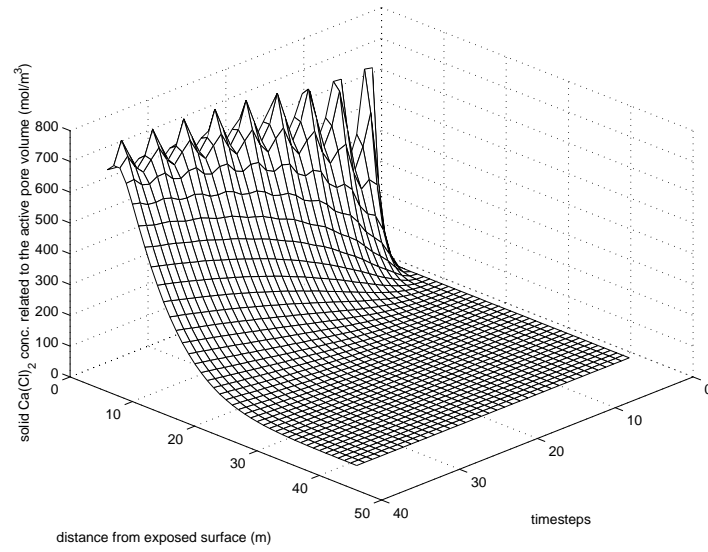


Figure 9.7: *Calculated bound calcium chloride concentration related to pore solution volume. 119 days of exposure. The test concerns an exposure of cycles of one week of exposure to a 3 wt% sodium chloride solution and one week of storage in room climate.*

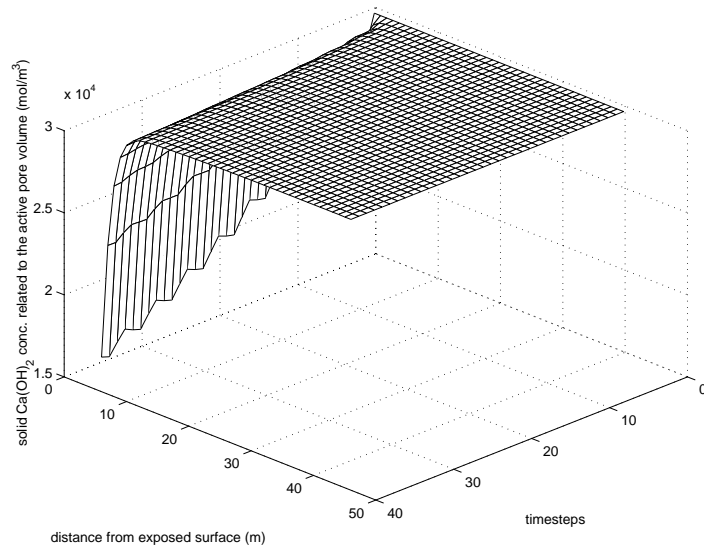


Figure 9.8: *Calculated bound calcium hydroxide concentration related to pore solution volume. 119 days of exposure. The test concerns an exposure of cycles of one week of exposure to a 3 wt% sodium chloride solution and one week of storage in room climate.*

10. Conclusions

It is concluded that the effect of the composition of the mixture of ions on the diffusion characteristics of the individual dissolved ion types is an important issue when dealing with chloride penetration into cement-based materials. It is shown in the paper that the requirement that dissolved ions should diffuse through the pore system in a way that the net charge at every material point and at every time level is very close to zero gives one possible explanation for obtaining the normally experimentally observed enrichment of chlorides near the exposed surface. By accounting for the dielectric effects it was possible to obtain a fairly good match between chloride profiles obtained by simulation and experiments. It should be carefully observed, however, that other mechanisms than the ones assumed here may be the cause of the measured response in terms of chloride ingress. In order to study this, other kinds of constitutive assumptions must be tested.

The results from the simulation showed that leaching of hydroxide ions in pore solution into the outer storage solution was small, see previous sections. At greater depths than 10 mm no leaching occurred. This is due to a combined effect of (i) the assumed dissolution rate of calcium and hydroxide ions from solid calcium hydroxide, as described by equation (5.3), and (ii) properties affecting diffusion of hydroxide ions in pore solution, i.e. concentration gradient dependent diffusion and (iii) effects on diffusion caused by dielectrics among different types of ions. The behavior also is dependent on the buffer of solid calcium hydroxide in concrete which is assumed to be high in the simulation made.

On the other hand, the simulation indicates an enrichment of calcium ions in pore solution in the whole domain with a maximum approximately at the depth 4 mm, after 119 days of exposure. This behavior is, again, due to the assumed dissolution reaction (5.3) and the rate of diffusion of calcium ions to outer storage solution and dielectric effects. It is the resulting shape of the calcium ions profiles in pore solution, which forces the chloride ions to be enriched near exposed surface. Loosely speaking, the chloride ions are forced to level out the electrical imbalance caused by calcium ions entering the pore solution due to dissolution of solid calcium hydroxide. It is also noted by the simulation that dissolved hydroxide ions cannot compensate for this behavior.

In order to verify the described model for diffusion and chemical reactions of ions in the pore solution of cement-based materials, an experimental determination of concentration profiles of all considered ions must be performed for given exposure conditions. In this work only the experimentally obtained chloride pro-

files were studied together with a model including several types of ions, besides chlorides. Further, one of the main issues is to find the relations of solubility properties of ions in the considered system of constituents.

It is also concluded that the method for dividing the total chloride content in two parts, one part being dissolved in pore solution and the other being bound, is very crucial. This makes possible a scaling of the diffusion coefficient valid for ions in bulk water with a tortuosity factor accounting for the shape of the microstructure. Further, this way of dividing the total concentration of chloride ions means that the effects caused by electrical forces among the positive and negative ions in pore solutions can be studied theoretically in a stringent manner.

The example concerning the tidal zone suffer from some serious inconsistencies, since the convection of the dissolved ions in pore solution, caused by capillary suction, not was considered. This type of phenomena has never been combined with multi-species calculations in concrete durability problems. The theoretical model is, however, described in [31] and cases where only the chloride ions are considered together with convection can be studied in [29]. Numerical issues for this application can be found in [30].

References

- [1] Bowen, R.M. (1976). *Theory of Mixtures*, Part 1, in Continuum Physics, Edited by A. Cemal Eringen, Princeton University of Technology.
- [2] Johannesson, B.F. (1998). *Modelling of Transport Processes Involved in Service Life Prediction of Concrete, Important Principles*, Division of Building Materials, Lund University of Technology.
- [3] Weast, R.C., Lide, D.R. Astle, M.J. and Beyer, W.H. (1989). *Handbook of Chemistry and Physics*, 70TH edition, CRC Press, Inc. Boca Raton, Florida.
- [4] Atkins, P.W. (1994). *Physical Chemistry*, Fifth Edition, Oxford University Press, Oxford.
- [5] Castellote, M., Andrade, C. and Cruz Alonso, M. (1999). *Changes in Concrete Pore Size Distribution Due to Electrochemical Chloride Migration Trials*, ACI Materials Journal, V. 96, No. 3, pp. 314-319.

- [6] Sharif, A. A., Loughlin K.F. Azad, A.K. and Navaz, C.M. (1997). *Determination of the Effective Chloride Diffusion Coefficient in Concrete via a Gas Diffusion Technique*, ACI Materials Journal, V. 94, No. 3, pp. 227-233.
- [7] Samson, E., Marchand, J. and Beaudoin, J.J. (1999). *Describing ion diffusion mechanisms in cement-based materials using the homogenization technique*. Cement and Concrete Research, V. 29, pp. 1341-1345.
- [8] Martys, N.S. (1999). *Diffusion in Partially-Saturated Porous Materials*. Materials and Structures, V. 32, pp. 555-562.
- [9] Glass, G.K., Hassanein, N.M. and Buenfeld, N.R. (1997). *Neural Network Modelling of Chloride Binding*. Magazine of Concrete Research, V. 49, No. 181, pp. 323-335.
- [10] Birnin-Yauri, U.A. and Glasser, F.P. (1998). *Friedel's Salt, $\text{Ca}_2\text{Al}(\text{OH})_6(\text{Cl}, \text{OH}) \cdot 2\text{H}_2\text{O}$: its Solid Solutions and their Role in Chloride Binding*, Cement and Concrete Research, V. 28, No. 12, pp. 1713-1723.
- [11] Wee, T.H., Wong, S.F., Swaddiwudhipong, S. and Lee, S.L. (1997). *A Prediction Method for Long-Term Chloride Concentration Profiles in Hardening Cement Matrix Materials*. ACI Materials Journal, V. 94, No. 6, pp. 565-579.
- [12] Sandberg, P. (1995). *Critical Evaluation of Factors Affecting Chloride Initiated Reinforcement Corrosion in Concrete*, Division of Building Technology, Lund Institute of Technology.
- [13] Tritthart, J. (1992). *Changes in Pore Water Composition and in Total Chloride Content at Different Levels of Cement Paste Plates Under Different Storage Conditions*, Cement and Concrete Research. Vol. 22, pp. 129-138.
- [14] Sergi, G., Yu, S.W. and Page, C.L. (1992). *Diffusion of Chloride and Hydroxyl Ions in Cementitious Materials Exposed to a Saline Environment*, Magazine of Concrete Research. 1992, Vol. 44, No. 158, Mar., pp. 63-69.
- [15] Page, C.L., Lambert, P. and Vassie, P.R.W. (1991). *Investigations of Reinforcement Corrosion. 1. The Pore Electrolyte Phase in Chloride-Contaminated Concrete*, Materials and Structures, Vol. 24, No. 139, pp. 234-252.

- [16] Glass, G.K. and Buenfeld, N.R. (1995). *The Determination of Chloride Binding Relationships*, Chloride Penetration into Concrete, Proceedings of the International Rilem Workshop, St-Rémy-lès-Chevreuse, France.
- [17] Midgley, H.G. and Illston, J.M. (1984). *The Penetration of Chlorides into Hardened Cement Pastes*, Cement and Concrete Research. Vol. 14, pp. 546-558.
- [18] Sandberg, P. (1996). *Durability of Concrete in Saline Environment*, Cementa AB, Sweden.
- [19] Tritthart, J. (1989). *The Influence of the Hydroxide Concentration in the Pore Solution of Hardened Cement Pastes on Chloride Binding*, Cement and Concrete Research. Vol. 19, pp. 683-691.
- [20] Ottosen, N.S. and Petersson, H. (1992). *Introduction to the Finite Element Method*, Prentice Hall, London.
- [21] Zienkiewicz, O.C. and Taylor, R.L. (1989). *The Finite Element Method, Fourth Edition, Vol. 2*, McGraw-Hill, London.
- [22] Bathe, K.J. (1996). *The Finite Element Procedures*, Prentice Hall, Englewood Cliffs, New Jersey.
- [23] Hughes, T.J.R. (1987). *The Finite Element Method, Linear Static and Dynamic Finite Element Analysis*, Prentice-Hall International Editions.
- [24] Janz, J. and Johannesson, B.F. (1993). *A Study of Chloride Penetration into Concrete* (in Swedish), Division of Building Technology, Lund University of Technology.
- [25] *Chloride Penetration into Concrete*, Proceedings of the International Workshop St. Rémy-lès-Chevreuse, France, 15-18 October 1995, Edited by Lars Olof Nilsson and Jean-Pierre Ollivier (RILEM Publications, France).
- [26] *Corrosion of Reinforcement, Field and Laboratory Studies for Modelling and Service Life*, Proceedings of the Nordic Seminar in Lund, Sweden, 1-2 February 1995, Edited by Kyösti Tuutti, Division of Building Technology, Lund University of Technology.

- [27] Lindmark, S. (1998). *Mechanisms of Salt Frost Scaling of Portland Cement-bound Materials: Studies and Hypothesis* (Doctoral Thesis), Division of Building Materials, Lund University of Technology.
- [28] RCT, Instructional and Maintenance Manual. (1998). Germann Instrument A/S, Copenhagen, Denmark.
- [29] Johannesson, B.F. (1997). *Nonlinear Transient Phenomena in Porous Media with Special Regard to Concrete and Durability*, Advanced Cement Based Materials, Vol. 6, pp. 71-75.
- [30] Johannesson, B.F. (1996). *Convection-diffusion Problems with Significant First-order Reversible Reactions*, Ninth Nordic Seminar on Computational Mechanics, Technical University of Denmark, Department of Structural Engineering and Materials, Edited by Lars Damkilde, pp. 231-236.
- [31] Johannesson, B.F. (2000). *Transport and Sorption Phenomena in Concrete and Other Porous Media*, Lund Institute of Technology, Division of Building Materials, Lund.

Nordic Mini Seminar on

Prediction Models for Chloride Ingress and Corrosion Initiation in Concrete Structures

Test application of DuraCrete Models

Sascha Lay, Institute for Building Materials of the Technical University of Munich, Germany

1 Model

The applied model for the prediction of chloride ingress has been developed in the Brite EuRam project DuraCrete /1/ and further sophisticated by Gehlen /2/:

$$C(x, t) = (C_{s, \Delta x} - C_i) \cdot \left[1 - \operatorname{erf} \left(\frac{x - \Delta x}{2\sqrt{t \cdot D_{\text{eff}}(t)}} \right) \right] + C_i \quad \text{Eq. 1-1}$$

and,

$$D_{\text{eff}}(t) = k_{RH} \cdot D_{RCM,0} \cdot k_t \cdot k_T \cdot \left(\frac{t_0}{t} \right)^n \quad \text{Eq. 1-2}$$

$C(x, t)$	chloride concentration in depth x at time t [M.-%/b]
$C_{s, \Delta x}$	chloride concentration in depth Δx at time of inspection [M.-%/b]
C_i	initial chloride concentration [M.-%/b]
erf	error function
x	depth with corresponding chloride concentration $C(x, t)$ [m]
Δx	depth of the "convection" zone in which the chloride profile deviates from behavior according to the 2 nd law of diffusion [m]
t	age of concrete [s]
$D_{\text{eff}}(t)$	effective diffusion coefficient of concrete at time t [10^{-12} m ² /s]
k_{RH}	environmental parameter accounting for the influence of the degree of saturation on D_{eff} [-]
$D_{RCM,0}$	chloride migration coefficient of water saturated concrete prepared and stored under predefined conditions, determined at the reference time t_0 [10^{-12} m ² /s]
k_t	test parameter to account for deviations of the chloride migration coefficient, determined under accelerated condition with the Rapid Chloride Migration method (RCM), and a diffusion coefficient determined under natural conditions [-]
k_T	temperature parameter, introduced in /2/ [-]

with

$$k_T = \exp \left(b_T \left(\frac{1}{T_{\text{ref}}} - \frac{1}{T} \right) \right) \quad \text{Eq. 1-3}$$

b_T	regression parameter [K]
T_{ref}	reference temperature [K]
T	temperature of the environment (micro climate) [K]
and	
n	exponent regarding the time-dependence of D_{eff} [-]
t_0	reference time [s]

The applied model is probabilistic, i.e. each parameter is inserted in terms of a mean value, standard deviation and distribution type.

Depassivation of the reinforcement will start when the critical corrosion inducing chloride content C_{crit} will be exceeded in the depth of the concrete cover d_c , expressed by the limit state function given in Eq. 1-4:

$$p_f = p \left\{ C_{crit} - C_i - (C_{s,\Delta x} - C_i) \cdot \left[1 - \operatorname{erf} \left(\frac{d_c - \Delta x}{2 \sqrt{k_{RH} \cdot k_t \cdot k_T \cdot D_{RCM,0} \cdot t \cdot \left(\frac{t_0}{t} \right)^n}} \right) \right] < 0 \right\} \quad \text{Eq. 1-4}$$

p_f	failure probability [-]
p	probability of a certain event to occur [-]
C_{crit}	critical chloride concentration [M.-%/b]
d_c	cover depth [mm]

2 Assumptions and Source of data

2.1 Substituted Surface Chloride Concentration $C_{s,\Delta x}$

For the marine environment the mean value was set to be the largest value of the “peak” concentration in depth Δx of the given chloride profiles /3/, whereas the co-variance was assumed to be 30%.

For the road environment a transition function, determined by a regression analysis of data from Tang and Utgenannt /4/, was applied:

$$k_{Cl} = \frac{Q_{Cl}}{M_{Cl}} = 20,67 - 0,90 \cdot a - 5,40 \cdot h \quad \text{Eq. 2-1}$$

k_{Cl}	ratio of chlorides reaching the concrete surface and the amount of chlorides spreaded [$10^{-3}/m$]
Q_{Cl}	chloride flow reaching the concrete surface [g Cl/m ²]
M_{Cl}	spreaded chloride [t/km]
a	horizontal distance from road [m]
h	vertical distance from road level [m]

The given distance of 3 m /3/ from the nearest lane was assumed to be the horizontal distance (safe side). The vertical distance was set to zero, as the chloride loading decreases more with increasing vertical as with horizontal distance.

The width of the street has been assumed to be 10 m leading to M_{Cl} in [t/km] with a given salt application m_{Cl} in [g/m²]. The co-variance (CoV) of $C_{s,\Delta x}$ was set to be 30%, since reliable data is yet lacking.

2.2 Migration Coefficient $D_{RCM,0}$

The migration coefficient $D_{RCM,0}$ measured at an age of 0,5 a was used for the calculations, assuming normal distribution. A clear age effect was not obvious throughout the given data. The CoV was set to 20% according to /2/.

2.3 Relative Humidity Factor k_{RH}

So far, reliable data on the influence of the saturation degree on the effective diffusion coefficient is scarce but nevertheless has to be accounted for. For the submerged (Sub), tidal (Tid) and splash (Sph) marine environment, full saturation was assumed on the safe side, giving a value of $k_{RH} = 1$. For the atmospheric marine environment (Atm) and the road-environment (road) a value of $k_{RH} = 0,5$ has been guessed, since data is not yet available.

2.4 Temperature Factor k_T

For the sea water the temperature input data was given. For the road environment the temperature was set to be equal to the sea water for comparison purposes.

2.5 The test method factor k_t and age factor n

Values for k_t and n were taken from DuraCrete /5/.

2.6 Depth Δx

For the submerged and tidal conditions Δx was set to be 4 mm according to the "peak" of the given chloride profiles. The "peak" of the profile is probably caused by an aggregation of cement paste in the surface area, since the specimens were stored submerged in seawater. Therefore Δx is assumed to remain constant over time for submerged and tidal conditions. The co-variance was set according to /2/.

For the splash, atmospheric and road-environment mean value and co-variance were chosen according to /2/, hereby accounting for possible effects as convection, chloride wash-off and carbonation in the surface near concrete layer.

2.7 Critical Chloride Concentration C_{crit} , initial concentration C_i and concrete cover d_{cover}

Values for C_{crit} were taken from /5/. The initial concentration was set constant to $C_i = 0,07$ M.-%/b. The mean of the concrete cover was given, whereas the co-variance was set to 8 mm according to /2/, assuming "standard" workman ship.

3 Input parameters

			D-Type	Sub	Tid	Sph	Atm	Road
$C_{s,\Delta x}$	[M.-%/b]	Mean	LogN	3,20	3,20	3,20	3,20	0,84
		StD		0,96	0,96	0,96	0,96	0,25
$D_{RCM,0}$	$[10^{-12} \text{ m}^2/\text{s}]$	Mean	ND	2,70	2,70	2,70	2,70	2,70
		StD		0,54	0,54	0,54	0,54	0,54
k_{RH}	[-]	Mean	Const	1,00	1,00	1,00	0,50	0,50
		StD		0,0	0,0	0,0	0,0	0,0
b_T	[K]	Mean	ND	4800	4800	4800	4800	4800
		StD		700	700	700	700	700
T_{ref}	[K]	Mean	Const	293	293	293	293	293
		StD		0,0	0,0	0,0	0,0	0,0
T	[K]	Mean	ND	284	284	284	284	284
		StD		9,00	9,00	9,00	9,00	9,00
k_t	[-]	Mean	ND	0,832	0,832	0,832	0,832	0,832
		StD		0,024	0,024	0,024	0,024	0,024
n	[-]	Mean	ND	0,30	0,30	0,30	0,65	0,65
		StD		0,12	0,12	0,12	0,05	0,05
t_0	[a]	Mean	Const	0,50	0,50	0,50	0,50	0,50
		StD		0,0	0,0	0,0	0,0	0,0
Δx	[mm]	Mean	BetaD	4,00	4,00	8,90	8,90	8,90
		StD	$0 \leq \Delta x \leq 50$	2,52	2,52	5,60	5,60	5,60
C_{crit}	[M.-%/b]	Mean	ND	2,10	0,80	0,80	0,80	0,80
		StD		0,20	0,10	0,10	0,10	0,10
d_c	[mm]	Mean	BetaD	60,00	60,00	60,00	60,00	60,00
		StD	$0 \leq d_c \leq 300$	8,00	8,00	8,00	8,00	8,00
C_i	[M.-%/b]	Mean	Const	0,07	0,07	0,07	0,07	0,07
		StD		0,0	0,0	0,0	0,0	0,0

D-Type: distribution type

StD: standard deviation

LogN: logarithmic normal distributed

ND: normal distribution

BetaD: beta distribution

4 Estimated Chloride Profiles

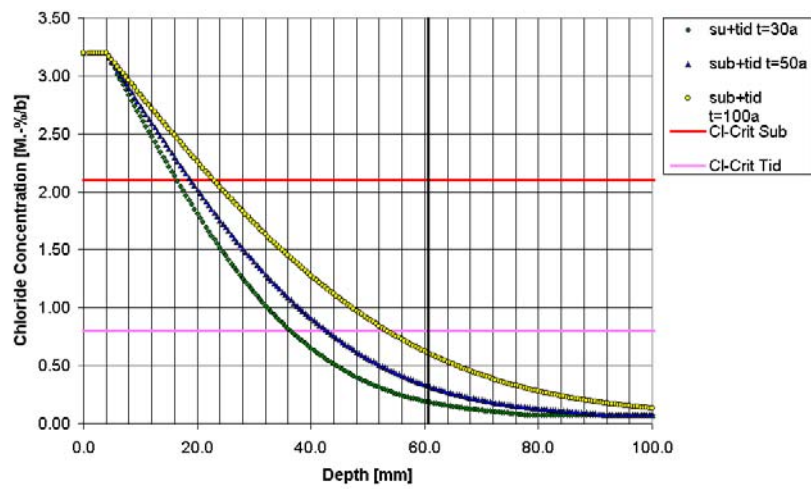


Figure 1: Submerged (Sub) and tidal (Tid) conditions

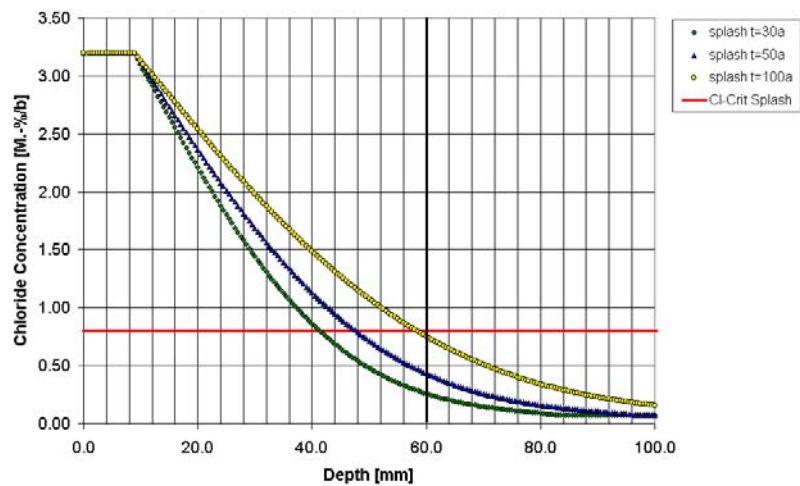


Figure 2: Marine splash conditions (Sph)

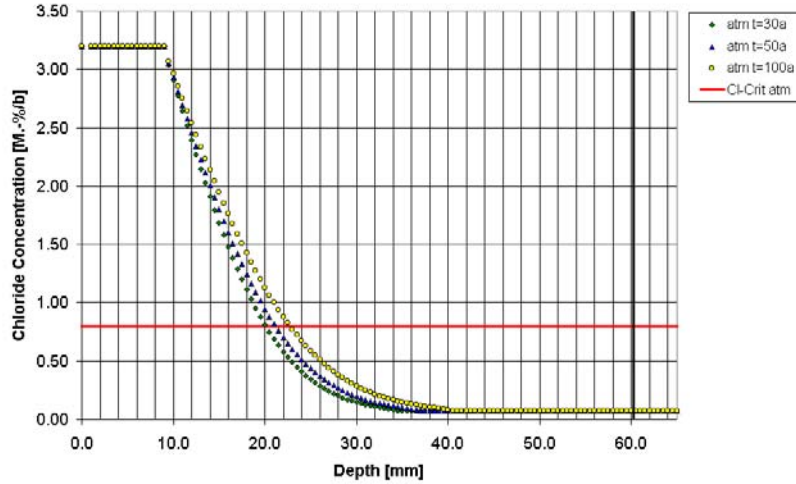


Figure 3: Marine atmospheric conditions (Atm)

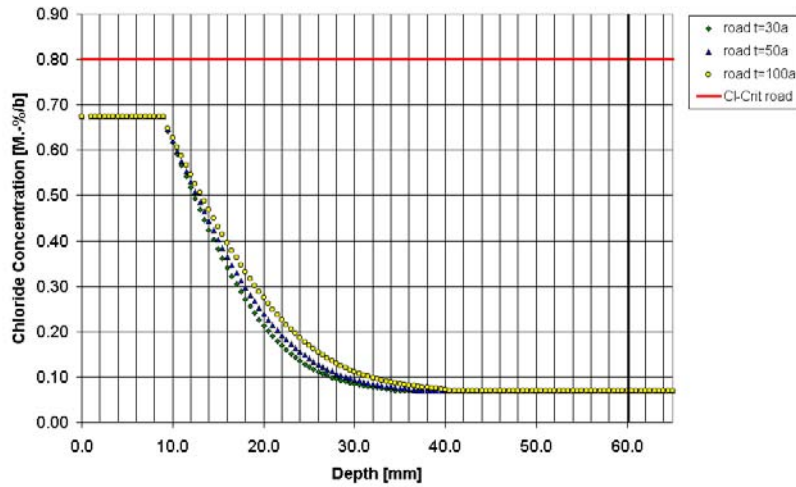


Figure 4: Estimated chloride profiles of a bridge column in a road environment (horizontal distance $a=3$ m from lane; $0,15 \text{ kg/m}^2 \text{ NaCl}$ spreaded)

5 Estimated Service Life

For the estimation of the service life of the case study structures, a safety requirement has to be introduced. Here, the chloride induced depassivation has been chosen as the limit state, which is regarded as a Serviceability Limit State (SLS 2 according to /2/). The required reliability index was set to $\beta_{\text{SLS}} = 2$, yielding a failure probability of $p_f = 2,275 \%$. The desired service life was assumed to be 100 years. Figure 5 to Figure 9 show the reliability index versus time for each environment. Table 1 depicts the reliability index after 100 years, and the service life yielding the reliability requirement.

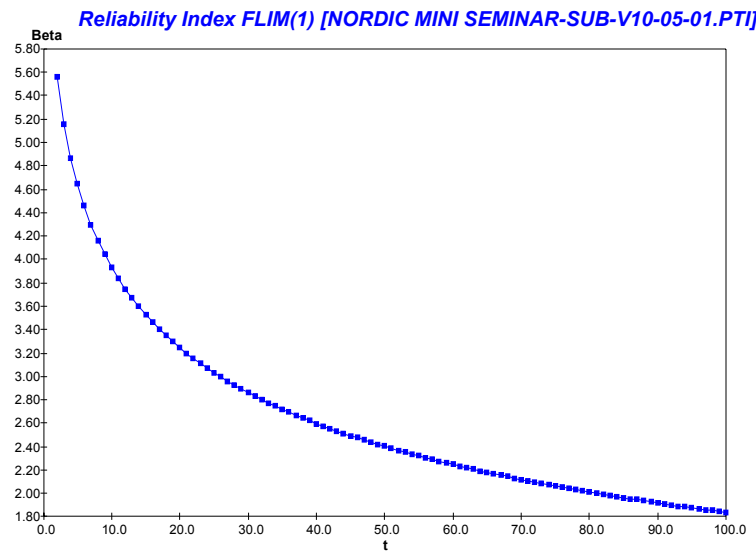


Figure 5: Reliability index for submerged marine conditions

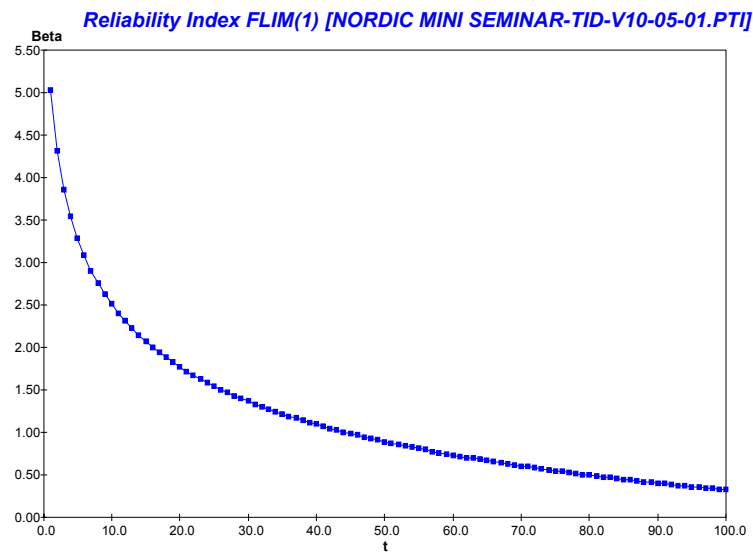


Figure 6: Reliability index for tidal marine conditions

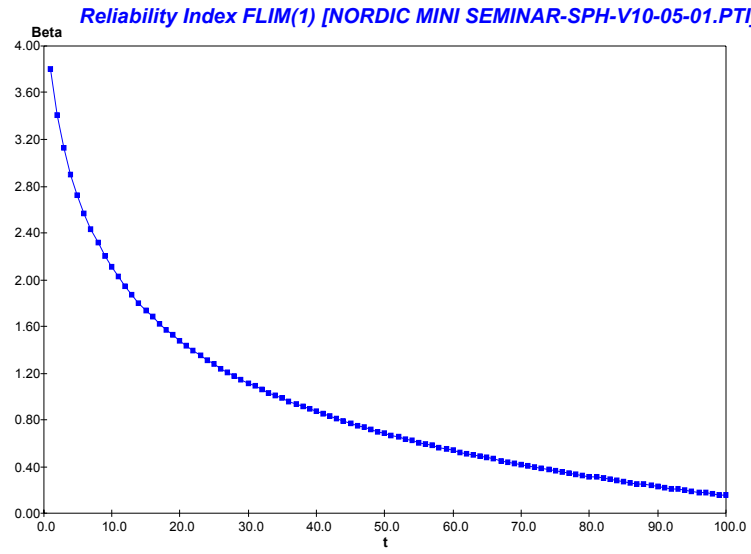


Figure 7: Reliability index for splash marine conditions

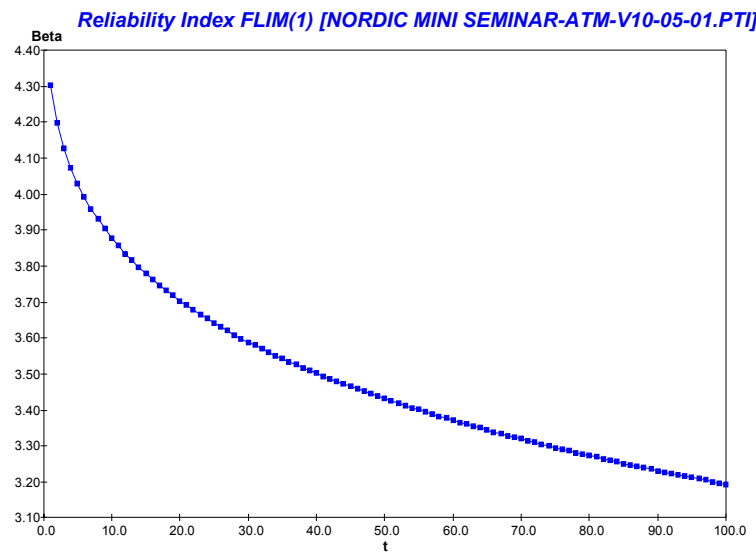


Figure 8: Reliability index for atmospheric marine conditions

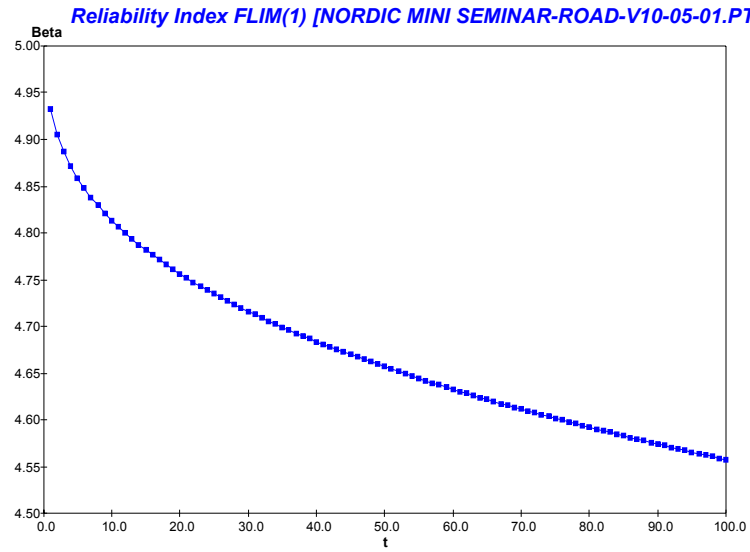


Figure 9: Reliability index for a road environment

Table 1: Estimated Service Life with a reliability $\beta \geq 2$ and reliability after 100 years $\beta(t = 100a)$

		Submerged	Tidal	Splash	Atmospheric	Road
Service Life	[a]	81	16	11	>100	>100
$\beta(t = 100a)$	[-]	1,837	0,329	0,157	3,194	4,558

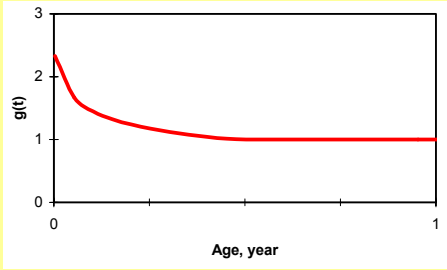
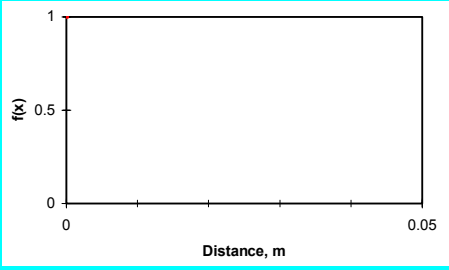
REFERENCES

- 1 BE95-1347: Modelling of Degradation – Report 4-5, 1998
- 2 Gehlen, C.: Probabilistische Lebensdauerbemessung von Stahlbetonbauwerken – Zuverlässigkeitsbetrachtungen zur wirksamen Vermeidung von Bewehrungskorrosion, Deutscher Ausschuss für Stahlbeton, Heft 510, Beuth Verlag, Berlin 2000
- 3 Nilsson, L.O.: Nordic Mini Seminar on Prediction Models for Chloride Ingress and Corrosion initiation in Concrete Structures – Data of the Case Studies, Göteborg, Sweden, 5/2001
- 4 Tang, L., Utgenannt, P.: Characterization of Chloride Environment along a Highway. In: Durability of Building Materials and Components 8 (Volume One), 1999
- 5 BE95-1347: Statistical Quantification of the Variables in the Limit State Functions – Report 9, 2000

Material Properties

Concrete Mix Design		H4	Density
Cement	399	kg/m ³	3150 kg/m ³
Silica fume	21	kg/m ³	2800 kg/m ³
Fly ash	0	kg/m ³	2300 kg/m ³
Slag	0	kg/m ³	2800 kg/m ³
Fine aggregate	842	kg/m ³	2650 kg/m ³
Coarse aggregate	843	kg/m ³	2650 kg/m ³
Max. size of aggregate	16	mm	
Water	168	kg/m ³	
Air pores	5.9	vol%	
Initial chlorides Cl ⁻	0.05	wt% of binder	
Sodium oxide Na ₂ O	0.01	wt% of binder	
Potassium oxide K ₂ O	0.6	wt% of binder	

Chloride Diffusivity		H4	Chloride Binding Capacity		
Applied potential in CTH Rapid Test U	60	V	Isotherm slope	3.57	
Specimen age	200	day	Non-linear exponent	0.38	
Specimen thickness L	50	mm	Time-dependent coefficient, a	0.36	
Temperature T	20	°C	Time-dependent coefficient, b	0.5	
Test duration t	24	hr	Activity energy	40000	J/mol
Chloride penetration depth x_d	12.0	mm			
Chloride diffusion coefficient D_{CTH}	2.7	$\times 10^{-12}$ m ² /s			
Friction factor f	71670				
Activity energy for D(T)	42000	J/mol			

Age-dependence			Distance-dependence		
Age when D becomes constant	180	days	Distance to constant D	0	m
			(Surface D)/(Bulk D)	0.52	
Exponent β_s	0.263		Exponent β_x	0.63	
					

Test Environments

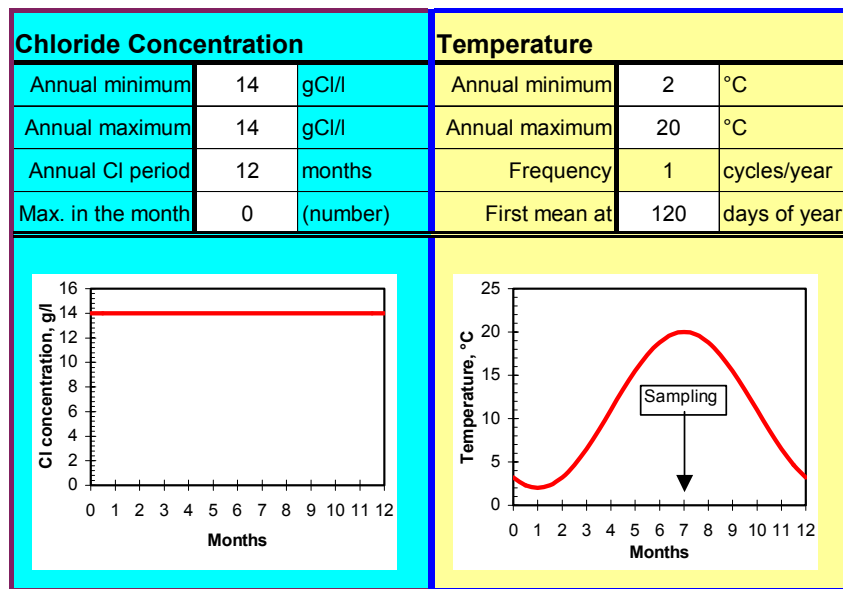


Fig. 1. Submerged zone.

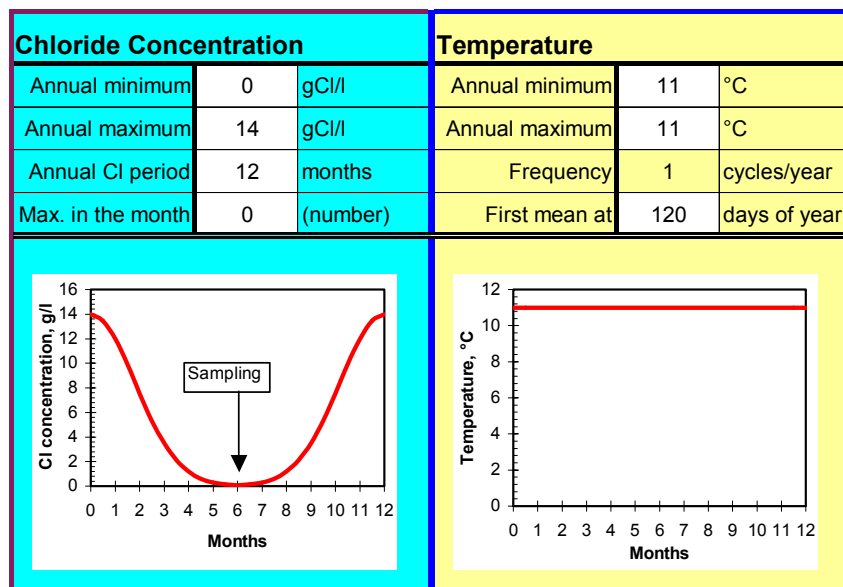


Fig. 2. Splash zone (0~30 cm above water).

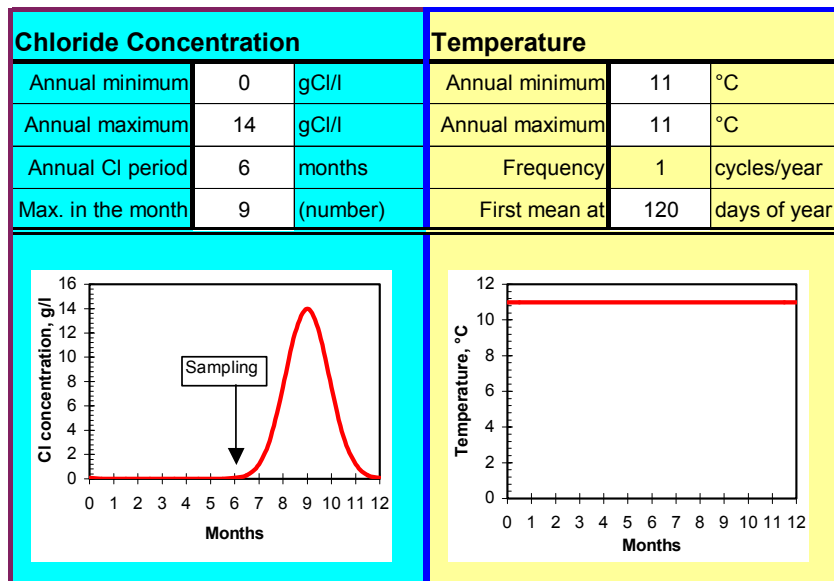


Fig. 3. Atmospheric zone (30~60 cm above water).

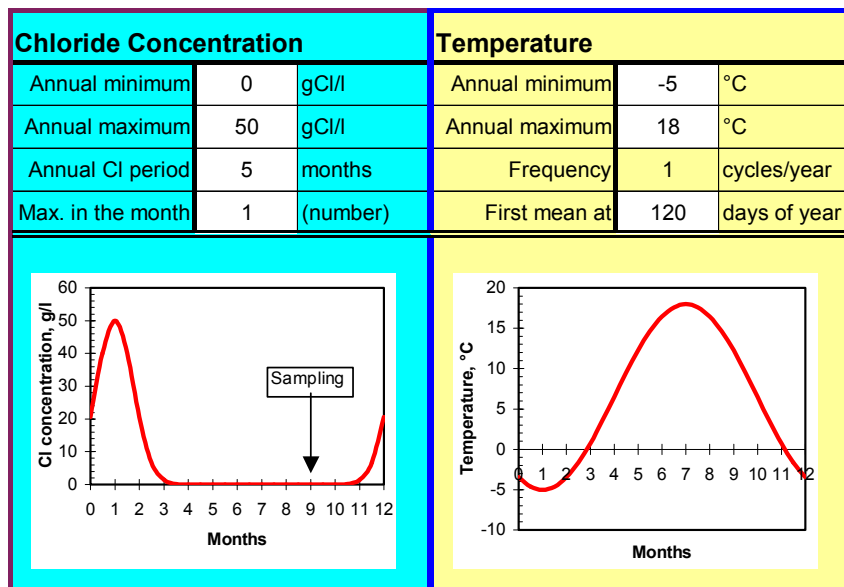


Fig. 4. Road environment (Rv 40 Borås-Göteborg).

Prediction Results

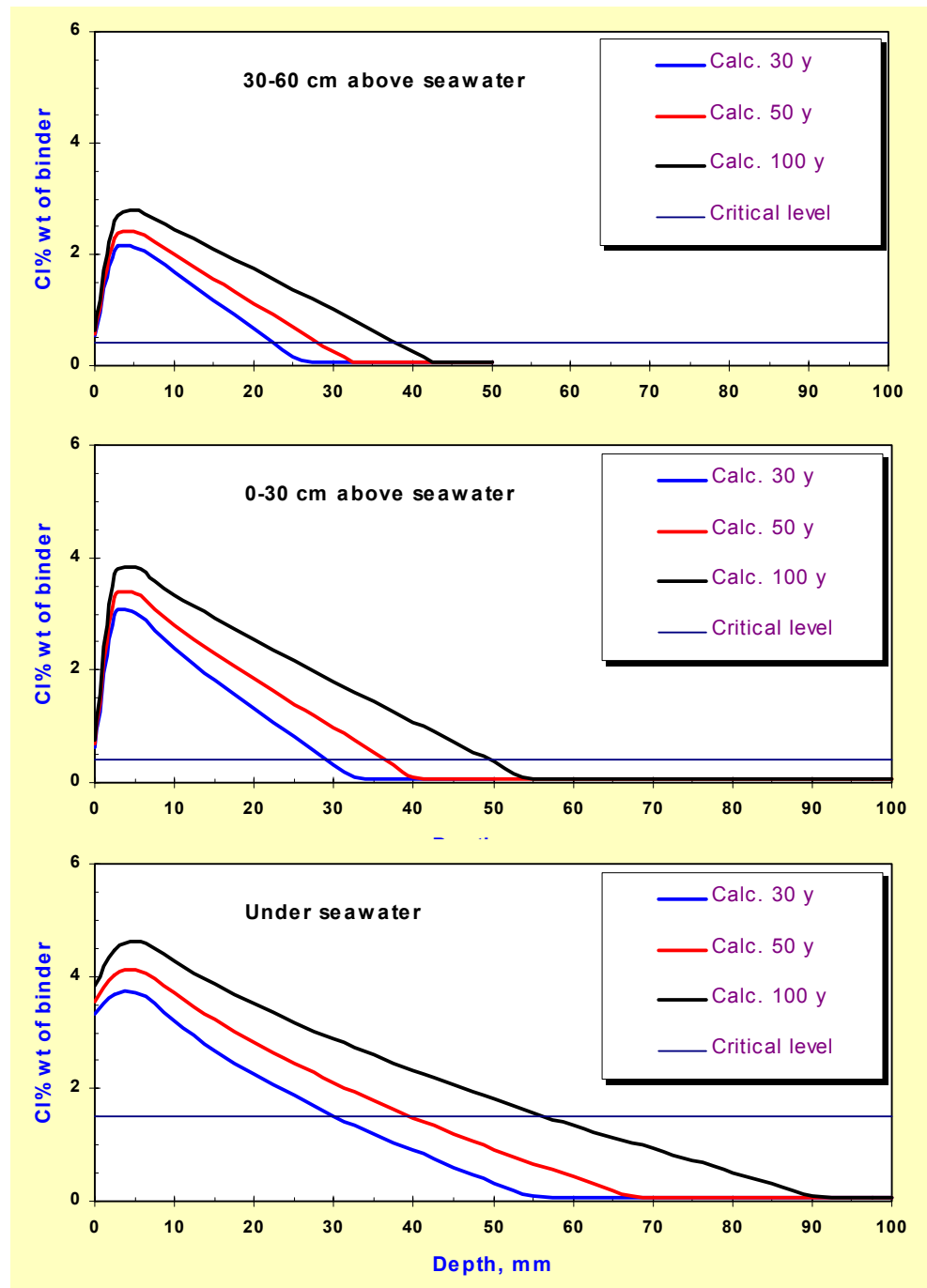


Fig. 4. Predicted results of the marine environment (Swedish west coast).

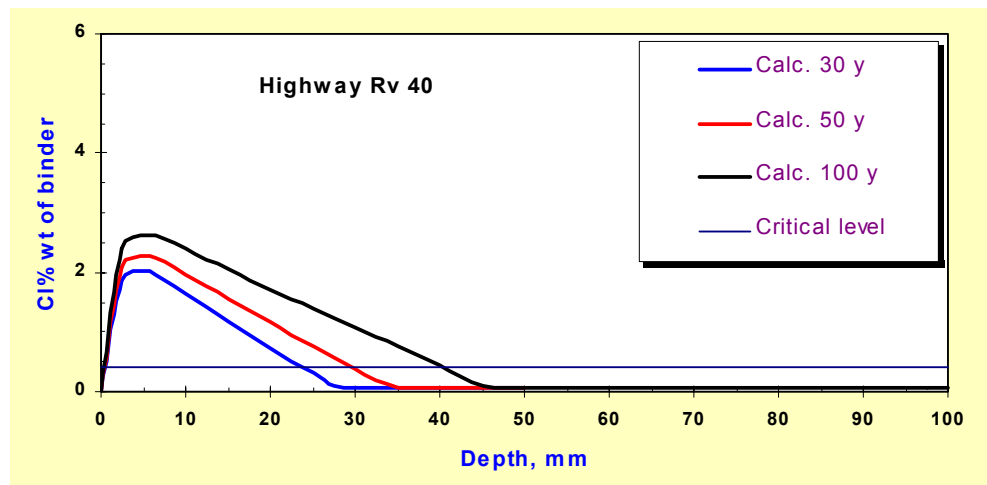


Fig. 5. Predicted results of the road environment (Rv 40 Borås-Göteborg).

A TEST OF PREDICTION MODELS FOR CHLORIDE INGRESS AND CORROSION INITIATION

Lars-Olof Nilsson

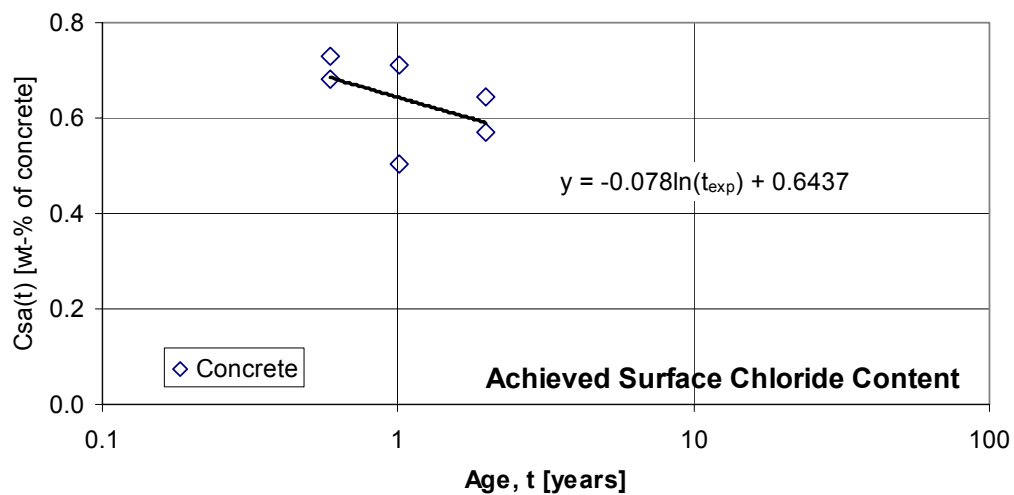
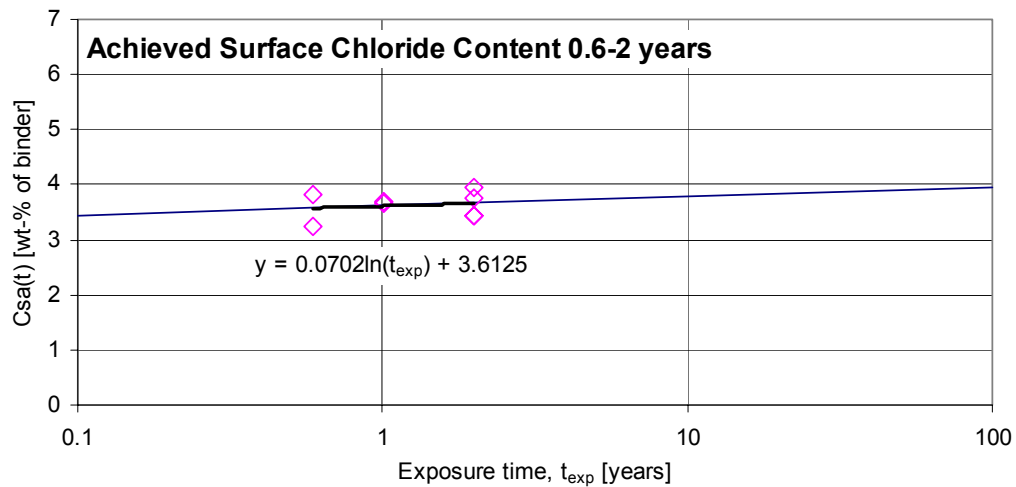
A False ERFC model, Nilsson (2001):

$$C(x, t) = C_{sa}(t_e) \cdot \operatorname{erfc}\left(\frac{x}{2\sqrt{D_a(t) \cdot t_e}}\right)$$

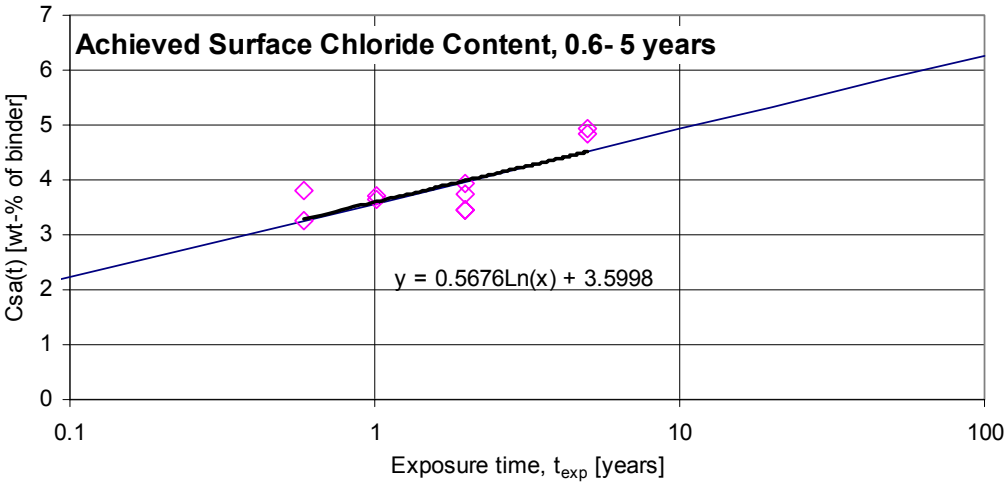
$$D_a(t_e) = D_{a,ref} \cdot \left(\frac{t_{ref}}{t_e}\right)^\alpha$$

$$C_{sa}(t_e) = A \cdot \ln(t_e + \Delta t_{ini}) + B$$

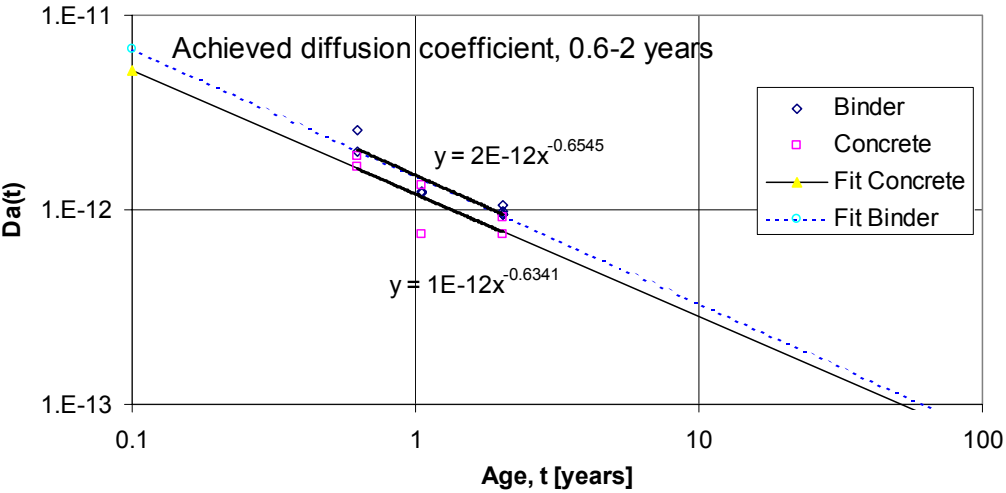
The provided chloride profiles give C_{sa} -values, depending on how many points the regression analysis utilizes and whether profiles as % of binder or concrete are used:



For the same concrete recent data from five years exposure show a more clear time-dependency of C_{sa} , also in submerged concrete (but this is ignored in the predictions):

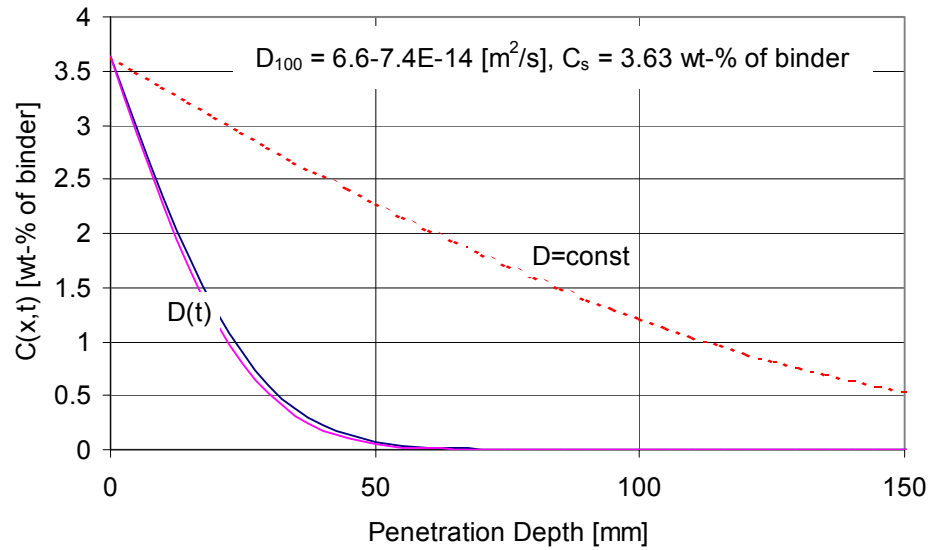


The profiles and laboratory tests gave these apparent diffusion coefficients $D_a(t)$:

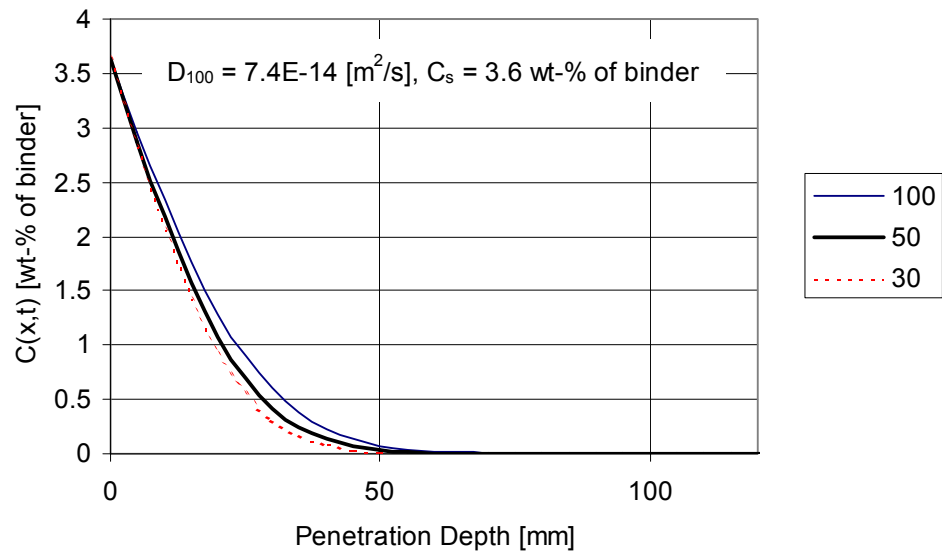


Fit Concrete				Fit Binder			
		alfa=0.6341				alfa=0.6545	
		0.1	100			0.1	100
		5.25363E-12	6.579E-14			6.77004E-12	7.36362E-14
		1.22E-12				1.50E-12	
		0.1	100			0.1	100
Da(t)	5.25E-12	6.58E-14		Da(t)	6.77E-12	7.36E-14	
	D ₁	D ₁₀₀			D ₁	D ₁₀₀	
Daex				Daex			
9.65E-12				1.27E-11			

A comparison with the erfc-model with constant D_a :



Predictions for the submerged, tidal and splash zones (no significant difference!), for 30, 50 and 100 years exposure:



DTI-predictions for the test case – sensitivity analysis

Marianne Tange Jepsen, DTI

Some results from the very simple model “what the engineer does, when he has nothing but the stated measurements and “Physical Chemistry” written by P.W. Atkins on the book shelf”, which means that these results are calculated with a numerical version of Fick’s 2. law.

Assumptions for all the profiles

- Constant surface chloride content: 3,63 wt% of binder

Assumptions for profiles labelled 1

- Constant diffusion coefficient: $1,7 \cdot 10^{-12} \text{ m}^2/\text{s}$

Assumptions for profiles labelled 2

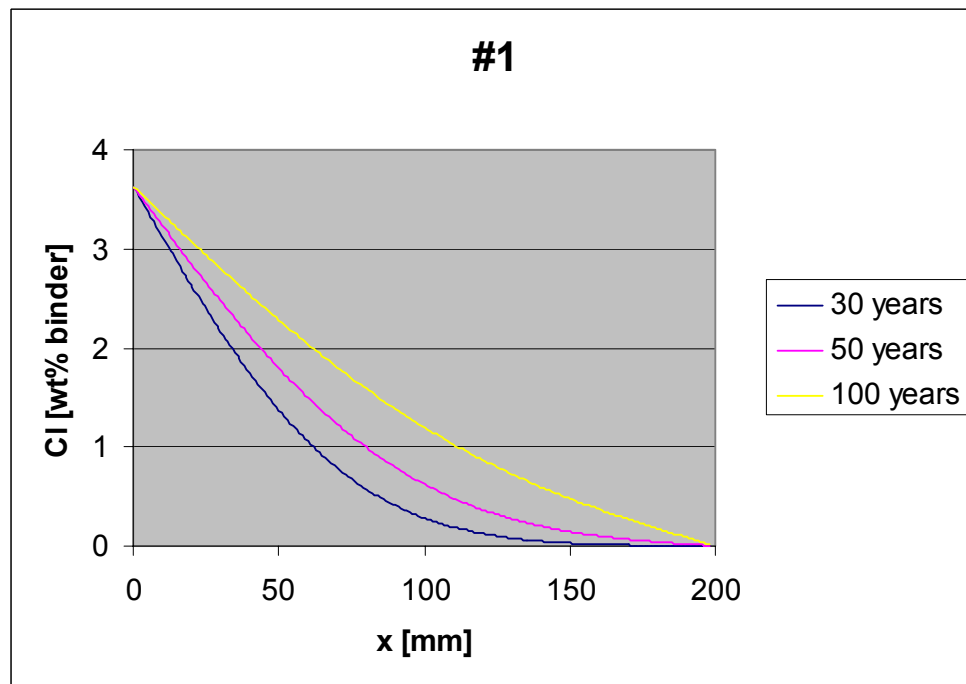
- Time dependent diffusion coefficient

$$D = a \cdot t^{-b}$$

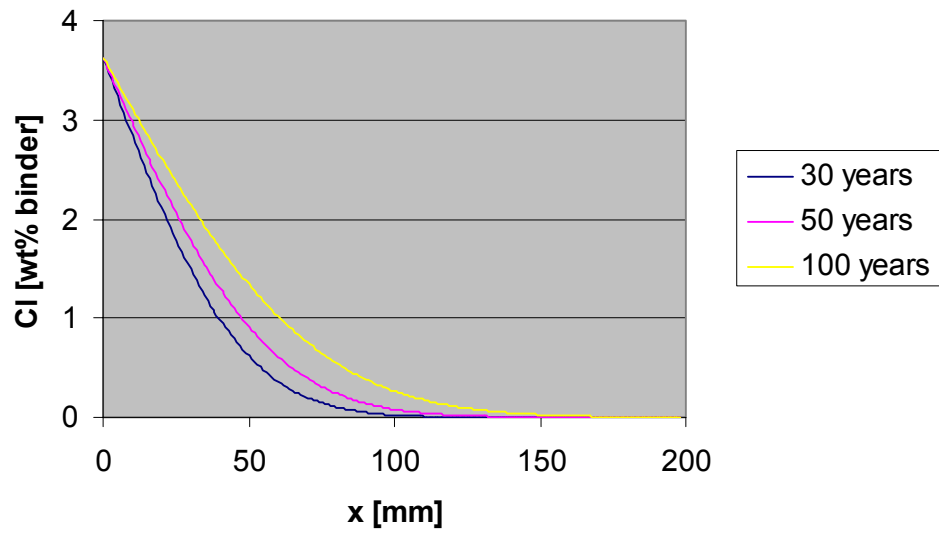
In case 2a $b=0.3$ (a is calculated so $=1,7 \cdot 10^{-12} \text{ m}^2/\text{s}$ after 0.5 years).

In case 2b $b=0.6$ (a is again calculated so $=1,7 \cdot 10^{-12} \text{ m}^2/\text{s}$ after 0.5 years).

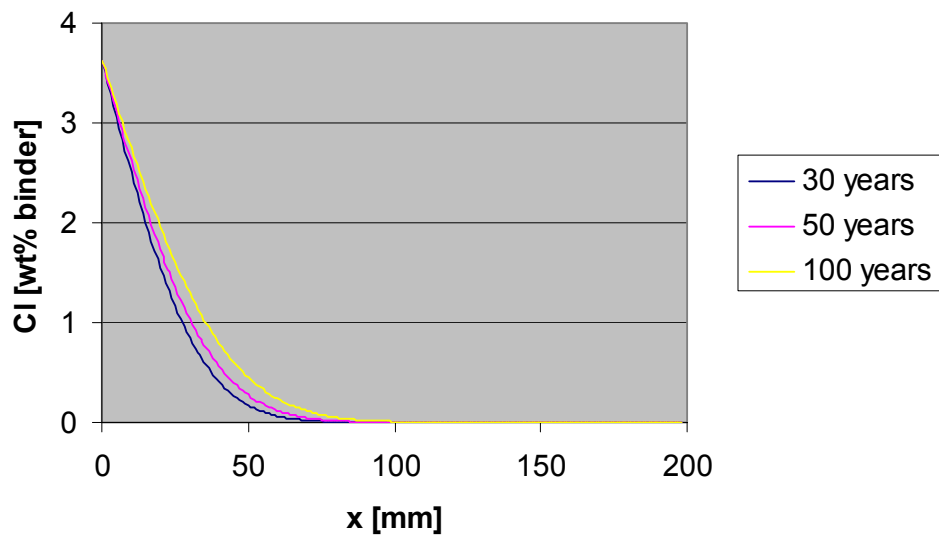
In case 2c $b=0.6$, but the D does only change the first year. After one year D is constant.



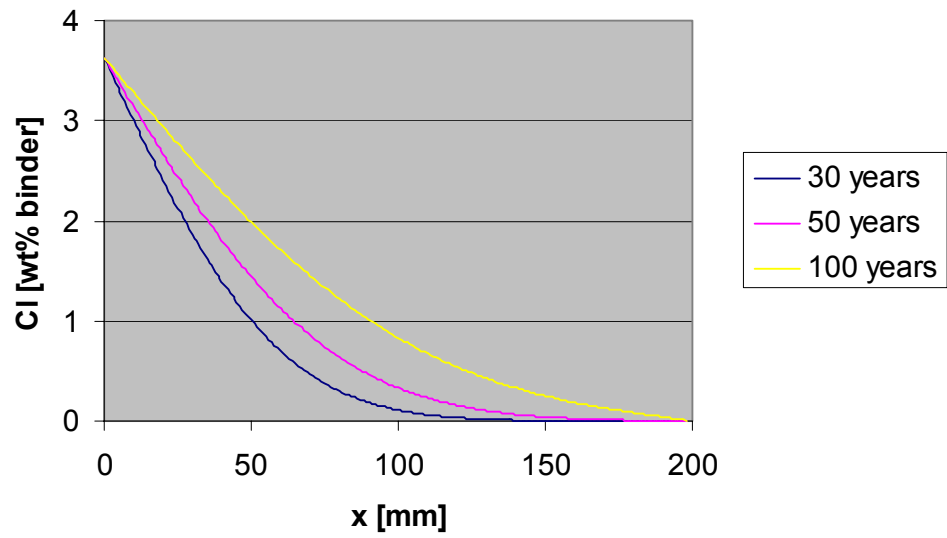
#2a



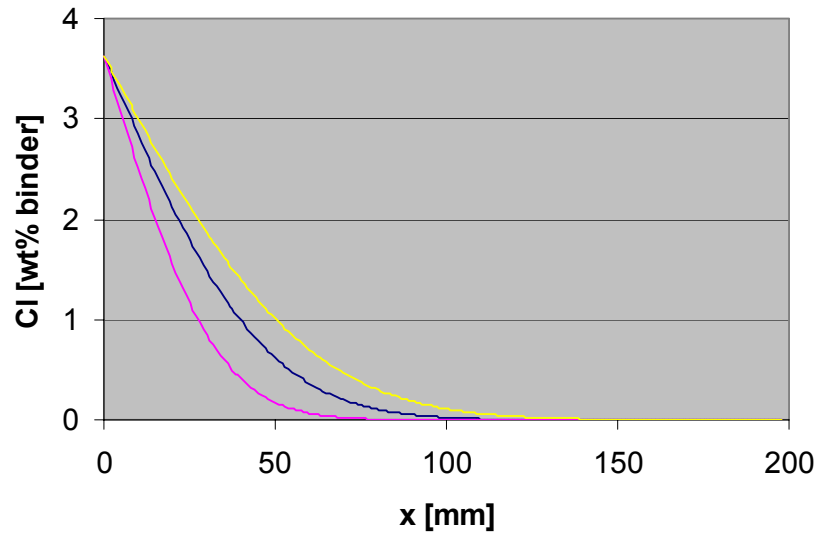
#2b



#2c

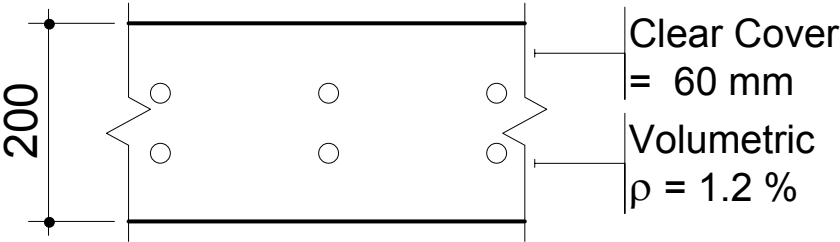


30 years



Description of Structure

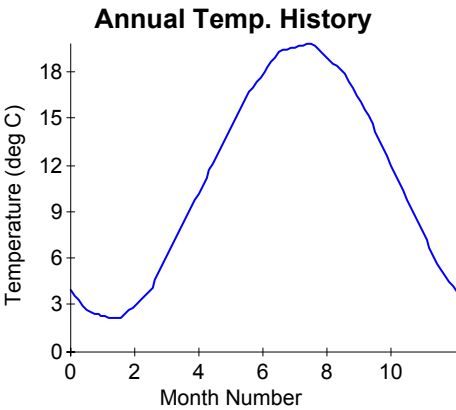
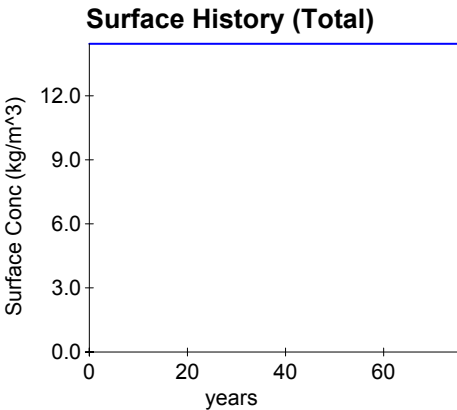
Properties of Scenarios



Base Case

Mix Design : w/cm = 0.40, Cost 100 \$/m³
Silica fume = 5 %
 $D_{28} = 3.49 \times 10^{-12}$ m²/s , m = 0.20 , $C_t = 1.2$ kg/m³
Black Steel (1.50 \$/kg) , Propagate = 6 years

Design Life = 75 years
Discount Rate = 3.0



L365

ClsemGOTtestcase

LON

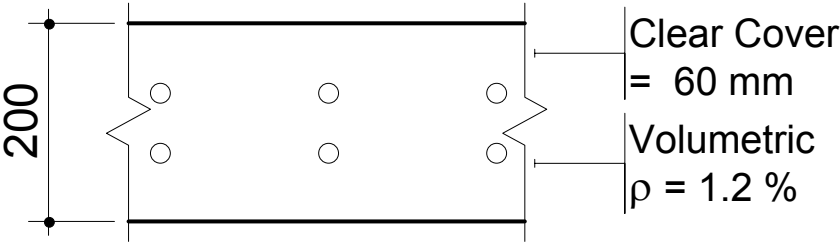
2001/6/9

Description of Structure

Properties of Scenarios

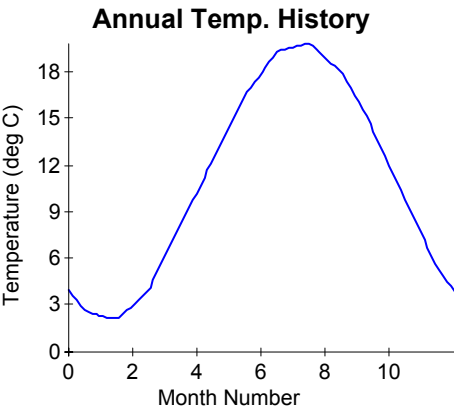
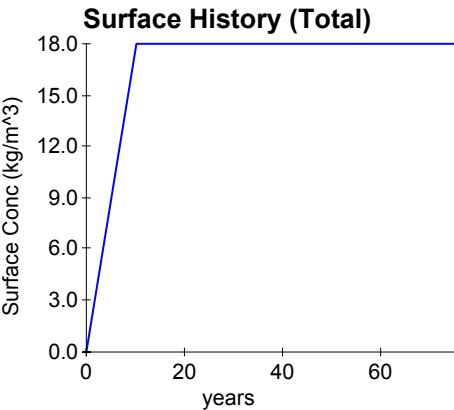
Base Case

Mix Design : w/cm = 0.40, Cost 100 \$/m³
Silica fume = 5 %
D₂₈ = 3.49x10⁻¹² m²/s , m = 0.20 , C_t = 1.2 kg/m³
Black Steel (1.00 \$/kg) , Propagate = 6 years



Design Life = 75 years

Discount Rate = 3.0



L365

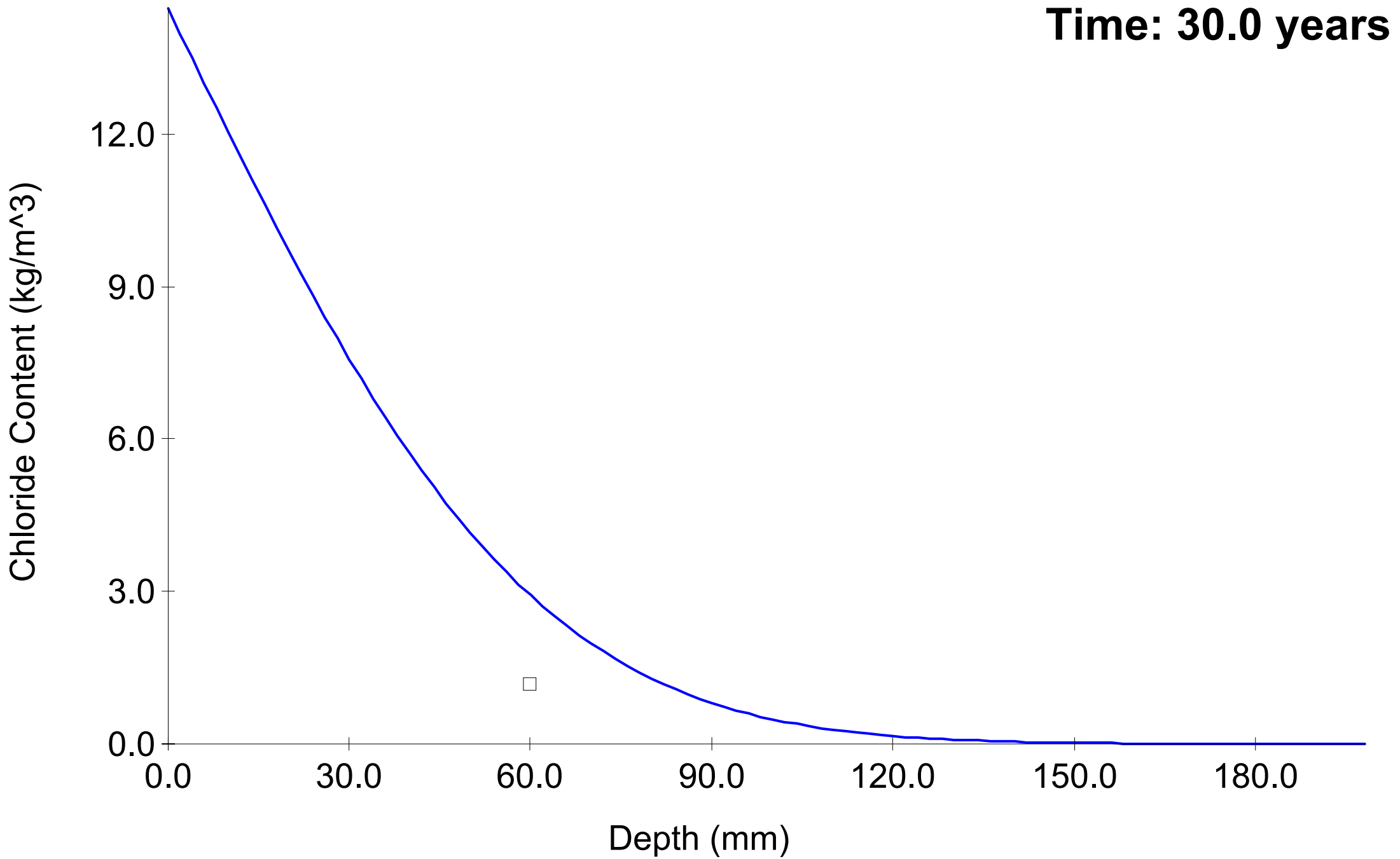
ClsemGOTtestcase

LON

2001/6/9

Concentration-Depth

Time: 30.0 years



Concentration-Depth

Time: 30.0 years

